The Effects of VEGF Over-expression on the Utero-placental Circulation

Vedanta Mehta

University College London

2011

A thesis submitted for the degree of Doctor of Philosophy

Declaration

I, Vedanta Mehta, confirm that the work presented in this thesis is my own. Where information has been derived from other sources, I confirm that this has been indicated in the thesis.

Abstract

Impaired uterine blood flow (UBF) leads to fetal growth restriction (FGR), one of the most challenging obstetric complications. FGR is associated with stillbirth, long-term neurological impairment and adult onset cardiovascular disease; there is no treatment currently available.

Previously, it was shown that sustained local over-expression of Vascular Endothelial Growth Factor (VEGF) in the uterine arteries (UAs) of pregnant sheep using an adenoviral vector results in increased UBF as measured by Doppler sonography, reduced vascular contractility and increased vascular relaxation 4-7 days after administration. The aim of this thesis is to examine the long-term effects on UBF, UA vascular reactivity, and the possible mechanism of action.

Telemetric transit-time flow probes were implanted around the UAs of mid-gestation pregnant sheep (n=10), and a telemetric blood-pressure sensitive catheter was inserted in the maternal (n=5) or fetal (n=4) carotid arteries. After obtaining baseline values for 7 days, we injected adenovirus vectors ($5x10^{11}$ particles) encoding the VEGF-A_{165} gene (Ad.VEGF) into one UA, and a reporter β-galactosidase gene (Ad.LacZ), contra-laterally. UBF and maternal haemodynamics were measured daily until term, when the UAs were harvested and their vascular reactivity studied. There was a significant increase in UBF in the Ad.VEGF transduced side (36.53% v/s 20.08%, p=0.02), a reduction in UA contractility but no difference in relaxation. A significantly greater number of adventitial blood vessels were observed in the Ad.VEGF treated UA. There were no significant changes in maternal or fetal blood pressure post-injection. Similar effects were observed with injection of an adenovirus encoding another member of the VEGF gene family, VEGF-$D^{\Delta N \Delta C}$ (n=5).

Endothelial cells (ECs) were isolated from the UAs of control mid-gestation pregnant sheep, cultured and infected with Ad.VEGF or Ad.LacZ vector. Protein extracted from UAECs infected *ex vivo* was assayed for eNOS and phosphorylated eNOS (Ser^{1177}) levels by Western blotting. eNOS and phospho-eNOS levels increased with rising Ad.VEGF concentrations in UAECs; Ad.LacZ vector transduction had no effect.

Local over-expression of VEGF effects a long-term increase in UBF by upregulation of eNOS, with neovascularization of the adventitia and reduced UA contractility. These changes may benefit pregnancies complicated by severe FGR. With clinical translation in mind, the last section of this thesis describes the optimization of a technique of gene targeting to the utero-placental circulation of growth-restricted guinea pigs, using a thermo-sensitive pluronic gel. Having optimized this technique, VEGF over-expression in the uteroplacental circulation is now being tested in this animal model of FGR.

Table of Contents

List of Figures

Chapter 1

Chapter 2

Chapter 4

Chapter 5

List of Tables

Chapter 2

Chapter 3

Chapter 4

Chapter 5

Publications

David AL, Torondel B, Zachary I, Wigley V, Abi-Nader K, Mehta V, Buckley SM, T Cook, Boyd M, Rodeck CH, Martin J, Peebles DM. Local delivery of VEGF adenovirus to the uterine artery increases vasorelaxation and uterine blood flow in the pregnant sheep. Gene Ther. 2008 Oct;15(19):1344-50

Abi-Nader KN, Mehta V, Wigley V, Filippi E, Tezcan B, Boyd M, Peebles DM, David AL. Doppler ultrasonography for the noninvasive measurement of uterine artery volume blood flow through gestation in the pregnant sheep. Reprod Sci. 2010 Jan;17(1):13-19.

Abi-Nader KN, Mehta V, Shaw SW, Bellamy T, Smith N, Millross L, Laverick B, Filippi E, Boyd M, Peebles DM, David AL. Telemetric monitoring of fetal blood pressure and heart rate in the freely moving pregnant sheep: a feasibility study. Lab Anim. 2011 Jan;45(1):50-54.

Mehta V, Abi-Nader KN, Waddington S, David AL. Organ targeted prenatal gene therapy-how far are we? Prenat Diagn. 2011 Jul;31(7):720-34.

Mehta V, Abi-Nader KN, Peebles DM, Benjamin E, Wigley V, Torondel B, Filippi E, Shaw SW, Boyd M, Martin J, Zachary I, David AL. Long-term increase in uterine blood flow is achieved by local over-expression of VEGF-A_{165} in the uterine arteries of pregnant sheep. Gene Therapy Epub Oct 2011

Acknowledgements

First and foremost, I would like to thank my supervisor Dr. Anna David. Her mentorship, encouragement, support and enthusiasm to teach goes beyond what may be expected, and this is genuinely appreciated. She would often tell me during the animal surgeries that she would make a surgeon out of me, and did succeed at it.

I am also grateful to my secondary supervisor, Prof Ian Zachary, for his guidance, encouragement and help with experimental design during the course of this Ph.D.

I would like to thank Prof. Donald Peebles and Prof. John Martin for their enthusiasm for this project and the very helpful discussions. Thanks to Dr. Elizabeth Benjamin for help with histology.

I am grateful to a number of colleagues in the lab, who were ever willing to help. Of particular mention are Khalil Abi-Nader, Steven Shaw, Elisa Filippi, Belen Torondel, David Sanz-Rosa, Paul Frankel, Ian Evans, Maiko Yamaji, Caroline Pellet-Many, Gary Britton, Dan Liu, Simon Waddington, Mariya Hristova, Alejandro Acosta-Saltos and Vijay Devineni.

During the course of this Ph.D., I had an opportunity to supervise several wonderful students in the lab and really enjoyed the experience. These included Berrin Tezcan, Marie Buitendyk, Panicos Shangaris, Gemma Petts, Beth Laverick, Neil Smith, Laura Millross-Jane, Alison Evans, Priyesh Patel and Rikesh Patel. I am thankful to them for their hard work.

I would also like to take this opportunity to thank all the staff at the BSU, Royal Veterinary College for taking excellent care of the experimental animals,

particularly Michael Boyd, Lynn Dorsett, David Manners, Tom Bellamy, Adnan, Hannah and Pauline Reading.

I am particularly grateful to Ark Therapeutics Ltd., who funded many of the experiments described in this thesis, and to the Dorothy Hodgkin Postgraduate Award Scheme, which funded my Ph.D.

Last but not the least, I owe it to my family for their encouragement, support and belief; particularly my Mum and Dad, for the numerous calls they made to me each day during the 'writing up' phase to make sure I was eating enough food and getting enough sleep.

Selected abbreviations

Ach	Acetylcholine
Ad	Adenovirus
AEDF	Absent end diastolic flow
AFI	Amniotic fluid index
AGA	Appropriate for gestational age
ALP	Alkaline phosphatase
ALT	Alanine aminotransferase
ANOVA	Analysis of Variance
AREDF	Absent or reversed end diastolic flow
AST	Aspartate aminotransferase
BK	Bradykinin
BP	Blood pressure
BPP	Biophysical profile
BrdU	5-bromo-2'-deoxyuridine
cAMP	Cyclic adenosine monophosphate
CAR	Coxsackievirus and adenovirus receptor
cDNA	Complementary DNA
cGMP	Cyclic guanosine monophosphate
CHD	Coronary heart disease
COX	Cyclooxygenase
CTG	Cardiotocograph
DNA	Deoxyribonucleic acid
dpc	Days post conception
E	Embryonic day
EBM	Endothelial basal medium
EC	Endothelial cell
ECM	Extracellular matrix
EDF	End diastolic flow
EDHF	Endothelium derived hyperpolarizing factor
EGF	Epidermal growth factor
EGM	Endothelial growth medium
eNOS	Endothelial nitric oxide synthase
FBS	Fetal bovine serum
FCS	Fetal calf serum
FGR	Fetal growth restriction
Flk-1	Fetal liver kinase-1
Flt-1	Fms-like tyrosine kinase-1
GA	Gestational age
GGT	Gamma-glutamyl transferase
GLDH	Glutamate dehydrogenase
GLiM	General Linear Model

HIF-1	Hypoxia inducible factor-1
HR	Heart Rate
HRE	Hypoxia response element
HRP	Horseradish peroxidase
HSPG	Heparan sulphate proteoglycan
HUVEC	Human umbilical vein endothelial cell
IGF-1	Insulin-like growth factor-1
im	Intra-muscular
iNOS	Inducible nitric oxide synthase
ip	Intra-peritoneal
KDR	Kinase domain region
MAP	Mean arterial pressure
MCA	Middle cerebral artery
MOI	Multiplicity of infection
MOPS	3-(N-morpholino)propanesulfonic acid
L-NAME	N^G-nitro-L-arginine methyl ester
L-NMMA	L-N^G-monomethyl Arginine citrate
nNOS	Neuronal nitric oxide synthase
NO	Nitric oxide
NRP	Neuropilin
NST	Non stress test
PAGE	Polyacrylamide gel electrophoresis
PBS	Phosphate buffered saline
PCR	Polymerase chain reaction
PDE5	phosphodiesterase type 5
PDGF	Platelet-derived growth factor
PE	Phenylephrine
PEDF	Preserved end diastolic flow
PET	Pre-eclampsia
pfu	Plaque forming unit
PGI_2	Prostacyclin
PI	Pulsatility index
PlGF	Placental growth factor
RCOG	Royal College of Obstetricians and Gynecologists
REDF	Reversed end diastolic flow
rh	Recombinant human
RI	Resistance index
RIPA	Radioimmunoprecipitation assay
RNA	Ribonucleic acid
RT	Reverse transcription
RTK	Receptor tyrosine kinase
sc	Sub-cutaneous
SD	Standard deviation
SDS	Sodium dodecyl sulphate
SEM	Standard error of mean
Ser	Serine

SFGR	Severe fetal growth restriction
SGA	Small for gestational age
siRNA	Small interfering ribonucleic acid
SUAL	Single umbilical artery ligation
TAFF	Transamniotic fetal feeding
TXA_2	Thromboxane-A_2
UA	Uterine artery
UABF	Uterine artery blood flow
UAEC	Uterine artery endothelial cell
UBF	Uterine blood flow
UtA	Uterine artery
VEGF	Vascular endothelial growth factor
VEGFR	Vascular endothelial growth factor receptor
vp	Viral particles
VSMC	Vascular smooth muscle cell
vWF	von-Willebrand Factor

Chapter 1

Introduction

Fetal growth restriction (FGR) is defined as a condition in which the fetus does not achieve its genetically determined growth potential (Figure 1.1). The term is often used inter-changeably with small for gestational age (SGA) infants, though the two are different and they describe different conditions. SGA infants fall below the 10^{th} percentile for a given gestational age. Approximately 50 to 70% of SGA babies are growth restricted. A substantial number however are not growth restricted, but are just small for gestational age when compared with the general population. Customised centile charts that take into consideration the genetic background of the neonate are very helpful in distinguishing SGA from FGR. Using the mother's height, weight, ethnicity and the sex of the neonate, the birthweight centile is adjusted to provide a more accurate centile (Gardosi J et al., 1992;McCowan LM et al., 2005). A typical birthweight centile chart commonly found in obstetric wards is represented in Figure 1.2. It is important to distinguish SGA from FGR, since SGA babies that are not growth restricted thrive and they have a lower morbidity and mortality when compared to their FGR counterparts .

FGR is a major problem for obstetricians, neonatologists, parents and society in general. It afflicts up to 7% of all pregnancies in the UK, and is severe in 1:500 cases (Romo A et al., 2009). FGR fetuses have higher incidences of

morbidity and mortality, and an increased pre-disposition to cardiovascular disorders and neurological handicaps (Bernstein IM et al., 2000;Romo A et al., 2009). The causes of FGR are manifold, some of which are described below.

Figure 1.1 – Picture of a neonate that is appropriately growth for gestational age (right) and another neonate that suffered fetal growth restriction (FGR, left).

The FGR neonate is smaller, with less fat deposition, and with dry wrinkly skin.Both these babies were born at the same gestational age. (Picture courtesy: Dr. A.L. David, UCL).

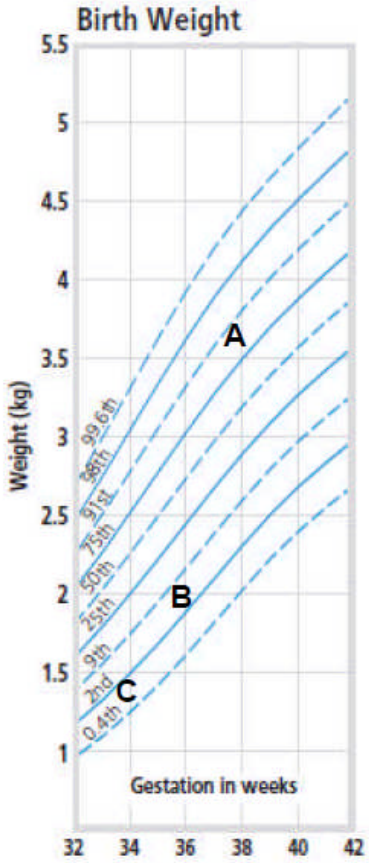

Figure 1.2 – A centile chart representing birthweight

These charts indicate the birthweight of a child in comparison with children of the same age and maturity who have shown optimum growth. The centile lines on the chart show the expected range of weights; each represents the proportion of children to be expected below that line. The points marked on the chart above are representative of a child that has grown (A) appropriately for its gestational age; (B) small for gestational age; or (C) developed severe fetal growth restriction. (Picture obtained from UK-WHO growth charts:early years; Royal College of Paediatrics and Child Health)

The FGR infant at birth may be symmetrically or asymmetrically small. The former are characterized by reduced weight, length and head circumference at birth. The etiological factors associated with symmetric growth restriction include intra-uterine infections, chromosomal abnormalities and intra-uterine toxins such as alcohol and smoking. The asymmetrically growth-restricted infants, seen most

commonly in instances of utero-placental vascular insufficiency, show sparing of head growth relative to weight and length.

1.1 Maternal Factors resulting in FGR

1.1.1 Maternal Hypertensive Conditions

Hypertensive disorders are present in 30-40% of pregnancies characterized by FGR. These disorders include pre-eclampsia, chronic hypertension with or without superimposed pre-eclampsia, autoimmune disorders, chronic severe nephropathy, and pregestational diabetes complicated with vasculopathy. The underlying cause of restricted fetal growth is believed to be constriction of the utero-placental blood vessels, thereby limiting perfusion. It has been observed that the worse the severity of pre-eclampsia and the earlier the onset of the disease, the more growth-restricted is the fetus (Maulik D, 2006a). According to one report, the decline in birth weight was 5% in mild pre-eclampsia, 12% with severe disease and 23% with early onset disease (Long PA et al., 1980). Unfortunately, maternal anti-hypertensive therapy does not improve fetal growth and some commonly prescribed β-blockers like atenolol may even exacerbate the condition. This is because the fetus is dependent on a higher pressure circulation and reducing it can precipitate hypoxia. This is sometimes seen in clinical practice when women with a very high BP are given a large dose of antihypertensive drugs, which results in fetal distress.

1.1.2 Maternal Autoimmune Disorders

Maternal autoimmune disorders, especially those that involve the vascular system, are associated with poor perinatal outcomes. Pregnant women with antiphospholipid (aPL) antibody syndrome have increased incidences of idiopathic recurrent fetal loss. For pregnant women with systematic lupus erythematosus, the risk of miscarriage is about 40% when aPL antibodies are positive compared to a risk of 15% when they are absent (McNeil HP et al., 1991). The presence of aPL antibodies is also correlated with adverse fetal

growth. In a prospective study, 24% of fetuses with birth weight below the 10th centile had positive aPL antibodies (Polzin WJ et al., 1991). In another prospective study, the relative risk of FGR with positive aPL antibodies was found to be significantly enhanced (Yasuda M et al., 1995). The correlation between positive aPL antibodies and the onset of FGR is not very well understood, and many authors have put forth different theories in an attempt to provide an explanation. One such study has reported that aPL antibodies suppress the production of prostacyclins in murine aortic endothelial cells, and may induce the production of thromboxane A_2, a potent vasoconstrictor and inducer of platelet aggregation, which in turn could lead to the formation of thrombi (Carreras LO et al., 1981). It is also possible that aPL antibodies may exert a direct toxic effect on the trophoblasts, independent of any thrombus formation (Yasuda M et al., 1995); or may disturb the intricate signaling transduction processes that are essential for the maintenance of normal pregnancy (Gleicher N et al., 1992).

1.1.3 Maternal Lifestyle

Maternal use of various recreational agents and narcotic substances is associated with FGR. For instance, maternal cigarette smoking leads to decreased fetal weight (Kramer MS, 1987). The effect is primarily mediated by carbon monoxide generation, which in turn reduces fetal oxygenation. In addition, the vasoconstrictive properties of nicotine also have a detrimental effect on utero-placental perfusion. In a prospective cohort study, it was found that there was an average birth weight reduction of 6% when smoking continued throughout gestation compared with only 1.7% when smoking was stopped after the first trimester. The effect is dose-dependent (Cliver SP et al., 1995).

Use of cocaine during pregnancy has been associated with significant maternal and fetal risks, including maternal stroke, hypertension, placental abruption, fetal brain injury and stillbirth. A multicentre study conducted by the National Institute of Child Health and Human Development Neonatal Research Network has demonstrated that exposure to cocaine *in utero* can retard fetal

growth symmetrically (Bada HS et al., 2002). The growth parameters most affected included birth weight, body length and head circumference.
Alcohol consumption in pregnancy has been associated with fetal alcohol syndrome or fetal alcohol spectrum disorders. Characterized by dysmorphic features and retardation of mental growth, FGR remains a central feature of these conditions (Sokol RJ et al., 2003). Current scientific opinion suggests that there is no conclusive evidence that very small amounts of alcohol consumption during pregnancy are harmful to the mother and baby. At the same time, there is uncertainty on the threshold of safe alcohol consumption during this period for pregnant women. For this reason, the Royal College of Obstetricians and Gynecologists (RCOG) has consistently stated that women should avoid drinking excessive amounts of alcohol when pregnant but there is no evidence that drinking 1 to 2 units once or twice a week is harmful (http://www.rcog.org.uk/what-we-do/campaigning-and-opinions/statement/rcog-statement-nice-guidelines-alcohol-consumption-dur)

1.1.4 Therapeutic Agents

Some commonly used therapeutic agents have been implicated in causing FGR. These include antineoplastic medication, anti-convulsants such as phenytoin, β-blockers (particularly atenolol) and steroids (Maulik D, 2006a). The underlying cause of the growth restriction associated with many of these drugs is unclear. Chemotherapeutic agents are known to inhibit rapidly dividing cells, which are richly abundant in the placenta and fetus and thus result in FGR. There is strong evidence that administration of a single course of steroids before 34 weeks of gestation induces fetal lung maturity in preterm labor. However, a number of animal and human studies suggest that administration of multiple doses leads to retardation of fetal somatic growth and neurodevelopmental handicap (Spinillo A et al., 2004).

1.1.5 Malnutrition

Maternal malnutrition characterized by an extremely low caloric intake can limit the supply of substrates to the developing fetus, and hence retard its

growth. The effect may span generations. During the harsh Dutch famine of 1944-1945, the average daily caloric intake was below 1500 kcal for many women during the third trimester. This was associated with significant reductions in fetal weight and size, as well as a possible intergenerational effect resulting in low fetal and neonatal weights (Stein Z and Susser M, 1975).

1.1.6 Environmental Pollution

Even relatively low concentrations of gaseous pollutants such as sulphur dioxide, nitrogen dioxide, carbon monoxide and ozone can have profound effects on retarding fetal growth (Liu S et al., 2003). One of the recent disasters which provided evidence for effects of environmental pollution on fetal growth has been the World Trade Centre (WTC) disaster. The WTC dust comprised pulverized cement, glass fibers, asbestos, lead, polycyclic aromatic hydrocarbons, polychlorinated biphenyls, polychlorinated furans and dioxins. A follow-up study of 182 pregnant women who were within 1 mile of the disaster on September 11, 2001 revealed a two-fold increase in infants whose growth had been compromised (Landrigan PJ et al., 2004;Perera FP et al., 2005).

1.1.7 Uterine and placental vascular insufficiency

Utero-placental vascular insufficiency is one of the most common causes of FGR. This thesis deals with FGR caused only by utero-placental vascular insufficiency. Hence, it has been discussed in greater detail in a separate section (1.3).

1.2 Fetal Factors resulting in FGR

1.2.1 Aneuploidy

Chromosomal abnormalities are strongly associated with FGR, which is commonly symmetrical and early onset. Traditionally, about 7% of FGR cases have been attributed to aneuploidy (abnormal number of chromosomes).

Approximately, 90% of the fetuses with trisomy 18 will develop FGR compared with only 30% of those with trisomy 21 (Snijders RJ et al., 1993b). Fetuses with aneuploidy have an increased incidence of multiple malformations and stillbirth (Maulik D, 2006a). A majority of the triploid fetuses are lost during the first trimester because of spontaneous abortions. The few that survive into the second trimester are characterized by profound anatomical defects and severe asymmetrical FGR (Doshi N et al., 1983).

1.2.2 Genomic Imprinting and Uniparental Disomy

Uniparental Disomy (UPD) is the inheritance of both homologs of a chromosome from a single parent. This condition, even though quite rare, has been implicated in FGR, the most commonly found example being maternal UPD of chromosome 16 (Maulik D, 2006a) and chromosome 14 (Sanlaville D et al., 2000).

Genomic imprinting is a developmental process which gives rise to differential expression of maternal or paternal genes or chromosomal regions because of the suppressed expression of either the maternal or paternal alleles, although both are present (Wutz A and Barlow DP, 1998). There are as many as 100 genes that are imprinted in mammals, and many of these are involved in fetal growth. According to the genetic conflict theory, paternally expressed imprinted genes are believed to enhance the availability of nutrients to the developing fetus, and hence enhance fetal growth. On the contrary, maternally expressed imprinted genes have a tendency towards conservation of maternal nutritional resources (Haig D, 1993;Haig D, 1997). This concept finds support in gene knockout animal models of paternally or maternally expressed growth factors such as the insulin-like growth factor. At the *insulin-like growth factor 2 (Igf2)* locus, only the paternal allele is expressed, and it produces a polypeptide (IGF-2) that promotes the transfer of substrates from the mother to the fetus. At the *insulin-like growth factor 2 receptor (Igf2r) locus*, the pattern of imprinting is reversed. The paternal allele is silent while the maternal allele encodes for a receptor that

degrades the IGF-2 peptide. *Igf2r* binds to and internalizes IGF-2, and transports it to intra-cellular compartments (early endosomes and lysosomes) where it is degraded. Knockout experiments have proven that normal fetal development depends on a balance between these two reciprocally imprinted genes; knockout of the *Igf2* alleles brings about a 40% reduction in birthweight (DeChiara TM et al., 1990), whereas knockout of the *Igf2r* gene in fetuses results in offspring that are oversized and ultimately nonviable (Lau MM et al., 1994).

It may appear paradoxical for a maternal allele to limit the supply of substrates to the fetus. A female mouse maximizes her reproductive success by producing a number of litters. If she invests too much of her resources in her current fetuses, she risks compromising her prospects for future progeny. However, because there can be different paternity amongst litters, paternal interest is best served by promoting nutrient transfer beyond what would be optimum for the mother.

Such genetic trends have evolved in humans as well, and they play an important role in regulating fetal development. The dominance of the maternally imprinted genes over paternally imprinted genes restricts fetal growth *in utero* (Haig D, 1993;Hitchins MP and Moore GE, 2002), as seen in cases of Prader-Willi syndrome, where there is loss of function of imprinted genes on the paternal allele of region 15q11-13 (Holm VA et al., 1993).

1.2.3 Fetal Malformations

The Centre for Disease Control and Prevention (CDC) found that approximately 22% of the infants with birth defects are growth-restricted (Khoury MJ et al., 1988). Some of the fetal malformations that are commonly associated with FGR or SGA infants include cardiac defects (tetralogy of Fallot, endocardial cushion defect, hypoplastic left heart, pulmonary stenosis, and ventricular septal defects), anencephaly and abdominal wall defects. A single umbilical artery (instead of the normally two present) is also associated with FGR. Thus, a

defective organ system/circulation appeared to be restricting the normal growth of the fetus.

1.2.4 Perinatal infections

Protozoan and viral infections are also known to commonly cause FGR. The viral pathogens that are commonly implicated in FGR include rubella, cytomegalovirus, human immunodeficiency virus, and varicella-zoster (Maulik D, 2006a). Protozoan infections that have been associated with FGR include malaria and toxoplasmosis. In Sub-Saharan Africa, about 40% of FGR cases are attributable to pregnancy-associated malaria (PAM). The malaria parasite, *Plasmodium falciparum*, expresses proteins called *P. falciparum* erythrocyte membrane protein-1 (PfEMP-1) on the surface of infected red blood cells (RBCs). These proteins cause the infected RBCs to sequester and block small blood vessels in the placenta, and hence limit the supply of substrates and oxygen to the growing fetus. The fact that PfEMP-1 is subject to a high level of antigenic variation has made the development of a vaccine for PAM difficult (Bir N et al., 2006).

1.2.5 Preterm birth

There is a strong association between spontaneous preterm birth and FGR (Tamura RK et al., 1984). In a case controlled study, it was determined that 30% of the fetuses born spontaneously before 35 weeks were growth-restricted compared to only 4.5% of those born at 37 weeks or later (Bukowski R et al., 2001). The onset of growth restriction not only precedes but also signals the premature onset of parturition, suggesting an adaptive response to *in utero* stress (Gardosi JO, 2005). Preterm delivery can also be iatrogenic, when doctors intervene to deliver a fetus prematurely in an attempt to prevent irreparable damage to the fetus or even stillbirth if the pregnancy were allowed to continue. This generally occurs when FGR is suspected and there is a high risk of intra-uterine demise.

1.3 Utero-placental vascular insufficiency

The provision of adequate nutrients and oxygen to the conceptus is a basic requirement for normal growth and development. The maternal vascular tree is able to provide all substrates and oxygen essential for the development of the fetus. During pregnancy uterine perfusion increases dramatically from 50ml/min in week 10 of human pregnancy to as much as 1300 ml/min at term as a result of increased maternal cardiac output and trophoblast-driven modification of the uterine spiral arteries (Lang U et al., 2003). Failure of this normal physiological process leads to preeclampsia (PET) and fetal growth restriction (FGR). The re-modelling of human utero-placental blood vessels in pregnancy is described below.

1.3.1 Development of human uteroplacental vessels

During the first half of human pregnancy, the uteroplacental (spiral) arteries undergo a series of pregnancy-specific changes to create the uteroplacental circulation, which include: (i) apparent replacement of endothelium and medial smooth muscle cells by invasive trophoblast; (ii) loss of elasticity; (iii) dilation to wide, non-contractile vessels; and (iv) loss of vasomotor control (Kaufmann P et al., 2003).

This remodelling of the spiral arteries reduces maternal blood flow resistance and increases uteroplacental perfusion to meet the requirements of the fetus (Figure 1.3). The loss of contractility and maternal vasomotor control ensures maternal blood supply to the placenta, irrespective of maternal attempts to regulate the blood distribution within the body. Local loss of vasomotor control also allows the fetus to gain control over the maternal blood flow resistance and blood flow distribution within the intervillous space. The extent and depth of trophoblast invasion is less in FGR compared with normal pregnancy which results in an inadequate re-modelling of the uterine spiral arteries (Figure 1.3).

This is the primary cause of uteroplacental insufficiency and the adverse fetal outcomes that are seen in affected pregnancies.

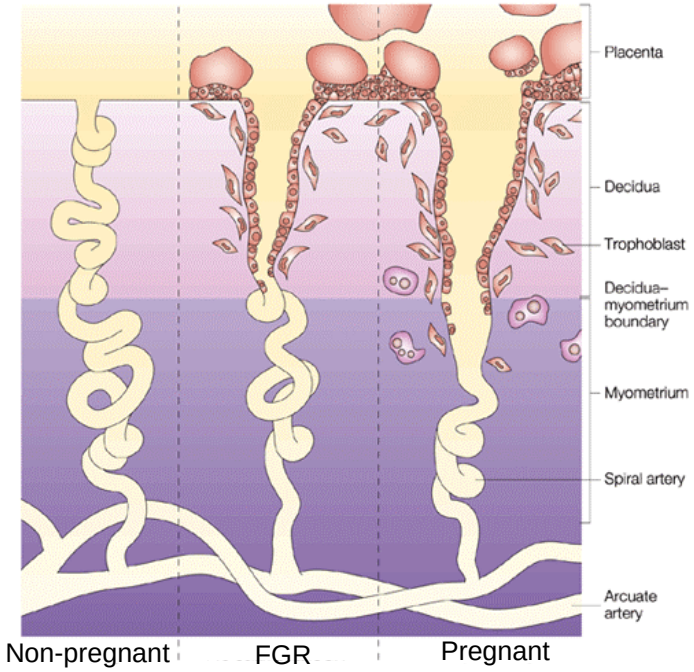

Figure 1.3: A comparison between non-pregnant (uninvaded), normal pregnant and pathological (FGR) pregnant uterine arteries.

The extent and depth of trophoblast invasion is less in pathological compared with normal pregnancy, with inadequate re-modelling of the myometrial spiral arteries in FGR. This results in reduced blood flow to the feto-placental unit, which manifests as fetal growth restriction. (Moffett-King A, 2002).

1.3.2 Uterine blood flow in normal human pregnancies

As discussed above, in normal human pregnancy the action of invasive trophoblasts on the maternal spiral arteries leads to the development of a low resistance uteroplacental circulation which facilitates the marked increase in blood flow seen in these vessels at term. Thaler *et al* evaluated low risk pregnancies by transvaginal duplex Doppler ultrasound (n = 24), and compared them to non-pregnant women (n = 27) (Thaler I et al., 1990). A steady increase in volume flow rate in the left ascending uterine artery from a mean of 94.5 mL/min before pregnancy to 342 mL/min in late gestation was observed, reflecting a 3.5-

fold increase. The mean diameter of the uterine artery in the non-pregnant state was 1.6 mm, and this increased to 3.7 mm towards term.

1.3.3 Uterine blood flow in pregnancies affected by uteroplacental insufficiency

Studies have shown that FGR is associated with abnormalities of the uteroplacental, umbilical and fetal circulations (Divon MY and Hsu HW, 1992). It is useful to look at some of the differences of two types of abnormal pregnancies, FGR and PET, which are proposed to be a result of uteroplacental insufficiency.

1.3.3.1 Fetal growth restriction due to uteroplacental insufficiency

Normal fetal growth is determined by the genetically predetermined growth potential modulated by maternal, fetal, placental, and external factors. FGR is a failure to reach this potential and is clinically suspected if sonographic estimates of fetal weight, size, or symmetry are abnormal. FGR is usually diagnosed when the fetus is at or below the tenth percentile for their estimated fetal weight (EFW) at a given gestational age. Cases of FGR are often considered to be severe when the EFW falls below the fifth percentile. Such examples are often first detected at the 20-week fetal ultrasound scan and are associated with asymmetric growth restriction.

In cases of FGR or severe FGR (SFGR) due to uteroplacental insufficiency there is defective trophoblast invasion and an inadequate development of maternal placentation. The uteroplacental circulation remains in a state of high resistance, which causes generalised endothelial cell injury (Papageorghiou AT et al., 2004). The local production of vasoactive substances such as prostaglandins, endothelins and nitric oxide is impaired and this leads to vasospasm in the small arterioles of the uteroplacental compartments as well as of other systemic vascular beds. Consequently there is an abnormal increase in the systemic vasopressor responses and this in turn may cause hypertension by

impairing renal function and increasing total peripheral resistance. Activated or injured endothelial cells lose their ability to maintain vascular integrity, which leads to an increase in capillary permeability, platelet thrombosis and increased vascular tone. Subsequent damage to the vascular wall promotes an atherosis-like process in the small arteries. The result of these processes is a local ischemia.

High resistance notched uterine artery Doppler waveforms have been observed in human pregnancies that go on to develop either PET or severe FGR (Papageorghiou AT et al., 2004). Konje JC *et al* quantified the reduction in uterine blood flow (UBF) in pregnancies complicated by FGR when compared to normal pregnancy: 12.5% reduction was observed at 20 weeks and 36.7% from 24 weeks of gestation until delivery. In absolute terms, the UBF in normal pregnancies at 20 weeks gestation was 328+159 ml/min v/s 287+117 ml/min in FGR pregnancies. At 38 weeks, the corresponding values were 830+284 ml/min and 534+332 ml/min, respectively (Konje JC et al., 2003).

Sheep studies have demonstrated an almost linear positive correlation between UBF and fetal size (Lang U et al., 2003), suggesting that this may be a useful non-clinical model to evaluate the efficacy of new treatments for FGR. Gelfoam embolisation of the proximal uterine arteries in sheep reduce UBF by 50% results in FGR and produces high resistance notched uterine artery Doppler waveforms similar to those seen in human FGR pregnancy (Ochi H et al., 1998).

1.3.3.2 Pre-eclampsia

Pre-eclampsia (PET) is a major cause of maternal mortality (15 – 20% in developing countries) and morbidities (acute and long-term), perinatal death and pre-term birth (Sibai B et al., 2005). It is characterised by an abnormal response to placentation that is associated with increased systemic vascular resistance, enhanced platelet aggregation, activation of the coagulation system and endothelial dysfunction. Typically after the uterus has been delivered of the fetus and placenta, the disease resolves. It is believed that one of the underlying causes

of PET is associated with defects in extravillous trophoblast invasion and failure to establish the maternal circulation correctly, resulting in uteroplacental hypoxia.

PET may manifest as early onset or late onset disease. Early onset disease, before 33 weeks gestation is generally associated with FGR and adverse pregnancy outcomes, including increased incidence of maternal and fetal morbidity and mortality. In contrast, maternal and perinatal outcomes are generally favourable in women with mild PET developing beyond 36 weeks gestation. It is believed that the pathophysiology of the disorder leading to early onset disease may differ from that of late onset disease (Sibai B et al., 2005;Steegers EA et al., 2010).

The traditional diagnosis of PET, based on new onset of both hypertension and proteinuria after 20 weeks gestation, is applicable to most women. Hypertension is defined as a blood pressure of at least 140 mmHg (systolic) or 90 mmHg (diastolic) on at least two separate occasions 4-6 hours apart in previously normotensive women. Proteinuria is defined as excretion of at least 300mg of protein every 24 hours. However, in some women, there may only be gestational hypertension without proteinuria, which is associated with a high rate of maternal and fetal morbidity. Additionally, both hypertension and proteinuria may be absent in 10-15% of women who develop haemolysis, elevated liver enzymes, and low platelet counts (HELLP syndrome) and in 38% of women who develop eclampsia. Both of these are associated with significantly higher rates of adverse pregnancy outcomes than mild PET (Sibai BM, 2004;Douglas KA and Redman CW, 1994).

1.3.3.3 Histological and morphological differences of human PET and FGR

The underlying abnormality in FGR and PET is a failure of oxygen transport from the intervillous space to the umbilical vein. Hypoxia can be present at any of three stages across the placenta: pre-placental, uteroplacental and post-

placental (Kingdom JC and Kaufmann P, 1997). In each case the placentae show very different histological structures.

Pre-placental hypoxia occurs in the presence of maternal anaemia or pregnancy at high altitude. The terminal placental villi are characterized by increased capillary volume fraction and increased capillary branching. The amount and proliferation of villous cytotrophoblasts is also increased. Because the hypoxia in this case is present before the placenta, it affects the entire organ resulting in uniform distribution of histological features (Kingdom JC and Kaufmann P, 1997). Concomitant with an increase in villous capillary density, there is also an increased secretion of vascular endothelial growth factor (VEGF) and erythropoietin (Zamudio S et al., 2006;Zamudio S et al., 2007). This is followed by reprogramming of the metabolic machinery, to augment energy supply by anaerobic pathways. In the placenta, this occurs by an increase in glucose consumption and lactate production, along with upregulation of various key elements of the glycolytic pathway (Illsley NP et al., 1984). Another characterisitic response triggered by hypoxia is termed “demand reduction”, which consists of attenuation of energy-expensive processes not essential for survival, such as fetal movements (Hooper SB, 1995). At the tissue level, this is manifested as inhibition of transcription and translation and related processes dependent on protein synthesis, such as cell growth and proliferation (Hochachka PW and Lutz PL, 2001). Although the mechanisms of demand reduction are not yet understood in the placenta, they are believed to result in the development of pathological pregnancies, as seen in FGR and PET, where placental and fetal growth are compromised in response to a low O_2 environment (Illsley NP et al., 2010).

Uteroplacental hypoxia occurs where normal oxygenated maternal blood has a restricted access to the uteroplacental circulation. This is seen in cases of utero-placental vascular insufficiency. Placentae derived from FGR pregnancies with abnormal but still preserved end-diastolic flow (PEDF) in the umbilical arteries, irrespective of whether complicated by PET or not, are classified under this category, and show a similar histological structure to that described for pre-

placental hypoxia (Kingdom JC and Kaufmann P, 1997). Placentae from this group display villi with elevated capillary volume fractions, amounts of cytotrophoblast and levels of syncytiotrophoblast knot formation. The capillaries grow by branching angiogenesis and vascular impedance is reduced. Neonates of such pregnancies are generally dehydrated and have elevated hematocrits, the placentae are thin, appear dark on sectioning and the villi are small and composed primarily of capillaries.

Post-placental hypoxia is where maternal oxygenated blood enters the intervillous space at a normal or reduced rate, but there is a major defect in fetoplacental perfusion (Kingdom JC and Kaufmann P, 1997). This form of hypoxia is seen in cases of severe FGR characterized by absent or reversed end diastolic flow (AREDF). The histopathological findings are homogeneous, but dissimilar to those observed in specimens from pre-placental or utero-placental hypoxia (Kingdom JC and Kaufmann P, 1997). The most characterisitic features are those of "terminal villi deficiency" where the villous placenta fails to transfer oxygen to the fetus despite normally oxygenated blood entering the intervillous space (Mayhew TM et al., 2003;Macara L et al., 1996;Kingdom J et al., 2000).

Mayhew TM et al (2003) quantified differences in placental morphology in PET, FGR, and PET with FGR pregnancies with particular focus on the dimensions and composition of peripheral (intermediate and terminal) villi. Placentae were sampled randomly. Fetal weights were reduced in all pregnancies complicated by PET, with or without FGR. However, only pregnancies complicated by FGR had a significantly smaller placenta. PET was not associated with any major effects on placental morphology (except for trophoblast thickness). In contrast, FGR was associated with placentae with reduced volumes of intervillous space as well as all types of villi (stem, intermediate and terminal) The impedance of growth of peripheral villi affected all tissues (trophoblast, stroma, capillaries) and was accompanied by smaller exchange areas and a thicker trophoblastic epithelium (Mayhew TM et al., 2003).

In another study, it was reported that that in cases of PET not accompanied by FGR, the placentae were morphologically very similar to control placentae in the volumes of parenchymal components, number of nuclei and the exchange areas of villi and capillaries (Teasdale F, 1985). This contrasts with the data from cases of PET accompanied with FGR (Teasdale F, 1987). Placentae were evaluated in this study: five from patients who suffered from severe PET and FGR and five age-matched controls. There was a decrease observed in the volumes of villi and intervillous space in the PET/FGR group. These findings were similar to alterations, which are observed with FGR alone, suggesting the main effects are due to FGR alone and not to interactions between PET and FGR.

Similar findings have been reported following comparison of twenty FGR placentae (ten at 20 – 22 weeks and ten at 23 – 25 weeks) with twenty aged matched controls. Placental and fetal weights in the FGR groups were smaller than in the controls. Poor vascularisation and immaturity of the villous tree were found in many FGR cases. The thickness of the placental membranes was increased from 10.74 ± 0.09 mm at 20 – 22 weeks and 10.92 ± 0.09 mm at 23-25 weeks in control groups, to 11.62 ± 0.1 mm and 11.87 ± 0.12 mm, respectively (Reshetnikova O et al., 2002).

Macara *et al*, (1996) evaluated the villous ultrastructure and immunohistochemistry in FGR pregnancies (n = 16, with absent end-diastolic flow velocity in the umbilical artery) and age-matched controls (n = 16). They found that the terminal villi from FGR cases were smaller in diameter, and had a reduced villous tissue per placental area (density of all classes of villi). This suggests that the cross-sectional area of terminal villi and the degree of vascularisation are reduced in FGR pregnancies with reduced umbilical artery perfusion. The number of cytotrophoblast cells, identified by the presence of nuclei, was reduced in the FGR group. These cells proliferate and fuse to form the syncytiotrophoblast layer, which might indicate a reduction in the turnover of the trophoblast layer in FGR.

In summary, differences between PET, FGR, and PET with FGR can be clearly seen when histological and morphological evaluations are performed. In general, the surface area of the syncytiotrophoblast is reduced whereas the thickness of the exchange barrier formed by the trophoblast and fetal capillary endothelium is increased in FGR (Sibley CP et al., 2005;Mayhew TM et al., 2003).

1.4 Diagnosis and Management of pregnancies complicated by FGR

The most important step in management of pregnancies complicated by FGR is an accurate diagnosis of the condition, along with the underlying etiological factor. This is often quite difficult, and easy to get wrong.

FGR caused by utero-placental insufficiency can be detected at the 24 week fetal ultrasound scan as a notched uterine artery waveform, the notch being indicative of increased resistance to the flow of blood in the uterine arteries (Figure 1.4). An increased pulsatility index (PI) and resistance index (RI) at this time point can also indicate uteroplacental circulatory resistance. Even at the 11-14 week scan, a notched uterine artery waveform and a raised PI can indicate that a pregnancy is at risk of developing FGR, although the sensitivity and specificity of these parameters are too poor to support their use in clinical risk prediction. Ultrasonography is also useful in identifying the restriction of body weight and length of long bones, with a relative “head sparing” effect. There may be reduced amniotic fluid around the fetus reflecting poor renal perfusion. (Ott WJ, 2006;Miller J et al., 2008)

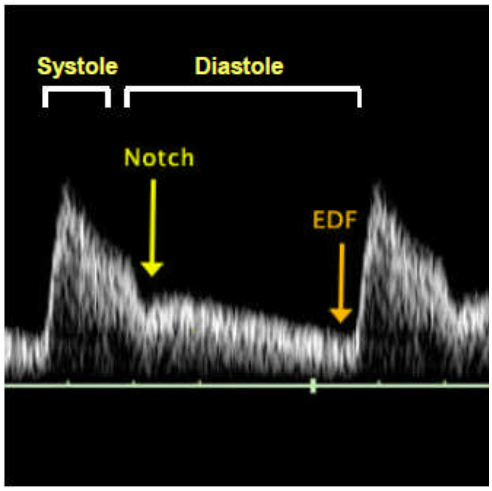

Figure 1.4 – Notched uterine artery waveform in pregnancies characterized by FGR.

The notch is indicative of high resistance to the flow of blood in the myometrial spiral arteries. EDF = End diastolic flow. (Picture courtesy: Dr. A.L. David, UCL)

Severely affected FGR fetuses weighing around 500 g or less have a high morbidity, and over 50% die postnatally. If fetal growth ceases completely in mid-pregnancy and the fetal weight remains below 500 g, the only management options currently available to parents are (i) to terminate the pregnancy, (ii) to await inevitable fetal death, or, (iii) to deliver the fetus by caesarean section if it weighs at least 450 - 500 g, in the knowledge that there is a high chance of postnatal death or disability. Small improvements in fetal growth and gestational age at delivery are associated with major improvements in survival and morbidity. A multi-centre observational study of severely growth restricted neonates showed a drop in major morbidity from 56.6% to 10.5% as gestational age advanced from 24 weeks to 32 weeks, and median survival gained per day *in utero* was 2% (range 1.1 – 2.6) between 24 and 27 weeks of gestation (Baschat AA et al., 2007).

The principal aim of fetal surveillance is the timely recognition of fetal stress and compromise so that delivery can be timed appropriately to prevent irreparable fetal damage or even demise. The risks of early delivery to the neonate need to be carefully balanced with the risks to the fetus of continuing intrauterine

life. Faced with the stresses of a compromised supply of nutrients and oxygen, the fetus mobilizes a number of adaptive responses that include preferential fetal growth over placental growth, deceleration of the fetal growth rate, reduction in fetal movements to conserve energy, increased number of red blood cells to improve the oxygen carrying capacity of fetal blood, and blood flow redistribution to vital organs (like the brain and heart) at the expense of less critical tissues and organs. Fetal surveillance tests aim to reflect this sequence of events and to deliver the fetus before irreparable damage has been done.

The most important fetal surveillance tests include Doppler sonography of the umbilical arteries and other fetal vascular beds, the biophysical profile (BPP), sonographic estimation of amniotic fluid volume, and the cardiotocograph (CTG) (Maulik D, 2006b).

Numerous studies have demonstrated the value of umbilical artery Doppler indices in predicting adverse outcomes in pregnancies complicated by FGR (Maulik D, 2006b). The absence of end-diastolic flow (AEDF) in the umbilical artery waveform is known to be associated with high incidences of morbidity and mortality (Karsdorp VH et al., 1994). Reversal of end-diastolic flow (REDF) is associated with an even worse prognosis. When used in a well defined high-risk pregnancy and combined with an appropriate plan of management, umbilical artery dopplers have been shown to be clinically useful as a predictive test for fetal/neonatal compromise (Morris RK et al., 2011)

The CTG is a non-invasive test during which the heartbeat of the fetus is measured while it is at rest, and during movement or kicking. Interpretation of the CTG test is relatively simple as it depends solely on the presence or absence of fetal heart rate accelerations which occur in response to fetal movements. The usual duration of a CTG is 20 minutes, during which observation of a minimum two accelerations of at least 15 bpm above baseline lasting at least 15 seconds need to be seen to classify the test as ‘reactive’ or normal. A non-reactive CTG can be associated with detrimental perinatal outcomes; however, more often than not it is related to the fetus sleep cycle or maternal sedation (Maulik D, 2006b). The CTG is used in conjunction with Doppler sonography of the umbilical

arteries to predict when is best to deliver a severely growth restricted fetus. However, it is considered to be of limited value as a stand alone test to monitor fetal condition.

Assessment of amniotic fluid volumes including the single deepest pocket and the amniotic fluid index (AFI), a measurement of the deepest pools of amniotic fluid in four uterine quadrants are considered useful in monitoring fetal condition. Oligohydramnios is associated with adverse perinatal outcome, and is highly prevalent in FGR. Its occurrence is therefore an important finding which signals the need to increase fetal monitoring (Chamberlain PF et al., 1984;Bastide A et al., 1986). The cause of oligohydramnios is believed to be a reduced renal blood flow, due to blood flow redistribution and decreased urine output (Arduini D and Rizzo G, 1991).

The biophysical profile (BPP) test is carried out to determine the health of the baby during pregnancy usually in combination with assessment of fetal blood flow (by Doppler) and fetal growth. The number and type of fetal movements, changes in the fetal heart rate with movement, muscle tone, breathing rate and AFI are combined to give a score which indicates the overall health of the fetus. A declining BPP score reflects deteriorating fetal condition and may indicate delivery to avoid fetal demise. Similar to CTG, the BPP is of limited value as a stand-alone test but useful when used in conjunction with other fetal surveillance tests.

As fetal condition deteriorates, the fetus adapts by dilatation of the fetal cerebral arteries, termed “brain sparing” which can be picked up on a Doppler scan of the middle cerebral artery (MCA) as an increased pulsatility index (Maulik D, 2006b;Baschat AA et al., 2001). In sheep fetuses, redistribution of blood in favour of the brain has been shown to be an effect of hypoxaemia (Peeters LL et al., 1979). Both in humans and sheep, this adaptation can be reversed temporarily by maternal hyperoxygenation (Goetzman BW et al., 1984;Arduini D et al., 1988). The CTG and BPP may also be improved using maternal oxygen administration, but there is a temporary impairment of the fetal heart rate pattern and increase in heart rate decelerations after discontinuation of

oxygen (Bekedam DJ et al., 1991). An important limitation of oxygen therapy is that it needs to be administered continuously without interruption.

The guidelines for managing FGR caused by utero-placental insufficiency are well established. Once other factors like chromosomal abnormalities, fetal structural abnormalities or maternal/fetal infections have been ruled out, Doppler assessment of the uterine arteries is performed at 22-24 weeks. A raised PI with a notched waveform is confirmatory of FGR caused by utero-placental insufficiency. It is then important to monitor the growth of the fetus serially by ultrasound examination every two weeks. Once the fetal growth velocity slows, scans are performed more frequently for assessment of umbilical artery Dopplers, fetal growth and AFI. Once fetal growth has ceased, abnormalities in the umbilical artery and middle cerebral blood flow are common and CTG montitoring can be instigated every few days. The mother is prescribed a course of steroids to mature the fetal lungs, and delivery is planned in liaison with the neonatal unit (Maulik D, 2006b).

The presence of umbilical artery AEDF or an abnormal CTG after 34 weeks would require immediate delivery. In a pregnancy less than 34 weeks, the administration of steroids to enhance fetal lung maturity is recommended. A recent multicentre randomized-controlled trial, the Growth Restriction Intervention Trial, compared the effects of delivering within 48 hours of steroid administration and delaying for as long as the fetal health *in utero* permitted. It found no difference in the still birth rate between the two groups (Walker DM et al., 2011).

If pregnancy is less than 28 weeks, the best plan of management of FGR remains uncertain and depends largely on the judgements of the obstetrician and neonatologist. If the fetal status dictates emergency delivery, it should be performed by caesarean section. However, delivery at this stage of gestation has a high morbidity and poor neonatal outcomes.

1.5 Perinatal Consequences of Fetal Growth Restriction

As has been described so far, fetal growth is dependent on multiple factors. These include the pre-determined genetic potential, the ability of the mother to provide sufficient nutrients, the ability of the placenta to transfer nutrients, intra-uterine hormones, and growth factors. An infant who fails to attain his growth potential *in utero* is described as growth-restricted. Some of the long-term and short-term consequences of FGR are described below:-

1.5.1 Mortality

The rates of perinatal mortality are markedly higher in FGR infants, irrespective of whether they are symmetrically or asymmetrically growth-restricted. One study reported a 5 to 6-fold increase in perinatal mortality in both pre-term and term FGR infants (Lackman F et al., 2001), while another reported a 10-fold rise in the death rate of FGR infants at term (McIntire DD et al., 1999). A higher number of fetal deaths are reported in those pregnancies characterized by AREDF on antenatal Doppler velocimetry (Hackett GA et al., 1987). Additionally, many stillbirths are undetected cases of FGR, when other causes have been ruled out.

1.5.2 Prematurity and Associated Complications

FGR fetuses are often not able to complete their *in utero* development until term and need to be delivered prematurely. FGR coupled with prematurity gives rise to a number of perinatal complications, which include respiratory distress syndrome (Tyson JE et al., 1995), chronic lung disease (Regev RH et al., 2003;Aucott SW et al., 2004), higher rates of necrotizing enterocolitis (Bernstein IM et al., 2000;Aucott SW et al., 2004) and intraventricular hemorrhage (Simchen MJ et al., 2000). It is believed that a non-favourable and hypoxic intra-uterine environment resulting from vascular placental insufficiency, results in a delay in metabolic adaptation responses and postnatal reperfusion injury, which manifests as prolonged lung disease.

1.5.3 Hypothermia

FGR infants have lower adipose tissue stores, resulting in less physiologic defenses against hypothermia. If thermally stressed, the FGR infant will increase caloric expenditure in order to maintain normothermia, which may result in acidosis and poor growth (Doctor BA et al., 2001).

1.5.4 Hypoglycemia

FGR infants are at elevated risk of hypoglycaemia after birth as they transition from a continuous supply of glucose to an intermittent one. Metabolic adaptations such as decreased glycogen and adipose tissue stores, increased insulin levels, altered insulin:glucagon ratios, impaired gluconeogenesis and ketogenesis all contribute to the inability of the FGR infant to maintain fasting glucose homeostasis (Pallotto EK and Simmons RA, 2002).

1.5.5 Polycythemia

One of the characteristic features of FGR is chronic *in utero* hypoxemia which leads to increased levels of erythropoietin, and consequent increase in RBC numbers (polycythemia) (Snijders RJ et al., 1993a). This may eventually exacerbate placental vascular dysfunction. Under the circumstances of hypoxemia-stimulated extramedullary hematopoiesis, the risk for thrombocytopenia may increase 10-fold; and increased blood viscosity, decreased erythrocyte pliability, as well as platelet aggregation worsen intra-placental blood flow dynamics further (Trudinger B et al., 2003).

1.5.6 Immune Deficiency and Sepsis

FGR infants generally have a compromised humoral and cellular immune system, which contributes to increased sepsis. They show a decrease in IgG concentrations, phagocytic index, lysozymes and neutrophil numbers, all of which explain their higher susceptibility to post-partum infections (Snijders RJ et al., 1993a;Chandra KR and Matsumura T, 1979).

These perinatal consequences of utero-placental insufficiency illustrate the multisystemic effects of FGR, and how detrimental it can be for neonatal health.

1.6 Long-term consequences of Fetal Growth Restriction

There is now strong evidence that FGR infants have an increased pre-dispostion to many adult onset disorders. These include cardiovascular disorders, type II diabetes and many neurological handicaps.

It is intriguing to consider how an adverse *in utero* environment can be an etiologic factor for diseases in adult life. The answer may lie in the developmental origins hypothesis. This hypothesis states that increased allocation of energy to any one trait during development, such as brain growth, would reduce allocation of resources to the other traits, such as tissue repair processes (Barker DJ, 2006). This makes such individuals more vulnerable to adult-onset disease in three ways.

(i) They have diminished functional capacity in key organs, like the kidney. It is believed that hypertension is initiated by the reduced number of glomeruli found in people who are small at birth (Brenner BM and Chertow GM, 1993).

(ii) They have altered hormonal levels and metabolism. Insulin resistance, which is often associated with low birth weight and FGR, may be viewed as persistence of a fetal adaptive response to maintain blood glucose concentrations for the benefit of the brain, but at the expense of glucose transport into muscles for general growth (Phillips DI, 1996).

(iii) It is believed that people who were born with smaller birth weights are more vulnerable to adverse environmental influences in later life. Animal experiments have proven that the environment faced by an individual *in utero* has a profound effect on shaping his responses to environmental stresses encountered in later life (Barker DJ, 2006).

Some of the diseases that afflict FGR infants early on in adulthood are discussed below.

1.6.1 Coronary Heart Disease

To exemplify the third point described above, a recent study conducted in Helsinki found that men with low taxable incomes had higher incidences of coronary heart disease (CHD) (Barker DJ et al., 2001). Furthermore, this association between low income and CHD was confined to men who had slow fetal growth and who were thin at birth, defined by a ponderal index (birthweight/length^3) of less than 26 kg/m^3. Men who were not small at birth showed no association of CHD with income, which suggests they were resilient to the effects of low income. It is believed that perceptions of low status and lack of success are associated with changes in neuroendocrine pathways that manifest as disease. People who were born SGA are believed to have elevated serum cortisol concentrations in response to stress, resulting in CHD (Phillips DI et al., 2000).

1.6.2 Type II Diabetes

A number of studies have found that differences in insulin sensitivity prevalent in individuals who are born small are associated with increased susceptibility to type II diabetes compared to individuals who are appropriately grown for gestational age (Hales CN et al., 1991;Lithell HO et al., 1996;Newsome CA et al., 2003).

One such study was conducted on a cohort of men who were born in Hertfordshire, UK from 1911 onwards and had their birth weight and weight at 1 year age recorded (Hales CN et al., 1991). Blood samples were collected from them when they were 59-70 years old and analysed for plasma glucose and insulin levels. The study revealed that there was a three-fold difference in the prevalence of diabetes and impaired glucose tolerance in men with the lowest (2.495 kg) and highest (4.309 kg) early weights.

The mechanisms which associate low fetal and infant weights with adult-onset diabetes and glucose intolerance are still not very well understood. It is

known that in humans, much of the development of Islets of Langerhans occurs between the 12th intra-uterine week and 5th post-natal month. FGR human babies have reduced numbers of cells in their organs (Widdowson EM et al., 1972). In some instances, this limitation in cell number may be directly associated with limitation in function. Experiments in rats fed a low protein diet during pregnancy demonstrated reduced numbers of β-cells and associated reduction in insulin secretion (Snoeck A et al., 1990). Similarly, growth-restricted human neonates may have fewer β-cells and a diminished capacity for insulin secretion (van Assche FA and Aerts L, 1979).

It is interesting to note that in pigs and rats, cell numbers increase most rapidly after birth, rather than before, and the animal can therefore recover to some extent from the effects of a malnourished *in utero* environment. Humans, on the other hand, accomplish a greater proportion of their growth before birth than do pigs. It has been calculated that the fertilized human ovum goes through approximately 42 rounds of cell division before birth (Milner RDG, 1989), whilst after birth there need be only a further five cycles of division. In humans, the effects of intra-uterine growth failure are therefore relatively more severe (Widdowson EM, 1971).

1.6.3 Hypertension

A strong association has also been found between low birthweight and hypertension. A one kg difference in birthweight is associated with around 3 mm Hg difference in systolic pressure (Barker DJ, 2006). This effect may appear small at first; however, the lesions that accompany poor fetal growth which tend to elevate blood pressure, and which may include a reduced number of glomeruli (oligonephropathy) have a marginal influence on blood pressure within the normal range as counter-regulatory mechanism maintain homeostasis. The lesions progress via hyperfiltration of the reduced number of glomeruli and the consequent glomerulosclerosis makes it difficult to maintain homeostasis. This leads to increased blood pressure, which initiates a cycling cascade that further deteriorates the lesions (Brenner BM and Chertow GM, 1993).

Histological examination of the kidneys of people killed in road accidents revealed that there were larger but fewer number of glomeruli in the kidneys of those being treated for hypertension (Keller G et al., 2003).

Another study found that there was more than 20 mmHg diference between the systolic pressures of hypertensive patients who weighed less than 2500g at birth and those who weighed more than 4000g at birth. This is consistent with the fact that those individuals with detrimental *in utero* development have a greater pre-disposition to develop clinical hypertension by the time they reach old age, which does not respond well to treatment (Barker DJ, 2006;Yliharsila H et al., 2003).

To conclude, associations between low birth weight and later diseases have been extensively replicated in studies in different countries. The associations between low birth weight and chronic disease are thought to be consequences of developmental plasticity, the phenomenon by which a single genotype can give rise to a range of different phenotypes in response to different environmental conditions during development. Poor nourishment during the *in utero* period, as in disorders like FGR make the individual highly susceptible to CHD, type II diabetes and hypertension later on in life.

1.7 Prenatal Therapies for FGR caused by utero-placental insufficiency

The choice of prenatal therapies for FGR depends on the nature of the etiological insult. Treatment of poor lifestyle habits (like stopping of cigarette smoking, alcohol use, and illicit drugs) may be of benefit. It is also important to rule out FGR caused by chromosomal disorders or perinatal infections before finalizing an appropriate management plan for FGR caused by vascular placental insufficiency. A number of antenatal treatments have been proposed such as maternal oxygen administration (hyperoxia) (Say L et al., 2003), low dose aspirin (Leitich H et al., 1997) and sildenafil citrate (Villanueva-Garcia D et al., 2007); however none have shown evidence of benefit on neonatal outcome. Some of these treatments are briefly described below.

1.7.1 Bed rest

Bed rest either at home or in the hospital has been widely proposed, particularly with the legs slightly elevated, with the aim of improving utero-placental perfusion by decreasing peripheral blood flow, preventing venocaval compression, increasing venous return and cardiac output (Figueroa R and Maulik D, 2006). Unfortunately, extended bed rest can have detrimental consequences for the mother such as an increased risk of thromboembolism, muscle atrophy, heartburn, constipation, a prolonged postpartum recovery period, and increased stress for the mother and her family (Kovacevich GJ et al., 2000;Heaman M and Gupton A, 1998). In addition, a review of the randomized trials to assess the benefits of extended bed rest at the hospital for women with FGR did not come to any conclusive evidence for bed rest to be beneficial over ambulation (Gulmezoglu AM and Hofmeyr GJ, 2000).

1.7.2 Oxygen supplementation

Maternal oxygen supplementation has been proposed since hypoxemia is a characteristic feature of many FGR pregnancies. In addition lowered oxygen tensions at high altitudes is associated with significantly lower birth weights than at sea level, probably because of reduced oxygen delivery (Giussani DA et al., 2007). Say and colleagues compared the therapeutic effects of maternal oxygen therapy with no oxygen therapy in suspected FGR cases (Say L et al., 2003). Their investigations included three studies with 94 women. The oxygen groups received 55% or 40% humidified oxygen at 8L/min by face mask, 24hours/day until delivery. Oxygenation compared with no oxygenation was associated with a reduction in the perinatal mortality rate (relative risk 0.50, 95% confidence interval 0.32-0.81) and a significant improvement in birthweight. However, two of these randomized trials did not involve a placebo. Moreover, the higher gestational age in the oxygen groups may have accounted for the difference in improved perinatal outcomes. Thus, there is not sufficient data to support the benefits of maternal oxygen administration on impaired fetal growth, and further investigations into this field are warranted.

Maternal oxygen supplementation has been associated with detrimental consequences in some FGR animal models and stopping the therapy in mid-gestation resulted in even poorer fetal oxygenation than the pre-therapy levels (Harding JE et al., 1992). Furthermore, prolonged oxygen supplementation is likely to result in maternal pulmonary dysfunction (Johanson R et al., 1995). The therapy is also difficult to administer. Thus, it is believed that maternal oxygen supplementation should not be used in cases of suspected FGR (Say L et al., 2003).

1.7.3 Aspirin

Low-dose aspirin has been used from mid-gestation to prevent the development of pre-eclampsia in women at high risk. Even though the underlying causes of pre-eclampsia and FGR are not well understood, biochemical studies have suggested there may be an imbalance in vasodilators such as prostacyclins and vasoconstrictors such as thromboxane. Low dose aspirin inhibits the cyclooxygenase-1 mediated synthesis of thromboxane-A_2 in the platelets (Kawabe J et al., 2010), without affecting prostacyclin synthesis. This alters the prostacyclin to thromboxane ratio and is believed to vasodilate the utero-placental vascular bed, thereby improving perfusion (Figueroa R and Maulik D, 2006).

Leitich and colleagues (1997) performed a meta-analysis that showed that the use of low-dose aspirin resulted in a significant reduction in FGR and a non-significant reduction in perinatal mortality. Their analysis revealed that aspirin was effective at doses of 50-80 mg/day. The preventive effect was further improved at higher doses between 100-150 mg/day. Importantly, aspirin was only effective if started before week 17 of gestation (Leitich H et al., 1997).

It is therefore important that pregnant women who are likely to benefit from low-dose aspirin should be carefully identified and started on the treatment early on in gestation, before 17 weeks (Leitich H et al., 1997). The majority of severe FGR cases occur in the first pregnancy, and thus once it is diagnosed, usually by 20 -24 weeks at the earliest, low dose aspirin is unlikely to be of benefit.

1.7.4 β-adrenergic receptor agonists

β-adrenergic receptors agonists or betamimetics relax the smooth muscle cells of the vasculature and myometrium, thereby dilating the utero-placental vascular bed and increasing placental perfusion. In addition, they also enhance blood glucose levels. Both these effects may relieve the detrimental effects of utero-placental vascular insufficiency to some extent. Betamimetics however, are able to cross the placenta and reach the fetal circulation, where they may cause adverse effects by altering fetal glucose levels and vasodilating the fetal vasculature (Figueroa R and Maulik D, 2006). In a randomized placebo controlled trial on betamimetic therapy in women with suspected FGR, no difference was found between the treatment group and control group, when comparing birthweight or neonatal morbidity and mortality. Thus, at the moment there is no evidence for their clinical usefulness in FGR (Gulmezoglu AM and Hofmeyr GJ, 2001).

1.7.5 Viagra

Some of the recent work aimed at mitigating FGR resulting from utero-placental insufficiency has included investigating the role of sildenafil citrate (Viagra). In *ex vivo* experiments, Viagra significantly reduced vasoconstriction and enhanced vasodilatation of myometrial small arteries from women whose pregnancies were complicated by FGR (Wareing M et al., 2005). It was therefore hypothesized that Viagra may offer a potential therapeutic strategy to improve uteroplacental blood flow in FGR pregnancies. Administration of Viagra as an intravenous bolus unexpectedly decreased uterine blood flow in pregnant ewes carrying either healthy or growth-restricted fetuses. It is believed that sildenafil results in a systemic reduction in vascular resistance and consequent blood flow "steal" from the uteroplacental circulation to the systemic vascular circuit (Miller SL et al., 2009). This indicates that sildenafil may be an inappropriate therapy for pregnancies complicated by FGR and should be used only with caution during pregnancy because of its detrimental effects. Furthermore a randomized control

trial of sildenafil citrate did not prolong gestation in pregnancies complicated by severe PET (Samangaya RA et al., 2009). Contrary to these results, a recent study demonstrated that oral silenafil therapy was associated with an improvement in the rate of fetal abdominal circumference growth in women with severe early-onset FGR (von Dadelszen P et al., 2011). This study is however limited by patient numbers (n=10), and a more detailed investigation into the benefits of sildenafil citrate therapy, including improvement in perinatal outcomes, if any, is warranted.

1.7.6 Growth Factor treatment

Transamniotic Fetal Feeding (TAFF) is the continuous infusion of hormones or nutrients into the amniotic fluid. As fetal swallowing occurs *in utero*, the enriched amniotic fluid is ingested and used for fetal anabolism. Transamniotic administration of recombinant human (rh)-IGF-1 by continuous infusion over a 7-day period towards the end of gestation in FGR rabbits enhanced serum IGF-1 levels and resulted in an increase in both fetal and placental weights in infused v/s sham catheterized but non-infused contra-lateral controls (Skarsgard ED et al., 2001). TAFF using Epidermal growth factor (EGF) also led to significant improvements in fetal weight and normalized neonatal birth weights equivalent to that of appropriately grown fetuses (Cellini C et al., 2004). Though proven to be beneficial in pre-clinical studies, the clinical translation of this methodology is unlikely. This is because chronic catheterization of the human amniotic cavity, particularly in high-risk pregnancies is not feasible.

It has been demonstrated that site-specific placental gene transfer of Angiopoietin-2 using an adenoviral vector resulted in a significant increase in fetal weights in normal pregnant mice, compared to control untreated mice. Other transgenes evaluated in the same study (Ang-1, bFGF, hepatocyte growth factor, IGF-1, PlGF, PDGF-B and VEGF-A_{121}) had no effect on fetal weight. The authors plan further experiments in models of placental vascular insufficiency, such as the naturally occurring FGR model in rabbits to assess the potential efficacy of these growth factors (Katz AB et al., 2009).

1.7.7 Treatment with melatonin and vitamin C

In a recent study, the potential of melatonin and vitamin C to increase umbilical blood flow was explored (Thakor AS et al., 2010). A fetal intra-venous infusion of melatonin and vitamin C significantly improved umbilical blood flow, via NO-dependent vasodilatation. The effects appeared to last for a short duration of time however, suggesting that chronic administration may be needed for any potential therapeutic benefit on fetal growth to be realized.

Work done by the same group in an FGR rat model, created by maternal nutrient restriction, has shown that administration of melatonin maternally in drinking water restores pup birthweight to that of control non growth-restricted pups. Interestingly, the fetal weights at day 20 were not significantly different between the undernourished group treated with melatonin and undernourished controls. This suggests that melatonin has a profound effect on enhancing neonatal birthweight only in the last 2 days of pregnancy (rat gestation = 22-23 days). It is believed that the beneficial effects of melatonin are mediated by an improvement in placental efficiency (Richter HG et al., 2009).

1.7.8 Nitric oxide donors

Studies in an FGR sheep model created by maternal under-feeding demonstrated that NO donors like L-arginine may be of potential benefit in ameliorating FGR (Lassala A et al., 2010). L-arginine is a nutritionally essential amino acid for fetal development (Wu G et al., 2009), and a precursor of NO biosynthesis (Wu G and Morris SM, Jr., 1998). Hence, it is believed that Arginine may play a critical role in placental development, utero-placental perfusion and transfer of nutrients from the mother to the fetus (Wu G et al., 2006).

In human patients, administration of L-arginine (3 g daily orally for 20 days) was found to have beneficial effects in ultrasound-diagnosed cases of FGR (cases of chromosomal abnormality, maternal diabetes, drug and alcohol use were excluded). There was a significant increase in estimated fetal weight in the treated group compared to control group, which received no treatment. The neonatal

weights were also significantly improved in the treated group (2823±85 g v/s 2495±147 g). The percentage of FGR neonates in the treatment group was significantly lesser than the control group (29% v/s 73%). (Sieroszewski P et al., 2004). The mechanism behind these effects is believed to be the enhanced production of NO, which improves utero-placental blood flow not only by vasodilatation, but also because of its anti-aggregative effects on platelets.

1.7.9 Pravastatin

Studies in a murine model of PET, created by lentiviral-mediated over-expression of sFlt-1 in the placenta, have demonstrated that statins may be of potential benefit in ameliorating PET (Kumasawa K et al., 2011). Statins have conventionally been used for the treatment of hypercholesterolemia, but it has recently been reported that they have a protective effect on vascular endothelial cells (Ludman A et al., 2009). Administration of pravastatin in pre-eclamptic mice (5µg/day intra-peritoneally; equivalent to a human therapeutic dose of 10mg/day) daily from embryonic day (E) 7.5 onwards resulted in significant improvements in maternal hypertension at E16.5 and later timepoints. There were also improvements in glomerular endotheliosis and proteinuria, concomitant with significant reduction in the levels of circulating sFlt-1 and significant increase in levels of mouse PlGF. VEGF levels remained unaltered (Kumasawa K et al., 2011). As PET and FGR commonly overlap with each other, statins may be of potential benefit for treating FGR too, even though this was not evaluated in the current study. The potential of pravastatin to treat PET in the clinics is currently under investigation in clinical trials, one of which is the StAmP trial (Statins for Amelioration of Pre-eclampsia), being conducted at University College London Hospitals.

1.7.10 Japanese Herbal Medicine

The traditional Japanese herbal medicine Toki-shakuyaku-san was found to have beneficial effects in a rat model of PET and FGR, caused by sub-cutaneous infusion of L-NAME (inhibitor of NO synthase activity). Administration of Toki-shakuyaku-san (1g/kg, 2g/kg) by gavage from day 14 of

gestation onwards brought about a reduction in maternal blood pressure. Furthermore, there was also improvement in fetal weight, when treated with the higher dose (2g/kg). Treatment with L-arginine, with the amount present in Toki-shakuyaku-san, was found to have no therapeutic effects. Additionally, there was no significant change in the serum levels of NO following treatment with Toki-shakuyaku-san. This suggests that the beneficical effects of Toki-shakuyaku-san on hypertension and fetal weight in this rat model of PET and FGR were NO-independent. (Takei H et al., 2004)

As has been discussed in this section, there is currently no treatment available which may convincingly ameliorate FGR and reliably reduce morbidity and mortality rates in the clinic, though several pre-clinical studies to develop a treatment are in progress. This thesis describes a novel gene therapy based approach that may be of potential therapeutic benefit in severe FGR caused by utero-placental insufficiency. The aim was to decrease the severity of FGR by adenovirus-mediated local over-expression of VEGF in the uterine arteries of pregnant sheep.

1.8 Types of placentation

In order to select the most appropriate animal models required to support the local administration of adenovirus-VEGF (Ad.VEGF) to pregnant women in their second trimester, it is useful to compare key aspects of human placentation to those found in animal models.

The maternofetal barrier refers to the tissue layers separating maternal and fetal circulations in the placenta. There is significant variation amongst different species in the completeness of this placental barrier depending on the extent of trophoblast invasion (Figure 1.5). This has been reviewed in detail by Kaufmann P (1981).

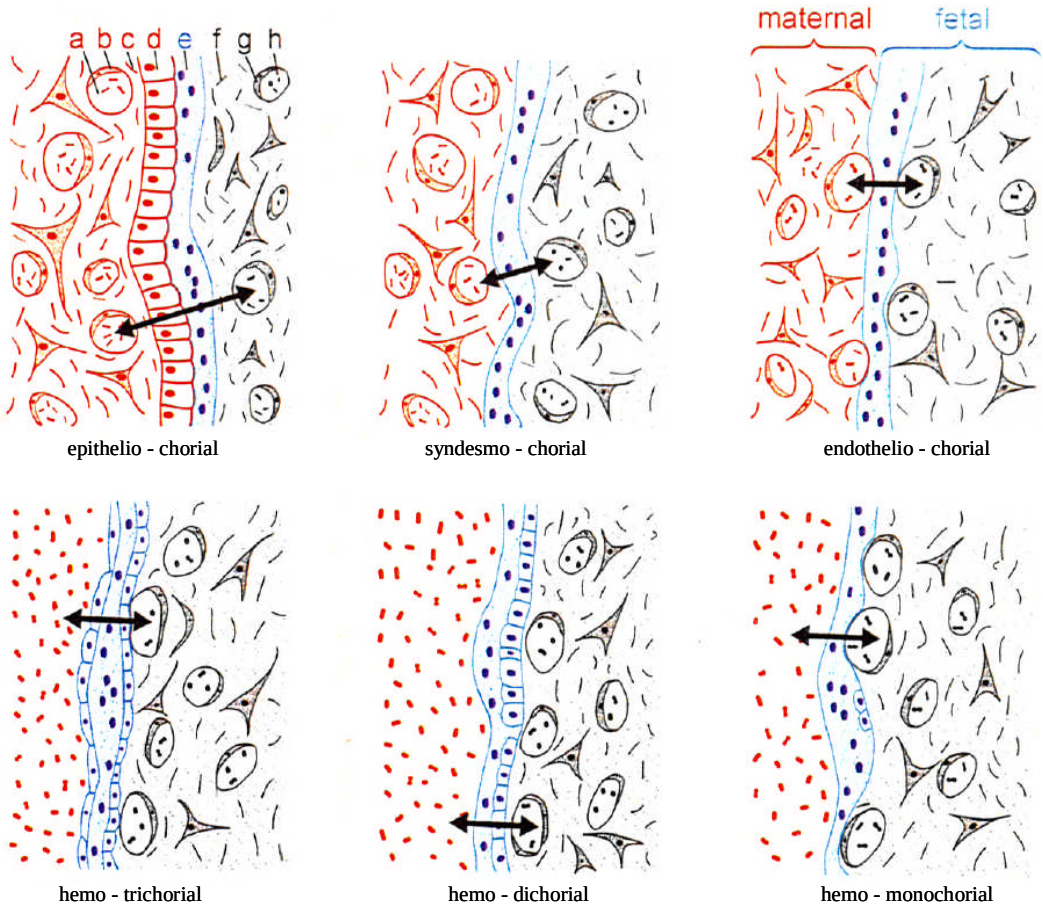

Figure 1.5 : Tissue layers of the maternofetal barrier according to the Grosser classification.

a-maternal blood (red dots); b-maternal endothelium (red); c-endometrial connective tissue (red); d-endometrial epithelium (red); e-trophoblast (blue); f-fetal connective tissue (black); g-fetal endothelium (black); h-fetal blood (black dots). The fetal components of the placental barrier (e – g) are collected under the term chorion. Maternal components are reduced step by step until the chorion comes into direct contact with the maternal blood (r, red dots). The trophoblast (blue) may be covered on one side (haemodichorial) or on both sides (haemotrichorial) by cytotrophoblast (Kaufmann P, 1981).

1.8.1 Epitheliochorial placenta

At one end of the spectrum the fetal chorion directly faces the intact endometrial epithelium. The blastocyst does not invade the endometrium, only remaining attached to it. Six tissue layers separate maternal and fetal blood: maternal capillary endothelium, maternal endometrial connective tissue and maternal endometrial epithelium and three layers of fetal origin - trophoblast, chorionic connective tissue, and fetal endothelium. From the six layers, the

trophoblast or the maternal epithelium may fuse syncytically. This kind of placentation is seen in sheep.

1.8.2 Syndesmochorial placenta

The stepwise removal of maternal tissue layers as a result of further blastocyst invasion results in destruction of the uterine epithelium. This placenta is found in camels.

1.8.3 Endotheliochorial placenta

Deeper invasion of trophoblasts and corresponding removal of endometrial connective tissue results in the development of endotheliochorial placenta. This placental barrier is characteristic for all carnivores.

1.8.4 Haemochorial placenta

The final step of trophoblast invasion results in erosion of the maternal vessels, which are finally completely destroyed. The trophoblastic surfaces now face the maternal blood directly (Enders AC, 1965). Depending on the number of trophoblastic epithelial layers a more detailed subdivision has been proposed: haemotrichorial (rat: Enders AC, 1965), haemodichorial (rabbit: Enders AC, 1965; human in the first trimester: (Hamilton WJ and Boyd JD, 1970), and haemomonochorial (guinea pig: (Kaufmann P and Davidoff M, 1977); human placenta at term Hamilton WJ and Boyd JD, 1970).

1.9 Animal Models of FGR

FGR can be artificially created in animal models by adopting a variety of strategies that affect the maternal, fetal or placental environments. In selecting an animal model of FGR, it is necessary to consider the size of the animal, its characteristic placentation, intra-uterine growth trends and gestational period. The commonly adopted experimental approaches to create FGR are described below.

Notably, about three quarter of all experiments using models of FGR have been performed in two rodent species, rats and mice (Schroder HJ, 2003). Advantages of the mouse include its small size and short generation time.

Additionally, the availability of murine embryonic stem cells facilitates gene targeting and the development of transgenic lines. The small size of mice, which make their maintenance easier compared to other species, may actually be a potential disadvantage for functional studies. The mouse placentation is quite different to human placentation. In contrast to humans, trophoblast invasion in the mouse is shallow. Uterine natural killer cells play a more important role than trophoblast in arterial remodelling in mice. The interhaemal barrier between the maternal and fetal circulations in mice consists of three trophoblast layers, outer one cellular and inner two syncytial, compared to only a single layer of syncytial trophoblast in humans. This difference is important when investigating the overall exchange of substrates across the placenta between the uterine and umbilical circulations.

The placental endocrine functions in the two species differ significantly. In mice, ovarian progesterone production is required throughout the length of gestation (3 weeks), and maintenance of the corpus luteum is dependent on pituitary prolactin and placental lactogen. In humans, maintenance of the corpus luteum is dependent on human chorionic gonadotropin (hCG) produced by the trophoblast. Furthermore, from 8 weeks of gestation, progesterone produced by the syncytiotrophoblast is sufficient to maintain pregnancy, even after ovariectomy (Schroder HJ, 2003).

One of the other drawbacks of working with mouse and rat models is their high rate of genetic mutation. This is believed to be on account of their shorter generation times, and consequently higher mutation rates, or possibly less accurate DNA replication systems. It is therefore suggested that murid rodents like mice, rats and hamsters are inappropriate models for most research on human conditions.

In contrast to mice and rats, the rabbit placentation (haemodichorial) and guinea pig placentation (haemomonochorial) is closer to the human situation, as discussed above.

The advantage of working with guinea pigs over rabbits though, is that being a smaller animal, they are easier to maintain. More importantly, they have a

longer gestation (~65 days) compared to the rabbit (~31 days). For our study, this is an advantage as it gives us the opportunity to intervene (by injecting gene therapy vectors) at mid-gestation, and be able to study the effects of the therapy for over a month.

While no animal truly recapitulates human pregnancy, the pregnant sheep has been extensively used over the past 40 years to study fetal physiology. The ovine fetus has a good tolerance to *in utero* manipulations allowing the surgical placement of catheters in both the maternal and fetal vasculature (Jellyman JK et al., 2004;Abi-Nader KN et al., 2011) and a consistent gestation period of 145 days, which is approximately half that of the human. As in humans, the gestational age of the fetus can be accurately determined by ultrasound using fetal measurements similar to those used in clinical practice (Barbera A et al., 1995). Ultrasound is routinely used in farming practice to check for multiple pregnancy early in gestation (Aiumlamai S et al., 1992). Considerable insights into placental oxygen and nutrient utilization and transfer has been obtained from pregnant sheep, and confirmed in humans once appropriate technology became available (Barry JS and Anthony RV, 2008). There are some important similarities and well as differences between human and sheep placentae.

In human pregnancy, the conceptus truly invades the uterine wall, which does not occur in ovine pregnancy. The sheep placenta consists of spot-like regions of maternofetal interdigitations (placentomes) containing a tuft of fetal villi, called a cotyledon, attached to 60-150 endometrial thickenings called caruncles. The placentomes are spread throughout the uterine cavity. The sheep cotyledon is anatomically very similar to the human placenta, and the vasculature within both is also very similar. Undoubtedly, the sheep placenta is far from being a perfect model for the human; nevertheless, the similarity in fetal placental vascular structure, relatively long duration of gestation, size and weight of the fetus make the sheep an appropriate model for human pregnancy (Meschia G et al., 1965;Battaglia FC et al., 1968).

The manifestations of FGR pregnancy in human and sheep are also very similar. Placental structural abnormalities that have been associated with FGR include reductions in placental villous number, diameter and surface area; along with reductions in villous arterial number, diameter and degree of branching (Krebs C et al., 1996;Macara L et al., 1996;Barry JS and Anthony RV, 2008). Severe early-onset FGR is associated with altered umbilical artery Doppler waveforms which are indicative of increased placental vascular resistance (described above). In incidences of ovine FGR as well (induced by hyperthermia), there is modification of placental vasculature in a similar fashion to that of the human FGR condition (Regnault TR et al., 2002). The near term uterine and umbilical blood flows are reduced, while umbilical artery Doppler velocimetry measures demonstrate increased pulsatility and resistance indices (Galan HL et al., 2005). Furthermore, fetal cotyledon VEGF levels are reduced in near term sheep FGR pregnancies (Regnault TR et al., 2003), which is very similar to what is observed in the human clinical setting (Lyall F et al., 1997).

The increase in uterine blood flow that occurs through the latter half of gestation is also very similar for humans and sheep. It increases two and a half times in humans (from 0.3 to 0.8 L/min) while in sheep, this increase is three fold (0.4 to 1.2 L/min) (Konje JC et al., 2003;Meschia G, 1984). This is concomitant with an increase in the supply of substrates and oxygen to the conceptus, failure of which manifests as asymmetric FGR. The rates of oxygen and glucose consumption in both near-term sheep and human fetuses are also similar (Barry JS and Anthony RV, 2008).

Based on the similarities between sheep and human pregnancy and the ability to place maternal and fetal catheters in pregnant sheep, it may be concluded that the pregnant sheep is an appropriate animal model to study human pregnancy.

Some of the specific methods used to create FGR in animal models are described below:-

1.9.1 Naturally occurring models

The rabbit is a useful species in which to investigate FGR. It provides a naturally occurring model of FGR which parallels the human situation in three ways: (a) the onset occurs in the third trimester; (b) brain sparing is seen; and (c) the underlying cause is vascular insufficiency via a “watershed region” between the vaginal and uterine arterial blood supplies. The bicornuate uterus carries multiple fetuses within individual amniotic cavities/gestational sacs. At term, the weight ratio of the growth-retarded fetus (third from ovarian end) to the favored fetus (closest to ovarian end) in each horn is consistently 0.85. The advantage of the bicornuate uterus is that there are two IUGR fetuses per litter, which enables comparative studies between the runt pairs, with one serving as the other’s control (Skarsgard ED et al., 2001;Thakur A et al., 2000).

1.9.2 Dietary manipulation

FGR may be created in animal models by either maternal nutrient restriction or maternal overnourishment. Both of these conditions are discussed below:-

1.9.2.1 Maternal undernutrition

One of the most commonly used strategies to create FGR is maternal nutrient restriction, particularly in rodents. In this thesis, we have worked with one such animal model of FGR-the maternal nutrient restricted guinea pig (Roberts CT et al., 2001a). Restricting maternal nutrition 4 weeks before and during pregnancy is a well-recognized method of creating FGR in small animals. In the guinea pig this impairs placental functional development, reduces the placental exchange and trophoblastic surface, and increases the thickness of the exchange barrier (Roberts CT et al., 2001a). Such actions are thought to be mediated by decreasing levels of the IGFs, which are important modulators of placental growth and differentiation (Roberts CT et al., 2001b;Roberts CT et al., 2002), and which are implicated in human FGR.

The maternal nutrient restriction model has also been created in other rodents by under-feeding the mother for different lengths of time during

gestation, reviewed in (Haugaard CT and Bauer MK, 2001). Woodall et al developed an FGR model in rats by nutrient restricting pregnant females by 30% of the *ad lib* intake, throughout gestation. After birth, all pups were cross-fostered by an *ad lib* intake mother. The mean fetal weight at late gestation, neonatal weight, placental weight as well as postnatal body weight at 18 weeks of age were all significantly lower in the undernourished group compared to the control group. Circulating IGF-I was significantly reduced in the restricted group from day 22 of gestation until postnatal day 9, but not at later time points (Woodall SM et al., 1996;Woodall SM et al., 1999).

1.9.2.2 Over-nourishment in adolescent pregnant sheep

Paradoxically, when adolescent sheep are over-nourished during pregnancy, fetal and placental weights are distinctly reduced from as early as 95 days of gestation and birth weight is significantly reduced (Wallace JM et al., 2004). There is also a reduction in both the uterine and umbilical blood flows. The decrease in placental weight is due to a reduction in both the number and weight of placentomes, though placental function is not altered. Furthermore, the fetus is hypoxic and exhibits brain sparing. There is an attenuated uptake of oxygen, glucose and amino acids by the umbilical circulation.

The etiology is believed to be the increased insulin and IGF-1 levels in maternal plasma, that are characteristic of over-nourishment, which provide a sustained anabolic stimulus for growth of maternal tissues that is so powerful that it shifts the supply of nutrients away from the feto-placental unit (Schroder HJ, 2003). In other words, the mother grows in size and weight at the expense of the fetus, which becomes growth-restricted.

1.9.3 Uterine artery ligation

Another commonly adopted strategy is uterine artery ligation, first demonstrated in rats (Wigglesworth JS, 1964). This reduces the blood flow in the uterine artery, and thereby limits the supply of nutrients and oxygen to the fetus. The model was originally designed to demonstrate the importance of uterine

blood supply as a controlling factor in fetal growth. One of the drawbacks with this model is the high incidence of fetal death and resorption among the fetuses in the manipulated horn.

In guinea pigs, the maternal side of the placentae is supplied with blood from an arcade between the uterine and ovarian artery. Ligation of this arcade between the uterine and ovarian arteries consistently results in growth restriction by about 50% compared to controls and there is no post-natal 'catch up' growth. However, the fetal mortality on the experimental side was found to be as high as 30% (Carter AM, 1993;Lafeber HN et al., 1984).

Tanaka *et al* mimicked a phenomenon called "postischemic hypoperfusion" of utero-placental circulation to create an FGR model with low mortality and favourable reproducibility. Instead of ligating the uterine artery, they used two small artery clamps to occlude the uterine artery vessels for a period of 5-60 minutes on day 17 of gestation. The fetuses were delivered by cesarean section on day 21. The fetuses on the ischemic side were found to be significantly lighter than control non-ischemic fetuses. Furthermore, they had significantly lowered liver:body weight ratios and significantly increased brain:body weight ratios compared to controls. Fetal mortality on the ischemic side was 14% (Tanaka M et al., 1994).

In large species like sheep, an adjustable occluder with exteriorized controller has been placed around the maternal common iliac artery which allows the operator to regulate uterine blood flow (Clark KE et al., 1982). Reduction in uterine blood flow is associated with significant reductions in fetal and placental weights (Lang U et al., 2003). Alternatively, the technique of embolizing the utero-placental vasculature with microspheres has been employed to create FGR in sheep (Clapp JF, 3rd et al., 1981;Creasy RK et al., 1972). Though successful in limiting fetal growth by reducing utero-placental perfusion, one of the main criticisms of this technique has been the simultaneous necrosis of placental tissue. Hence, the effects of a compromised uteroplacental circulation on fetal growth cannot be distinguished from those caused by a reduced placental exchange capacity for nutrients and substrates.

1.9.4 Single umbilical artery ligation

Single umbilical artery ligation (SUAL) has also been used to create FGR in the sheep fetus. At 108-119 days of pregnancy, one umbilical artery is isolated and ligated close to the fetal abdomen. Although this model was developed in the late 1960s (Emmanouilides GC et al., 1968), it is prevalent even currently in FGR studies (Miller SL et al., 2009). A reduced umbilical blood flow limits the supply of substrates and oxygen from the ewe to the fetus (Oh W et al., 1975), resulting in asymmetric growth restriction. The SUAL fetuses are characterized by relatively greater brain and adrenal weights, compared to control fetuses (Morrison JL, 2008). There is a significant reduction in fetal and placental weights. Furthermore, gross and microscopic examination of the placenta revealed evidence of infarction of about one-half of its surface (Oyama K et al., 1992).

1.9.5 Placental injury or reduction

Experimentally induced thermal placental injury causes FGR in pregnant rabbits. The optimum exposure to create the FGR condition was determined to be 15mA direct current for 40 seconds, which created growth-restriction in 71% of all treated fetuses and relatively low abortion rates. The fetuses and placentae showed reductions in weight of about 31% and 41% respectively relative to controls, and brain:liver weight ratio was increased in the FGR group compared to controls (Rosati P et al., 1995). The basis of this model is interference with the placental exchange function by creating a wide area of ischemic tissue.

Likewise, growth restriction has been created in the sheep by surgical reduction in the number of endometrial caruncles from the uterus of the non-pregnant ewe prior to mating. During pregnancy, the maternal caruncles are in close apposition with the fetal cotyledons, and the two together form placentomes. Reducing the number of caruncles leads to a reduction in placental weight, which clearly influences fetal weight (Alexander G, 1964;Robinson JS et al., 1979) because there is reduced placental exchange area and function. The removal of

100 uterine caruncles before mating has been shown to reduce lamb birthweight by about 17% (Mellor DJ et al., 1977). These placentally restricted fetuses also show evidence of redistribution of cardiac output and brain sparing, a common manifestation of asymmetric FGR.

1.9.6 Hypoxia

A number of FGR models have been created by exposing the pregnant rat to low oxygen tension in the last half of gestation. In the rat, even brief intermittent episodes of hypoxia for 1-2 hours/day acutely decrease fetal oxygen delivery, and this can have deleterious consequences on fetal growth (Schwartz JE et al., 1998).

More recently, the importance of fetal oxygenation for prenatal growth was demonstrated in the chicken model (Giussani DA et al., 2007). Incubation of fertilized eggs laid by sea level hens at high altitude markedly reduced fetal growth. However, this growth restriction could be completely prevented by oxygen supplementation to the fertilized eggs during incubation at high altitude, thereby proving that oxygen was the limiting factor resulting in growth retardation. These growth restricted embryos were also characterized by an increased relative brain weight, expressed as a percentage of fetal body mass. Interestingly, incubation at high altitude of fertilized eggs laid by high altitude hens also restricted fetal growth, albeit to a lesser extent than sea level hens.

1.9.7 Hyperthermia

A high ambient temperature in the first trimester of pregnancy is associated with lower birth weight (Lawlor DA et al., 2005). The underlying physiological mechanisms of this relationship have been explored in the sheep. This model can be created in pregnant ewes by raising the ambient temperature to 40°C for 12 hours and then to 35°C for 12 hours of each 24-hour period, with relative humidity maintained at 30-40%, from 45 days of gestation onwards. Under this regimen, the maternal core body temperature is raised by 0.6-1.0°C within 7 days, which decelerates fetal growth (Wallace JM et al., 2005). Placental

and fetal weights are reduced by as much as 50% in FGR fetuses of hyperthermic ewes at 135 days gestation (Thureen PJ et al., 1992).

Maternal hyperthermia results in smaller placentomes with a diminished capacity for the transfer of oxygen and substrates (like glucose) to the fetus. The fetal adaptations cause a slowing of fetal growth to match the placental substrate supply. The uterine and umbilical blood flows are also reduced (Bell AW et al., 1987). FGR created by exposing pregnant ewes to hyperthermia is also characterized by relative sparing of the fetal heart, and an increase in the ratio of brain to liver weight, which is evident as early as 55 days of gestation.

1.9.8 Transgenic models

There are a number of transgenic mouse models of FGR available. One of them is the placental-specific *Igf2*-knockout mouse. As mentioned previously (Section 1.2.2.), the *Igf2* gene is paternally expressed in the fetus and placenta, and promotes the transfer of nutrients from the mother to the fetus. Deletion of this gene from the labyrinthine trophoblast of the mouse placenta has been shown to reduce the nutrient transfer functions and growth of the placenta, and result in FGR. Fetuses from the knockout animals were found to weigh only 78% of wild type fetuses at E19 (Constancia M et al., 2002).

Mice in which the gene for eNOS had been knocked out also showed evidence of FGR and reduced placental development at E17, as well as a slower growth trajectory postnatally. The etiology is believed to be a compromised utero-placental circulation, on account of reduced production of NO by the endothelium (Hefler LA et al., 2001). Prolonged blockade of nitric oxide synthesis in pregnant rats, by continuous infusion with L-nitro-arginine, results in chronic maternal hypertension and substantial FGR, reducing weights of newborn pups by as much as 40% (Molnar M et al., 1994).

1.10 Adenovirus mediated gene therapy: background and considerations for treatment of FGR

This thesis discusses the potential of local administration of recombinant therapeutic adenoviruses to reverse utero-placental vascular insufficiency. To appreciate the potential hazards of intra-arterial injection of an adenovirus encoding for VEGF, it is necessary to briefly review the nature and background history of adenovirus infections. A concise account is provided by (Russell WC, 1998).

1.10.1 Natural history of adenoviral infections

Adenoviruses are frequent causes of spontaneous, short-lived infections of the respiratory and gastrointestinal tracts and ocular infections in humans of all ages, which commonly result in brief pyrexia (fever) and signs of temporary inflammation and epithelial damage in the affected tissues. Systemic infection, such as meningoencephalitis, is very uncommon. Infection normally occurs via aerosol spread. Natural infectivity is low because adenoviruses are frequently found in the atmosphere, whereas people rarely develop a clinically apparent infection. Recovery is considered to be due to clearance of the virus and infected cells by humoral and cellular mechanisms (Russell WC, 1998;O'Riordan C, 2002;Trapnell BC and Shanley TP, 2002).

Adenoviruses do not integrate into the host genome (Russell WC, 1998;Evans JD and Hearing P, 2002). For that reason, and because of the efficacy of the immune response, active adenoviral infection is short-lived and chronic infection does not occur in people with a normal immune system. Serotype 5 adenovirus infections commonly occur in children in the community, so antibodies are often found in young people and in most adults (Russell WC, 1998).

There is limited data on adenovirus infection during pregnancy and the association of adenovirus with miscarriage and FGR (Reddy UM et al., 2005;Montone KT et al., 1995). However the evidence is only circumstantial and

there is none to confirm adenovirus infection to be the etiological factor for abnormal pregnancies. Infact, the presence of viral infection in amniotic fluid samples (collected at amniocentesis) was found to be not significantly associated with postamniocentesis pregnancy loss (Wenstrom KD et al., 1998). The adenovirus-VEGF construct used in the studies described in this Ph.D. has been genetically modified by deletion of E1 and partial deletion of E3, the former making it replication deficient, which is a major defence against any disease in humans (Figure 1.6)

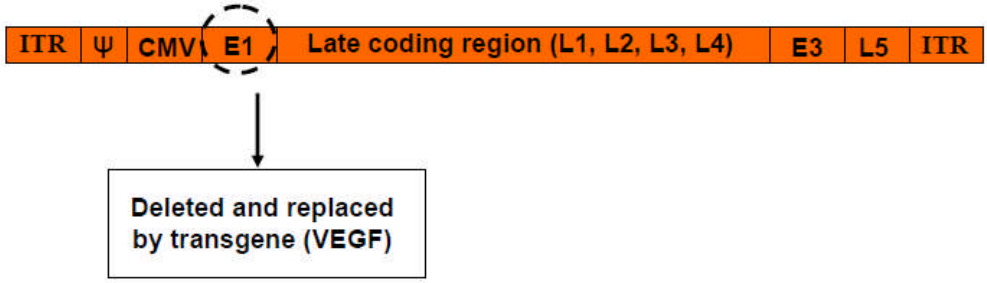

Figure 1.6 – Recombinant adenoviral construct used in the experiments described in this thesis.

The adenoviral backbone has been modified by deletion of E1 and partial deletion of E3, the former resulting in the construct becoming replication incompetent. ITR = Inverted terminal repeats; ψ = packaging signal.

1.10.2 Infection with replication deficient adenoviruses

Adenovirus virions normally infect susceptible species (*e.g.* humans, pigs, and cotton rats) by entering cells via attachment to Coxsackie and Adenovirus Receptor (CAR), followed by binding to integrins $\alpha_v\beta_3$ and $\alpha_v\beta_5$ which promote virus internalization (Bergelson JM et al., 1997;Tomko RP et al., 1997;Nemerow GR and Stewart PL, 1999). They become uncoated in the cytoplasm, transported to the nucleus and divert the cell's synthetic mechanisms to produce more viral DNA, proteins etc, which are assembled into further virons that are subsequently

released and are available to infect other cells and organisms (Russell WC, 1998;Evans JD and Hearing P, 2002;Nemerow GR, 2002). The adenoviral DNA remains episomal and is not integrated into the host genome (Evans JD and Hearing P, 2002).

It has been demonstrated that expression of CAR on trophoblast cells varies with gestational age and trophoblast phenotype (Koi H et al., 2001). CAR was found to be continuously expressed in invasive cytotrophoblast (fetal side) but not in syncytiotrophoblast (outermost fetal component), thus rendering the syncytiotrophoblast resistant to adenoviral infection and limiting transplacental transmission. The ability of adenoviruses to infect trophoblasts is also related to the state of trophoblast differentiation (MacCalman CD et al., 1996;Parry S et al., 1998). Recombinant adenoviruses efficiently transduce the inner cytotrophoblast, but there is a significant reduction in the transduction efficiency of these vectors after the terminal differentiation of the mononucleated cytotrophoblast into the multinucleated syncytiotrophoblast.

These reports (MacCalman CD et al., 1996;Parry S et al., 1998;Koi H et al., 2001) and others (Nemerow GR, 2002) do suggest that species susceptibility to adenovirus infection is related to the absence or scarcity of appropriate CAR receptors. Based on these reports, it is evident that administration of adenoviral vectors into the utero-placental vasculature is likely to limit fetal transmission because of the placental barrier, which is refractory to infection. However, it is important to note that this hypothesis relies on assays of CAR in tissue culture, which can itself alter expression of the virus receptor and may not fully reflect events *in vivo*. 'Susceptibility' may be only a relative state as there are experimental and clinical results showing adenoviral infection of cells and animals of non-susceptible species after exposure to high concentrations of wild-type and modified viruses to become gene therapy agents (Evans JD and Hearing P, 2002;Kim M et al., 2002;Batra RK and Sharma SWL, 2002).

To conclude, it is important to be aware that there are now experimental and clinical results showing that adenoviral vectors may infect cells from animals of so-called 'non-susceptible' species, and the details of expression and the metabolic activities of the viral and imported transgenes in these circumstances are not yet clear. Thus, in the context of developing a safe gene therapy candidate for treatment of FGR, the potential for transplacental transmission needs to be thoroughly investigated to assess the safety of administration.

1.11 Rationale for use of Adenovirus-vegf and mechanism of action

Vascular Endothelial Growth Factor (VEGF, especially VEGF-A) is essential in several processes during embryonic development, including vasculogenesis, whereby primordial vessels arise from blood islands and endothelial cell progenitors undergo differentiation; and angiogenesis, which is the formation of new blood vessels (capillaries) from pre-existing ones (Carmeliet P, 2003;Sadler TW, 2004) (Figure 1.7).

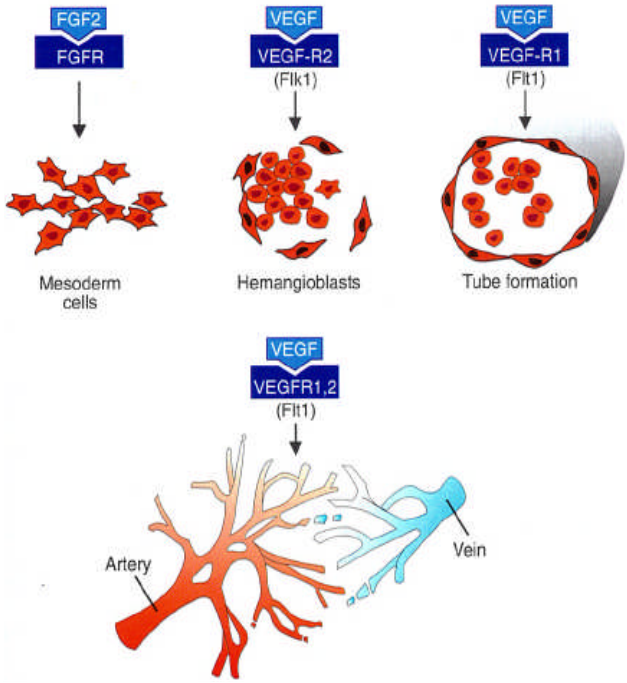

Figure 1.7 - Embryonic blood vessel formation involves two major processes: vasculogenesis (top), in which vessels arise from blood islands, and angiogenesis (bottom), in which new vessels sprout from existing ones.

During vasculogenesis, fibroblast growth factor 2 (FGF-2) binds to its receptor on subpopulations of mesoderm cells and induces them to form hemangioblasts. Then under the influence of VEGF acting through two different receptors, these cells become endothelial and coalesce to form vessels. Angiogenesis is also regulated by VEGF, which stimulates proliferation of endothelial cells at points where new vessels will sprout from existing ones (Sadler TW, 2004).

Several groups have suggested that VEGF gene or protein therapy may be therapeutically useful in local perivascular applications by stimulating vascular protective endothelial functions (Zachary I et al., 2000) and as a potential treatment for ischaemic heart disease (Simons M et al., 2000;Yla-Herttuala S and Martin JF, 2000;Khurana R et al., 2001). Importantly, VEGF has been found to cause vasodilatation and an increase in blood flow in diverse animal blood vessels and vascular beds (Ku DD et al., 1993;Takeshita S et al., 1998). These effects are mediated partly through its ability to stimulate endothelial production of nitric oxide (NO) and prostacyclin (PGI_2) (Laitinen M et al., 1997;Wheeler-Jones C et al., 1997;Horowitz JR et al., 1997).

Several studies have shown VEGF production and secretion in the human placental and fetal membranes. VEGF is expressed in the syncytiotrophoblast, chorionic and amniotic membranes and decidua (Ahmed A et al., 1995), secreted by villous fibroblasts (Anthony FW et al., 1994), and the villous trophoblasts (Lash GE et al., 2002). The fall in uteroplacental resistance in normal pregnancy is mediated by interstitial extravillous trophoblast secretion of angiogenic and vasodilator signals such as VEGF to promote local blood flow to the uterus (discussed in Section 1.13.5). In FGR and PET, there is decreased depth and density of trophoblast invasion (Naicker T et al., 2003;Reister F et al., 2001), and myometrial small arteries show increased vasoconstriction and decreased endothelium-dependent vasodilatation (Ong SS et al., 2005;Wareing M et al., 2005).

In PET, placental derived soluble (s) Flt-1, an antagonist (decoy receptor) for VEGF is upregulated, and is thus proposed to cause lowered circulating concentrations of free VEGF and endothelial dysfunction (Sibai B et al., 2005;Ahmad S and Ahmed A, 2004). Analysis of supernatants from pre-eclamptic placental villous explant cultures revealed a four-fold rise in sFlt-1 compared to normal pregnancies. Conditioned medium from normal villous explants induced endothelial cell migration and *in vitro* tube formation, both of which were attenuated by pre-incubation with sFlt-1. Endothelial cells treated with pre-eclamptic conditioned medium showed substantially reduced angiogenesis compared with normal conditioned ($P < 0.001$) medium, which was not further decreased by the addition of exogenous sFlt-1, indicating a saturation of the soluble receptor (Ahmad S and Ahmed A, 2004).

Similarly, maternal serum concentrations of VEGF have been found to be significantly diminished in pregnancies complicated by FGR (Bersinger NA and Odegard RA, 2005). Another study found that women with established FGR have significantly elevated levels of sFlt-1, but importantly, the increase in sFlt-1 does not precede the clinical onset of FGR, as it does in PET. The same study showed that VEGF levels in cases of established FGR were significantly lower than in normal pregnant women (Savvidou MD et al., 2006).

For several years, there have been suggestions that placental angiogenic and vasoactive factors might serve as therapeutic targets in compromised pregnancies in humans (Reynolds LP et al., 2006;Ahmad S and Ahmed A, 2004). I have carried out experiments in this thesis to test this hypothesis in pregnant sheep.

1.12 Vascular Endothelial Growth Factor (VEGF)

VEGF is a vascular endothelial cell-specific mitogen, initially called vascular permeability factor because of its ability to render microvessels hyperpermeable to plasma proteins at sites where it was over-expressed along with its receptors (Leung DW et al., 1989;Dvorak HF et al., 1991). Its role as a potent endothelial mitogen was confirmed only a few years later. Since these initial findings it has been shown that VEGF-$A_{165,}$ the substance characterized in these early studies, is a member of a wider family encompassing a number of related genes, which have multiple effects on endothelial and other cells, and play a pivotal role in vascular development. The pro-angiogenic role of VEGF has attracted clinical interest for its possible uses in gene therapy to improve the blood supply to ischaemic tissues (therapeutic angiogenesis) and as a target for anti-angiogenic drugs that prevent tumour vascularization. In addition to its role in blood vessel development during embryogenesis and post-natal growth, VEGF also has roles in adult angiogenesis during wound healing, the menstrual cycle and exercise-induced muscle enlargement, and in vascular maintenance (Maharaj AS and D'Amore PA, 2007;Ferrara N, 1999).

The VEGF family of growth factors comprises a group of homodimeric glycoproteins and belongs to a super-family of growth factors also comprising the Platelet derived growth factors (PDGFs). Both growth factors consist of antiparallel homodimers covalenly linked by two interchain disulphide bonds and possessing a characteristic cysteine knot structure that confers important binding properties (Keyt BA et al., 1996).

The VEGF family includes VEGF-A, -B, -C, -D, the related placental growth factor (PlGF), the *orf* virus-encoded factor VEGF-E, and VEGF-F found in snake venom. The human VEGF-A gene is organized in eight exons, separated by seven introns (Tischer E et al., 1991), and is localized in chromosome 6p21.3 (Vincenti V et al., 1996). Alternative exon splicing of a single VEGF-A gene results in the generation of at least five different molecular species, having respectively 121, 145, 165, 189, and 206 amino acids, following signal sequence cleavage ($VEGF_{121,}$ $VEGF_{145}$, $VEGF_{165}$, $VEGF_{189}$ and $VEGF_{206}$) (Figure 1.8). The different VEGF-A isoforms have different biochemical and physical properties due to the presence or absence of the C-terminal domains, encoded by exons 6 and 7. $VEGF_{165}$ is deficient in the residues encoded by exon 6, while $VEGF_{121}$ lacks the residues encoded by exons 6 and 7. $VEGF_{165}$ is the predominant and most potent molecular species produced by a variety of normal and transformed cells. Native $VEGF_{165}$ is a basic, heparin-binding, homodimeric glycoprotein of 45 kDa (Ferrara N and Henzel WJ, 1989). Transcripts encoding $VEGF_{121}$ and $VEGF_{189}$ have been detected in a majority of cells and tissues which express the VEGF-A gene, whilst $VEGF_{206}$ is a rare form (Houck KA et al., 1991). $VEGF_{121}$ is a freely diffusible protein. $VEGF_{165}$ is also secreted, although a significant fraction remains bound to the cell surfaces and extracellular matrix (ECM) on account of its affinity to heparan sulphate, while $VEGF_{189}$ and $VEGF_{206}$ are almost completely sequestered in the ECM (Park JE et al., 1993). The heparin binding activity of VEGF-A is due to the presence or absence of exons 6 and/or 7 that encode for heparin binding domains (Robinson CJ and Stringer SE, 2001).

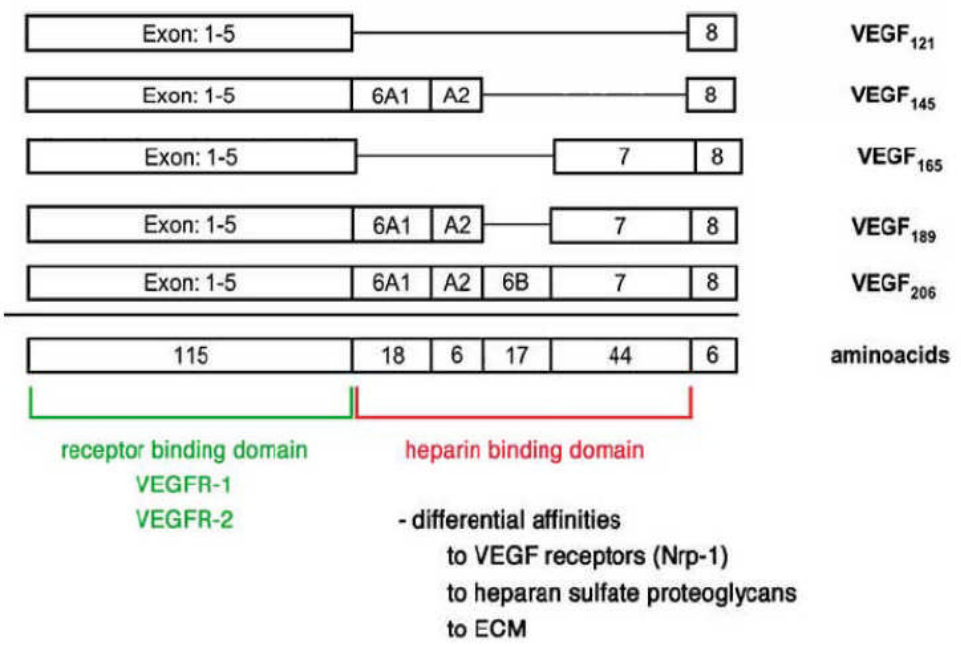

Figure 1.8 – VEGF-A isoforms result from alternative splicing

VEGF-A isoforms are generated by alternative splicing from a single gene, and are 121, 145, 165, 189 and 206 amino acids long. The larger isoforms contain a heparin binding domain which mediates binding to the extracellular matrix (ECM), Neuropilin-1 and HSPG. Domains 1 to 5 are conserved between all VEGF-A isoforms and constitute the VEGFR-1 and VEGFR-2 binding domains. Figure adapted and modified from (Eming SA and Krieg T, 2006).

The physiological importance of VEGF-A is discussed in Section 1.13.

VEGF-B is expressed in a wide range of tissues and particularly in the heart and skeletal muscle. VEGF-B knockout mice are healthy and fertile (Bellomo D et al., 2000;Aase K et al., 2001). Both of these studies performed in knockout mice noted that VEGF-B appears to have a role in cardiac development, but the reported phenotypes differed. Bellomo et al (2000) reported that one-month old VEGF-B-null mice have smaller hearts than wild-type mice, while Aase et al (2001) reported that the electrocardiogram PQ interval was slightly extended, which they attributed to an atrial conduction defect.

VEGFs-C and D are believed to play an important role in the development of the lymphatic system. VEGF-$C^{-/-}$ mice die during late embryogenesis due to a

defect in lymph vessel formation (Karkkainen MJ et al., 2001). In contrast, VEGF-D$^{-/-}$ mutant mice are viable and do not display any abnormal phenotype (Baldwin ME et al., 2005), suggesting that any key developmental roles of VEGF-D are compensated by another molecule, possibly VEGF-C. However, VEGF-D may play an important role in lymphangiogenesis, as ectopic expression of VEGF-D in the skin of transgenic mice under the control of the keratin 14 gene promoter induced the growth of lymphatic vessels in the dermis, whereas blood vessels were unaffected (Veikkola T et al., 2001). It may also be possible that VEGF-D may be less important in mice than humans, given that mouse VEGF-D lacks VEGFR2 binding capacity.

VEGF-E is encoded in the Orf virus, a parapox virus infecting sheep, goats and sometimes humans and inducing a transient angiogenesis in the skin (Lyttle DJ et al., 1994).

1.13 Physiological significance of VEGF

Hereafter VEGF denotes VEGF-A. VEGF is a potent biological molecule, which plays an important role in several physiological and disease-related functions. These include angiogenesis, vasodilatation, vascular permeability, vascular protection and endothelial cell survival, which in turn have been implicated in developmental and pathological roles.

1.13.1 Angiogenesis

VEGF is known to play a critical role in embryonic vasculogenesis and angiogenesis. Loss of a single VEGF allele in mice is known to result in embryonic lethality between day 11 and 12. The VEGF$^{+/-}$ heterozygous embryos are growth retarded and exhibit a number of developmental abnormalities such as under-development of the fore-brain region, malformation of the outflow region of the heart, rudimentary dorsal aortae and reduced thickness of the ventricular wall. The yolk sac revealed a markedly reduced number of nucleated red blood cells within the blood islands. There were significant defects in the vasculature of a number of tissues and organs, including the placenta and nervous system

(Ferrara N et al., 1996;Carmeliet P et al., 1996). All these defects are believed to result directly or indirectly from the reduced levels of VEGF.

The effects of VEGF on post-natal development have also been assessed. Partial inhibition of VEGF achieved by inducible *Cre-loxP*-mediated gene ablation resulted in increased mortality, stunted body growth, and impaired organ development, primarily of the liver (Gerber HP et al., 1999). Administration of a soluble VEGF receptor chimeric protein, mFlt(1-3)-IgG, which achieves a greater level of VEGF inhibition (than the conditional *Cre-loxP*-mediated gene ablation strategy), resulted in a nearly complete arrest of somatic growth and lethality within 4-6 days, when administered soon after birth. The primary cause of death in these mice appeared to be liver and renal failure. On isolation, endothelial cells from the liver exhibited increased apoptotic index, thereby suggesting that VEGF is required not only for proliferation but also survival of endothelial cells. However, the dependence on VEGF was gradually lost after the fourth postnatal week, after which time VEGF inhibition did not result in any serious defects (Gerber HP et al., 1999).

In a fully grown animal, VEGF is primarily required for processes dependent on active angiogenesis, such as corpus luteum formation and wound healing. The development and endocrine functions of the ovarian corpus luteum are dependent on the growth of new capillary vessels (Bassett DL, 1943). VEGF mRNA is temporally and spatially upregulated during the proliferation of blood vessels in the rat, mouse and primate ovary and the rat uterus, suggesting that VEGF mediates the cyclical growth of blood vessels in the female reproductive tract (Ravindranath N et al., 1992;Cullinan-Bove K and Koos RD, 1993).

The angiogenic role of VEGF is also important for wound healing, as re-vascularisation of injured/damaged tissue is essential for repair. It is believed that VEGF also increases the permeability of capillaries surrounding wounds. This leads to fibrin deposition in the damaged tissue, which in turn acts as a substrate for tissue regrowth, including angiogenesis. The regulation of VEGF expression and angiogenesis is disturbed in abnormally healing wounds (Bates DO and Jones RO, 2003).

However, not all angiogenesis mediated by VEGF is beneficial. Many tumour cell lines secrete VEGF *in vitro*, suggesting that this molecule is an important mediator of tumour vascularisation. Without attracting blood vessel growth, many tumours are unable to grow to dangerous sizes due to the limitations of obtaining nutrients via diffusion. In situ hybridisation studies have demonstrated that VEGF mRNA is up-regulated in many human tumours, including lung, breast, ovary, kidney and cancers of the gastrointestinal tract (Ferrara N, 1999). The discovery of the involvement of VEGF in tumour vascularisation and progression launched a huge effort to develop anti-VEGF therapies for the treatment of cancer, including anti-VEGF antibodies and VEGF receptor tyrosine kinase inhibitors. Bevacizumab (Avastin), a humanised anti-VEGF-A monoclonal antibody, received FDA approval in 2004 for the treatment of colorectal cancer. A phase III trial showed that Bevacizumab slowed tumour growth and improved survival when used in combination with other chemotherapeutic agents (Hurwitz H et al., 2004), and other trials have shown varying degrees of efficacy of Bevacizumab with different cancers (Jain RK et al., 2006).

VEGF-mediated angiogenesis is also involved in eye disease. Inappropriate blood vessel growth in the eye often interferes with vision, leading to visual impairment. A common cause of blindness in older people is wet age-related macular degeneration whereby blood vessels grow into the eye with advancing age, particularly in the retinal region around the optic nerve (the macula). VEGF is synthesized by retinal epithelial cells (Adamis AP et al., 1993), and is over-expressed in retinopathies in, for example, diabetes (Aiello LP et al., 1994). Anti-VEGF therapies Pegaptanib (Macugen) and Ranibizumab (Lucentis) are FDA-approved for the treatment of age-related macular degeneration, working in part by preventing VEGF-stimulated blood vessel growth in the retina (Ciulla TA and Rosenfeld PJ, 2009). In clinical trials, both Pegaptanib and Ranibizumab have been shown to slow the onset of macular degeneration and in some patients improve visual performance (Gragoudas ES et al., 2004;Rosenfeld PJ et al., 2006;Brown DM et al., 2006;Ciulla TA and Rosenfeld PJ, 2009).

VEGF-reducing therapies may suffer from a number of unwanted side-effects however, due to loss of VEGF-dependent vascular protection, including bleeding, oedema, clotting and hypertension (Kamba T and McDonald DM, 2007).

In some other pathologies, a pro-angiogenic strategy may be beneficial. Atherosclerosis leads to build-up of plaques in artery walls, narrowing the lumen and increasing the likelihood of plaque rupture and thrombosis. Atherosclerosis of the coronary or cerebral arteries may lead to life-threatening events such as myocardial infarction or stroke. Stimulation of collateral vessel growth to bypass a narrowing vessel has been of major interest in treating conditions such as angina and peripheral vascular disease, and preventing future heart attacks. VEGF may have a role in collateral growth under normal and ischaemic conditions (Rissanen TT et al., 2005;Clayton JA et al., 2008) and adenovirus-mediated over-expression of VEGF has beneficial effects in animal models of peripheral and cardiac ischaemia (Zachary I et al., 2000), though so far convincing therapeutic effects have not been demonstrated in clinical trials (Zachary I and Morgan RD, 2011).

1.13.2 Vasodilatation

VEGF increases endothelial production of the vasoactive molecules NO and PGI_2 (Laitinen M et al., 1997;Wheeler-Jones C et al., 1997). The importance of both these molecules in vasodilatation is discussed in greater detail below (Section 1.16). VEGF induces sustained eNOS activation in endothelial cells (ECs) via Phosphoinositide 3-kinase (PI3K) dependent Akt-catalysed phosphorylation of eNOS at Ser^{1177}, the same site phosphorylated in response to shear stress (Dimmeler S et al., 1999). Phosphorylation of this site renders eNOS active at resting Ca^{2+} concentrations. PI3Ks are a family of enzymes which play an important role in cellular physiology, particularly cell growth, proliferation, differentiation, motility, survival and intracellular trafficking. They mediate these functions in response to the binding of different growth factors to cell surface receptors (Vanhaesebroeck B et al., 2010).

VEGF also promotes long-term NO production by inducing expression of both eNOS and the highly active isoform iNOS (Kroll J and Waltenberger J, 1998). Short-term (less than 10 minutes after VEGF administration) NO production is independent of PI3K, and may involve VEGF-stimulated Ca^{2+} mobilisation (Gelinas DS et al., 2002). VEGF-stimulated PGI_2 production in ECs involves PKC- and ERK-mediated activation of cytosolic phospholipase 2, and also requires intracellular Ca^{2+} (Gliki G et al., 2001;Wheeler-Jones C et al., 1997).

1.13.3 Vascular and Neuro-protection

It has been proposed that low levels of VEGF protect the adult vasculature partly via NO and prostacyclin production (Zachary I et al., 2000). Common side effects for anti-VEGF therapies (such as Bevacizumab) include bleeding, oedema, unwanted clotting and hypertension (Kamba T and McDonald DM, 2007). Mice with an endothelial-specific VEGF knockout survive to birth but show progressive endothelial degeneration, with 50% of them dying before 25 weeks of post-natal life (Lee S et al., 2007). Interestingly, exogenous VEGF administration is unable to compensate for loss of endothelial-produced VEGF in endothelial survival, suggesting that an intracellular VEGF signalling loop may be important.

A role for VEGF in neuroprotection (and other aspects of the nervous system including axonal outgrowth) has been noted (Sondell M et al., 2000). While this may partially occur via regulation of neural vascularisation or maintenance of the neural vasculature, VEGF acts as a direct pro-survival factor for cultured neurons (Oosthuyse B et al., 2001). In addition, loss of VEGF isoforms showed a defect similar to that observed in patients with amyotrophic lateral sclerosis (ALS), an adult-onset motor neuron disease. Virus-mediated over-expression of VEGF in muscles of mice with experimental ALS reduced disease symptoms and improved survival (Azzouz M et al., 2004), suggesting that VEGF-dependent neuroprotection is biologically relevant.

1.13.4 Endothelial cell migration

VEGF also plays important roles in modulating endothelial cell migration and vascular permeability. Such effects are important for processes like wound healing. VEGF mediates endothelial cell migration by activating proteins involved in chemotaxis. As the ECM plays an essential role in stabilising blood vessels through interactions with endothelial cells and vascular smooth muscle cells (VSMCs) sheathed in a basement membrane, breakdown of the latter is a pre-requisite for endothelial cell migration and formation of new vessels during development and disease (Zachary I, 2005). This is triggered by the induction of matrix-degrading metalloproteinases (MMPs). MMP-2 and MMP-9 appear to play an important role in promoting angiogenesis and are upregulated along with VEGF and VEGFR2 in angiogenic lesions in a model of tumour angiogenesis (Bergers G et al., 2000).

1.13.5 Physiological re-modelling of spiral arteries in pregnancy

In humans, the fall in utero-placental vascular resistance that occurs in pregnancy, is mediated by local factors including VEGF. For example, leucocyte/trophoblast cell interactions result in substantial increases in both VEGF and PlGF (Zhou Y et al., 2003b). The human cytotrophoblast cells secrete angiogenic and vasodilator signals (Zhou Y et al., 2003a) that affect local blood flow to the uterus and mediate the normal maternal response to pregnancy, which includes vasodilatation in the utero-placental vascular circuit and increased maternal cardiac output and blood volume. As already described, in PET, placental-derived sFlt, an antagonist of VEGF and PlGF, is upregulated resulting in lowered circulating concentrations of free VEGF and PlGF and endothelial dysfunction (Sibai B et al., 2005). Trophoblast expression of various vasodilatory and anticoagulative factors such as VEGF is related to the depth of invasion by trophoblast giant cells (Hemberger M et al., 2003). Invading cytotrophoblasts secrete VEGF to regulate their acquisition of an endothelial-like phenotype which allows them to replace the maternal cells that line the uterine vessels (Zhou Y et

al., 2002). These cells are also dependent on VEGF for their maintenance and growth (Zhou Y et al., 2003a).

1.14 Regulation of VEGF gene expression

Upregulation of VEGF-A by hypoxia is mediated via the binding of hypoxia inducible facor-1 (HIF-1) to the hypoxia response element (HRE) in the VEGF promoter. HIF-1 is composed of a 120 kDa HIF-1α subunit complexed with a HIF-1β subunit. Under physiological conditions (in normoxia), HIF-1α undergoes rapid degradation. Two key prolines within its oxygen degradation domain (ODD) are hydroxylated by one of a three member family of prolyl-hydroxylase domain-containing proteins (PHDs 1-3), the activity of these enzymes being oxygen dependent (Semenza GL, 2001). Their actions allow HIF-1α interaction with ubiquitin ligase thus promoting the formation of a larger complex which is rapidly destroyed by proteasome activity. Under hypoxic conditions, the hydroxylation of HIF-1α is reduced, preventing degradation and allowing HIF-1α to accumulate and to combine with HIF-1β at nuclear HREs of target genes such as VEGF, thereby allowing gene transcription. Not only is hypoxia able to increase the production of VEGF, it also allows stabilization of its mRNA (Ikeda E et al., 1995). These two mechanisms provide a system by which ischemic tissues can increase VEGF production and secretion, so attracting the growth of new blood vessels (Shweiki D et al., 1992).

In a study investigating the role of HIF-1α in tumour growth, Ryan et al showed that HIF-1α inactivation led to a dramatic reduction of tumorigenesis and increased apoptosis, concomitant with reduced hypoxia-induced expression of VEGF (Ryan HE et al., 1998).

1.15 VEGF Receptors

VEGFs bind to three major receptor tyrosine kinases (RTK): VEGFR-1/Flt-1 (fms-like tyrosine kinase-1), VEGFR2/KDR/Flk-1 (fetal liver kinase-1)

and VEGFR-3/Flt-4. In addition, heparan sulphate proteoglycans (HSPGs) and Neuropilins (NRPs) are also able to bind VEGF isoforms in an isoform-specific manner.

VEGFR-1 and VEGFR-2 comprise an extracellular domain of seven immunoglobulin-like (Ig-like) domains containing ligand binding activity, a single hydrophobic transmembrane domain and a cytoplasmic region, containing a bipartite tyrosine kinase domain divided into two parts by an inert sequence. VEGFR-3 is slightly different from the structures of VEGFR-1 and VEGFR-2 because the fifth Ig-like domain (in VEGFR-3) is cleaved into disulfide-linked subunits (Iljin K et al., 2001). Analysis of mutant and chimeric forms of VEGFR1 and VEGFR2 have shown that ligand binding occurs primarily to the second and third Ig-like domains (Barleon B et al., 1997b;Davis-Smyth T et al., 1996). Figure 1.9 (Page 98) summarises the interactions between the different VEGF isoforms and their receptors. Briefly, VEGF-A_{165} binds to VEGFR1 and VEGFR2 (Neufeld G et al., 1999). VEGF-C and –D also recognize VEGFR2 but with lower affinity and bind to a third receptor, VEGFR3. PlGF and VEGF-B bind with high affinity only to VEGFR1, and VEGF-E only binds to VEGFR-2. VEGFR-1 has a 10-fold higher affinity for VEGF-A_{165} than VEGFR-2 (Petrova TV et al., 1999). Nevertheless, VEGFR-1 undergoes little detectable phosphorylation and weak signaling when bound to VEGF-A_{165}, whereas, VEGF-A_{165} binding to VEGFR-2 results in autophosphorylation on several major sites and is followed by the activation of multiple downstream signaling pathways (Waltenberger J et al., 1994). All three VEGF receptors possess a similar overall structure, the tyrosine kinase domains being 80% identical at the amino acid level in the three receptors.

1.15.1 VEGFR-1

VEGFR-1 is a 180kDa protein which binds VEGF and can be alternatively spliced to generate a soluble, secreted form, sFlt-1. VEGFR-1 null mice die *in utero*, apparently from a vascular defect, with lethality occurring around E8.5 (Fong GH et al., 1995). Endothelial cells are present, but these are not correctly assembled into functional vascular channels. This indicates that while VEGFR-1

is not required for endothelial cell differentiation, it may be necessary for vascular organization. Blood cells were also formed. This is in contrast to the defect in VEGFR-2 mice, where endothelial and blood cells were lacking (Shalaby F et al., 1995). The lack of vessel formation in VEGFR-1 null mice has been associated with an abnormally high number of endothelial precursor cells, due to increased commitment of mesenchymal stem cells to the hemangioblast lineage (Fong GH et al., 1999). Using chimeric mice generated from mixtures of VEGFR-1 null and wild-type embryonic stem cells in various proportions, the same study showed that when diluted, the VEGFR-1 null EC progenitors formed apparently normal vascular channels. This indicates that the vascular disorganization observed in VEGFR-1 null mice is because of a dramatic increase in the number of endothelial progenitors. It also suggests that endothelial expression of VEGFR1 may not be a pre-requiste for an EC to participate normally in vessel formation.

VEGFR-1 tyrosine kinase activity is not essential for normal vascular development. Hiratsuka *et al* deleted exons encoding the C-terminus of VEGFR-1 in mice, so preserving the extracellular and transmembrane regions but removing the intracellular tyrosine kinase domain. Mice homozygous for the deletion were viable and fertile, and blood vessel development was unaffected (Hiratsuka S et al., 1998).

Overall, this suggests that VEGFR-1 may act as a negative regulator (decoy receptor) of VEGF function during embryonic development which sequesters this ligand, rendering it less available to VEGFR-2 and preventing excessive VEGF signaling through the latter. Soluble VEGFR-1, lacking either the tyrosine kinase domain or the transmembrane domain, can still sequester VEGF away from VEGFR-2, allowing normal vascular development.

The pathological role of sFlt-1 in the etiology of PET has already been discussed above.

Even though VEGF signaling through VEGFR-1 is not essential in ECs; it is very important in some non-endothelial cells. Both monocytes and

macrophages require the tyrosine kinase signaling activity of this receptor for chemotaxis in response to VEGF and PlGF (Barleon B et al., 1996;Clauss M et al., 1996).

1.15.2 VEGFR-2

VEGFR-2, also known as kinase domain receptor (KDR) in humans or fetal liver kinase-1 (Flk-1) in mice, binds VEGF-A_{165} resulting in phosphorylation of its tyrosine residues (Millauer B et al., 1993;Quinn TP et al., 1993). VEGFR-2 binds to VEGF-A, fully processed VEGFs C and D, and VEGF-E.

VEGFR-2 is expressed in endothelial cells and their progenitors (Millauer B et al., 1993;Quinn TP et al., 1993;Yamaguchi TP et al., 1993), and was thought to be specific for endothelial cells, but has more recently been identified on other cell types including neurons and their progenitors (Yang X and Cepko CL, 1996;Nishijima K et al., 2007).

VEGFR-2 null mice die *in utero* at E8.5-9.5 due to a massive defect in vasculogenesis, whereas heterozygous mice were fertile and apparently normal (Shalaby F et al., 1995). In knockout animals, no blood vessels were observed in either the embryo or yolk sac, and yolk sac blood islands were not formed. VEGFR-2 null mice contained cells expressing early endothelial markers including VEGFR3 and tie2, but not the later endothelial marker tie1, and no recognizable endothelial cells were present, indicating an essential early role of VEGFR2 in endothelial differentiation. Interestingly, VEGF-A knockout mice do form some endothelial cells, showing that some roles of VEGF-A in endothelial development can be compensated to some extent by another VEGFR-2 ligand, such as VEGF-C. VEGFR-2 null mice also developed few committed haematopoietic progenitor cells, indicating a role for VEGFR2 in blood development. VEGFR2 has been reported as a marker which defines the haemangioblast (Yamaguchi TP et al., 1993), the blood island precursor which forms endothelial and blood cells in the yolk sac, explaining the association between absence of blood and endothelial cells in VEGFR-2 deficient mice.

Porcine aortic endothelial cells which lack endogenous VEGF receptors, display chemotaxis and mitogenesis in response to VEGF when transfected with a plasmid coding for KDR. On the contrary, transfected cells expressing Flt-1 lack such responses (Waltenberger J et al., 1994). While VEGFR-2/Flk-1/KDR is known to undergo strong ligand-dependent tyrosine phosphorylation in intact cells, Flt-1 undergoes only a weak or undetectable response (Seetharam L et al., 1995;Waltenberger J et al., 1994). Furthermore, VEGF mutants which bind selectively to VEGFR-2, are fully active EC mitogens (Keyt BA et al., 1996) and VEGFR-2 activation is required for antiapoptotic effects of VEGF for human umbilical vein endothelial cells (HUVECs) in serum-deprived conditions (Gerber HP et al., 1998). Thus, it is suggested that the major signaling receptor for VEGF, mediating most of its biological activities in ECs (such as migration, proliferation, survival and changes in permeability) is VEGFR-2.

1.15.3 VEGFR-3

VEGFR-3 is expressed only in venous endothelial cells in the embryo, and is confined to the lymphatic system in the adult (Iljin K et al., 2001). It has roles in cardiovascular development in the embryo, particularly lymphangiogenesis, and binds to VEGF-C and VEGF-D. In VEGFR-3 deficient mice, large vessels become abnormally organized with defective lumens, leading to fluid accumulation in the pericardial cavity and cardiovascular failure at embryonic day 9.5 (Dumont DJ et al., 1998).

1.15.4 Neuropilins

Neuropilins (NRPs), [reviewed by (Pellet-Many C et al., 2008)] are transmembrane glycoproteins that bind some VEGFs, and class 3 semaphorins (mainly sema3A), the latter being secreted proteins involved in directing the growth cones of growing axons. Two neuropilin genes are known, NRP1 and NRP2, which like VEGFR1 can produce either a transmembrane receptor or, by alternative splicing, can result in soluble forms (sNRP1 and 2) composed of part of the extracellular region only. NRP1 binds to some isoforms of VEGF-A (including VEGF-A_{165}) (Soker S et al., 1998), VEGFs B-E and PlGF2 (and mouse

PlGF), whereas NRP2 binds to some VEGF-A isoforms (including VEGF-A_{165}), and VEGFs C and D (Gluzman-Poltorak Z et al., 2000;Karpanen T et al., 2006). Both NRP1 and NRP2 are expressed in vascular endothelial cells, but in the adult vasculature NRP1 is mainly expressed by arterial ECs, whereas NRP2 is expressed by venous and lymphatic ECs (Yuan L et al., 2002).

NRPs have no known signaling role acting alone, but are believed to act as co-receptors for VEGF and semaphorins. When co-expressed in cells with KDR, NRP1 enhanced the binding of VEGF-A_{165} to KDR and VEGF-A_{165}-mediated chemotaxis. Conversely, inhibition of VEGF-A_{165} binding to NRP-1, inhibits its binding to KDR and its mitogenic activity for endothelial cells (Soker S et al., 1998). These findings suggest that neuropilin-1 binding of VEGF and its complexation with KDR enhances KDR signaling, causing increased migratory and proliferative effects of VEGF-A_{165}. The potentiation of VEGF-stimulated cell signaling by NRP-1 could occur via a number of mechanisms, such as stabilization of the VEGF/VEGFR-2 signaling complex at the cell surface so increasing the duration of VEGFR-2 signaling, or by transducing signals directly (e.g. via the NRP-1 associated molecule synectin) which feed in to VEGFR-2 signaling.

NRP-1 null mice die *in utero* around E12.5-13.5. Multiple cardiovascular defects are seen with sparse capillaries in the yolk sac and some major vessels in the brachial region incorrectly branched, incomplete or not formed at all (Kawasaki T et al., 1999). Neurogenic defects are also observed, with nerves following incorrect paths, probably due to a blockade of semaphorin 3-mediated signaling (Kitsukawa T et al., 1997). The vascular and neural functions of NRP-1 were further delineated by producing mice deficient in NRP-1 specifically in the endothelium, or mice expressing mutant NRP-1 specifically unable to bind Sema3A but able to bind VEGF-A_{165} (Gu C et al., 2003). Endothelial-specific NRP-1 null mice died *in utero*, displaying abnormalities in major arteries and reduced vessel branching at E12.5. In contrast, mice expressing a mutant NRP-1 which binds VEGF-A_{165} but not Sema3A, are born alive, but exhibit nervous

system defects and die soon after birth. Together these data indicate that endothelial expression of NRP-1 but not Sema3A binding to NRP-1, is required for normal vascular development, while Sema3A binding to NRP-1 plays a restricted role in neurogenesis. However, the precise contribution of VEGF binding to NRP-1 in vascular development is not yet known.

NRP-2 null mice are viable, with no apparent cardiovascular defects but a reduced number of small lymphatic vessels (Chen H et al., 2000;Yuan L et al., 2002). The major defect appears to be neural, with abnormal guidance of cranial and spinal nerves. NRP-1/NRP-2 double knockout mice die *in utero* at E8, earlier than for single NRP-1 null mice (Takashima S et al., 2002), suggesting that NRP-2 may compensate to a certain extent for NRP-1 during early cardiovascular development. NRP-1/NRP-2 double-null mice display a severe cardiovascular abnormality with large avascular areas in the yolk sac and embryo, and reduced connections between blood vessel sprouts. This severe phenotype, similar to that observed for VEGF-A null and VEGFR-2 null mice, may reflect insufficient VEGF-A/VEGFR-2 signalling as NRP-mediated potentiation of the VEGF-A signal is lost.

1.15.5 Heparan sulphate proteoglycans

Several VEGF isoforms, including VEGF-A_{165}, contain a heparin binding domain, and so are able to bind to HSPGs. HSPGs are transmembrane proteins abundant on the surface of endothelial cells, where the covalently-linked heparan sulphate moiety, similar to the mast cell-produced polysaccharide mixture, heparin, binds to the plasma protein antithrombin III. This binding accelerates the action of antithrombin III to inactivate thrombin, so limiting the extent of thrombus formation during the clotting cascade. HSPGs are highly negatively charged, and bind to strongly positive regions on a variety of secreted growth factors including VEGFs (Bernfield M et al., 1992).

The heparin binding domain of VEGF-A is not present in some isoforms such as VEGF-A_{121} and differences in heparin binding, as well as NRP1 binding,

have been suggested to account for some of the differences in, for example, biological activity between VEGF-A splice variants. Even though heparin binding itself does not appear essential for VEGF biological activity, at least in cell based studies, a complete loss of heparin-binding ability may have more dramatic effects. Heparin has been reported to affect the interaction of VEGF-A_{165} with VEGFR-2 (Tessler S et al., 1994), and to increase VEGF-A_{165}-stimulated tubulogenesis (Ashikari-Hada S et al., 2005).

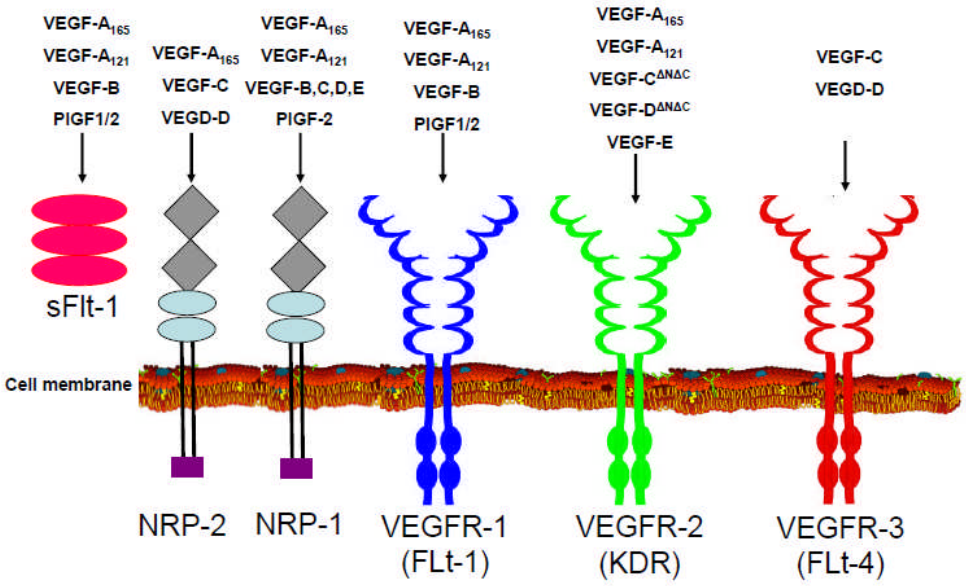

Figure 1.9 – Family of VEGF ligands and their receptors.

1.16 Pathways of endothelium-dependent vascular relaxation

There are three characterized pathways of endothelium-dependent relaxation – production of Nitric oxide, Prostacyclins and Endothelial derived hyperpolarizing factor. These are discussed below.

1.16.1 Nitric oxide

Nitric oxide (NO) is a gas produced by the NO synthase (NOS) family of proteins. There are three cognate forms of NOS, neuronal NOS (nNOS), inducible NOS (iNOS) and endothelial NOS (eNOS). eNOS and nNOS are expressed constitutively, dependent on Ca^{2+} and calmodulin, and generate relatively small amounts of NO for maintenance of vascular tone and neurotransmission, respectively. On the other hand, iNOS is an inflammation-inducible, high activity, Ca^{2+} independent enzyme that liberates large amounts of NO (Sessa WC, 2009;Valdes G et al., 2009)

NO serves as a second messenger in diverse physiological responses in the cardio-vascular system, particularly vasodilatation, anti-coagulation, vascular remodeling and angiogenesis. NO is known to be the most potent vasodilator in large blood vessels. In the aorta and carotid arteries of eNOS knockout mice, endothelium-dependent vasodilatation is completely eliminated (Sessa WC, 2009;Huang PL et al., 1995;Faraci FM et al., 1998). Furthermore, it has been shown that these mice exhibit a hypertensive phenotype (Huang PL et al., 1995) whereas transgenic mice which chronically over-express eNOS are characterized by hypotension (Ohashi Y et al., 1998).

An effector cell, such as an endothelial cell gets stimulated by a chemical mediator like VEGF, acetylcholine, bradykinin or physical force like shear stress (frictional force generated by blood flow against endothelium). These stimuli activate eNOS to promote the conversion of L-arginine to nitric oxide by increasing the intracellular calcium (Vane JR, 1994). The nitric oxide then acts upon the guanylate cyclase of the same cell or diffuses to another cell such as a

smooth muscle cell to increase the cyclic (c) GMP (by the guanylate cyclase reaction) and bring about vascular relaxation (Griffith TM et al., 1985) (Figure 1.10). As NO is soluble in water, there are no barriers to its diffusion. Hence, one can visualize arterial endothelial cells releasing small amounts of NO each time they are stretched by the pulsations of the heart (Vane JR, 1994), resulting in a small degree of vascular relaxation.

When L-arginine is metabolized by NOS to form NO, L-citrulline is formed (Palmer RM and Moncada S, 1989). This reaction is inhibited by N^G-mono-methyl-L-arginine (L-NMMA), a commonly used inhibitor of NOS activity in pharmacology studies. L-citrulline is very quickly recycled through arginine succinate back to L-arginine, so that the endothelial cells have a mechanism for maintaining intracellular L-arginine concentrations (Hecker M et al., 1990). This is important for the maintenance of vascular tone.

It has been demonstrated that VEGF not only upregulates but also mediates some of its biological effects by upregulation of reactive oxygen species, particularly hydrogen peroxide. This generation of reactive oxygen species by VEGF is dependent upon the activity of PI-3 kinases (Colavitti R et al., 2002). These reactive oxygen species have relevance for vascular biology as they decrease the bioavailability of NO. Both superoxide and hydrogen peroxide are highly reactive with NO and form peroxynitrites as the major product. Even though peroxynitrites can cause vasodilatation, the concentrations required to do so are far in excess of the effective vasorelaxant concentrations of NO. There is now an increasing amount of evidence suggesting that a large number of cardiovascular diseases stem from the increased generation of reactive oxygen species, which impair the physiological functions of eNOS. These include hypercholesterolemia, hypertension, CHD and diabetes (Kojda G and Harrison D, 1999).

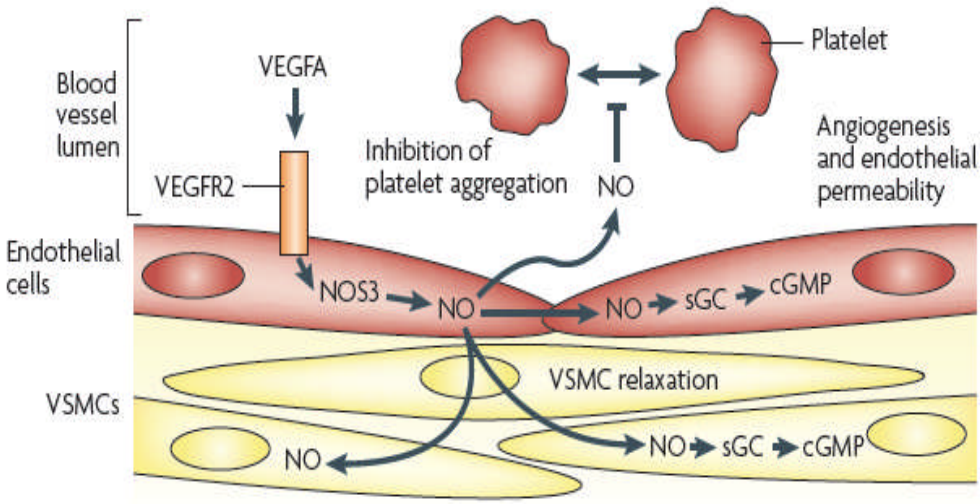

Figure 1.10 – Role of nitric oxide (NO) signaling in angiogenesis, vascular tone and haemostasis

VEGF binding to its receptor VEGFR2 on endothelial cells activates endothelial nitric oxide synthase (NOS3, eNOS) to produce the diffusible signaling molecule NO. NO plays an important role in a number of physiological processes. It diffuses into vessel walls, and brings about an increase in cyclic GMP (via the guanylate cyclase pathway) in vascular smooth muscle cells (VSMCs), resulting in vascular relaxation and increase in blood flow. NO also stimulates endothelial cell growth and motility, which leads to angiogenesis. VEGF signaling through NO contributes to increased vascular permeability. In addition, NO also prevents thrombosis by inhibiting platelet adhesion and aggregation. Figure adapted from (Isenberg JS et al., 2009).

1.16.2 Prostacyclins (PGI_2)

Prostacyclin is one member of the prostaglandin family of lipid mediators derived from arachidonic acid, of which there are now close to 90 members. Arachidonic acid is an unsaturated constituent of the phospholipid bilayer in cell membranes. It is metabolized by constitutive cyclooxygenases (COX-1) and inducible COX-2 into prostaglandins and related compounds (Dubois RN et al., 1998). COX-2 is the key enzyme involved in synthesis of PGI_2, particularly in response to treatment with growth factors (Kawabe J et al., 2010).

PGI_2 is a major vasodilator within the prostaglandin cascade and synthesized predominantly by the endothelium (Gryglewski RJ, 2008). Its main effects are mediated either directly (through activation of soluble adenylate cyclase, which increases cyclic AMP levels), or by opposing the vasoconstrictor

and pro-aggregating effects of platelet-derived thromboxane-A_2 (TXA_2), which is also an intermediate produced during arachidonic acid metabolism (by COX-1 enzyme). The ability of the large vessel wall to synthesize PGI_2 is greatest at the intimal surface and progressively decreases towards the adventitia (Moncada S et al., 1977).

Prostacyclins relax isolated vascular strips and are strong hypotensive agents on account of their property to induce vasodilatation in all vascular beds studied, including the pulmonary and cerebral circulations. The vasorelaxant effects of prostacyclin have been reviewed in detail (Moncada S and Vane JR, 1978).

During normal pregnancy, the urinary metabolites of prostacyclin increase progressively to up to 5-fold above their original levels during the last month of pregnancy (Ylikorkala O et al., 1986). A large scale prospective study showed that women afflicted by PET had lower urinary levels of prostacyclin metabolites as early as weeks 13-16 (but no change in levels of TXA_2), which yielded a higher TXA_2/PGI_2 ratio (Mills JL et al., 1999). This imbalance in favour of the vasoconstrictive and pro-coagulant TXA_2 is believed to be the underlying cause of the main features that charcterize PET, including hypertension, platelet aggregation and reduced utero-placental perfusion (Wang YP et al., 1991). Following this discovery that the levels of prostacyclins and thromboxane were perturbed in PET pregnancies, the use of low-dose aspirin as a therapeutic strategy has been tested in a number of clinical trials. The rationale behind this was that COX inhibitors, like aspirin at low doses, could prevent or ameliorate PET by reducing platelet thromboxane production while sparing endothelial PGI_2 production. However, this strategy was of limited therapeutic benefit, indicating that there is more to PET than an alteration in levels of PGI_2 and thromboxane (CLASP, 1994).

1.16.3 Endothelial derived hyperpolarizing factor (EDHF)

Endothelium-dependent relaxation/vasodilatation in response to chemical agonists and physical forces such as shear stress exerted by the flow of blood, are generally attributed to the release of NO and/or PGI_2. However, in a number of vascular beds, these responses cannot be completely explained by these two mediators only. The relaxation observed in the presence of NOS and COX inhibitors has been associated with hyperpolarization of vascular smooth muscle (VSMCs) and an endothelium derived hyperpolarizing factor or EDHF has been postulated (Feletou M and Vanhoutte PM, 2009). The hyperpolarization of VSMCs has been attributed to an increase in conductance to K^+ ions. Increased K^+ ion efflux from a cell results in a more negative resting membrane potential and thus hyperpolarization, which is followed by relaxation (Feletou M and Vanhoutte PM, 2005).

Selective K^+ channel inhibitors have been used *in vitro* to characterize the types of potassium channel involved in the EDHF response. The channels that most commonly appear to mediate EDHF responses are charybdotoxin-sensitive large conductance Ca^{2+} activated potassium channels and apamin-sensitive small conductance Ca^{2+} activated potassium channels (Edwards G et al., 1998).

The identity of EDHF is a topic of much heated debate. Some of the compounds that have been proposed as potential candidates include epoxyeicosatrienoic acids, hydrogen peroxide, K^+ ions, C-type natriuretic peptide, hydrogen sulphide, carbon monoxide, etc. The exact identity of EDHF may differ in different vascular beds (Feletou M and Vanhoutte PM, 2009).

Electrophysiological and pharmacological investigations in human arteries have demonstrated that there appears to be a larger contribution of EDHF in the microvessel circulation than in large arteries (Urakami-Harasawa L et al., 1997). The generation of double-knockout mice, which lack both eNOS and COX-1, i.e., the “EDHF mouse” has facilitated the assessment of contribution of EDHF in

endothelium-dependent relaxation in resistance arteries (COX-2 expression was found to be absent in the resistance vessels of these mice). In these mice, males become hypertensive while females are normotensive. Furthermore, the endothelium-dependent relaxation was intact in the resistance arteries of female mice (and associated with vascular smooth muscle hyperpolarization) but greatly attenuated in vessels from male mice. This suggests that EDHF may be more important in female arteries to confer endothelium-dependent dilatation, while NO and PGI_2 may play an important role in male arteries (Scotland RS et al., 2005).

A previously published study investigated the role of EDHF from myometrial blood vessels in non-pregnant, normotensive and PET women. The relative contributions of NO, PGI_2 and EDHF were investigated by using inhibitors of all three alone and in combination. The vessels from non-pregnant and PET women showed minimal residual relaxation in the presence of L-NAME, suggesting that NO is the prinicipal mediator of endothelium dependent relaxation in these vessels. COX and EDHF inhibitors had no effect on relaxation. On the contrary, normal pregnant vessels were able to compensate and relax via either a NO or EDHF dependent mechanism. Hence, normal pregnancy is associated with the development of parallel EDHF and NO pathways in the myometrial bed, ensuring that if one of the pathways is functioning poorly, there is a compensatory back-up mechanism in place. This 'back-up' system is lacking in PET pregnancy, with the endothelium-dependent relaxation solely being mediated via NO (Kenny LC et al., 2002).

Thus, endothelium-dependent relaxation of blood vessels is primarily mediated through three different pathways of relaxation – NO, PGI_2 and EDHF. The relative contribution of these different pathways of relaxation varies in different species and different vascular beds. These three pathways may be selectively blocked by the addition of inhibitors such as L-NAME, N^G,N^G-Dimethylarginine dihydrochloride (for NOS); Indomethacin or NS-398 (for PGI_2); and, Apamin and Charybdotoxin (which inhibit the effects of EDHF)

(Figure 1.11). While Indomethacin is a non-selective inhibitor of both the COX-1 and COX-2 pathways, NS-398 specifically inhibits the COX-2 pathway.

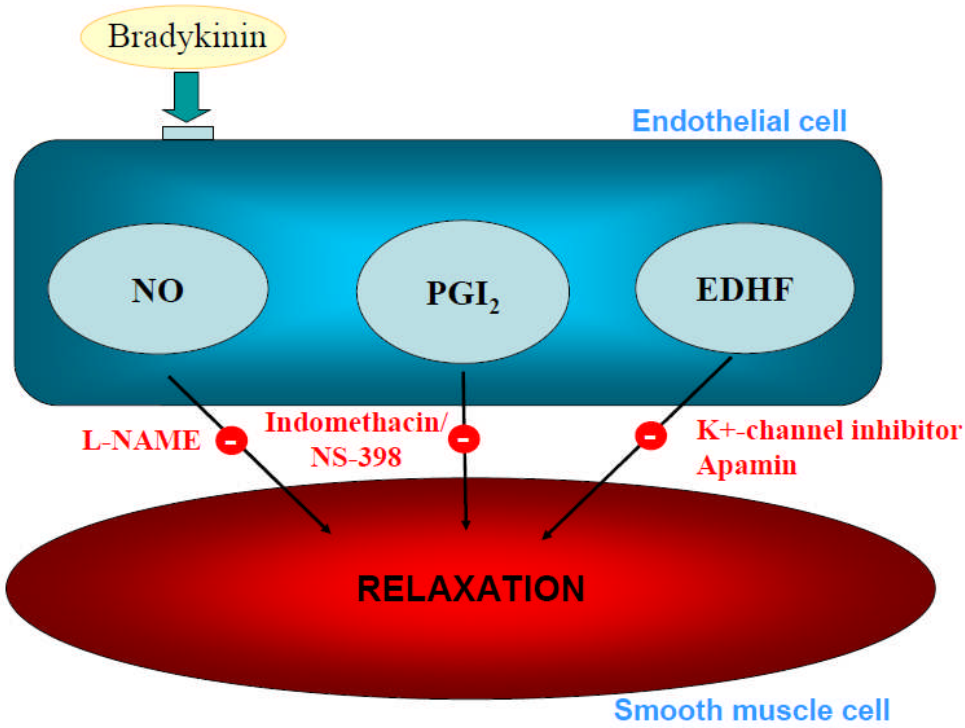

Figure 1.11 – Pathways of endothelium-dependent relaxation.

Bradykinin acts on endothelial cells, stimulating the release of nitric oxide (NO), prostacyclins (PGI_2) and Endothelium-derived hyperpolarizing factor (EDHF). These molecules act on the vascular smooth muscle layer of a blood vessel and bring about relaxation. The action of either of these pathways may be blocked by treatment with specific inhibitors. L-NAME is an inhibitor of the NOS pathway, Indomethacin/NS-398 blocks the synthesis and effects of PGI_2, and Apamin inhibits the effects of EDHF.

1.17 Biology of Endothelial Cells (ECs)

In this study, I have attempted to understand the mechanism of action of VEGF by carrying out *ex vivo* experiments on sheep uterine artery endothelial cells. The ECs form a monolayer lining called the endothelium, in all of the blood vessels of our circulation. Initially, they were thought to act as a dialysis membrane allowing nutrients from the blood stream to diffuse through to the underlying tissue without letting proteins or blood cells escape. It is now known that these highly sophisticated cells are virtually in control of the blood

circulation, and have been appropriately referred to as the ‘maestro’ of blood circulation (Vane JR, 1994).

1.17.1 Structure

Being composed of a single layer of flat scale-like cells that are all in contact with a basement membrane, the endothelium is described as a squamous epithelium. ECs are very flat, between 20-50 μm in diameter and up to 5μm in depth (Limaye V and Vadas M, 2007). The cytoplasm is relatively simple with few organelles, mostly concentrated in the perinuclear zone. Another prominent feature of ECs is the presence of many pinocytotic vesicles which are involved in the process of transport of substances from one side of the cell to the other.

1.17.2 Cell junctions and basement membrane

ECs are connected to one another by three types of junctions commonly found in other epithelia: tight, adherens and gap (Dejana E, 2004). All junction types consist of a trans-membrane protein on one cell, interacting homotypically with another molecule of the same protein on an adjacent cell. Other proteins bind the cytoplasmic tail of the transmembrane molecule, linking it directly or indirectly to the actin cytoskeleton.

Tight junctions form a belt around the endothelial cell, the zona occludens, and act as a barrier to the transport of substances across the endothelium via the paracellular route (between cells). Tight junctions also have fence-like properties, restricting the diffusion of membrane components and allowing the maintenance of differing compositions of the apical and basolateral plasma membrane.

Adherens junctions also form a belt around endothelial cells, the zonula adherens, and provide mechanical strength to cell-cell contacts but are also involved in signaling EC-EC contact. Cadherins, the key transmembrane proteins involved, are indirectly linked to the actin cytoskeleton by binding to intracellular catenins. All ECs express vascular endothelial (VE)-cadherin, which is the main cadherin present in endothelial cell adherens junctions (Vestweber D, 2008). VE-

cadherin associates with vascular endothelial growth factor receptor 2 (VEGFR2) in confluent cells, regulating endothelial cell survival (Carmeliet P et al., 1999).

Catenins, including β-catenin, plakoglobin/γ-catenin and p-120, are able to bind to the cytoplasmic tail of VE-cadherin, and link it to the actin cytoskeleton. Catenins can translocate to the nucleus, and regulate transcription, allowing EC-EC contact to influence gene expression. Sequestering of β-catenin by VE-cadherin in juxtaposed endothelial cells is thought to be involved in contact inhibition of cell growth (Gumbiner BM and McCrea PD, 1993).

Gap junctions do not form a belt, but exist as fluid-filled channels (connexons) which form direct links between the cytoplasm of adjacent ECs, allowing the passage of ions and small molecules, so aiding cell-cell communication. Connexons are composed of individual protein subunits called connexins (Cx) – ECs express Cx43, Cx40 and Cx37, forming channels around 20nm in diameter. ECs also form gap junctions with underlying smooth muscle cells.

Platelet endothelial cell adhesion molecule (PECAM, also known as CD31), a transmembrane immunoglobulin-like molecule which can participate in homophilic or heterophilic interactions, is concentrated at EC-EC junctions. Although not part of a defined junctional complex, PECAM is important in EC-EC adhesion. PECAM staining is often used as a marker for endothelium in immunohistochemistry.

The endothelium, as for other epithelia, rests on a basement membrane produced by the endothelial cells themselves (Kramer RH et al., 1984). The basement membrane is usually continuous but may be discontinuous, and encloses ECs in a sheath in intact vessels. Pericytes are enclosed within the basement membrane, smooth muscle cells are not. All basement membranes consist primarily of type IV collagens, laminins, nidogens (entactins) and HSPGs such as perlecan, with lower amounts of other components such as thrombospondin, fibronectin and vitronectin (Hallmann R et al., 2005). The

basement membrane may influence cell behaviour by binding growth factors such as VEGF (via HSPGs), and through the binding of integrins to components such as laminins.

1.17.3 Function

Endothelial cells are involved in many aspects of vascular biology, including:

*Vasoconstriction and vasodilatation, and hence the control of blood flow and blood pressure

*Coagulation

*Atherosclerosis

*Formation of new blood vessels (angiogenesis)

*Inflammation and oedema

*Filtering and trafficking functions, particularly in the renal glomerulus and in the blood-brain barrier to allow transit of white blood cells in and out of the bloodstream.

Some of these essential functions will be briefly reviewed below.

1.17.3.1 Control of blood flow and blood pressure

ECs regulate basal vasomotor tone, and therefore vascular blood flow and blood pressure, by the tightly controlled release of vasodilators like NO, PGI_2 and EDHF as well as vasoconstrictors like endothelins and thromboxane A_2 as discussed in detail in a preceding section.

The endothelins (ETs) are a family of 21 amino acid peptides, of which ECs and smooth muscle cells produce mainly the ET-1 isoform. Production of ET-1 is induced by hypoxia, ischaemia and shear stress, which induce the

transcription of ET-1 mRNA, with rapid secretion of ET-1 within minutes. The majority of ET-1 secretion is towards the abluminal side of the EC and thus it acts in a paracrine manner by binding to ET_A receptors on smooth muscle cells, to cause vasoconstriction. It also has some autocrine effects through the ET_B receptors on endothelial cells, activation of which causes NO and prostacyclin release (Rosendorff C, 1997).

1.17.3.2. Coagulation

The quiescent endothelium possesses anticoagulant activity by providing an anti-thrombotic surface which inhibits the coagulation cascade. One of the major strategies used by ECs to maintain anticoagulant activity is to prevent activation of thrombin. Activated thrombin converts soluble fibrinogen into insoluble strands of fibrin, which stimulates coagulation by causing platelet activation and the activation of several coagulation factors (Limaye V and Vadas M, 2007). ECs express HSPGs, which along with glycosaminoglycans in the ECM, are able to stimulate antithrombin-III (Rosenberg RD, 1985). They also express tissue factor pathway inhibitor (TFPI) that prevents thrombin formation, and express thrombomodulin (Dielis AW et al., 2008). Therefore, in the healthy endothelium, the balance is towards the expression of anticoagulant factors to ensure smooth uninterrupted blood flow in the vessels.

1.17.3.3. Angiogenesis

Angiogenesis is the formation of new blood vessels from pre-existing ones. This process involves the degradation of ECM by ECs, as well as their migration, proliferation and the formation of tubes in association with mural cells. In the process of vessel formation, it is essential for ECs to carry out efficient cell-matrix attachments and cell-cell contacts.

Attachments between the EC and surrounding ECM are mediated by the integrin family of cell surface adhesion molecules. Integrins provide adhesive and signaling functions between ECs and the ECM, and this interaction is critical in maintaining the EC polarity and alignment along the vasculature. The integrins

link the cell with the ECM at focal adhesion points and interact with the actin cytoskeleton. This interaction stimulates cell contraction, thus allowing cell movement on adhesive contacts (Silva R et al., 2008).

In addition to interaction with the ECM, ECs must form cell-cell contacts in order to produce a viable capillary like network. This cell-cell adhesion is mediated by molecules like VE-cadherin and PECAM-1, as described above.

1.17.3.4. Inflammation and oedema

Endothelial cells are responsive to local agents such as histamine, which is released when local tissues are damaged. As a result, the intercellular junctions between endothelial cells allow the passage of large amounts of fluid from blood plasma into the extravascular space, so that the surrounding tissues become engorged with fluid and swollen, a condition called oedema.

The endothelium also plays a critical function in regulating the trafficking of leucocytes from the intravascular space to extravascular sites of inflammation. The first step in leucocyte transmigration is the arrest of leucocytes and contact with the ECs. This is mediated by the selectins, which allow the rolling and docking of the leucocyte on the endothelium (Vestweber D, 2007). During the second step of the transmigration process, the leucocytes flatten and migrate along the endothelium, a process known as diapedesis. Finally, extravasation occurs by leucocyte migration through EC junctions and their subsequent attachment/migration on ECM components (collagen and fibronectin) (Vestweber D, 2007). The main families of molecules involved in this trafficking process are the selectins, integrins, immunoglobulin supergene family and variants of the CD44 family (Limaye V and Vadas M, 2007).

1.18 Previous work from our lab which has led up to this project

Some of the previous experiments from our lab which laid the foundation for the research described in this Ph.D. are discussed below.

The hypothesis proposed was that local over-expression of VEGF in the uterine arteries of normal pregnant sheep would increase uterine blood flow, and alter vascular reactivity. The first experiments were analysed at a short term time point after adenovirus gene transfer, to determine firstly whether local VEGF over-expression was occurring and secondly what effect it might have. First generation (E1, E3-deleted) replication-deficient adenovirus vectors (5×10^{11} viral particles in 10 mL Phosphate buffered saline) containing the VEGF-A_{165} gene (Ad.VEGF-A_{165}) or the nuclear localising beta-galactosidase reporter gene (Ad.LacZ, the same dose) as a control, were injected into the uterine arteries of pregnant sheep (n = 5) at 88 – 102 days of gestation (term = 145 days). Uterine blood flow was quantified using Doppler sonography just before vector injection. The operators were unaware as to which side had received the Ad.VEGF-A_{165} vector.

Between 4 to 7 days after adenovirus injection, the ewe was re-anaesthetised, and uterine blood flow and umbilical artery Doppler measurements were repeated. When compared with measurement of blood flow before vector injection, uterine artery blood flow increased by over three-fold (mean ± SD increased from 233 ± 156 mL/min to 753 ± 415 mL/min) in Ad.VEGF-A injected vessels and this increase was significant (Figure 1.12).

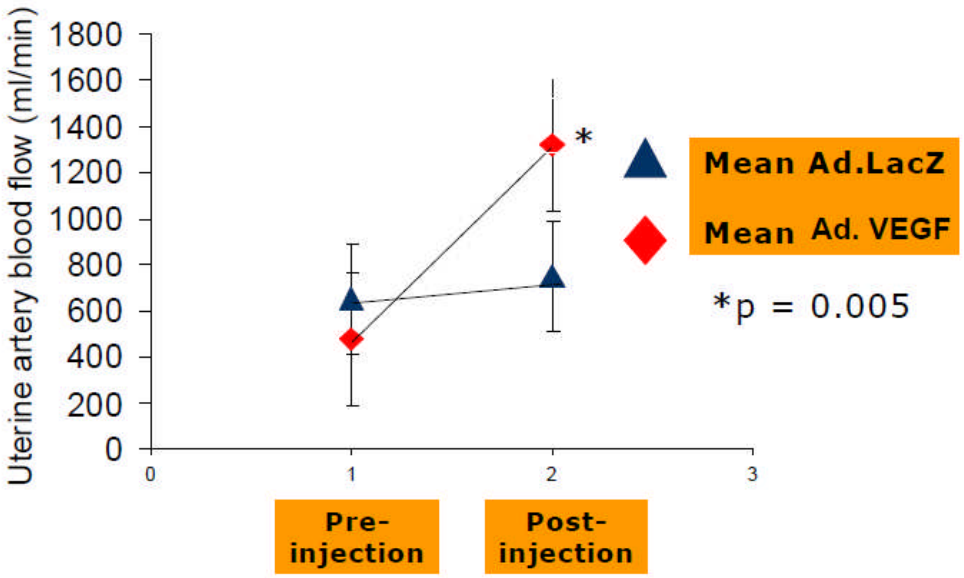

Figure 1.12 - Changes in uterine blood flow (UBF) 4 - 7 days after injection of Ad.VEGF-A_{165} or Ad.LacZ.

UBF was determined in mid-gestation pregnant sheep by Doppler ultrasonography, just prior to administration of Ad.VEGF-A_{165} and Ad.LacZ to the uterine arteries contralaterally (n=5). 4-7 days later, UBF was again measured in the injected animals under terminal anaestheia. There was a dramatic and significant three-fold increase in UBF in the Ad.VEGF-A_{165} transduced uterine arteries. Blood flow increased in the Ad.LacZ transduced uterine arteries as well, though this increase was not significant (David AL et al., 2008).

Post-injection uterine blood flow was also higher than pre-injection levels in the Ad.LacZ injected vessels but the increase was not significant (mean uterine blood flow pre-injection was 320 ± 160 mL/min and post-injection was 430 ± 110 mL/min). There were no significant changes in the umbilical artery diameter, PI, resistance index (RI) or fetal heart rate 4 – 7 days after injection of adenoviral vectors. Cross-flow of vector from injection in one uterine artery on one side to the other uterine artery on the contra-lateral side is unlikely to have taken place. The uterine arteries supply only one uterine horn each and we believe the volume of injection (10 mL) is only sufficient to reach the uterine artery branches and maternal villi on that side of injection. No evidence of vector spread to the contra-lateral artery was detected using RT-PCR analysis for vector expression or ELISA analysis for transgenic protein expression in uterine arteries samples.

Furthermore, the transduced vessels harvested at post-mortem examination were examined on an organ bath set-up to investigate changes in vascular reactivity. A significant reduction in the contractile response and significant increase in relaxation was observed in Ad.VEGF-A_{165} transduced uterine arteries relative to Ad.LacZ transduced vessels. The endothelium-dependent relaxation was also studied in the presence of different inhibitors of relaxation, and it was found that the major contributors to relaxation in pregnant sheep uterine arteries were the NOS and EDHF pathways (David AL et al., 2008).

To conclude, local administration of Ad.VEGF-A_{165} into the uterine artery of pregnant sheep increases uterine blood flow short term, as measured in a blinded fashion by Doppler ultrasonography. This increase in UBF is concomitant with a diminished contractile response and enhanced relaxation response of Ad.VEGF-A_{165} transduced vessels.

1.19 Aims of the thesis

With the aim of developing a treatment for FGR, the aim of this thesis is to investigate the effect of local VEGF gene therapy on the uteroplacental circulation, particularly :

1) To study the effects of local VEGF over-expression on the uterine arteries of pregnant sheep.

2) To study the effects of local VEGF over-expression on eNOS, phospho-eNOS and iNOS levels in uterine artery endothelial cells from pregnant sheep

3) To optimize a technique of gene targeting to the utero-placental circulation of pregnant guinea pigs, with the aim of using this technique to study the

effects of VEGF gene transfer on fetal growth in an FGR model of guinea pig pregnancy.

.

Chapter 2

Methods

2.1 Care of Sheep and Animal Husbandry

Sheep of Romney breed were used. Each ewe was ear tagged twice with an identification number and the sheep flock was vaccinated against Toxoplasma, Chlamydia and Clostridium annually. All procedures on animals were conducted in accordance with the UK Home Office regulations and the Guidance for the Operation of Animals (Scientific Procedures) Act (1986) under Project Licence number 70/6546 titled 'Fetal gene therapy *in utero*'. All animal surgeries were under general anaesthesia and conducted by personal licencees (Anna David, Donald Peebles, Khalil Abi-Nader, Vedanta Mehta, Steven Shaw and Michael Boyd).

2.2 Timed Mating of Ewes

All experiments were conducted on time-mated sheep to ensure the gestational age of fetus was consistent. Tupping of sheep was begun in early autumn during the sheep breeding season and approximately 20 sheep were tupped each year. To enable timed mating of sheep, Chronogest® sponges (Flugestone acetate) containing 30mg of progesterone were placed in the vagina of ewes for 2 weeks to induce ovulation. Forty-eight hours after removal of the progesterone sponges, ewes were placed in a pen with the ram overnight. The

abdomen of the ram had been marked beforehand with Ram Raddle®, a coloured powder mixed with liquid paraffin that permanently marks the fleece on the back of the ewe once she has been tupped. Ewes that had been marked the next morning were presumed to have been successfully tupped. Two weeks later ewes were placed back in with the ram overnight in case of unsuccessful tupping the first time. A different coloured Ram Raddle was used to be able to differentiate the two tupping dates. Ewes were scanned by the technical staff at the Royal Veterinary College at approximately 60 days of gestation to confirm pregnancy. Non-pregnant ewes were re-sponged and re-tupped a month later. The success rate of sheep pregnancy on tupping was 85%.

2.3 Transport of tupped sheep and housing

Pregnant ewes were sent from the Royal Veterinary College (RVC) Hawkshead Campus to the Biological Services Unit (BSU), RVC Camden Campus in a lorry one week before use to allow acclimatization. At the BSU in Camden, they were housed together in pairs in specially designed sheep pens at ambient temperature. The floor of the pens was covered with straw and the ewes had *ad lib* access to hay and running water and were given a daily portion of Super Ewe and Lamb 6mm pencils compound feed (Appendix 1). The feed is a concentrated source of oil, protein and vitamins and the amount given to sheep was increased as gestation progressed or when there was more than one fetus. This ensures adequate nutrition for the ewe and reduces the risk of toxaemia caused by the large late gestation fetus compressing the rumen and reducing the ability of the ewe to digest enough hay for nutrition.

The straw bedding was changed and the room thoroughly washed weekly. The room dimensions exceeded the guidelines of the UK Home Office, to ensure that the animals were comfortable and not distressed. A picture of the sheep pen with all the dimensions is shown in Figure 2.1.

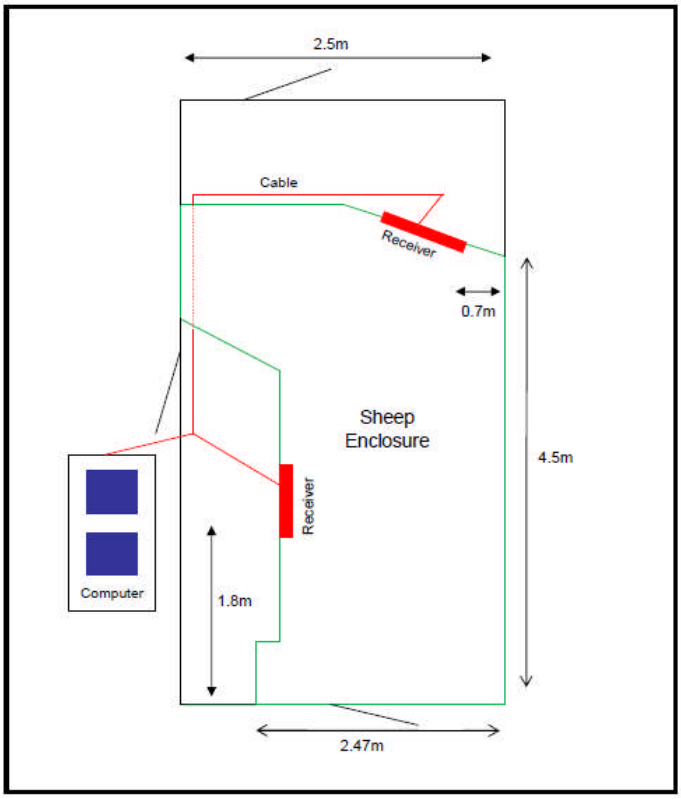

Figure 2.1 – Diagram of sheep enclosure

The monitoring space consisted of an animal enclosure room adjacent to a computer room. The two receivers, which were fixed at 53cm above ground level on the inside of the enclosure, were arranged in a way to maximize free animal movement in the space available while maintaining a good signal. The green line indicates the area of the enclosure in which the sheep were free to roam. Cables ran from each receiver to the computer outside the sheep enclosure and above the height of the ewe to avoid damage.

2.4 Confirmation of pregnancy and gestational age using ultrasound

All pregnant sheep were scanned the day after arrival at the BSU, Camden to confirm pregnancy, fetal number and gestational age. Ewes were caught, turned up and held in a sitting position for scanning by an experienced animal technician. The fleece was then clipped from the abdomen. Using gel (Ultragel Vete, Transpharma Sas, Italy) applied to the suprapubic area and lower abdomen, an experienced fetal medicine specialist (Anna David, Khalil Abi-Nader, Steven Shaw) scanned the uterus using an Acuson 128 XP10 ultrasound scanner

(Siemens, Bracknell, United Kingdom) with a C3 3.5 MHz curvilinear transducer. Fetal number was checked and the gestational age of the fetuses was confirmed by comparing the biparietal diameter (BPD) and occipito-snout length (OSL) with published data. (Barbara A et al 1995, Kelly RW and Newnham JP, 1989).

Figure 2.2 - Acuson 128 XP10 ultrasound machine (Siemens, Bracknell, United Kingdom) used to scan pregnant sheep and guinea pigs.

2.5 Sheep anaesthesia and preparation for surgery

Prior to surgery, the sheep were starved overnight on wood chip bedding with free access to water. During this fasting period, a companion animal was also placed and fasted with the sheep that had to undergo surgery the next morning to prevent distress. The overnight fasting was to prevent bloating which may occur when sheep under anaesthesia are unable to belch (eructate) normally and release methane gas, which is a by-product of the fermentation of their food. (Wolfensohn S and Lloyd M, 1998).

On the morning of surgery, the sheep was run down the corridor to the theatre room where she was ‘turned’ and restrained. The wool was clipped from

her neck, the jugular vein was cannulated using a 19 Gauge butterfly winged perfusion set (Terumo Europe NV, Leuven, Belgium) and general anaesthesia was induced with thiopental sodium 20mg/kg intravenously (IV, Thiovet, Novartis, Animal Health UK Ltd., Hertfordshire, UK). Once asleep, the ewe was lifted onto the operating table and intubated supine with a 9.0 mm cuffed endotracheal tube (Portex, UK) using a laryngoscope (Penlon, UK) to visualize the vocal cords. A cuff was inflated on the endotracheal tube to prevent inhalation of regurgitated ruminal contents and the ewe's head was lowered to allow drainage of saliva and ruminal fluid (Taylor PM, 1991). Because access to the whole abdomen was needed for procedures, the animals were kept in dorsal recumbency. Anaesthesia was maintained with 2%-2.5% Isoflurane in oxygen (Isoflurane-vet, Merial Animal Health Ltd., Essex, UK) using a Magill circuit (Medishield ventilator, Manley Serovent).

The induction and maintenance of general anaesthesia was performed by Mr. Michael Boyd, Theatre Manager, Biological Services Unit, RVC Camden.

Once anaesthetized, the wool was clipped from the ewe's abdomen and a detailed ultrasound examination of the uterus and its contents was performed using a 3.5MHz probe as before. Fetal measurements were collected, namely biparietal diameteter, occipito-snout length, abdominal circumference, femur length and umbilical artery Doppler pulsatility and resistance indices.

Ultrasound examination was performed by Dr. Anna David, Dr. Khalil Abi-Nader, Vedanta Mehta and Dr. Steven Shaw.

The abdominal surface, right flank and the neck area of the ewe was scrubbed with 'Hibiscrub' (Chlorhexidine gluconate 4% w/v, Regent Medical, Manchester, UK) followed by 'Povidone' (1% w/w Iodine solution, Vetasept Animal Care Ltd., York, UK). The neck and abdomen were exposed with sterile drapes.

A pulse oximeter (5250 RGM, Ohmeda) placed on the ewe's ear was used to monitor oxygen saturation and pulse rate during general anaesthesia and this data was documented every 15 minutes together with respiration rate, isoflurane concentration and level of anaesthesia. Maternal blood was taken for pre-

operative haematological and biochemical analysis. Blood was collected into BD Vacutainer tubes (BD Vacutainer systems, Plymouth, UK) containing 0.105 M sodium citrate for plasma (9C, blue topped bottle), silica clot activator polymer gel for serum (yellow top bottle) and potassium EDTA (K_3EDTA) for whole blood (purple top bottle).

2.6 Insertion of Blood pressure catheter to monitor maternal haemodynamics

The blood pressure in the ewe was measured by inserting a blood pressure sensitive catheter into the carotid artery. The instrument used was a TA11 PA-D70 device (Data Sciences International, Tilburg, Netherlands), which has a 35cm long catheter connected to a transmitter (Figure 2.3) that can be switched on/off with a magnet waved 3-4 cm over the skin surface. The tip of the catheter is filled with a bio-compatible gel, to prevent coagulation of blood.

Figure 2.3 – A PA-D70 implant (Data Sciences International, Tilburg, Netherlands) used to measure maternal blood pressure and heart rate in pregnant sheep.

In preparation for the BP catheter insertion surgery, the transmitter was switched ‘on’ with the magnet and confirmed to be ‘on’ by bringing it close to a radio tuned into 530 KHz AM. When the transmitter is on, it is reflected on a ‘tuned’ radio as a characteristic humming sound. A metallic receiver RMC-1

(Data Sciences International, USA) was placed under the operating table, to catch the signal from the transmitter during the surgery.

The skin of the ewe's neck to the right of the trachea in the midline was incised longitudinally for 5cm with a number 11 blade (Swann-Morton, Sheffield, UK) and exposed to reveal the trachea and the strap (infrahyoid) muscles. The muscles were gently pushed aside to the midline to expose the carotid artery, which was dissected free of underlying connective tissue. Two 1-0 sterile silk vessel ties (Ethicon, New Jersey, USA) were placed around the carotid artery, about 1 cm apart. The upper vessel tie was tied tightly around the vessel to occlude it, the lower suture was loosely tied. The carotid artery between the two ties was raised slightly to suspend the vessel between the ties and occlude it. A small incision was made at an angle in the suspended vessel wall with scissors. Using a fine forceps the vessel incision was opened and the tip of the catheter was gently inserted into the carotid artery lumen, and pushed towards the heart until a clean blood pressure waveform could be observed on the computer placed nearby. The lower vessel tie was then tied tightly around the vessel and catheter to keep it in place. A further tie was placed around the vessel and catheter within to secure it.

The body of the transmitter was placed in a cavity made between the subcutaneous neck tissue and underlying neck muscles. The subcutaneous tissue was closed with continuous 2-0 Vicryl (Johnson & Johnson Intl, St. Stevens-Woluwe, Belgium). The skin incision was closed with continuous 2-0 vicryl suture. Terramycin antibiotic (3.92% cutaneous spray containing oxytetracycline hydrochloride; Pfizer, Kent, UK) was sprayed over the incision.

2.7 Implantation of flow probes around uterine arteries

A 6mm 6-PS transit-time flow probe (Transonic Systems Inc, New York), which can measure blood flow within a $\pm$10% limit of error was used to measure blood flow in the uterine arteries. Flow probes were placed around the main

uterine artery on either side where they measured the real time flow measurements. Data was telemetrically transmitted to a computer located in the adjacent room using Bluetooth technology. Before implantation, the flow probes were tested by shaking their reflection bracket in a container full of water, and observing if there was any change in the waveform on the acquisition computer.

A midline lower abdominal incision was made in the skin using a number 11 blade from just below the umbilicus to the pubic bone. The rectus sheath was carefully incised avoiding any vessels, and the peritoneal cavity was opened carefully. The ruminant bowel was packed to one side using sterile lap sponges. The disassembled flow probes were sterilized by placing in Vetguard cold sterilant (Steritech, Cheltenham, UK) for 15 minutes after which the flow probes were reassembled just before placement. A trocar and cannula were passed from the peritoneal cavity through the skin to exit at the right flank of the ewe. The sterilized flow probes were then internalized by passing them through the cannula into the maternal peritoneal cavity. The lower lateral aspect of each uterine horn was exposed to observe each main uterine artery as it passed over the anterior wall of the uterus within its mesometrium (a picture of the uterine artery tree of pregnant sheep is shown in Figure 2.14). The visceral peritoneum was dissected to expose the uterine artery 5cm from its most lateral aspect, and to free a short loop segment from its underlying connective tissue.

A flow probe was placed around each main uterine artery and secured in place using the screws provided with the kit (Figure 2.4). The overlying visceral peritoneum was closed using 4-0 Prolene suture (Ethicon, Edinburgh, UK). The lap sponges were removed from the abdomen and intra-muscular Penstrep 3ml (200mg/ml procaine penicillin and 250mg/ml dihydrostreptomycin; Norbrook Laboratories Ltd., County Down, UK), intra-peritoneal Crystapen 3g (Sodium benzylpenicillin G, Schering-Plough, Uxbridge, UK) + gentamicin 80mg (Geneticin Injectable, Roche Products Ltd., Hertfordshire, UK) were administered for antibiotic prophylaxis. The abdomen was closed in layers. The rectus sheath was closed with continuous 6mm nylon tape (Johnson and Johnson, Belgium) to prevent herniation of the abdominal contents. The subcutaneous tissue and the

skin were closed with 1-0 PDS and 1-0 Vicryl (Ethicon, Norderstedt, Germany) respectively.

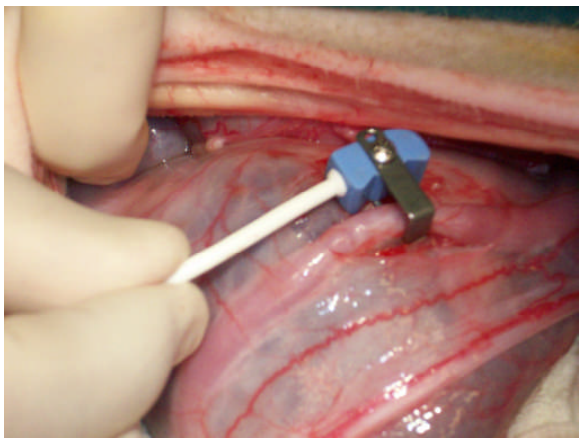

Figure 2.4 – A transit-time flow implanted around the main uterine artery for telemetric measurement of uterine artery blood flow.

The ewe was turned slightly more to the left side to allow access. The skin buttons were tunneled under the skin a further 10cm higher up and brought out onto the maternal right flank. The opening into the abdomen was closed with 1-0 PDS (Ethicon, Norderstedt, Germany) for the sheath and 1-0 Vicryl (Ethicon, Norderstedt, Germany) for the skin. The skin buttons were sutured in place with 1-0 PDS (Figure 2.5).

Figure 2.5 – The skin buttons sutured on the maternal right flank of the sheep.

(Continued from overleaf) The physiometer system was connected with flow probes implanted around the uterine arteries through the skin buttons. Once connected, the flow probes beamed the real-time uterine artery blood flow measurements to an acquisition computer in close proximity by bluetooth technology.

Terramycin was sprayed over the abdominal incision and the flank incisions. Analgesia (0.1 mg/ml IM buprenorphine) was administered to the ewe. The ewe was then allowed to recover, extubated and placed in its pen under observation. Early standing (within 1 hour) was encouraged to prevent bloating.

2.8 Vector Injection

Approximately 1 week (range 6 to 10 days) after the probe placement surgery, the ewe was re-anaesthetized and the mid-line laparatomy scar was reopened. The location of the transonic flow probes was checked. A short section of the main uterine artery, just proximal to the flow probe was cleared of the surrounding visceral peritoneum and the vessel was stabilized using a 45 cm vessel loop (Bard UK, London) (Figure 2.6). The vessel was digitally occluded, while vector ($5x10^{11}$ viral particles in 10ml PBS in a 10ml syringe) was injected into the lumen, just distal to the site of occlusion using a 23 gauge butterfly needle (Figure 2.7). Blood was first withdrawn into the butterfly cannula to ensure the needle was inside the uterine artery lumen and then, the vector was slowly injected over one minute. The butterfly needle was removed and the vessel was digitally occluded over the injection site as well. The vessel occlusion was maintained for a further four minutes giving a total occlusion time of 5 minutes. This ensured there was sufficient time for the adenovirus to infect the endothelium of the uterine artery vessel and branches locally and to prevent excessive systemic spread of the vector.

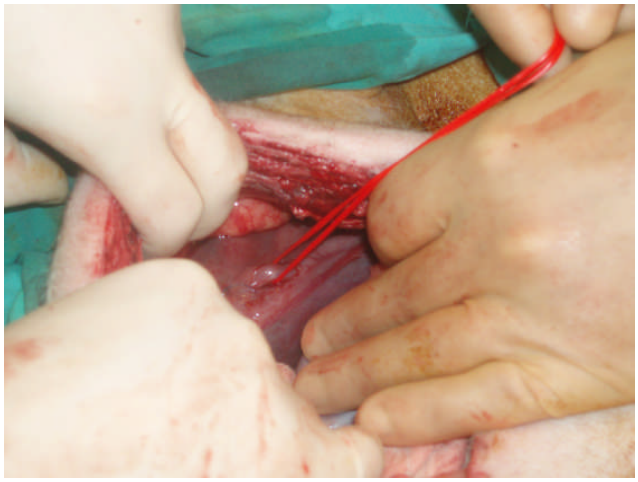

Figure 2.6 – Isolation of the proximal part of the uterine artery before vector injection.

Before vector injection, a short section of the main uterine artery, just proximal to the flow probe was cleared of the surrounding visceral peritoneum and the vessel was stabilized using a 45 cm vessel loop. This enabled the vector to be injected into the vessel more reliably.

Figure 2.7 - Injection of vector into the occluded uterine artery

The vector ($5x10^{11}$ viral particles in 10 ml PBS) was injected slowly into the lumen of the uterine artery just distal to the site of occlusion but proximal to the flow probe, over a period of one minute. Following vector injection, the vessel occlusion was maintained for a further four minutes to ensure sufficient time for the adenovirus to infect the endothelium of the uterine artery vessel and branches locally.

The occlusion was then released, the vessel loops were removed and the site of injection was carefully observed for any signs of bleeding. The peritoneum

was again sutured over the exposed section of the uterine artery using a 4-0 Prolene suture (Ethicon, Norderstedt, Germany).

Antibiotics were administered and the body wall was closed as described above. Intra-muscular analgesia was given as before, and the sheep was allowed to recover in its pen.

2.9 Insertion of blood pressure catheter to monitor fetal haemodynamics

The animals were prepared for surgery and anaesthetized as described in previous sections. Laparotomy was performed using a midline incision as before and the abdomen was opened in layers. A 6PS transit-time flow probe (Transonic Systems Inc., NY, USA) was then placed around each main uterine artery on both sides to measure uterine artery blood flow. The flow probe cables were then exteriorised on the upper right flank of the ewe. This procedure is described in greater detail in the preceding section (Section 2.7).

In preparation for the fetal BP catheter insertion surgery, the transmitter was switched 'on' with the magnet and confirmed to be 'on' by bringing it close to a radio tuned into 530 KHz AM. A metallic receiver RMC-1 (Data Sciences International, USA) was placed under the operating table, to catch the signal from the transmitter during the surgery.

Following this the uterus was palpated and the fetal parts identified. In an area of myometrium away from placentomes, a 5cm uterine incision was made just above the fetal head using a No21 blade (Swann-Morton, Sheffield, UK). The fetal head was exteriorized through the uterine incision and Babcock clamps were used to compress the amniotic membrane against the uterine wall in order to minimize bleeding (Figure 2.8). A 3cm longitudinal incision was made in the fetal neck 1cm to the right of the trachea and the right common carotid artery was identified and mobilized from beneath the strap muscles. Two 3-0 silk ties (Mersilk, Ethicon Ltd, Edinburgh, UK) were passed under the vessel proximally and distally and held without tying using Kelly clamps. The right common carotid

artery was then elevated under tension from the two sides to prevent excessive bleeding, while an incision was made in the vessel wall using a fine-tipped scissors until the lumen could be identified. A fine-tipped curved forceps was inserted into the arterial lumen and the jaws were held apart to maintain luminal patency. One of the hemodynamic catheters of the telemetric D70-PCTP device (Data Sciences International, Tilburg, Netherlands) was inserted into the arterial lumen and threaded upstream towards the aorta for a distance of around 5-7cm until a clear signal to the nearby receiver could be obtained. The silk lines were then tied, one to occlude the vessel distally and one to secure the catheter within the vessel proximally. The neck skin was closed over the catheter using 2-0 Vicryl (Ethicon, St. Stevens-Woluwe, Belgium). The fetal head was returned to the amniotic cavity. The other hemodynamic catheter was inserted into the amniotic cavity to record background pressure. The uterine incision was closed in two layers using 2-0 PDS (Ethicon, St. Stevens-Woluwe, Belgium) in a running fashion with the catheters passing through the incision at a distance from the angles. While the first layer incorporated the whole thickness of the uterine wall along with the amniotic membrane, the second layer buried the first to provide a water-tight seal. The transmitter was then attached to the inner surface of the abdominal wall slightly lateral to the laparotomy incision using 3-0 Prolene (Ethicon, Norderstedt, Germany). This step is necessary to allow easy accessibility since an external magnet is needed to turn the transmitter On and Off. A 3ml intramuscular injection of Penstrep (200mg/ml procaine penicillin and 250mg/ml dihydrostreptomycin; Norbrook Laboratories Ltd., County Down, UK) and a 75% intraperitoneal/25% intrauterine injection of sodium benzylpenicillin G 3g (Crystapen, Schering-Plough, Uxbridge, UK) + gentamicin 80mg (Genticin Injectable, Roche Products Ltd, Hertfordshire, UK) were given at the end of the procedure for infection prophylaxis. The abdomen was then closed in layers and buprenorphine 0.01mg/kg IM (Vetergesic, Alstoe Animal Health, York, UK) was administered every 6-12 hrs for analgesia during the first 48-72 hours after the operation and the ewe was allowed to recover.

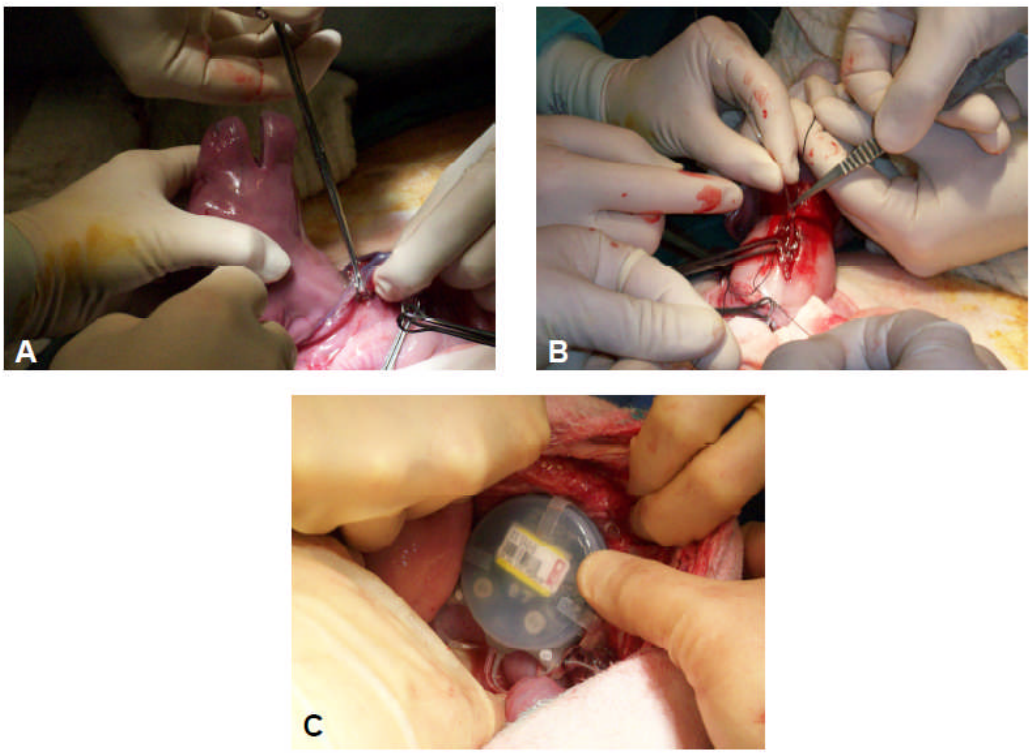

Figure 2.8 – Implantation of blood pressure sensitive catheter in the fetal carotid artery to monitor haemodynamics.

A D70-PCTP telemetric device (Data Sciences International, Tilburg, Netherlands) was used to measure blood pressure and heart rate in the fetal sheep. The device has two pressure sensitive catheters, one of which was inserted into the fetal carotid artery to measure fetal haemodynamics, while the other was inserted into the amniotic cavity to record background pressure. A – Exteriorization of fetal head to expose the fetal carotid artery after making a longitudinal incision in the neck. B – Insertion of blood pressure sensitive catheter into the fetal carotid artery. C – Attachment of the body of the implant to the inner surface of the abdominal wall.

The surgeries described above were performed by Dr. Anna David, Prof. Donald Peebles, Dr. Khalil Abi-Nader, Vedanta Mehta and Dr. Steven Shaw.

2.10 Haemodynamic monitoring

Between the probe placement and vector injection surgeries, the blood pressure and uterine blood flow of the sheep were monitored every day. The uterine artery flow probe gave a signal once the amplitude of the detected blood flow rose above 35%. This depended on how rapidly a fluid interface developed

between the probe and the vessel, a function of vessel size and took between 48-72 hours.

In order to monitor the uterine blood flow, the rechargeable battery packs and physiometer (Transonic Systems Inc, NY, USA, Figure 2.9) were placed in a back pack attached to the wool on the sheep's back. The physiometer was connected to the flow probes via the skin buttons on the upper right flank of the sheep. Once connected, the flow probes transmitted the real time uterine blood flow measurements to an acquisition computer located in close proximity by wireless Bluetooth technology. The data was acquired using the Physioview software (Transonic Systems Inc, NY, USA). A sample uterine artery blood flow waveform is represented in Figure 2.10. The wireless communication equipment operates at a worldwide available standard 2.4 GHz frequency band. The real time pulsatile flow was sampled at a frequency of 128 Hz.

Figure 2.9 – Battery pack and Physiometer

In order to monitor uterine artery blood flow in pregnant sheep, cables from the physiometer were attached to the skin buttons on the right flank of the ewe. This enabled the real-time blood flow data from the flow probes around the uterine arteries to be transmitted to an acquisition computer in close proximity, by bluetooth technology.

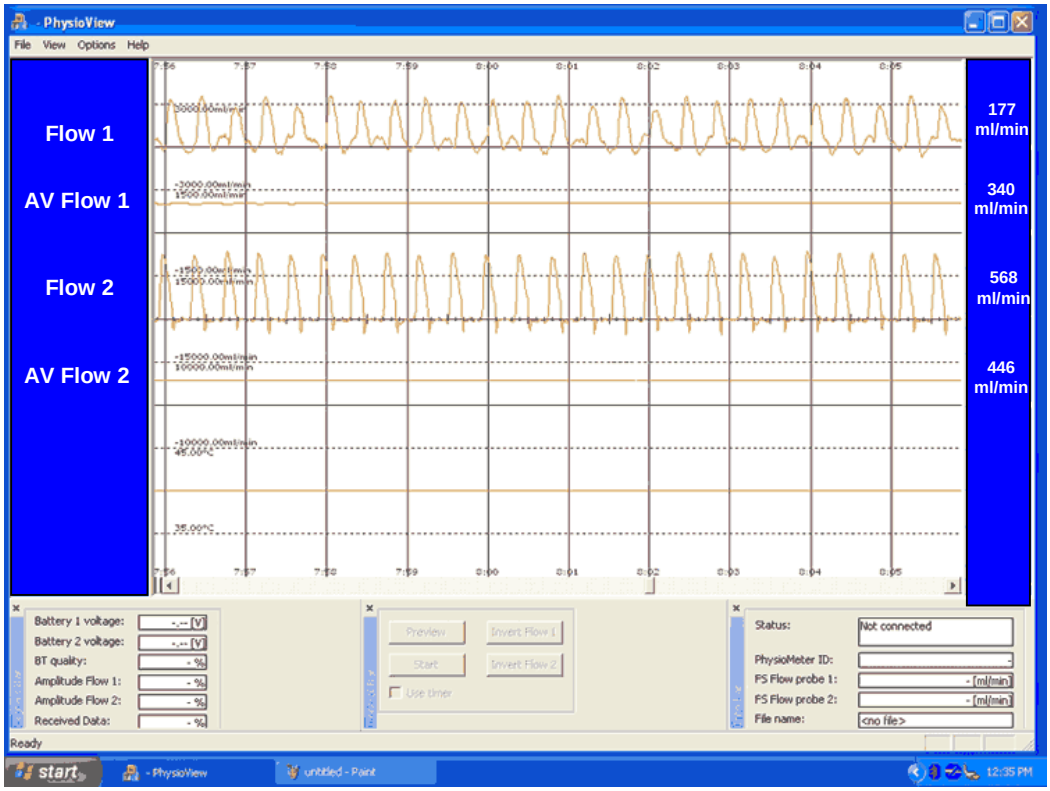

Figure 2.10 – Sample uterine artery blood flow waveform acquired using Physioview software

The uterine blood flow was monitored for 6-7 hours daily for 3 days before and 7 days after the vector injection surgery in a sub-set of the sheep. This was to investigate whether the administration of the vector had any short-term effects on the diurnal rhythm of uterine artery blood flow (UABF). Thereafter, the monitoring was reduced to one hour daily (till the day of post-mortem) at the same time everyday to eliminate the effect of any diurnal variation on uterine blood flow. The uterine artery waveforms were exported to Notepad (Microsoft Inc, NY, USA) and analysed in AcKnowledge 3.9.1 (Acknowledge Inc, Somerville, MA, USA) to derive an average value and standard deviation for each hour of monitoring.

For every sheep monitored, a baseline UABF was established for each of the two uterine arteries by averaging the values of UABF recorded for three consecutive days immediately before the administration of the vector. Each

subsequent daily reading of UABF was then compared with this baseline and converted into a percentage increase in blood flow from baseline. The latter was plotted on a line graph (MS Office Excel, Microsoft Inc, NY, USA) and the slope/gradient of increase in UABF for each uterine artery was calculated. The gradient of increase of blood flow in the uterine arteries transduced with Ad.VEGF (-A_{165} or D) and Ad.LacZ were compared using the General Linear Model Test (Minitab 5.1) to determine statistical significance.

The blood pressure signal was immediately available from the time of catheter placement. The blood pressure and heart rate were monitored continuously round the clock for 3-5 days before and ~7 days after the administration of the vector. This was to investigate if the administration of the vector had any acute detrimental effects on systemic blood pressure. Thereafter, the blood pressure was monitored for one hour daily (till the day of post-mortem) at the same time each day to eliminate the effect of diurnal variation on blood pressure.

When the blood pressure of a sheep needed to be monitored, the transmitter placed in the maternal or fetal neck was switched on with a magnet. The turned on transmitter beamed the real time blood pressure signal to the metallic receivers RMC-1 (Data Sciences International, USA) which further relayed it to an acquisition computer placed in close proximity (Figure 2.11). At the end of the monitoring period, the transmitter was turned off by swiping the magnet over the skin of the neck.

Figure 2.11 – A sheep being monitored for uterine artery blood flow and blood pressure.

In order to monitor blood pressure, the transmitter implanted in the ewe's neck was switched on with a magnet. Once 'on', the transmitter beamed the blood pressure signal to two metallic receivers (visible in picture), which further relayed the signal to an acquisition computer. To monitor UABF, the battery pack and physiometer were placed in back packs hooked on to the sheep's fleece, and connected to the skin buttons on the flank. Once connected to the flow probes (via skin buttons), the physiometer telemetrically transmitted the real time blood flow data to an acquisition computer by bluetooth technology.

The real time blood pressure waveforms were acquired using the software 'Acquisition' (Data Sciences International, USA, Figure 2.12). The acquired traces were opened up in another program 'Analysis' (Data Sciences International, USA) on which plots for Diastolic blood pressure, Systolic blood pressure and Heart Rate were constructed from the original BP waveform. These plots were exported into Microsoft Office Excel and further analysed to derive an average value of Diastolic blood pressure, Systolic blood pressure and Heart Rate for each hour of monitoring. The Mean Arterial Pressure (MAP) for each hour of monitoring was calculated from the analysed data using the formula;-

$$\text{Mean Arterial Pressure} = \frac{2\text{xDiastolic pressure} + \text{Systolic pressure}}{3}$$

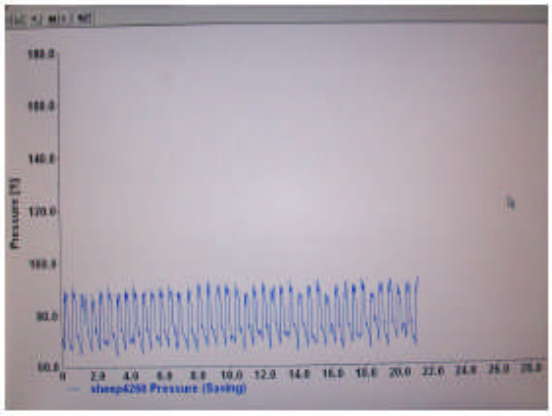

Figure 2.12 – Sample blood pressure waveform acquired using Dataquest Acquisition Software (DSI, Tilburg, Netherlands)

Statistical analysis was performed by comparing the MAP values before and after the administration of the vector (at the same time of the day) using paired t-test.

2.11 BrdU infusion for assessment of cell division

A sub-set of sheep received an intravenous infusion of BrdU 48 hours before their scheduled post-mortem examination in order to assess endothelial cell proliferation. Normal saline was warmed to 40-50°C and BrdU (B5002, Sigma Aldrich, Gillingham, Dorset, UK) was slowly dissolved in it by gentle vortexing to yield a final concentration of 20mg/ml. Once completely dissolved, the BrdU injection solution was allowed to cool down to room temperature (22-25°C).

The weight of the sheep was taken using special scales designed for large animals. Half an hour before the infusion, the sheep was administered Diazepam (1 mg/kg, Hameln Pharmaceuticals, Gloucester, UK) sub-cutaneously and restrained in a crate. The fleece on her ear was shaved with an electric clipper, cleaned with 70% ethanol, followed by the application of EMLA cream (Lidocaine/prilocaine mixture in 5% oil-in-water emulsion) for at least 30 minutes to provide local anaesthesia. A 21-gauge butterfly needle was then inserted into the marginal vein of the ear. Blood was withdrawn to confirm the placement of the needle in the vein. The catheter and needle were flushed with heparinised

saline, and the needle was secured in its position by wrapping it up in tape. The sheep's head was supported during the procedure to prevent her pulling the needle out.

A total of 20mg BrdU/kg of body weight was slowly infused into the venous catheter over 20 to 25 minutes (Figure 2.13). The needle was then withdrawn from the vein, and the injection site was digitally compressed for a minute to achieve hemostasis. The sheep was released from the crate and returned to her pen at the end of the procedure.

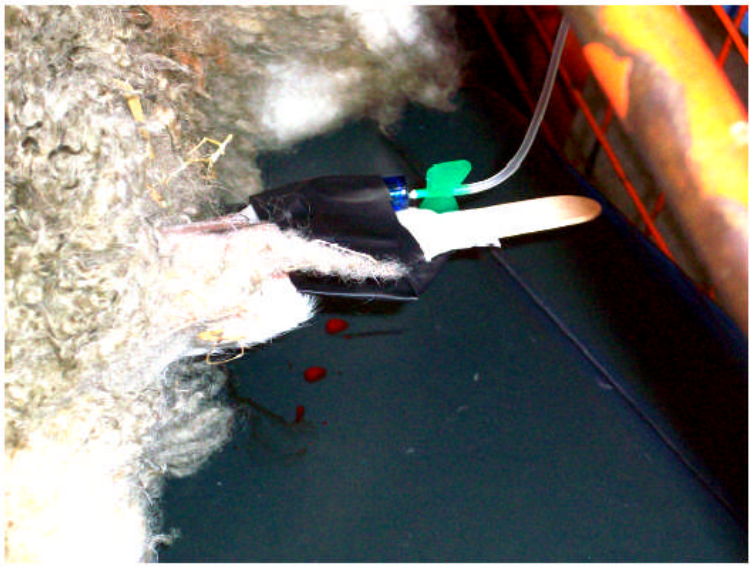

Figure 2.13 – Infusion of BrdU into the marginal vein of the ewe's ear.

The endothelial cell proliferation in uterine arteries of pregnant ewes in response to over-expression of VEGF was examined by BrdU immunohistochemistry. The animals received an intravenous BrdU infusion (20 mg/kg bodyweight) into the marginal vein of the ear after application of EMLA cream for local anaesthesia. The infusion was carried out 48 hours before post-mortem examination.

The BrdU infusion was carried out by Mr. Michael Boyd, Dr. Anna David and Vedanta Mehta.

2.12 Post-mortem examination

The post-mortem examination was performed approximately five days before the expected date of delivery (range 3 to 7 days, delivery usually at 145

days of gestation). The ewe was anaesthetized as before, and fetal measurements and umbilical artery Doppler examination were recorded by ultrasound. The post-mortem was performed under terminal anaesthesia to maintain perfusion to the uterine arteries during clearing. This was essential to prevent any endothelial damage that occurs rapidly after death.

Maternal blood was sampled for biochemistry and haematological analysis. The abdomen was reopened using the previous scar. The uterine arteries were stripped gently of their surrounding serosa and two loose ties were placed around the proximal segment of each uterine artery, just below the flow probe, which was then removed. The uterine arteries were then gently cleared of the surrounding serosa down to the third branch (Figure 2.14). Once the vessels had been cleared, the ewe was put down by injecting 40ml of Euthatal (sodium pentobarbitone, Rhône Merieux, Essex UK) into the carotid vein. Once the cessation of heart beat was confirmed, the proximal tie was tied securely round the uterine arteries which were then divided distally. The entire uterine artery tree to the third branch was then removed gently in one piece and placed immediately into cold Kreb's buffer (K0507, Sigma Aldrich, Gillingham, Dorset, UK). The uterine arteries were further cleared in cold Kreb's buffer and the branches were separated.

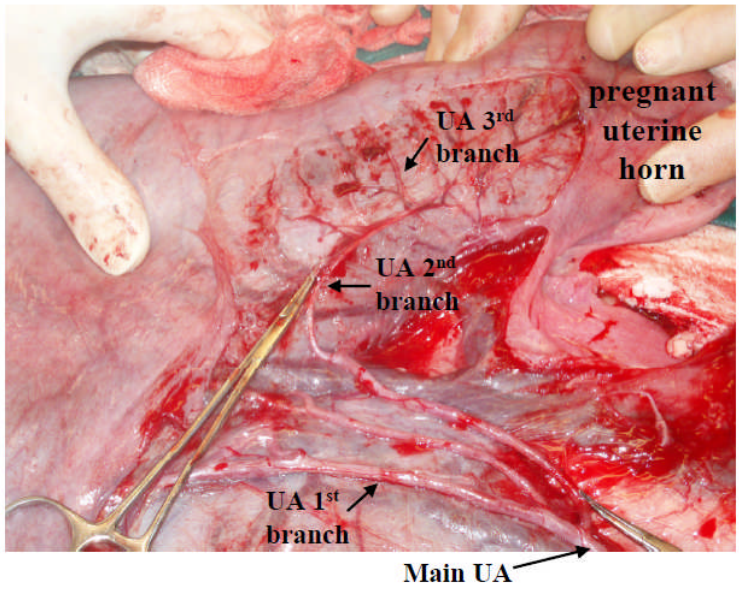

Figure 2.14 – The branches of the uterine artery dissected out at post-mortem examination.

The different braches of the uterine artery (main branch, 1st branch, 2nd branch and 3rd branch) were dissected out under terminal anaesthesia. Samples were taken from each of the branches for RNA extraction, protein extraction, histology, immunohistochemistry and organ bath pharmacology.

The uterus was opened and amniotic fluid was collected and snap frozen. The umbilical cord was tied and cut and the fetal sheep was removed from the uterine cavity. Fetal blood was sampled from the umbilical veins for VEGF ELISA, biochemistry and haematological analysis. Maternal and fetal organs were sampled widely according to a standard proforma, organs were weighed and measurement of fetal parameters was undertaken (Appendix IV).

Samples from each tissue were snap-frozen in liquid nitrogen for future nucleic acid/protein extraction. One sample from each tissue was placed in a histology cassette and dropped into 4% paraformaldehyde (pH 7.4) overnight before transfer into 70% ethanol.

2.13 Organ Bath Studies

2.13.1 Principle:

Organ bath is an *in vitro* technique that allows us to examine functional responses and vascular reactivity of isolated arterial or venous segments. In organ bath experiments, a blood vessel is cleared of surrounding fat and connective tissue and mounted between two L-shaped pins in physiological medium. The medium is bubbled with oxygen and maintained at 37°C. The contractility and relaxation of the vessel is examined by subjecting it to increasing doses of agonists. A force transducer calculates the tension changes in response to different agents under isometric conditions, i.e, the vessel diameter is kept constant and displays this information as a real-time trace on a computer (Figure 2.15).

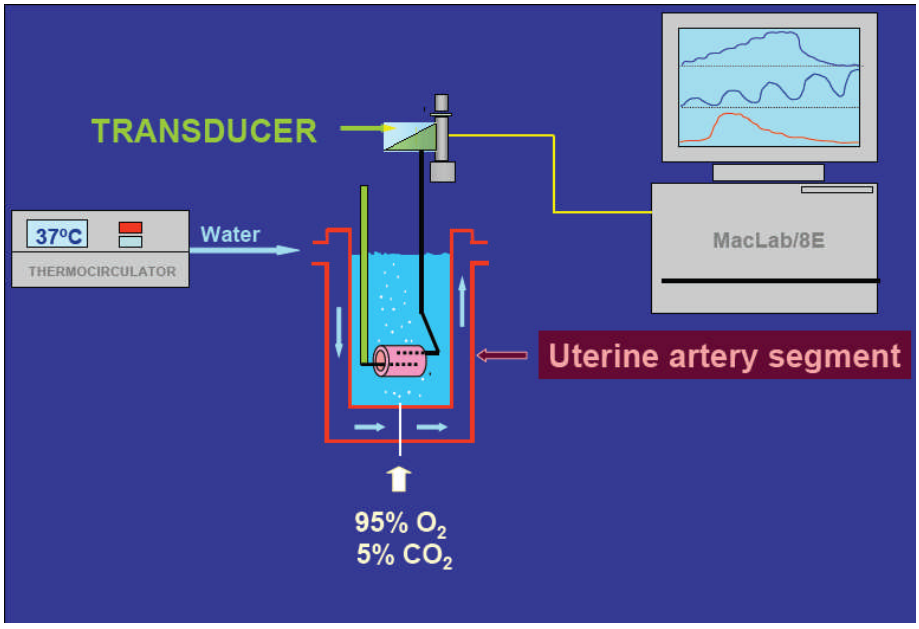

Figure 2.15 – Principle of organ bath analysis

A small segment of a blood vessel is suspended between two L-shaped pins in an organ bath chamber. The chamber is filled with Kreb's buffer through which carbogen gas (95% O_2, 5% CO_2) is constantly bubbled. The solution in the chamber is maintained at 37°C using a water thermocirculator. Agonists added directly into the organ bath chamber cause the vessel ring to either contract or relax. The change in the tension of the vessel is measured by a force transducer and recorded on an acquisition computer as a real-time trace.

2.13.2 Method:

The uterine arteries were transported from the BSU Camden to the Rayne Institute, UCL in freshly made Kreb's buffer within 1 hour of retrieval from the ewe. Their pharmacologic responses were analysed on an 8 chambered organ bath set-up. Under a microscope, the branches were cleared of surrounding connective tissue within a petri-dish containing Kreb's buffer and cut into 3mm long rings. Each ring was carefully mounted between the two L-shaped pins of a 25ml organ bath, ensuring the endothelium was not damaged. The composition of the Kreb's buffer used is described in Appendix II. The Kreb's buffer was bubbled with carbogen gas (95% oxygen, 5% carbon dioxide) to maintain a physiological pH of 7.4, and the temperature was maintained at 37°C with a water thermocirculator.

Following mounting, the vessels were allowed to equilibrate for one hour, with washing every 15 minutes. During this time, the basal tension was also gradually increased to 1.0g in small steps, to allow the vessels to generate their optimum response to the agonists in future steps.

After one hour, the vessels were challenged with 48mM Potassium chloride (KCl) to test for viability and also to determine the maximum contractility. They were then washed 3 times with Kreb's buffer, and challenged again after 20 minutes. In all, they were challenged 3-4 times with KCl, till the maximum contractile response generated was equal to the previous response ($\pm$5%). A contractile response greater than 1.5g was considered viable.

After the KCl stimulation, the vessels were again allowed to rest for 30 minutes, during which time they were washed 3 times with Kreb's buffer. Then, a dose response curve to L-phenylephrine (L-1286 Sigma Aldrich) was generated (10^{-9} to $3x10^{-5}$M). The next higher dose was added only after the contraction induced by the previous dose had stabilized.

The vessels were again allowed to rest for 30 minutes, during which they were washed 4-5 times with Kreb's buffer, until they attained the basal tone. After attaining the basal tone, they were pre-contracted with phenylephrine, until they achieved an absolute contraction between 2-4 grams. Once the contraction had stabilized, they were made to relax to bradykinin (B-3259, Sigma Aldrich, 10^{-11} to

$3x10^{-7}$M). After the bradykinin dose-response curve, the vessels were washed and different inhibitors of relaxation were added to the organ bath chamber. Following appropriate incubation times; 20 minutes for L-NAME, ($3x10^{-4}$ M, N5751, Sigma Aldrich, a NOS inhibitor), 20 minutes for Indomethacin/NS-398, (10^{-5} M, I7378/N-194, Sigma Aldrich, a COX inhibitor), and 30 minutes for Apamin, (10^{-6} M, A-1289, Sigma Aldrich, an inhibitor of the EDHF pathway), the vessels were again pre-contracted and then relaxed exactly as described previously. The contractility of the vessels to L-phenylephrine in the presence of L-NAME was also examined.

The real-time traces were analysed using Chart Wizard 4.2.1. The extracted data was plotted in the form of a points-graph with non-linear regression using GraphPad Prism 5.0, and statistical significance was assessed using two-way ANOVA.

2.14 Histology of tissues and determination of intima/media ratios

Tissues samples were fixed in 4% paraformaldehyde overnight, transferred to 70% ethanol the next day and processed into paraffin in cassettes using a Thermo Shandon Pathfinder Histology processor (Thermo Scientific, Surrey, UK). The paraffinised tissue blocks were cut into 3-micron thick sections using a microtome, and the ribbon was floated in a water bath (37°C) until it had completely stretched. The stretched paraffin ribbon was placed in the centre of a glass slide and air dried. The slides used were coated with Polylysine (631-0107 VWR, Leuven, Germany) to ensure that the tissue stuck firmly and did not fall off during subsequent immunohistochemistry steps.

One slide of each section was used for H&E staining to look for pathological changes. H&E staining was performed by immersing the slide in hematoxylin solution made up in PBS pH 7.2 for 5 minutes and washed 3 times in PBS before being immersed in 1% eosin counterstain solution made up in PBS pH 7.2 for 5 seconds and washed 3 times in PBS. Sections were processed

through an increasing alcohol gradient into xylene and then mounted in DPX mounting medium. A coverslip was placed over the section and the slide was allowed to dry. Slides were analysed under normal light microscopy with the assistance of Dr. Elizabeth Benjamin, Department of Pathology and Institute for Women's Health, University College London.

H&E stained sections of the uterine arteries were photographed under 10x magnification on a microscope (Nikon Eclipse E600, Amstelveen, Netherlands), and the photomicrographs were imported into Image J (National Institute of Health, USA) for further analysis. The relative thicknesses of the intimal and medial layers were determined using the 'Track and Trace' Function to calculate the intima/media ratios.

2.15 Adventitial Vessel enumeration

One of the important functions of VEGF is angiogenesis or formation of new blood vessels. In order to confirm this, the number of adventitial blood vessels was assessed in ovine uterine arteries that been transduced with either Ad.VEGF-A_{165} or Ad.LacZ.

The number of adventitial blood vessels was first counted in H&E stained sections by light microscopy. However, it was considered more appropriate and informative to perform this count on immunohistochemically stained sections, using an antibody that specifically stains the endothelium. Hence, the uterine artery sections of pregnant sheep were stained with two antibodies that are commonly used to stain the endothelium – anti-von Willebrand Factor (vWF) and anti-CD31.

2.15.1 Principle of Immunohistochemistry

Immunohistochemistry (IHC) refers to the process of localizing antigens (proteins) in cells of a tissue section exploiting the fundamental principle of antibodies binding specifically to antigens in biological tissues. Visualising an

antibody-antigen interaction can be accomplished in a number of ways. In the most common instance, an antibody is conjugated to an enzyme, such as peroxidase, that can catalyse a colour-producing reaction on addition of an appropriate substrate. Alternatively, the antibody can also be tagged to a fluorophore, such as fluorescein. rhodamine or alexafluor (this is known as immunofluorescent staining).

The advantage of IHC over techniques like Enzyme-linked Immunosorbent Assay (ELISA) or Western blotting (which function on the same principle) is the ability to identify and locate specific proteins within the tissue structure, which adds a whole new dimension to the technique. The target immunogens may sometimes be physically "hidden" from the antibody, because of protein folding or formation of cross-linking methylene bridges during 'fixation'. An antigen retrieval step, where enzymes or heat are used to re-model the protein structure and break down methylene bridges, may be required to visualise some antigens.

2.15.2 Method

Paraffin sections on slides were dewaxed and hydrated, by sequentially passing through the following steps: xylene (3 min, BDH), xylene (3 min), xylene (3 min), absolute ethanol (2 min, BDH), absolute ethanol (2 min), 95% ethanol (1 min), 95% ethanol (1 min), 70% ethanol (2 min), 70% ethanol (2 min), distilled water (5 min). Endogenous peroxidase activity was blocked by immersing the slide in 0.6% Hydrogen peroxide (Sigma Aldrich) for 15 minutes. The slide was then rinsed in tap water. A boundary was made around the tissue section using a DAKO pen (DAKO, Glostrup, Denmark). Antigen retrieval was performed by trypsin digestion to unmask the antigen sites that may have become cross-linked during fixation. A fresh solution of 0.1% trypsin (Difco Trypsin-250, 215240, BD Biosciences, Oxford, UK) and 0.1% calcium chloride was prepared in 0.005M Tris buffered saline at 37°C, pH 7.8. Slides were immersed for 10 minutes and then rinsed in PBS.

Non-specific antibody binding to proteins in tissue preparations was prevented by applying 5% non-immune goat serum (X0907, Dako, Glostrup, Germany) to each slide for 30 minutes at room temperature, the serum being from the species which provided the second layer antibody. The primary antibody rabbit anti-human von Willebrand factor (anti-vWF, A0082, Dako) was diluted in PBS with 0.1% BSA (PBS/BSA) at varying concentrations (1:50, 1:100, 1:200, 1:400 and 1:800) and pipetted on the tissue sections within the boundary (~200 µl). The slides were then placed at 4°C overnight in a humidified chamber. Negative controls were obtained by omitting the incubation with primary antibody.

Next morning, secondary goat anti-rabbit biotinylated IgG (E0432, Dako, Glostrup, Denmark) was diluted 1:100 in PBS/BSA and added to the slides after washing with PBS/BSA. The slides were kept at room temperature for one hour. During the last half hour of incubation, the ABC Solution (PK 4000, Vector Laboratories, Peterborough, UK) was prepared as per manufacturer's protocol, and allowed to stand at room temperature for at least 30 minutes.

The slides were then washed with PBS/BSA (1 wash), followed by PBS (2 washes). The ABC solution was then added to the tissue sections after gently drying off the excess buffer. The slides were further incubated at room temperature for 1 hour.

Towards the end of incubation, the 3-3'diaminobenzidine (DAB) substrate solution (D5905, Sigma Aldrich) was prepared. 25mg of DAB were added to 50 ml of PBS and the solution was vigorously vortexed and filtered. The slides were rinsed with PBS. Just before use, 16.7µl of 30% Hydrogen peroxide was added to the DAB solution which was mixed and transferred to a cuvette. The slides were transferred into the solution and allowed to stain for about 15 minutes, before the reaction was stopped by transferring the slides to water.

The stained sections were counterstained with Mayer's haematoxylin solution (51275, Fluka, USA), differentiated in Scott's tap water and destained in acid alcohol. The slides were then dehydrated by passing through an ascending

alcohol gradient, followed by 3 changes in xylene. They were finally mounted in DPX and covered with a cover slip.

The appropriate primary antibody concentration was determined, and all remaining slides were stained using this concentration. The blood vessels in the perivascular adventitia were observed under a microscope (Nikon Eclipse E600, Amstelveen, Netherlands). The number of positively stained vessels with a distinct lumen was counted in duplicate sections and compared between the uterine arteries from both the Ad.VEGF and Ad.LacZ injected sides. The statistical significance was determined using unpaired t-test.

2.16 Immunohistochemistry for VEGF receptors

The paraffinised tissue sections were dewaxed and hydrated as described above. Antigen retrieval was performed by treating the tissue sections in Pronase (10165921001, Roche Diagnostics, Germany) for 15 minutes at room temperature (for Neuropilin-1 staining) or boiling in Citrate buffer pH 6.0 for 20 minutes (for VEGFR-1 and VEGFR-2). The sections were then treated with 3% Hydrogen peroxide for 15 minutes to block endogenous peroxidases, washed with PBS and permeabilized by treating in PBS with 0.1% Tween-20 (PBST) for 15 minutes. The slides were washed again and blocked in rabbit serum (X0902, Dako) (for Neuropilin-1 and VEGFR-2) or goat serum (for VEGFR-1). A goat polyclonal neuropilin-1 (1:50, sc-7239 Santa Cruz Biotechnology USA), rabbit polyclonal VEGFR-1 (1:50, sc-316 Santa Cruz Biotechnology) or mouse monoclonal VEGFR-2 (1:50, sc-6251 Santa Cruz Biotechnology) primary antibody was applied to the tissue sections overnight at 4°C in a humidified chamber.

Next morning, the slides were washed and the appropriate secondary antibody was applied at 1:400 dilution, polyclonal rabbit anti-goat biotinylated IgG (E0466 Dako Glostrup Denmark) for neuropilin-1, polyclonal rabbit anti-mouse biotinylated IgG (E0464 Dako Glostrup Denmark) for VEGFR-2 and polyclonal goat anti-rabbit biotinylated IgG (E0432 Dako Glostrup Denmark) for

VEGFR-1. The slides were then stained and fixed as has been described for anti-vWF staining.

2.17 Immuno-Fluorescence Double Labeling for BrdU and vWF

Uterine arteries from sheep that had been infused with BrdU were fixed, processed, paraffin embedded and sectioned as has been described previously. The tissue sections were used for double labeling with anti-BrdU antibody (a cell proliferation maker) and anti-vWF antibody (an endothelial marker) to specifically identify proliferating endothelial cells.

The dewaxing, blocking of endogenous peroxidases, antigen retrieval (with trypsin), blocking of non-specific binding sites with pre-immune serum and application of primary anti-vWF were performed as has been described previously (Section 2.15.2). The only difference is that in place of non-immune goat serum, non-immune donkey serum (D9663, Sigma Aldrich) was used for the blocking step (as donkey is the species in which both the secondary and tertiary antibodies had been raised).

Next morning, the slides were rinsed with PBS/BSA, followed by a one hour room temperature incubation with biotinylated donkey anti-rabbit secondary antibody (1:100, 711-065-152, Jackson ImmunoResearch, West Grove, PA, USA). The slides were then rinsed with PBS, and the sections were incubated for another one hour with the avidin-biotinylated horseradish peroxidase complex (ABC, PK 4000, Vector Laboratories, Peterborough, UK). The deposited ABC Complex was detected via covalent conjugation of biotinylated tyramide (1:1000 in PBS, Dupont, UK), reacted in the presence of 0.01% Hydrogen peroxide in PBS for 10 minutes at room temperature (Werner A et al., 1998). This treatment with biotinylated tyramide allowed us to transform an initially noncovalent form of biotin labeling into a covalent one, to allow the label to withstand the post-treatment with 2N Hydrochloric acid (HCl) for 45 minutes at room temperature needed to expose the BrdU antigen (by dissociating the histones and partially

denaturing DNA). The HCl-treated sections were briefly washed in PBS, exposed for 30 minutes to 0.1M boric acid/sodium borate buffer (pH 8.5), washed in PBS again, pre-incubated with 0.5% Triton X-100 and 5% donkey serum in PBS and then incubated with the primary mouse antibody against BrdU (1:100 Dako, Glostrup, Germany M0744) overnight at 4°C. This step was followed by a one hour incubation with a secondary Alexafluor-488 conjugated goat anti-mouse IgG (1:200, 11001, Invitrogen, Paisley, UK) and then enhanced with a tertiary Alexafluor-488 conjugated donkey anti-goat antibody (1:200, 11055, Invitrogen, Paisley, UK), in combination with Texas Red Streptavidin (016-070-084, Jackson Immunoresearch) for one hour at room temperature. The sections were covered with mounting medium with DAPI (H-1200, Vector Laboratories, UK) and stored in the dark at 4°C before use. Negative controls were obtained by not exposing the tissue section to either of the primary antibodies.
This analysis was performed by Vedanta Mehta and Panicos Shangaris.

2.18 Confocal Microscopy

For visualizing the immuno-fluorescence double labeling, digital micrographs of the Alexafluor-488 for the BrdU staining and Texas red fluorescence for vWF were taken representing an area of 1mm x 1mm (1024 pixels x 1024 pixels; grayscale 0-255) with a Leica TCS 4D confocal laser microscope using a 20X objective (Milton Keynes, UK). The fluorescence was excited using low ArKr laser power (0.25V) at wavelengths of 488 nm for Alexafluor-488, 568 nm for Texas Red and 358 nm (ultraviolet) for DAPI, and detected using the BP-FITC filter for Alexafluor-488, the LP590 filter for Texas Red and the LP360 filter for DAPI, respectively. Nine consecutive, equidistant levels were recorded and condensed to a single bitmap using the MaxIntens algorithm.

Confocal Microscopy was performed by Vedanta Mehta under the supervision of the technical staff at the Imaging Facility, Rockefeller Building, UCL.

2.19 RT-PCR

To determine the extent of vector expression, Reverse-Transcription (RT)-PCR was performed on a number of maternal and fetal samples (maternal uterine arteries, uterus and placentomes; maternal and fetal gonad, adrenal, lung, liver, kidney, spleen, brain and thymus) obtained at post-mortem examination.

For RT-PCR, total RNA was isolated from 30-40mg of snap-frozen tissues using the Qiagen RNeasy Mini Kit (74104, Qiagen Ltd, Crawley, West Sussex, UK) as per manufacturer's instructions, with an additional proteinase-K (19131, Qiagen) digestion step (following homogenization) at 55°C for 10 minutes. The yield and purity of RNA was estimated on a spectrophometer by measuring the A_{260}/A_{280} ratio, and considered to be suitable for analysis if the ratio was 1.80-1.95. Total RNA (1µg) was reverse transcribed to cDNA using the QuantiTect Reverse Transcription Kit (205311, Qiagen). The RT step was carried out at 42°C for 30 minutes.

PCR was performed on the cDNA generated using the Taq PCR Master Mix Kit (201443, Qiagen). For Ad.VEGF-A_{165} detection, the forward primers used (Table 2.1) were designed to span the vector transgene boundary (Viita H et al., 2008) to ensure that the reaction was sensitive only for the transgenic *vegf*, and not endogenous *vegf*. In all cases, a PTC-100 Thermocycler (MJ Research Inc., Watertown, MA, USA) was used and the PCR final reaction volume was 20 µl. Each reaction contained 10 µl Taq PCR Master Mix, 6 µl sterile double distilled water, 1 µl forward primer (to yield a final concentration of 1 µM), 1 µl reverse primer (to yield a final concentration of 1 µM) and 2 µl cDNA. The PCR cycle was 94°C for 4 minutes, followed by 30 cycles of denaturation at 94°C for 1 minute, annealing at 64°C for 1 minute and extension at 72°C for 1 minute, followed by a final extension step of 72°C for 10 minutes.

The RT-PCR, described as above was further sensitized by following it with a semi-nested approach. 2 µl of the first round reaction product was transferred to a fresh tube and used as the template for the second round PCR step. The second round forward primer was identical to the first round forward

primer, but the reverse primer bound to the template at a site more internal than the complementary binding site of the first round reverse primer (Table 2.1, Figure 2.16). The annealing temperature was kept at 54°C. All other thermocyling steps were identical to the first round reaction protocol. The primer sequence and thermocycling protocol for both the first round and second round PCR is described in Table 2.1. *The optimization of the semi-nested PCR has been described in the Results Section.*

Table 2.1 – Primer sequence and protocol to determine Ad.VEGF-A_{165} expression in ovine maternal and fetal samples

Primer	Sequence	Annealting Temperature and Time	Expected Product size
1st round Forward Primer	5`-TCAGATCCATGAACTTTCTGC-3`	64°C for 60 seconds	366 base pairs
1st round Reverse Primer	5`-TCTCTCCTATGTGCTGGCCT-3`	64°C for 60 seconds	
2nd round Forward Primer	5`-TCAGATCCATGAACTTTCTGC-3`	54°C for 60 seconds	330 base pairs
2nd round Reverse Primer	5`-GATCCGCATAATCTGCATGGT-3`	54°C for 60 seconds	

Figure 2.16 – Sites of primer binding for first round and second round of semi-nested RT-PCR to determine Ad.VEGF-A_{165} expression

Ψ = packaging signal, ITR = Inverted terminal repeats, CMV = Cytomegalovirus promoter

As a positive control to show the presence of sheep cDNA in the reverse transcribed samples, primers to endogenous sheep sequences (kindly provided by Dr. Jill Maddox, University of Melbourne) were tested for specificity. These primers were designed from cattle sequences and amplified sheep sequences of transcription factor COUP-TF1 (COUPTF1, GenBank ref AJ249440), TATA box

binding protein (TBP, GenBank ref L47974) and scavenger receptor class B type 1 (SRB1, GenBank ref AF019384). The TBP primer was found to be the most specific for sheep DNA and the one that gave no non-specific amplification signal with adenovirus alone (David AL, 2005, Ph.D. Thesis). It was thus used as a positive control for sheep cDNA in future investigations. The reaction conditions for the amplification of the TBP gene are summaried in Table 2.2.

Table 2.2 – PCR conditions for Tatabox binding protein in sheep tissues.

Product size	127 base pairs
Forward primer	5`-TCTGTCTATTCTGGAGGAGCAGCAAC-3`
Reverse primer	5`-TGCCTGCTGGGACGTCGACT-3`
Annealing temperature	65°C

All products of PCR amplification were subjected to electrophoresis alongside a 1kb+ DNA ladder on a 1% agarose gel containing ethidium bromide (10mg/ml) at 80V for 1 hour. The gel was visualized on an ultra-violet transilluminator and photographed on Gel Documentation System (Syngene, Cambridge, UK). For the Ad.VEGF-A_{165} PCR, RNA samples from uninjected sheep, non-infected HUVECs and a water blank were used as negative controls; while RNA from HUVECs or sheep uterine artery endothelial cells transduced with Ad.VEGF-A_{165} was used as a positive control. For the TBP PCR, water blank was used as a negative control. Each tissue was subjected to PCR analysis twice.

Analysis was performed by Vedanta Mehta and assisted by Gemma Petts.

2.20 Blood Investigations

Analysis of blood count, biochemistry, liver function and bile acids was performed on maternal and fetal blood samples at the Royal Veterinary College pathology department (Clinical Sciences Division), Hawkshead Campus, Potters Bar. Maternal samples were analysed before vector injection and at post-mortem,

while fetal samples could only be analysed at post-mortem. An optimum data set for blood analysis was investigated (Table 2.3, David AL, 2005, Ph.D. Thesis)

Table 2.3 – Blood analysis performed on samples from experimental maternal and fetal sheep

Haematological analysis	Serum biochemistry	Liver function tests
White blood cell count	Total protein conc.	Glutamate dehydrogenase
Neutrophil count and %	Albumin conc.	Aspartate transaminase
Lymphocyte count and %	Globulin conc.	Gamma-glutamyltransferase
Monocyte count and %	Sodium conc.	Creatine kinase
Eosinophil count and %	Potassium conc.	Total bilirubin conc.
Basophil count and %	Chloride conc.	Bile acids
Red blood cell count	Bicarbonate conc.	
Haemoglobin conc.	Anion gap	
Haematocrit	Calcium conc.	
Mean red cell volume and haemoglobin conc.	Inorganic phosphorous conc.	
Platelet count	Urea conc.	
	Creatinine conc.	

conc.:concentration

2.21 Isolation of primary uterine artery endothelial cells (UAECs)

The uterine arteries from mid-gestation pregnant sheep (approximately 90-100 days, n=6) were dissected free of surrounding connective tissue and cleared right from their origin at the internal iliac artery up to the level of the 2nd division, under terminal anaesthesia, as previously described. The ewe was then put down

with an overdose of intravenous pentobarbitone (40ml, Euthatal, Rhône, Merieux, Essex, UK) and the uterine arteries were ligated at the two ends using 1-0 silk ties and removed as a single piece (which included the main, first and second branches). They were transported from the BSU to the tissue culture laboratory in UCL in falcon tubes containing Endothelial Cell Basal Medium (EBM, CC3124, Lonza, Walkersville, USA) supplemented with 1.5µg/ml Fungizone (15290-026, Invitrogen, Paisley, UK).

The uterine arteries were then placed in a petri-dish in a sterile laminar flow hood and cleared further of surrounding connective tissue and blood clots. At the proximal end of the uterine arteries, a 23 gauge butterfly needle was introduced and secured tightly with a haemostat. About 50ml of M-199 (41150-020, Invitrogen, Paisley, UK) was flushed through the vessel to remove all blood clots. The distal end of the vessel was then tied off and it was inflated with EBM containing 5mg/ml collagenase (11088815001, Roche Diagnostics, Mannheim, Germany) and 0.5% bovine serum albumin (BSA) (A4503, Sigma Aldrich, UK) to help dissociate endothelial cells from the vessel wall. The inflated vessel was placed in the 37°C incubator for varying lengths of time, either 15 minutes or 55 minutes (Bird IM et al., 2000;Grummer MA et al., 2009). The distal tie was then cut and the contents of the vessel were flushed into a falcon tube using Endothelial Cell Growth Medium (EGM, described in Appendix III). The contents of the falcon were centrifuged at 1000rpm for eight minutes two times to concentrate the endothelial cell fraction. After each cycle, the supernatant was removed and the pellet was re-suspended in EGM to remove all debris.

The freshly isolated cells were considered to be at passage 0 and plated in 4 wells of a 6-well plate (140675, Nunc, Roskilde, Denmark) in EGM containing 10% Fetal bovine serum, 1% penicillin-streptomycin (15140-122, Invitrogen, Paisley, UK). All cell surfaces on which endothelial cells were cultured were treated with gelatin (G1393, Sigma Aldrich) to enhance adhesion to the surface. Cells were grown for approximately 6 days and passaged (passage 1) to T-25 flasks (136196, Nunc). To passage the UAECs, they were first rinsed with EBM (containing no serum) as serum is known to inhibit the action of trypsin. The cells

were then treated with 0.25% trypsin (25200-056, Invitrogen) and kept in the incubator for 2 minutes. Detachment of cells from the culture dish surface was confirmed under the microscope. If a large number of cells were still adherent, the incubation time with trypsin was prolonged. Following this, the reaction with trypsin was quenched by the addition of EGM. This medium containing free floating cells was transferred to a falcon tube for centrifugation. After two washes in EGM, cells were plated to new dishes (T-25 flasks).

Cells were then grown to 70% confluence in T-25 flasks and then passaged (passage 2) to T-75 flasks (178905, Nunc). Cells were again grown to approximately 70% confluence and passaged once more (passage 3) to T-175 flasks (178883, Nunc). Once ready for passage, the cells were passaged (passage 4) to 6-well plates for adenovirus infection experiments. The number of cells seeded per well was $3.5x10^5$, as determined by a haemocytometer-based automated cell counter (Adam-MC Cell Counter, Digital Bio, Korea).

For immunofluorescent staining, a gelatinized cover slip was placed at the bottom of the 6-well plate before seeding the cells.

2.22 Experiments to confirm identity of uterine artery endothelial cells

To ensure that isolated and cultured cells were of endothelial origin, three experiments were performed.

2.22.1 Immunofluorescent staining

$3.5x10^5$ cells/well were seeded on a gelatinized cover-slip in a 6-well plate and allowed to grow until completely confluent (usually overnight). Next morning, the medium was aspirated and 4% formaldehyde was added gently along the edge of each well to fix the cells. The plate was kept on a shaking platform for 15 minutes, after which the formaldehyde was discarded and the cells were washed twice with PBS. 0.1% Triton X-100 (diluted in PBS) was then added

to each well to permeabilize the cell membrane. The solution was aspirated after 10 minutes and the cells were washed twice with PBS.

Primary antibodies were prepared in PBS containing 0.1% Tween-20 and 1% BSA. The antibodies used are outlined in the Table 2.4. After the addition of the primary antibody, the plate was left overnight at 4°C on the shaking platform. Next morning, the cells were washed three times in PBS. The appropriate secondary antibodies (Table 2.4) were prepared in the same solution and added to the cells for one hour at room temperature. The wells were again washed three times with PBS. The coverslip was then gently lifted up and flipped over a drop of 4',6-diamidino-2-phenylindole (DAPI) solution on a glass slide (with the cell adhering surface of the coverslip facing down). After five minutes, the slides were observed under a fluorescent microscope and subsequently photographed on a confocal microscope. Negative controls were obtained by omission of the primary antibody.

Table 2.4 – Antibodies used for detecting sheep uterine artery endothelial cells

Target antigen for immuno-staining	Primary and secondary antibodies
vWF	1° = polyclonal rabbit anti-human vWF (1:400, A0082, Dako, Glostrup, Germany) 2° = Alexafluor-488 donkey anti-rabbit IgG (1:1000, A21206, Invitrogen, Paisley, UK)
β-catenin	1° = rabbit monoclonal anti- β-catenin (1:2000, C2206, Sigma Aldrich, Gillingham, Dorset, UK) 2° = Alexafluor-488 donkey anti-rabbit IgG (1:1000, A21206, Invitrogen, Paisley, UK)
VE-cadherin	1° = mouse monoclonal anti-VE cadherin (1:500, sc9989, Santa Cruz Biotechnology, Heidelberg, Germany) 2° = Alexafluor-488 goat anti-mouse IgG (1:1000, A11001, Invitrogen, Paisley, UK)

2.22.2 Acetylated LDL analysis

Endothelial cells internalize and degrade Acetylated Low Density Lipoprotein (Ac-LDL) 7-15 faster than smooth muscle cells via the "scavenger cell pathway" of LDL metabolism. This has enabled the identification of endothelial cells distinctly from smooth muscle cells based on their increased metabolism of Ac-LDL (Voyta JC et al., 1984).

The UAECs were incubated with Ac-LDL tagged with Alexafluor-488 to confirm their endothelial identity (L-23380, Invitrogen, UK). Ac-LDL was added directly to cells growing in culture in 1 ml EBM (serum-free) to yield a final concentration of 10μg/ml and left to incubate for four hours at 37°C. The medium was then aspirated and fresh PBS was added. Cells were then observed under a fluorescent microscope and photographed on a confocal microscope.

2.22.3 VEGF challenge

UAECs grown to confluence in a 6-well plate were serum deprived overnight. Next morning, VEGF-A_{165} protein (293-VE-010, R&D Systems) was added to a well to yield a final concentration of 25μg/ml. Control wells were serum deprived overnight but not challenged with the VEGF-A_{165} protein. The plate was returned to the 37°C incubator for 10 minutes, after which, the cells were rinsed in cold PBS and protein extracted, as described below (Section 2.25). The protein extract was probed with an antibody to phosphorylated-ERK Thr^{202} Tyr^{204} (1:1000, 9101, Cell Signaling Technology, Danvers, MA, USA) following which the membrane was stripped and re-probed with an antibody to total ERK (1:1000, 9102, Cell Signaling Technology) by western blotting. The secondary antibody used was goat anti-rabbit IgG-HRP (1:8000, sc-2004, Santa Cruz Biotechnology). Detailed protocol for western blotting is described in Section 2.27.2.

2.23 Infection of UAECs with Adenovirus vectors

Cultured UAECs were seeded in a six well plate at a concentration of $3.5x10^5$ cells/well as determined by an automated cell counter. Next day, the cells were incubated for an hour with a minimal volume (1ml/well) of EBM containing 2% FBS. As FBS is very rich in growth factors, including VEGF, we wished to reduce the concentrations of growth factors in the culture medium so that they do not mask the effects of endogenously over-expressed VEGF. Ad.VEGF-A_{165}, Ad.VEGF-D or Ad.LacZ were then added to the medium at multiplicities of infection of 0, 1, 10, 100, 1000 and 10000. Protein was extracted after 24 or 48 hours of infection for analysis by western blotting.

For cells that were incubated for 48 hours after infection with the adenovirus, the medium was replaced with fresh EBM (containing 2% FBS) after 24 hours of infection.

2.24 Determination of infection efficiency by X-gal staining

An additional plate was infected with Ad.LacZ at increasing multiplicities of infection (as described above). The medium was changed at 24 hours and fresh medium was added. After 48 hours of incubation, 100% Ethanol was added to each well for 20 minutes, in order to fix the cells. The wells were then washed in PBS four times. 3ml of freshly prepared X-gal stain (composition described in 2.36) was then added to each well, and the plate was incubated in the dark overnight on a shaking platform. Next morning, the cells were washed with PBS and viewed under a light microscope. For each well, 10 high powered fields (40X) were randomly selected and the number of stained cells and total cells were counted to determine the infection efficiency.

2.25 Protein extraction (from intact uterine arteries and uterine artery endothelial cells)

Frozen tissues from the main, first, second and third branches of uterine arteries, both left and right sides of the uterus were analysed from ewes injected with Ad.VEGF-A_{165}/Ad.VEGF-D and Ad.LacZ *in vivo* for both short and long-term studies. Approximately, 30-50mg of tissue was pulverised in liquid nitrogen using a metallic bijoux to extract protein for western blot analysis. After crushing, 1mL of Radio ImmunoPrecipitation Assay (RIPA) Buffer (R0278, Sigma Aldrich, USA) containing Complete Protease Inhibitor Cocktail (11873580001, Roche, Mannheim, Germany) and phosphatase inhibitor cocktail 1 and 2 (P5726 and P2850, Sigma Aldrich USA), as per manufacturers' recommended dosages, was added to the powdered tissue. Samples were then homogenized for 30 seconds on ice using a polytron in a 1.8ml cryovial (Nunc). The homogenised sample was transferred to a 15ml falcon tube and centrifuged at 3000rpm for 10 minutes at 4°C. The supernatant was transferred to a 1.5ml Eppendorf tube and centrifuged at 13000 rpm for 10 minutes at 4°C. The supernatant was then transferred to a clean tube and stored at -20°C.

For protein extraction from cultured cells, the culture medium was aspirated and the cells washed with cold PBS. The plate was kept on ice and 100µl of RIPA buffer (with protease and phosphatase inhibitors) was added to each well. The cells were then scraped off with a cell scraper (3010, Corning Life Sciences, Amsterdam, Netherlands) and transferred to a 1.5ml eppendorf tube. The tube was centrifuged at 13,000 rpm for 10 minutes at 4°C. The supernatant was then transferred to a clean tube and stored at -20°C.

2.26 Determination of protein concentration

The concentration of each protein sample was determined using the Bio-Rad Protein Assay Kit (Bio-Rad, Herts, UK), based on the method of Bradford. The Bradford protein assay is a colorimetric assay based on the absorbance shift

of the dye Coomassie Brilliant Blue G-250 under acid conditions when a redder form of the dye is converted into a bluer form on binding to protein. The amount of the blue-coloured complex in solution is a measure of protein concentration, and can be quantified by means of an absorbance reading at 595 nm to determine the protein concentration.

Protein standards were prepared using BSA (23209, Pierce, Northumberland, UK) diluted in the same buffer in which protein extraction had been performed. The following dilutions of BSA were prepared – 2.0, 1.5, 1.0, 0.5, 0.25, 0.125, 0.0625 and 0 mg/ml protein. The standard or sample (5 µl per well) was incubated with the dye reagent (200 µl per well) in a 96 well plate at room temperature for 15 minutes. The absorbance of the wells was then read on a spectrophotometer (Tecan) at 595 nm. Every serial dilution or tissue sample was tested on two wells and the final result taken as the average. The absorbance values for the calibration dilutions were plotted against the standard concentrations of BSA to produce a linear calibration curve (Figure 2.17) and the protein concentration of the tissue samples was determined against it. Tissue samples that gave a higher absorbance reading than that of the highest standard (2.0 mg/ml) were re-diluted so that their absorbance fell within the linear range of the assay.

Analysis was performed by Vedanta Mehta and Marie Buitendyk.

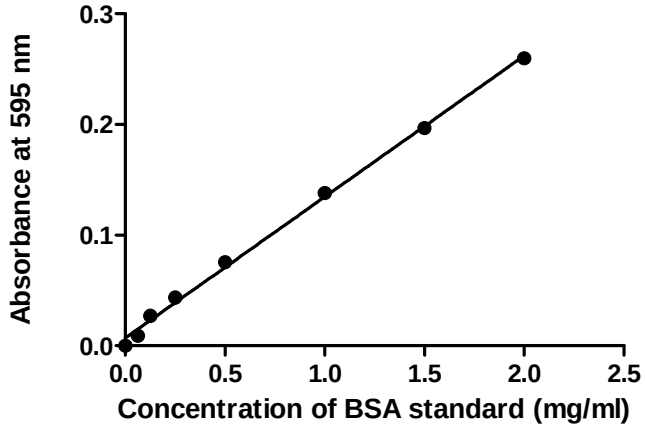

Figure 2.17 – An example of a standard curve generated with BSA, used to determine the concentration of protein extracts from uterine arteries and UAECs.

2.27 SDS-PAGE and Western blotting

SDS-PAGE separates proteins migrating through a gel under the influence of an electric field. When coupled with antibody detection steps, the relative abundance of a particular protein in two or more protein extracts can be determined.

2.27.1 Principle of Western blotting

Heating of cell lysates with sodium dodecyl sulphate (SDS)- and Dithiothreitol (DTT)- containing sample buffer denatures proteins, by reducing protein disulphide bonds to thiol groups and covering the protein with SDS molecules, forming a negatively-charged complex. Under the influence of an electric field, proteins migrate through a gel whose pore size is determined by the concentration of acrylamide and cross-linker in the gel. Larger proteins are obstructed more than smaller proteins, resulting in a separation of proteins largely based on molecular size. During transfer, the protein/SDS complex is transferred out of the gel onto a protein-binding membrane under the influence of an electric field. For antibody detection, protein-binding sites on the membrane are blocked by incubating with a protein solution such as 5% milk or 3% BSA, and the protein of interest is then specifically bound with an antibody. This primary antibody is then detected with a secondary antibody conjugated to an enzyme, often a peroxidase. A liquid substrate is then added, which in the presence of the peroxidase enzyme emits light in a chemiluminescent reaction, and this light is detected using photographic film.

Western blotting is often described as a semi-quantitative technique, with the amount of protein originally present in the lysate proportional to the amount of peroxidase enzyme bound to protein on the membrane, and thus the amount of

light generated and area and intensity of the band present on the film. For routine western blotting, samples were protein assayed before loading. Blotting with an antibody such as GAPDH, total ERK, α-tubulin or β-actin serves as a loading control and helps to visually confirm comparable protein loading.

2.27.2 Western Blot Analysis

25μg of extracted protein (from either intact uterine arteries or transduced uterine artery endothelial cells) was assayed for levels of eNOS, iNOS, phosphorylated eNOS (Ser^{1177}) by Western blotting. The protein samples were reduced with 4x Laemelli reducing buffer (NP007, Invitrogen) by boiling at 100°C for 5 minutes. The reduced samples were run on a 4-12% Bis-Tris Gel (NP0335BOX, Invitrogen) in MOPS-SDS Running buffer (NP0001, Invitrogen) alongside Rainbow Molecular Weight Marker (RPN800E, GE Healthcare, Bucks, UK), at 200V for 50 minutes.

The protein was then transferred to a PVDF membrane (LC2005, Invitrogen) using a wet transfer apparatus in 1x NuPAGE transfer buffer (NP00061, Invitrogen) containing 10% methanol. The transfer was performed at 40V for 1.5 hours. Following the transfer, the membrane was blocked using 5% skimmed milk in PBST for one hour at room temperature. The primary antibody was diluted in 5% milk at an appropriate dilution (Table 2.5). Following the blocking step, the membrane was incubated with the primary antibody overnight at 4°C on a shaking platform.

Next morning, the membrane was washed three times with PBST. This was followed by an incubation with the appropriate secondary antibody (diluted in 5% milk) for one hour at room temperature. The membrane was washed again three times with PBST and then dried. The protein bands were visualized using the Enhanced Chemiluminescence Plus Reagent Detection system (RPN2132, GE Healthcare). The hyperfilm was scanned using the HP Deskscan system and densitometric analysis was performed on the bands using the software Image J. After probing with one antibody, the membrane was stripped using the Re-blot

Plus Strong solution (2504, Millipore, Watford, UK) as per manufacturer's instructions, and re-probed with another antibody.

Table 2.5 – Antibodies used for western blotting

Target antigen	Primary and secondary antibodies
eNOS	1° = monoclonal mouse anti-eNOS (1:3000, 610296, BD Biosciences, Oxford, UK) 2° = sheep anti-mouse IgG-horseradish peroxidase (1:3000, RPN 4201, GE Healthcare, Bucks, UK)
iNOS	1° = monoclonal mouse anti-iNOS(1:3000, 610328, BD Biosciences, Oxford, UK) 2° = sheep anti-mouse IgG-horseradish peroxidase (1:3000, RPN 4201, GE Healthcare, Bucks, UK)
phosphorylated eNOS (Ser^{1177})	1° = monoclonal rabbit anti-p-eNOS(Ser^{1177}) (Cell Signaling Technology, Danvers, MA, USA) 2° = donkey anti-rabbit IgG-horseradish peroxidase (1:8000, Santa Cruz Biotechnology, Heidelberg, Germany)

2.28 ELISA for VEGF-A_{165} and VEGF-D

2.28.1 Principle of the VEGF Assay

This assay employs the quantitative sandwich enzyme immunoassay technique. A monoclonal antibody specific for VEGF has been pre-coated onto a microplate. Standard and samples are pipetted into the wells and any VEGF present is bound by the immobilized antibody. After washing away the unbound substances, an enzyme-linked polyconal antibody specific for VEGF is added to the wells. The unbound substances are again washed away, followed by the addition of a chromogenic substrate. The colour developed is proportional to the

amount of VEGF bound in the initial step. The colour development is stopped after an appropriate time and the absorbance of the wells is measured to determine VEGF concentration.

2.28.2 Method

A commercially available kit was used to quantify the levels of VEGF-A_{165} (DVE00, R&D Systems, Minneapolis, MN, USA) or VEGF-D (DVED00, R&D Systems) expression as per manufacturer's instructions. The sensitivity of this assay falls in the range of 5.0 – 10.0 pg/ml of VEGF. The protein extraction and estimation were performed as has been described previously (Sections 2.25 and 2.26).

Tissue samples were diluted so that the absorbance of the sample fell within the linear range of the VEGF assay (usually at a protein level of less than 1000 pg/ml). The VEGF assay consisted of a microtiter plate containing 12 x 8 wells precoated with a monoclonal mouse antibody to VEGF (-A_{165} or –D). The VEGF protein standard dilutions were prepared to obtain a calibration curve. To each well was added 50 µl of assay diluent (provided as part of the kit) and 200 µl of the calibration dilution or tissue extract containing 300 ng protein and the plate was incubated for 2 hours at room temperature. The plate was washed three times with washing solution and then incubated with 'Conjugate' solution (polyclonal antibody against VEGF conjugated to horseradish peroxidase) for 2 hours at room temperature. The wells were again washed three times with washing solution and the bound peroxidase revealed by incubation with the 'Substrate' solution (containing the chromogen tetramethylbenzidine) for 20 minutes at room temperature yielding a blue coloured reaction product. The reaction was quenched by the addition of 'Stop' solution (containing 2N Sulphuric acid). On addition of the 'Stop' solution, the blue colour in the wells turned yellow. The absorbance of the wells was measured at 450 nm with wavelength correction at 560 nm using a microplate reader (Tecan). Every serial dilution or sample was tested on two wells

and the final result taken as the average. The absorbance values for the calibration dilutions were plotted against the standard concentrations of VEGF to produce a nearly linear calibration curve and the VEGF concentration in tissue samples was determined against it.

Analysis was done by Vedanta Mehta, Khalil Abi-Nader, Alison Evans and Rikesh Patel.

2.29 Guinea Pig Experiments

Guinea Pigs of Dunkin Hartley breed were used. Female virgin guinea pigs were purchased from Harlan Animal Research Laboratory, UK and housed in groups of 2-3 in cages. The cages carried a card with an identification number for each guinea pig. The guinea pigs housed within the same cage were distinguished by making different coloured marks on the back of their heads. The room in which the guinea pig cages were placed had a 12 h : 12 h light : dark cycle, at a constant temperature of 25°C.

All procedures on animals were conducted in accordance with UK Home Office regulations and the Guidance for the Operation of Animals (Scientific Procedures) Act (1986) under Project Licence number 70/6546 titled 'Fetal gene therapy *in utero*'.

2.29.1 Guinea Pig Diet

The guinea pigs had *ad lib* access to food. They were fed a commercially available guinea-pig/rabbit ration (Appendix 1). Tap water supplemented with Vitamin C (400mg/L) was available *ad lib.*

2.30 Timed Mating of Guinea Pigs

In order to time mate guinea pigs, their vaginas were visually observed every day to check for the rupture of hymen. The guinea pig estrus cycle lasts approximately 16 days. A pro-estrus of approximately 36 hours is characterized by vaginal swelling, increased sexual activity and rupture of the vaginal membrane.

The membrane remains open for 2-3 days, covering the period of ovulation. Estrus lasts 8-12 hours and is characterized by the copulatory reflex (lordosis), an open vaginal membrane and vaginal congestion. Estrus most commonly occurs at night.

On finding the hymen ruptured and vagina open, female guinea pigs were deemed to be in estrus and placed with a male for 3 nights. After 3 nights, the male was separated from the female. The occurrence of coitus during this period is usually marked by a copulatory plug, containing hardened semen. However, even if a copulatory plug was not found, mating was presumed to have occurred during these 3 days. The middle day of this 3-day period was considered to be day 0, and the next day was considered to be 1 day post-conception (dpc).

Guinea pigs were scanned at 22-24 dpc to confirm pregnancy. They were restrained by a trained animal technician (Figure 2.18) and scanned using a 7-10 MHz probe (Siemens, Bracknell, United Kingdom). If a fetus was detected, an attempt was made to get a measurement of BPD, and this was compared with published data to confirm the gestational age (Turner AJ and Trudinger BJ, 2000). Pregnant guinea pigs were used for surgeries subsequently.

In some cases, guinea pigs were mated but were not pregnant when scanned. In such cases, a re-scan was performed one week later. If a fetus was still not detected after one week, the non-pregnant guinea pigs were returned to the routine of daily hymen examination for re-mating.

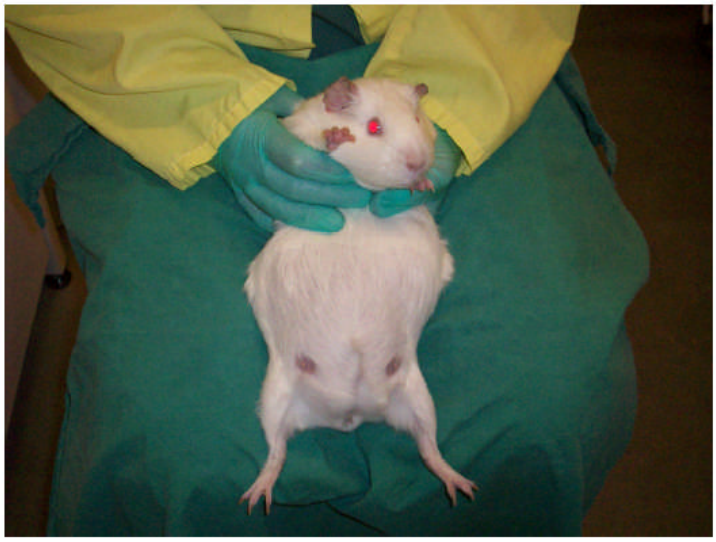

Figure 2.18 – Restraint of a guinea pig in preparation for ultrasound scanning

2.31 Creating Growth-Restricted Guinea Pigs (Method adapted from Roberts CT et al 2001)

Virgin female guinea pigs were divided into two groups, with the members of the two groups having similar body weights. One group was maintained on the *ad lib* diet, while the other group was fed 70% of the *ad lib* intake. The body weights of all animals were measured three times/week, as was the food in the hopper of the *ad lib* fed animals before feeding each day to determine the amount of food consumed per gram body weight. The nutrient restricted group was fed 70% of the *ad lib* intake per gram body weight. The guinea pigs were maintained on this control (normal) or nutrient-restricted diet for approximately 4 weeks. During this period, the routine vaginal checks were carried, as described in the preceding section.

After 4 weeks, the female guinea pigs were placed with a male for 3 nights on the day they were deemed to be in estrus, that is, had a ruptured vaginal membrane. The guinea pigs were scanned at 22-24 dpc to confirm pregnancy. If a fetus was detected by ultrasound scanning, the nutrient restricted animals were continued to be fed 70% of the *ad lib* intake per gram body weight until day 34

post-conception, and from day 35 onwards, food was increased to 90% of the *ad lib* intake. If a fetus was not detected, a re-scan was performed 1 week later. If the uterine horns were found to be 'empty' on the second re-scan, the guinea pig was returned to the original diet (control or nutrient-restricted) until the next estrus 16 days later, at which time she was mated again with a male.

2.32 Guinea Pig Anaesthesia

Surgery was performed at either 30 or 45 dpc in pregnant guinea pigs. Before surgery, guinea pigs were starved overnight with free access to water to reduce the volume of stomach contents during surgery, thereby reducing the risk of regurgitation/aspiration. General anaesthesia was induced with Diazepam, Atropine and Ketamine. Atropine (0.5mg/kg, Martindale Pharmaceuticals, Essex, UK) and Diazepam (5mg/kg, Hameln Pharmaceuticals, Gloucester, UK) were administered by the sub-cutaneous route. Following a 20 minute wait, Ketamine (40 mg/kg, Hameln Pharmaceuticals, Gluocester, UK) was administered by the intra-muscular route to the sedated animal.

A face mask was then applied to the animal, through which Isoflurane (Isoflurane-vet, Merial Animal Health Ltd., Essex, UK) was administered. General anaesthesia was maintained with 1.5-2.0% isoflurane in oxygen. The animal was placed supine on a heated operating table for rodents. A diathermy pad was placed underneath the animal.

Once anaesthetized, the fur was clipped from the guinea pig's abdomen and a detailed ultrasound examination of the uterus and its contents was performed using a 7-10 MHz probe. Fetal measurements were collected, namely biparietal diameteter, occipito-snout length, abdominal circumference, femur length, placental length and thickness and crown-rump length.

The abdominal surface of the guinea pig was scrubbed with 'Hibiscrub' (Chlorhexidine gluconate 4% w/v, Regent Medical, Manchester, UK) followed by 'Povidone' (1% w/w Iodine solution, Vetasept Animal Care Ltd., York, UK), and then exposed with sterile drapes.

A pulse oximeter (5250 RGM, Ohmeda) placed on the guinea pig's ear was used to monitor oxygen saturation and pulse rate and this data was documented every 15 minutes together with respiration rate, isoflurane concentration and level of anaesthesia. Maternal blood was taken for pre-operative haematological and biochemical analysis. Blood was collected into BD Vacutainer tubes (BD Vacutainer systems, Plymouth, UK) containing 0.105 M sodium citrate for plasma (9C, blue topped bottle), silica clot activator polymer gel for serum and potassium EDTA (K_3EDTA) for whole blood.
The guinea pig anaesthesia was performed by Mr. Michael Boyd. The fetal measurments by ultrasound scanning were initially collected by Dr. Anna David. During the course of the work for this thesis, she trained Vedanta Mehta to collect fetal measurments by ultra-sound scanning, who performed all ultrasound analysis in the latter part of the project.

2.33 Guinea Pig Surgery

To begin with, all surgeries were carried out on pregnant guinea pigs at 30 dpc and under direct vision. However, because of the difficulties associated with finding the uterine arteries, we moved to pregnant guinea pigs at 45 dpc and began operating under a surgical microscope - Discovery V8 Stereomicroscope (Carl Zeiss Ltd., Herts UK).

A midline lower abdominal incision was made in the skin using a number 10 blade (Swann-Morton, Sheffield, UK). The edges of the skin incision were injected with a 10% solution of Lidocaine hydrochloride (0.5ml, Hameln Pharmaceuticals, Gloucester, UK) to provide local anaesthesia. The rectus sheath was incised and the peritoneal cavity was opened carefully by blunt dissection. This is primarily because the rectus sheath in a guinea pig is very thin, and it is easy to accidentally rupture the bowel when using sharp surgical instruments to gain access to the peritoneal cavity. Once inside the peritoneal cavity, the bowel was packed to one side by either using sterile damp gauze or being retracted by a

surgical assistant. The utero-placental circulation was transduced with Ad.LacZ or Ad.VEGF-A_{165} by four different methods, which are described below.

2.33.1 Direct injection into uterine arteries

Experiments began by attempting to directly inject the vector into the uterine arteries. The uterine arteries in a pregnant guinea pig at 45 dpc have a very small diameter, ~200-350 μm and are deeply embedded in fat. To locate the uterine artery, the perivascular fat tissue was gently lifted up. A strong light was shone directly across the fat pad from back to front, so that the bright red coloured uterine artery could be visualized inside it. Once the precise location of the uterine artery had been determined, the fat was very gently dissected using a small straight vannas scissors (103102, John Weiss and Company, Milton Keynes, UK) to expose the uterine artery. In case of any accidental bleeds while cutting through the highly vascularized fat, haemostasis was achieved by electrical cauterization (VIO 300D Electrosurgical Generator, ERBE, Georgia, USA). During this surgery, it was sometimes necessary to deliver the uterus outside the body cavity in order to gain easy access to the uterine artery. In such cases, the uterus and its contents were kept warm by wrapping them up in sterile gauze soaked in warm saline solution.

Once the uterine artery had been cleared of surrounding fat and just before injecting the vessel, the uterine artery segment proximal to the injection site was occluded using a microvascular clip (610195, Harvard Apparatus, Kent, UK). The injection ($1x10^{10}$ viral particles of Ad.LacZ in a volume of 0.5-1.3 ml PBS) was then administered distal to the occlusion over approximately 1 minute. Initially a 31 gauge Hamilton needle was used, but this was too large for some of the uterine artery vessels. A custom made 34 gauge needle was then used, with a catheter attached, made by Dr. Simon Waddington (Lecturer, Institute for Women's Health, UCL) which helped in improving the injection technique.

A second microvascular clip was then placed over the injection site once the needle was removed to compress the injection site, for a minimum of 3

minutes (Figure 2.19). After this time both occluders were removed and the vessel was carefully observed for bleeding. On some occasions re-occlusion of the vessel was necessary to achieve haemostasis. Additionally, adrenaline (Hameln Pharmaceuticals, Gluocester, UK) was applied to the vessel to achieve haemostasis when further occlusion had been unsuccessful.

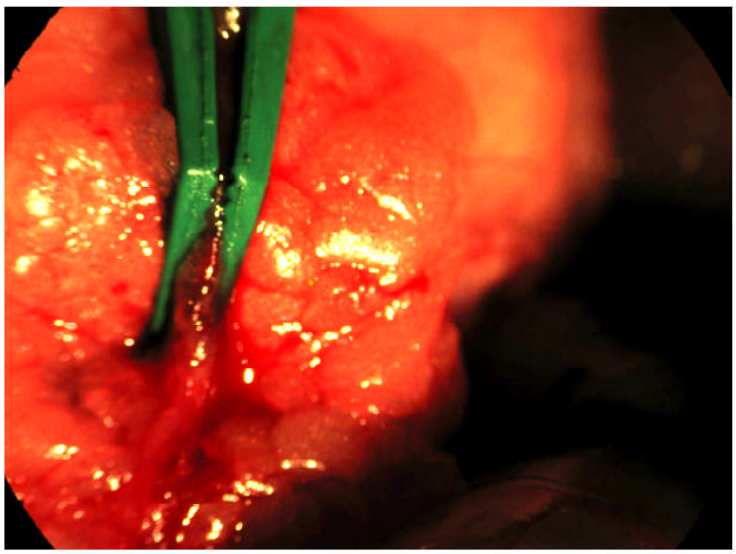

Figure 2.19 – A microvascular clip placed around a uterine artery at the site of injection

After injection of Ad.LacZ to the uterine arteries of pregnant guinea pigs, a microvascular clip was placed over the injection site to compress it, for a minimum of 3 minutes. After this time, the clip was removed and the vessel was carefully watched for bleeding. If haemostasis was not achieved, the clip was placed for longer duration and adrenaline was administered over the site of bleeding.

A successful injection was defined as the vector seen moving down the vessel during injection. Failed injections were due to vector being inadvertently injected into the vessel wall, leaking out of the vessel or coming out the other side of the vessel, opposite the injection site. In case of failed injections, 1-2 re-attempts were made to inject the uterine artery. As the uterine artery is very unsupported within the fat, it is quite difficult and technically challenging to inject it reliably.

The post-mortem examination was scheduled 3-5 days post-surgery to achieve good transgene expression, unless necessitated earlier because of maternal death or miscarriage.

2.33.2 External transduction of uterine and radial arteries

The effect of external gene transfer to the uterine and radial arteries was also studied in some animals. In some cases, these were animals in which attempts to inject the uterine artery vessel were unsuccessful either because the vessel was deemed to be too small to be injected, or because the injection attempt failed. The vector dose administered on each side (left or right) was $1x10^{10}$ viral particles of Ad.LacZ in a total volume of 0.5-1.0 ml PBS. For uterine artery gene transfer the vector was either injected alongside the vessel as it ran within the fat (6 uterine arteries) or dropped onto the exposed vessel within the fat (2 uterine arteries) and left to transduce for 5 minutes. Vector was also dropped onto the radial arteries as they ran within their mesentery (2 uterine horns) and left for 5 minutes before the uterus was subsequently mobilized. During this 5 minute time period the uterine horn was kept warm and moist by wrapping it in a sterile gauze soaked with warm saline. No vessel occlusion was used in this technique. The radial arteries were kept as flat as possible during transduction to avoid vector running off, but this did occur in all cases.

2.33.3 Injection of internal iliac arteries

The internal iliac artery gives off 6 branches in a guinea pig. These are **umbilical** (which further forms the superior vesical artery that sends numerous branches to the upper bladder and ureter), **inferior vesical artery** (supplying the lower bladder and also forming the middle rectal artery supplying the rectum), **cranial gluteal** (supply the dorsolateral wall of pelvis), **internal pudendal artery** (supplying the external genitalia), **vaginal** and **uterine** arteries. Hence, we believed that intra-arterial injection of adenovirus in the internal iliac, which is more easily accessible than the uterine artery would also lead to transduction of the latter. Figure 2.20 shows the vessels given off from the internal iliac artery

before the uterine artery origin in a guinea pig. As can be seen, the uterine artery is one of the most distal branches of the internal iliac artery, an approximate distance of 3.5cm from the origin of the internal iliac artery.

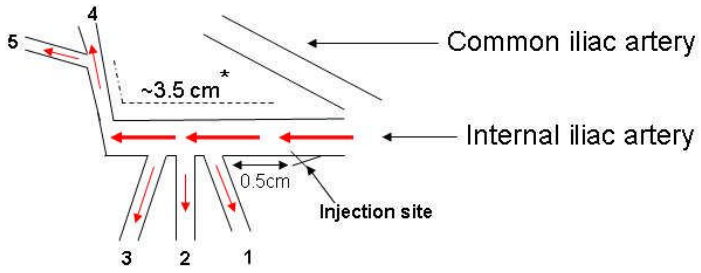

1- cranial gluteal artery (dorsolateral wall of pelvis and pelvic muscles) ~1-1.5 cm long

2- internal pudendal artery (external genitalia) ~ 1.5 cm long

3- vesical artery (branches to supply bladder, ureter and rectum) ~ 3 cm long

4- vaginal artery ~ 3 cm

5- uterine artery ~ 5 cm

* Distance from site of injection to origin of uterine artery

Figure 2.20 – Distal branches of the internal iliac artery in a guinea pig

The internal iliac artery was easily identified running with a neurovascular bundle along the pelvic side wall beneath the posterior aspect of the peritoneum at the level of the cervix (Figure 2.21). Careful dissection of the peritoneum with a small straight vannas scissors revealed the prominent internal iliac vein, and behind it lay the smaller sized artery. The vessel is 200 – 250 μm in diameter and runs transversely from its origin at the common iliac artery towards the cervical parametrium. Its first branch, the cranial gluteal artery was occasionally seen after dissection of the fat within the cervical parametrium.

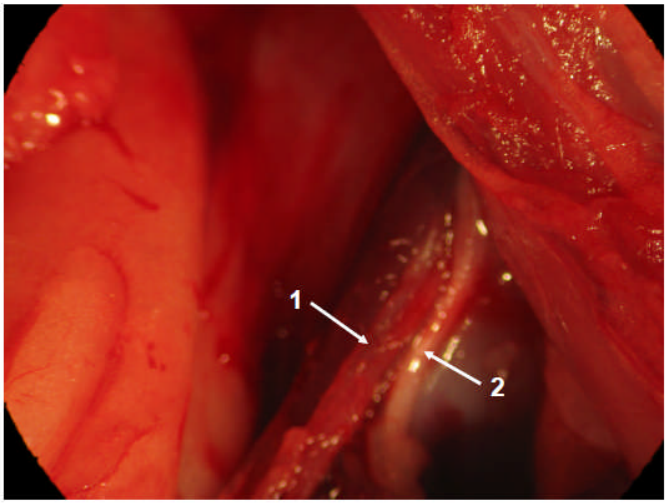

Figure 2.21 – The internal iliac artery of the guinea pig

1 = The internal iliac artery of a guinea pig running along the pelvic wall; 2= pelvic neurovascular bundle running adjacent to the internal iliac artery.

We initially performed the internal iliac injections with a 31 Gauge Hamilton needle, but moved to the 34 Gauge needle thereafter as it is easier to use. The vector dose injected was $1x10^{10}$ viral particles in 1.0-1.5 ml of PBS. All animals were injected at 45 – 47 days of gestation.

The internal iliac artery segment proximal to the injection site was occluded using a microvascular clip, and the injection was administered distal to the occlusion over approximately 1 minute. On 2 occasions, the internal iliac artery distal to the origin of the cranial gluteal artery was dissected out and injected, when attempts at injection at sites on the internal iliac artery proximal to this failed.

Following the administration of the vector, a second micro-vascular clip was placed over the injection site once the needle was removed to compress the injection site, for a minimum of 3 minutes. After this time both clips were removed and the vessel was carefully observed for bleeding. On some occasions re-occlusion of the vessel was necessary to achieve haemostasis. Additionally, adrenaline was applied to the vessel to achieve haemostasis when further occlusion had been unsuccessful.

A successful injection was defined as the vector fluid seen moving down the vessel during injection. Failed injections were due to vector being inadvertently injected into the vessel wall, leaking out of the vessel or coming out of the other side of the vessel, opposite the injection site. In case of failed injections, 1-2 re-attempts were made to inject the internal iliac artery. After this time the vessel was so constricted that it could not be injected.

Animals were left for a maximum of 4 days to achieve good transgene expression after which they were put down, and vessels, maternal and fetal tissues dissected out. The post-mortem examination had to performed earlier when there were peri-operative complications or maternal deaths post-operatively.

2.33.4 External Administration of Vector-Pluronic Gel Combination

Pluronic F-127 is a thermo-sensitive polymer gel that is liquid when cold, but gelatinizes when brought to room temperature. It has been used as a vehicle for virus-mediated gene delivery (Iaccarino G et al., 1999;Khurana R et al., 2004;Mallawaarachchi CM et al., 2005), but not to the utero-placental circulation.

2.33.4.1 Re-constitution of vector in pluronic gel

A 25% (w/v) solution of Pluronic F-127 (P2443, Sigma Aldrich, USA) was prepared by dissolving the powder in cold double distilled de-ionized water. The solution was placed on a rotating platform overnight at 4°C to ensure the polymer was homogenously mixed.

Next morning, the vector (Ad.LacZ, $1x10^{10}$ viral particles) was re-constituted in 1 ml of Pluronic gel and mixed by gently pipetting up and down, on ice. The vector was re-constituted just before the time of its administration.

2.33.4.2 Surgery for pluronic gel-vector administration

A mid-line laparotomy was performed under general anaesthesia as above. For administration on the uterine artery, the fat either side of the lower uterine horns was exposed. A light (KL 1500 LCD, Schott, Mainz, Germany) was shone through from the far side of the fat as it was held up to visualize the uterine artery. The uterine artery was gently cleared of surrounding fat and exposed. On each side, 1 ml of the vector-Pluronic gel combination was applied to the uterine artery with a 1ml micro-pipette. The pluronic gel solidified as soon as it came in contact with the guinea pig tissues. It was allowed to remain in place for at least 5 minutes, to ensure maximal tissue transduction. The procedure was repeated on the contra-lateral side.

For radial artery gene transfer, the uterine horn on one side was moved across to expose the arteries as they ran within the uterine parametrium. Occasionally the uterine horn needed to be lifted out of the peritoneal cavity to expose the radial arteries adequately and in these cases the uterus was kept warm by wrapping in sterile gauze soaked in warm saline.

Sometimes, it was not possible to transduce the uterine artery and radials at the same time because of difficulties in exposing all these vessels together. In such instances, the uterine artery was transduced first. After a 5 minute wait, the radials were exposed and transduced. Thereafter, the uterine horns and artery were gently returned to the body cavity and the incision closed.

2.33.5 Closure of incision

After vector administration (by either of the four methods described above), the abdomen was closed in layers. The rectus sheath was closed with continuous 2-0 Vicryl with Tapercut needle (Ethicon, St. Stevens-Woluwe, Belgium) to prevent herniation of the abdominal contents. The subcutaneous tissue and skin were closed with continuous 2-0 Vicryl with Tapercut needle

(Ethicon, St. Stevens-Woluwe, Belgium) and continuous 2-0 Vicryl with Cutting needle (Ethicon, St. Stevens-Woluwe, Belgium) respectively. A 10% solution of lidocaine hydrochloride (0.5ml) was again administered subcutaneously just before closing the skin to provide local anaesthesia.

No antibiotics were administered intra-peritoneally prior to closing the incision. There are only few antibiotics that are well-tolerated in guinea pigs and many of those commonly used such as Penicillin-streptomycin kill the symbiotic gut flora of the guinea pig, thereby interfering with their digestion. In extreme cases, administration of antibiotics can even be lethal for guinea pigs. The antibiotic regimen included intra-muscular administration of Baytril (2.5% w/v Enrofloxacin, Bayer Health Care, Kiel, Germany), which is deemed safe to use in guinea pigs.

The post-operative analgesia included administration of 0.1 mg/ml Vetergesic (Buprenorphine, Alstoe Animal Health, York, UK) and Carprofen (5mg/kg, Pfizer Animal Health, Kent, UK) sub-cutaneously. The guinea pig was then allowed to recover and placed in her cage which was pre-warmed with a hot water bottle. She was kept under close observation and not returned to the home cage until she regained the righting reflex (ability of rodents to regain footing when placed with the back down on a flat surface) and showed some slight movements within the cage.

2.34 Post-operative care

Guinea pigs were closely observed for 3-4 days post-operatively for any signs of miscarriage or distress. This included observations such as withdrawal from food and water, loud vocalization in the form of squealing, sitting in one corner of the cage and none or little movement when stimulated by touch. The analgesic regimen (as described above) was administered once daily for 2-3 days post-operatively, or for longer if needed.

Guinea pigs are well known for their lack of appetite post-operatively. In order to promote their eating, they were fed commercially available probiotic

yoghurts, baby food formulations and ‘Lectade’ Oral Rehydration Therapy for small animals (Pfizer Animal Health, Kent, UK). All of these are known to function as appetite stimulants for guinea pigs.

2.35 Post-mortem

The post-mortem examination was performed 4-7 days after the administration of the vector, unless necessitated earlier by miscarriage or maternal distress. The animal was put down with 3.5 ml of Euthatal (sodium pentobarbitone, Rhône Merieux, Essex UK) by intra-peritoneal or intra-cardiac administration. Once death was confirmed by cessation of breathing and heart movement, an abdominal incision was made. The uterine and radial arteries running alongside the uterus were harvested in one piece, along with all the surrounding fat and placed in cold Kreb’s Ringer solution for subsequent pharmacological analysis. Small sections of the uterine and radial arteries were also preserved for histological studies, DNA, RNA and protein extraction.

The uterus was opened and amniotic fluid was collected with a 21G needle attached to a 2ml syringe. Fetal blood was sampled for biochemistry and haematological analysis from the umbilical vein and fetal heart. Maternal and fetal organs were sampled widely according to a standard proforma (Appendix V), and fetuses and organs were weighed. Fetal parameters were measured with a calipers (biparietal diameter, occipito-snout length, crown rump length and femur length). Placental weight, diameter and thickness were also noted down.

Samples from each tissue were snap-frozen in liquid nitrogen for future nucleic acid/protein extraction. One sample from each tissue was placed in a histology cassette and dropped into 4% paraformaldehyde (pH 7.4) overnight before transfer into 70% ethanol. Some tissues (uterine and radial arteries, uterus, cervix, placentae, bladder, pelvic muscles, maternal and fetal liver, heart, kidney, lung, adrenal, spleen and gonad) were analysed by X-gal histochemistry to determine transgene expression.

2.36 Detection of β-galactosidase transgene expression by X-gal histochemistry

Tissue samples were placed in 100% ethanol at post-mortem and fixed for atleast 2 hours before washing with PBS. Samples were then incubated in X-gal staining solution containing 40mM potassium ferrocyanide, 40mM potassium ferricyanide, 1mM $MgCl_2$ in PBS and 5-Bromo-4-chloro-3-indolyl β-D-galactopyranoside (X-gal, B4252, Sigma Aldrich) dissolved in DMSO (D2650, Sigma Aldrich) at 40mg/ml overnight in a rotary shaker protected from the light. Next morning, the stained samples were washed in PBS and photographed with a camera attached to a microscope (Discovery V8 Stereomicroscope, Carl Zeiss Ltd., Herts UK and Canon Powershot A620 digital camera).

2.37 Wire Myography

2.37.1 Principle

Wire myography is an *in vitro* technique that allows examination of functional responses and vascular reactivity of isolated small arteries (with internal diameter 60 μm to 3 mm). The basic principle of wire myography is very similar to that described previously for an organ bath. It involves the mounting of small vessels as ring preparations by threading them onto two stainless steel wires and securing the wires to two supports. One support is then attached to a micrometer, allowing control of vessel circumference, while the other support is attached to a force transducer for measurement of tension development. The whole vessel preparation is kept in a chamber with physiological salt solution at 37°C, bubbled with oxygen (Figure 2.22). Vessels are viable for many hours while maintained in the myography chamber.

During the experiments, the circumferences of the vessels are kept constant, i.e., the vessels are examined under isometric conditions. Different

agonists are then added directly to the chamber and vessel tension is monitored for possible contractile or relaxant effects.

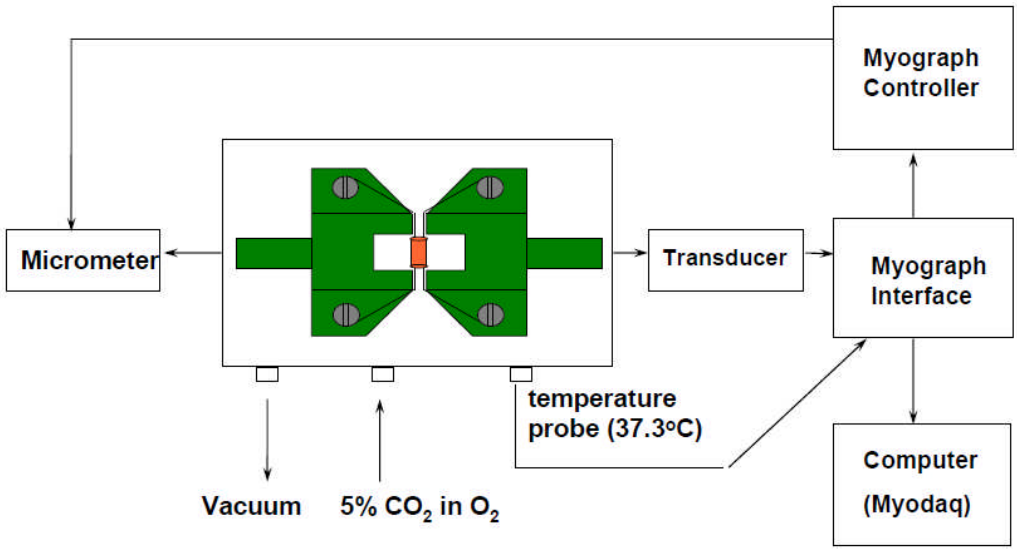

Figure 2.22 – Principle of wire myography

A small segment of a blood vessel is suspended between two stainless steel wires in a myograph chamber. The chamber is filled with Kreb's buffer through which carbogen gas (95% O_2, 5% CO_2) is constantly bubbled. The solution in the chamber is maintained at 37°C. Agonists added directly into the myograph chamber cause the vessel ring to either contract or relax. The change in the tension of the vessel is measured by a force transducer and recorded on an acquisition computer as a real-time trace.

2.37.2 Procedure

The uterine and radial arteries were transported from the BSU Camden to the Pharmacology Lab at the Rayne Institute, UCL in freshly prepared cold Kreb's buffer solution. At UCL, the guinea pig uterine and radial arteries were cleared of surrounding fat and connective tissue under a dissection microscope and cut into 1mm long ring segments. Each vessel ring was gently threaded between two stainless steel wires (40μm thick) with the minimum possible manipulation, to preserve endothelial integrity. Each wire was secured to a stable

support, one of which is connected to a force transducer for measurement of tension development.

In these experiments, dual chamber wire myographs were used (DMT 410A, Danish Myotechnology, Aarhus, Denmark) which allow the analysis of two vessel preparations simultaneously. Each chamber was filled with 5ml of Kreb's Ringer solution (supplemented with 2.5mM $CaCl_2$). The Kreb's buffer was bubbled with carbogen gas (95% oxygen, 5% carbon dioxide) to maintain a physiological pH of 7.4, and the temperature was maintained at 37°C.

Following mounting, the vessels were allowed to equilibrate for one hour, with washing every 15 minutes. Each vessel was then normalized to determine the maximum active tension development using the automatic feature on the acquisition software. This allows the standardization of initial experimental conditions, an important consideration when examining pharmacological differences between vessels.

After one hour of equilibration, the vessels were challenged with 48mM Potassium chloride (KCl) to test for viability and also determine the maximum contractility. They were then washed 3 times with Kreb's buffer, and challenged again after 20 minutes. In all, the vessels were challenged 3-4 times with KCl, until the maximum contractile response generated was equal to the previous response ($\pm$5%). A contraction greater than 1.5g (14.7 mN) was considered viable.

The vessels were allowed to rest for 30 minutes to recover, during which time they were washed 3 times with Kreb's buffer. They were then challenged with a bolus dose of L-phenylephrine (1 μm, L-1286 Sigma Aldrich), and made to relax with a bolus dose of Acetycholine (1 μM, A7725, Sigma Aldrich). Only those segments which relaxed >70% (and therefore had an intact endothelium) were used for subsequent analysis.

Following the endothelial integrity test, a dose response curve to L-phenylephrine was generated (10^{-9} to $3x10^{-5}$M). The next higher dose of L-phenylephrine was added only after the contraction induced by the previous dose had stabilized and reached a plateau.

The vessels were again allowed to rest for 30 minutes, during which time they were washed 4-5 times with Kreb's buffer until they attained the pre-contraction basal tone. They were then contracted sub-maximally with L-phenylephrine (1μm) so that they attained ~70% of the maximum contractile response. Once the contraction had stabilized, they were made to relax with increasing doses of Acetylcholine (10^{-9} to $3x10^{-5}$M).

The real-time traces were acquired using Myodaq software **(**MyoDaq V.2.01, Danish Myo Technology, Aarhus, Denmark) and analysed using Myoview software (Danish Myo Technology). The extracted data was plotted in the form of a points-only graph with non-linear regression using GraphPad Prism 5.0, and statistical significance was assessed using two-way ANOVA.

Chapter 3

Results: The Effects of Local Over-expression of VEGF on the Uterine Arteries of Pregnant Sheep

This chapter describes the effects of adenovirus-mediated over-expression of VEGF-A_{165} on uterine arteries from pregnant sheep 30-45 days after administration of the vector. We studied the effects of VEGF-A_{165} on various physiological parameters which included uterine artery blood flow, vascular reactivity, neovascularization, maternal and fetal blood pressure and eNOS levels. The rationale behind carrying out these studies was to determine if local over-expression of VEGF in pregnant uterine arteries can be of potential therapeutic benefit in treating FGR.

In this study, sixteen pregnant Romney ewes underwent surgery to implant telemetric flow probes, followed by injection four to seven days later of an adenovirus containing the VEGF-A_{165} gene (Ad.VEGF-A_{165}) into one uterine artery and the LacZ gene (Ad.LacZ) in the contralateral uterine artery (n=11), or the VEGF-$D^{\Delta N \Delta C}$ gene (Ad.VEGF-$D^{\Delta N \Delta C}$) into one uterine artery and Ad.LacZ in the contralateral uterine artery (n=5). A sub-set of these pregnant sheep had blood-pressure sensitive catheters implanted in their maternal carotid artery (n=4 for Ad.VEGF-A_{165} group) or fetal carotid artery (n=4, Ad.VEGF-A_{165} group) to monitor maternal and fetal blood pressure, respectively. Each sheep was monitored to give a mean daily reading of the uterine blood flows, maternal/fetal blood pressure and maternal/fetal heart rate before and after injection until a few days before expected delivery.

The results of the analysis performed on the sheep have been described in the following chapter. In twin pregnancies, both the uterine horns carried a fetus each and have been referred to as 'gravid'. In singleton animals, the uterine horn carrying a fetus has been referred to as the 'gravid' horn, and the contra-lateral horn not carrying a fetus has been referred to as the 'non-gravid' horn. We found the uterine artery supplying the gravid horn was generally more developed and larger in size than the uterine artery supplying the non-gravid horn. The baseline blood flow values were also always higher in the uterine artery supplying the gravid horn.

Each sheep underwent surgery approximately 90-110 days into the pregnancy. As the ewes were time-mated, this date was very accurate and ultrasound scanning confirmed the gestation. The details of the analysis performed on the Ad.VEGF-A_{165} sheep has been described in Table 3.1. A similar table (Table 3.13) has been presented for the Ad.VEGF-$D^{\Delta N \Delta C}$ sheep later in this chapter.

Table 3.1 – Details of experimental analysis performed on sheep injected with Ad.VEGF-A_{165} and Ad.LacZ contra-laterally

Animal	Fetal No.	GA at probe placement (days)	GA at vector injection (days)	GA at PM (days)	UABF	MBP	FBP	Organ Bath	vWF	RT-PCR	eNOS
UA7	**1**	**102**	**108**	**139**	+	-	-	+	-	-	-
UA8	**2**	**102**	**109**	**140**	+	-	-	+	-	-	-
UA9	**1**	**90**	**95**	**137**	+	-	-	+	-	-	-
UA10	**1**	**89**	**93**	**144**	+	-	-	+	-	-	-
UA11	**2**	**97**	**104**	**139**	+	-	-	+	+	-	-
UA12	**1**	**95**	**102**	**140**	+	-	-	+	-	-	-
UA13	**2**	**80**	**87**	**139**	+	+	-	+	+	+	+
UA14	**2**	**80**	**90**	**137**	+	+	-	+	+	+	+
UA15	**1**	**80**	**88**	**136**	+	+	-	+	-	+	-
UA16	**2**	**96**	**103**	**136**	+	+	-	+	+	-	+
UA18	**1**	**89**	**97**	**136**	+	-	-	-	-	-	-
UA20	**2**	**101**	**109**	**115**	-	-	+	+	-	-	-
UA25	**1**	**101**	**107**	**111**	-	-	+	+	-	-	-
UA26	**1**	**101**	**108**	**138**	-	-	+	+	-	-	-
UA29	**1**	**102**	**110**	**4 mths PN**	-	-	+	+	-	-	-
UA22*	**1**	**78**	**84**	**134**	-	+	-	+	+	-	-
UA24*	**2**	**84**	**97**	**133**	-	+	-	+	+	-	-

* indicates uterine artery injection with PBS bilaterally; GA=gestational age; UABF = measurement of uterine artery blood flow; MBP = measurement of maternal blood pressure; FBP= measurement of fetal blood pressure; vWF = adventitial vessel enumeration by anti-vWF immunohistochemistry; PM: post mortem examination; mths: months; PN: postnatal

3.1 Uterine artery injection of Ad.VEGF-A_{165} has a minimal long term fetal and maternal morbidity and mortality rate

In the group of fetuses that underwent telemetric fetal haemodynamic monitoring (n=4), two fetal deaths occurred 7 and 10 days after vector injection. One ewe developed a haematoma underneath the site of skin button placement on the flank. There were no other cases of maternal or fetal morbidity or mortality. One ewe gave birth to a healthy lamb on the day of scheduled post mortem examination, 2 days earlier than expected. The delivery was uncomplicated without any postpartum haemorrhage or retained placenta. The ewe and lamb were monitored for 4 months until weaning and showed no adverse development or abnormal growth velocity. Gross examination at the time of post-mortem of all ewes, fetuses and the one lamb did not reveal any pathology.

3.2 Ad.VEGF-A_{165} transduction of uterine arteries in the pregnant sheep results in long-term increase in uterine artery blood flow

Uterine artery blood flow (UABF) was measured successfully long term in ten (6 singletons and 4 twins) out of 11 pregnant ewes in the Ad.VEGF-$_{A165}$ group. In the sheep where UABF failed, the flow probe had a manufacturing fault and no long-term UABF data could be obtained. In all other cases, UABF data was available within 48 – 72 hours of flow probe placement.

The telemetric flow probes used in this study permitted measurements of the blood flow to be collected over periods of time while allowing the ewe to remain in her usual environment and without the need to restrain her to connect up implanted flow probes. Flow probes were implanted bilaterally up to a week before vector injection and uterine artery blood flow was measured for 1 hour each day, at the same time of the day to avoid diurnal variation. Before administration of the vector, the measured uterine artery blood flow was averaged over three consecutive days to derive a baseline value. The daily measurements of blood flow post-injection for each uterine artery were compared with this baseline

value and converted into a percentage increase from baseline. Figure 3.1 depicts the absolute values of uterine blood flow for one sheep. Figure 3.2 shows the uterine blood flow data from the same animal expressed as a percentage increase from baseline, while Figure 3.3(a) shows this data averaged for all 10 animals in the cohort. Figure 3.3(b) depicts the UABF data in terms of conductance (blood flow/pressure), which has greater physiological relevance for whole animal studies as it is dependent on both uterine blood flow and mean arterial pressure.

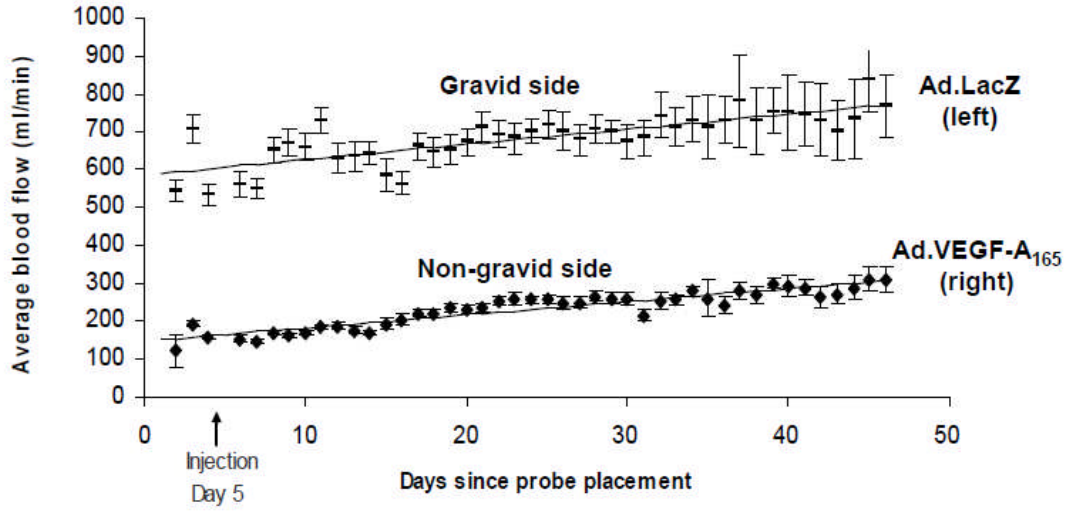

Figure 3.1 – Representative graph for daily uterine artery blood flow in a singleton pregnant sheep

Pregnant sheep underwent a laparotomy at mid-gestation to implant transit-time flow probes around their uterine arteries. Uterine artery blood flow was measured for one hour each day at the same time in the morning, before and after the administration of Ad.VEGF-A_{165} and Ad.LacZ contralaterally. The daily uterine artery blood flow values for each uterine artery were plotted on a graph. In this particular animal represented (UA9), the left uterine artery (injected with Ad.LacZ) supplied a gravid horn, while the opposite uterine artery supplied a non-gravid horn. As can be observed from the graph, the uterine artery blood flow in the vessel supplying the gravid horn is higher at all time points, compared to the vessel supplying the non-gravid horn.

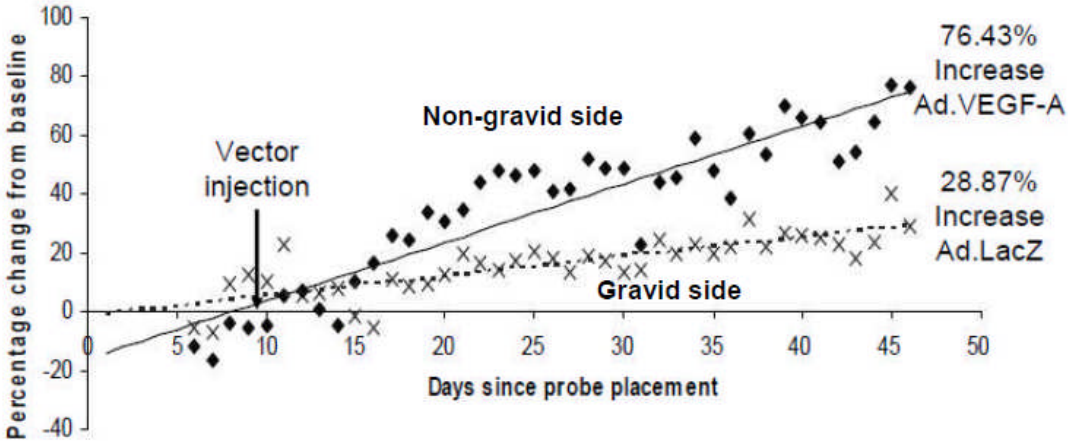

Figure 3.2 – Representative graph for percentage increase in uterine artery blood flow from baseline in a singleton pregnant sheep

Pregnant sheep underwent a laparatomy at mid-gestation to implant transit-time flow probes around their uterine arteries. Uterine artery blood flow was measured for one hour each day at the same time in the morning, before and after the administration of Ad.VEGF-A_{165} and Ad.LacZ contralaterally. The post-injection values were compared with a pre-injection baseline, which was obtained by averaging the values of uterine artery blood flow obtained for 3 consecutive days before the administration of the vector. In this graph, the percentage increase in uterine artery blood flow from baseline is greater in the Ad.VEGF-A_{165} transduced uterine artery compared to the Ad.LacZ transduced uterine artery.

There was a slight fall in UABF from baseline directly after vector administration, that reached a nadir at days 2-4 after vector injection and recovered completely by days 5-7. The percentage fall in UABF from baseline to the nadir at days 2-4 after vector injection was not significantly different in the Ad.VEGF-A_{165} (n=10) compared with the Ad.LacZ (n=9) injected uterine arteries (mean -10.85%$\pm$ SD16.94% v/s mean -8.42%$\pm$SD15.69%, p=0.74). This slight but non-significant fall in UABF just after vector injection was most likely due to trauma during vector delivery into the uterine artery lumen and the resultant vasoconstriction.

As anticipated, UABF increased as gestation advanced. The extent of increase in UABF in the last trimester of pregnancy, as noted in our study was similar to what has been reported by other authors (Wallace JM et al., 2008). For

each animal (n=10), the maximum increase in blood flow from baseline was calculated at 4 different time points - 7 days, 14 days, 21 days and 28 days post-vector injection. The UABF percent change at each time-point was calculated using the average of 3 consecutive daily mean UABF measurements. The gradient of the percentage increase in blood flow from baseline in each uterine artery was calculated for the same time points. A two-way general linear model (GLiM) was used to compare the UABF percent change in Ad.VEGF-A_{165} and Ad.LacZ injected uterine arteries at each time point and also the gradients of UABF %change over the length of gestation (Table 3.2). The two factors accounted for in the GLiM analysis were whether the uterine artery supplied a gravid or non-gravid horn and whether Ad.VEGF-A_{165} or Ad.LacZ vector was injected.

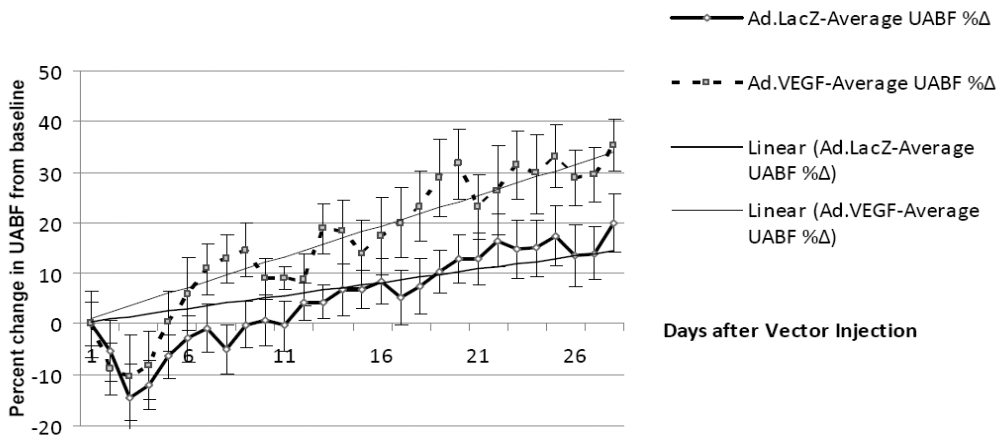

Figure 3.3 – Percentage increase in uterine artery blood flow from baseline and gradient of percentage increase in uterine blood flow from baseline in 10 pregnant sheep injected with Ad.VEGF-A_{165} and Ad.LacZ contra-laterally

Pregnant sheep underwent a laparotomy at mid-gestation to implant transit-time flow probes around their uterine arteries. Uterine artery blood flow was measured for one hour each day at the same time in the morning, before and after the administration of Ad.VEGF-A_{165} and Ad.LacZ contralaterally. The post-injection values were compared with a pre-injection baseline, which was obtained by averaging the values of uterine blood flow obtained for 3 consecutive days before the administration of the vector. In this graph, the mean percentage increase in uterine artery blood flow from baseline is significantly greater in the Ad.VEGF-A_{165} transduced uterine arteries (36.53%) compared to the Ad.LacZ transduced uterine arteries (20.08%), p=0.02, n=10.

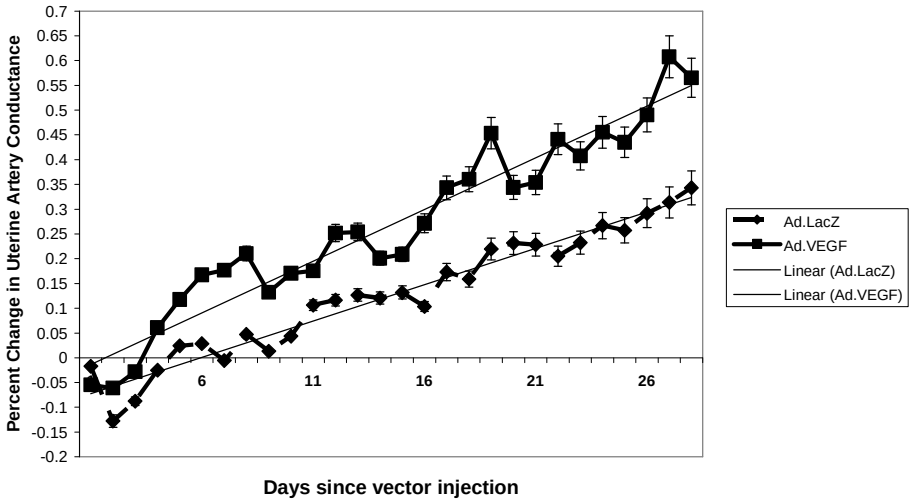

Figure 3.3(b) – Percentage increase in uterine artery conductance from baseline and gradient of percentage increase in uterine artery conductance from baseline in 10 pregnant sheep injected with Ad.VEGF-A_{165} and Ad.LacZ contra-laterally

Pregnant sheep underwent a laparotomy at mid-gestation to implant transit-time flow probes around their uterine arteries. Uterine artery blood flow and mean arterial pressure were measured for one hour each day at the same time in the morning, before and after the administration of Ad.VEGF-A_{165} and Ad.LacZ contralaterally. The post-injection values were compared with a pre-injection baseline, which was obtained by averaging the values of uterine blood flow/mean arterial pressure obtained for 3 consecutive days before the administration of the vector. In this graph, the mean percentage increase in uterine artery conductance from baseline is significantly greater in the Ad.VEGF-A_{165} transduced uterine arteries compared to the Ad.LacZ transduced uterine arteries.

Table 3.2 - Percentage change in uterine artery blood blow (UABF) and Gradient of Percentage Change in UABF at one week intervals post-Ad.VEGF-A_{165}/Ad.LacZ injection to the uterine arteries of pregnant sheep

Time-point after vector injection	% Increase in UABF ± SEM		p value (GLiM)	Gradient of % Increase in UABF		p value (GLiM)
	Ad.VEGF-A_{165} (n=10)	Ad.LacZ (n=9)		Ad.VEGF-A_{165} (n=10)	Ad.LacZ (n=9)	
7 days	12.83± 4.76	-1.93± 4.23	0.02	1.00	-1.05	0.043
14 days	18.00± 5.62	6.19± 3.96	0.10	1.28	0.08	0.037
21 days	28.38± 6.36	12.81± 5.17	0.07	1.30	0.35	0.042
28 days	36.53± 4.51	20.08± 5.28	0.02	1.27	0.51	0.042

GLiM:General Linear Model

Table 3.3 summarizes the maximum increase in blood flow from baseline in each uterine artery at 28 days after the administration of the vector. The maximum increase in blood flow in each uterine artery was seen only on the last day of pregnancy, before post-mortem examination.

Table 3.3 – Percentage change in uterine artery blood flow from baseline 28 days after administration of Ad.VEGF-A_{165} or Ad.LacZ to the uterine arteries of mid-gestation pregnant sheep.

Animal	**Fetal no.**	Side of vector injection		% change in UABF at 28d	
		Ad. VEGF-A_{165}	**Ad.LacZ**	**Ad. VEGF-A_{165}**	**Ad.LacZ**
UA7	Singleton	Gravid	Non-gravid	47.01	13.59
UA8	Twin	Gravid	Gravid	9.9	-8.8
UA9	Singleton	Non-gravid	Gravid	49.47	22.57
UA10	Singleton	Non-gravid	Gravid	42.35	16.96
UA11	Twin	Gravid	Gravid	27.82	NA
UA12	Singleton	Non-gravid	Gravid	28.55	11.56
UA13	Twin	Gravid	Gravid	44.33	32.52
UA14	Twin	Gravid	Gravid	NA	NA
UA15	Singleton	Non-gravid	Gravid	57.89	25.52
UA16	Twin	Gravid	Gravid	24.39	17.53
UA18	Singleton	Gravid	Non-gravid	33.62	49.34

NA: data not available; UABF: Uterine artery blood flow

Considering singleton and twin gestations together, at 28 days post vector injection, the mean increase in blood flow in the uterine arteries injected with Ad.VEGF-A_{165} (n=10, 36.53%± 4.51%) was significantly higher (p=0.02) than in the uterine arteries injected with Ad.LacZ (n=9, 20.08%±5.28%). The difference in UABF %increase was apparent and significantly different as early as 7 days

after vector injection, although statistical significance was not reached at the 14 and 21 days post-injection time-points (Table 3.2). Also, the extent of increase in UABF was highest when Ad.VEGF-A_{165} was injected on the non-gravid side in singleton pregnancies (Table 3.4).

Table 3.4 - Percentage mean increase in UABF from baseline 28 days post-injection in the different groups.

No. of fetuses	Side of Ad.VEGF-A_{165} injection	Max. increase in UABF at 28 days post injection			
		Ad.VEGF-A_{165} injected UtA		Ad.LacZ injected UtA	
Twins	Gravid	26.61%	n=4	13.75%	n=3
Singleton	Non-gravid	44.56%	n=4	19.15%	n=4
Singleton	Gravid	40.31%	n=2	31.46%	n=2

UtA = Uterine artery

Using GLiM analysis, the mean gradient of percentage increase in UABF was significantly higher in the Ad.VEGF-A_{165} transduced vessels at all time points analysed, that is, 7, 14, 21 and 28 days after vector injection (Table 3.2). Of the two factors accounted for in the GLiM, only the vector played a significant contribution towards the higher gradient in Ad.VEGF-A_{165} transduced vessels, and not the pregnancy status of the uterine horn (i.e., gravid or non-gravid). That is, the more rapid increase in uterine artery blood flow seen in the Ad.VEGF-A_{165} injected uterine arteries was significantly related to the effect of Ad.VEGF-A_{165} rather than to whether the vessel was supplying a gravid or non-gravid uterine horn.

In two sheep, we measured UABF for 8 hours/day for 1 week after administration of the vector, to see if there were any acute detrimental changes in UABF. No acute adverse effects were observed on UABF.

In summary, local administration of Ad.VEGF-A_{165} to the uterine arteries of pregnant sheep results in a sustained increase in uterine artery blood flow, that

is apparent as early as 7 days post-injection and lasts for at least 28 days post-injection.

3.3 Ad.VEGF-A_{165} transduction of uterine arteries in the pregnant sheep results in a significant increase in fetal weight compared to uninjected controls

Fetal weights from singleton pregnancies undergoing long-term UABF monitoring (n=6) were measured at post-mortem examination and compared to a historical singleton fetal control group from the same sheep breed (n=9) (David AL, 2005, Ph.D Thesis). The gestational age of the two groups was not statistically different (mean 139$\pm$3.1 days v/s mean 137.8$\pm$3.9 days, p=0.61, unpaired t-test). The mean fetal weight in the experimental group was significantly higher than that in the control group (5990$\pm$951 grams v/s 4698$\pm$1004 g, p=0.03, unpaired t-test). The relative fetal liver weights from the experimental group (n=16) were compared to a historical fetal control group (n=10). The mean gestational age of the two groups was not statistically different (139$\pm$2.9 v/s 138.9$\pm$6.5 days, p=0.95, unpaired t-test). The relative fetal liver weight was significantly higher in the experimental group (0.024 v/s 0.017g, p=0.01). The relative fetal kidney weights were also significantly higher in the treatment group (0.020 v/s 0.014, p=0.02). There was no significant difference in the relative weights of other tissues and organs.

3.4 Local administration of Ad.VEGF-A_{165} to the uterine arteries does not lead to significant changes in maternal blood pressure

VEGF is known to have a vasodilatory and hypotensive effect (Henry TD et al., 2003). We were concerned that uterine artery administration of Ad.VEGF-A_{165} might lead to a sudden and detrimental drop in maternal blood pressure. In order to assess the safety of adenoviral mediated VEGF gene transfer, maternal haemodynamic parameters were monitored telemetrically continuously 3 days

before and 4 to 7 days after Ad.VEGF-A_{165} vector injection in 4 animals. For these experiments, a PhysioTel® Implantable Transmitter with a blood-pressure sensitive catheter (PA-D70 device, Data Sciences International Tilburg, Netherlands) was inserted into the maternal carotid artery just before placement of flow probes around the uterine arteries. Blood pressure and heart rate were measured for 3 days before vector injection in order to derive baseline values (to compare the post-injection values with) and to examine the diurnal variation. Measurements were then taken continuously round the clock after vector injection over the period that would coincide with the time of maximum gene expression, which is normally from 12 hours post-infection to 1 week.

To study the long-term effects of Ad.VEGF-A_{165} vector injection, I also recorded maternal haemodynamic parameters daily until the end of gestation. Measurements were taken for 1 hour at the same time of the day in each animal to avoid diurnal variation. It was not possible to continuously monitor all 4 animals until the end of pregnancy because only one animal could be monitored at one time.

There was no significant change in maternal mean arterial pressure (MAP) from pre-injection baseline values in the time period immediately following the vector injection. Five days after vector injection, the MAP had fallen from 92.78$\pm$6.34 mmHg to 90.41$\pm$8.05 mmHg (n=4, paired t-test p=0.28). In normal ovine pregnancy, there is a small non-significant fall in MAP during the third trimester (105-136 days) (Kitanaka T et al., 1989). Maternal HR was not significantly different and changed from 106$\pm$9.4 beats per minute (bpm) to 108$\pm$8.6 bpm (p=0.46) in the five days following Ad.VEGF-A_{165} administration. The MAP and heart rate at term were not significantly different than the values at vector injection. The following figures (3.4-3.7) summarize the changes in MAP and heart rate short term and long term after the administration of the vector.

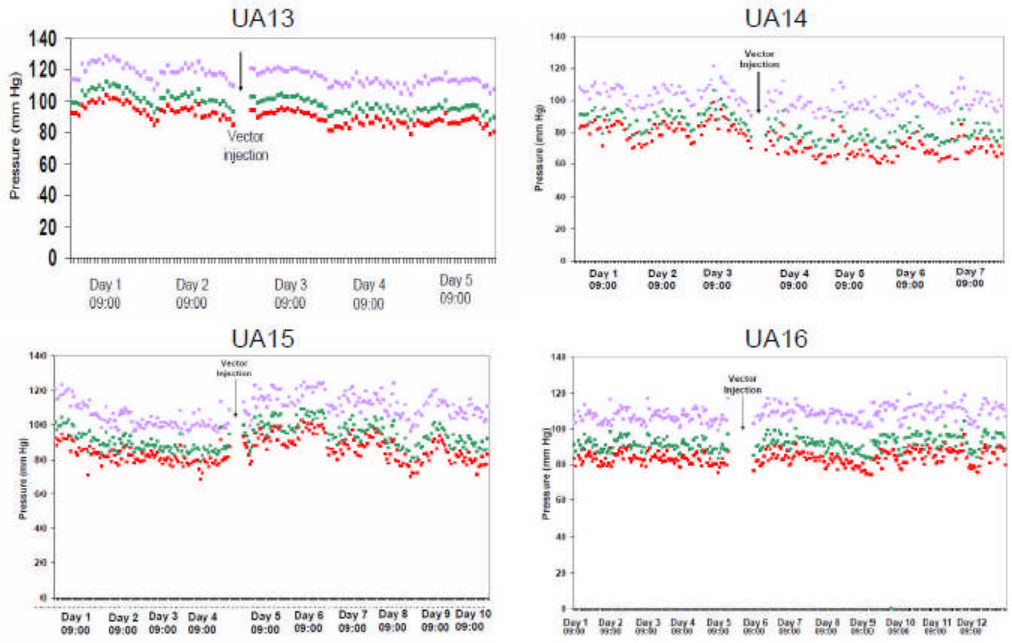

Figure 3.4 – Diurnal variation in maternal blood pressure before and after administration of Ad.VEGF-A_{165} and Ad.LacZ to the uterine arteries of pregnant sheep

A blood pressure-sensitive haemodynamic catheter was implanted in the carotid artery of mid-gestation pregnant sheep. The uterine arteries were injected with Ad.VEGF-A_{165} and Ad.LacZ contra-laterally one week later. The maternal blood pressure was monitored continuously day and night for 2-5 days before, and 3-7 days after the administration of the vector. There was no significant acute change in maternal blood pressure in the period following the vector injection. **Purple = Systolic blood pressure, Green = Mean arterial pressure; Red = Diastolic pressure**

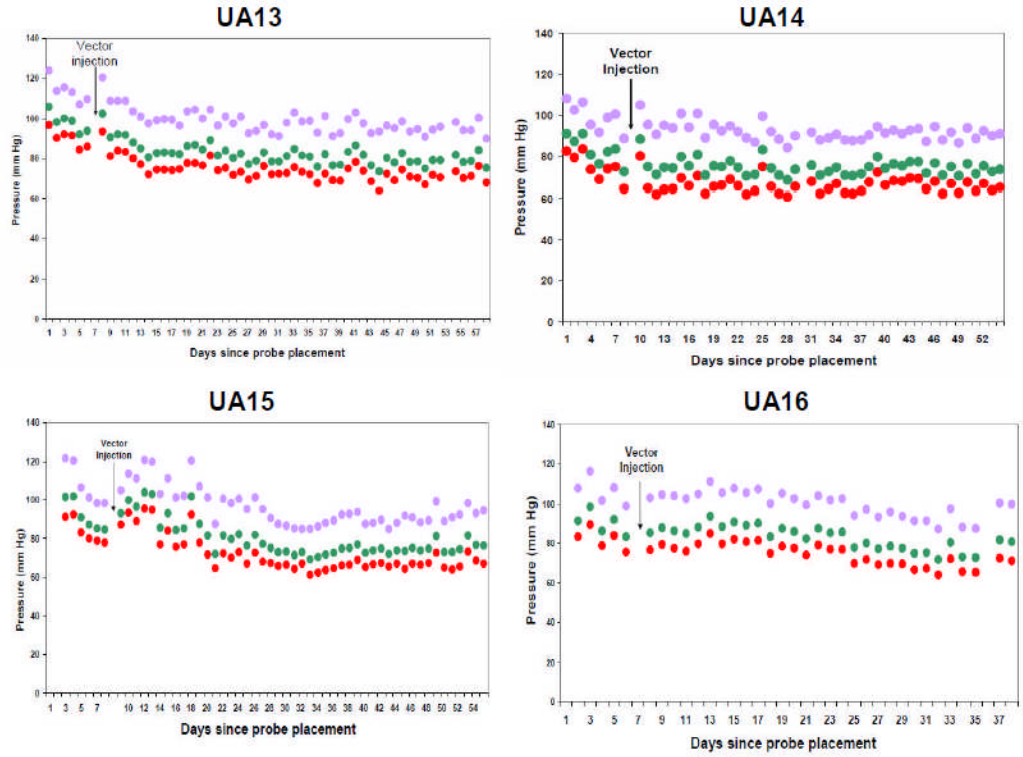

Figure 3.5 – Daily variation in maternal blood pressure before and after administration of Ad.VEGF-A_{165} and Ad.LacZ to the uterine arteries of pregnant sheep

A blood pressure-sensitive haemodynamic catheter was implanted in the carotid artery of mid-gestation pregnant sheep. The uterine arteries were injected with Ad.VEGF-A_{165} and Ad.LacZ contra-laterally one week later. The maternal blood pressure was monitored for one hour each morning at the same time of the day, before and after the administration of the vector, until term. There was no significant change in maternal blood pressure following the vector injection. **Purple = Systolic blood pressure**, **Green = Mean arterial pressure**; **Red = Diastolic pressure**

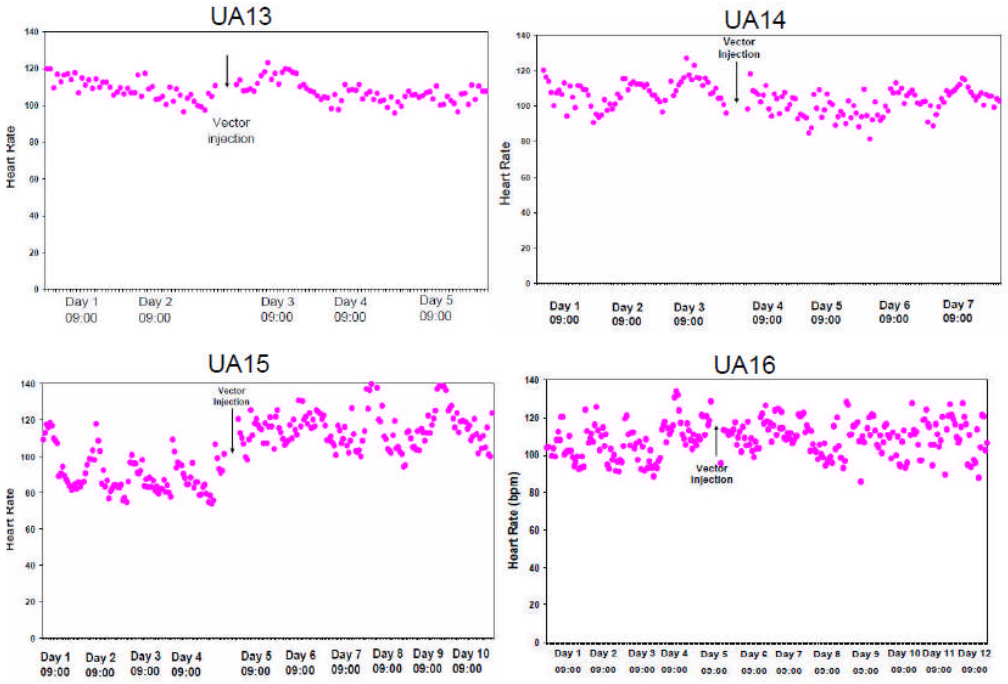

Figure 3.6 – Diurnal variation in maternal heart rate before and after administration of Ad.VEGF-A_{165} and Ad.LacZ to the uterine arteries of pregnant sheep

A blood pressure-sensitive haemodynamic catheter was implanted in the carotid artery of mid-gestation pregnant sheep. The uterine arteries were injected with Ad.VEGF-A_{165} and Ad.LacZ contra-laterally one week later. The maternal heart rate was monitored continuously day and night for 2-5 days before, and 3-7 days after the administration of the vector. There was no significant acute change in maternal heart rate in the period following the vector injection.

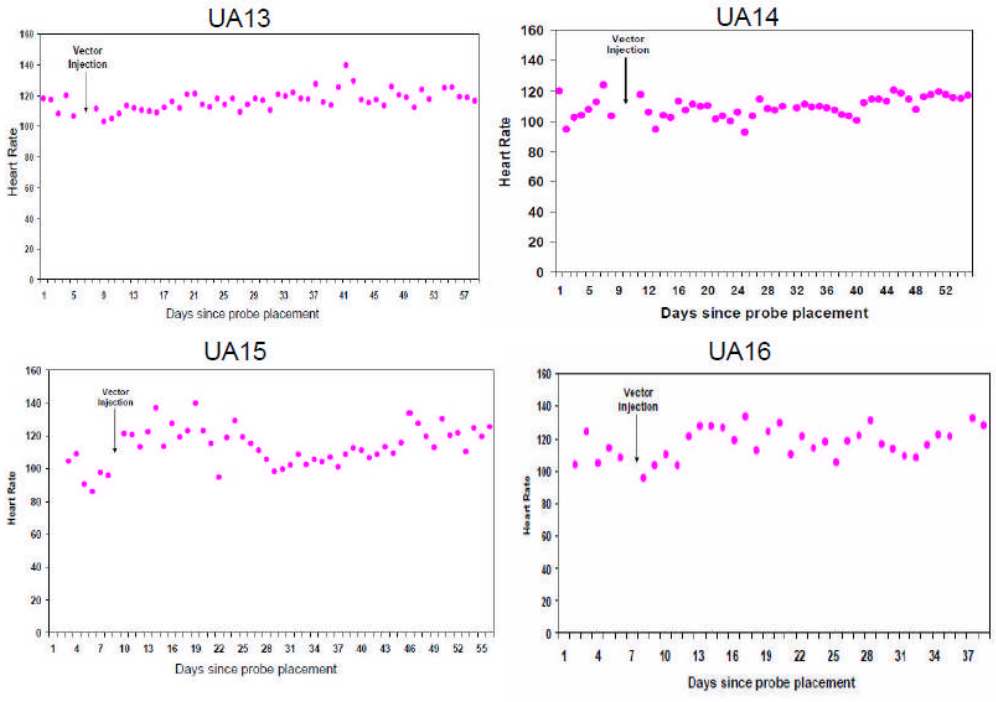

Figure 3.7 – Daily variation in maternal heart rate before and after administration of Ad.VEGF-A_{165} and Ad.LacZ to the uterine arteries of pregnant sheep

A blood pressure-sensitive haemodynamic catheter was implanted in the carotid artery of mid-gestation pregnant sheep. The uterine arteries were injected with Ad.VEGF-A_{165} and Ad.LacZ contra-laterally one week later. The maternal heart rate was monitored for one hour each morning at the same time of the day, before and after the administration of the vector, until term. There was no significant change in maternal heart rate following the vector injection.

Overall this data shows that there was no statistically significant effect seen on systemic maternal haemodynamics upon vector administration either short-term or long-term, suggesting there is unlikely to be any acute or chronic clinically important manifestation. A clinically important effect may be one wherein the magnitude of difference may be 20 mm Hg or greater, as in the case of severe haemorrhage. However, our experimental animals showed no

detrimental signs of health. They resumed normal feeding a couple of hours after surgery, were active and displayed no evident signs of distress.

3.5 Local administration of Ad.VEGF-A_{165} to the uterine arteries does not lead to significant changes in fetal blood pressure

In order to further assess the safety of Ad.VEGF-A_{165} administration to the uterine arteries of pregnant sheep, fetal haemodynamic parameters were monitored telemetrically (n=4). For these experiments, a PhysioTel® Implantable Transmitter with two blood-pressure sensitive catheters (D70-PCTP device, Data Sciences International Tilburg, Netherlands) was used, with one catheter being chronically implanted in the fetal carotid while the other one was placed in the amniotic cavity. This device can transmit in a range slightly exceeding one meter and hence, we arranged our two receivers in a way to maximize free animal movement while maintaining a good signal. The monitoring room set-up is graphically illustrated in Figure 2.1. Fetal blood pressure and heart rate data were transmitted telemetrically to the receivers which were in turn connected by cable to a computer in the adjacent room. Uploaded traces were viewed using the Dataquest software (Data Sciences International, Tilburg, Netherlands) then, selected traces were copied onto a database (Microsoft Office Excel 2003 software, Microsoft Corporation, USA) for further analysis. The difference between the fetal arterial and amniotic fluid pressure was used to calculate the true fetal BP. Data were collected continuously for 3 days before and 7 days after vector injection and then for 1 hour a day until the end of gestation (n=2 ewes).

During the monitoring schedule, short intermittent periods of signal loss were initially noticed when the ewe strayed away from the receivers. After repositioning of the receivers, this was kept to a minimum. Using this set-up, the signal could be detected by one of the two receivers at any one time, providing data for hourly monitoring in 100% of the diurnal and daily monitoring periods.

3.5.1 Fetal blood pressure and heart rate can be measured telemetrically long term

In the first procedure we performed, the catheter was placed into the common carotid artery. Fetal BP and HR data were collected and appeared to be in the normal range for the first 11 days after catheter placement. Adenovirus vector injection was performed uneventfully 7 days after catheter placement. On the 12th day after catheter placement, there was a sudden drop in BP and HR followed by fetal death. Post-mortem examination performed 48 hours later showed no fetal abnormality, haemorrhage or structural damage, and culture of tissues from the uterus and fetus revealed no evidence of microbial invasion. The tip of the catheter was found lying in the bicarotid trunk where it may have caused a partial obstruction of blood flow to both common carotid arteries. As there is some evidence that cannulation of the fetal sheep carotid arteries can result in ischemic brain damage especially when bilateral obstruction has occurred (Dodic M et al., 1998), we attempted to cannulate the second fetus through the femoral artery as an alternative route. On examining the fetal femoral artery at hysterotomy, this proved impossible to achieve at this gestational age due to the discrepancy between the small diameter of the femoral artery when compared to the catheter tip. The second fetus was thus cannulated through the common carotid artery as before. Fetal death again occurred suddenly, on the 8th day after catheter placement, and one day after vector injection. The catheter tip was observed at the bicarotid trunk in a similar way to the preceding fetus. There were no abnormal findings at post mortem examination.

In the subsequent two procedures we adjusted our technique to thread the catheter tip further upstream the carotid artery in an attempt to bypass the bicarotid trunk and reach the descending aorta (Figure 3.8). We used the distance between the point of insertion and the middle third of the sternum as an estimate of the threading distance which was approximately 7cm in both fetuses. The cannulation of the common carotid artery in these two fetuses was uncomplicated, and both survived until the end of gestation. At scheduled post mortem examination in one fetus (138 days of gestation), the catheter tip was found to be

lying in the right common carotid artery just below the point of insertion. This migration of the catheter tip might have been a result of fetal growth and movement. We were not able to ascertain the position of the catheter tip in the other fetus, which was unexpectedly born overnight on the day of the scheduled post mortem at term (139 days of gestation). During birth the catheter was pulled out from the carotid artery without obvious haemorrhage or structural damage to the fetal neck. This lamb survived until planned post mortem examination at four months of age.

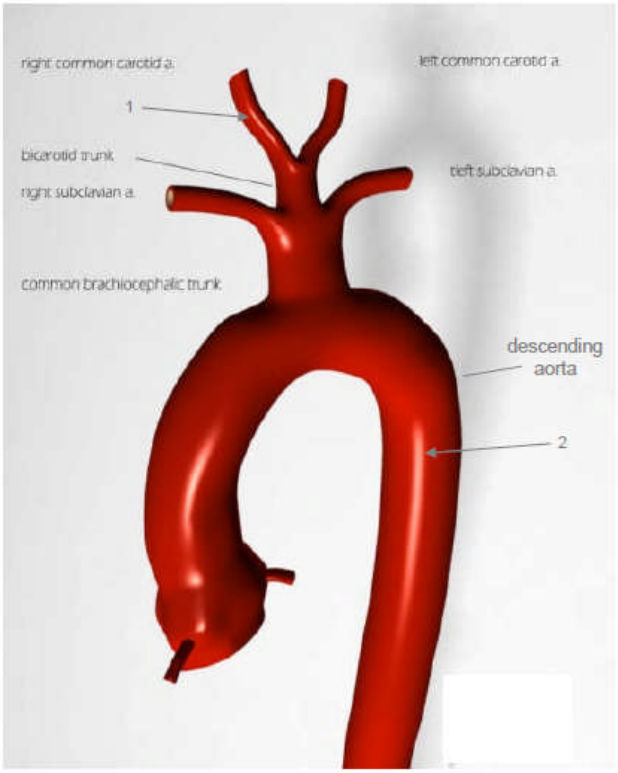

Figure 3.8 – Vascular anatomy of the neck arteries of fetal sheep

1 – Position of blood pressure sensitive catheter tip in first two experiments (placement in the right common carotid artery) which resulted in fetal death due to downward migration of catheter tip and obstruction of the bicarotid trunk. 2 – Position of catheter tip in subsequent two experiments (placement in the descending aorta) which allowed long-term monitoring of fetal haemodynamics. Picture adapted and modified from http://www.wikidoc.org/index.php/Image:Aortic_variations_truebovine.jpg

3.5.2 Short-term and long-term changes in fetal blood pressure

There was no significant change in fetal MAP from baseline values in the time period immediately following the vector injection. Three days after vector injection, the fetal MAP had fallen from 38.29±3.17 mmHg at baseline to 37.97±3.72 mmHg (n=3, paired t-test, p=0.28). Fetal heart rate was not significantly different and changed from 178±12.4 bpm to 171±10.9 bpm in the three days following Ad.VEGF-A_{165} administration. In one fetal sheep, the change in MAP and heart rate was investigated during vector injection and subsequent occlusion. The fetal MAP and heart rate increased by a maximum of 8mm Hg and 14 bpm respectively 3 minutes after occlusion and remained elevated until 30 minutes after release of occlusion. Figure 3.9 summarize the changes in MAP and heart rate short-term and long-term after vector injection.

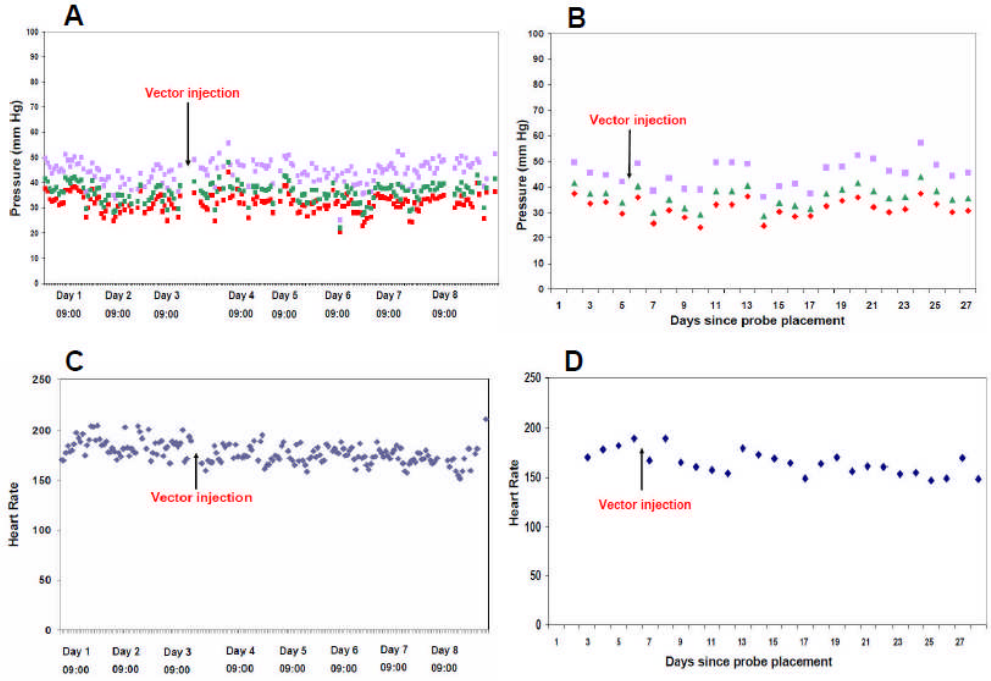

Figure 3.9 – Representative figures showing changes in fetal blood pressure and heart rate after administration of Ad.VEGF-A_{165} and Ad.LacZ to the uterine arteries of one pregnant sheep (UA29)

A blood pressure-sensitive haemodynamic catheter was implanted in the carotid artery of fetal sheep between 100-110 days gestational age (term=145 days). The maternal uterine arteries were

injected with Ad.VEGF-A_{165} and Ad.LacZ contra-laterally one week later. The fetal blood pressure and heart rate were monitored continuously round the clock for 3 days before and 5 days after the administration of the vector (A and C respectively). Fetal blood pressure and heart rate were also monitored for one hour each morning at the same time of the day, before and after the administration of the vector, until term (B and D respectively). There were no significant or detrimental changes in fetal haemodynamics following vector administration. **Purple = Systolic blood pressure, Green = Mean arterial pressure; Red = Diastolic pressure; Blue = Heart Rate**

Overall this data shows that there is no statistically significant effect seen on systemic maternal haemodynamics upon vector administration either short-term or long-term, suggesting there is unlikely to be any acute or chronic clinically important manifestation.

3.6 Ad.VEGF-A_{165} transduction of uterine arteries in the pregnant sheep results in long term changes in vascular reactivity.

I investigated the vascular responses of uterine arteries transduced with Ad.VEGF-A_{165} and Ad.LacZ long-term, approximately 30-45 days after local administration of the adenovirus vector. At 4 – 7 days after adenovirus-mediated gene transfer of VEGF to the uterine arteries, a significant reduction in the contractile response and a significant enhancement of the relaxation response were seen (David AL et al., 2008). We therefore studied both types of response in these long term transduced vessels.

3.6.1 Local over-expression of VEGF-A_{165} in the uterine arteries of pregnant sheep results in a diminished contractile response in twin and singleton pregnancies.

Organ bath experiments were conducted on the 2nd and 3rd branches of the main uterine artery. I initially studied all the four branches (main, 1st, 2nd and 3rd branches). The magnitude of the contractile responses generated in the main uterine artery and its 1st branch however were very large resulting in deformation of the L-shaped pins of the organ bath. Hence, I studied only the 2nd and 3rd branches for our pharmacology experiments. This is in keeping with published

literature where most studies on sheep uterine arteries have studied only these branches (Xiao D and Zhang L, 2002). Two-way analysis of variance (ANOVA) was used to statistically compare the vascular responses of the Ad.VEGF-A_{165} and Ad.LacZ transduced vessels, as it enables a variety of factors affecting uterine artery vascular response to be considered such as the type of vector applied, and whether the uterine artery was supplying a gravid or non-gravid horn.

We first studied twin pregnancies (n = 3) where a fetus was present in each horn of the bicornuate uterus. Figure 3.10 shows that there was a significant reduction in the mean contractile response to phenylephrine (PE) in vessels from twin pregnancies transduced with Ad.VEGF-A_{165} (E_{max} 155.7$\pm$13.65) compared to Ad.LacZ (E_{max} 180.7$\pm$10.39, $p<0.001$, two-way ANOVA). There was no significant difference in the magnitude of the KCl responses between the Ad.VEGF-A_{165} and Ad.LacZ treated sides (16.63±3.05g v/s 15.89±2.65g respectively, p=0.92).

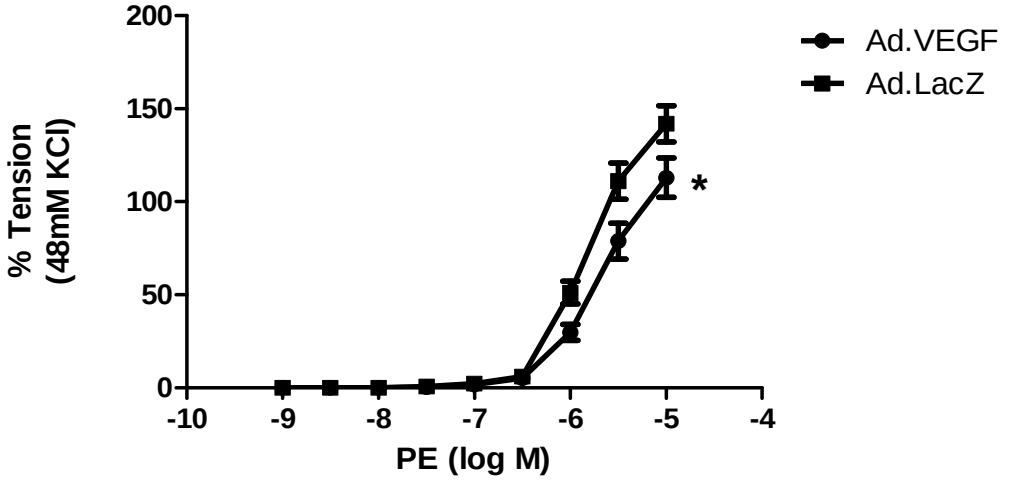

Figure 3.10 – Contractility of twin pregnant Ad.VEGF-A_{165} and Ad.LacZ transduced uterine arteries to L-phenylephrine (PE) 30-45 days after gene transfer.

At mid-gestation and in twin pregnancies (n=3), one uterine artery was injected with Ad.VEGF-A_{165} and the contra-lateral uterine artery was injected with Ad.LacZ. The second and third branches of the main uterine arteries were harvested 30-45 days after injection, cut into 3mm ring segments and analysed on an 8-chambered organ bath system. Concentration response curves to PE were constructed for each vessel in quadruplicate. The contractility of the vessel is expressed as a percentage of the response to KCl. PE produced concentration-dependent contractions, which

were of significantly lesser magnitude in Ad.VEGF-A_{165} transduced vessels compared to Ad.LacZ transduced vessels. Error bars denote standard error of mean. * denotes $p<0.005$

We next investigated this in animals that had a singleton pregnancy (n=5). Animals either received Ad.VEGF-A_{165} into the uterine artery supplying the non-gravid horn (n=4, Figure 3.11) or the gravid horn (n=1, Figure 3.12).

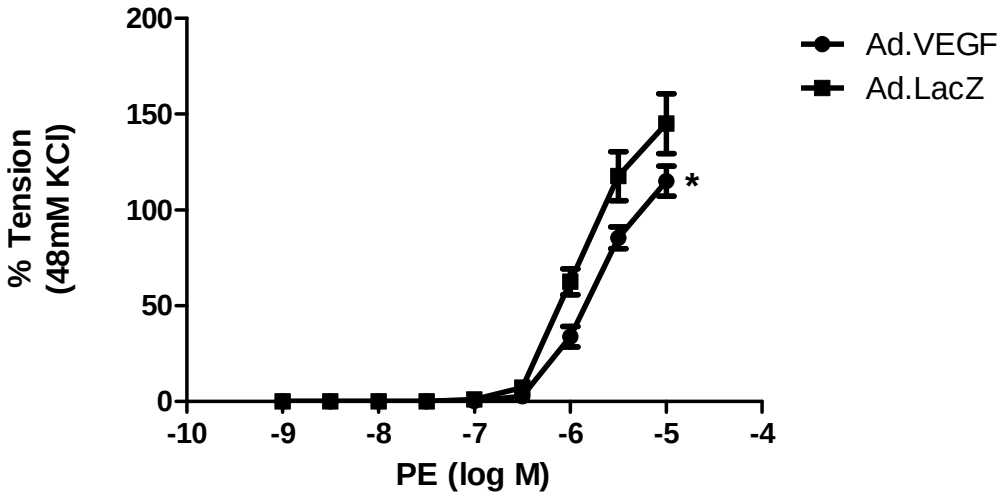

Figure 3.11 – Contractility of singleton pregnant Ad.VEGF-A_{165} and Ad.LacZ transduced uterine arteries to L-phenylephrine 30-45 days after gene transfer (Ad.VEGF-A_{165} administered on non-gravid side).

At mid-gestation, the uterine artery supplying the non-gravid horn was injected with Ad.VEGF-A_{165} and the contra-lateral uterine artery was injected with Ad.LacZ in singleton pregnant animals (n=4). The second and third branches of the main uterine arteries were harvested 30-45 days after injection, cut into 3mm ring segments and analysed on an 8-chambered organ bath system. Concentration response curves to PE were constructed for each vessel in quadruplicate. The contractility of the vessel is expressed as a percentage of the response to KCl. PE produced concentration-dependent contractions, which were of significantly lesser magnitude in Ad.VEGF-A_{165} transduced vessels compared to Ad.LacZ transduced vessels. Error bars denote standard error of mean. * denotes $p<0.005$

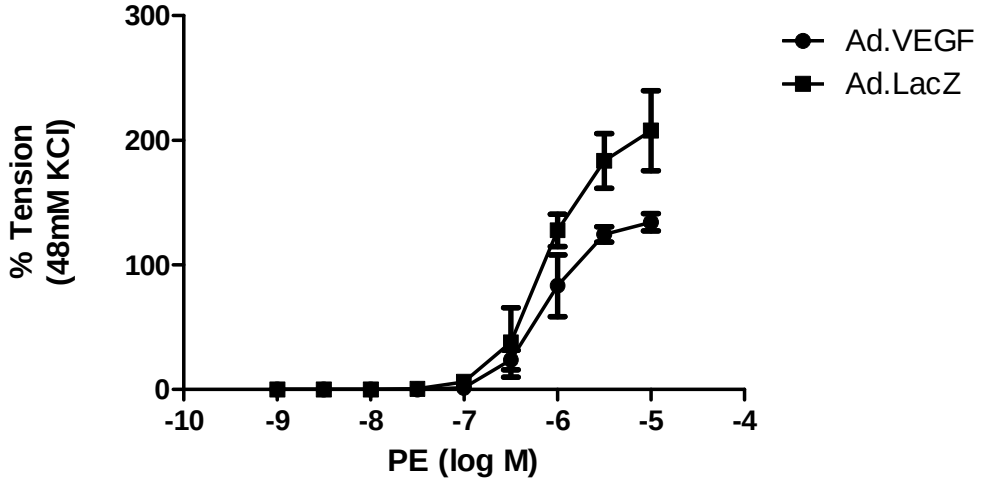

Figure 3.12 – Contractility of singleton pregnant Ad.VEGF-A_{165} and Ad.LacZ transduced uterine arteries to L-phenylephrine 30-45 days after gene transfer (Ad.VEGF-A_{165} administered on gravid side).

At mid-gestation, the uterine artery supplying the gravid horn was injected with Ad.VEGF-A_{165} and the contra-lateral uterine artery was injected with Ad.LacZ in a singleton pregnant animal (n=1). The second and third branches of the main uterine arteries were harvested 31 days after injection, cut into 3mm ring segments and analysed on an 8-chambered organ bath system. Concentration response curves to PE were constructed for each vessel in quadruplicate. The contractility of the vessel is expressed as a percentage of the response to KCl. PE produced concentration-dependent contractions, which were of lesser magnitude in Ad.VEGF-A_{165} transduced vessels compared to Ad.LacZ transduced vessels. Error bars denote standard error of mean.

When Ad.VEGF-A_{165} was administered to the uterine artery supplying the non-gravid horn, there was a significant reduction in the contractile response compared to the Ad.LacZ transduced vessel (E_{max} 153.9 ± 9.23 v/s 178.3 ±12.59, n=4, $p<0.001$, two-way ANOVA, Figure 3.11). Similarly when Ad.VEGF-A_{165} was administered to the uterine artery supplying the pregnant horn in a singleton pregnancy, there appeared to be a reduced contractile response compared to the Ad.LacZ transduced uterine artery (E_{max} 155.1 ±11.32 v/s 235.9 ± 19.62, Figure 3.12). The change in contractile response appeared to be more marked in this configuration. No statistical analysis could be performed in this case because only one animal which received this combination of factors was studied.

Combining the data for the three different experimental groups described above by two-way ANOVA (to factor in the effects of the vector and whether the uterine artery was supplying a gravid or non-gravid horn), I observed there was a significant reduction in the contractile response to phenylephrine in the Ad.VEGF-A_{165} transduced vessels (E_{max} 154.1$\pm$6.95) when compared to the Ad.LacZ transduced vessels (E_{max} 184.7$\pm$8.33, p=0.0001).

Table 3.5 summarizes the maximum contractile response (E_{max}) to phenylephrine observed in singleton and twin experiments.

Table 3.5 – Maximum response (E_{max}) to L-phenylephrine in uterine arteries from twin and singleton pregnant animals injected with Ad.VEGF-A_{165} and Ad.LacZ contra-laterally.

At mid-gestation, one uterine artery was injected with Ad.VEGF-A_{165} and the contra-lateral uterine artery was injected with Ad.LacZ in pregnant sheep. The second and third branches of the main uterine artery were harvested 30-45 days after injection and analysed on an 8-chambered organ bath system. Concentration response curves to PE were constructed for each vessel in quadruplicate. The contractility of the vessel is expressed as a percentage of the response to KCl. The p value is for the contraction dose response curve.

Number of fetuses	Side of Ad.VEGF-A_{165} vector injection	Number of animals	Observed E_{max} % (Mean$\pm$SEM)		p value
			Ad.VEGF-A_{165} vector	Ad.LacZ vector	
Twins	Gravid	3	155.7 ±13.65	180.7±10.39	0.0003
Singleton	Non-gravid	4	153.9 ± 9.23	178.3±12.59	0.0009
Singleton	Gravid	1	155.1 ±11.32	235.9±19.62	na
All 3 groups	-	8	154.1 ± 6.95	184.7 ± 8.33	0.0001

Table 3.6 summarizes the EC_{50} with phenylephrine observed in singleton and twin experiments. EC_{50} is the dose required to produce 50% of the maximal effect. As was expected, the EC_{50} was higher for the Ad.VEGF-A_{165} transduced vessels than for the Ad.LacZ transduced ones since the former are less contractile

Table 3.6 – EC_{50} in response to L-phenylephrine in uterine arteries from twin and singleton pregnant animals injected with Ad.VEGF-A_{165} and Ad.LacZ contra-laterally.

At mid-gestation, one uterine artery was injected with Ad.VEGF-A_{165} and the contra-lateral uterine artery was injected with Ad.LacZ in pregnant sheep. The second and third branches of the main uterine artery were harvested 30-45 days after injection and analysed on an 8-chambered organ bath system. Concentration response curves to PE were constructed for each vessel in quadruplicate. The contractility of the vessel is expressed as a percentage of the response to KCl. EC_{50} was calculated by plotting a sigmoidal dose response curve. The p value is for the contraction dose response curve.

Number of fetuses	Side of Ad.VEGF-A_{165} vector injection	Number of animals	EC_{50} (M)		p value
			Ad.VEGF-A_{165} vector	Ad.LacZ vector	
Twins	Gravid	3	3.48×10^{-6}	2.33×10^{-6}	0.0003
Singleton	Non-gravid	4	2.97×10^{-6}	1.88×10^{-6}	0.0009
Singleton	Gravid	1	9.84×10^{-7}	9.91×10^{-7}	na
All 3 groups	-	8	2.60×10^{-6}	1.82×10^{-6}	0.0001

In summary this data demonstrates that 30-45 days after local administration of Ad.VEGF-A_{165} to the uterine arteries of mid-gestation pregnant sheep, there is a significant reduction in uterine artery contractility compared to Ad.LacZ transduced vessels.

3.6.2 Local over-expression of VEGF-A_{165} in the uterine arteries of pregnant sheep has no significant effect on the relaxation response to bradykinin 30-45 days after gene transfer

I next analysed the relaxation response to bradykinin in the uterine arteries that had been transduced with Ad.VEGF-A_{165} or Ad.LacZ, approximately 30-45 days after vector injection. Data is first presented on twin gestations (n=3), in which there was a fetus in each uterine horn. Figure 3.13 shows that there was no difference in the relaxation response to bradykinin between the Ad.VEGF-A_{165} transduced side (E_{max} 62.16±1.84) and the Ad.LacZ transduced side (E_{max} 59.01±1.90).

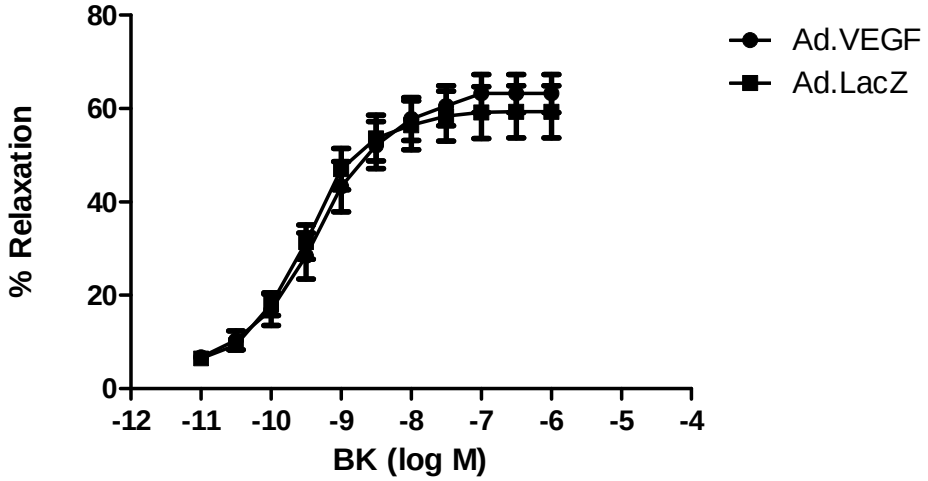

Figure 3.13 – Endothelium-dependent relaxation of twin pregnant Ad.VEGF-A_{165} and Ad.LacZ transduced uterine arteries to bradykinin (BK) 30-45 days after gene transfer.

At mid-gestation, one uterine artery was injected with Ad.VEGF-A_{165} and the contra-lateral uterine artery was injected with Ad.LacZ in twin pregnant animals (n=3). The second and third branches of the main uterine arteries were harvested 30-45 days after injection, cut into 3mm ring segments and analysed on an 8-chambered organ bath system. Concentration response curves to BK were constructed for each vessel in quadruplicate. The relaxation of the vessel is expressed as a percentage of inhibition of PE-induced contraction. There was no significant difference in the relaxation response between the Ad.VEGF-A_{165} and Ad.LacZ transduced vessels (statistical significance assumed at $p<0.05$). Error bars denote standard error of mean.

I investigated this similarly in 4 animals that had a singleton pregnancy, all of which had Ad.VEGF-A_{165} injected into the vessel supplying the non-gravid side. As in the case of twins, no significant difference was observed in the endothelium-dependent relaxation to bradykinin between the Ad.VEGF-A_{165} transduced side (E_{max} 48.83$\pm$2.63) and Ad.LacZ transduced side (E_{max} 40.13$\pm$1.86, Figure 3.14). In one singleton pregnant animal, Ad.VEGF-A_{165} was injected into the vessel supplying the gravid horn, and Ad.LacZ into the uterine artery supplying the non-gravid horn. However, the vessels from this animal failed the endothelial integrity test, that is, they did not relax more than 30% in response to a bolus dose of bradykinin (1 μm) suggesting compromise of endothelial integrity (either during dissection or mounting). Hence, the results of this animal were excluded from the analysis.

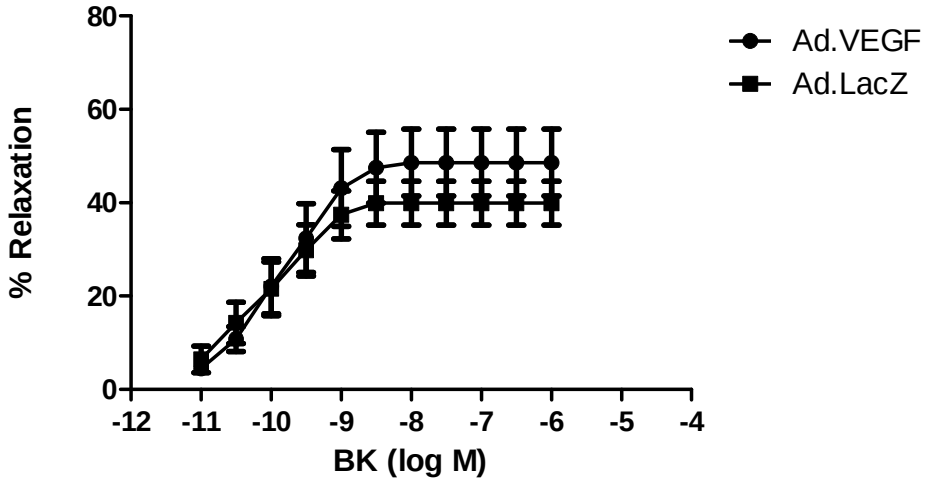

Figure 3.14 – Endothelium-dependent relaxation of singleton pregnant Ad.VEGF-A_{165} and Ad.LacZ transduced uterine arteries to bradykinin 30-45 days after gene transfer (Ad.VEGF-A_{165} administered on non-gravid side).

At mid-gestation, the uterine artery supplying the non-gravid horn was injected with Ad.VEGF-A_{165} and the contra-lateral uterine artery was injected with Ad.LacZ in singleton pregnant animals (n=4). The second and third branches of the main uterine arteries were harvested 30-45 days after injection, cut into 3mm ring segments and analysed on an 8-chambered organ bath system. Concentration response curves to BK were constructed for each vessel in quadruplicate. The relaxation of the vessel is expressed as a percentage of inhibition of PE-induced contraction. There was no significant difference in the relaxation response between the Ad.VEGF-A_{165} and Ad.LacZ transduced vessels (statistical significance assumed at $p<0.05$). Error bars denote standard error of mean.

Table 3.7 summarizes the maximum relaxation response (E_{max}) to bradykinin from singleton and twin experiments.

Table 3.7 – Maximum response (E_{max}) to bradykinin in uterine arteries from twin and singleton pregnant animals injected with Ad.VEGF-A_{165} and Ad.LacZ contra-laterally.

At mid-gestation, one uterine artery was injected with Ad.VEGF-A_{165} and the contra-lateral uterine artery was injected with Ad.LacZ in pregnant sheep. The second and third branches of the main uterine artery were harvested 30-45 days after injection and analysed on an 8-chambered organ bath system. Concentration response curves to BK were constructed for each vessel in quadruplicate. The relaxation of the vessel is expressed as a percentage of inhibition of PE-induced contraction. The p value is for the relaxation dose response curve.

Number of fetuses	Side of Ad.VEGF-A_{165} vector injection	Number of animals	Observed E_{max} % (Mean±SEM)		p value
			Ad.VEGF-A_{165} vector	Ad.LacZ vector	
Twins	Gravid	3	62.16±1.84	59.01±1.90	0.995
Singleton	Non-gravid	4	48.83± 2.63	40.13±1.86	0.968
Both groups	-	7	57.53± 1.55	52.25±1.47	0.954

Table 3.8 summarizes the pD_2 (-log EC_{50}) to bradykinin from singleton and twin experiments.

Table 3.8 – pD_2 (-log EC_{50}) in response to bradykinin in uterine arteries from twin and singleton pregnant animals injected with Ad.VEGF-A_{165} and Ad.LacZ contra-laterally.

At mid-gestation, one uterine artery was injected with Ad.VEGF-A_{165} and the contra-lateral uterine artery was injected with Ad.LacZ in pregnant sheep. The second and third branches of the main uterine artery were harvested 30-45 days after injection and analysed on an 8-chambered organ bath system. Concentration response curves to BK were constructed for each vessel in quadruplicate. The relaxation of the vessel is expressed as a percentage of inhibition of PE-induced contraction. pD_2 was calculated by plotting a sigmoidal dose-response curve. The p value is for the relaxation dose response curve.

Number of fetuses	Side of Ad.VEGF-A_{165} vector injection	Number of animals	pD_2 (Mean±SEM)		p value
			Ad.VEGF-A_{165} vector	Ad.LacZ vector	
Twins	Gravid	3	9.27 ± 0.12	9.50 ± 0.13	0.995
Singleton	Non-gravid	4	9.83 ± 0.25	9.97 ± 0.25	0.968
Both groups	-	7	9.43 ± 0.11	9.61 ± 0.12	0.954

To summarize, these results show that 30-45 days after local over-expression of VEGF-A_{165} in the uterine arteries of pregnant sheep, there is no significant difference in the relaxation response to bradykinin between uterine artery segments transduced with either Ad.VEGF-A_{165} or Ad.LacZ. This is observed in both twin and singleton pregnancies.

3.6.3 The long-term relaxation response to Bradykinin is primarily mediated via the Nitric oxide Synthase (NOS) and Endothelium Derived Hyperpolarizing Factor (EDHF) pathways

The reduced contractility associated with local VEGF-A_{165} over-expression in uterine arteries long-term prompted me to examine the mechanisms involved. To do this it was first established which mechanisms mediated relaxation of uterine arteries using inhibitors of specific relaxation pathways. Vessels from 3 animals (all twins) were used for these experiments. I used three inhibitors known to affect different components of the relaxation pathway. L-

NAME is an inhibitor of the NOS pathway, indomethacin blocks the action of prostacyclins while apamin is a small conductance Ca^{2+} activated K^+ channel blocker which inhibits the functions of EDHF. Uterine arteries were incubated for 20 minutes (for L-NAME and indomethacin) or 30 minutes (for apamin) with the inhibitor either individually or in combination, then pre-contracted with phenylephrine, followed by a dose-response curve to bradykinin. The concentrations used for the different inhibitors were L-NAME - 300μM, Indomethacin - 10 μM and Apamin - 1 μM. The vascular relaxation in uterine arteries (2^{nd} and 3^{rd} branches of the main uterine artery) was compared in vessels exposed or unexposed to inhibitors.

Treatment with L-NAME reduced the relaxation response to bradykinin in uterine artery segments (Figure 3.15, Table 3.9). L-NAME significantly reduced relaxation relative to control vessels (not treated with L-NAME). There was no significant difference however in the amount of reduced relaxation response in the uterine arteries with L-NAME inhibition, between the Ad.VEGF-A_{165} and Ad.LacZ transduced sides. Treatment with the cyclooxygenase inhibitor Indomethacin did not change the endothelium dependent relaxation, indicating that PGI_2 does not modulate the relaxation in these vessels. The remaining endothelium-dependent relaxation, that was resistant to inhibition by L-NAME and Indomethacin, was significantly reduced by pre-treatment with apamin (the E_{max} was lowered by 43.21% in Ad.VEGF-A_{165} transduced vessels v/s 48.26% in Ad.LacZ transduced vessels, n=3). There was no significant difference in the small amount of residual relaxation that remained after NOS, PGI_2 and EDHF inhibition between the Ad.VEGF-A_{165} and Ad.LacZ transduced sides (n=3). Incubation with Indomethacin alone or Apamin alone also did not significantly alter the bradykinin-induced relaxation (data not shown).

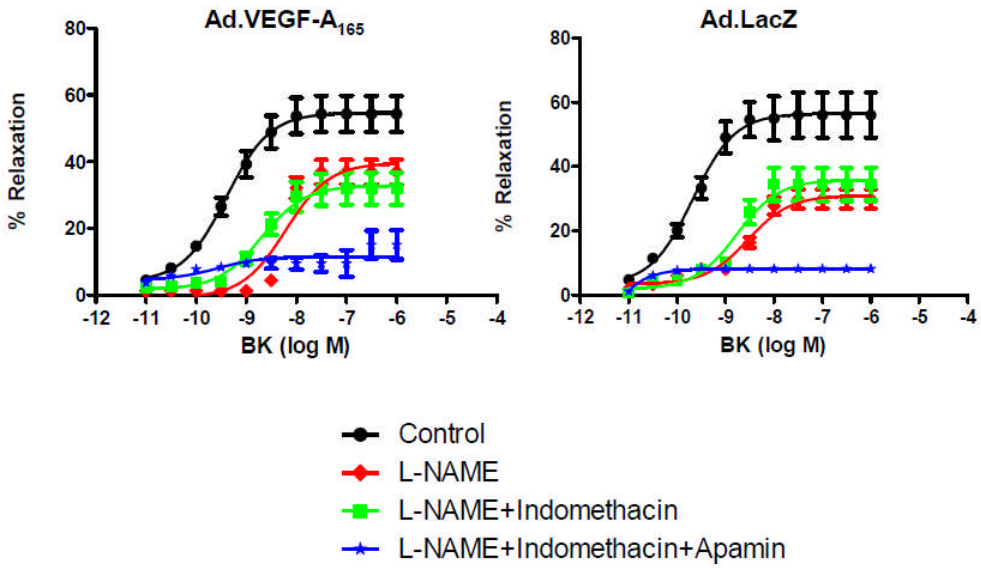

Figure 3.15(a) – The endothelium-dependent relaxation to bradykin in the presence of different inhibitors of the relaxation pathway in pregnant sheep uterine arteries, 30-45 days after Ad.VEGF-A_{165} or Ad.LacZ transduction.

The contribution of nitric oxide (NO), prostacyclin (PGI_2) and endothelium-derived hyperpolarizing factor (EDHF) on the relaxation response to BK were investigated in vessels precontracted with PE. Cumulative relaxation curves of BK (10^{-11}M to 10^{-6}M) were constructed under the following conditions: (1) control (no inhibitors); (2) in the presence of G -nitro-L-Arginine-Methyl Ester (L-NAME, NO synthase inhibitor, 300 µM); (3) in the presence of L-NAME and indomethacin (PGI_2 inhibitor, 10 µM); (4) in the presence of L-NAME, indomethacin and apamin (small-conductance Ca^{2+}-activated K^+ channel inhibitor, 1 µM). Relaxation was expressed as a percentage of inhibition of PE-induced contraction. The mean relaxation response of vessels from twin pregnant sheep (n=3) was calculated. Statistical significance was assumed at $p<0.05$. The BK relaxant effect was not modified by indomethacin but reduced by L-NAME ($p<0.05$, n=3). The remaining endothelium-dependent relaxation (E_{max}), that was resistant to indomethacin and NO synthase inhibition, was significantly reduced by pretreatment with apamin in both Ad.VEGF-A_{165} and Ad.LacZ treated arteries ($P<0.05$, n=3).

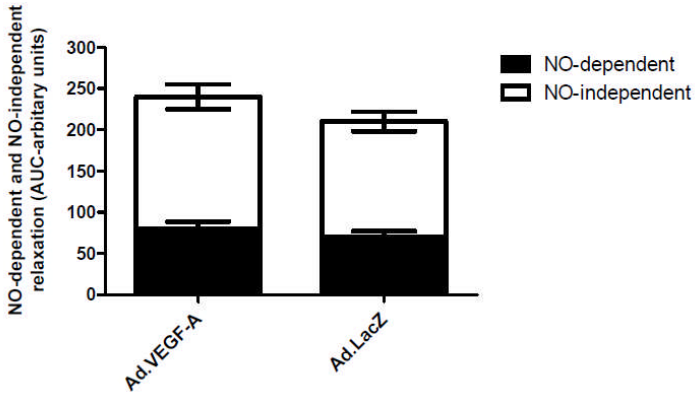

Figure 3.15(b) – Partial contribution of NO-dependent and NO-independent mechanisms to the endothelial-dependent relaxation

Values are the mean±SEM for the area under the curve (AUC) for BK-induced relaxation (complete bar with positive SEM), the AUC for BK-induced relaxation following treatment with L-NAME (NO-independent component, white bar), and the remaining AUC after BK with L-NAME (NO-dependent component, black bar). No significant differences were observed in the overall relaxation as well as NO-dependent and NO-independent relaxations between the treated and control sides.

Table 3.9 –– E_{max} in response to bradykinin in uterine arteries from pregnant sheep injected with Ad.VEGF-A_{165} and Ad.LacZ contra-laterally, in the presence of different inhibitors of endothelium-dependent relaxation.

At mid-gestation, one uterine artery was injected with Ad.VEGF-A_{165} and the contra-lateral uterine artery was injected with Ad.LacZ in pregnant sheep. The second and third branches of the main uterine artery were harvested 30-45 days after injection and analysed on an 8-chambered organ bath system. Concentration response curves to BK were constructed for each vessel in the absence and presence of different inhibitors of relaxation, namely, L-NAME, Indomethacin and Apamin. The relaxation of the vessel is expressed as a percentage of inhibition of PE-induced contraction. The p value indicates the significance of the effect of individual inhibitors on the dose response curve.

Inhibitor	E_{max} % (Mean ±SEM)		p value
	Ad.VEGF-A_{165} transduced side	Ad.LacZ trandsduced side	
No inhibitor	54.73±2.36	56.52±2.15	
L-NAME	39.66±4.96	31.03±4.40	p<0.05
L-NAME+ Indomethacin	32.89±3.74	35.88±4.65	p=0.2
L-NAME+ Indomethacin+ Apamin	11.52±2.01	8.26±1.65	p<0.05

In summary, this data demonstrates that the bradykinin-mediated endothelium-dependent relaxation in pregnant sheep uterine arteries is mediated

via NO and EDHF. Inhibition by L-NAME significantly reduces the relaxation response compared to untreated vessels. There is a further significant attenuation of relaxation when Apamin is added. Prostacyclins do not appear to play a significant role in the bradykinin-mediated relaxation. In all cases, that is, both in the presence and absence of different inhibitors, the vascular relaxation responses in the Ad.VEGF-A_{165} and Ad.LacZ transduced uterine arteries were not significantly different.

3.6.4 The long-term reduction in contractility to Phenylephrine in Ad.VEGF-A_{165} transduced vessels is mediated via the Nitric oxide Synthase (NOS) pathway

In order to investigate the mechanism behind the reduced contractility of Ad.VEGF-A_{165} transduced vessels long-term, the contractility to phenylephrine was studied in the presence of the NOS inhibitor, L-NAME. Uterine arteries from twin pregnant sheep (n=3) were incubated with L-NAME (300 μM) for 20 minutes, and a dose-response curve to phenylephrine was generated. The contractile response in uterine arteries (2^{nd} and 3^{rd} branch) was compared in vessels exposed or unexposed to L-NAME.

I observed a significant increase in the contractile response to phenylephrine in the Ad.VEGF-A_{165} transduced vessels when pre-treated with L-NAME (E_{max} 106.6$\pm$3.94 v/s 132.9$\pm$6.07, p=0.002). Vessels transduced with Ad.LacZ also contracted in response to phenylephrine when pre-treated with L-NAME, but the increase in contractility was less and was non-significant (E_{max} 124.6$\pm$8.51 v/s 131.9$\pm$8.69). With the inhibition of the NOS pathway by L-NAME, the E_{max} in response to phenylephrine in both the Ad.VEGF-A_{165} and Ad.LacZ transduced vessels were very similar. (Figure 3.16, Table 3.10)

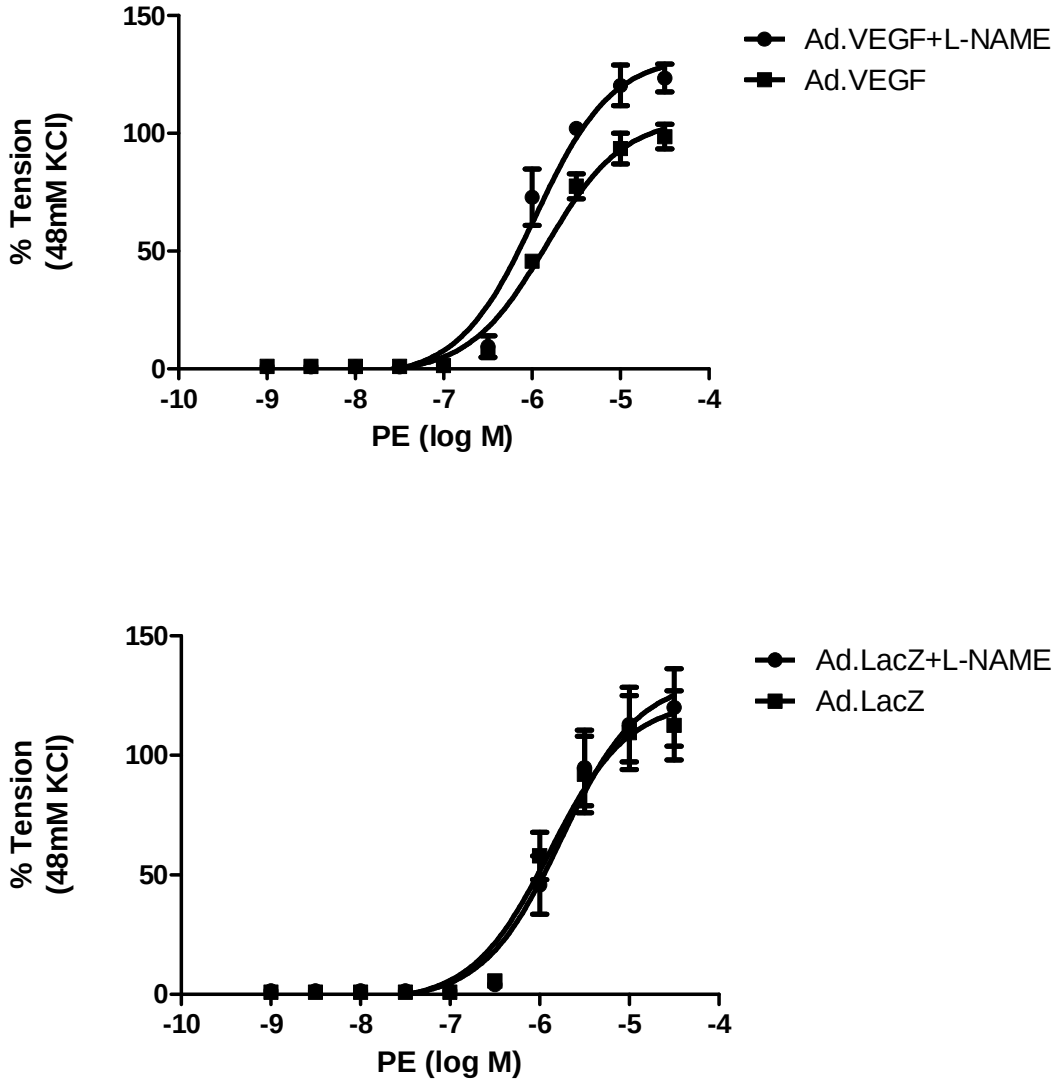

Figure 3.16 - The contractility to phenylephrine in the presence of L-NAME in pregnant sheep uterine arteries, 30-45 days after Ad.VEGF-A_{165} (top) or Ad.LacZ (bottom) transduction.

The effect of NOS inhibition on the contractile response to PE was investigated in uterine arteries transduced with either Ad.VEGF-A_{165} or Ad.LacZ. Cumulative relaxation curves of PE (10^{-9}M to 10^{-4}M) were constructed under the following conditions: (1) control (no inhibitor); and (2) in the presence of L-NAME (300 µM). The contractility of the vessel is expressed as a percentage of the response to KCl. The mean contractile response of vessels from twin pregnant sheep (n=3) was calculated. Statistical significance was assumed at $p<0.05$. The PE-produced contractility was significantly enhanced in the presence of L-NAME in Ad.VEGF-A_{165} treated uterine arteries (top graph), but there was no significant increase seen in the Ad.LacZ treated uterine arteries (bottom graph).

Table 3.10 –– Maximum response (E_{max}) in response to phenylephrine in uterine arteries from pregnant sheep injected with Ad.VEGF-A_{165} and Ad.LacZ contra-laterally, in the presence of L-NAME.

At mid-gestation, one uterine artery was injected with Ad.VEGF-A_{165} and the contra-lateral uterine artery was injected with Ad.LacZ in twin pregnant sheep (n=3). The second and third branches of the main uterine artery were harvested 30-45 days after injection and analysed on an 8-chambered organ bath system. Concentration response curves to PE were constructed for each vessel in the absence and presence of L-NAME. The contractility of the vessel is expressed as a percentage of the response to KCl. The p value indicates the significance of the effect of addition of inhibitor compared to control vessels (i.e., unexposed to inhibitors).

Inhibitor	E_{max} % (Mean±SEM)		p value
	No inhibitor	L-NAME	
Ad.VEGF-A_{165} transduced side	106.6±3.94	132.9±6.07	0.002
Ad.LacZ trandsduced side	124.6±8.51	131.9±8.69	0.987

Thus, the reduction in phenylephrine-induced contractility in pregnant sheep uterine arteries transduced with Ad.VEGF-A_{165} appears to be mediated by NO. When the NOS pathway is blocked by pre-treatment with L-NAME, there is no longer any difference in the maximum contractile response between the Ad.VEGF-A_{165} and Ad.LacZ transduced uterine arteries.

3.7 There is no difference in the vascular reactivity of the contra-lateral uterine arteries in sham-operated term pregnant sheep

Uterine arteries from two sham-operated long-term sheep (one twin pregnant and one singleton pregnant) that were injected only with the vehicle (PBS) were examined on an organ bath 36-50 days after injection. I was interested in investigating whether there are any inherent differences between the vascular

reactivity of the contra-lateral uterine arteries in the absence of over-expression of VEGF. Figure 3.17 and Figure 3.18 show that there was no difference in the contractility or relaxation between the left and right uterine arteries.

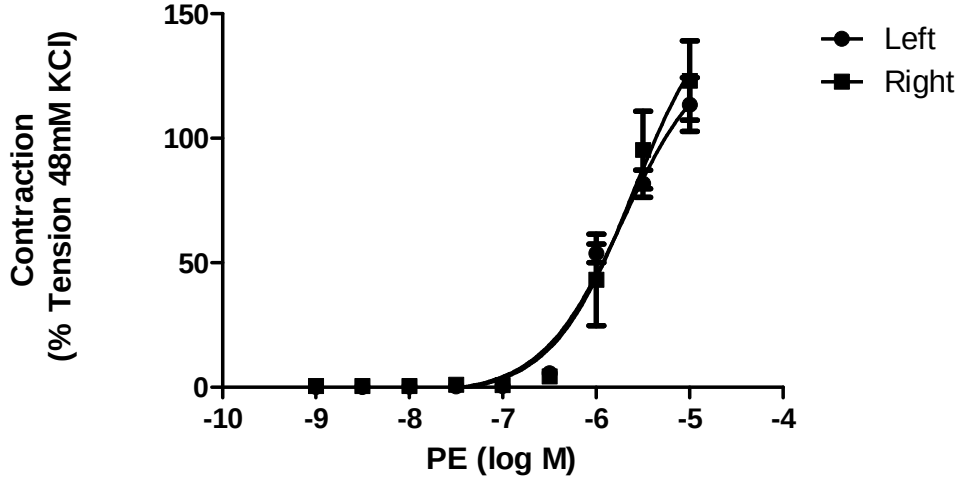

Figure 3.17 - Contractility of pregnant sheep uterine artery sham-injected with phosphate buffered saline (PBS) 30 days after injection.

At mid-gestation, the uterine arteries of one twin pregnant sheep and one singleton pregnant sheep were injected with PBS bilaterally. The second and third branches of the main uterine arteries were harvested over 30 days after injection, cut into 3mm ring segments and analysed on an 8-chambered organ bath system. Concentration response curves to PE were constructed for each vessel in quadruplicate. The contractility of the vessel is expressed as a percentage of the response to KCl. PE produced concentration-dependent contractions, which were no different between the left and right sides. Error bars denote standard error of mean.

In response to phenylephrine, the E_{max} in the left uterine artery was 135.7$\pm$8.35 and that in the right uterine artery was 158.3$\pm$19.19. The p value for difference in the dose-response curve to phenylephrine was 0.90 (Two-way ANOVA).

The relaxation dose response curve to bradykinin was also not significantly different between the left and right uterine arteries (p=0.96, Two-way ANOVA, Figure 3.18). The E_{max} in the left uterine artery was 63.73$\pm$2.45, while the E_{max} in the right uterine artery was 65.33$\pm$2.05.

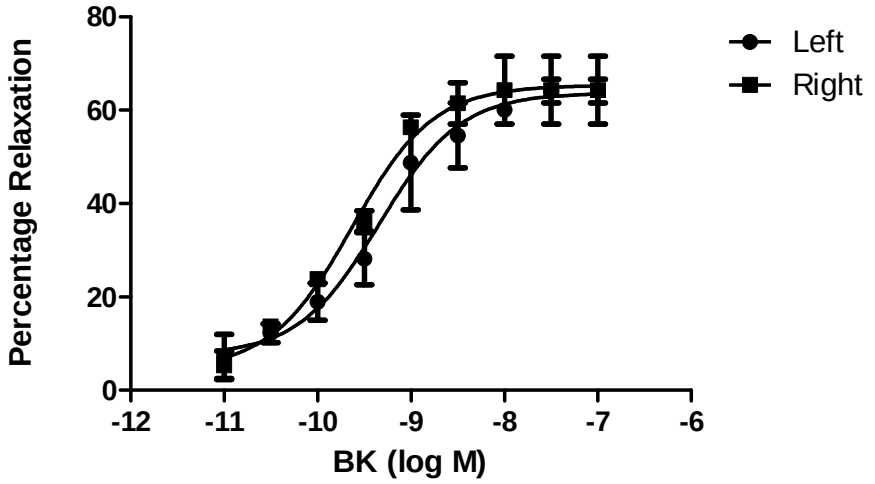

Figure 3.18 – Endothelium-dependent relaxation of pregnant sheep uterine artery sham-injected with phosphate buffered saline (PBS) 30 days after injection

At mid-gestation, the uterine arteries of one twin pregnant sheep and one singleton pregnant sheep were injected with PBS bilaterally. The second and third branches of the main uterine arteries were harvested over 30 days after injection, cut into 3mm ring segments and analysed on an 8-chambered organ bath system. Concentration response curves to BK were constructed for each vessel in quadruplicate. The relaxation of the vessel is expressed as a percentage of inhibition of PE-induced contraction. BK produced concentration-dependent relaxation, which was not different between the left and right sides. Error bars denote standard error of mean.

3.8 The vascular reactivity of sheep uterine arteries can not be studied on a wire myograph

I was interested in examining the effects of Ad.VEGF-A_{165} transduction on the vascular reactivity of smaller utero-placental blood vessels (which resemble the diameter of the human spiral arteries more closely). Hence, the 4^{th} and 5^{th} branches of the main uterine artery were dissected out for pharmacology experiments. I attempted to study the vascular reactivity of these segments on an organ bath set-up, but failed to do so because their internal diameter was too small for the two L-shaped pins to pass through their lumen.

Next, I attempted to study their vascular reactivity on a wire myograph using 40 μm thick stainless steel wires to mount them. However, the thick

muscular layer of the sheep uterine arteries resulted in the generation of excessive contractions to KCl and PE. The magnitude of these contractile tensions was beyond the limits of accurate measurement of the wire myograph. In addition, the large force of contraction also deformed the delicate wires of the myograph, making it impossible to continue with the experiment.

Hence, it was concluded that the vascular reactivity of the fourth and fifth branches of pregnant sheep uterine arteries cannot be analysed on a wire myograph.

3.9 Ad.VEGF-A_{165} transduction of uterine arteries in the pregnant sheep does not lead to any significant difference in the vascular reactivity of the umbilical vessels

I also investigated the changes in vascular reactivity of the umbilical arteries and umbilical veins in the Ad.VEGF-A_{165}/Ad.LacZ transduced sheep long-term. This experiment was only performed in twin pregnant sheep (n=3) in order to have appropriate internal controls from within the same animal.

The umbilical arteries and umbilical veins were cut into 3mm long segments and mounted on the organ bath. Their contractility and relaxation was studied with phenylephrine and bradykinin respectively, similarly to as was done for the uterine arteries. I found no observable difference in the vascular responses of the umbilical arteries and veins between the Ad.VEGF-A_{165} and Ad.LacZ transduced sides (data not shown).

3.10 Local over-expression of VEGF-A_{165} in the uterine arteries of pregnant sheep upregulates eNOS levels short-term but not long-term

The organ bath pharmacology experiments described previously (David AL et al., 2008) and above, suggest that eNOS plays an important role in the altered uterine artery vascular reactivity associated with Ad.VEGF-A_{165} transduction. In order to verify this, protein extracts of uterine artery samples from short-term studies (4-7 days after vector injection) and long-term studies

(30-52 days after vector injection) were analysed for changes in eNOS levels by western blotting. I observed an upregulation in the levels of eNOS in Ad.VEGF-A_{165} transduced compared to Ad.LacZ transduced uterine arteries short-term (Figure 3.19 A). However, this difference was not sustained long-term. There was no difference in eNOS levels between the Ad.VEGF-A_{165} and Ad.LacZ transduced uterine arteries obtained from pregnant sheep at term (Figure 3.19 B).

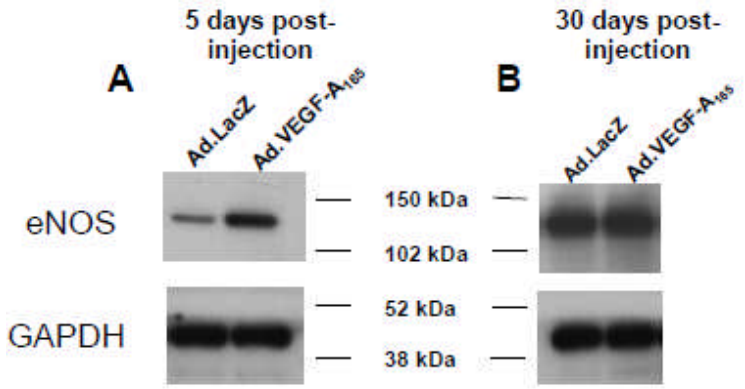

Figure 3.19 - Representative western blot showing upregulation of eNOS in Ad.VEGF-A_{165} transduced uterine arteries compared to Ad.LacZ transduced uterine arteries (A) 5 days after vector administration but not (B) 30 days after vector administration

Uterine arteries from pregnant sheep were injected with Ad.VEGF-A_{165} and Ad.LacZ contra-laterally at mid-gestation, and harvested either (A) 5 days post-injection; or (B) 30 days post-injection. Protein extracts from the uterine artery tissue samples were analysed by western blotting using a mouse monoclonal antibody to eNOS. Results are representative of 3 independent experiments each at the short-term and long-term time points. GAPDH was used as a loading control.

3.11 Microscopic examination of tissues from Ad.VEGF-A_{165} transduced sheep does not reveal any significant pathology.

Maternal and fetal tissues collected at post-mortem examination (complete list of samples in post-mortem sheet in Appendix IV) from Ad.VEGF-A_{165} transduced sheep (n=5) were stained with H&E and observed microscopically under the supervision of Dr. Elizabeth Benjamin.

The uterine arteries did not show any evidence of edema, leucocyte infiltration or inflammation. Sections of the maternal heart from three ewes showed evidence of low-grade myocarditis (Figure 3.20). A similar cardiac histology was observed in sham operated ewes which received only PBS and in ewes which had no surgical intervention prior to post-mortem (used for uterine artery endothelial cell extraction). Hence, it was concluded that the presence of low-grade myocarditis was unrelated to the administration of the vector. Nevertheless, none of these ewes demonstrated any symptoms of ill-health or anomalous maternal haemodynamics.

All other maternal and fetal tissues examined, including the liver had an unremarkable histology.

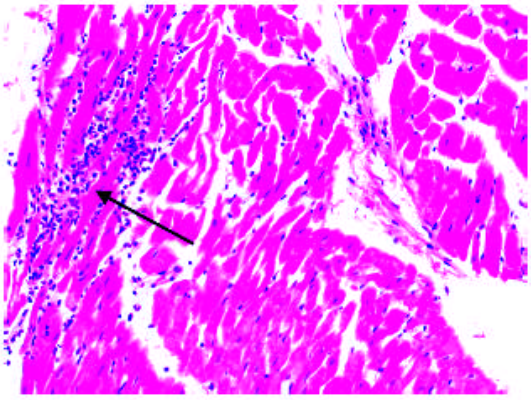

20X mag.

Figure 3.20 – H&E stained section of pregnant sheep heart 30 days after administration of Ad.VEGF-A_{165} and Ad.LacZ to the uterine arteries at mid-gestation

Maternal tissue samples collected at post-mortem examination were analyzed for routine histology. Tissues were fixed in 4% paraformaldehyde overnight, transferred to 70% ethanol and processed into paraffin. Sections were stained with hematoxylin and eosin for morphological assessment. A mild inflammatory response (myocarditis) was observed in sections of the maternal heart from n=3 sheep (arrow pointing at site of inflammation). The histology of all other maternal and fetal specimens was unremarkable.

3.12 Ad.VEGF-A_{165} transduction of uterine arteries in the pregnant sheep results in long term changes in adventitial angiogenesis

VEGF is known to have an angiogenic effect, that is, it leads to the formation of new blood vessels from pre-existing ones. We hypothesized that this may be one of the mechanisms of action of VEGF-A_{165} over-expression in pregnant ovine uterine arteries, and therefore we studied the angiogenic response to Ad.VEGF-A_{165} transduction in these vessels.

3.12.1 Vessel counting in H & E stained sections

We started by counting the number of blood vessels in the perivascular adventitia of the uterine arteries in H&E stained sections. Twins (n=4) were used for the analysis to avoid any inherent differences between the gravid and non-gravid sides. Vessels were cut in cross-section so that the lumen, intima, media and adventitia were all visible in the same field. The counting was done under a light microscope by two observers independently and blinded to the vector given. Ten high-powered fields per vessel section were counted. An example of a vessel stained with H&E is given in Figure 3.21.

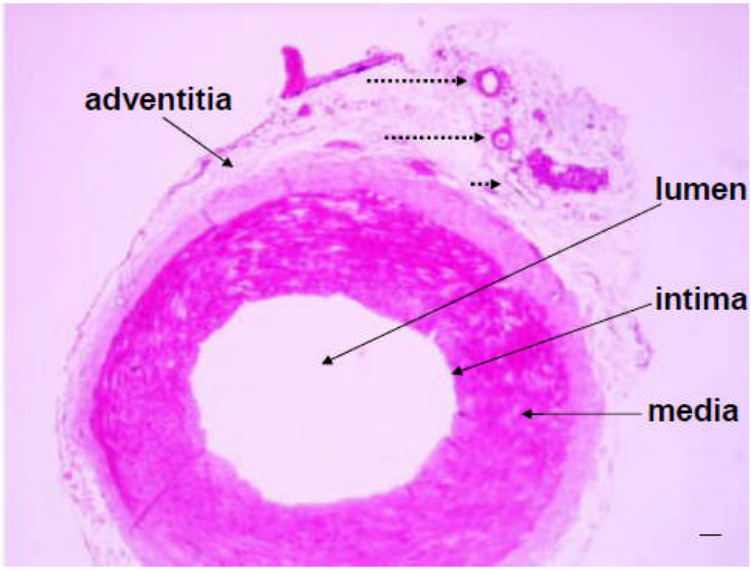

Figure 3.21 – Adventitial vessel enumeration in H&E stained uterine artery sections from pregnant sheep, 30-45 days after a local injection of Ad.VEGF-A_{165} or Ad.LacZ.

Maternal uterine artery samples collected at post-mortem examination were analyzed for routine histology. Tissues were fixed in 4% paraformaldehyde overnight, transferred to 70% ethanol and processed into paraffin. Sections were stained with hematoxylin and eosin for morphological assessment and adventitial vessel enumeration. No inflammatory inflammation or edema was observed. Dotted arrows point to adventitial blood vessels. We observed a significant increase in the number of adventitial blood vessels in uterine arteries transduced with Ad.VEGF-A_{165} compared to Ad.LacZ. Scale bar = 40µm.

A significant increase in the number of blood vessels in the perivascular adventitia of the uterine arteries tranduced with Ad.VEGF-A_{165} (11.64 ± 0.79) was observed, when compared with the Ad.LacZ transduced side (8.75 ± 0.83), n=28 sections, $p<0.05$ (Student's t-test).

One of the drawbacks of vessel enumeration in H&E stained sections is that it is quite subjective, leaving it to the discretion of the observer what structure to identify as a blood vessel. Hence, it is not very reproducible or reliable.

3.12.2 Immunohistochemical staining of endothelial cells

In order to make our analysis more reliable and reproducible, a more objective method was used to identify adventitial blood vessels, using tissue sections stained immunohistochemically with markers of endothelial cells. It is

important to note that only animals carrying twin pregnancies (n=4) were selected for this experiment, so as to exclude any intrinsic confounding factors that may exist between the uterine arteries supplying the gravid and non-gravid horns of the uterus, which might influence adventitial neovascularization.

Slides were stained with endothelial specific markers, namely anti-von Willebrand Factor (vWF) and anti-CD31. Unfortunately, the latter antibody failed to cross-react with the sheep antigen and did not yield any results.

First, the optimum concentration of anti-vWF antibody to stain endothelial cells was determined (Figure 3.22) and a dilution of 1:400 was observed to be the most appropriate concentration to use. The total number of positively stained adventitial blood vessels associated with a distinct lumen were then counted by two observers independently and blinded to the vector given. The advantage of this method over H&E staining is that it is much more objective as only the endothelium is positively stained. This enables the experimenter to unambiguously identify and count a blood vessel.

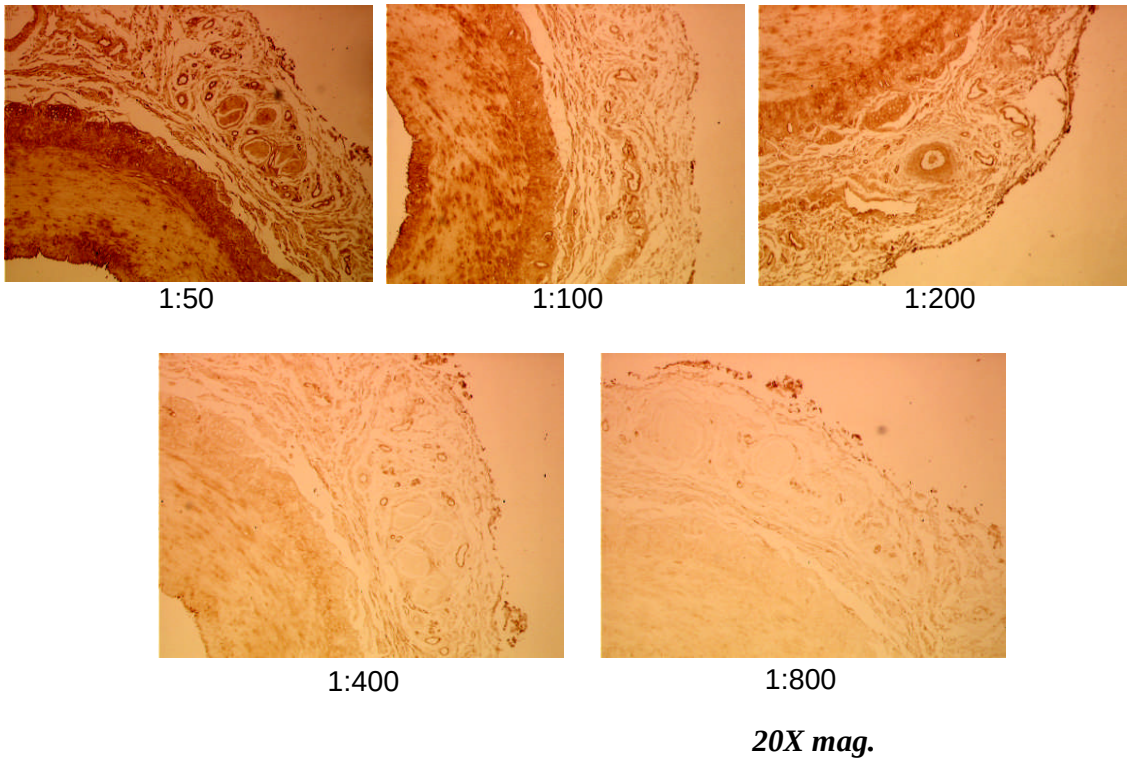

Figure 3.22 – Optimization of anti-von Willebrand Factor (anti-vWF) staining in pregnant sheep uterine artery sections.

(Continued from overleaf) Maternal uterine artery samples collected at post-mortem examination were analyzed by anti-vWF immunohistochemistry. Tissues were fixed in 4% paraformaldehyde overnight, transferred to 70% ethanol and processed into paraffin. Sections were stained with primary rabbit anti-human vWF antibody immunohistochemically at different concentrations, using the avidin-biotin-peroxidase system; 3,3`-diaminobenzidine was used as a substrate for visualization. The optimum concentration of the primary antibody was determined to be 1:400.

The number of positively stained adventitial blood vessels (Figure 3.23) was significantly greater in the uterine arteries transduced with Ad.VEGF-A_{165} compared to Ad.LacZ (141.56$\pm$14.61 v/s 92.75$\pm$9.64 respectively, n=16 sections for each vector in duplicate, p=0.013, unpaired t-test), when data was averaged over all the uterine artery branches counted. The data for the individual branches has been presented in Table 3.11.

As mentioned, each uterine artery section was stained and counted in duplicate by two observers. The inter-observer variability between both the counts was 4.2%.

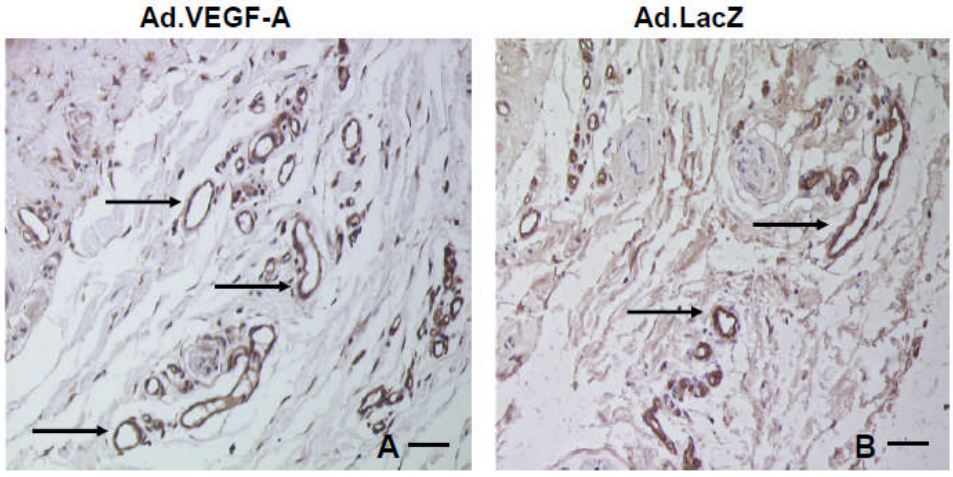

Figure 3.23 – Representative images of anti-vWF stained sections of pregnant sheep uterine arteries.

Maternal uterine artery samples collected at post-mortem examination were analyzed by anti-vWF immunohistochemistry. Tissues were fixed in 4% paraformaldehyde overnight, transferred to 70% ethanol and processed into paraffin. Sections were stained with primary rabbit anti-human vWF antibody immunohistochemically at a concentration of 1:400, using the avidin-biotin-peroxidase system; 3,3`-diaminobenzidine and a light hematoxylin counterstain were used as substrates for visualization. The positively stained adventitial blood vessels with a distinct lumen were counted under a light microscope. The number of adventitial blood vessels was found to be significantly greater in Ad.VEGF-A_{165} transduced uterine arteries (A), compared to Ad.LacZ transduced uterine

arteries (B). Arrows point to positively stained adventitial blood vessels with a distinct lumen. Scale bar = 40 μm.

Table 3.11 – Number of adventitial blood vessels in different branches of the uterine artery, determined by enumeration of anti-vWF stained sections

Maternal uterine artery samples collected at post-mortem examination were analyzed by anti-vWF immunohistochemistry. Tissues were fixed in 4% paraformaldehyde overnight, transferred to 70% ethanol and processed into paraffin. Sections were stained with primary rabbit anti-human vWF antibody immunohistochemically at a concentration of 1:400, using the avidin-biotin-peroxidase system; 3,3`-diaminobenzidine and a light hematoxylin counterstain were used as substrates for visualization. The positively stained adventitial blood vessels with a distinct lumen were counted in the different branches of the uterine arteries under a light microscope.

Uterine artery branch	Number of adventitial blood vessels		p value
	Ad.VEGF-A_{165} side (Mean±SEM)	Ad.LacZ side (Mean±SEM)	
Main uterine artery	227.09±18.61 (n=4)	152.67±13.17 (n=4)	0.0001
1st branch	144.80±17.62 (n=4)	89.8±8.24 (n=4)	0.032
2nd branch	114.11±18.49 (n=4)	83.50±8.52 (n=4)	0.247
3rd branch	80.27±2.64 (n=4)	45.06±7.81 (n=4)	0.035
Average of all branches	141.56±14.61 (n=16)	92.75±9.64 (n=16)	0.013

Thus, our vessel enumeration results showed that local administration of Ad.VEGF-A_{165} to the uterine arteries of pregnant sheep results in significant adventitial neovascularization compared to control uterine arteries transduced with Ad.LacZ.

3.13 There is no detectable difference in the level of VEGF expression at the protein level between the Ad.VEGF-A_{165} and Ad.LacZ transduced arteries long-term

Snap-frozen tissue samples collected at post-mortem examination were used for protein extraction and analysed by VEGF-A_{165} ELISA (R&D Systems, Minneapolis, MN, USA) to quantify the level of VEGF-A_{165} protein present 30-45

days after vector injection (that is, at term). However, at the end of gestation, human VEGF-A_{165} was not detectable by ELISA in any uterine artery, uterine wall, or placentome samples of all pregnant ewes injected with Ad.VEGF-A_{165} (n=10). Similarly, blood samples obtained from the ewes before vector injection as well as samples obtained from the ewes and fetuses at post-mortem examination did not show any detectable human VEGF-A_{165} expression using ELISA.

We also performed immunohistochemistry for VEGF-A_{165} in the uterine artery sections from six sheep (4 twins and 2 singleton pregnancies). The stained slides showed specific staining of VEGF around the adventitial blood vessels on both the Ad.VEGF-A_{165} and Ad.LacZ treated sides, though there was no difference in the level of expression quantitatively (around the blood vessels) between both the sides (Figure 3.24).

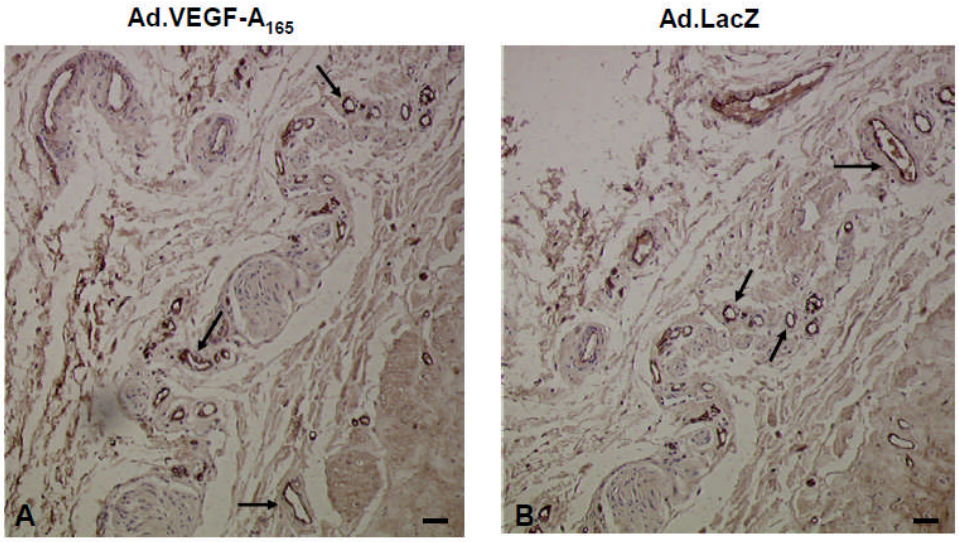

Figure 3.24 - Representative images of anti-VEGF stained sections of pregnant sheep uterine arteries , 30-45 days after local administration of (A) Ad.VEGF-A_{165} or (B) Ad.LacZ.

Maternal uterine artery samples collected at post-mortem examination were analyzed by anti-VEGF immunohistochemistry. Tissues were fixed in 4% paraformaldehyde overnight, transferred to 70% ethanol and processed into paraffin. Sections were stained immunohistochemically with a mouse monoclonal antibody to VEGF-A_{165} at a concentration of 1:400, using the avidin-biotin-peroxidase system; 3,3`-diaminobenzidine was used as a substrate for visualization. Positive staining was observed around small blood vessels in the perivascular adventitia of the uterine

artery. Though the number of adventitial vessels was significantly greater in the Ad.VEGF-A_{165} transduced segments (A) relative to Ad.LacZ transduced ones (B), we were not able to detect any quantitative difference in the levels of VEGF expression between both the sides. Scale bar = 40 μm.

Hence, the ELISA and immunohistochemistry data suggest that there are no detectable differences in the levels of VEGF protein expression between the Ad.VEGF-A_{165} and Ad.LacZ injected sides in long-term transduced animals.

3.14 Local administration of Ad.VEGF-A_{165} to the uterine arteries of pregnant sheep results in upregulation of VEGFR-2 short-term

Uterine artery sections obtained from experimental animals (after 5 days and 30 days of Ad.VEGF-A_{165} transduction) were stained immunohistochemically for VEGFR-1, VEGFR-2 and Neuropilin-1. The stained slides showed the presence of VEGFR-1, VEGFR-2 and Neuropilin-1 in the intimal and adventitial endothelia (lining small blood vessels) (Figure 3.25). The presence of these three receptors in the sheep uterine artery suggests that all of them may be mediating the biological effects of VEGF-A_{165}. There was an upregulation of VEGFR-2 in the uterine arteries transduced with Ad.VEGF-A_{165} compared to Ad.LacZ, 4-7 days after injection (Figure 3.25). There was no detectable difference in the level of any of the receptors at 1 month post-injection (Figure 3.26).

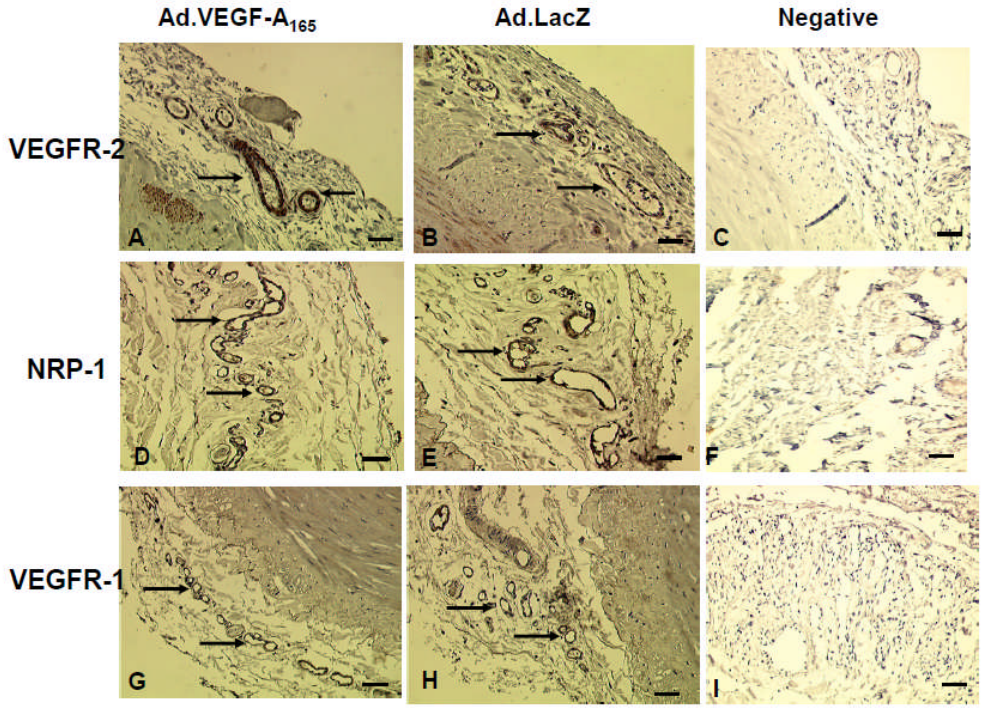

Figure 3.25 - Representative images of short-term Ad.VEGF-A_{165}/Ad.LacZ transduced sheep uterine artery sections stained with antibodies to (A-B) VEGFR-2, (D-E) Neuropilin-1, and (G-H) VEGFR-1. (C), (F) and (I) are respective negative controls for the stainings.

Maternal uterine artery samples from sheep injected with Ad.VEGF-A_{165} and Ad.LacZ contra-laterally at mid-gestation were collected at post-mortem examination 4-7 days later. Tissues were fixed in 4% paraformaldehyde overnight, transferred to 70% ethanol and processed into paraffin. Sections were stained immunohistochemically with antibodies to the three VEGF receptors, namely (A-B) VEGFR-2, (D-E) Neuropilin-1, and (G-H) VEGFR-1 at a concentration of 1:50, using the avidin-biotin-peroxidase system; 3,3`-diaminobenzidine and a light haematoxylin counter-stain were used as substrates for visualization. (C), (F) and (I) are respective negative controls obtained by omitting the primary antibody. Positive staining (pointed at by arrows) was observed around small blood vessels in the perivascular adventitia of the uterine artery. We detected the presence of all three receptors in the uterine arteries of pregnant sheep, and noted an upregulation of VEGFR-2 in the Ad.VEGF-A_{165} transduced uterine artery segments. Scale bar = 40 μm.

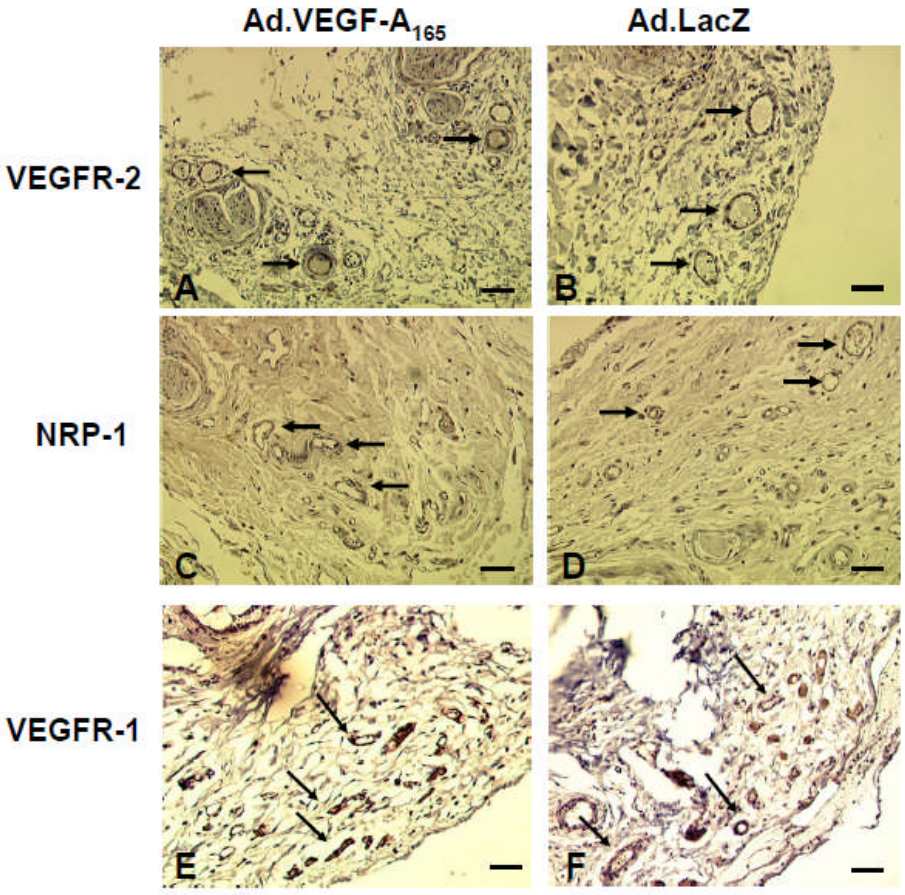

Figure 3.26 - Representative images of long-term Ad.VEGF-A_{165}/Ad.LacZ transduced sheep uterine artery sections stained with antibodies to (A-B) VEGFR-2, (C-D) Neuropilin-1, and (E-F) VEGFR-1.

Maternal uterine artery samples from sheep injected with Ad.VEGF-A_{165} at mid-gestation were collected at post-mortem examination 30-45 days later. Tissues were fixed in 4% paraformaldehyde overnight, transferred to 70% ethanol and processed into paraffin. Sections were stained immunohistochemically with antibodies to the three VEGF receptors, namely (A-B) VEGFR-2, (C-D) Neuropilin-1, and (E-F) VEGFR-1 at a concentration of 1:50, using the avidin-biotin-peroxidase system; 3,3`-diaminobenzidine and a light haematoxylin counter-stain were used as substrates for visualization. Positive staining (pointed at by arrows) was observed around small blood vessels in the perivascular adventitia of the uterine artery. We detected the presence of all three receptors in the uterine arteries of long-term transduced pregnant sheep. Scale bar = 40 µm.

I also performed immunohistochemistry with an antibody specific for the phosphorylated form of VEGFR-2. The tyrosine residues of this receptor are known to be phosphorylated in response to VEGF stimulation and thus, I was interested to investigate whether there were specific sites in the uterine artery of receptor phosphorylation. Unfortunately, three antibodies used for the

immunohistochemical detection of phosphorylated VEGFR-2 failed to cross-react with ovine samples.

It is well known that the ligand-dependent phosphorylation of VEGFR-2 is critical for mediating the wide spectrum of biological effects of VEGF (Ferrara N, 1999). Hence, the presence of phosphorylated (activated) VEGFR-2 in the uterine artery was expected, especially because VEGF-induced effects on uterine blood flow, vascular reactivity and neovascularization were evident long-term.

3.15 Local administration of Ad.VEGF-A_{165} to the uterine arteries does not result in systemic vector expression

In order to assess the safety of intra-arterial Ad.VEGF-A_{165} administration into the utero-placental vasculature long-term, I determined the extent of systemic vector expression. I performed Reverse Transcriptase (RT)-PCR with primers specific for Ad.VEGF-A_{165} on RNA isolated from a wide selection of maternal and fetal tissues. The RNA extracts used for all experiments were of high quality, as judged by an A_{260}/A_{280} reading of 1.80-1.95 and production of a doublet band on agarose gel electrophoresis (Figure 3.27).

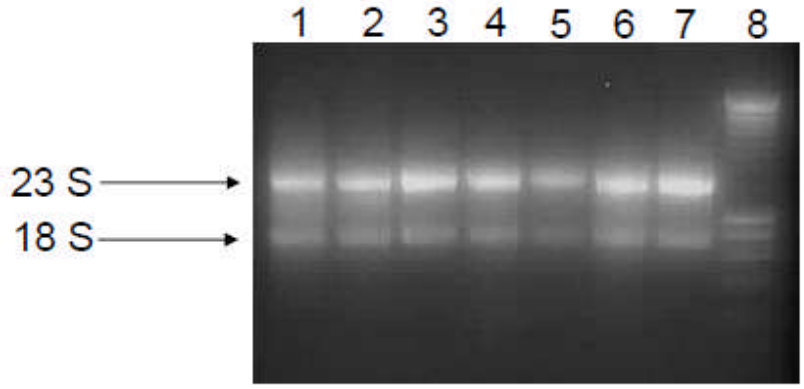

Figure 3.27 – Representative image for agarose gel electrophoresis of total RNA extract from sheep tissues.

1 – Ad.VEGF-A_{165} injected UtA; 2 – Ad.LacZ injected UtA; 3 – maternal heart; 4 – maternal ovary; 5 – maternal liver; 6 – maternal adrenal; 7 – maternal spleen; 8 – 1kb+ DNA ladder

I also performed RT-PCR for a sheep housekeeping gene, Tata-box binding protein (TBP), GenBank reference L47974, to use as a positive control. This has previously been shown to give no amplification signal from adenovirus DNA alone (David AL, 2005, Ph.D Thesis).

The first round PCR with primers specific for Ad.VEGF-A_{165} was negative in all maternal and fetal samples analysed, including the uterine arteries that had been transduced with the adenovirus. The RT-PCR with primers specific for TBP was positive in all maternal and fetal samples. This confirmed that good quality RNA had been extracted from all sheep samples that could be reverse-transcribed into cDNA and subsequently amplified.

We speculated that first round PCR might not be sensitive enough to detect long term transgene expression, which might be at quite low levels. Consequently, a semi-nested PCR was carried out wherein the forward primer was identical to the first round PCR forward primer, but the reverse primer bound to a sequence more internal to the complementary binding site of the first round reverse primer. Three reverse primer candidates were designed and tested at different annealing temperatures on HUVECs transduced with Ad.VEGF-A_{165} (positive control) (Table 3.12). We chose oligonucleotide 2 which worked consistently at the highest annealing temperature, (54°C) as the reverse primer for the second round of the semi-nested PCR. Even though oligonucleotide 3 gave a positive amplification signal at a lower annealing temperature, the advantage of using a primer that works at a higher annealing temperature is that it minimizes the possibility of contaminating bands from non-specific amplification.

Table 3.12 – Optimisation of semi-nested RT-PCR to determine Ad.VEGF-A_{165} expression in maternal and fetal tissues, 30-45 days after gene transfer to the uterine arteries.

Sequence of reverse primer candidates for 2nd round of Semi-nested RT-PCR to determine Ad.VEGF-A_{165} expression	RT-PCR amplification at different annealing temperatures			
	50°C	52°C	54°C	56°C
Oligonucleotide 1 5`-GATCCGCATAATCTGCA-3`	-	-	-	-
Oligonucleotide 2 5`-GATCCGCATAATCTGCATGGT-3`	+	+	+	-
Oligonucleotide 3 5`-CGCATAATCTGCATGGTGAT-3`	+	-	-	-

'+': Positive amplification; '-': No amplification

Using this approach, a positive band was observed in the Ad.VEGF-A_{165} transduced vessel but the Ad.LacZ transduced vessel was negative, as were all other tissues (Figure 3.28). This indicated there was no systemic expression of transgenic *vegf* long-term.

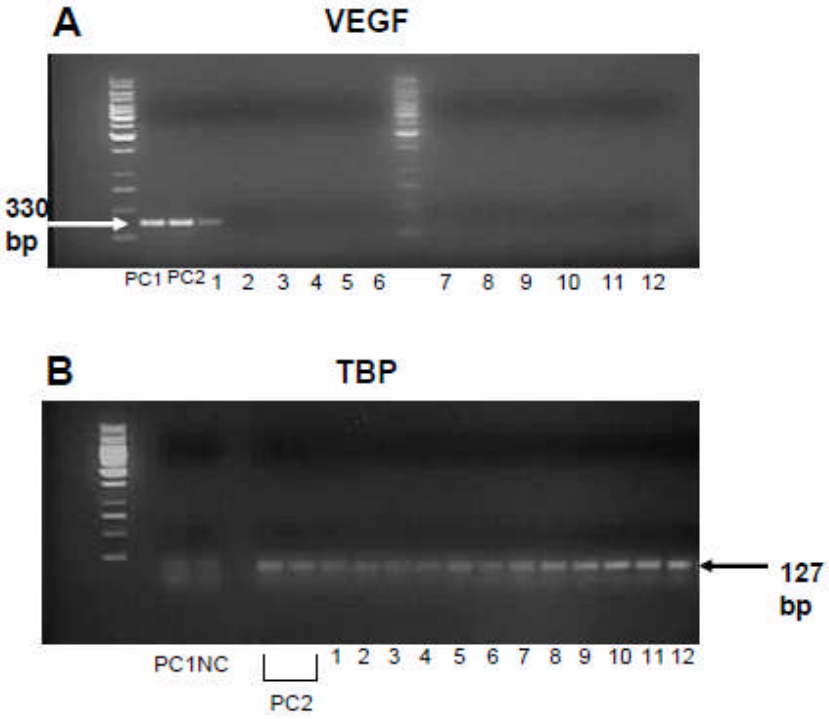

Figure 3.28 – RT-PCR to determine transgenic *vegf* experession in maternal and fetal tissues, 30-45 days after Ad.VEGF-A_{165} gene transfer.

(A) Semi-nested RT-PCR with primers specific for Ad.VEGF-A_{165} in sheep maternal and fetal samples was positive only in the Ad.VEGF-A_{165} transduced vessel, but negative in all other tissues. Gel pictures are representative from one sheep. 1 – Ad.VEGF-A_{165} injected UtA; 2 – Ad.LacZ injected UtA; 3 – maternal heart; 4 – maternal ovary; 5 – maternal liver; 6 – maternal adrenal; 7 – maternal spleen; 8 – maternal uterus; 9 – maternal placentome; 10 – fetal heart; 11- fetal liver; 12 – fetal gonad. The positive control used is either human umbilical vein endothelial cells (HUVECs, PC1) or sheep uterine artery endothelial cells (PC2) infected with Ad.VEGF-A_{165} and the negative control (NC) is uninfected HUVECs. The ladder used is 1kb+ DNA ladder (Fermentas). (B) RT-PCR with primers specific for sheep housekeeping gene TATA-box Binding Protein (TBP) is positive for all ovine samples.

3.16 Local administration of Ad.VEGF-A_{165} to the uterine arteries of pregnant sheep results in reduced intima:media ratios

Uterine artery sections from animals carrying twin pregnancies (n=4) were stained with H&E and examined for changes in intimal thickness, medial thickness and intima:media ratios. This was done by analyzing cross-sectional photomicrographs of uterine artery segments in ImageJ software to obtain the

relative lengths of the intimal and medial layers and their respective ratios. All measurements were performed twice by the same observer, who was blinded to the vector injected into the uterine artery. The results of this analysis have been summarized in Figure 3.29 (a-c).

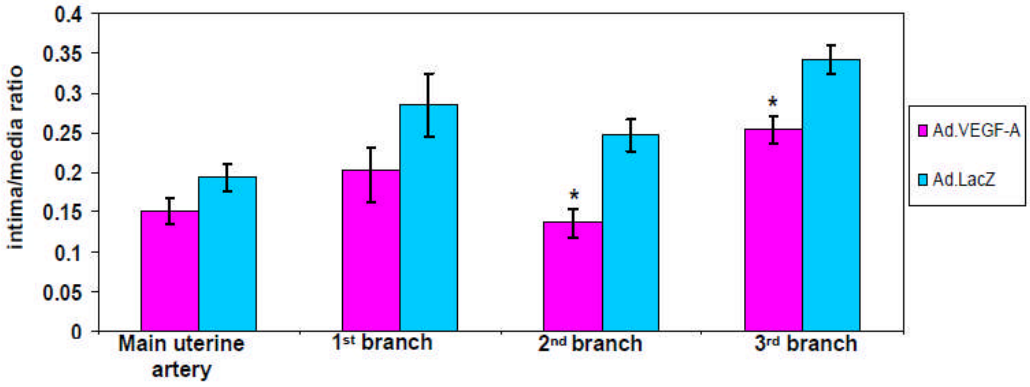

Figure 3.29(a) – intima/media ratios in the uterine arteries of twin pregnant sheep 30-45 days after administration of Ad.VEGF-A_{165} and Ad.LacZ to the uterine arteries at mid-gestation

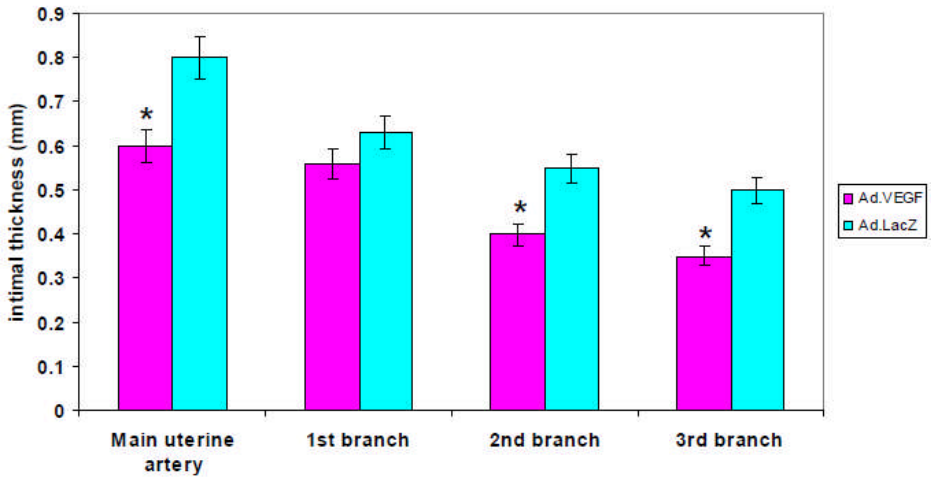

Figure 3.29(b) – Relative intimal thickness in the uterine arteries of twin pregnant sheep 30-45 days after administration of Ad.VEGF-A_{165} and Ad.LacZ to the uterine arteries at mid-gestation

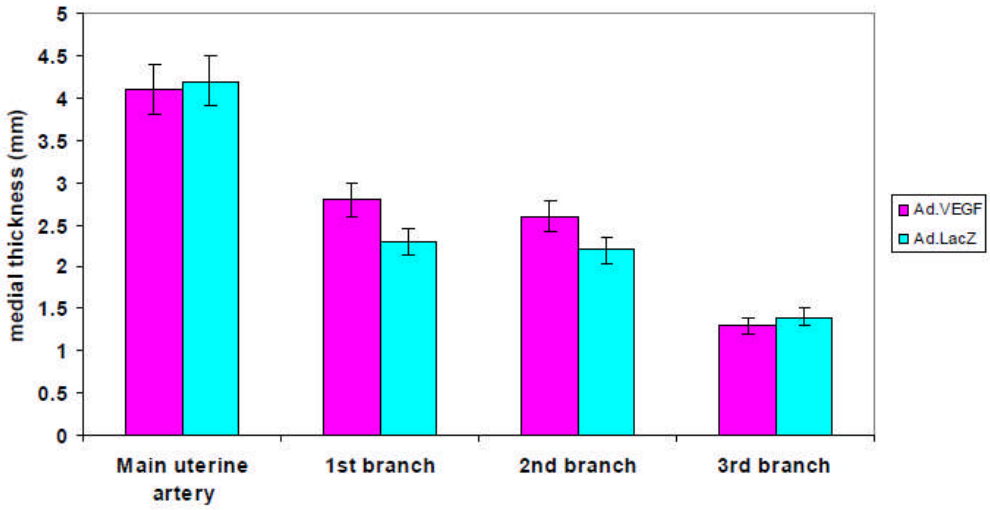

Figure 3.29(c) – Relative medial thickness in the uterine arteries of twin pregnant sheep 30-45 days after administration of Ad.VEGF-A_{165} and Ad.LacZ to the uterine arteries at mid-gestation

Maternal uterine artery samples collected at post-mortem examination were fixed in 4% paraformaldehyde overnight, transferred to 70% ethanol and processed into paraffin. Sections were stained with hematoxylin and eosin for morphological assessment. Photomicrographs of stained sections were analysed using 'ImageJ' to determine the relative thicknesses of the intimal and medial layers and intima/media ratios. Analysis was conducted on twin pregnant sheep (n=4). There was a reduction in the intima/media ratios and intimal thickness in Ad.VEGF-A_{165} transduced vessels compared to Ad.LacZ transduced segments. * indicates $p<0.05$

We observed there was a reduction in the intima:media ratios in the Ad.VEGF-A_{165} transduced segments compared to Ad.LacZ transduced segments in the main uterine artery and its subsequent three branches, though this difference was significant only in 2nd and 3rd branches (n=4, p=0.03 and 0.05 respectively). The intra-observer variability of measurement was 5.2%.

The reduction in intima/media ratios appeared to be primarily on account of a reduction in the intimal thickness rather than an increase in medial thickness, as is evident from Figure 3.29 (b and c).

3.17 Local administration of Ad.VEGF-A_{165} to the uterine arteries of pregnant sheep results in normal postnatal growth

One ewe gave birth to a healthy female lamb (Figure 3.30) on the day of scheduled post mortem examination (139 days gestational age), 2 days earlier than expected. The delivery was uncomplicated without any postpartum haemorrhage or retained placenta. This animal (UA29) had undergone chronic fetal catheterization to monitor fetal haemodynamics. During birth the catheter was pulled out from the carotid artery without obvious haemorrhage or structural damage to the fetal neck. The next morning, the small wound in the lamb's neck through which the catheter had pulled out was cleaned with povidone antiseptic solution.

Figure 3.30 – Pictures of the lamb born to an ewe injected with Ad.VEGF-A_{165} and Ad.LacZ at mid-gestation.

The lamb was unexpectedly born on the day of its scheduled post-mortem. These pictures were taken at 4 months age.

After discussion with the local Home Office Inspector, the ewe and lamb were allowed to continue being monitored and this was done for 4 months until weaning. The lamb showed no adverse development or abnormal growth velocity. The maternal and neonatal haematology, biochemistry, liver function tests as well as the weight and blood oxygen saturation of the lamb were assessed at weekly intervals for the first month and thereafter once a month until post-mortem

examination. All haematological values and serum biochemistry were within the normal ranges for both mother and lamb. The liver enzyme Glutamate dehydrogenase (GLDH) was elevated in the lamb (range 19-37 U/l at different time-points examined; normal levels <20 U/l), as were the Gamma-glutamyl transferase (GGT) levels (range 85-100 U/l at different time points examined; normal levels < 76 U/l). Previous studies in lambs born to control ewes which have not had any intervention have shown levels of GLDH to be elevated compared to the normal range quoted for adult sheep (20 U/l), thus suggesting that the normal adult range cannot be applied to young lambs (Meyer DJ and Harvey JW, 1998;David AL, 2005). GGT is present in colostrum and this may have resulted in the elevation during the period the lamb is suckling. All other liver enzymes were within the normal range.

The blood oxygen saturation of the lamb as measured by a pulse oximeter was in the range of 97-99% at all time points examined.

Figure 3.31 shows the post-natal weight gain of the lamb compared to Suffolk sheep (a sheep breed of similar size to Romneys) at regular intervals after birth. Similar post-natal growth velocity data was not available for Romney breed for comparison.

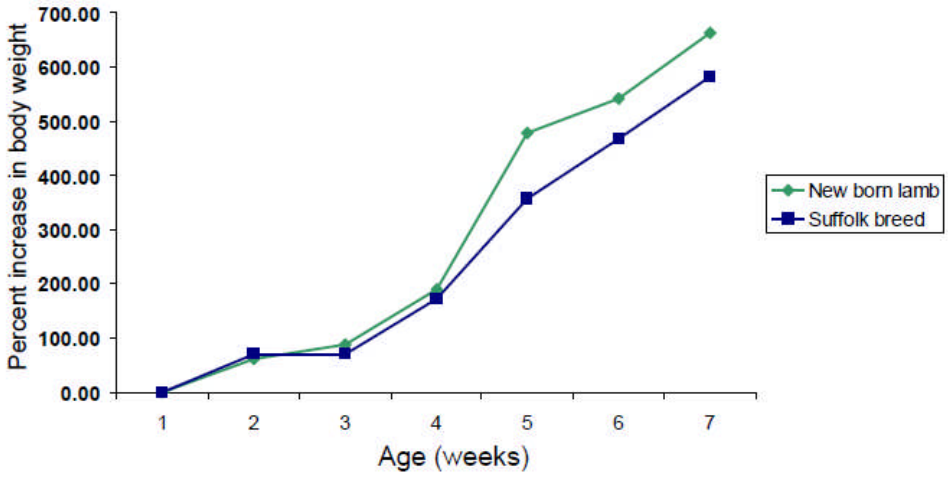

Figure 3.31 – Percentage increase in body weight (relative to birthweight) in the new born lamb compared to Suffolk breed sheep

At 4 months after birth, both mother and lamb were euthanized. Maternal and fetal tissue samples collected at post-mortem were examined microscopically after H&E staining. All tissue samples examined had an unremarkable histology.

Even though post-natal data was acquired for only one lamb in this study, it indicates that the neonatal growth and development is normal following Ad.VEGF-A_{165} administration to the uterine arteries at mid-gestation.

3.18 The effects of adenovirus-mediated over-expression of VEGF-A_{165} in the uterine arteries at mid-gestation are not sustained post-partum

As mentioned in the preceding section, sheep UA29 gave birth to a healthy female lamb on the day of her scheduled post-mortem. Both mother and lamb were kept alive for a further 4 months to monitor development. At post-mortem examination, maternal and lamb samples were snap-frozen for subsequent semi-nested RT-PCR analysis for vector expression. All samples analysed (listed in post-mortem sheep, Appendix IV) were negative.

The vascular reactivity of the maternal uterine arteries was studied on an organ bath set-up. The contractility and relaxation to increasing doses of phenylephrine and bradykinin respectively were investigated (Figure 3.32 and Figure 3.33 respectively).

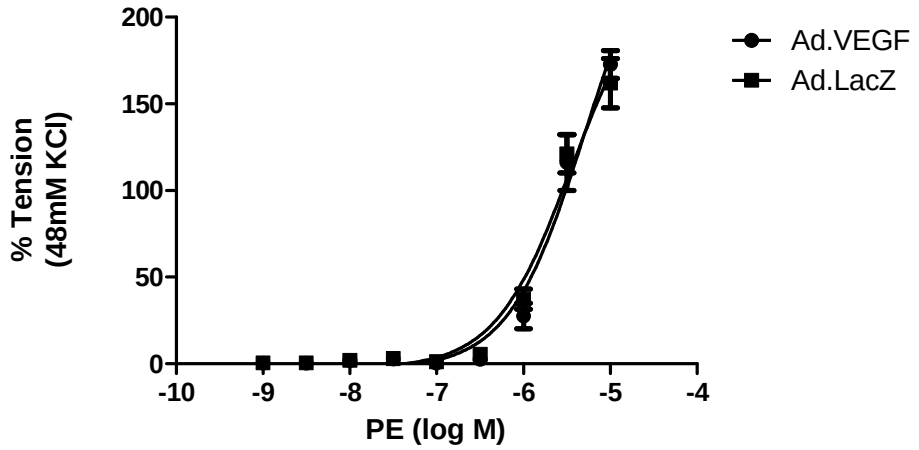

Figure 3.32 - Contractility of pregnant sheep uterine arteries injected with Ad.VEGF-A_{165} and Ad.LacZ contralaterally at mid-gestation, 4 months post-partum

At mid-gestation, one uterine artery was injected with Ad.VEGF-A_{165} and the contra-lateral uterine artery was injected with Ad.LacZ in a singleton pregnant sheep. The second and third branches of the main uterine arteries were harvested 4 months post-partum, cut into 3mm ring segments and analysed on an 8-chambered organ bath system. Concentration response curves to PE were constructed for each vessel in quadruplicate. The contractility of the vessel is expressed as a percentage of the response to KCl. PE produced concentration-dependent contractions, which were not different in magnitude between the Ad.VEGF-A_{165} transduced vessels and Ad.LacZ transduced vessels (n=1). Error bars denote standard error of mean.

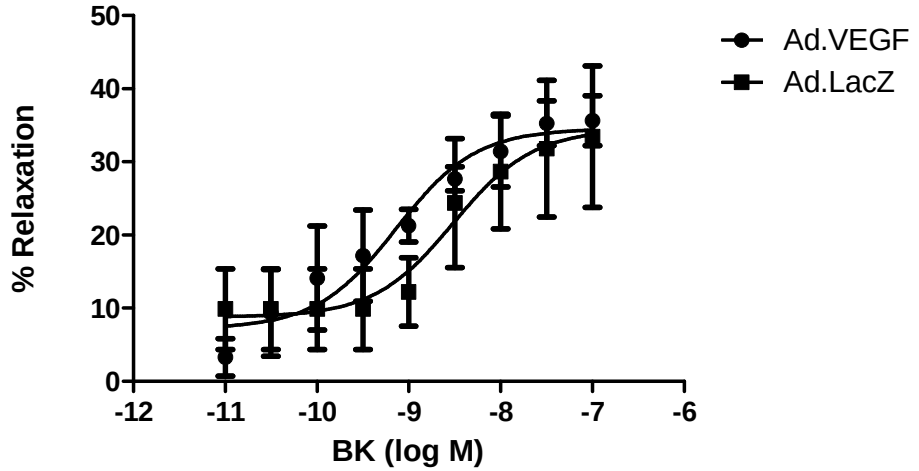

Figure 3.33 -Relaxation of pregnant sheep uterine arteries injected with Ad.VEGF-A_{165} and Ad.LacZ contralaterally at mid-gestation, 4 months post-partum

(Continued from overleaf) At mid-gestation, one uterine artery was injected with Ad.VEGF-A_{165} and the contra-lateral uterine artery was injected with Ad.LacZ in a singleton pregnant sheep. The second and third branches of the main uterine arteries were harvested 4 months post-partum, cut into 3mm ring segments and analysed on an 8-chambered organ bath system. Concentration response curves to BK were constructed for each vessel in quadruplicate. The relaxation of the vessel is expressed as a percentage of inhibition of PE-induced contraction. There was no apparent difference in the relaxation response between the Ad.VEGF-A_{165} and Ad.LacZ transduced vessels (n=1). Error bars denote standard error of mean.

There was no difference in the contractile and relaxation responses of the uterine arteries that had received either Ad.VEGF-A_{165} or Ad.LacZ. Even though we only have data from one animal, it shows that the effects of adenovirus-mediated transgene expression on vascular reactivity are not sustained 5 months post-administration. This is to be expected since the maximum duration of adenovirus mediated gene transfer is usually believed to be 4 – 6 weeks after transduction.

3.19 Local administration of Ad.VEGF-A_{165} to the uterine arteries of pregnant sheep does not lead to haematological and biochemical pathological changes.

Blood and serum samples were taken from experimental sheep (n=3) at three different time points – vector injection, 1 week post-injection and post-mortem examination. Fetal samples could only be collected at post-mortem. The samples were sent to the Clinical Diagnostics Lab, RVC Hawkshead for routine haematological, biochemical and liver function analysis and were compared with standard normal ranges for adult and fetal sheep. All maternal and fetal haematological and biochemical values examined were within the normal range.

3.20 Analysis of maternal and fetal liver function tests after Ad.VEGF-A_{165} injection does not indicate any liver pathology

The serum levels of liver enzymes can indicate whether hepatic disease is present and assess its functional aspect. The diagnostic usefulness of particular liver enzymes depends on the domestic animal species investigated and their age, and this must be considered when interpreting results (Meyer DJ and Harvey JW, 1998). The serum levels of aspartate transaminase (AST) were within the normal range in all samples examined. While abnormal levels of AST provide only a general indicator of hepatic injury in ruminants, the serum concentration of the liver enzyme GLDH is the most specific for hepatocellular injury. In ruminants, GLDH is raised in hepatic necrosis and bile-duct obstruction (Kaneko JJ et al., 1997).

Two of the three sheep examined showed elevated levels of GLDH in the samples taken just before vector injection (UA25 – 108 U/l and UA26 – 184 U/l; normal levels <20 U/l). However, when examined 1 week post-injection, the levels of GLDH had fallen to within the normal ranges (UA25 – 13 U/l and UA 26 – 17 U/l). These levels were normal when examined again at the time of the post-mortem examination. It is unlikely that administration of Ad.VEGF-A_{165} may have played a role in restoring the normal levels of GLDH in pregnant ewes, but the data at least suggests that vector administration does not appear to cause any hepatocellular injury.

GGT and alkaline phosphatase (ALP) are markers of cholestasis, GGT being associated with epithelial cells comprising the bile ductular system and ALP associated with the canalicular membrane. GGT levels were within the normal range for all maternal and fetal sheep samples analysed. Serum levels of ALP fluctuate widely in normal ruminants and are not considered to be very valuable in the evaluation of cholestatic disorders. ALP levels were therefore not measured in our sheep.

Bilirubin was not raised in any of the maternal and fetal serum samples analysed. The levels of alanine aminotransferase (ALT) were normal. There is

only low level ALT activity in the hepatocytes of ruminants in contrast to rodent hepatocytes and therefore the level of this liver enzyme in the serum is not diagnostically useful.

Overall, these results suggest that administration of Ad.VEGF-A_{165} to the uterine arteries of pregnant ewes does not cause any clinically important changes in the levels of maternal and fetal liver enzymes.

Section II – Experiments with Ad.VEGF-D$^{\Delta N \Delta C}$

Following on from the encouraging results of the Ad.VEGF-A_{165} study, we became interested in investigating the effects of another member of the VEGF family, VEGF-$D^{\Delta N \Delta C}$ on the utero-placental circulation. VEGF-$D^{\Delta N \Delta C}$ is angiogenic but may elicit a more restricted range of biological responses compared with VEGF-A_{165} (Rissanen TT et al., 2003;Jia H et al., 2004). It may also be less likely to cause unwanted side effects, such as making the vessels less leaky/permeable as compared to VEGF-A_{165}, and thus we felt it may be of greater therapeutic benefit in treating FGR caused by vascular placental insufficiency. For the current study, we used adenoviral vectors encoding the mature (processed/truncated) form of the VEGF-D gene, i.e., VEGF-$D^{\Delta N \Delta C}$ (Achen MG et al., 1998) to transduce the uterine arteries of pregnant sheep. Previous experiments with the long-form of the VEGF-D gene were found to not alter uterine blood flow or vascular reactivity in pregnant sheep (David AL et al., 2008). Published studies have demonstrated that VEGF-$D^{\Delta N \Delta C}$ has a substantially greater angiogenic effect and significantly increased affinity for VEGFR-2 than the full length form (Rissanen TT et al., 2003;Stacker SA et al., 1999). For simplicity, VEGF-$D^{\Delta N \Delta C}$ and Ad.VEGF-$D^{\Delta N \Delta C}$ have been referred to as VEGF-D and Ad.VEGF-D respectively in this chapter.

Initially, the short-term effects of Ad.VEGF-D on uterine artery vascular reactivity were studied. Long-term experiments requiring chronic implantation of flow-probes are technically more difficult and intensive. Hence, I first wanted to determine if Ad.VEGF-D transduction actually has any biological effect on the uterine arteries short-term, before carrying out any long-term experiments. Two kinds of short-term experiments were performed – (i) uterine artery injection of Ad.VEGF-D or Ad.LacZ bilaterally (n=2 each); and (ii) uterine artery injection of Ad.VEGF-D and Ad.LacZ contra-laterally within the same animal (n=6). The rationale behind conducting these two experiments was that VEGF-D is believed to be more highly soluble than VEGF-A_{165}. We were thus initially concerned that

VEGF-D protein from the transduced side would be carried systemically to the contra-lateral side and influence its vascular reactivity, thereby eliminating any differences in vascular responses in experiments wherein the two vectors were injected contra-laterally (Seppo Yla-Hertulla, personal communication). Hence, we designed experiments to test both the combinations - bilateral and unilateral administration of Ad.VEGF-D/Ad.LacZ.

We then studied the long-term effects of Ad.VEGF-D transduction on vascular reactivity, neovascularization, endothelial cell proliferation and UABF (by chronic implantation of telemetric flow probes, n=5). UABF was measured successfully in all 5 ewes.

Some sheep in this study (n=9) had an intravenous administration of 5-Bromo-2′-deoxyuridine (BrdU) 48 hours before post-mortem. Uterine artery samples from these sheep were stained with an anti-BrdU antibody to assess cell proliferation.

The details of the analysis performed on the Ad.VEGF-D sheep have been described in Table 3.13.

Table 3.13 - Details of experimental analysis performed on sheep injected with Ad.VEGF-D and Ad.LacZ.

Animal	Fetal No.	Vector injected	GA at Probe placement	GA at Vector injection	GA at PM	UABF	Organ Bath	vWF	BrdU	eNOS analysis
UA17	2	Ad.VEGF-D bilaterally	-	87	91	-	+	-	-	-
UA19	1	Ad.VEGF-D bilaterally	-	96	100	-	+	-	-	-
UA21	2	Ad.LacZ bilaterally	-	91	95	-	+	-	-	-
UA23	1	Ad.LacZ bilaterally	-	95	99	-	+	-	-	-
UA31	1	Ad.VEGF-D/ Ad.LacZ contralaterally	-	83	87	-	+	-	-	-
UA32	1	Ad.VEGF-D/ Ad.LacZ contralaterally	-	108	114	-	+	-	-	-
UA34	1	Ad.VEGF-D/ Ad.LacZ contralaterally	-	109	116	-	+	+	+	-
UA36	1	Ad.VEGF-D/ Ad.LacZ contralaterally	-	82	89	-	+	+	+	+
UA37	1	Ad.VEGF-D/ Ad.LacZ contralaterally	-	108	113	-	+	+	+	+
UA41	1	Ad.VEGF-D/ Ad.LacZ contralaterally	-	95	99	-	+	+	+	+
UA38	2	Ad.VEGF-D/ Ad.LacZ contralaterally	89	96	139	+	+	+	+	+
UA39	1	Ad.VEGF-D/ Ad.LacZ contralaterally	89	95	136	+	+	+	+	+
UA42	1	Ad.VEGF-D/ Ad.LacZ contralaterally	98	112	142	+	+	+	+	-
UA43	1	Ad.VEGF-D/ Ad.LacZ contralaterally	95	105	139	+	+	+	+	-
UA45	1	Ad.VEGF-D/ Ad.LacZ contralaterally	82	95	140	+	+	+	+	+

GA=gestational age; UABF = measurement of uterine artery blood flow; vWF = adventitial vessel enumeration by anti-vWF immunohistochemistry; BrdU = administration of 5`-bromo-2`-deoxyuridine to measure endothelial cell proliferation

The detailed results of the analysis performed on the Ad.VEGF-D transduced sheep have been described in the following section. There was no maternal or fetal mortality in this study. Gross examination at the time of post-mortem of all ewes and fetuses did not reveal any pathology.

3.21 Ad.VEGF-D transduction of uterine arteries in the pregnant sheep bilaterally results in short term changes in vascular reactivity.

I investigated the vascular responses of uterine arteries transduced with Ad.VEGF-D and Ad.LacZ bilaterally, 4 days after gene transfer. Both the contraction and relaxation responses of the vessels were examined.

3.21.1 Local over-expression of VEGF-D in the uterine arteries of pregnant sheep bilaterally results in a diminished contractile response in twin and singleton pregnancies.

Organ bath experiments were conducted on the 2nd and 3rd branches of the main uterine artery from 4 sheep – two carrying twin pregnancies (UA17 and UA21) and two carrying singleton pregnancies (UA19 and UA23). One twin pregnant and one singleton pregnant animal were injected with Ad.VEGF-D bilaterally (UA17 and UA19 respectively), while the other twin and singleton pregnant animal were injected with Ad.LacZ bilaterally (UA 21 and UA23 respectively). The post-mortem examination was performed 4 days after injection, and the vascular contractility of the harvested uterine arteries was examined with phenylephrine.

I observed a reduction in the vascular contractility of uterine arteries from both the twin (Figure 3.34) and singleton (Figure 3.35) pregnant animals injected with Ad.VEGF-D, compared to the corresponding controls which had received Ad.LacZ. Table 3.14 summarizes the E_{max} and EC_{50} to phenylephrine in the animals studied in this group.

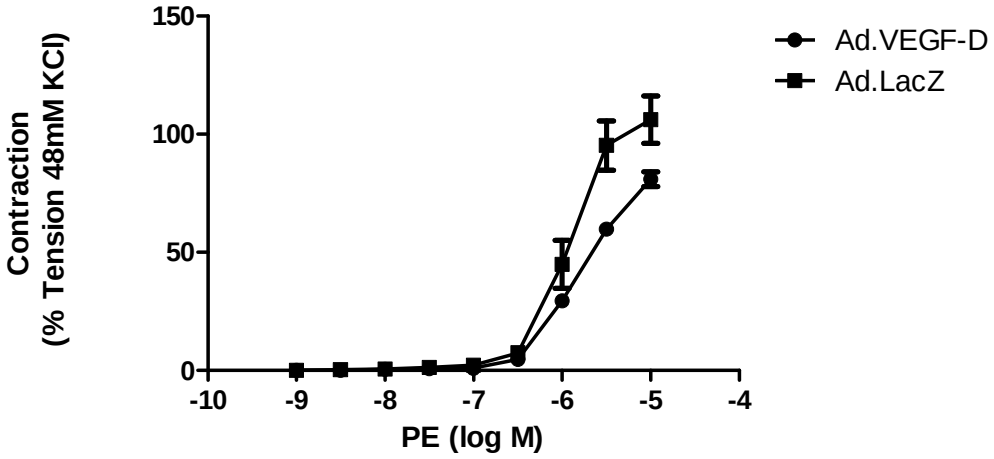

Figure 3.34 - Contractility of twin pregnant Ad.VEGF-D and Ad.LacZ transduced uterine arteries to L-phenylephrine (PE) 4 days after gene transfer.

At mid-gestation, the uterine arteries of one twin pregnant sheep were injected with Ad.VEGF-D bilaterally, and those of another were injected with Ad.LacZ bilaterally (n=1 animal each). The second and third branches of the main uterine arteries were harvested 4 days after injection, cut into 3mm ring segments and analysed on an 8-chambered organ bath system. Concentration response curves to PE were constructed for each vessel in quadruplicate. The contractility of the vessel is expressed as a percentage of the response to KCl. PE produced concentration-dependent contractions, which were of lesser magnitude in Ad.VEGF-D transduced vessels compared to Ad.LacZ transduced vessels. Error bars denote standard error of mean.

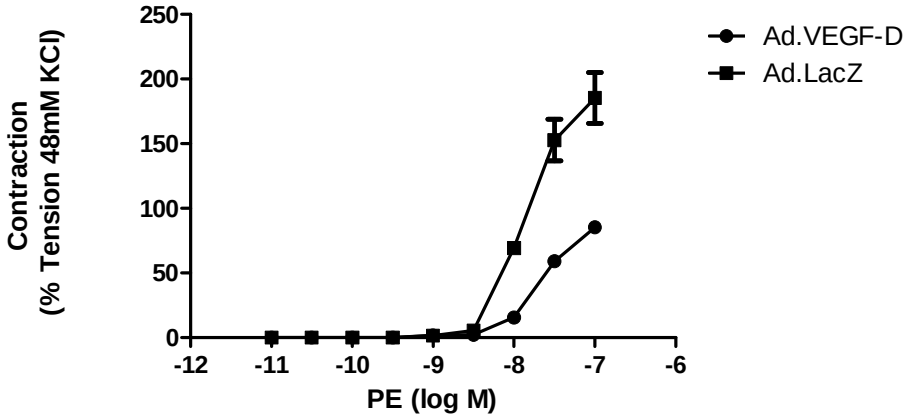

Figure 3.35 - Contractility of singleton pregnant Ad.VEGF-D and Ad.LacZ transduced uterine arteries to L-phenylephrine (PE) 4 days after gene transfer.

At mid-gestation, the uterine arteries of one singleton pregnant sheep were injected with Ad.VEGF-D bilaterally, and those of another were injected with Ad.LacZ bilaterally (n=1 animal

each). The second and third branches of the main uterine arteries were harvested 4 days after injection, cut into 3mm ring segments and analysed on an 8-chambered organ bath system. Concentration response curves to PE were constructed for each vessel in quadruplicate. The contractility of the vessel is expressed as a percentage of the response to KCl. PE produced concentration-dependent contractions, which were of lesser magnitude in Ad.VEGF-D transduced vessels compared to Ad.LacZ transduced vessels. Error bars denote standard error of mean.

Table 3.14 – E_{max} and EC_{50} in response to L-phenylephrine in uterine arteries from twin and singleton pregnant sheep injected with Ad.VEGF-D or Ad.LacZ bilaterally.

At mid-gestation, the uterine arteries of one twin and one singleton pregnant sheep were injected with Ad.VEGF-D bilaterally, and those of another twin and singleton sheep were injected with Ad.LacZ bilaterally. The second and third branches of the main uterine artery were harvested 4 days after injection and analysed on an 8-chambered organ bath system. Concentration response curves to PE were constructed for each vessel in quadruplicate. The contractility of the vessel is expressed as a percentage of the response to KCl.

Animal	Number of fetuses	Vector injected	Number of animals	E_{max} % (Mean±SEM)	EC_{50}
UA17	Twin	Ad.VEGF-D	1	102.8±3.45	$2.46x10^{-6}$M
UA21	Twin	Ad.LacZ	1	131.8±10.09	$1.73x10^{-6}$M
UA19	Singleton	Ad.VEGF-D	1	126.1±7.62	$4.34x10^{-8}$M
UA23	Singleton	Ad.LacZ	1	235.5±17.60	$2.16x10^{-8}$M

In summary, this data suggests that 4 days after local administration of Ad.VEGF-D to the uterine arteries of mid-gestation pregnant sheep bilaterally, there is a reduction in uterine artery contractility compared to Ad.LacZ transduced vessels. Because only one animal was studied in each configuration, it was not possible to do any statistical test on these results. However, if the data is analysed from a different perspective so that the contractile response of the 3 sets of gravid vessels transduced with Ad.VEGF-D (2 sets from the twin pregnant animal and 1 set from the singleton pregnant animal) is compared with the contractile response of the 3 sets of gravid vessels transduced with Ad.LacZ, the contractile response of the former is significantly lesser than the latter (E_{max} 108.3±3.83 v/s 144.1± 10.22, n=3, p=0.013, Figure 3.36).

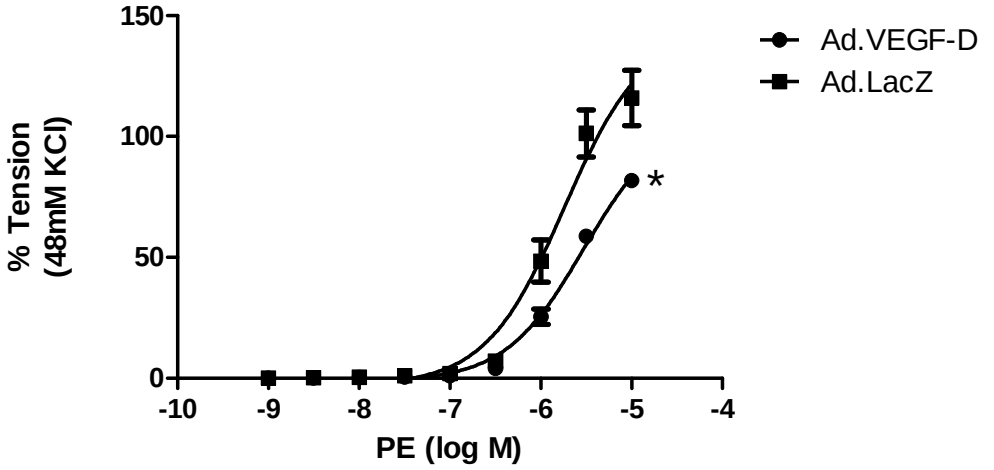

Figure 3.36 - Contractility of gravid Ad.VEGF-D and Ad.LacZ transduced uterine arteries to L-phenylephrine (PE) from one twin and one singleton pregnant animal 4 days after gene transfer.

At mid-gestation, the uterine arteries of one twin and one singleton pregnant sheep were injected with Ad.VEGF-D bilaterally, and those of another twin and another singleton pregnant sheep were injected with Ad.LacZ bilaterally. The second and third branches of the main uterine arteries supplying the gravid uterine horn were harvested 4 days after injection, cut into 3mm ring segments and analysed on an 8-chambered organ bath system. Concentration response curves to PE were constructed for each vessel in quadruplicate. The contractility of the vessel is expressed as a percentage of the response to KCl. PE produced concentration-dependent contractions, which were of significantly lesser magnitude in Ad.VEGF-D transduced vessels compared to Ad.LacZ transduced vessels. Error bars denote standard error of mean. * denotes $p<0.05$

3.21.2 Studies on the uterine artery relaxation response after local over-expression of VEGF-D in the uterine arteries of pregnant sheep bilaterally are inconclusive.

I also studied the endothelium-dependent relaxation to bradykinin in the uterine arteries from sheep that had been injected with Ad.VEGF-D or Ad.LacZ bilaterally. I observed an enhancement in the relaxation of uterine arteries from the twin pregnant animal (Figure 3.37), though the uterine arteries from the singleton pregnant animals did not yield any conclusive results (Figure 3.38) Table 3.15 summarizes the E_{max} and pD_2 to bradykinin in the animals studied in this group.

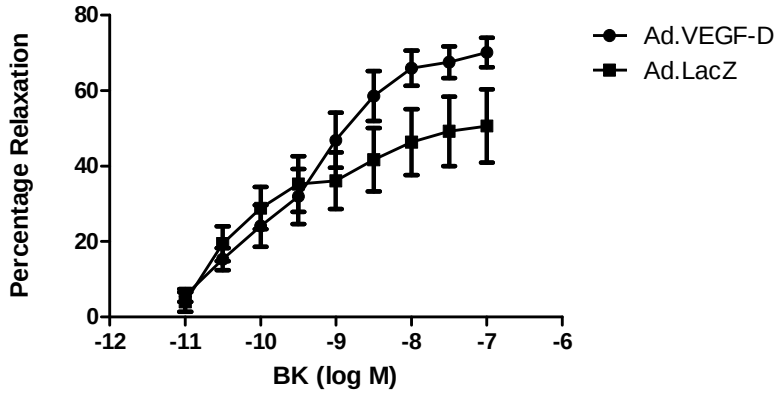

Figure 3.37 – Endothelium-dependent relaxation to bradykinin in twin pregnant Ad.VEGF-D and Ad.LacZ transduced uterine arteries 4 days after gene transfer.

At mid-gestation, the uterine arteries of one twin pregnant sheep were injected with Ad.VEGF-D bilaterally, and those of another were injected with Ad.LacZ bilaterally (n=1 animal each). The second and third branches of the main uterine arteries were harvested 4 days after injection, cut into 3mm ring segments and analysed on an 8-chambered organ bath system. Concentration response curves to BK were constructed for each vessel in quadruplicate. The relaxation of the vessel is expressed as a percentage of inhibition of PE-induced contraction. BK produced concentration-dependent relaxation, which was of greater magnitude in Ad.VEGF-D transduced vessels compared to Ad.LacZ transduced vessels. Error bars denote standard error of mean.

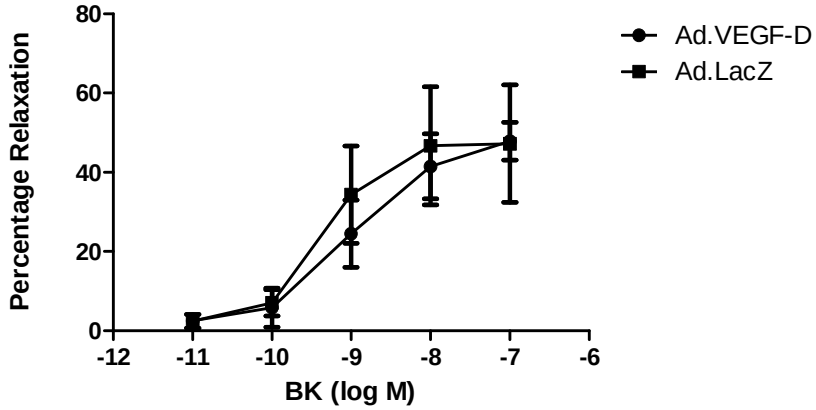

Figure 3.38 – Endothelium-dependent relaxation to bradykinin in singleton pregnant Ad.VEGF-D and Ad.LacZ transduced uterine arteries 4 days after gene transfer.

At mid-gestation, the uterine arteries of one singleton pregnant sheep were injected with Ad.VEGF-D bilaterally, and those of another were injected with Ad.LacZ bilaterally (n=1 animal

each). The second and third branches of the main uterine arteries were harvested 4 days after injection, cut into 3mm ring segments and analysed on an 8-chambered organ bath system. Concentration response curves to BK were constructed for each vessel in quadruplicate. The relaxation of the vessel is expressed as a percentage of inhibition of PE-induced contraction. BK produced concentration-dependent relaxation, which was not different between the Ad.VEGF-D transduced segments and Ad.LacZ transduced segments. Error bars denote standard error of mean.

Table 3.15 – E_{max} and pD_2 in response to bradykinin in uterine arteries from twin and singleton pregnant sheep injected with Ad.VEGF-D or Ad.LacZ bilaterally.

At mid-gestation, the uterine arteries of one twin and one pregnant singleton sheep were injected with Ad.VEGF-D bilaterally, and those of another twin and singleton sheep were injected with Ad.LacZ bilaterally. The second and third branches of the main uterine artery were harvested 4 days after injection and analysed on an 8-chambered organ bath system. Concentration response curves to BK were constructed for each vessel in quadruplicate. The relaxation of the vessel is expressed as a percentage of inhibition of PE-induced contraction.

Animal	Number of fetuses	Vector injected	Number of animals	E_{max} % (Mean±SEM)	pD_2
UA17	Twin	Ad.VEGF-D	1	68.54±3.01	9.29±0.15
UA21	Twin	Ad.LacZ	1	45.51±3.37	10.20±0.36
UA19	Singleton	Ad.VEGF-D	1	47.28±4.99	8.97±0.28
UA23	Singleton	Ad.LacZ	1	48.33±7.99	9.34±0.51

Because we only studied one animal in each configuration, it was not possible to do any statistical test on these results and make definite conclusions about the effects of Ad.VEGF-D on uterine artery relaxation. This study was limited by animal numbers, and a greater number of animals are warranted to come to any definite conclusion. However, if the data is analysed from a different perspective so that the relaxation response of the 3 sets of gravid vessels transduced with Ad.VEGF-D (2 sets from the twin pregnant animal and 1 set from the singleton pregnant animal) is compared with the relaxation response of the 3 sets of gravid vessels transduced with Ad.LacZ, the endothelium-dependent relaxation response of the former is significantly greater than the latter (E_{max} 66.07±2.03 v/s 41.50±3.40, n=3, p=0.036, Figure 3.39).

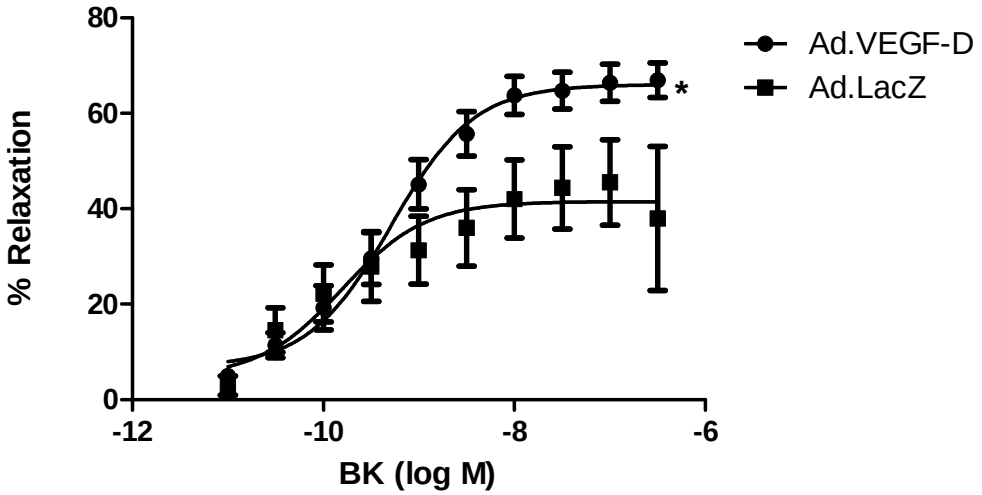

Figure 3.39 – Relaxation of gravid Ad.VEGF-D and Ad.LacZ transduced uterine arteries to bradykinin (BK) from one twin and one singleton pregnant animal 4 days after gene transfer.

At mid-gestation, the uterine arteries of one twin and one singleton pregnant sheep were injected with Ad.VEGF-D bilaterally, and those of another twin and another singleton pregnant sheep were injected with Ad.LacZ bilaterally. The second and third branches of the main uterine arteries supplying the gravid uterine horn were harvested 4 days after injection, cut into 3mm ring segments and analysed on an 8-chambered organ bath system. Concentration response curves to BK were constructed for each vessel in quadruplicate. The relaxtion of the vessel is expressed as a percentage of inhibition of PE-induced contraction. BK produced concentration-dependent relaxations, which were of significantly greater magnitude in Ad.VEGF-D transduced vessels compared to Ad.LacZ transduced vessels. Error bars denote standard error of mean. * denotes $p<0.05$

3.22 Ad.VEGF-D transduction of uterine arteries in the pregnant sheep unilaterally results in short term changes in vascular reactivity.

We also performed experiments wherein we injected the uterine arteries with Ad.VEGF-D and Ad.LacZ contra-laterally in the same animal. The animals were sacrificed 4-7 days post-injection, and the contractility and relaxation of their vessels was studied in an organ bath set-up. The vascular reactivity of uterine arteries depends on a number of factors, which include weight of the animal, age and gravidity status. We therefore considered that an intra-animal comparison (between both the uterine arteries of animals that had been injected

with two different vectors) was likely to be more informative than an inter-animal comparison (between animals injected bilaterally with the same vector) to elucidate the effect of the vector. More importantly, we felt this data would give us a better opportunity to put the results in perspective and compare with our previous data from Ad.VEGF-A_{165} injected sheep (all of whom had received Ad.VEGF-A_{165} and Ad.LacZ contra-laterally).

3.22.1 Local over-expression of VEGF-D in the uterine arteries of pregnant sheep results in a diminished contractile response

The uterine arteries from mid-gestation pregnant sheep were injected with Ad.VEGF-D and Ad.LacZ contra-laterally (n=6). All of the sheep used in this study carried singleton pregnancies. In half of the animals (n=3), Ad.VEGF-D was injected into the uterine artery supplying the gravid horn, while in the other half (n=3), Ad.VEGF-D was injected into the uterine artery supplying the non-gravid horn.

The results for contractility to phenylephrine have been presented individually for each group first and then combined for both the groups. Two-way ANOVA was used to statistically compare the vascular responses of the Ad.VEGF-D and Ad.LacZ transduced vessels.

Injection of Ad.VEGF-D into the uterine artery supplying the gravid horn significantly reduced the contractile response to phenylephrine when compared to injection of Ad.LacZ vector on the non-gravid side (Figure 3.40). The E_{max} in the Ad.VEGF-D transduced vessels was 115.1$\pm$7.81 v/s 158.7$\pm$11.75 in Ad.LacZ transduced vessels (n=3, $p<0.001$, two-way ANOVA).

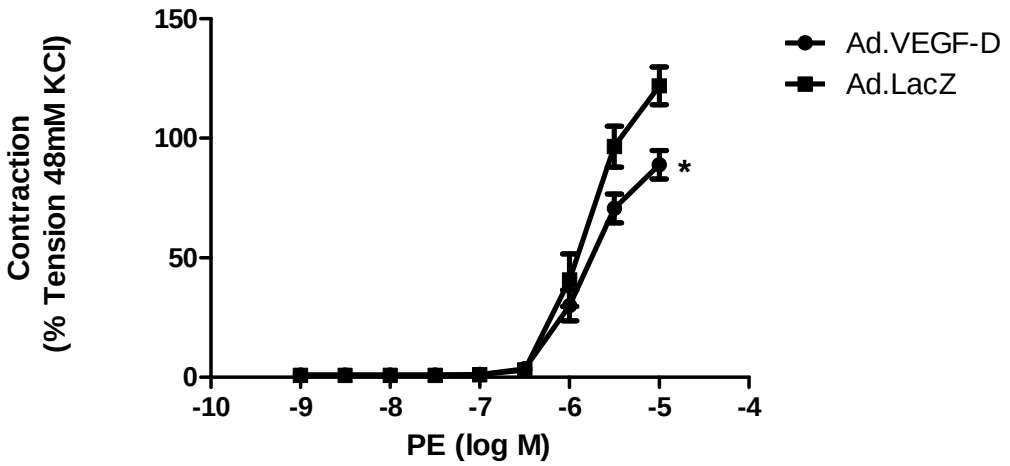

Figure 3.40 - Contractility of singleton pregnant Ad.VEGF-D and Ad.LacZ transduced uterine arteries to L-phenylephrine 4-7 days after gene transfer (Ad.VEGF-D administered on gravid side).

At mid-gestation, the uterine artery supplying the gravid horn was injected with Ad.VEGF-D and the contra-lateral uterine artery was injected with Ad.LacZ in singleton pregnant animals (n=3). The second and third branches of the main uterine arteries were harvested 4-7 days after injection, cut into 3mm ring segments and analysed on an 8-chambered organ bath system. Concentration response curves to PE were constructed for each vessel in quadruplicate. The contractility of the vessel is expressed as a percentage of the response to KCl. PE produced concentration-dependent contractions, which were of significantly lesser magnitude in Ad.VEGF-D transduced vessels compared to Ad.LacZ transduced vessels. Error bars denote standard error of mean. * denotes $p<0.005$

Injection of Ad.VEGF-D into the uterine artery supplying the non-gravid horn resulted in no differential response between the Ad.VEGF-D and Ad.LacZ transduced vessels (Figure 3.41). The E_{max} in the Ad.VEGF-D transduced vessels was 163.2+17.87 v/s 173.3$\pm$30.05 in Ad.LacZ transduced vessels (n=3, p=0.863, two-way ANOVA).

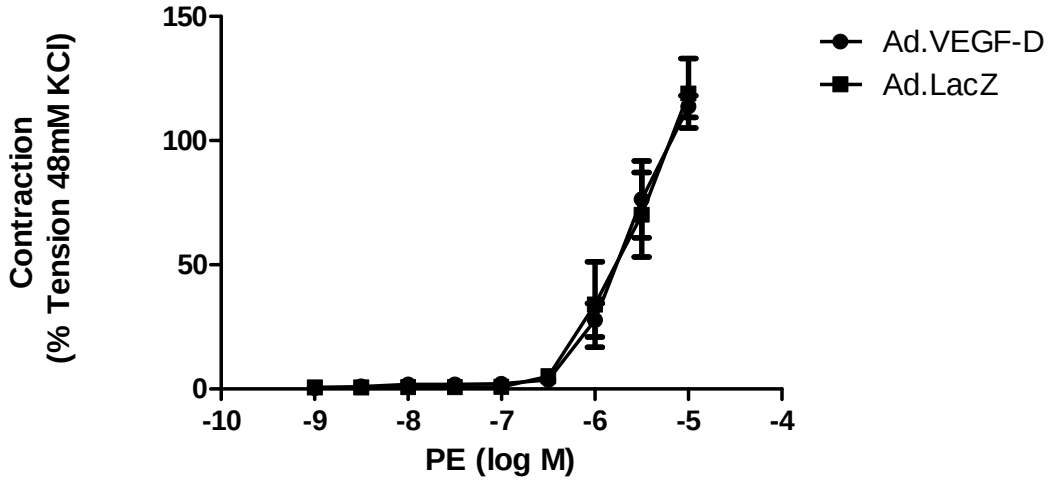

Figure 3.41 - Contractility of singleton pregnant Ad.VEGF-D and Ad.LacZ transduced uterine arteries to L-phenylephrine 4-7 days after gene transfer (Ad.VEGF-D administered on non-gravid side).

At mid-gestation, the uterine artery supplying the non-gravid horn was injected with Ad.VEGF-D and the contra-lateral uterine artery was injected with Ad.LacZ in singleton pregnant animals (n=3). The second and third branches of the main uterine arteries were harvested 4-7 days after injection, cut into 3mm ring segments and analysed on an 8-chambered organ bath system. Concentration response curves to PE were constructed for each vessel in quadruplicate. The contractility of the vessel is expressed as a percentage of the response to KCl. PE produced concentration-dependent contractions, which were no different between the Ad.VEGF-D transduced segments and Ad.LacZ transduced segments. Error bars denote standard error of mean.

When contractility data from these experiments was combined, analysis using two-way ANOVA to control for factors such as the injection side and the vector demonstrated that Ad.VEGF-D transduced vessels were significantly less contractile to phenylephrine compared to Ad.LacZ transduced vessels (Figure 3.42). Table 3.16 and 3.17 summarize the E_{max} values and EC_{50} respectively, in response to L-phenylephrine, observed in the animals in this cohort.

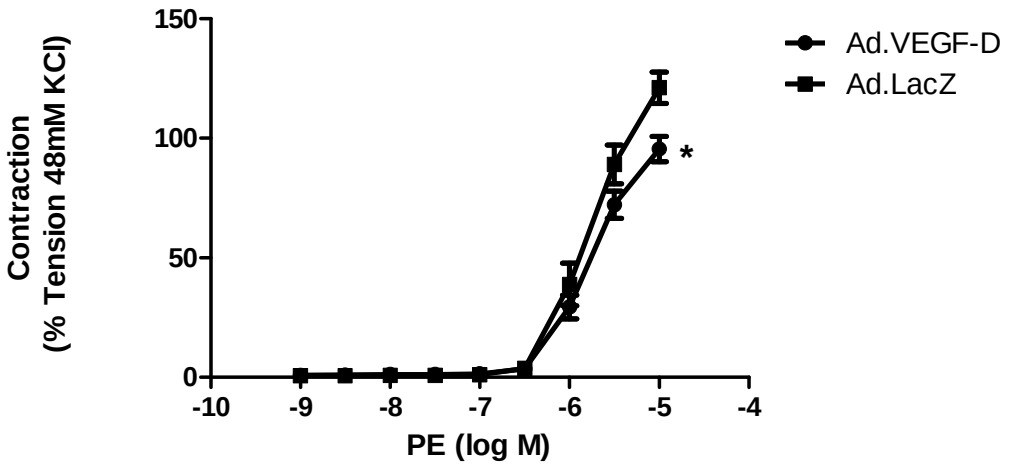

Figure 3.42 - Contractility of singleton pregnant Ad.VEGF-D and Ad.LacZ transduced uterine arteries to L-phenylephrine 4-7 days after gene transfer (combined data).

At mid-gestation, the uterine artery supplying the gravid horn (n=3) or non-gravid horn (n=3) was injected with Ad.VEGF-D and the contra-lateral uterine artery was injected with Ad.LacZ in singleton pregnant animals (n=6). The second and third branches of the main uterine arteries were harvested 4-7 days after injection, cut into 3mm ring segments and analysed on an 8-chambered organ bath system. Concentration response curves to PE were constructed for each vessel in quadruplicate. The contractility of the vessel is expressed as a percentage of the response to KCl. PE produced concentration-dependent contractions, which were of significantly lesser magnitude in Ad.VEGF-D transduced vessels compared to Ad.LacZ transduced vessels. Error bars denote standard error of mean. * denotes $p<0.005$

Table 3.16 - E_{max} in response to L-phenylephrine in uterine arteries from singleton pregnant animals injected with Ad.VEGF-D and Ad.LacZ contra-laterally.

At mid-gestation, the uterine artery supplying the gravid horn (n=3) or non-gravid horn (n=3) was injected with Ad.VEGF-D and the contra-lateral uterine artery was injected with Ad.LacZ in singleton pregnant animals (n=6). The second and third branches of the main uterine artery were harvested 4-7 days after injection and analysed on an 8-chambered organ bath system. Concentration response curves to PE were constructed for each vessel in quadruplicate. The contractility of the vessel is expressed as a percentage of the response to KCl. The p value is for the contraction dose response curve.

Number of fetuses	Side of Ad.VEGF-D vector injection	Number of animals	Observed E_{max} % (Mean±SEM)		p value
			Ad.VEGF-D vector	Ad.LacZ vector	
Singleton	Gravid	3	115.1±7.81	158.7±11.75	0.0001
Singleton	Non-gravid	3	163.2+17.87	173.3±30.05	0.863
Singleton	Gravid and non-gravid data combined	6	126.6+7.54	159.9±10.96	0.0001

Table 3.17 – EC_{50} in response to L-phenylephrine in uterine arteries from singleton pregnant animals injected with Ad.VEGF-D and Ad.LacZ contra-laterally.

At mid-gestation, the uterine artery supplying the gravid horn (n=3) or non-gravid horn (n=3) was injected with Ad.VEGF-D and the contra-lateral uterine artery was injected with Ad.LacZ in singleton pregnant animals (n=6). The second and third branches of the main uterine artery were harvested 4-7 days after injection and analysed on an 8-chambered organ bath system. Concentration response curves to PE were constructed for each vessel in quadruplicate. EC_{50} was determined by plotting a sigmoidal dose response curve. The p value is for the contraction dose response curve.

Number of fetuses	Side of Ad.VEGF-D vector injection	Number of animals	EC_{50} (M)		p value
			Ad.VEGF-D vector	Ad.LacZ vector	
Singleton	Gravid	3	$2.49x10^{-6}$	$2.53x10^{-6}$	0.0001
Singleton	Non-gravid	3	$4.08x10^{-6}$	$4.52x10^{-6}$	0.863
Singleton	Gravid and non-gravid data combined	6	$2.86x10^{-6}$	$2.87x10^{-6}$	0.0001

To summarize, these results show that 4-7 days after adenovirus-mediated local over-expression of VEGF-D and LacZ in the uterine arteries of pregnant sheep contra-laterally, there is a significant reduction in the contractile response to L-phenylephrine in the Ad.VEGF-D transduced vessel segments. We have demonstrated that the reduction in contractile response was only seen when Ad.VEGF-D was injected into the gravid side uterine artery, but not when it was injected into the non-gravid uterine artery. Nevertheless, the overall data obtained by combining the results of the gravid and non-gravid side still shows a trend towards a significant reduction in contractile response for the Ad.VEGF-D transduced vessel segments.

3.22.2 Local over-expression of VEGF-D in the uterine arteries of pregnant sheep results in a significantly enhanced relaxation response

We also investigated the endothelium-dependent relaxation to bradykinin in the uterine arteries of pregnant sheep (n=6) which had received an Ad.VEGF-D injection and Ad.LacZ injection contra-laterally. As in the preceding section, the results for each group (Ad.VEGF-D injection on gravid side and Ad.VEGF-D injection on non-gravid side) have been presented individually, followed by the combined results for both groups. Two-way ANOVA was used to statistically compare the vascular responses of the Ad.VEGF-D and Ad.LacZ transduced vessels.

The uterine arteries from one sheep (UA41) which had received Ad.VEGF-D on the non-gravid side failed the endothelial integrity test (the vessel segments relaxed less than 10% to a bolus dose of bradykin). Consequently, the relaxation data from this animal had to be excluded from our analysis.

Administration of Ad.VEGF-D to the uterine artery supplying the gravid horn resulted in a significant enhancement of relaxation (Figure 3.43). The E_{max} in the Ad.VEGF-D transduced vessels was 77.76$\pm$3.90 v/s 44.42$\pm$3.87 in Ad.LacZ transduced vessels (n=3, p=0.010, two-way ANOVA)

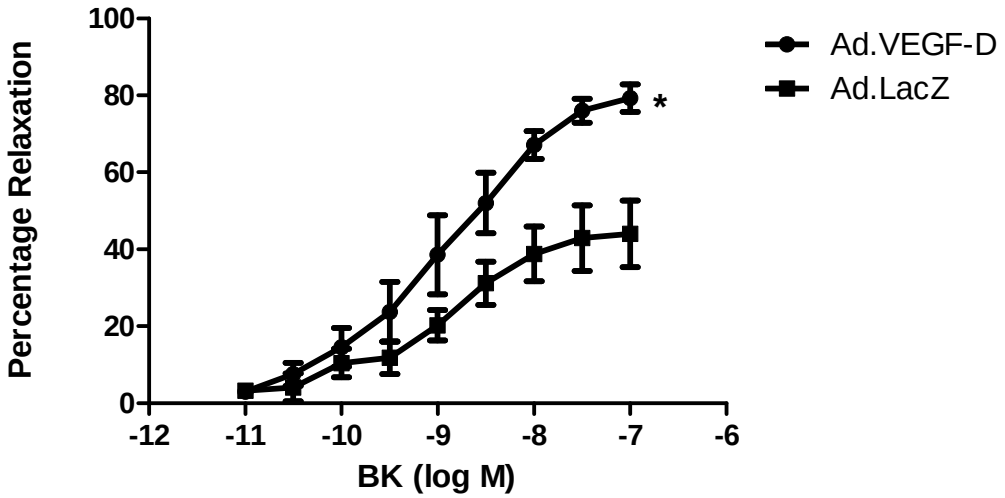

Figure 3.43 – Endothelium-dependent relaxation to bradykin in singleton pregnant Ad.VEGF-D and Ad.LacZ transduced uterine arteries 4-7 days after gene transfer (Ad.VEGF-D administered on gravid side).

At mid-gestation, the uterine artery supplying the gravid horn was injected with Ad.VEGF-D and the contra-lateral uterine artery was injected with Ad.LacZ in singleton pregnant animals (n=3). The second and third branches of the main uterine arteries were harvested 4-7 days after injection, cut into 3mm ring segments and analysed on an 8-chambered organ bath system. Concentration response curves to BK were constructed for each vessel in quadruplicate. The relaxation of the vessel is expressed as a percentage of inhibition of PE-induced contraction. BK produced concentration-dependent relaxation, which was of significantly greater magnitude in Ad.VEGF-D transduced vessels compared to Ad.LacZ transduced vessels. Error bars denote standard error of mean. * denotes $p<0.05$

Administration of Ad.VEGF-D to the uterine artery supplying the non-gravid horn indicated a trend towards increased relaxation on this side (Figure 3.44), even though the E_{max} values for both the sides were very similar – 38.75$\pm$2.24 (Ad.VEGF-D) v/s 37.71$\pm$1.61 v/s (Ad.LacZ). No statistical test was performed on this group of results because of the small number of animals (n=2).

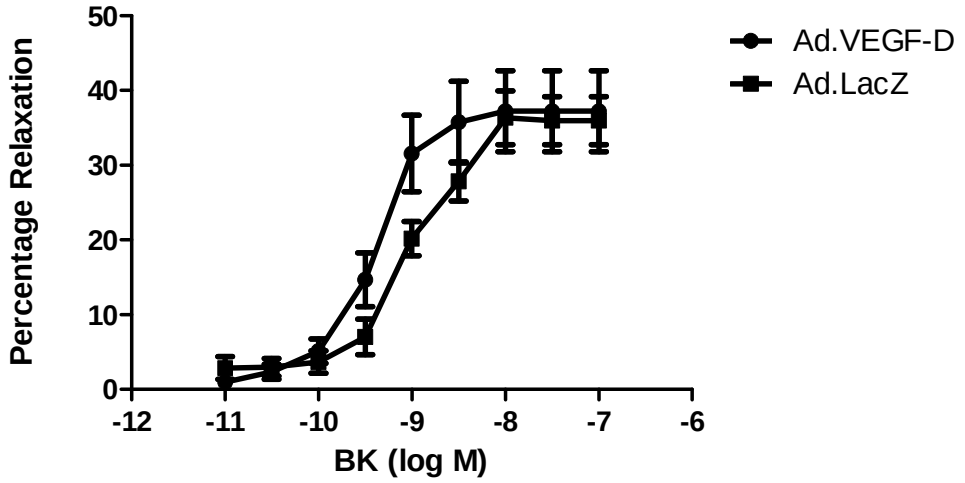

Figure 3.44 – Endothelium-dependent relaxation to bradykin in singleton pregnant Ad.VEGF-D and Ad.LacZ transduced uterine arteries 4-7 days after gene transfer (Ad.VEGF-D administered on non-gravid side).

At mid-gestation, the uterine artery supplying the non-gravid horn was injected with Ad.VEGF-D and the contra-lateral uterine artery was injected with Ad.LacZ in singleton pregnant animals (n=2). The second and third branches of the main uterine arteries were harvested 4-7 days after injection, cut into 3mm ring segments and analysed on an 8-chambered organ bath system. Concentration response curves to BK were constructed for each vessel in quadruplicate. The relaxation of the vessel is expressed as a percentage of inhibition of PE-induced contraction. BK produced concentration-dependent relaxation, which demonstrated a trend towards enhancement in the Ad.VEGF-D transduced segments compared to the Ad.LacZ transduced segments. Error bars denote standard error of mean.

When the data for both these groups was combined (using two-way ANOVA), the relaxation response in the Ad.VEGF-D transduced vessels was significantly greater than the Ad.LacZ transduced vessels (p=0.052, Figure 3.45, Table 3.18). Table 3.18 and 3.19 summarize the E_{max} values and pD_2 in response to bradykinin observed in the animals in this cohort.

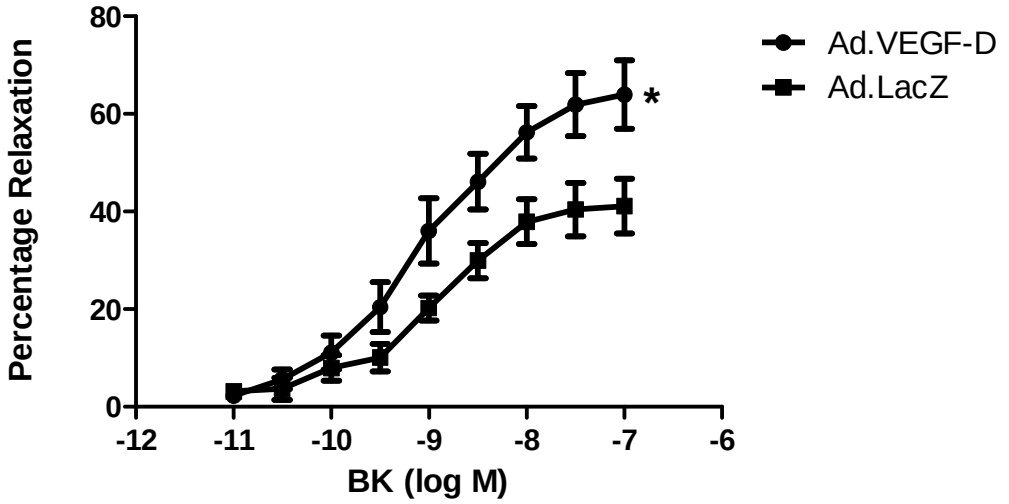

Figure 3.45 – Endothelium-dependent relaxation to bradykin in singleton pregnant Ad.VEGF-D and Ad.LacZ transduced uterine arteries 4-7 days after gene transfer (combined data)

At mid-gestation, the uterine artery supplying the gravid horn (n=3) or non-gravid horn (n=2) was injected with Ad.VEGF-D and the contra-lateral uterine artery was injected with Ad.LacZ in singleton pregnant animals (n=5). The second and third branches of the main uterine arteries were harvested 4-7 days after injection, cut into 3mm ring segments and analysed on an 8-chambered organ bath system. Concentration response curves to BK were constructed for each vessel in quadruplicate. The relaxation of the vessel is expressed as a percentage of inhibition of PE-induced contraction. BK produced concentration-dependent relaxation, which was of significantly greater magnitude in Ad.VEGF-D transduced vessels compared to Ad.LacZ transduced vessels. Error bars denote standard error of mean. * denotes $p \leq 0.05$

Table 3.18 - E_{max} in response to bradykinin in uterine arteries from singleton pregnant animals injected with Ad.VEGF-D and Ad.LacZ contra-laterally.

At mid-gestation, the uterine artery supplying the gravid horn (n=3) or non-gravid horn (n=2) was injected with Ad.VEGF-D and the contra-lateral uterine artery was injected with Ad.LacZ in singleton pregnant animals (n=5). The second and third branches of the main uterine artery were harvested 4-7 days after injection and analysed on an 8-chambered organ bath system. Concentration response curves to BK were constructed for each vessel in quadruplicate. The relaxation of the vessel is expressed as a percentage of inhibition of PE-induced contraction. The p value is for the relaxation dose response curve.

Number of fetuses	Side of Ad.VEGF-D vector injection	Number of animals	Observed E_{max} % (Mean±SEM)		p value
			Ad.VEGF-D vector	Ad.LacZ vector	
Singleton	Gravid	3	77.76±3.90	44.42±3.87	0.010
Singleton	Non-gravid	2	38.75±2.24	37.71±1.61	na
Singleton	Gravid and non-gravid data combined	5	62.50±3.25	41.89±2.49	0.052

Table 3.19 – pD_2 in response to bradykinin in uterine arteries from singleton pregnant animals injected with Ad.VEGF-D and Ad.LacZ contra-laterally.

At mid-gestation, the uterine artery supplying the gravid horn (n=3) or non-gravid horn (n=2) was injected with Ad.VEGF-D and the contra-lateral uterine artery was injected with Ad.LacZ in singleton pregnant animals (n=5). The second and third branches of the main uterine artery were harvested 4-7 days after injection and analysed on an 8-chambered organ bath system. Concentration response curves to BK were constructed for each vessel in quadruplicate. pD_2 was determined by plotting a sigmoidal dose response curve. The p value is for the relaxation dose response curve.

Number of fetuses	Side of Ad.VEGF-D vector injection	Number of animals	pD_2		p value
			Ad.VEGF-D vector	Ad.LacZ vector	
Singleton	Gravid	3	8.86±0.13	8.82±0.23	0.010
Singleton	Non-gravid	2	9.42±0.17	8.95±0.11	na
Singleton	Combined data from both groups above	5	9.05±0.14	8.87±0.16	0.052

To summarize, these results demonstrate that 4-7 days after adenovirus-mediated local over-expression of VEGF-D and LacZ in the uterine arteries of pregnant sheep contra-laterally, there is a significant increase in the endothelium-dependent relaxation response to bradykinin in the Ad.VEGF-D transduced vessels. The extent of enhancement of endothelium-dependent relaxation was greater when Ad.VEGF-D was injected into the gravid uterine artery rather than the non-gravid uterine artery.

3.22.3 The endothelium dependent relaxation in the uterine arteries of pregnant sheep transduced with Ad.VEGF-D short-term is mediated via NO and EDHF

The relaxation response to bradykinin was investigated in the presence of different inhibitors of relaxation, to examine the mechanism of action of local VEGF-D expression in uterine arteries short-term. Vessels from 5 singleton pregnant animals (which had a good relaxation response) were used for this study. These experiments were performed using the same methodology described in Section 3.6.3, the only difference being that in place of Indomethacin, an alternative COX-2 inhibitor, NS-398 (10 μM) was used. NS-398 is a specific

inhibitor of the COX-2 enzyme, a key mediator in the synthesis of PGI_2 (Kawabe J et al., 2010). Indomethacin, on the other hand is a non-selective inhibitor of both COX-1 and COX-2 pathways and thus blocks the synthesis of Thromboxane-A_2 (a vasoconstrictor) and PGI_2 (a vasodilator). As we intended to investigate only the contribution of PGI_2 towards endothelium-depend relaxation in uterine arteries transduced with Ad.VEGF-D, use of a more specific inhibitor, such as NS-398, was considered to be more appropriate.

Treatment with L-NAME significantly reduced the relaxant effect to bradykinin in uterine artery segments from both the Ad.VEGF-D and Ad.LacZ transduced vessels. Even though the E_{max} values in the presence of L-NAME were not significantly different from that of vessels unexposed to this inhibitor (Table 3.20), addition of L-NAME resulted in a significant shift of the dose-response curve to the right (Figure 3.46).

Further addition of NS-398 (with L-NAME) did not result in any significant change in the endothelium dependent relaxation, even though there was a trend towards a reduction in the relaxation response in the Ad.VEGF-D transduced segments. Pre-treatment with Apamin (in the presence of L-NAME and NS-398) resulted in a further significant attenuation of the endothelium-dependent relaxation. The residual relaxation that was resistant to the cumulative inhibition by all three inhibitors was significantly greater in the Ad.VEGF-D transduced vessels (19.57%) compared to Ad.LacZ transduced vessels (9.21%, n=5, p=0.05). NS-398 and Apamin alone had no significant influence on relaxation (data not shown). Table 3.20 summarizes the results of the relaxation response in the presence of different inhibitors.

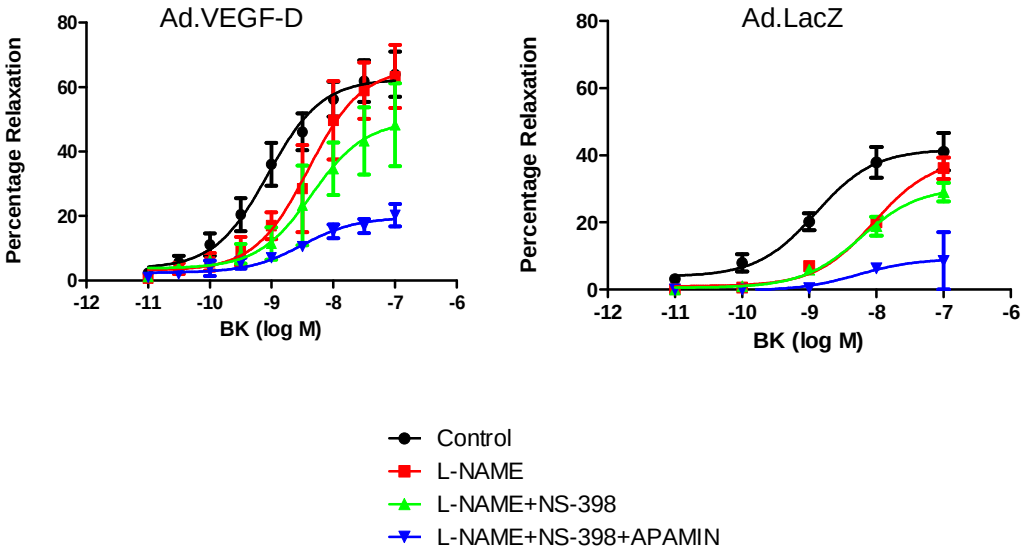

Figure 3.46(a) - The endothelium-dependent relaxation to bradykin in the presence of different inhibitors of the relaxation pathway in pregnant sheep uterine arteries, 4-7 days after Ad.VEGF-D or Ad.LacZ transduction.

The contribution of NO, PGI_2 and EDHF on the relaxation response to BK were investigated in vessels precontracted with PE. Cumulative relaxation curves of BK (10^{-11}M to 10^{-6}M) were constructed under the following conditions: (1) control (no inhibitors); (2) in the presence of L-NAME (300 µM); (3) in the presence of L-NAME and NS-398 (COX-2 inhibitor, 10 µM); (4) in the presence of L-NAME, NS-398 and apamin (1 µM). Relaxation was expressed as a percentage of inhibition of PE-induced contraction. The mean relaxation response of vessels from singleton pregnant sheep was calculated (n=5). Statistical significance was assumed at $p<0.05$. The BK relaxant effect was not significantly modified by NS-398 but reduced by L-NAME ($p<0.05$, n=5). The remaining endothelium-dependent relaxation (E_{max}), that was resistant to NS-398 and NO synthase inhibition, was significantly reduced by pretreatment with apamin in both Ad.VEGF-D and Ad.LacZ treated arteries ($P<0.05$, n=5). The residual relaxation that was resistant to the cumulative addition of all three inhibitors was significantly greater in the Ad.VEGF-D transduced segments compared to Ad.LacZ transduced segments.

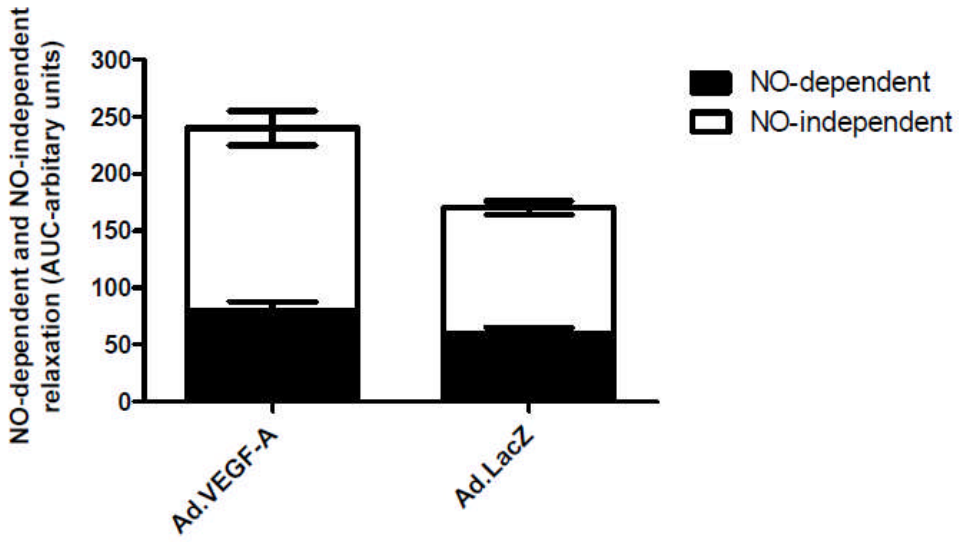

Figure 3.46(b)- Partial contribution of NO-dependent and NO-independent mechanisms to the endothelial-dependent relaxation

Values are the mean±SEM for the area under the curve (AUC) for BK-induced relaxation (complete bar with positive SEM), the AUC for BK-induced relaxation following treatment with L-NAME (NO-independent component, white bar), and the remaining AUC after BK with L-NAME (NO-dependent component, black bar). A significant reduction in the overall relaxation as well as NO-dependent and NO-independent relaxations was observed between the treated and control sides ($p<0.05$).

Table 3.20 - E_{max} in response to bradykinin in uterine arteries from pregnant sheep transduced short-term with Ad.VEGF-D and Ad.LacZ contra-laterally, in the presence of different inhibitors of endothelium-dependent relaxation.

At mid-gestation, one uterine artery was injected with Ad.VEGF-D and the contra-lateral uterine artery was injected with Ad.LacZ in singleton pregnant sheep (n=5). The second and third branches of the main uterine artery were harvested 4-7 days after injection and analysed on an 8-chambered organ bath system. Concentration response curves to BK were constructed for each vessel in the absence and presence of different inhibitors of relaxation, namely, L-NAME, NS-398 and Apamin. The relaxation of the vessel is expressed as a percentage of inhibition of PE-induced contraction. The p value indicates the significance of the effect of individual inhibitors on the dose response curve.

Inhibitor	E_{max} % (Mean±SEM)		p value
	Ad.VEGF-A_{165} transduced side	Ad.LacZ trandsduced side	
No inhibitor	62.50±3.25	41.79±3.09	
L-NAME	66.00±6.17	39.12±2.29	$p<0.05$
L-NAME + NS-398	49.55±6.25	30.45±2.11	$p=0.2$
L-NAME + NS-398 + Apamin	19.57±1.49	9.21±3.92	$p<0.05$

Overall, this data demonstrates that NO and EDHF play a significant contribution in mediating the endothelium-dependent relaxation in both Ad.VEGF-D and Ad.LacZ transduced vessels. PGI_2 may play a role as well in Ad.VEGF-D transduced vessels, but our results currently show this contribution is non-significant. The residual relaxation that remains after blocking all the three pathways is significantly greater in the Ad.VEGF-D transduced vessels compared to Ad.LacZ transduced vessels.

3.23 Ad.VEGF-D transduction of uterine arteries in the pregnant sheep results in long-term changes in uterine artery blood flow.

We were interested in investigating whether the short-term changes in uterine artery vascular reactivity observed in response to VEGF-D over-expression resulted in any long-term changes in UABF. The UABF was measured long-term in 5 pregnant ewes which were injected with Ad.VEGF-D and Ad.LacZ contra-laterally. Telemetric flow probes were implanted around the uterine arteries of these sheep (Table 3.22) up to a week before vector injection and uterine artery blood flow was measured for 1 hour each day. Before the administration of the vector, the measured uterine artery blood flow was averaged over three consecutive days to derive a baseline value. The daily measurements of blood flow post-injection for each uterine artery were compared with this baseline value and converted into a percentage increase from baseline.

We were aware that if Ad.VEGF-D had a similar effect in magnitude to Ad.VEGF-A_{165} on utero-placental perfusion, we would need to measure uterine artery blood flow in at least 10-11 ewes to reach statistically significant results. However, we were more interested in investigating if Ad.VEGF-D had a biological effect on uterine blood flow, rather than aiming for significance *per se*.

Hence, a smaller number of animals were used for this study as compared to the Ad.VEGF-A_{165} study.

As was seen with the Ad.VEGF-A_{165} injected ewes, there was a slight fall in UABF from baseline for the first 1-3 days after vector injection, but it had recovered completely by day 4 in all cases. The mean percentage fall in UABF from baseline 1-3 days after vector injection was not significantly different in Ad.VEGF-D (n=5) compared with Ad.LacZ (n=5) injected uterine arteries (9.01±5.95% v/s 9.14±23.50%, p=0.99).

Figure 3.47 shows the average increase in blood flow from baseline in all 5 pregnant ewes, calculated in the same way as described earlier in Section 3.2.

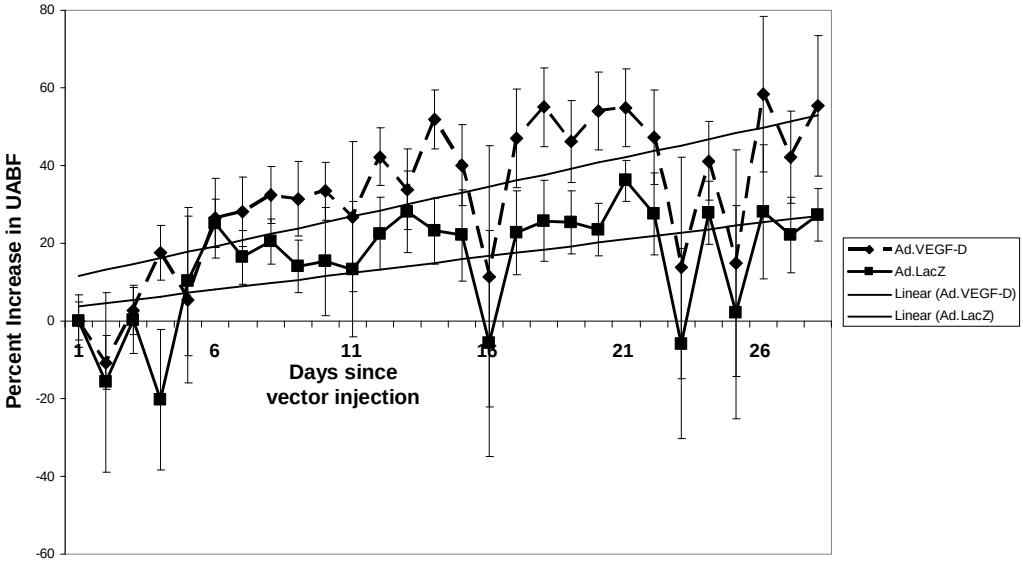

Figure 3.47 - Percentage increase in uterine artery blood flow (UABF) from baseline and gradient of percentage increase in UABF from baseline in 5 pregnant sheep injected with Ad.VEGF-D and Ad.LacZ contra-laterally

Pregnant sheep underwent a laparotomy at mid-gestation to implant transit-time flow probes around their uterine arteries. UABF was measured for one hour each day at the same time in the morning, before and after the administration of Ad.VEGF-D and Ad.LacZ contralaterally. The post-injection values were compared with a pre-injection baseline, which was obtained by averaging the values of UABF obtained for 3 consecutive days before the administration of the vector. In this graph, the mean percentage increase in UABF from baseline is greater in the Ad.VEGF-D transduced uterine arteries (50.58%) compared to the Ad.LacZ transduced uterine arteries (26.94%), though statistical significance was not reached, most probably because of the limited animal numbers.

For each animal (n=5), the maximum increase in blood flow from baseline was calculated at 4 different time points - 7 days, 14 days, 21 days and 28 days post-vector injection. The UABF percent change at each time-point was calculated using the average of 3 consecutive daily mean UABF measurements. The gradient of the percentage increase in blood flow from baseline in each uterine artery was calculated for the same time points. A two-way GLiM was used to compare the UABF percent change in Ad.VEGF-D and Ad.LacZ injected uterine arteries at each time point and also the gradients of UABF %change over the length of gestation (Table 3.21). The two factors accounted for in the GLiM analysis were whether the uterine artery supplied a gravid or non-gravid horn and whether Ad.VEGF-D or Ad.LacZ vector was injected.

Table 3.21 - Percentage change in uterine artery blood blow (UABF) and Gradient of Percentage Change in UABF at one week intervals post-Ad.VEGF-D/Ad.LacZ injection to the uterine arteries of pregnant sheep (n=5)

Time-point after vector injection	% Increase in UABF ± SEM		p value (GLiM)	Gradient of % Increase in UABF		p value (GLiM)
	Ad.VEGF-D	Ad.LacZ		Ad.VEGF-D	Ad.LacZ	
7 days	28.86± 8.23	20.91± 5.28	0.496	3.32	0.99	0.145
14 days	41.93± 8.70	24.41± 10.04	0.223	3.25	1.68	0.224
21 days	52.09± 9.83	29.11± 6.52	0.102	2.70	1.34	0.093
28 days	50.58± 15.81	26.94± 7.84	0.152	2.05	1.00	0.058

GLiM :General Linear Model

Table 3.22 summarizes the maximum increase in blood flow from baseline in each uterine artery at 28 days after the administration of the vector.

Table 3.22 - Percentage change in uterine artery blood flow (UABF) from baseline 28 days after administration of Ad.VEGF-D or Ad.LacZ to the uterine arteries of mid-gestation pregnant sheep.

Animal	**Fetal no.**	Side of vector injection		% change in UABF at 28 days post-injection	
		Ad. VEGF-D	**Ad.LacZ**	**Ad. VEGF-D**	**Ad.LacZ**
UA38	Twin	Gravid	Gravid	23.60	21.23
UA39	Singleton	Non-gravid	Gravid	66.14	47.86
UA42	Singleton	Gravid	Non-gravid	24.77	4.48
UA43	Singleton	Non-gravid	Gravid	32.65	19.85
UA45	Singleton	Non-gravid	Gravid	105.76	41.32

As anticipated, UABF increased with advancing gestation (Figure 3.47). Considering singleton and twin gestations together, at 28 days post vector injection, the mean increase in blood flow in the uterine arteries injected with Ad.VEGF-D (50.58$\pm$15.81%, n=5) was higher than in the uterine arteries injected with Ad.LacZ (26.94$\pm$7.84%, n=5). This increase was however not significant (p=0.152, GLiM Test), most probably because of the limited number of animals in this study.

At 28 days post-injection, it is encouraging to note that even with the limited number of animals, the difference in gradient of the %increase in UABF from baseline, between the Ad.VEGF-D and Ad.LacZ transduced sides (2.05 v/s 1.00 respectively) is close to significance (p=0.058).

These results propose that Ad.VEGF-D is playing a role in enhancing utero-placental perfusion long-term. This is also supported by the data presented in Table 3.22 which shows that the percentage increase in UABF from baseline in the Ad.VEGF-D transduced uterine artery was always higher than the contra-

lateral Ad.LacZ injected uterine artery. However, it must be emphasized that this trend is not significant (most probably on account of the limited number of experimental animals), thereby preventing us from making any firm conclusions. Experiments in greater number of animals are warranted to obtain statistically meaningful results.

3.24 The effect of Ad.VEGF-D transduction of uterine arteries in the pregnant sheep on fetal weights

Fetal weights from singleton pregnancies undergoing long-term uterine artery blood flow monitoring (n=4) were measured at post-mortem examination and compared to a historical singleton fetal control group from the same sheep breed (n=9) (David AL, 2005, Ph.D Thesis). The mean gestational age of the two groups was not statistically different (139.3$\pm$2.5 days v/s 137.8$\pm$3.9 days, p=0.97, unpaired t-test). The mean fetal weight in the experimental group was not significantly different than that in the control group (4863$\pm$492 grams v/s 4698$\pm$1004 grams, p=0.45, unpaired t-test).

Fetal liver weights from the experimental group (n=4) were compared to a historical singleton fetal control group from the same sheep breed (n=10). The mean gestational age of the two groups was not statistically different (139.3$\pm$2.5 days v/s 138.9$\pm$6.5 days, p=0.68, unpaired t-test). Mean fetal liver weight was higher in the experimental group (123.60$\pm$24.67 grams vs 106.10$\pm$21.18 grams), although this increase was not significant (p=0.20).

Although statistical significance was not reached, there was a trend observed, and higher numbers of experimental animals may have enabled a significant difference to be observed.

3.25 Ad.VEGF-D transduction of uterine arteries in the pregnant sheep results in long term changes in vascular reactivity

The results described in the previous section demonstrate that Ad.VEGF-D infection significantly alters uterine artery vascular reactivity 4-7 days after administration. I was interested in investigating if these short-term findings were sustained until term, and therefore examined the vascular reactivity of uterine arteries from long-term transduced sheep (30-45 days post-injection) on an organ bath. At 4 – 7 days after adenovirus gene transfer, changes in the contractile and relaxation response had been seen. I therefore studied both types of responses in these long term transduced vessels.

3.25.1 Local over-expression of VEGF-D in the uterine arteries of pregnant sheep results in a diminished contractile response long-term

Five mid-gestation pregnant sheep were used for this experiment, only one of which was pregnant with twins. Of the four singleton pregnant ewes, three had Ad.VEGF-D injected into the uterine artery supplying the non-gravid horn while one had Ad.VEGF-D injected into the uterine artery supplying the gravid horn (the operators were blinded to the vector injected at the time of surgery). At post-mortem examination 30-45 later, the uterine arteries were carefully dissected out and their vascular reactivity was studied with escalating doses of phenylephrine. Two-way ANOVA was used to statistically compare the vascular responses of the Ad.VEGF-D and Ad.LacZ transduced vessels.

Two of the study groups (twin pregnant animals and singleton pregnant animals with Ad.VEGF-D injected into the gravid uterine artery) had only animal each, making their results ineligible for any statistical assessment and logical conclusion. Hence, data from all 5 animals has been presented together to get statistically meaningful results. The statistical test used (two-way ANOVA)

factors in not only the effect of the vector but also whether the uterine artery is supplying a gravid or non-gravid horn.

I observed a significant reduction in the contractile response to phenylephrine in the Ad.VEGF-D transduced vessels compared to Ad.LacZ transduced vessels (Figure 3.48). The E_{max} and EC_{50} in the Ad.VEGF-D transduced vessels were 144.0±4.64 and $2.89x10^{-6}$ respectively v/s 184.2±8.58 and $2.63x10^{-6}$ in the Ad.LacZ transduced vessels, n=5, p=0.002. There was no significant difference in the magnitude of the KCl responses between the Ad.VEGF-D and Ad.LacZ treated sides (18.45±4.87g v/s 17.63±4.34g respectively, p=0.87).

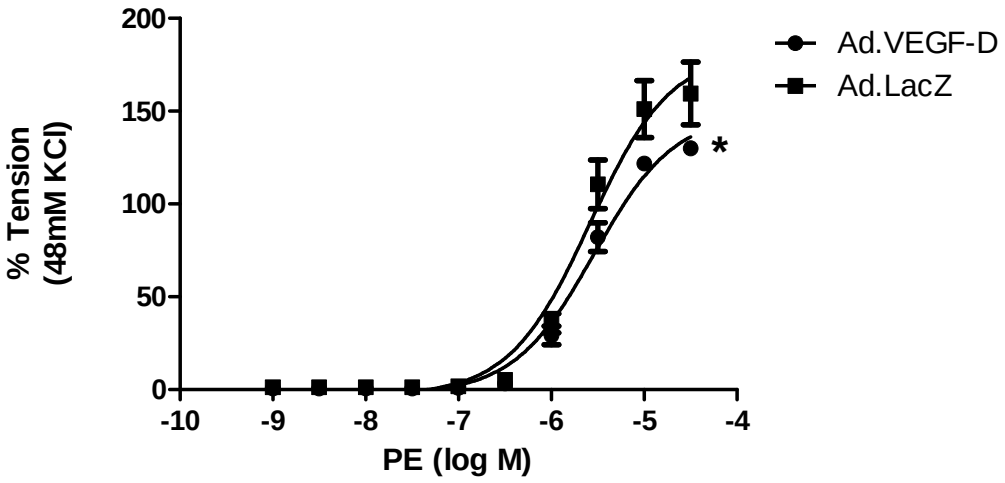

Figure 3.48 – Contractility of pregnant Ad.VEGF-D and Ad.LacZ transduced uterine arteries to L-phenylephrine 30-45 days after gene transfer.

At mid-gestation, one uterine artery was injected with Ad.VEGF-D and the contra-lateral uterine artery was injected with Ad.LacZ in pregnant animals (n=5). The second and third branches of the main uterine arteries were harvested 30-45 days after injection, cut into 3mm ring segments and analysed on an 8-chambered organ bath system. Concentration response curves to PE were constructed for each vessel in quadruplicate. The contractility of the vessel is expressed as a percentage of the response to KCl. PE produced concentration-dependent contractions, which were of significantly lesser magnitude in Ad.VEGF-D transduced vessels compared to Ad.LacZ transduced vessels. Error bars denote standard error of mean. * denotes $p<0.005$

3.25.2 Local over-expression of VEGF-D in the uterine arteries of pregnant sheep does not significantly change the endothelium-dependent relaxation long-term

The uterine arteries from 5 mid-gestation pregnant sheep (described above) were also examined for changes in endothelium-dependent relaxation to bradykinin. Data from all 5 animals has again been presented together and analysed using two-way ANOVA.

I observed no significant changes in the vascular relaxation between the Ad.VEGF-D and Ad.LacZ transduced vessel segments (Figure 3.49). The E_{max} and pD_2 in the Ad.VEGF-D transduced vessels were 48.39±2.66 and 9.19±0.18 respectively v/s 43.92±2.99 and 9.12±0.22 respectively in the Ad.LacZ transduced vessels, n=5, p=0.163.

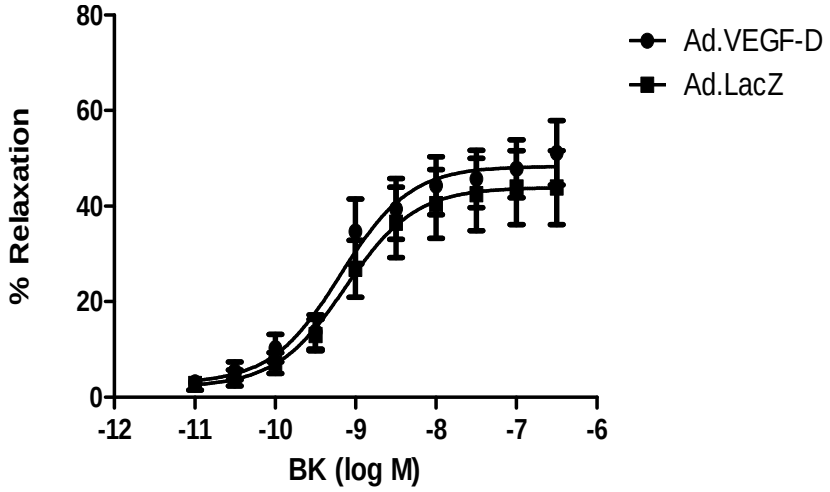

Figure 3.49 - Endothelium-dependent relaxation of pregnant Ad.VEGF-D and Ad.LacZ transduced uterine arteries to bradykinin 30-45 days after gene transfer.

At mid-gestation, one uterine artery was injected with Ad.VEGF-D and the contra-lateral uterine artery was injected with Ad.LacZ in pregnant sheep (n=5). The second and third branches of the main uterine arteries were harvested 30-45 days after injection, cut into 3mm ring segments and analysed on an 8-chambered organ bath system. Concentration response curves to BK were constructed for each vessel in quadruplicate. The relaxation of the vessel is expressed as a percentage of inhibition of PE-induced contraction. There was no significant difference in the relaxation response between the Ad.VEGF-D and Ad.LacZ transduced vessels (statistical significance assumed at $p<0.05$). Error bars denote standard error of mean.

3.25.3 The endothelium dependent relaxation in the uterine arteries of pregnant sheep transduced with Ad.VEGF-D long-term is mediated via NO and EDHF

Similar to the short-term experiments described in section 3.22.3, the relaxation response of long-term transduced uterine arteries was investigated in the presence of different inhibitors of relaxation. Treatment with L-NAME significantly reduced the relaxant effect to bradykinin in uterine artery segments from both the Ad.VEGF-D and Ad.LacZ transduced vessels; there was no differential response between the two kinds of vessels. Addition of NS-398 did not result in any significant alterations in the relaxation response. Pre-treatment with Apamin (in the presence of L-NAME and NS-398) resulted in a further significant attenuation of the endothelium-dependent relaxation. The residual relaxation that was resistant to the cumulative inhibition by all three inhibitors was not significantly different between the Ad.VEGF-D and Ad.LacZ transduced sides (Figure 3.50). Table 3.23 summarizes the results of the relaxation response in the presence of different inhibitors.

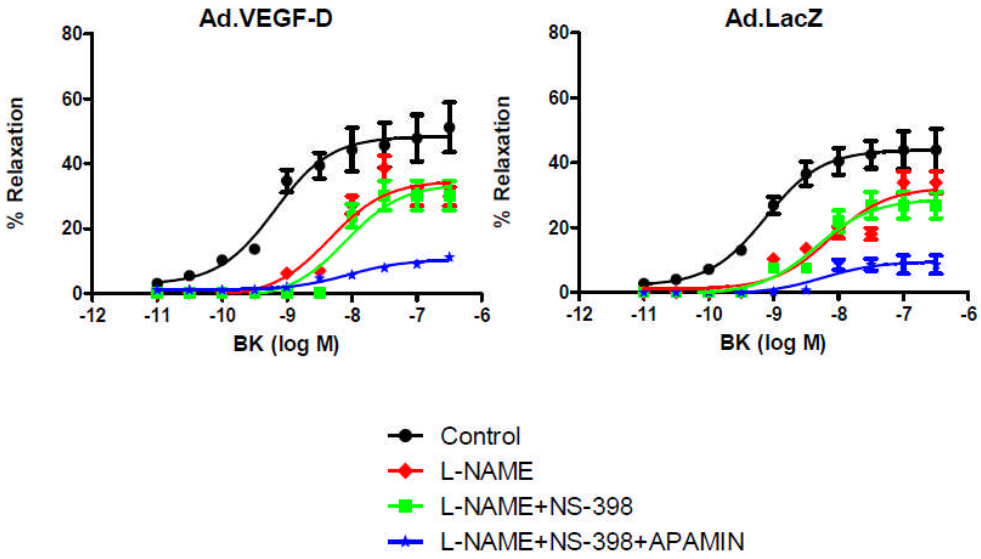

Figure 3.50(a) -The endothelium-dependent relaxation to bradykin in the presence of different inhibitors of the relaxation pathway in pregnant sheep uterine arteries, 30-45 days after Ad.VEGF-D or Ad.LacZ transduction.

The contribution of NO, PGI_2 and EDHF on the relaxation response to BK were investigated in vessels precontracted with PE. Cumulative relaxation curves of BK (10^{-11}M to 10^{-6}M) were constructed under the following conditions: (1) control (no inhibitors); (2) in the presence of L-NAME (300 µM); (3) in the presence of L-NAME and NS-398 (10 µM); (4) in the presence of L-NAME, NS-398 and apamin (1 µM). Relaxation was expressed as a percentage of inhibition of PE-induced contraction. The mean relaxation response of vessels from n=5 pregnant sheep was calculated. Statistical significance was assumed at $p<0.05$. The BK relaxant effect was not modified by NS-398 but reduced by L-NAME ($p<0.05$, n=5). The remaining endothelium-dependent relaxation (E_{max}), that was resistant to NS-398 and NO synthase inhibition, was significantly reduced by pretreatment with apamin in both Ad.VEGF-D and Ad.LacZ treated arteries ($P<0.05$, n=5). There was no difference in the small amount of residual relaxation between the Ad.VEGF-D and Ad.LacZ transduced vessels.

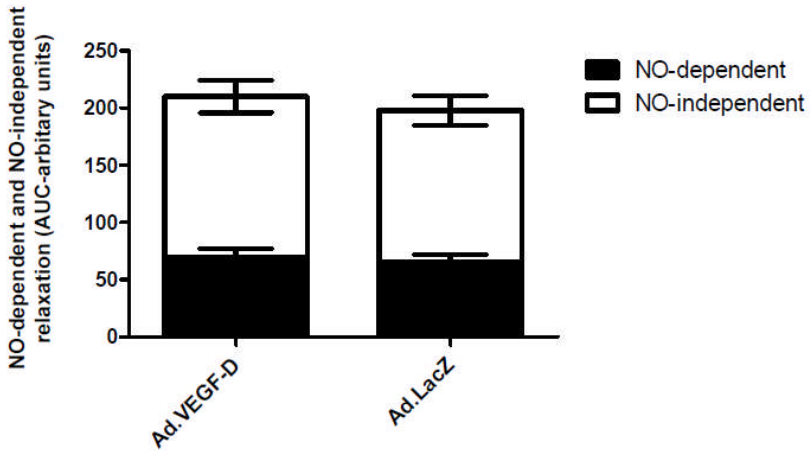

Figure 3.50(b) - Partial contribution of NO-dependent and NO-independent mechanisms to the endothelial-dependent relaxation

Values are the mean±SEM for the area under the curve (AUC) for BK-induced relaxation (complete bar with positive SEM), the AUC for BK-induced relaxation following treatment with L-NAME (NO-independent component, white bar), and the remaining AUC after BK with L-NAME (NO-dependent component, black bar). No significant differences were observed in the overall relaxation as well as NO-dependent and NO-independent relaxations between the treated and control sides.

Table 3.23 - E_{max} in response to bradykinin in uterine arteries from pregnant sheep transduced long-term with Ad.VEGF-D and Ad.LacZ contra-laterally, in the presence of different inhibitors of endothelium-dependent relaxation.

At mid-gestation, one uterine artery was injected with Ad.VEGF-D and the contra-lateral uterine artery was injected with Ad.LacZ in pregnant sheep. The second and third branches of the main uterine artery were harvested 30-45 days after injection and analysed on an 8-chambered organ bath system. Concentration response curves to BK were constructed for each vessel in the absence and presence of different inhibitors of relaxation, namely, L-NAME, NS-398 and Apamin. The relaxation of the vessel is expressed as a percentage of inhibition of PE-induced contraction. The p value indicates the significance of the effect of individual inhibitors on the dose response curve.

Inhibitor	E_{max} % (Mean±SEM)		p value
	Ad.VEGF-A_{165} transduced side	Ad.LacZ trandsduced side	
No inhibitor	48.39±2.66	43.92±2.99	
L-NAME	37.13±4.30	32.38±4.08	p=0.05
L-NAME + NS-398	33.74±5.76	28.73±4.25	p=0.48
L-NAME + NS-398 + Apamin	10.47±1.84	9.52±2.33	p<0.05

In summary, these results show that local over-expression of VEGF-D in the uterine arteries of pregnant sheep at mid-gestation results in a significant reduction in vascular contractility long-term, but no significant difference in relaxation compared to Ad.LacZ transduced vessels. The vascular relaxation response to bradykinin is primarily mediated by NO and EDHF in both the Ad.VEGF-D and Ad.LacZ infected uterine arteries. There is no significant difference between the small amount of residual relaxation in the presence of NOS, PGI_2 and EDHF inhibitors, between the Ad.VEGF-D and Ad.LacZ transduced vessels.

3.26 Local over-expression of VEGF-D in the uterine arteries of pregnant sheep upregulates eNOS levels short-term but not long-term

Protein extracts of uterine artery samples from short-term studies (4-7 days after vector injection) and long-term studies (30-45 days after vector injection) were analysed for changes in eNOS levels by western blotting. I observed an upregulation in the levels of eNOS in Ad.VEGF-D transduced uterine arteries compared to Ad.LacZ transduced uterine arteries short-term (Figure 3.51 A). However, this difference was not sustained long-term. There was no difference in eNOS levels between the Ad.VEGF-D and Ad.LacZ transduced uterine arteries obtained from term pregnant sheep (Figure 3.51 B)

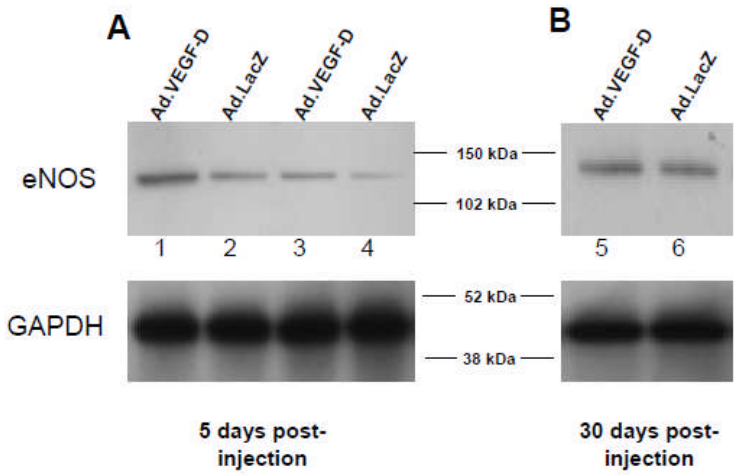

Figure 3.51 - Representative western blot showing upregulation of eNOS in Ad.VEGF-D transduced uterine arteries compared to Ad.LacZ transduced uterine arteries (A) 5 days after vector administration but not (B) 30 days after vector administration

Uterine arteries from pregnant sheep were injected with Ad.VEGF-D and Ad.LacZ contra-laterally at mid-gestation, and harvested either (A) 5 days post-injection; or (B) 30 days post-injection. Protein extracts from the uterine artery tissue samples were analysed by western blotting using a mouse monoclonal antibody to eNOS. Results are representative of n=3 independent experiments each for the short-term and long-term time points. GAPDH was used as a loading control. There was an upregulation in eNOS 5 days after gene transfer in the Ad.VEGF-D transduced vessels compared to Ad.LacZ transduced vessels (the protein extracts run in lanes 1 and 2 are from the contra-lateral uterine arteries of one sheep, similarly for lanes 3 and 4; and lanes 5 and 6).

This result is similar to what was observed in the Ad.VEGF-A_{165} transduced ewes.

3.27 Ad.VEGF-D transduction of uterine arteries in the pregnant sheep results in changes in endothelial cell proliferation and adventitial neovascularization

On examination of H&E stained uterine artery sections from short-term transduced animals, we observed a dramatic proliferation of cells in the perivascular adventitia (Figure 3.52). We speculated that these may be endothelial cells which had been stimulated to proliferate by VEGF-D, a known mitogen. In order to confirm this, we carried out immunohistochemistry with two antibodies

on the same section – (i) anti-BrdU, a cell proliferation marker and (ii) anti-vWF, an endothelium marker.

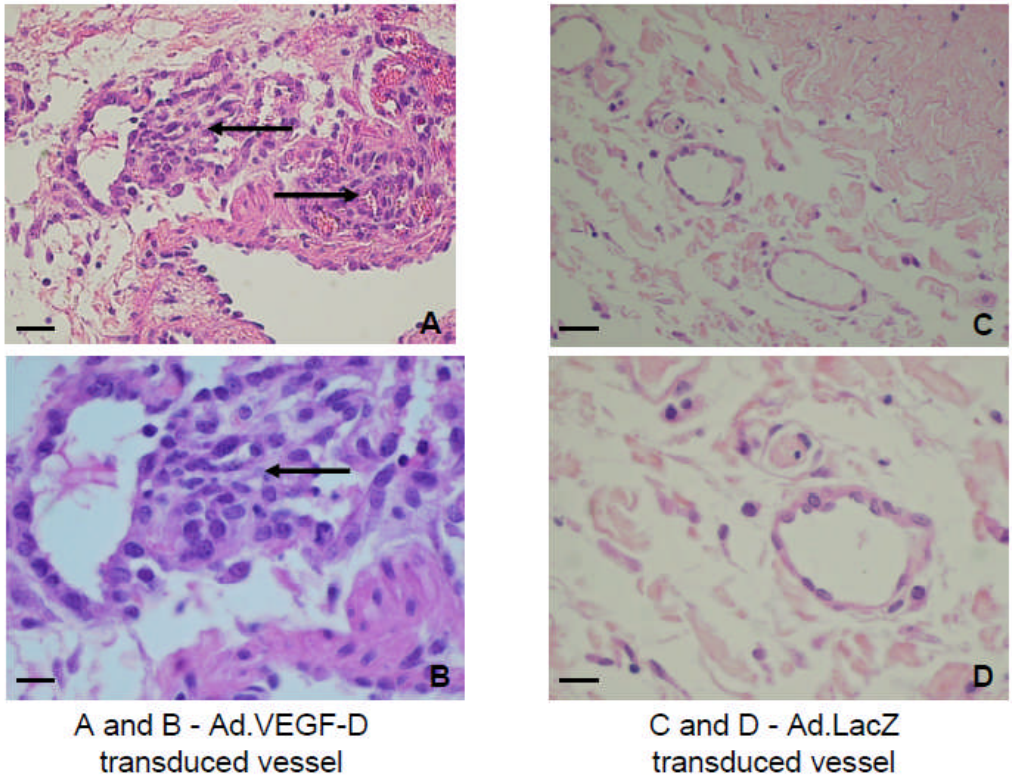

Figure 3.52 – Endothelial cell proliferation in the perivascular adventitia of uterine arteries transduced with Ad.VEGF-D, 5 days after gene transfer.

Maternal uterine artery samples collected at post-mortem examination (5 days after vector injection) were analyzed for routine histology. Tissues were fixed in 4% paraformaldehyde overnight, transferred to 70% ethanol and processed into paraffin. Sections were stained with hematoxylin and eosin for morphological assessment. Sections from uterine arteries injected with Ad.VEGF-D showed distinct nodules of proliferating endothelial cells (A and B), pointed at by arrows. These were not observed in sections from Ad.LacZ injected uterine arteries (C and D). Scale bar = 40 µm (A and C); 20 µm (B and D).

The protocol for anti-BrdU immunohistochemistry was adapted from David AL, Ph D Thesis, 2005 while the protocol for anti-vWF staining had previously been optimized in our lab. Both these protocols were combined together into a double immunofluorescent staining protocol, as described by (Hristova M et al., 2010).

3.27.1 Local over-expression of VEGF-D in the uterine arteries of pregnant sheep short-term increases the number of proliferating endothelial cells but does not significantly increase the number of adventitial blood vessels.

Uterine arteries from 4 singleton pregnant animals which had received a BrdU infusion 48 hours before post-mortem (Table 3.13) were used for immunohistochemical analysis of endothelial cell proliferation. The double-stained slides were observed under a fluorescent microscope and the number of proliferating endothelial cells (anti-BrdU positive and anti-vWF positive) was counted in 10 randomly selected high powered fields in all branches of the uterine arteries. As the sections had been stained with anti-vWF, we were also able to count the number of adventitial blood vessels in order to assess neovascularization (Figure 3.53). The counting was done by two observers who were blinded to the vector injected into the uterine artery. The inter-observer and intra-observer variability were 6.0% and 4.8% respectively.

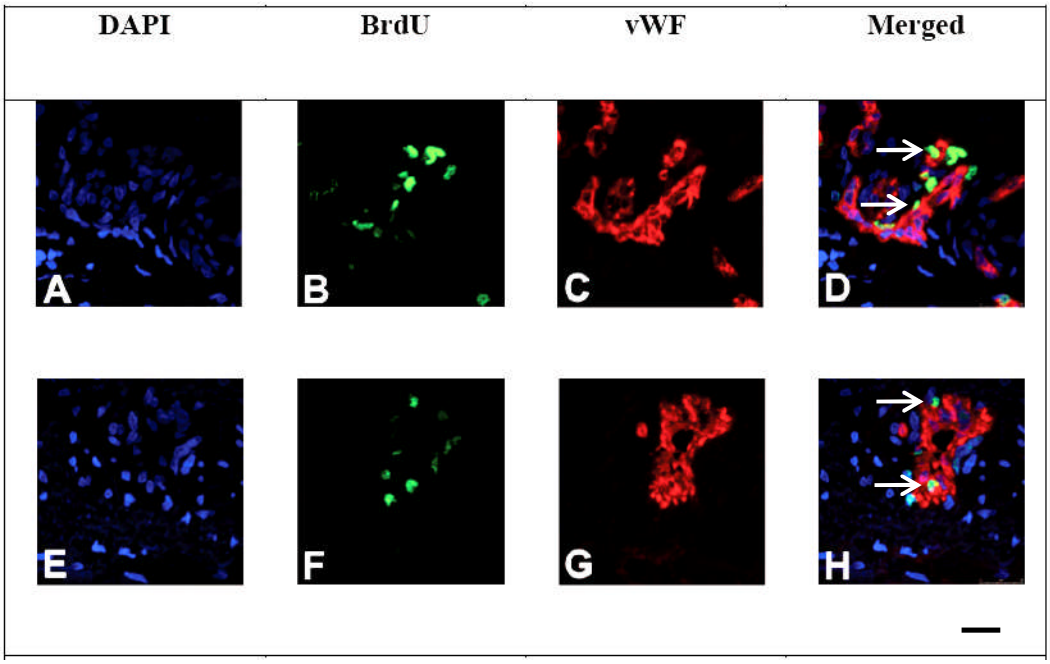

Figure 3.53 – Representative images of proliferating endothelial cells in the perivascular adventitia of uterine arteries injected with Ad.VEGF-D, 5 days after gene transfer.

(Continued from overleaf) Maternal uterine artery samples collected at post-mortem examination were analyzed by double labeling using anti-vWF and anti-BrdU fluorescent immunohistochemistry. Tissues were fixed in 4% paraformaldehyde overnight, transferred to 70% ethanol and processed into paraffin. Sections were stained with primary rabbit anti-human vWF and monoclonal mouse anti-BrdU antibodies, using the avidin-biotin-peroxidase system; Texas Red (red) and Alexafluor-488 (green) were used for visualization of the sites of antibody binding respectively. The sections were observed under a confocal microscope using excitation lasers of the appropriate wavelength. A and E represent the nuclei (blue) stained with DAPI, B and F represent proliferating nuclei that have been stained positively with anti-BrdU, C and G represent clusters of endothelial cells stained positively with anti-vWF. D and H are obtained by merging images of all three stainings A green nucleus surrounded by red cytoplasm represents a proliferating endothelial cell (white arrows). The number of proliferating endothelial cells was found to be significantly greater in Ad.VEGF-D transduced vessels compared to Ad.LacZ transduced ones. Scale bar = 40μm.

We observed a significant increase in the number of proliferating endothelial cells in Ad.VEGF-D transduced vessels compared to Ad.LacZ transduced vessels and untransduced vessels from control sheep (used for endothelial cell studies) at the same gestational age ($p=0.013$, $n=4$, Two-way ANOVA). The ANOVA showed that the vector type had a significant effect on the number of proliferating endothelial cells but pregnancy status (gravid or non-gravid uterine horn) did not ($p=0.563$). There was no significant difference in the number of adventitial blood vessels ($p=0.301$, $n=4$, Two-way ANOVA) between the Ad.VEGF-D transduced vessels and Ad.LacZ transduced vessels. The mean number of proliferating endothelial cells and adventitial blood vessels in the Ad.VEGF-D/Ad.LacZ transduced uterine arteries and untransduced vessels is summarized in Table 3.24.

Table 3.24 – Mean number of proliferating endothelial cells and adventitial blood vessels in the uterine arteries of pregnant sheep transduced with Ad.VEGF-D or Ad.LacZ (4-7 days after gene transfer) and uninjected sheep.

Treatment administered	Mean no. of proliferating endothelial cells (±SEM)	Mean no. of adventitial blood vessels (±SEM)
Ad.VEGF-D	22.83±6.03*	55.10±6.82
Ad.LacZ	9.16±2.68	50.41±5.51
No treatment	7.75±1.89	47.68±5.40

* indicates $p<0.05$

Overall, this data demonstrates that over-expression of VEGF-D in the uterine arteries of pregnant sheep at mid-gestation leads to a significant increase in the number of proliferating endothelial cells in the perivascular adventitia 4-7 days after injection, though there is no significant effect on adventitial vessel number.

3.27.2 Local over-expression of VEGF-D in the uterine arteries of pregnant sheep long-term increases the number of adventitial blood vessels but does not significantly increase the number of proliferating endothelial cells.

The pregnant sheep used to study the long-term effects of VEGF-D over-expression (n=5) were also administered an intravenous BrdU infusion 48 hours before post-mortem examination. In one animal (UA38) which was pregnant with twins, part of the uterine artery adventitia was lost during histology processing and sections from this animal were therefore not used for vessel enumeration or cell proliferation studies. We only used tissues from the other 4 singleton animals (UA39, UA42, UA43 and UA45) for this study.

The double immunofluorescent stained sections (with anti-BrdU and anti-vWF) were observed under a fluorescent microscope as before. Proliferating endothelial cells and adventitial blood vessels were counted blinded in 10 randomly selected high-powered fields (Figure 3.54-3.56).

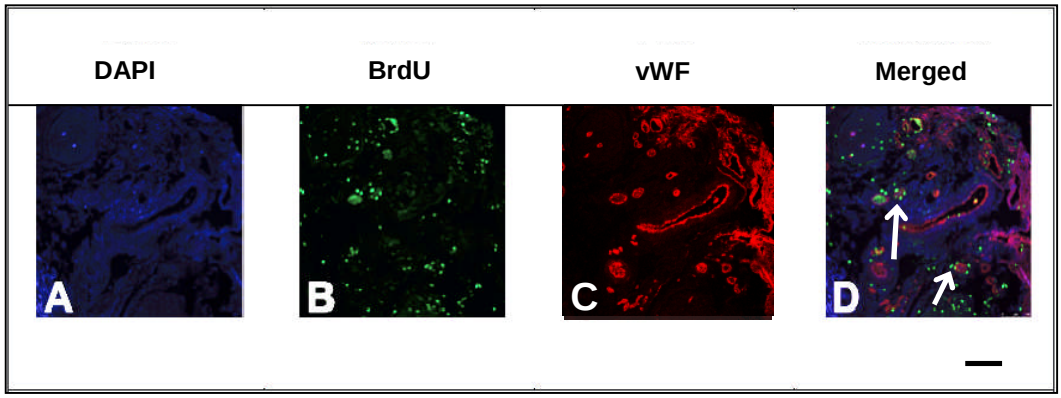

Figure 3.54 – Representative images of proliferating endothelial cells and adventitial blood vessels in the perivascular adventitia of uterine arteries injected with Ad.VEGF-D, 30 days after gene transfer.

Maternal uterine artery samples collected at post-mortem examination were analyzed by double labeling using anti-vWF and anti-BrdU fluorescent immunohistochemistry. Tissues were fixed in 4% paraformaldehyde overnight, transferred to 70% ethanol and processed into paraffin. Sections were stained with primary rabbit anti-human vWF and monoclonal mouse anti-BrdU antibodies, using the avidin-biotin-peroxidase system; Texas Red (red) and Alexafluor-488 (green) were used for visualization of the sites of antibody binding respectively. The sections were observed under a confocal microscope using excitation lasers of the appropriate wavelength. A represents the nuclei (blue) stained with DAPI, B represents proliferating nuclei that have been stained positively with anti-BrdU, C represents adventitial blood vessels stained positively with anti-vWF. D has been obtained by merging images of all three stainings A green nucleus surrounded by red cytoplasm (pointed at by white arrows) represents a proliferating endothelial cell. The number of adventitial blood vessels was found to be significantly greater in Ad.VEGF-D transduced vessels compared to Ad.LacZ transduced ones. Scale bar = 100µm.

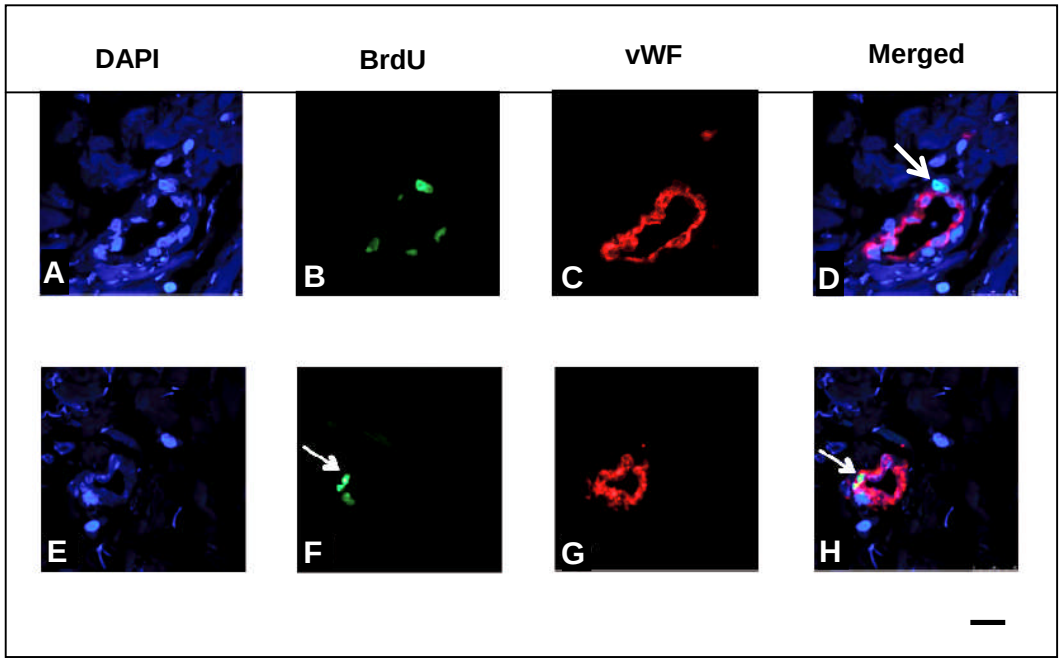

Figure 3.55 – Representative images of proliferating endothelial cells and adventitial blood vessels in the perivascular adventitia of uterine arteries injected with Ad.VEGF-D, 30 days after gene transfer (high power).

Maternal uterine artery samples collected at post-mortem examination were analyzed by double labeling using anti-vWF and anti-BrdU fluorescent immunohistochemistry. Tissues were fixed in 4% paraformaldehyde overnight, transferred to 70% ethanol and processed into paraffin. Sections were stained with primary rabbit anti-human vWF and monoclonal mouse anti-BrdU antibodies, using the avidin-biotin-peroxidase system; Texas Red (red) and Alexafluor-488 (green) were used for visualization of the sites of antibody binding respectively. The sections were observed under a confocal microscope using excitation lasers of the appropriate wavelength. A and E represent the nuclei (blue) stained with DAPI, B and F represent proliferating nuclei that have been stained positively with anti-BrdU, C and G represent adventitial blood vessels stained positively with anti-vWF. D and H have been obtained by merging images of all three stainings A green nucleus surrounded by red cytoplasm (pointed at by white arrows) represents a proliferating endothelial cell. The number of adventitial blood vessels was found to be significantly greater in Ad.VEGF-D transduced vessels compared to Ad.LacZ transduced ones. Scale bar = 40μm.

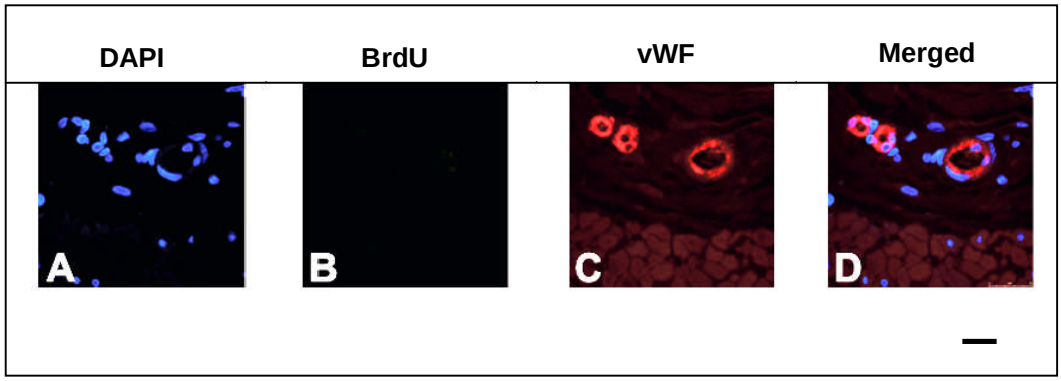

Figure 3.56 – Representative images of adventitial blood vessels in the perivascular adventitia of uterine arteries injected with Ad.LacZ, 30 days after gene transfer.

Maternal uterine artery samples collected at post-mortem examination were analyzed by double labeling using anti-vWF and anti-BrdU fluorescent immunohistochemistry. Tissues were fixed in 4% paraformaldehyde overnight, transferred to 70% ethanol and processed into paraffin. Sections were stained with primary rabbit anti-human vWF and monoclonal mouse anti-BrdU antibodies, using the avidin-biotin-peroxidase system; Texas Red (red) and Alexafluor-488 (green) were used for visualization of the sites of antibody binding respectively. The sections were observed under a confocal microscope using excitation lasers of the appropriate wavelength. A represents the nuclei (blue) stained with DAPI, B represents proliferating nuclei that have been stained positively with anti-BrdU, C represents adventitial blood vessels stained positively with anti-vWF. D has been obtained by merging images of all three stainings. Note the absence of any proliferating nuclei in panel B in Ad.LacZ transduced vessels. Scale bar = 40µm.

We observed an increase in the number of proliferating endothelial cells in the Ad.VEGF-D transduced vessels compared to Ad.LacZ transduced and uninfected vessels, though this increase was not significant. ($p=0.159$, $n=4$, Two-way ANOVA). However, the number of adventitial blood vessels was significantly greater in the Ad.VEGF-D transduced vessels compared to Ad.LacZ transduced and uninjected vessels ($p=0.043$, $n=4$, Two-way ANOVA). The ANOVA showed that the vector type played a significant effect on the number of adventitial blood vessels but whether the uterine artery was supplying a gravid or non-gravid uterine horn did not ($p=0.436$). The mean number of proliferating endothelial cells and adventitial blood vessels in the Ad.VEGF-D/Ad.LacZ transduced uterine arteries and untransduced vessels is summarized in Table 3.25.

Table 3.25 – Mean number of proliferating endothelial cells and adventitial blood vessels in the uterine arteries of pregnant sheep transduced with Ad.VEGF-D or Ad.LacZ (30-45 days after gene transfer) and untransduced vessels.

Treatment administered	Mean no. of proliferating endothelial cells (±SEM)	Mean no. of adventitial blood vessels (±SEM)
Ad.VEGF-D	23.47±6.16	77.91±6.76*
Ad.LacZ	15.5±4.37	58.06±5.78
No treatment	7.8±3.74	54.33±7.26

* indicates $p<0.05$

In summary, this data demonstrates that in uterine arteries transduced long-term with Ad.VEGF-D, there is a significant increase in the number of adventitial blood vessels, but the number of proliferating endothelial cells is not significantly different compared to controls.

3.28 Local administration of Ad.VEGF-D to the uterine arteries of pregnant sheep leads to increased levels of VEGF-D protein expression short-term

Protein extracts of uterine arteries, uterus and placentomes from 2 short-term transduced, 2 long-term transduced and one control uninjected sheep were used to detect levels of VEGF-D protein by ELISA. An ELISA to detect VEGF-A_{165} protein in tissues from sheep which had been injected with Ad.VEGF-A_{165} has previously been optimized in our lab. We used the same protocol for the VEGF-D ELISA, keeping all buffers (for protein extraction and plate washes) the same.

To estimate the VEGF-D and total protein concentrations in the samples, calibration curves to rhVEGF-D and bovine serum albumin (BSA) were constructed respectively. These were unique to each assay, so a calibration was performed for each experiment. Using these standard curves and optical density measurements of the protein extracts, the concentration of the unknown sample

could be determined using the 'Linear Regression' and 'Interpolate Unknowns from Standard' feature in GraphPad Prism 5.0.

The values obtained for protein concentrations were used to calculate equal amounts of protein to add to each well of the ELISA plate (0.3 μg in 200 μl buffer). Each protein extract needed to be appropriately diluted to achieve this. The ELISA protocol was followed as per manufacturer's instructions.

Table 3.26 summarizes the VEGF-D protein levels in each sample from the short-term transduced sheep as determined by ELISA.

Table 3.26 – Amount of VEGF-D protein detected by ELISA in uterine artery, uterus and placentome samples 4-7 days after injection of Ad.VEGF-D or Ad.LacZ vectors

Sample	VEGF-D protein concentration (pg/ml)
UA 34 left uterine artery (main)	-
UA34 left uterine artery (1st branch)	-
UA34 left uterine artery (2nd branch)	-
UA34 left uterine artery (3rd branch)	-
UA34 left uterus sample	-
UA34 left placentome sample	-
UA34 right uterine artery (main)	-
UA34 right uterine artery (1st branch)	*335.58*
UA34 right uterine artery (2nd branch)	*429.61*
UA34 right uterine artery (3rd branch)	*228.46*
UA34 right uterus sample	*358.16*
UA34 right placentome sample	-
UA 36 left uterine artery (main)	*632.96*
UA36 left uterine artery (1st branch)	*577.53*
UA36 left uterine artery (2nd branch)	-
UA36 left uterine artery (3rd branch)	*269.76*
UA36 left uterus sample	-

UA36 left placentome sample	-
UA36 right uterine artery (main)	-
UA36 right uterine artery (1st branch)	-
UA36 right uterine artery (2nd branch)	-
UA36 right uterine artery (3rd branch)	-
UA36 right uterus sample	-
UA36 right placentome sample	-

Samples in *italics* are from the side injected with Ad.VEGF-D. '-' indicates a negative result.

Even though not all the expected branches had detectable levels of protein in this assay, it shows that there was no VEGF-D protein detected in the uterine artery branches contra-lateral to the side that had been injected with Ad.VEGF-D. VEGF-D could also not be detected in maternal or fetal blood samples obtained at vector injection and post-mortem (in short-term experiments).

For long-term transduced ewes and sham controls, human VEGF-D was not detectable by ELISA in any uterine artery, uterine wall, or placentome sample. Similarly, blood samples obtained from the ewes before vector injection as well as samples obtained from the ewes and fetuses at post-mortem examination did not show any detectable human VEGF-D expression using ELISA.

In summary, VEGF-D protein was detectable by ELISA only in the Ad.VEGF-D injected uterine arteries of the short-term transduced sheep. It was not detectable in the Ad.LacZ injected uterine arteries. Likewise, it could also not be detected in any sample from the long-term transduced or uninjected ewes.

3.29 Local administration of Ad.VEGF-D to the uterine arteries of pregnant sheep results in upregulation of VEGFR-2 short-term

Uterine artery sections obtained from experimental animals injected with Ad.VEGF-D/Ad.LacZ contra-laterally (both at the short-term and long-term time points) were stained immunohistochemically for VEGFR-1, VEGFR-2 and Neuropilin-1. The stained slides showed the presence of VEGFR-1, VEGFR-2 and Neuropilin-1 in the intimal and adventitial endothelia (lining small blood vessels). Similar to our findings in the Ad.VEGF-A_{165} transduced sheep, I observed an upregulation of VEGFR-2 in the uterine arteries transduced with Ad.VEGF-D compared to Ad.LacZ, 4-7 days after injection (Figure 3.57). There was no detectable difference in the level of any of the receptors at 1 month post-injection between the Ad.VEGF-D and Ad.LacZ transduced vessels (data not shown).

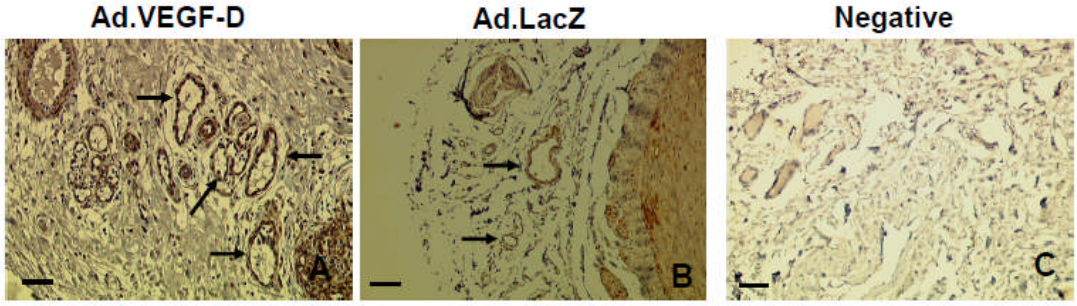

Figure 3.57 - Representative images of short-term Ad.VEGF-D/Ad.LacZ transduced sheep uterine artery sections stained with an antibody to VEGFR-2.

Maternal uterine artery samples from sheep injected with Ad.VEGF-D/Ad.LacZ at mid-gestation were collected at post-mortem examination 4-7 days later. Tissues were fixed in 4% paraformaldehyde overnight, transferred to 70% ethanol and processed into paraffin. Sections were stained immunohistochemically with an antibody to VEGFR-2 at a concentration of 1:50, using the avidin-biotin-peroxidase system; 3,3`-diaminobenzidine and a light haematoxylin counter-stain were used as substrates for visualization. (C) is a negative control obtained by omitting the primary antibody. Positive staining was observed around small blood vessels in the perivascular adventitia of the uterine artery. We noted an upregulation of VEGFR-2 in the Ad.VEGF-D transduced uterine artery segments compared to Ad.LacZ transduced ones. Scale bar = 40 μm.

3.30 Microscopic examination of tissues from Ad.VEGF-D transduced sheep does not reveal any significant pathology.

Maternal and fetal tissues collected at post-mortem examination (complete list of samples in post-mortem sheet in Appendix) from Ad.VEGF-D transduced sheep (n=3 short-term experiments and 3 long-term experiments) were stained with H&E and observed microscopically under the supervision of Dr. Elizabeth Benjamin.

The uterine arteries from all three short-term transduced sheep showed a dramatic proliferation of cells in the perivascular adventitia of the Ad.VEGF-D transduced segments relative to Ad.LacZ transduced segments (Figure 3.52). We performed further staining with anti-BrdU and anti-vWF antibodies to confirm the identity of these cells (Section 3.27), and found most of them to be proliferating endothelial cells.

There were no inflammatory responses observed in the uterine arteries from the short-term or long-term transduced sheep. Two sections of the maternal heart from the short-term transduced sheep and one from the long-term transduced sheep showed evidence of low-grade myocarditis, but this was believed to be unrelated to the administration of the vector.

All other maternal and fetal tissues examined, including the liver had an unremarkable histology.

3.31 Local administration of Ad.VEGF-D to the uterine arteries of pregnant sheep does not lead to any pathological haematological and biochemical changes.

Blood and serum samples were taken from experimental sheep (n=3) at three different time points – vector injection, 1 week post-injection and post-mortem. Fetal samples could only be collected at post-mortem. The samples were

sent to the Clinical Diagnostics Lab, RVC Hawkshead for routine haematological and biochemical analysis.

All maternal and fetal haematological and biochemical values examined were within the normal range.

3.32 Analysis of maternal and fetal liver function tests after Ad.VEGF-D injection does not indicate any liver pathology

The serum levels of liver enzymes were analysed to assess for functional hepatocellular injury in 3 short-term transduced and 3 long-term transduced animals. Maternal samples were collected from the former group before vector injection and at post-mortem, while for the latter group, an additional time point – 1 week post injection was included. Fetal samples could only be obtained at post-mortem.

The levels of maternal AST and GLDH were within the normal range in all samples examined. Levels of fetal AST were below normal in one short-term sheep UA19 (15 U/l; normal range 48-156 U/l) and both the fetuses of one long-term twin pregnant sheep UA38 (14 U/l and 18 U/l). Abnormal levels of AST are only a general indicator of hepatocellular injury in ruminants, with GLDH being the most reliable indicator.

The levels of fetal GLDH were elevated in 2 short-term and 2 long-term sheep. This is summarized in Table 3.27:-

Table 3.27 – Levels of glutamate dehydrogenase (GLDH) in sheep fetuses at post-mortem examination, after administration of Ad.VEGF-D to the maternal uterine arteries.

Sheep Number	Duration of experiment	Number of fetuses	GLDH levels	
			1st fetus	2nd fetus
UA17	Short-term	Twin	17.0 U/l	25.0 U/l
UA19	Short-term	Singleton	24.0 U/l	-
UA38	Long-term	Twin	36.0 U/l	31.0 U/l
UA45	Long-term	Singleton	31.0 U/l	-

Short-term experiment = 4-7 days after gene transfer; long-term experiment = 30-45 days after gene transfer; values indicated in red are above the normal range (<20U/l)

The normal range for GLDH in adult sheep is < 20 U/l. The GLDH levels for fetal sheep are not very well known. In our study, fetal GLDH levels from ewes which had only been injected with PBS were in the range of 39.0 – 54.0 U/l, thus suggesting that the normal adult range cannot always be applied to fetal sheep.

Bilirubin was not raised in any of the serum samples analysed. The levels of alanine aminotransferase (ALT) were normal in all samples examined.

Overall, these results suggest that administration of Ad.VEGF-D to the uterine arteries of pregnant ewes does not cause any clinically important changes in the levels of maternal and fetal liver enzymes.

To conclude, the data presented in this section suggest that over-expression of VEGF-D affects UABF, uterine artery vascular reactivity, eNOS levels and adventitial neovascularization in a similar way to VEGF-A_{165}.

Discussion

The effects of local adenovirus-mediated over-expression of two members of the VEGF gene family – VEGF-A_{165} and VEGF-D on the utero-placental circulation of pregnant sheep have been explored in this chapter. The effects of Ad.VEGF-A_{165} were only examined long term, at least 30 days after transduction since data on the short term effect, 4 – 7 days after transduction, has been previously published by our group (David AL et al., 2008). The effects of Ad.VEGF-D have been studied both short-term and long-term.

3.33 Adenovirus-mediated over-expression of vegf in uterine arteries results in a local upregulation of transgenic vegf gene and protein short-term; however, in long-term transduced vessels, only an upregulation of vegf mRNA level is detectable.

In this thesis, VEGF (-A_{165} and -D) expression in maternal and fetal samples was evaluated using a variety of techniques; at the mRNA level by RT-PCR and at the protein level by ELISA and immunohistochemistry. Overall, it was demonstrated that in short-term transduced vessels, VEGF expression was upregulated at the protein level (both by ELISA and immunohistochemistry) and at the transcriptional level (by RT-PCR) (David AL et al., 2008). In contrast, in long-term transduced vessels, *vegf* upregulation was detectable only at the transcriptional level, but not at the protein level.

Using ELISA for analysis of uterine artery, uterus and placentomes from the short-term transduced animals, rhVEGF-D was primarily detected in the uterine arteries that had been injected with Ad.VEGF-D. The contra-lateral uterine artery (which had received Ad.LacZ) and all other samples were negative. These findings are similar to the ELISA analysis of tissues from the short-term transduced animals that were administered Ad.VEGF-A_{165} (David AL et al., 2008)

in two important ways – (i) short-term expression of VEGF-D was restricted to the uterine artery that had been injected with Ad.VEGF-D and (ii) there was no expression of VEGF-D in the contra-lateral uterine artery (that had been injected with Ad.LacZ). ELISA was unable to detect any VEGF-D (or VEGF-A_{165}) in the long-term transduced uterine arteries.

Immunohistochemical analysis for VEGF-A_{165} in the uterine arteries showed specific staining of VEGF around the adventitial blood vessels on both the Ad.VEGF-A_{165} and Ad.LacZ treated sides, though there was no difference in the level of expression quantitatively between both the sides in long-term transduced vessels. In our previously published short-term experiments, we noted increased expression levels of VEGF in the adventitia of Ad.VEGF-A_{165} transduced uterine artery segments (David AL et al., 2008). A limitation of both VEGF immunohistochemistry and ELISA is that the antibody is not able to discriminate between endogenous and transgenic VEGF. I speculate that the positive staining was due to endogenous VEGF while the lack of any differential staining between both the sides was on account of low levels (or absence) of transgenic VEGF being expressed long-term

Vegf-A_{165} expression at the messenger RNA level was investigated in a number of maternal and fetal tissues by RT-PCR. The advantage of this technique over protein/antigen analysis is that the primers can be customized to span the vector-transgene boundary, thus enabling the amplification of only adenoviral expressed *vegf*. Using this method, the first round RT-PCR was negative in all maternal and fetal tissues sampled 30 days after gene transfer including the uterine arteries that had been transduced with Ad.VEGF-A_{165}. In order to make the technique more sensitive, second round PCR was performed using a semi-nested approach. This yielded a positive band only in the Ad.VEGF-A_{165} transduced vessels, but not in any other tissue. A similar result was obtained in short-term transduced vessels, sampled 4-5 days after gene transfer, wherein a positive band was only present in the Ad.VEGF-A_{165} transduced uterine arteries. However, an important difference is that a second-round amplification step was not required to detect transgene expression in the short-term samples, as the first

round was sensitive enough to detect adenoviral expressed *vegf*, suggesting higher levels of VEGF expression at the short term time point. This is to be expected, given the short term nature of expression mediated by adenovirus vectors.

It is of note that the technique of RT-PCR is based on the principle of reverse transcription of mRNA to cDNA, which then gets amplified in a PCR. This means that only actively transcribed genes can be detected by RT-PCR. During the toxicology studies conducted by Ark Therapeutics Ltd. for another adenoviral gene therapy candidate (Trinam), simple PCR detected the presence of viral DNA (and transgene) in the liver and spleen of pigs a few days after intra-vascular administration. However, RT-PCR was not able to detect any expression in these tissues. It was hypothesized that these viral particles were in a quiescent state, and may not have infected any cells so that they were not actively transcribing (Tim Farries, Ark Therapeutics Ltd., personal communication). This highlights the importance of conducting both PCR and RT-PCR to detect vector spread and vector expression respectively, in maternal and fetal tissues. Knowledge of global distribution of the vector is important for safety assessment, as even quiescent viral particles could mount a strong immune and inflammatory response. These PCR experiments are currently being performed in collaboration with Ark Therapeutics Ltd.

Notably, we were not able to detect any transgene expression in the maternal liver either short-term or long-term. Administration of viral vectors in rodents inevitably leads to strong transgenic expression in the liver, possibly because of the very high density of Coxsackievirus Adenovirus Receptors in this organ. I have observed this in guinea pig studies described elsewhere in this thesis. These varying results may be due to the different animal models being studied. Alternatively the injection technique used in combination with occlusion, may be restricting the virus primarily to the utero-placental vasculature.

In summary, I have shown that within the first week of vector injection, VEGF (-A_{165}/-D) levels are upregulated in the Ad.VEGF transduced uterine arteries as determined by ELISA and immunohistochemistry. However, there is no detectable difference in VEGF protein levels when analysed at more than a

month after injection. In the long-term transduced vessels, any differential expression of the transgenic *vegf* between Ad.VEGF-A_{165} and Ad.LacZ transduced segments is only detectable at the transcriptional level by semi-nested RT-PCR.

3.34 Adenovirus mediated over-expression of VEGF in the uterine arteries of pregnant sheep results in an upregulation of VEGFR-2 short-term, but this difference is not sustained long-term

Using immunohistochemistry and western blotting techniques, expression of the VEGF receptors VEGFR-1, VEGFR-2 and Neuropilin-1 was evaluated in Ad.VEGF-A_{165}/Ad.VEGF-D/Ad.LacZ transduced uterine arteries short-term and long-term. Immunohistochemistry showed presence of all three receptors in the endothelium of the uterine artery lumen and adventitial blood vessels, whether transduced with Ad.VEGF-A_{165}/Ad.VEGF-D/Ad.LacZ.

I observed an upregulation in the level of only VEGFR-2 in short term Ad.VEGF-A_{165} and Ad.VEGF-D transduced vessels (compared to Ad.LacZ transduced vessels). However, there were no detectable differences in the level of receptor expression (by immunohistochemistry) between the Ad.VEGF-A_{165}, Ad.VEGF-D and Ad.LacZ injected vessels long-term. The lack of any detectable difference after long term adenovirus mediated gene transfer is likely to be because the analysis was performed at a time-point when adenovirus-mediated VEGF expression had decreased.

Exogenous VEGF treatment has been shown to upregulate levels of VEGFR-1 mRNA in HUVECs from 1-24 hours after treatment (Barleon B et al., 1997a); and also levels of VEGFR-2 in cultures of mouse cerebral slices from 6-24 hours after treatment (Kremer C et al., 1997). Later time points were not analysed in these studies.

The fact that I observed an upregulation of VEGFR-2 levels in the short-term transduced vessels (coinciding with the peak of VEGF expression) is not surprising. The pattern of VEGFR-2 expression has been shown to resemble that

of VEGF expression very closely. Both are upregulated during developmental angiogenesis, downregulated in adult tissue and upregulated in adult pathological conditions like malignant tumours. It is therefore possible that a common mechanism may regulate the expression of VEGF and VEGFR-2 (Kremer C et al., 1997;Plate KH et al., 1993). Reduced VEGFR-2 expression is a characteristic of atherosclerotic arteries, and may be associated with the development of vasculopathies and their complications (Belgore F et al., 2004). It has also been demonstrated that there is a significant reduction in the maternal serum levels of soluble (s) VEGFR-2 in women whose pregnancies are complicated by FGR (Wallner W et al., 2007). As VEGFR-2 is primarily derived from the vascular endothelial cells, it is possible that the enhanced endothelial expression of VEGFR-2 observed in this study may be of benefit in an FGR situation.

I did not observe any change in the level of VEGFR-1 and Neuropilin-1 in the short-term or long-term transduced vessels. Although VEGFR-1 and VEGFR-2 have been reported in ovine uterine artery endothelial cells (Grummer MA et al., 2009), I am the first to document the presence of Neuropilin-1 in the ovine uterine artery.

It is important to note that VEGFR-1 functions primarily as a decoy receptor of VEGF, rendering it less available to VEGFR-2 to prevent excessive VEGF signaling. Neuropilin has no known signaling activity alone, but acts as a co-receptor that potentiates VEGF cell signaling through VEGFR-2. VEGFR-2 is believed to be the major signaling receptor for VEGF, mediating most of its biological activity. Its upregulation in the short-term transduced tissue provides evidence of enhanced VEGF signaling and a possible explanation for the changes in endothelial cell proliferation, vasodilatation, eNOS upregulation and UABF that were observed in this study.

Western blotting is likely to be a more informative and reliable technique than immunohistochemistry to detect any differences in the levels of the receptors quantitatively. However, our western blot analysis did not yield any conclusive results – either there were multiple bands and it was impossible to correctly identify the VEGFR band, or there was no band at all. Previously published work

has identified specific antibodies which cross-react with sheep VEGFR-1 and VEGFR-2 (Grummer MA et al., 2009), but all these studies were carried out on sheep endothelial cells rather than intact tissue. We tried these and a few other antibodies on protein extracts from intact uterine artery tissue, both short-term and long-term, but had no success.

In summary, I have shown the presence of all three receptors – VEGFR-1, VEGFR-2 and Neuropilin-1 in the uterine arteries of pregnant sheep by immunohistochemistry. VEGFR-2, but not VEGFR-1 or Neuropilin-1, is upregulated in the short-term transduced uterine arteries in response to VEGF-A_{165} and VEGF-D over-expression. However, there is no difference in the levels of either of the VEGF receptors in the long-term transduced uterine arteries.

3.35 Adenovirus mediated gene transfer of VEGF to the uterine arteries of mid-gestation pregnant sheep leads to long-term changes in uterine blood flow

In this study we showed a statistically significant increase in UABF apparent as early as 7 days after Ad.VEGF-A_{165} injection, and significantly different at 28 days post-injection at which point the mean maximum increase in UABF from baseline was 37% compared to 20% on the Ad.LacZ injected side. A similar trend was observed in the Ad.VEGF-D injected ewes, although significance was not demonstrated within the limited number of experimental animals.

This observation is similar to our previously published finding of a significant increase in utero-placental perfusion as measured by Doppler sonography, seen 4-7 days after delivery of Ad.VEGF-A_{165} into the uterine arteries of mid-gestation pregnant ewes. However, the importance of this new result as compared to the previously published short term data is that the increase in blood flow is maintained over at least 4 weeks, a critical finding that implies a possible therapeutic potential for our intervention. Importantly, the use of the ‘gold standard’ transit time flow probes, instead of Doppler ultrasonography

(David AL et al., 2008), provides a far more reliable and accurate estimate of the true increase in UABF (Abi-Nader KN et al., 2010), and thus, unequivocally confirms an effect for local over-expression of VEGF-A_{165} on UABF.

Perivascular transit-time technology, which uses piezoelectric transducers positioned around a vessel during surgery, is considered a highly accurate method for volume blood flow estimation and has been already evaluated in vitro (Lundell A et al., 1993) and in vivo (Sokol GM et al., 1996). On the contrary, estimation of uterine artery blood flow by colour Doppler is subjective and prone to large errors. Although Doppler readings correlate well with those obtained using transit-time flow probes in mid-gestation pregnant sheep (Acharya G et al., 2007), use of Doppler derived blood volume flow data is too inaccurate in this kind of study, where relatively minor differences in blood flow may be of significance.

For volume blood flow estimation, colour Doppler requires the use of pulsed-wave Doppler (an ultrasound imaging technique that can detect moving liquids). For accurate velocity measurements, it is essential that the pulsed-wave Doppler insonation angle should be as close to zero as possible because angles of insonation less than 30° will underestimate the maximal velocity (Palmer SK et al., 1992) by less than 15%, while large insonation angles can induce substantial errors in the measurement of maximal velocity (Dickerson KS et al., 1993). Factors that can limit the accuracy of pulsed-wave Doppler in estimating blood velocity also include nonlaminar flow, vessel shape, and estimation of mean velocity (Taylor KJ and Holland S, 1990). In the sheep the error in blood volume flow data changes as pregnancy advances. The uterine artery in mid-gestation pregnant sheep follows a relatively tortuous pathway (compared to late gestation) and corrections in the angle of insonation that are required for Doppler derived blood flow measurements, would not be adequate enough to accurately reflect the direction of blood flow.

There are also inaccuracies inherent in the pulsed-wave Doppler technique because these systems are designed to achieve high spatial resolution rather than uniformity of insonation. There is also overweighting of the higher velocity components at the center of the vessel, resulting in flow overestimation (Ho SS et

al., 2002). When measuring vessel diameter, the blooming effect is common to both color and power Doppler, which results in overwriting of the vessel walls in an attempt to maximize vessel filling. Errors in measuring vessel diameter have a large impact on the calculated uterine artery blood flow since the measurement is squared when calculating the vessel area $A = \pi(D/2)^2$. In the sheep, our group observed a larger relative error in vessel diameter estimation associated with the smaller vessel diameter at mid-gestation when compared to late gestation measurements (Abi-Nader KN et al., 2010).

Another important advancement in our method of uterine blood flow monitoring was the use of a telemetric set-up. While transit-time flow probes have been used previously to measure uterine blood flow in sheep (Wallace JM et al., 2008;Miller SL et al., 2009), they involved connecting the sheep by cables to an acquisition set-up. In order to do so, the sheep had to be restrained to a small pen or cart. Our telemetric set-up for uterine blood flow monitoring allows the pregnant ewe unrestricted movement in her pen. Thus, the animal is relatively unstressed during monitoring, which is an important cornerstone of the principle of 3Rs – Reduction, Refinement and Replacement, advocated by the UK Home Office for experimental work with animals (Robinson V, 2005).

Uterine blood flow is known to be highly variable between animals. To allow for this inter-animal variation, it is common practice to compare post-treatment uterine blood flow data with a pre-treatment baseline (Miller SL et al., 1999;Miller SL et al., 2009). In this study, baseline blood flow values were acquired for 3 days before vector injection. The post-injection uterine blood flow measurements were then compared with the pre-injection baseline to obtain a value for percentage change in blood flow from baseline. Thus, using an objective and reliable method of haemodynamic monitoring, we have shown a significant increase in uterine blood flow for at least 4 weeks following Ad.VEGF-A_{165} injection.

We have shown an increase in blood flow in both gravid and non-gravid uterine arteries, though the maximum increase was seen when Ad.VEGF-A_{165} was injected into the non-gravid uterine artery in singleton pregnancies. This might be

explained by the fact that non-gravid uterine arteries have undergone less vascular remodeling than gravid vessels in animals that have a bicornuate uterus, such as sheep and rodents (Osol G and Mandala M, 2009), which may make them more susceptible to the effects of VEGF over-expression. During normal pregnancy, the utero-placental vascular bed is significantly developed and the vascular channels are dilated to facilitate the maximal supply of substrates and oxygen to the developing fetus (Barry JS and Anthony RV, 2008). In cases of FGR or PET where utero-placental perfusion is impaired, it is possible that VEGF expression may provide an even greater enhancement of perfusion than is seen here.

The drop in UABF observed during the first few days after vector injection was limited to approximately 10% of the pre-injection baseline UABF, and may be due to the vessel occlusion during injection and subsequent trauma to the vessel itself. UABF recovered in all treated sheep by days 5-7 after vector injection. However, this is still a point of concern if our protocol is to be applied in the clinical setting, where growth restricted fetuses are frequently hypoxemic (Akalin-Sel T et al., 1994). In the last trimester of pregnancy, fetal PO_2 as determined by sampling blood from the umbilical vein under ultrasound guidance, has been found to be significantly lower in growth-restricted fetuses (median=2.70 kPa; range=1.71-3.51 kPa) than control fetuses (median=6.10 kPa; range 4.47 – 7.58 kPa) (Nicolini U et al., 1990). A minimally invasive technique such as trans-femoral uterine artery catheterization (Delotte J et al., 2009) would reduce uterine artery trauma and post-injection constriction, and has been used to inject the uterine arteries for embolization of fibroids in clinical practice. The procedure itself, and in particular the temporary occlusion of the lumen, could reduce the oxygen supply to the fetus, particularly if the other uterine artery supply was significantly compromised. Hypoxaemic FGR fetuses may have little reserve to tolerate further compromise of the uteroplacental circulation during the catheterisation procedure. This could result in immediate death of the fetus, or brain damage. On the other hand, they may be more tolerant of a temporary interruption to the uteroplacental circulation, since they are already tolerant to it. Data from sheep studies (Skillman CA et al., 1985) suggest that the uterus of the

pregnant sheep is perfused to sufficient excess to protect the fetus during short-term reductions of less that 50% UABF. In addition during the surgeries described in this thesis, the operators did not observe any deleterious effects on fetal blood pressure and heart rate following short-term occlusion of the uterine artery. Although there is a risk of profound fetal hypoxaemia or even death during the procedure, with pre-oxygenation of the mother, and sonographic fetal heart rate monitoring via the mother's abdomen this risk will be minimised. The alternative option, of not treating the fetus, carries a high risk of intra-uterine death; therefore the risk is considered acceptable. Further experiments to determine the optimal vector dose and whether extra-luminal administration of vector results in equally efficient gene delivery are required.

Some of the other therapeutic candidates being investigated with the aim of reversing FGR include sildenafil citrate, an inhibitor of type 5 phospho-diesterase (PDE5). This enzyme is responsible for the degradation of cGMP to guanosine monophosphate. Administration of sildenafil delays the breakdown of cGMP and increases vasodilatation. In myometrial arteries taken at Caesarean delivery from women whose pregnancies were complicated by FGR, sildenafil citrate reduced vasoconstriction and enhanced vasodilatation (Wareing M et al., 2005). This and other studies on utero-placental vascular reactivity in human pregnancy often employ myometrial arteries as a surrogate for investigations on uterine arteries (Ashworth JR et al., 1996;Robinson NJ et al., 2008), because of the extreme difficulty in obtaining the latter tissue. For instance, at University College London Hospital, a tertiary referral centre with a high throughput of deliveries (approximately 5500 per annum), there are not more than 1-2 cases of uterine artery removal in pregnant women in a year (David AL, personal communication). These primarily occur in cases of cervical cancer during pregnancy or of massive obstetric haemorrhage.

Miller *et al* examined the effects of intra-venous administration of sildenafil citrate on utero-placental circulation in normal pregnant and FGR pregnant sheep at 0.7 gestation (110-115 days). The FGR was induced by single umbilical artery ligation (SUAL) which is known to reduce uteroplacental

perfusion and produce fetal hypoxemia, acidemia and asymmetric growth restriction as observed in severe human FGR secondary to placental insufficiency. SUAL carried out at 105-110 days of gestation (0.7 gestation) reduces fetal body weight by about 20% compared with control animals (Miller SL et al., 2007). Contrary to expectation, sildenafil citrate infusion reduced uterine blood flow in all animals, whether normal or FGR, and this was associated with a significant deterioration in fetal well-being as evidenced by decreased fetal oxygenation, increased fetal CO_2 (as determined by analysis of fetal blood samples collected at specific time-points after infusion), hypotension and tachycardia (Miller SL et al., 2009). The unexpected poor outcome is hypothesized to result from the vasodilatory effect of the sildenafil citrate on the maternal vasculature systemically, which results in a "steal" of blood flow from the utero-placental circulation to the systemic vascular circuit. Even in normal pregnant sheep where there is no reduction in UABF and yet, infused sildenafil citrate had a detrimental effect on fetal growth and wellbeing. It is possible that this effect is likely to be exacerbated in a pregnancy where there is already reduced UABF.

In yet another pre-clinical study, it was demonstrated that site-specific placental gene transfer of Angiopoietin-2 using an adenoviral vector resulted in a significant increase in fetal weights in normal pregnant mice, compared to control untreated mice. $1x10^8$ pfu of the recombinant adenoviral vector was injected into the placentae of pregnant mice at E14, and the fetuses were harvested at day 17 of gestation (Katz AB et al., 2009). Vector spread and expression in this study was not evaluated by PCR or RT-PCR, and is an important parameter to consider for clinical translation of the therapy. Moreover, other transgenes evaluated in the same study (Ang-1, bFGF, hepatocyte growth factor, IGF-1, PlGF, PDGF-B and VEGF-A_{121}) had no effect on fetal weight.

Eremia SC *et al* demonstrated that intra-amniotic IGF supplementation improved growth rate in ovine fetuses with FGR caused by placental embolization (Eremia SC et al., 2007). The IGF-1 was administered as an intra-amniotic injection three times/week (dose of each injection = 120 µg). Treatment was commenced from day 100 of gestation, and post-mortem examination was

performed 28 days later. The IGF-1 treatment improved fetal weight at post-mortem examination to values intermediate between control (not growth-restricted) and saline-treated FGR fetuses. The liver weight, perirenal fat weight and carcass growth were also significantly improved.

Even though all these studies appear to hold great promise for the treatment of FGR, it is unlikely for them to be translated to the clinic. This is primarily because their delivery requires chronic catheterization of the amniotic cavity, which is likely to lead to infection and preterm birth with its inherent morbidity and mortality. Furthermore, it is important to note that in human pregnancy characterized by utero-placental insufficiency, fetal growth is retarded by both nutrient and oxygen deprivation. While growth factor treatment may enhance metabolism of nutrients, oxygen would still remain a limiting factor. The importance of oxygen for prenatal growth has been demonstrated by Dino Giussani in the chick model (Giussani DA et al., 2007). Hence, it is likely that a therapy that reverses the utero-placental insufficiency and requires only a single intervention rather than a chronically invasive procedure is likely to hold more potential for translation to the clinic. The finding that the increase in uterine blood flow was sustained through pregnancy in our studies is therefore of critical importance.

In our experiments, we noted a significant increase in singleton fetal weight compared to data from historical controls using the same sheep breed. Even though encouraging at first sight, the results could have been affected by other factors such as differences in fetal growth year by year for example. Further studies on the effects of Ad.VEGF-A_{165} gene therapy on fetal growth and birth weight in cohorts of sheep are currently ongoing. A single measure of fetal weight at post-mortem is a much less sensitive measure of fetal growth than repeated, direct and precise measures of growth rate. It is for this reason that we are measuring uterine blood flow, growth velocity (by serial weekly ultrasound scanning), birth weight, neonatal growth and development in an FGR sheep model, induced by maternal over-nourishment (Wallace JM et al., 2008). Preliminary data from these studies have indicated a significantly increased fetal

and neonatal growth velocity in FGR lambs whose mothers received uterine artery injection of Ad.VEGF-A_{165} bilaterally at mid-gestation compared with injection of Ad.LacZ vector (Carr D and David AL, personal communication).

Individuals born after growth restricted pregnancies have an increased predisposition to cardiovascular disorders and neurological damage. It is therefore important to design experiments to evaluate whether Ad.VEGF-A_{165} gene therapy is only limited to producing bigger individuals, or if it can also reverse the adverse developmental programming associated with FGR. This information would be best explored in a clinical trial, owing to the lack of availability of ideal animal models.

In summary, we have shown that adenovirus-mediated over-expression of VEGF-A_{165} in the uterine arteries of pregnant sheep leads to a sustained and significant increase in utero-placental perfusion for at least 4 weeks post-injection. This is associated with an improvement in fetal weight.

3.36 Local over-expression of VEGF in the uterine arteries of mid-gestation pregnant sheep leads to changes in vascular reactivity

Changes in uterine artery vascular reactivity were seen in response to VEGF over-expression both short-term and long-term. Vessels transduced with Ad.VEGF-D and examined 5-7 days later were significantly less contractile to phenylephrine and relaxed significantly more to bradykinin than control vessels transduced with Ad.LacZ vector. In previously published data (David AL et al., 2008), a similar effect was observed with Ad.VEGF-A_{165} at the short term time point after vector administration. However, vessels examined over 30 days later (long-term), irrespective of whether transduced with Ad.VEGF-A_{165} or Ad.VEGF-D, only showed a diminished contractile response, but no significant difference in relaxation response when compared to Ad.LacZ transduced vessels.

While the long-term effects of Ad.VEGF-A_{165} and Ad.VEGF-D on vascular contractility and relaxation were similar, VEGF-D appeared to have a more profound effect on relaxation in the short-term transduced vessels, as can be

noted in Table 3.18 and 3.19. The pD_2 in response to bradykinin between the Ad.VEGF-D and Ad.LacZ transduced sides differed by an order of magnitude.

VEGF stimulates endothelial cells to produce nitric oxide (Laitinen M et al., 1997;van der Zee R et al., 1997) and PGI_2 (Wheeler-Jones C et al., 1997) both of which molecules are involved in vascular relaxation. VEGF-D has also been shown to stimulate eNOS phosphorylation at Ser^{1177} (Jia H et al., 2004). Hence, the effects of VEGF over-expression described above are not unexpected. The lack of any detectable difference in the long-term relaxation response to bradykinin could be explained by the fact that at term, the utero-placental blood vessels are maximally dilated (Lumbers ER, 1997); hence, VEGF over-expression may be unable to further enhance the relaxation of uterine arteries. It is possible that over-expression of VEGF may enhance vasodilatation in term-pregnant vessels from an FGR pregnancy characterized by utero-placental vascular insufficiency, impaired vasodilatation and endothelial dysfunction, wherein there exists the potential of enhancing vascular relaxation responses.

When term pregnant vessels were contracted with phenylephrine in the presence of L-NAME, both Ad.VEGF-A_{165} and Ad.LacZ transduced vessels demonstrated an enhancement of contractile response. This increase in contractility was however significant only in the Ad.VEGF-A_{165} transduced vessels and not in the Ad.LacZ transduced vessels. I also observed that with NOS blockade, the E_{max} in the Ad.VEGF-A_{165} and Ad.LacZ transduced vessels was similar. This supports the concept that NO is a key mediator in the differential contractile response to phenylephrine between the Ad.VEGF-A_{165} and Ad.LacZ transduced vessels.

The vascular relaxation responses of the uterine arteries were also studied in the presence of different inhibitors of relaxation – L-NAME, Indomethacin/NS-398 and Apamin. I observed that L-NAME, and Apamin (in the presence of NS-398 and L-NAME), significantly attenuated the relaxation response, while PGI_2 inhibitors did not play any significant role. While previous studies have demonstrated that PGI_2 plays an important role in the relaxation of pregnant ovine uterine arteries compared to uterine arteries from non-pregnant ewes (Magness

RR and Rosenfeld CR, 1993;Magness RR et al., 1996), our experiments are different because we have only examined uterine arteries from pregnant ewes, that were transduced with adenovirus vectors. PGI_2 is a known to be an important vasodilator in several vascular beds, which include the utero-placental, pulmonary and cerebral circulations (reviewed by Moncada S and Vane JR, 1978). However, the results presented in this thesis suggest that in response to VEGF over-expression in pregnant ovine uterine arteries, the contributions of NO and EDHF towards vascular relaxation are more important than PGI_2.

When the vascular response of vessel segments was examined after pre-treatment with Apamin alone, there was no change in the relaxation response. Apamin is an inhibitor of small conductance Ca^{2+} activated K^+ channels and inhibits the actions of EDHF. While the identity of EDHF remains a topic of much debate, it is largely accepted that EDHF is a mediator of endothelium-dependent relaxation in the presence of NOS and COX inhibitors (Feletou M and Vanhoutte PM, 2009). It is proposed that the continuous generation of NO by endothelial cells counteracts the generation of EDHF and/or the mechanism of its action, and that EDHF acts as a backup endothelium-dependent vasodilator when NO production is compromised. Exogenously applied NO, at concentrations comparable to those achieved after endothelial stimulation with different agonists, attenuated EDHF-mediated relaxation responses in rabbit carotid and porcine coronary arteries. This inhibitory effect most likely resulted from an interference with the synthesis and/or release of EDHF rather than its mechanism of action (Bauersachs J et al., 1996). In concurrence with these studies in other vascular beds, our results too indicate that in the absence of NOS blockade, EDHF does not play any significant contribution to the endothelium dependent relaxation. The importance of EDHF-mediated relaxation in the utero-placental vascular bed was demonstrated by Kenny LC et al (2002). The relative contributions of NO, PGI_2 and EDHF were investigated in myometrial blood vessels from non-pregnant, pregnant and PET women, by using inhibitors of all three alone and in combination. The non-pregnant and PET vessels showed minimal residual relaxation in the presence of L-NAME, suggesting that NO is the prinicipal

mediator of endothelium dependent relaxation in these vessels. COX and EDHF inhibitors had no effect on relaxation. On the contrary, normal pregnant vessels were able to compensate and relax via either an NO or EDHF dependent mechanism. Hence, normal pregnancy is associated with the development of parallel EDHF and NO pathways in the myometrial bed, ensuring that if one of the pathways is malfunctional, there is a compensatory back-up mechanism in place. This 'back-up' system is lacking in PET pregnancy, with the endothelium-dependent relaxation solely being mediated via NO.

The residual relaxation that remained after cumulative inhibition with inhibitors of all three relaxation pathways was significantly greater in the vessels transduced short-term with Ad.VEGF-A_{165} or Ad.VEGF-D (compared to Ad.LacZ). However, in the long-term transduced vessels, there was no significant difference in the small amount of residual relaxation that remained after NOS, COX and EDHF inhibition between the Ad.VEGF and Ad.LacZ transduced sides. It is possible that VEGF over-expression is activating an as yet unknown pathway of relaxation short-term, and this effect is not sustained long-term when transgene expression is on the decline.

Previous studies investigating the effects of pregnancy on uterine artery vascular reactivity found that pregnancy brings about a reduction in contractility and increase in relaxation in ovine uterine arteries (Xiao D et al., 1999). These alterations are primarily NO-dependent. Quantitative western blotting showed that eNOS protein expression in term pregnant sheep UAECs (harvested at ~140 days gestational age) was increased to 197% of non-pregnant values.

An important strength of our study design is that uterine arteries were injected with Ad.VEGF and Ad.LacZ contra-laterally and their vascular reactivity was compared within the same animal. This controlled for inter-animal variation on account of factors such as maternal weight, age, parity, etc. As discussed above, transgenic *vegf* expression was only detectable in the uterine arteries that had been injected with Ad.VEGF, and never in the contra-lateral Ad.LacZ injected uterine arteries, thereby validating our findings. In singleton pregnancies, there was the obvious issue of one vessel supplying a gravid horn while the other

supplying a non-gravid horn. However, two-way ANOVA analysis allowed for this factor while determining the relative contribution of the different vectors used, on the vascular response.

The most commonly used agonist to study endothelium-dependent relaxation in vascular beds is acetylcholine (ACh). We used bradykinin for our experiments however, as stimulation with ACh had no relaxant effect on ovine uterine arteries. Other groups working on pregnant ovine uterine arteries obtained similar results, and it is believed that these vessels lack muscarinic receptors (Xiao D et al., 2001). In this respect, the sheep uterine artery differs from the human uterine artery, as the latter has been shown to relax in response to ACh stimulation (Jovanovic A et al., 1994).

Though sheep and human pregnancy are quite different from each other, the extent of increase in utero-placental perfusion, changes in uterine artery dimensions and vascular reactivity in pregnancy are similar in both species. During the latter half of gestation, uterine blood flow increases two and a half times in humans (from 0.3 to 0.8 L/min) while in sheep, this increase is three fold (0.4 to 1.2 L/min) (Konje JC et al., 2003;Meschia G, 1984). This is concomitant with an increase in the supply of substrates and oxygen to the conceptus, failure of which manifests as asymmetric FGR. The rates of oxygen and glucose consumption in both near-term sheep and human fetuses are also similar, and sheep are considered an ideal animal model for human reproductive physiology (Barry JS and Anthony RV, 2008). I therefore believe that the magnitude of the responses observed in ovine vessels would be reproducible and similar in the human clinical scenario as well.

No difference was observed in the vascular reactivity of the umbilical vessels between the Ad.VEGF and Ad.LacZ sides. The sheep placenta is epitheliochorial and there are 6 maternal-fetal layers which would need to be transgressed to reach the umbilical circulation from the maternal circulation, compared to only a single trophoblastic layer in late human gestation. I thus believe that the adenoviral vector or any VEGF protein released into the uterine circulation in sheep is unable to cross the placenta and influence the umbilical

circulation. In humans, the placenta has a high density of CAR that are capable of sequestering adenovirus. CAR was found to be continuously expressed in invasive cytotrophoblast (fetal side) but not in syncytiotrophoblast (outermost fetal component), thus rendering the syncytiotrophoblast resistant to adenoviral infection and limiting transplacental transmission (Koi H et al., 2001). Nevertheless, in human pregnancy, limited amounts of VEGF protein may reach the umbilical circulation and have therapeutic effects on umbilical vascular reactivity, which may be of potential benefit in FGR.

Previous studies have demonstrated that the human placenta is capable of synthesizing VEGF (Lash GE et al., 2002) and sVEGFR1 , which are released into both the maternal and fetal circulations. Using the *in vitro* dually perfused human placental lobule, it has been shown that the levels of VEGF and VEGFR1 secreted into the maternal circulation are greater than the fetal circulation. As VEGFR1 is a decoy receptor for VEGF, it sequesters most of its ligand in the uterine circulation, resulting in free VEGF being detectable only in the fetoplacental circulation, where it is a potent vasodilator of the umbilical vasculature (Brownbill P et al., 2007).

Using the same placental lobule perfusion model, it has been demonstrated that the placental release of sVEGFR-1 into the maternal and fetal circulations is significantly increased in pregnancies complicated by PET. This is concomitant with a significant decrease in the levels of free VEGF in the umbilical circulation, which probably contributes to a diminished vasodilatory response *in vivo* in this disease. It is of interest to note that exogenous VEGF induced vasorelaxation in the fetoplacental vasculature in perfused placental lobules from both normal and PET pregnancies, but the magnitude of relaxation was significantly greater in PET than in normal specimens. Furthermore, the recovery time from VEGF addition was significantly longer in PET pregnancies than in normal pregnancies (Brownbill P et al., 2008), thus proving that VEGF can induce vasodilatation and consequently enhance perfusion in the umbilical vasculature.

Myometrial arteries from women with pregnancies complicated by FGR are known to exhibit enhanced vasoconstriction and decreased endothelium-

dependent vasodilatation (Wareing M et al., 2005). I therefore believe that the alterations in uterine artery vascular reactivity brought about by VEGF over-expression, presented in this thesis, are likely to confer a beneficial effect in pregnancies complicated by FGR. These changes in vascular reactivity may also partly explain the increase in uterine blood flow that was demonstrated in this investigation.

3.37 Adenovirus mediated local over-expression of VEGF in the uterine arteries of mid-gestation pregnant sheep leads to elevated eNOS levels short-term but does not affect eNOS levels 30 days after transduction

Levels of eNOS were examined in protein extracts of uterine arteries from both short-term and long-term transduced animals by Western blotting. I observed an upregulation in the level of eNOS in Ad.VEGF (-A_{165} and -D) transduced vessels short-term compared to Ad.LacZ transduced vessels. However, this difference was not sustained long term. These findings suggest two possible mechanisms, of which either or both may be at work. Firstly continued significant VEGF expression may be needed for long-term NOS upregulation and secondly, upregulation of NOS at term in normal sheep pregnancy may already be at its peak and cannot be upregulated further by VEGF overexpression.

VEGF phosphorylates KDR, resulting in phospholipase Cγ activation and inositol 1,4,5-triphosphate formation, which evokes an elevation in intra-cellular Ca^{2+} levels and consequent eNOS activation (He H et al., 1999). In addition to the calcium dependent pathway, VEGF can also bring about NO synthesis using a Ca^{2+}-independent pathway, perhaps using the phosphatidylinositol-3-OH-kinase/Akt associated eNOS pathway, which is also stimulated by insulin and shear stress (Fulton D et al., 1999).

The ability of adenovirus-mediated VEGF-A_{165} gene therapy to stimulate upregulation of eNOS and NO and consequent increase in blood capillary density and perfusion (at 7 days post-administration) has previously been demonstrated in

a rat model of skin ischaemia (Huang N et al., 2006). The upregulation of eNOS appears to be one of the underlying mechanisms of action of VEGF, by which it produces therapeutic effects on vascular reactivity and blood flow.

Incubation of cultured HUVECs with VEGF protein has been shown to upregulate eNOS and NO levels in both an acute (1 hour) and chronic (>24 hours) manner (Hood JD et al., 1998), thus proving VEGF has an effect on human endothelial cells. I therefore believe that the results obtained from sheep uterine arteries presented in this thesis are likely to be similar to what we may expect from human uterine arteries, if examined. However, it remains to be seen whether chronic over-expression of VEGF in the uteroplacental circulation can upregulate eNOS and NO levels in women with a pregnancy affected by severe FGR, where there is evidence of endothelial dysfunction.

Even though I measured levels of eNOS protein in this study by Western blotting, it would have been valuable to quantify the levels of eNOS activity and/or NO levels. Increases in eNOS levels do not necessarily translate into increased NO levels as the activation of eNOS is regulated by numerous post-translational modifications and other processes, including protein-protein interactions, phosphorylation, and subcellular localization.

Following activation, eNOS shuttles between caveolae and other subcellular compartments such as the noncaveolar plasma membrane portions, Golgi apparatus, and perinuclear structures. This subcellular distribution is variable depending upon cell type and mode of activation and has a profound effect on the ability of eNOS to produce NO as the availability of its substrates and cofactors will vary with location (Fleming I and Busse R, 2003;Ostrom RS et al., 2004). To this end, it has been demonstrated that in HUVECs obtained from pregnancies complicated by FGR, there is an upregulation of eNOS protein levels (1.7 fold) compared to cells obtained from normal pregnancies. In spite of this increase, there is a dramatic reduction in eNOS activity (67$\pm$6%) and diminished NO synthesis in HUVECs from FGR pregnancies, thus indicating that most of the upregulated NOS is in its non-functional/dysfunctional conformation (Casanello P et al., 2005;Casanello P and Sobrevia L, 2002). As mentioned further above, it is

difficult to obtain pregnant uterine artery tissue for such experiments, but it is possible that the mechanisms found to be operating in HUVECs may be operating on the maternal side of the vasculature as well.

In summary, this data shows that VEGF over-expression results in increased levels of eNOS in the short-term transduced vessels, but this increase is not sustained long-term. Importantly, an increase in eNOS levels only, is not sufficient to justify that this therapy would be of likely benefit in improving utero-placental perfusion, and requires further investigation into levels of eNOS activity/NO generation.

3.38 Local over-expression of VEGF in the uterine arteries of mid-gestation pregnant sheep leads to changes in endothelial cell proliferation and neovascularization

A significant increase in adventitial endothelial cell proliferation was observed 4 – 7 days after transduction with Ad.VEGF-D vector in comparison with control adenovirus vector. The number of proliferating endothelial cells however was not significantly different between the Ad.VEGF-D and Ad.LacZ transduced sides when vessels were analysed at 30 days after gene transfer. On the other hand, the number of positively stained anti-vWF blood vessels was significantly greater in uterine arteries examined 30 days after Ad.VEGF (-A_{165} and –D) transduction but not in vessels examined 4 – 7 days after adenovirus gene transfer. We speculate that endothelial cells which are stimulated to proliferate by relatively high levels of VEGF at the peak of adenovirus vector expression (2-7 days) subsequently organize themselves into adventitial blood vessels, which results in an increase in perivascular blood vessel number seen in term pregnant uterine arteries.

The role of VEGF as a key regulator of angiogenesis has been very well characterized in pre-clinical models. Site-specific arterial gene transfer with plasmid vectors encoding VEGF-A_{165} cDNA leads to revacularization in a rabbit model of hindlimb ischaemia, to an extent superior than that achieved with a single intra-arterial bolus dose of the recombinant protein alone (Takeshita S et

al., 1996a;Takeshita S et al., 1996b). The gene transfer in this case was performed by transfecting the internal iliac artery of the ischemic limb with recombinant plasmids percutaneously, using a hydrogel-coated balloon catheter. It has further been demonstrated that an adenovirus vector encoding VEGF-A_{165} cDNA stimulated a physiologically relevant angiogenic response that was adequate to attenuate the detrimental effects of vascular occlusion in the setting of pre-existing ischaemia in a rat model of hindlimb ischaemia. These results have been used to propose that adenovirus-mediated VEGF expression may be useful in the prevention of advancing arterial occlusive diseases (Mack CA et al., 1998). In another recent study, cardiac fibroblasts engineered to express VEGF and transplanted into the hearts of rats resulted in significant cardiac neovascularization and attenuation of cardiac dysfunction, when compared to control groups (Goncalves GA et al., 2010).

Based on these results, I believe that adenovirus-mediated VEGF gene therapy to the utero-placental circulation, in the setting of pre-existing utero-placental insufficiency, may be of potential benefit in improving utero-placental perfusion. This is because the ability of VEGF to stimulate neovascularization and improve collateral circulation, as demonstrated in the studies above, is likely to enhance blood supply to the compromised fetus and overcome the detrimental effects of FGR to some extent.

Nevertheless, it is important to note that even though the ability of VEGF to promote therapeutic angiogenesis by stimulating proliferation, development and survival of endothelial cells is well documented in diverse animal models, compelling evidence that this translates to humans is so far lacking (Zachary I and Morgan RD, 2011). The VIVA (VEGF in Ischemia for Vascular Angiogenesis) phase II trial which investigated the effects of intracoronary and intravenous infusions of rhVEGF in patients of exertional angina demonstrated no significant improvements beyond that of placebo in exercise treadmill time, angina class and quality of life assessments at 60 days post-treatment. At 120 days post-treatment, there was only a significant improvement in angina class and modest improvement in overall outcomes compared to placebo (Henry TD et al., 2003).

These findings have been considered to be a huge setback for therapeutic angiogenesis (Zachary I and Morgan RD, 2011).

The Kuopio angiogenesis trial evaluated the effects of Ad.VEGF-A_{165} on restenosis and myocardial perfusion in patients with coronary heart disease, compared with plasmids encoding VEGF-A_{165} or placebo; the vectors were delivered by catheter during angioplasty and stent placement. The primary end points of the study were minimal luminal diameter and percent diameter stenosis, while the secondary end points included myocardial perfusion, exercise tolerance, incidence of new cardiac events and working ability. At the 6-month follow-up, there was no difference in the clinical restenosis rate and minimal luminal diameter in the treated patients. Significant improvement was seen only in myocardial perfusion in the Ad.VEGF-A_{165} treated patients (Hedman M et al., 2003).

Despite the treatment of more than 2500 patients using angiogenic cytokines, clinical trials have not demonstrated any long term beneficial consequences of VEGF on cardiovascular disease. The findings of most of these trials have been disappointing (Zachary I and Morgan RD, 2011), and the promise shown by therapeutic angiogenesis in pre-clinical models yet remains to be translated to the clinics. One of the reasons responsible for the poor clinical outcomes of VEGF gene therapy is believed to be low transduction efficiency. It is estimated that even using the most effective vectors, only 5-10% of the target cell population can be transduced in humans, which is considerably less than the transduction efficiency attained in smaller mammalian species (like mice and rats), most commonly used to generate pre-clinical data.

An important limitation of our study is that it was performed in healthy pregnant sheep, rather than in a model of FGR pregnancy. Normal human and ovine pregnancies are characterized by elevated VEGF levels and increased utero-placental angiogenesis that maximizes the supply of substrates and oxygen to the developing fetus (McKeeman GC et al., 2004;Vonnahme KA et al., 2005). Nevertheless, VEGF over-expression resulted in further angiogenesis, over and above that demanded by the physiological changes in normal sheep pregnancy.

Human pregnancies affected by FGR are characterized by lower baseline levels of VEGF, dysfunctional endothelium and only partially re-modelled utero-placental vasculature. We speculate that in human FGR pregnancy, VEGF over-expression provided by recombinant protein or gene therapy will restore some if not all of the deficient angiogenesis that characterizes this condition. While a short acute exposure to VEGF treatment such as that provided by VEGF infusion, may be insufficient, a chronic exposure to VEGF using gene therapy may potentially have some therapeutic effects.

To determine the extent of adventitial neovascularization, I used two endothelial markers to stain adventitial blood vessels – anti vWF and anti CD31. Two previous studies have investigated anti-vWF antibody staining of endothelial cells in sheep tissues; with good positive staining seen in one study (Bobryshev YV et al., 2001), but only weak/unconvincing staining in the other (Preziuso S et al., 2002). The immunohistochemical and fluorescent staining that we observed with anti-vWF appeared to be specific and convincing. This may be on account of the choice of antibody and methodology, particularly the antigen retrieval technique which differed from the study wherein anti-vWF staining was weak. I performed antigen retrieval using trypsin digestion, while the latter study employed no antigen retrieval at all (Preziuso S et al., 2002). Bobyryshev YV et al (2001) who also obtained good results with anti-vWF antibody used proteinase-K for antigen retrieval. I did not observe any endothelial cell staining with the anti-CD 31 antibody, in common with other authors (Preziuso S et al., 2002). This is probably because of inter-species antigenic diversity and the consequent inability of an antibody designed to rodent/human antigens to recognize the corresponding ovine antigen.

The advantage of immunohistochemical evaluation of neovascularization over other methods such as H&E staining is that it allows the researcher to objectively identify and count a blood vessel. On H&E stained sections, it is difficult to reliably identify a blood vessel as nerve fibers can appear very similar. We observed that some of the positively stained blood vessels had small blood

clots within their lumen, indicating there was blood flow through them and that they were functional.

The number of proliferating endothelial cells was quantified by anti-BrdU immunohistochemistry. H&E stained sections revealed dramatic cell proliferation in the perivascular adventitia of uterine arteries that had been injected with Ad.VEGF-D and these appeared to be proliferating endothelial cells. In order to confirm this, it was necessary to perform double staining using a cell proliferation marker (anti-BrdU) and an endothelial marker (anti-vWF). BrdU is a thymidine analogue that is incorporated into dividing cells during DNA synthesis, and which is passed down to daughter cells following division. Antibodies to BrdU thus stain the DNA of actively dividing cells and BrdU immunohistochemsitry has often been regarded as the 'gold standard' technique to determine cell proliferation. To achieve results, the pregnant ewes received an intra-venous administration of BrdU 48 hours before post-mortem which has the obvious disadvantages of a stressful injection procedure for the animal and uncertain penetration of the targeted cells with a uniform concentration of the compound. In contrast, antibodies to endogenously expressed proliferation markers like Ki67 and Proliferating Cell Nuclear Antigen (PCNA) stain protein antigens rather than DNA.

Another sensitive technique to estimate cell proliferation is the use of radiolabelled thymidine, which like BrdU, is incorporated during the S phase of the cell cycle. The disadvantages of this technique include the need to use a radioactive substance, and the fact that [3H]-thymidine is non-specifically incorporated in several tissues. Thus, BrdU labeling appeared to be the optimum method of assessing endothelial cell proliferation in this study.

As discussed further above, we again compared the effect of VEGF with control vector on vessels from within the same animal. We observed significant differences in the neovascularization data (long-term) and proliferation data (short-term) provided by just 4-6 animals. The study is limited slightly because sections from each branch of the uterine artery were obtained only at 1-2 levels. It would have been more informative to examine sections from multiple levels of

the utero-placental tree or from serial sections, and investigate if the rate of adventitial neovascularization and endothelial cell proliferation is consistently higher in all levels of all branches. The experimental protocol had to be limited to only 2 levels at most because of the need to use large amounts of uterine artery vessel tissue for organ bath analysis, DNA/RNA extraction and protein extraction.

We have demonstrated an increase in the number of adventitial blood vessels in uterine arteries transduced with Ad.VEGF-A_{165}/Ad.VEGF-D relative to controls. We speculate that these adventitial blood vessels are *vasa vasora*. The *vasa vasora* is a microvasculature network that originates primarily in the adventitial layer of large arteries and supplies oxygen and nutrients to the outer layers of the arterial wall (Heistad DD et al., 1981). Thus, increases in the *vasa vasora* may augment the function of the uterine artery thereby enhancing uterine perfusion.

There has been considerable debate about the role of adventitial microvasculature/vasa vasora in the amelioration or deterioration of vasculopathies. While some authors believe adventitial neovascularization may be of therapeutic benefit, others are of the opinion that it may lead to progression of vascular disease (Hoefer IE et al., 2007). Studies have demonstrated that prolonged treatment with inhibitors of angiogenesis like endostatin and TNP-470 resulted in a reduction of intimal neovascularization and plaque growth in apolipoprotein E-deficient mice (Moulton KS et al., 1999). Conversely, VEGF administration (intra-peritoneally) in mice deficient in apolipoprotein E and apolipoprotein B100, and fed on a cholesterol diet, resulted in a dramatic increase in atherosclerotic plaque area (Celletti FL et al., 2001). Some animal studies have shown increased neointima formation following VEGF delivery. Additionally, VEGF and other markers of angiogenesis have been shown to be expressed in atherosclerotic plaques (Inoue M et al., 1998).

Contrary to these results, other studies have demonstrated that VEGF-A protein and adenoviral gene transfers of VEGF-A, VEGF-B, VEGF-C and VEGF-D have no effects on atherosclerosis in hypercholesterolemic LDL-receptor/ApoB48-deficient mice in which the lipoprotein profile and

atherosclerosis closely mimic the human disease (Leppanen P et al., 2005). Furthermore, inhibition of VEGFR2 using an anti-Flk antibody has no effect on plaque size and vessels in ApoE-deficient mice and did not halt disease progression (Luttun A et al., 2002). Delivery of VEGF and other angiogenic cytokines in patients with ischaemic heart disease did not promote or accelerate atherosclerosis and any of its clinical complications (Zachary I and Morgan RD, 2011).

Even though the studies in this thesis were not performed in a model of atherosclerosis, the increased adventitial neovascularization and chronic VEGF exposure did not result in any adverse outcomes on the vascular health of the uterine arteries. It has been demonstrated that hypertrophied *vasa vasora* have the potential of revascularizing occluded atherosclerotic carotid arteries, by developing a collateral circulation, in human patients (Colon GP et al., 1999). Furthermore, it is believed that adventitial microvessels/vasa vasora in the utero-placental and ovarian vascular beds play an important role in facilitating the changes in blood flow in pregnancy (Zezula-Szpyra A et al., 1997).

I also measured the intima/media ratios in uterine arteries from twin pregnant animals to examine if VEGF gene therapy altered the vessel morphology. This was done by measuring the relative thickness of the intimal and medial layers in H&E stained sections of uterine arteries that had been transduced with Ad.VEGF-A_{165} or Ad.LacZ long-term. I observed a reduction in the intima/media ratios of Ad.VEGF-A_{165} transduced uterine artery segments compared to Ad.LacZ transduced segments in all branches examined, which was significant in the two smallest branches of the main uterine artery that were examined. It is likely that statistical significance would have been reached in the main and first branch of the uterine artery as well, if a few additional twin pregnant animals had been included in the study.

Studies in other vascular beds have demonstrated that an increase in the intima/media ratios is associated with vasculoproliferative disorders such as atherosclerosis and restenosis after angioplasty. It has further been demonstrated that disruption of the function of vasa vasorum is associated with neointimal

thickening. In pigs, ligation of the side branches of the femoral artery occludes blood flow to the vasa vasora, and results in significant intimal hyperplasia. The authors' interpretation of these results was that occlusion of the vasa vasorum promoted intimal thickening (Barker SG et al., 1993). Although oxygenation measurements were not carried out following the ligation, they believed that occlusion of the vasa vasorum would lead to a hypoxic environment, a condition which would make the vessel prone to atherosis. Hence, intimal hyperplasia and periadventitial blood flow may be inversely related.

Intimal hyperplasia observed in the uterine arteries of premenopausal women is accompanied by impaired cyclic GMP production, and altered arginase and NOS activities (Marinova GV et al., 2008). It has been demonstrated that there exists a positive correlation between intima/media ratios and endogenous NOS inhibitors in endothelial cells (like L-NMMA and ADMA), as well as endothelin-1 within the vessel wall of perimenopausal human uterine arteries (Beppu M et al., 2002). Accumulation of endogenous NOS inhibitors in endothelial cells is known to be associated with diminished NO production and intimal hyperplasia (Azuma H et al., 1995;Masuda H et al., 1999).

In another study, it was shown that uterine artery atherosclerosis may be used as a surrogate marker for atherosclerosis in other critical vascular beds, like the coronary and carotid arteries, as well as the development of cardiovascular disease. Indeed other risk factors for the development of cardiovascular disease, such as ECG abnormalities and cholesterol levels greater than 200 mg/dl (normal range = 180-200 mg/dl) have been found to be associated with greater intimal thickness and intima/media ratios in the uterine arteries (Crawford BS et al., 1997). There is now strong evidence that developing both FGR and/or PET during pregnancy confers an increased predisposition to cardiovascular disease (Smith GC et al., 2001;Manten GT et al., 2007). The reduction in intima/media ratios we observed in our study therefore may confer an arterioprotective effect on the uterine arteries, which may potentially benefit FGR.

The importance of these findings has also been demonstrated in a study investigating the effects of 17β-Estradiol (E_2) in perimenopausal human arteries

(Obayashi S et al., 2001). Incubation with E_2 significantly augmented endothelium-dependent relaxation, and was accompanied by significant increases in cyclic AMP and GMP production, but only in uterine arteries that had normal intima/media ratios. In perimenopausal human uterine arteries characterized by intimal hyperplasia and increased intima/media ratios however, E_2 failed to alter the acetylcholine-induced relaxation as well as the cyclic nucleotide production. NO is known to relax vascular smooth muscle through activation of soluble guanylate cyclase, which in turn increases intracellular levels of cyclic GMP (Ignarro LJ, 1989). PGI_2 on the other hand, exerts its relaxation effect through activation of soluble adenylate cyclase, which increases cyclic AMP levels (Moncada S and Vane JR, 1978). Although this investigation was carried out using uterine artery specimens from non-gravid women, the results underscore the clinical importance of the intima/media ratio in this vascular bed.

3.39 Ad.VEGF administration to the uterine arteries does not lead to detrimental changes in maternal and fetal haemodynamics

In this study, we investigated changes in maternal and fetal haemodynamics in response to Ad.VEGF-A_{165} injection to the uterine arteries using implanted telemetric blood pressure sensitive catheters in the maternal or fetal carotid arteries. We observed no significant difference in the maternal or fetal blood pressure and heart rates in the week following vector injection. There was a small non-significant drop in maternal blood pressure at term, but this is normally observed in sheep (Kitanaka T et al., 1989). In one of the instrumented fetuses, there was a rise in blood pressure at term. This too is a normal occurrence in sheep. During the occlusion for vector administration, we observed a small and non-signficant rise in fetal blood pressure and heart rate, which returned to baseline levels within 30 minutes.

An intravenous injection of VEGF (250 µg/kg) has been shown to produce transient tachycardia, hypotension and a decrease in cardiac output in conscious

instrumented rats (Yang R et al., 1996). VEGF also caused a dose-dependent reduction in mean arterial pressure and an associated increase in heart rate. Pre-treatment with L-NAME significantly attenuated the depressor and tachycardic responses to VEGF, suggesting that VEGF-induced hypotension is mediated by NO. Conversely, drugs and antibodies that disrupt VEGF signaling are used to treat cancer by inhibiting tumour growth, but are associated with significant hypertension. The hypertension is believed to occur due to a decreased production of NO in the wall of arterioles and other resistance vessels (Kamba T and McDonald DM, 2007;Facemire CS et al., 2009).

The lack of a detectable systemic effect of VEGF expression suggests that the technique of gene delivery used results in sustained over-expression only in the uterine arteries and not in the systemic vasculature. This is borne out by the RT-PCR data showing transgene expression only on the maternal side of the placenta, as discussed above. VEGF is a large protein and is therefore unlikely to be able to cross the epitheliochorial placenta of sheep to reach the fetal circulation from maternal circulation and vice-versa (Vonnahme KA et al., 2005). However, this is not the case in the human patient, where only a single syncytiotrophoblast layer needs to be crossed in the third trimester of pregnancy to reach the fetal circulation from the maternal circulation. Thus, there is a possibility of VEGF protein entering the fetal circulation in humans and causing hypotension. An appropriate way to assess if Ad.VEGF has any effects on fetal blood pressure in a pre-clinical ovine model would be to inject the vector directly into the umbilical vein, and then monitor fetal haemodynamics.

The technique of blood pressure monitoring we used has been regarded as the ‘gold standard’ for measurement of haemodynamic parameters. Some previously published studies on haemodynamic monitoring used chronic maternal and/or fetal catheterization, and connection of the animal physically via the catheters with a polygraph (Marsh AC et al., 2002). Furthermore, these catheters need to be flushed with heparinised saline daily to prevent blood coagulation around the pressure-sensitive tip, which would render the catheter useless. This type of experiment involves space restriction and animal restraint, which is a

significant stressor (Rivalland ET et al., 2007;Niezgoda J et al., 1993). Refinement of animal experiments to reduce the potential for suffering and stress and to enhance animal welfare improves the quality of the data obtained. It is also one of the cornerstones of the 3Rs, a widely accepted ethical framework for conducting scientific experiments using animals humanely (Robinson V, 2005). We believe that telemetric monitoring of maternal or fetal blood pressure and heart rate in the freely moving pregnant ewe would meet these expectations. One of the advantages of traditional chronic catheterization using implanted externalized catheters is that it permits access to the maternal/fetal circulation and amniotic cavity for fluid sampling over time, which is not feasible using the telemetric monitoring method described here.

As mentioned above, refinement of technique is associated with a reduction in stress levels for the experimental animals. However, this project was not designed to investigate this issue. For any true comparison to be made, the same experiment would need to be repeated in animals monitored by traditional methods. Comparing our data to those obtained by traditional methods in other studies, we can only accurately compare the baseline (pre-intervention) data. In a study investigating the effect of 50% reduction in maternal nutrient intake on fetal blood pressure in sheep, the blood pressure of control fetuses was found to be 38$\pm$0.7 mm Hg at about 115 days of gestation (Edwards LJ and McMillen IC, 2001). In our study, the pre-injection baseline value of fetal blood pressure at approximately 110-112 days of gestation was 38.29$\pm$3.17 mm Hg. Thus, even though the values of fetal blood pressure in both the investigations are similar, it is to be noted that this is only a snapshot comparison rather than a chronic long-term one. Hence, little can be inferred about the difference in stress caused by the two techniques of haemodynamic monitoring.

In animals that had maternal blood pressure catheters implanted, there was no morbidity or mortality. However, in the four animals used for fetal telemetry studies, there were 2 fetal deaths, that occurred 8 days and 12 days after catheter placement. This is likely to have been due to displacement of the catheter as the fetuses grew. In both cases the tip of the catheter was found lying in the bicarotid

trunk at post-mortem, which may have resulted in obstruction of blood flow to both common carotid arteries. Cannulation of the fetal sheep carotid arteries has been shown to result in ischaemic brain damage especially when bilateral obstruction has occurred (Dodic M et al., 1998). The insertion technique was adjusted by threading the catheter tip further upstream the carotid artery in an attempt to bypass the bicarotid trunk and reach the descending aorta, and the problem was overcome. The two fetuses subsequently operated with this adjustment were monitored successfully till term.

In summary, using a 'gold standard' technique of maternal and fetal haemodynamic monitoring, we have demonstrated that local administration of Ad.VEGF to the uterine arteries of mid-gestation pregnant sheep has no detrimental consequences on maternal/fetal blood pressure and heart rate.

3.40 Administration of Ad.VEGF to the uterine arteries of pregnant sheep is found to be safe in preliminary investigations.

The preliminary analysis designed to assess the safety of Ad.VEGF gene transfer in pregnant ewes suggested that there were no obvious signs of toxicity from the viral vector. The ewes resumed normal feeding and behaviour the day after vector injection and displayed no signs of suffering or distress. Analysis of maternal blood and serum samples collected before vector injection, one week after injection and at post-mortem; and fetal blood and serum samples collected at post-mortem for routine haematology, biochemistry and liver function showed no detectable abnormality. This further supports the safety of Ad.VEGF gene transfer. Notably, there was no evidence of liver function abnormality despite the high dose of vector injected. This is important because the liver is a major site of Ad vector-induced inflammation and clearance in many experimental studies in animals (Worgall S et al., 1997). In the study cited, the adenovirus vector was administered intravenously. There are two possible explanations for the lack hepatic toxicity – firstly the delivery technique restricts the vector to the uterine

vasculature and does not allow it to leak into the systemic circulation; and secondly, the vector preparations used in our studies were of a clinical-grade and highly purified, in contrast to many experimental virus preparations which are contaminated with replication-competent adenoviruses.

Gross examination of maternal and fetal tissues at post-mortem examination or microscopic histology of H&E stained tissues did not reveal any significant pathology. Some ewes showed evidence of low-grade myocarditis, this was believed to be unrelated to the administration of viral vectors and is a common finding in this breed of sheep (David AL personal communication and PhD thesis). Sham operated ewes who received only the vehicle (PBS), also showed evidence of myocarditis. All other tissues examined had an unremarkable histology. The uterine arteries showed no evidence of oedema, inflammation or leucocyte infiltration.

The sheep placentation is very different to that of humans, and therefore the sheep is a relatively poor model in which to test for toxicity or safety. Work is currently ongoing in another pre-clinical model, the FGR guinea pig, to assess vector spread and expression in fetal tissue. The guinea pig placenta is very similar to human placenta, and hence, this species can provide more valuable and relevant data for pre-clinical assessment of safety.

More advanced toxicology studies are being conducted by Ark Therapeutics to assess the safety of this potential therapy. These include administration of very high doses of Ad.VEGF ($2x10^{12}$ viral particles) to pregnant rabbits to determine the LD_{50}, as well as detailed microscopic histological examination of maternal and fetal tissues from these experimental animals. In a further series of experiments in collaboration with the University of Manchester, *in vitro* studies with human placental villous explants exposed to Ad.VEGF have been performed. Placental villous explants were grown in culture for 5 days, and then infected with adenovirus at high concentrations or control material, and then analysed 48 hours later. This exposure to adenovirus had no detrimental effect on villous function as measured by hormone secretion or enzyme activity. Neither was there any adverse effect on the cellular structure of the placental tissue.

Toxic effects such as the formation of vascular tumours, uncontrolled angiogenesis and inflammation have been seen after unregulated myoblast-mediated VEGF over-expression in murine hearts (Lee RJ et al., 2000). These results underscore the need for regulated expression of a gene encoding such a potent product. In contrast with these results, transient modes of VEGF gene delivery based on the injection of an adenovirus or plasmid DNA have been reported as safe to administer in animal models and human patients (Losordo DW et al., 1998;Rosengart TK et al., 1999;Patel SR et al., 1999). Adenovirus-mediated gene transfer peaks at 24 hours post-transduction, is maximum during the first one week, after which it begins to decline, and there is only minimal residual expression remaining after one month. This is considered to be a disadvantage of adenoviral vector systems, and renders them useless for many therapeutic applications which require long-term gene expression. However, in our study, the short-term expression by adenoviral vectors makes their use highly desirable, as therapeutic transgenic protein expression is required for only a few weeks of gestation to achieve the desired beneficial outcome.

In summary, we have shown that adenovirus-mediated VEGF gene transfer to treat utero-placental vascular insufficiency appears to be safe. More advanced toxicology studies are currently being performed, which are pivotal before clinical application can be contemplated.

3.41 Conclusion

The results presented in this chapter demonstrate that local adenovirus-mediated VEGF-A_{165}/VEGF-D over-expression in the pregnant sheep uterine arteries at mid-gestation results in a significant long-term increase in UABF, a reduction in uterine artery vascular contractility, increased adventitial angiogenesis and increased fetal weight. It gives hope that impaired utero-placental perfusion found in cases of FGR and pre-eclampsia may be potentially reversed. Vector administration appears to be safe leading to no undesirable vector expression, change in maternal or fetal haemodynamics, or pathology.

Studies in growth-restricted small and large animal models, optimization of the delivery technique, and further safety evaluation will be required before clinical application could be contemplated.

Chapter 4

Results: The Effects of VEGF Over-expression on Pregnant Uterine Artery Endothelial Cells

I was interested in elucidating the mechanism of action of VEGF in pregnant ovine uterine arteries. To do this, experiments were carried out in endothelial cells isolated from the uterine arteries of mid-gestation pregnant sheep. The advantage of the uterine artery endothelial cell (UAEC) model is that it provides an opportunity to investigate the response of the endothelium, which is the first vascular layer infected by the adenovirus, to over-expression of the transgenic protein. As the endothelium is believed to be the principal regulator of the circulatory system, it is important to know how it reacts to different ligands, such as VEGF in this case, to understand their mode of action and effects on blood flow.

The UAEC model can be used to create several different experimental conditions within a single culture plate, for instance, by altering the viral vector dose or the incubation time post-infection. In addition, experimental conditions can be controlled more clearly and experiments can be easily repeated. To carry out such experiments in pregnant sheep would be technically demanding, expensive and unethical. In contrast, endothelial cells can be isolated relatively easily from sheep vessels by enzymatic digestion. It has been shown that these cells retain their primary character and have similar responses to those of freshly isolated UAECs, for up to 4 passages *ex vivo* (Bird IM et al., 2000).

The following chapter describes the results of optimization of a technique to isolate pure ovine UAECs, their characterization and their responses to Ad.VEGF-A_{165} and Ad.VEGF-D infection. In order to obtain uncontaminated cultures of endothelial cells from pregnant sheep uterine arteries, the first step was to determine the optimum incubation time with collagenase. Following this, a number of different methods were used to confirm the purity of our endothelial cell preparation. This is primarily because it is easy to get contamination from smooth muscle cells and fibroblasts in primary endothelial cell preparations. Hence, confirming the purity of our primary cell cultures was critical to validate our observations from subsequent experiments.

4.1 To extract uterine artery endothelial cells from pregnant sheep, the optimum time for incubation of uterine arteries with collagenase is 15 minutes.

In the first two experiments performed, endothelial cells were extracted in accordance with the only previously published protocol (Bird IM et al., 2000;Grummer MA et al., 2009), by incubating the uterine arteries with collagenase for 55 minutes. Following this long incubation time, we observed that our cell preparations did not consist of cobblestone-shaped cells, which is a characteristic of endothelial cell morphology but instead, they had an elongated and fibrous appearance, which is typical of smooth muscle cells. Following this, the incubation time with collagenase was reduced to 15 minutes, as has been suggested in papers for primary endothelial cell extraction from human blood vessels (Crampton SP et al., 2007) which resulted in a pure culture of endothelial cells. Immunofluorescent staining and other tests described below were used to confirm these findings.

4.1.1. Immunofluorescent staining confirms that endothelial cells can be extracted from the pregnant mid-gestation sheep uterine artery

Anti-vWF, a marker specific for endothelial cells and megakaryocytes, was first used to distinguish endothelial cells from other cell types. vWF is a glycoprotein produced uniquely by endothelial cells and megakaryocytes (Zanetta L et al., 2000) which forms a complex with coagulation factor VIII and is involved in the formation of platelet plugs at the site of endothelial cell damage (Mannucci PM, 1998). Its use as an endothelial cell marker has been well established for several years (Zanetta L et al., 2000).

As was suspected, staining of cells isolated following a 55 minute collagenase digestion, with anti-vWF antibody, showed that many nuclei lacked any fluorescent staining (Figure 4.1A). This indicated contamination with other cell types, most probably smooth muscle cells and macrophages.

Following this, the incubation time with collagenase was reduced to 15 minutes. Figure 4.1A depicts the photomicrograph of positive immuno-staining with anti-vWF antibody on cells isolated after a reduced incubation time. The vWF can be seen as a fluorescent green stain in the cytoplasm, specifically in the Weibel-Palade bodies, and the nuclei are counterstained by DAPI, indicated by blue dots. As is evident, all the blue dots are surrounded by green cytoplasm after an incubation time of 15 minutes. This confirms that all the cells in the culture preparation are of endothelial origin, and there is no contamination evident with smooth muscle cells.

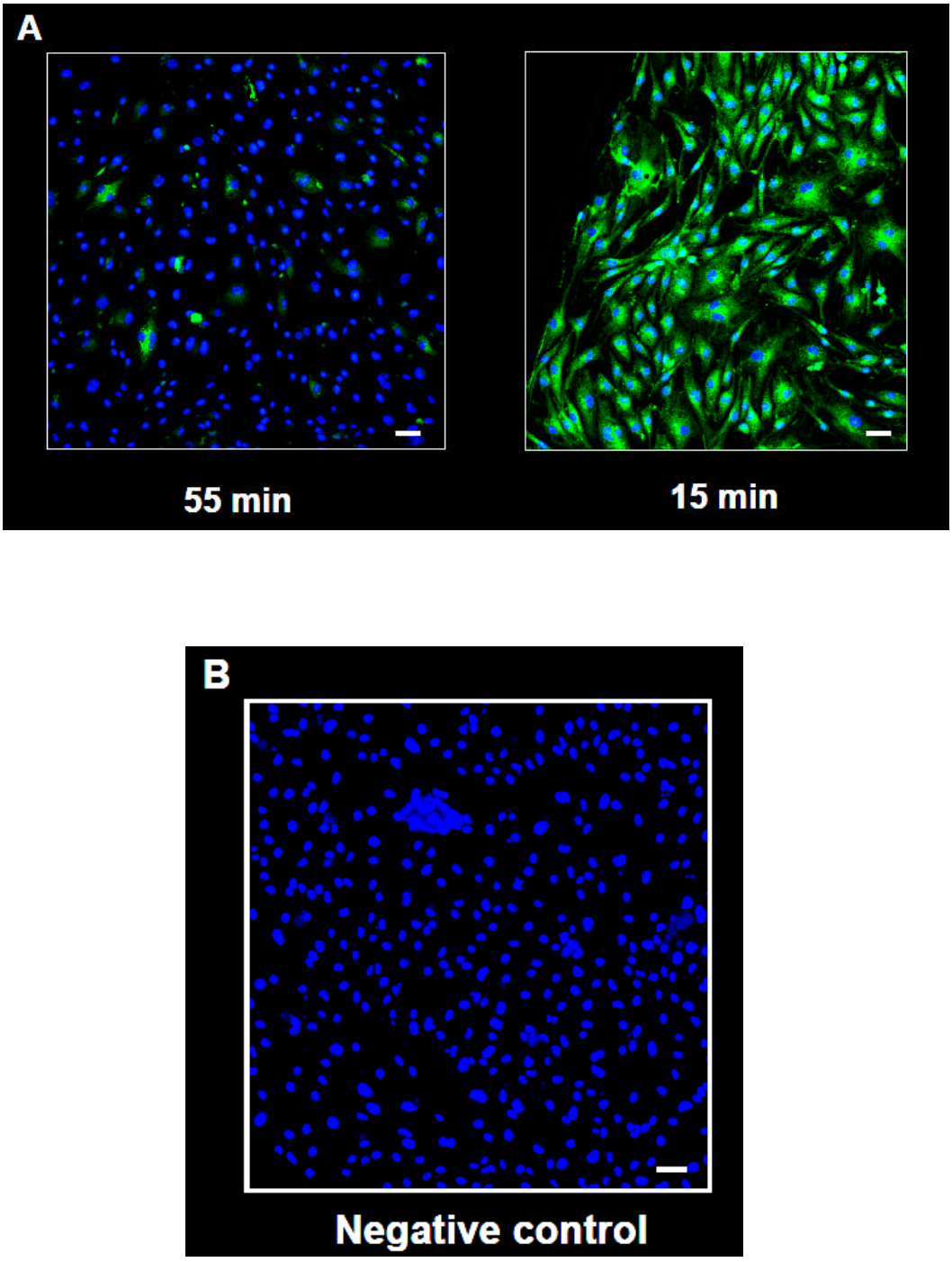

Figure 4.1 – Anti-vWF staining to optimize the incubation time of pregnant sheep uterine arteries with collagenase to isolate pure endothelial cell preparations

(Continued from overleaf) Uterine arteries from mid-gestation pregnant sheep were incubated with collagenase (5mg/ml) for either 55 minutes or 15 minutes to detach endothelial cells. Detached cells were grown in culture for up to 4 passages and then stained with primary rabbit anti-human von Willebrand Factor antibody (1:400), followed by a secondary Alexafluor-488 donkey anti-rabbit IgG to confirm endothelial cell identity. The nuclei were counterstained with DAPI. The top panel 'A' shows that digestion for 55 minutes resulted in contamination with other cell types, which did not stain with anti-vWF. However, digestion for 15 minutes resulted in a pure culture of endothelial cells, all of which were positively stained with anti-vWF. The bottom panel 'B' shows anti-vWF staining on smooth muscle cells (negative control). Scale bar = 40μm

Staining with two additional antibodies anti-VE cadherin and anti-β-catenin, was performed to verify the identity of cell types. VE cadherin and β-catenin are essential for the early assembly of inter-cellular junctions in endothelial cells (Lampugnani MG et al., 1995). Previous studies have described their localization in areas of cell-to-cell contact in confluent cultured endothelial cell monolayers. This indicates that these proteins may be used to recognize endothelial cells (Lampugnani MG et al., 1995). While VE-cadherin is specifically found in endothelial cells, β-catenin may also occur in the adherence junctions of other cell types. Nevertheless, staining with both these antibodies would demonstrate the morphology of adherence junctions between cells. As seen in Figure 4.2, the fluorescent green staining shows the adherence junctions between the cells bearing a cobble-stone or pavement-stone like appearance, which is characteristically seen in endothelial cells. Hence, this staining further confirms the successful isolation of endothelial cells from ovine uterine arteries. Smooth muscle cells were used as a negative control for all staining experiments and gave no positive staining with any of the fluorescent antibodies.

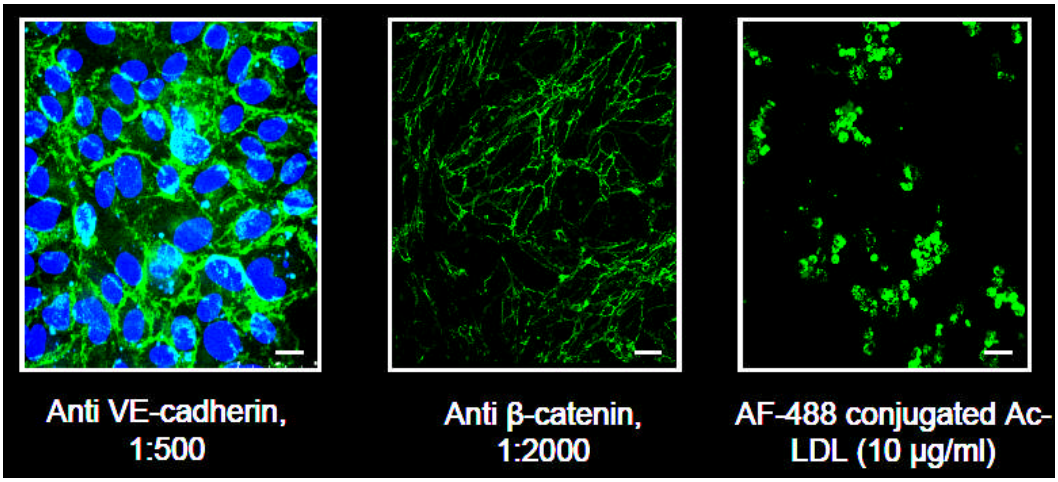

Figure 4.2 – Confirmation of the identity of pregnant sheep UAECs by immunofluorescence and Ac-LDL staining

Uterine arteries from mid-gestation pregnant sheep were incubated with collagenase (5mg/ml) for 15 minutes to detach endothelial cells. Detached cells were grown in culture for up to 4 passages and then stained with primary anti-VE cadherin (1:500) or anti-β-catenin (1:2000) antibodies, followed by the appropriate Alexafluor-488 conjugated secondary antibodies. These antibodies stain the adherence junctions between endothelial cells, which give a cobblestone-like appearance. Cultured cells were also incubated with acetylated LDL, a lipoprotein that endothelial cells metabolize, that had been conjugated with Alexafluor-488. This resulted in a positive staining, further confirming the endothelial origin of the cells. Blue dots (where present) represent the DAPI-stained nuclei. Scale bar = 40µm

4.1.2 Staining with Ac-LDL confirms the isolation of pregnant sheep uterine artery endothelial cells

Endothelial cells internalize and degrade Ac-LDL 7-15 times faster than smooth muscle cells via the 'scavenger cell pathway' of LDL metabolism (Voyta JC et al., 1984). This has enabled the identification of endothelial cells distinctly from smooth muscle cells based on their increased metabolism of fluorescently labeled Ac-LDL. Figure 4.2 shows the uptake of Ac-LDL by endothelial cell specific receptor-mediated endocytosis into endosomes and lysosomes where it will be metabolized. Smooth muscle cells were used as a negative control for all staining experiments and gave no positive staining with Ac-LDL (data not shown). As can be seen from the figure, all cells took up and metabolized the Ac-

LDL to yield a fluorescent product, and are therefore endothelial in origin. There is no contamination with smooth muscle cells.

4.1.3 Challenge with VEGF protein confirms the isolation of pregnant sheep uterine artery endothelial cells

VEGF receptors are known to be present on the endothelium where they bind VEGF and signal downstream activation of different signal transduction pathways, including phosphorylation of ERK. Upregulation of the phosphorylated form of ERK after challenge with VEGF-A_{165} protein was thus also used to confirm that the isolated cells were of endothelial origin.

Western blotting with a phospo-ERK antibody was carried out on protein extracts from cells challenged with VEGF-A_{165} for 10 minutes and unchallenged cells. There was an observable increase in phospho-ERK levels as seen by a denser band when compared with the band from unchallenged cells (Figure 4.3). This further confirmed the endothelial origin of the isolated cells.

Figure 4.3 – Upregulation of phospho-ERK following challenge of pregnant sheep uterine artery endothelial cells with rhVEGF-A_{165} protein

Uterine arteries from mid-gestation pregnant sheep were incubated with collagenase (5mg/ml) for 15 minutes to detach endothelial cells. Detached cells were grown in culture for up to 4 passages. Prior to experimentation, cultured endothelial cells were serum-deprived overnight. Next morning, they were challenged with rhVEGF-A_{165} protein (25 ng/ml, R&D Systems) for 10 minutes. Protein extracts from challenged (V) and control (C) cells were analysed by western blotting for phosphorylated (p) ERK and total-ERK levels. Upregulation of p-ERK following VEGF-A_{165} challenge indicates the endothelial origin of these cells.

4.2 Adenovirus vector can infect pregnant ovine UAECs

To determine whether adenovirus vectors could infect the cultured ovine UAECs, cells were infected with Ad.LacZ at increasing multiplicities of infection (MOI, 0, 1, 10, 100, 1000 and 10000) in a 6-well plate. The culture medium was replaced with fresh EGM (supplemented with 2% FBS) after 24 hours. After a further 24 hours of incubation, the cells were fixed in 100% ethanol and stained with X-gal staining solution. The percentage of positively stained cells in each well was determined under a light microscope by direct counting in 10 randomly selected high-powered fields. Figure 4.4 shows some representative images of stained cells infected at different MOIs. The results of this analysis are shown in Table 4.1.

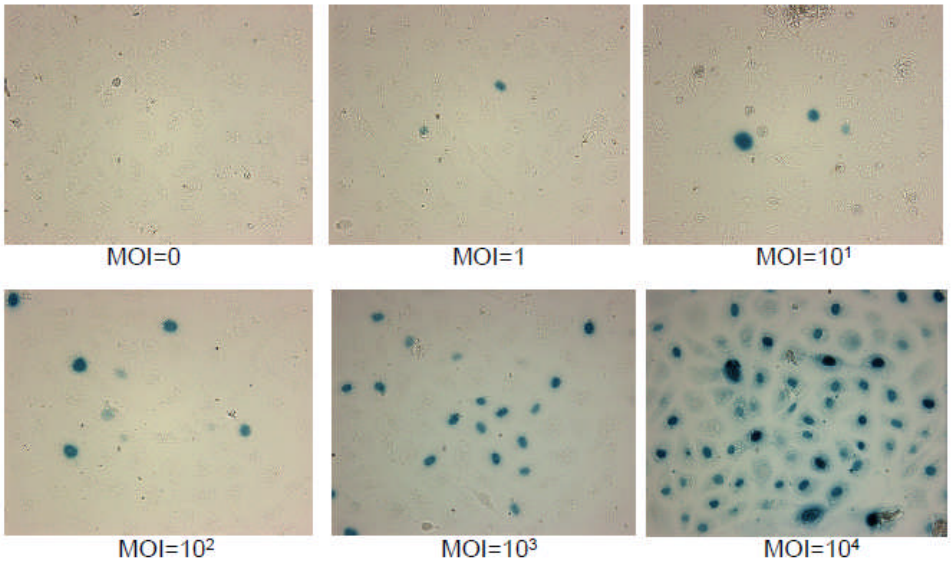

20x mag.

Figure 4.4 – Improvement in transduction efficiency in sheep UAECs with an increase in adenovirus vector MOI

Pregnant sheep UAECs were grown in culture for up to 4 passages, and then infected at increasing multiplicities of infection (MOIs) with Ad.LacZ in 6-well plates. After 48 hours of infection, the cells were fixed in 100% ethanol and stained with X-gal staining solution overnight. Infection

efficiency was determined by counting the number of positively stained blue cells and unstained cells in 10 randomly selected high powered fields.

Table 4.1 – Infection efficiency of pregnant sheep UAECs with Ad.LacZ

Multiplicity of Infection	Percentage of cells positively stained in 10 randomly selected high powered fields (Mean±SEM)
0	0
1	0.70±0.08
10	6.39±2.73
100	32.55±3.82
1000	63.12±1.79
10000	90.23±3.98

Thus, adenovirus vectors are capable of infecting pregnant ovine UAECS, and the infection efficiency improves with increasing MOI.

4.3 eNOS, iNOS and phosphorylated eNOS (Ser^{1177}) are upregulated in cultured ovine UAECs 48 hours after Ad.VEGF-A_{165} and Ad.VEGF-D transduction, but not after 24 hours of infection

In order to understand the mechanism of VEGF action on pregnant sheep uterine arteries, I was interested in studying the effects of VEGF-A_{165} and VEGF-D over-expression on eNOS, p-eNOS (Ser^{1177}) and iNOS levels in pregnant sheep UAECs. Ovine UAECs were passaged four times before seeding them in 6-well plates. The cells in each plate were infected with Ad.VEGF-A_{165}, Ad.VEGF-D or Ad.LacZ at increasing multiplicities of infection (0, 1, 10, 100, 1000 and 10000).

After 24 hours of infection with either Ad.VEGF-A_{165} or Ad.LacZ, protein was extracted from the cells and used for western blotting analysis with antibodies specific to eNOS, iNOS and p-eNOS (Ser^{1177}). Experiments were carried out three times on cells from different sheep. I observed no change in the levels of any of these proteins 24 hours after adenovirus infection (Figure 4.5). Similar results were obtained with Ad.VEGF-D (data not shown).

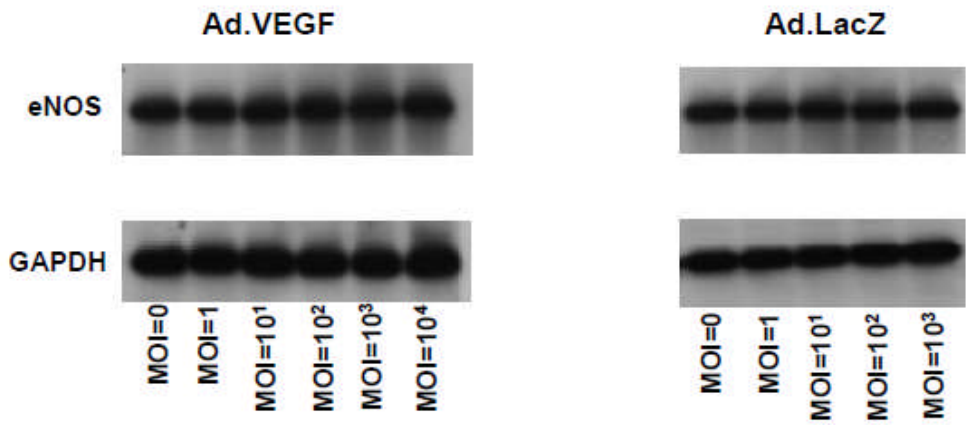

Figure 4.5 – Representative western blot showing no change in eNOS levels 24 hours after Ad.VEGF-A_{165} infection in pregnant sheep UAECs

Pregnant sheep UAECs were grown in culture for up to 4 passages, and then infected at increasing multiplicities of infection (MOIs) with Ad.VEGF-A_{165} or Ad.LacZ in 6-well plates. Protein was extracted from infected cells 24 hours later, and assayed for eNOS levels by western blotting. There was no change in the levels of eNOS in Ad.VEGF-A_{165} or Ad.LacZ infected cells. Phospho-eNOS (Ser^{1177}) and iNOS levels were also analysed, and found to be unchanged (data not shown). GAPDH was used as a loading control for gels.

These experiments were also carried out 48 hours after infection with Ad.VEGF-A_{165}, Ad.VEGF-D and Ad.LacZ at increasing MOIs (0, 1, 10, 100, 1000 and 10000). The medium was replaced with fresh culture medium (EGM supplemented with 2% FBS) 24 hours post-infection.

After 48 hours of virus vector infection, protein was extracted from the cells and used for western blotting analysis with antibodies specific to eNOS, iNOS and p-eNOS (Ser^{1177}). Experiments were performed three times on cells from different sheep. I observed an upregulation in the levels of all three proteins 48 hours post-infection in the Ad.VEGF-A_{165} and Ad.VEGF-D infected cells. There was no change in the levels of eNOS, iNOS or p-eNOS (Ser^{1177}) in the Ad.LacZ infected cells (Figure 4.6 and Figure 4.7).

While the levels of eNOS and iNOS appeared to increase in a dose-dependent manner in response to Ad.VEGF (-A_{165}/-D) infection, the levels of p-eNOS (Ser^{1177}) were significantly raised only at the highest MOI of Ad.VEGF-A_{165}/Ad.VEGF-D.

A.

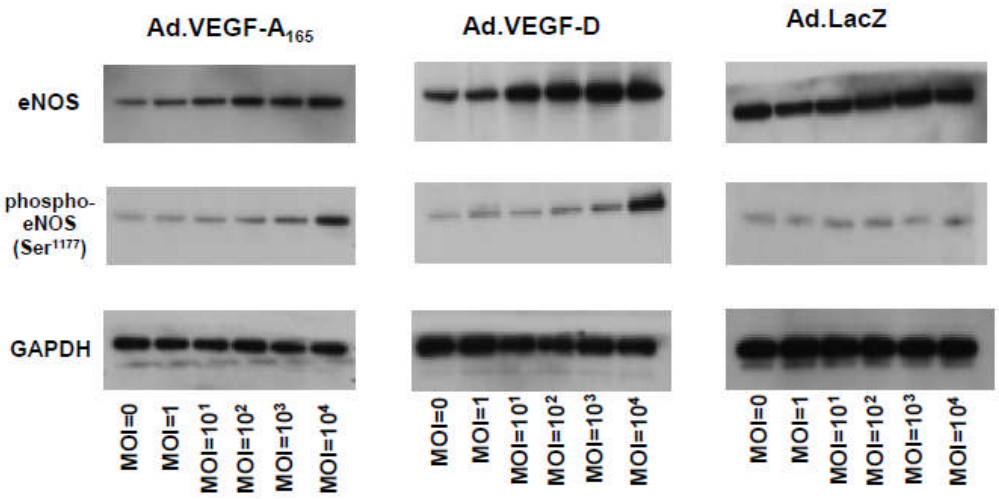

B. Change in eNOS levels

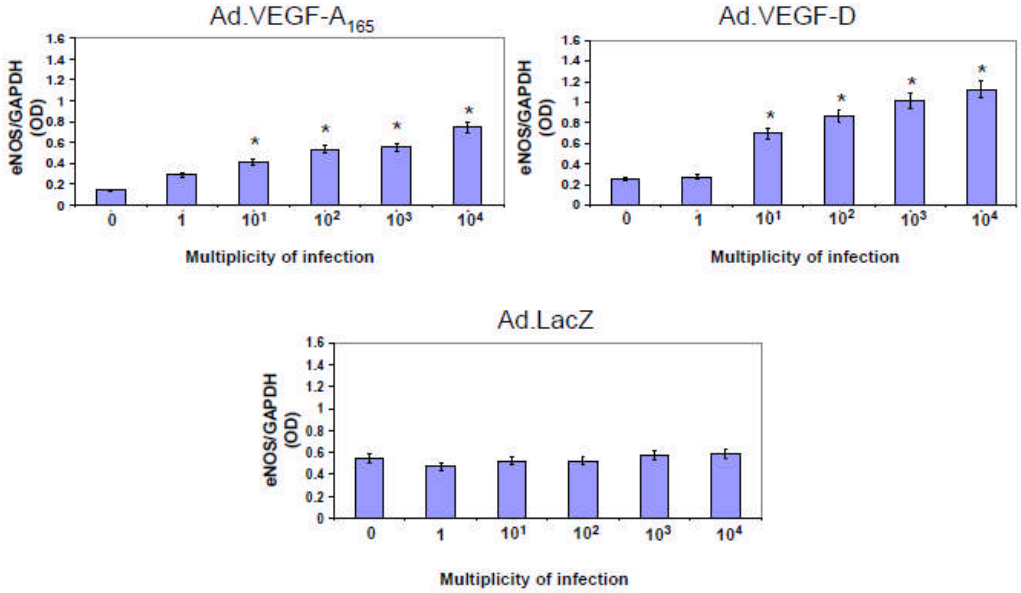

C. Change in p-eNOS levels

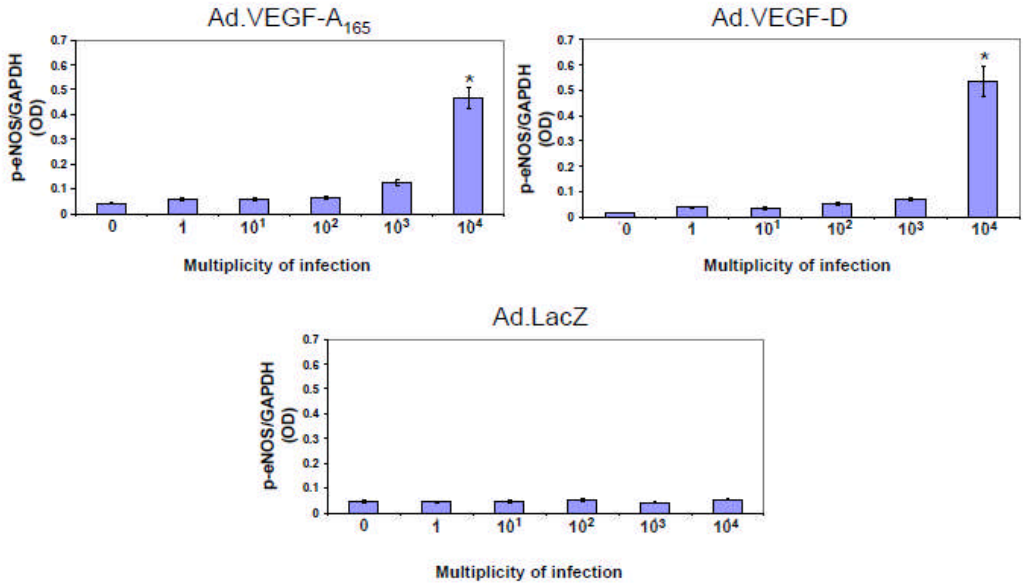

Figure 4.6 - Representative western blots showing an upregulation in eNOS and phospho(p)-eNOS (Ser^{1177}) levels 48 hours after Ad.VEGF (-A_{165}/-D) infection in pregnant sheep UAECs

Pregnant sheep UAECs were grown in culture for up to 4 passages, and then infected at increasing multiplicities of infection (MOIs) with Ad.VEGF-A_{165}, Ad.VEGF-D or Ad.LacZ in 6-well plates. Protein was extracted from infected cells 48 hours later, and assayed for eNOS and p-eNOS (Ser^{1177}) levels by western blotting. (A) An increase in eNOS and p-eNOS (Ser^{1177}) levels with increasing MOI was observed in Ad.VEGF-A_{165} and Ad.VEGF-D infected cells, but not Ad.LacZ infected cells. (B) Densitometric analysis was performed on the eNOS bands using Image J software, after normalizing against the density of GAPDH bands. Results are representative of n=3 independent experiments. (C) Densitometric analysis was performed on the p-eNOS (Ser^{1177}) bands using Image J software, after normalizing against the density of GAPDH bands. Results are representative of n=3 independent experiments. * indicates $p<0.05$ in comparison to the relative density of the corresponding band from uninfected cells (MOI=0) by t-test.

A.

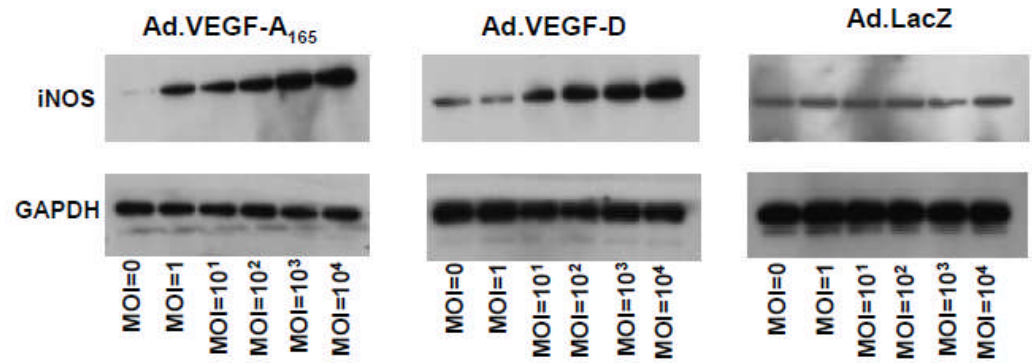

B.

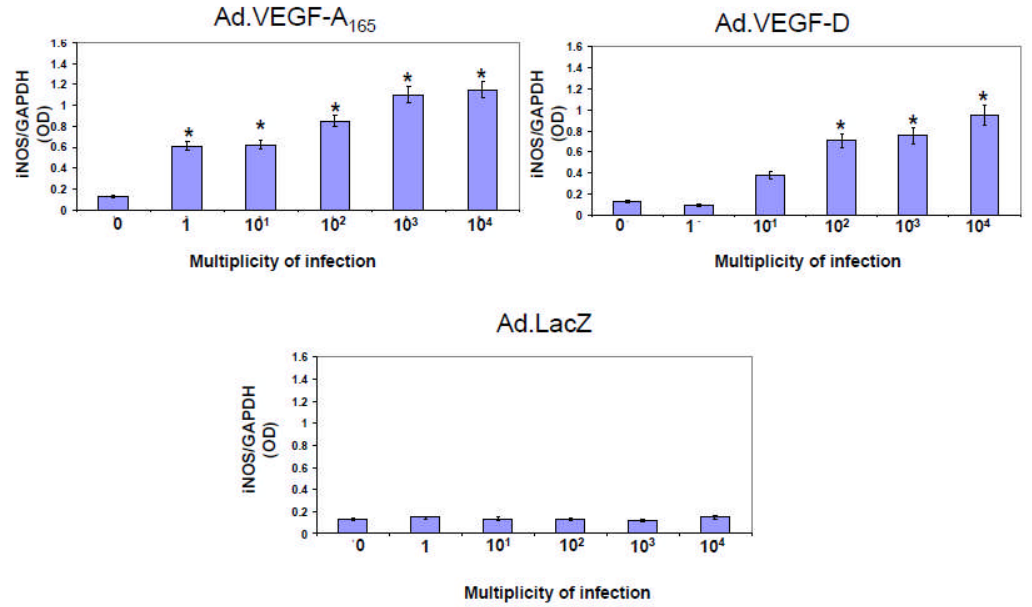

Figure 4.7 - Representative western blots showing an upregulation in iNOS levels 48 hours after Ad.VEGF (-A_{165}/-D) infection in pregnant sheep UAECs

Pregnant sheep UAECs were grown in culture for upto 4 passages, and then infected at increasing multiplicities of infection (MOIs) with Ad.VEGF-A_{165}, Ad.VEGF-D or Ad.LacZ in 6-well plates. Protein was extracted from infected cells 48 hours later, and assayed for iNOS levels by western blotting. (A) A dramatic increase in iNOS levels with increasing MOI was observed in Ad.VEGF-A_{165} and Ad.VEGF-D infected cells, but not Ad.LacZ infected cells. (B) Densitometric analysis

was performed on the iNOS bands using Image J software, after normalizing against the density of GAPDH bands. Results are representative of n=3 independent experiments. * indicates $p<0.05$ in comparison to the relative density of the corresponding band from uninfected cells (MOI=0) by t-test.

In summary, these results demonstrate that adenovirus-mediated over-expression of VEGF-A_{165} and VEGF-D in pregnant ovine UAECs results in an upregulation of eNOS, iNOS and p-eNOS(Ser^{1177}).

4.4 Western blotting for VEGF receptors in adenovirus transduced pregnant ovine UAECs did not lead to any conclusive results

Treatment with VEGF has been shown to upregulate the levels of its receptors (Kremer C et al., 1997;Barleon B et al., 1997a). In order to investigate how the levels of VEGF receptors were altered in ovine UAECs in response to adenovirus-mediated over-expression, we performed western blotting on protein extracts from infected cells with antibodies specific to VEGFR-1, VEGFR-2 and Neuropilin-1. These antibodies (described in Section 2.16) have previously been showed to react very well with sheep tissue by immunohistochemistry on paraformaldehyde-fixed paraffin-embedded tissue sections. However, when these and few other antibodies were used for western blotting on sheep endothelial cell extracts, the results were disappointing. Either there was no band present at all, or there were multiple bands and it was difficult to determine which one was the actual receptor band.

Hence, it was not possible to come to any conclusion about changes in the levels of the VEGF receptors in pregnant sheep UAECs in response to adenovirus-mediated over-expression of VEGF-A_{165} or VEGF-D.

4.5 Discussion

This chapter describes the effects of Ad.VEGF-A_{165}/Ad.VEGF-D gene transfer on UAECs from mid-gestation pregnant sheep. UAECs were isolated by collagenase digestion, grown in culture for up to 4 passages and then infected

with Ad.VEGF-A_{165}, Ad.VEGF-D or Ad.LacZ at increasing multiplicities of infection. I observed an increase in the levels of eNOS, p-eNOS (Ser^{1177}) and iNOS in the Ad.VEGF-A_{165} and Ad.VEGF-D infected cells, but not in the Ad.LacZ infected cells.

At the beginning of these experiments, collagenase digestion was performed for 55 minutes to isolate endothelial cells from pregnant uterine arteries, according to previously published work from Prof. Ian M. Bird's group at the University of Wisconsin (Bird IM et al., 2000;Grummer MA et al., 2009). This is the only other group which has worked extensively on ovine UAECs, and the isolation technique was discussed with them. However, we found that this long incubation time resulted in extensive smooth-muscle cell contamination in our cultures. It was therefore decided to reduce the incubation time to 15 minutes, which is in conformity with other published studies for primary endothelial cell isolation from human vessels (Crampton SP et al., 2007). Using this shorter incubation time, we were able to obtain pure endothelial cell preparations. The discrepancy in the results from the 55 minute incubation time between our studies and those of Bird et al may be on account of differences in technique amongst different operators, or perhaps the use of a different sheep breed.

The different results obtained lead us to use a variety of different techniques to confirm the identity of the cells retrieved from the pregnant sheep uterine arteries. I performed immunostaining with anti-vWF, anti-VE cadherin and anti-β-catenin to confirm the identity of endothelial cells. While anti-vWF is a cytoplasmic stain, the latter two antibodies stain the adherence junctions between endothelial cells. The pattern of staining observed with anti-VE cadherin and anti-β-catenin antibodies had a cobblestone-like appearance, which is a characteristic of endothelial cells. In addition to the immunofluorescent staining, the cells were also treated with fluorescently labeled Ac-LDL. Endothelial cells internalize and degrade Ac-LDL 7-15 times faster than smooth muscle cells via the "scavenger cell pathway" of LDL metabolism. This has enabled the identification of endothelial cells distinctly from smooth muscle cells based on their different metabolism of Ac-LDL (Voyta JC et al., 1984).

Furthermore, serum-deprived cells were challenged with VEGF-A_{165} protein, and the levels of phosphorylated ERK examined. VEGF protein has been shown to upregulate the phosphorylated form of ERK in endothelial cells (Bird IM et al., 2000). I observed this trend in our primary cell cultures. Hence, all these findings confirm that I had obtained pure cultures of endothelial cells.

It is important to note that all experiments in this investigation were conducted at passage four. It has previously been shown that up to this passage, ovine UAECs retain their primary *in vivo* characteristics. This means, expression of key proteins and mRNA, as evident on the day of isolation, are sustained when cells are maintained in culture up to passage four. In addition, levels of eNOS protein and mRNA show higher expression in cells from pregnant ewes than in cells from nonpregnant ewes at the fourth passage, indicating the retention of characteristics present at the time of isolation (Bird IM et al., 2000;Gifford SM et al., 2003). The retention of this primary character is important for the validation of our results.

The UAEC model provided the opportunity to investigate the effects of Ad.VEGF transduction, using multiple MOIs and incubation times post-infection, while harvesting cells obtained from only a few animals. All the experiments described in this chapter were performed on cells obtained from as few as 6 sheep. In addition, I was also able to prepare frozen stocks of cells for future analysis. Carrying out such experiments directly on pregnant sheep would not only be very expensive, but also unethical.

Previous studies have demonstrated that stimulation with VEGF-A_{165} protein for 24 hours results in an upregulation of eNOS and iNOS in cultures of porcine aortic endothelial cells (Kroll J and Waltenberger J, 1998) and HUVECs (Hood JD et al., 1998). VEGF also induces sustained eNOS activation in cultured endothelial cells via PI-3-K dependent Akt-catalysed phosphorylation of eNOS at Ser^{1177}. This is the same site phosphorylated in response to shear stress (Dimmeler S et al., 1999) and phosphorylation of this site renders eNOS active at resting Ca^{2+} concentrations.

However, when uterine artery endothelial cells from pregnant sheep were challenged with VEGF-A_{165} protein for 24 hours, there was no change in the level of eNOS or iNOS (Bird IM, personal communication). A significant short-term increase in NO release was observed in response to VEGF-A_{165} protein stimulation for one hour in cultured pregnant UAECs (Bird IM et al., 2000), but this could occur on account of increased activation of eNOS or enhanced iNOS activity for a short duration, without any change in the levels of these proteins.

In contrast to these findings, we have shown upregulation of eNOS, p-eNOS and the high-activity isoform iNOS in response to chronic VEGF exposure resulting from Ad.VEGF transduction of pregnant sheep UAECs. These results were visible 48 hours post-infection but there was no upregulation in the first 24 hours of infection. This is likely to be because transgene expression peaks during the first 12-24 hours, and downstream signaling pathways are activated/upregulated only following this period.

Levels of NO were not analysed in our study. The reason why we observed a difference in eNOS and iNOS levels in response to adenovirus-mediated over-expression, but the same was not noted by Bird IM, may be on account of the method by which VEGF is presented to the cells, that is, endogenous or exogenous. The prevailing view until recently had been that endothelial cells do not produce VEGF (Maharaj AS et al., 2006). However, in a report by Lee *et al*, it was demonstrated that endogenous VEGF produced by endothelial cells is crucial for vascular homeostasis and maintenance (Lee S et al., 2007). The authors specifically deleted VEGF in the endothelial cells and mature haematopoietic cells of mice by using a vascular endothelial cadherin-driven Cre recombinase system. Using this mouse model, it was shown that in the absence of their own autocrine VEGF, endothelial cells undergo apoptosis, causing collateral damage by blocking vascular traffic and initiating thrombosis. Accumulation of these detrimental changes in the entire vascular network leads to haemorrhage, endothelial cell rupture, neointimal hyperplasia, circulatory collapse and consequent death of 55% of mice deficient in endothelial VEGF by 25 weeks of age. Furthermore, in this mouse model, exogenous administration of VEGF was

unable to compensate for the loss of endogenous VEGF in endothelial cells, despite the fact that signaling through VEGFR-2 activated many cell signaling pathways, including the PI3K/AKT pathway, which is essential for cell survival. Extracellular inhibitors of VEGF (Avastin) are not known to affect the survival of endothelial cells in culture, but a small molecular weight inhibitor of VEGFR-2 (SU4312), which blocks VEGF signaling at the intra-cellular level, has been shown to be cytotoxic.

All these findings support the concept that endogenous/autocrine VEGF signaling is essential for endothelial cell survival, and acts by a pathway that is independent of exogenous/paracrine VEGF signaling.

A recent study has demonstrated that human pregnancies complicated by FGR and early-onset PET are characterized by endothelial dysfunction, which persists not only until term but also several weeks post-partum (Yinon Y et al., 2010). This is manifested as an impaired vasodilatory response to shear-stress. Extrapolating from the studies of Lee *et al* (2007), I believe that a therapy that corrects the underlying endothelial dysfunction at the intra-cellular/endogenous level rather than exogenous growth factor supplementation may be of potential therapeutic benefit in FGR and early-onset PET. Though as already mentioned in the previous chapter, this hypothesis is difficult to test in pregnant human uterine endothelial cells because of the difficulty in procuring this tissue.

One of the limitations of this study was that levels of NO were not measured. Even though upregulation of eNOS, p-eNOS (Ser^{1177}) and iNOS would suggest an increased release of NO, this may not necessarily hold true in every case (as discussed in Chapter 3). It is therefore important to quantify the amount of this gas to get a more reliable estimate of the amount of vasorelaxant effect that can be expected. One of the commonly used techniques for NO estimation is the use of a colorimetric assay, the Griess Method. Additionally, it would be helpful to quantify the amount of VEGF protein released into the cell culture supernatant and also the amount of intra-cellular VEGF, to get an estimate of the amount of protein produced in response to adenovirus infection at the different MOIs. This can be performed by ELISA on cell culture supernatants and UAEC protein

extracts. I have preserved samples of cell culture supernatants and UAEC proteins extracts, and intend to use them for estimation of VEGF and NO levels.

Further experiments in animal models of FGR characterized by utero-placental insufficiency and endothelial dysfunction are warranted, to understand the true mechanism of Ad.VEGF action and to explore the benefits of endogenous VEGF treatment, if any, over exogenous VEGF treatment. To this end, we plan to investigate the effects of adenovirus-mediated VEGF expression in UAECs isolated from sheep with pregnancies complicated by FGR. Work alongside this project is ongoing in the adolescent-overnourished ewe, a sheep model of FGR in which there is mid-gestation reduction in uterine artery blood flow that correlates with the reduction in fetal weight (Wallace JM et al., 2008). Additionally, using siRNA technology we plan to knockdown VEGF expression in pregnant sheep UAECs to mimic a dysfunctional endothelium (likely seen in FGR/PET), and then investigate if Ad.VEGF infection can rescue the anomalous phenotype. The rationale behind these experiments is to find out if Ad.VEGF infection and consequent endogenous VEGF production can reverse the endothelial dysfunction that characterizes utero-placental vascular insufficiency.

In this study, I attempted to measure the levels of VEGF receptors, VEGFR-1, VEGFR-2 and neuropilin-1 in protein extracts from the infected UAECs. However, we did not get any conclusive results in this study, due to the poor quality of the western blots. Even though previous studies have shown the presence of VEGFR-1 and VEGFR-2 in UAECs (Grummer MA et al., 2009) by western blotting, we were unable to get clear results. It may be on account of an inferior batch of antibodies that we used, or perhaps our choice of lysis buffer for protein extraction, which is different to what was used by Grummer MA (2009). I believe, however, the latter is unlikely to have played any role as our western blots for eNOS, p-eNOS (Ser^{1177}), iNOS and GAPDH were clean (showing only a single band at the correct molecular weight). Nevertheless, we plan to repeat this experiment using a fresh batch of antibodies and the same lysis buffer as was used by Grummer MA. Another alternative to circumvent this problem would be to extract RNA from the transduced UAECs, and use it for RT-PCR with primers

specific for the different VEGF receptors. In this way, we would be able to investigate changes in VEGF receptors at the messenger level, using a very sensitive and reliable technique.

In these studies, it was noted that even at very high MOIs such as 10^4, the infection efficiency only reached 90% and never 100% as would be anticipated at this vector dose. It is unusual to have such a low infection efficiency with such a high titre of adenoviral vector. It is possible that the titre of the virus provided was over-estimated by Ark Therapeutics Ltd., which produced the virus, or that a number of freeze-thaw cycles had been performed on the virus stocks, which can lead to a reduction in infection efficiency. The titres were not re-checked in our lab before experimentation, and in the future, this would be important to do.

The *ex vivo* experiments on uterine artery vascular reactivity using an organ bath revealed that in addition to the NOS pathway, EDHF plays an important role in the bradykinin-mediated endothelium-dependent relaxation in pregnant sheep. However, the very identity of EDHF is unknown and there are no known antibodies to recognize it currently. Hence, it was not possible to perform any western blot analysis to investigate changes in EDHF levels in response to Ad.VEGF infection in the UAEC model. But in future experiments, we intend to measure the levels of small Ca^{2+} activated potassium (SK) channels by western blotting on UAEC protein extracts. These channels mediate the effects of EDHF in blood vessels and it would be of interest to see if there is any difference in their level in response to chronic VEGF exposure.

In conclusion, I have demonstrated that Ad.VEGF transduction leads to an upregulation in eNOS, p-eNOS and iNOS levels in pregnant ovine UAECs. This may be one of the important mechanisms by which VEGF is able to mediate the beneficial outcomes on uterine artery vascular reactivity and uterine blood flow. Exogenous administration of VEGF protein has been shown to have no effect on the different NOS isoforms analysed. It is possible therefore, that sustained local endogenous over-expression of VEGF may be necessary to increase NOS levels in the uteroplacental vasculature. Future experiments to investigate the receptors involved and effects of Ad.VEGF infection on UAECs from an FGR sheep model

may give insights into the potential of VEGF gene therapy to reverse utero-placental insufficiency, and its mechanism of action.

Chapter 5

Results: Optimisation of gene transfer to the utero-placental circulation of pregnant guinea pigs

The work described in the previous chapters has shown that local adenovirus-mediated over-expression of VEGF-A_{165} in the uterine arteries of pregnant sheep brings about a significant increase in UABF. The effects appear to be mediated by changes in vascular reactivity, eNOS upregulation and neovascularization. It is well known that there exists a direct positive co-relation between UABF and fetal size and weight (Lang U et al., 2003). A compromised utero-placental circulation is known to limit the rate of fetal growth and produce either SGA or FGR infants, but the converse of this has not been proven. Hence, the next phase of this investigation logically progresses to study if an increase in blood flow can actually translate into an increase in fetal growth. These experiments were carried out in guinea pigs – an appropriate small animal model for human pregnancy. The advantage of using guinea pigs is that they have a haemomonochorial placentation, which is the most similar to human placentation in an animal model, with the exception of some non-human primates. Thus, experimental results obtained from pregnant guinea pigs as well as toxicology studies conducted in this species are likely to hold more relevance for clinical translation. Furthermore, they have a relatively long gestation (65 days) for a small animal, in contrast to mice, rats and rabbits. This gives the opportunity to administer therapy at mid-gestation, and study the effects of treatment for 30-35 days post-administration.

The following chapter describes the results of pilot experiments for this project, firstly to set up the FGR model in pregnant guinea pigs and secondly to

develop a method of targeting gene therapy to the utero-placental circulation of pregnant guinea pigs. Most of these optimization experiments were carried out in normal pregnant guinea pigs rather than nutrient-restricted ones, because they are easier and quicker to obtain than FGR guinea pigs.

5.1 Timed mating of guinea pigs yields a good conception rate when females are left with males for 3 nights

The model of FGR pregnancy that we chose to adopt was the peri-conceptual under-nutrition model in guinea pigs (Roberts CT et al., 2001a). Previous work developing this model showed that when males were left in the same cage as nutrient restricted females for a single night (on the day the vaginal membrane was found to be ruptured), conception rates were in the range of 50-60% (Roberts CT, personal communication).

Initially we left males in with females only for a single night (on the day the hymen was found to be open) so that mating could be timed accurately. Unfortunately this resulted in a very low conception rate (Table 5.1) in our study cohort. We considered that the most likely cause was that mating was occurring outside the time period when we deemed the guinea pigs to be in estrus phase. Even though the hymen remains open for 2-3 days, the estrus phase lasts only 8-12 hours in the night, during which the female guinea pig is receptive to the male.

Table 5.1 – Conception rate in female guinea pigs left with a male for a single night and 3 nights

Time male left in with female	Conception rate
Overnight	2 out of 7 (28.57%)
3 days	6 out of 10 (60%)
3 days with new boar	7 out of 10 (70%)

After discussion with Dr. Claire Roberts and her research group, Adelaide University, South Australia, who originated this particular FGR model, it was decided that the males be left in with the females for a longer period of time, to ensure they were together during the receptive phase. This change boosted conception rates as shown in Table 5.1. We have further improved the conception rate in normal guinea pigs up to 70% in the most recent animals, by buying in some new boars (Table 5.1).

5.2 Nutrient-restricted guinea pigs have a lower conception rate than guinea pigs on ad lib diet

To develop the nutrient restricted diet that is known to generate pregnant guinea pigs with FGR according to the protocol of Roberts CT et al (2001), the daily dietary intake of normal pregnant guinea pigs was first determined. We used virgin Dunkin Hartley guinea pigs at 5-7 months of age, that weighed at least 800 grams. Guinea pigs below this threshold weight showed a tendency towards rapid weight loss when put on the nutrient restricted diet and nil conception rate. The daily food intake and body weights of normal guinea pigs (n = 10) were measured daily for 1 month before conception. Animals were then left in with the male for 3 days, after which (assuming the animal got pregnant), the body weight and food intake were measured throughout the length of gestation.

To create the FGR model, guinea pigs were nutrient restricted to 70% of the normal intake for 4 weeks before conception until day 34 of pregnancy, and then to 90% of the normal intake until the end of gestation. Normal pregnant animals were found to be consuming an average of 0.6g of feed daily per 100g body weight before and during early pregnancy. Animals on the growth restricted diet were therefore fed 0.42g of feed daily (70%) per 100g body weight when put on the under-nutrition regime.

Initially guinea pigs on a nutrient restricted diet failed to get pregnant, even after being placed in the same cage as a male for over one month (n=6). However, with the improved conception rates in normal pregnant animals, leaving

males in with females for a longer duration during estrus and bringing in new males into the breeding programme, we have currently started obtaining FGR pregnancies with a success rate of 60-70%. This compares well with previously published results (Roberts CT et al., 2001a), wherein the success rate of FGR guinea pig pregnancy was 60%. Guinea pigs maintained on an *ad lib* diet generally have conception rates >90%.

Guinea pigs that failed to get pregnant after being put on the nutrient restricted diet were maintained on the same diet for a further 2-4 weeks (until the next 1-2 estrus cycle) and re-mated. If they still failed to conceive after three occasions to mate, they were returned to a normal diet for 4-6 weeks until they regained their original baseline body weight, and then made to enter the under-nutrition regime again.

5.3 It is possible to confirm pregnancy in guinea pigs by ultrasound scanning

Guinea pigs were first scanned at 18-20 days post-conception, while restrained by a trained animal technician, to confirm pregnancy. However, at this gestational age, we were able to see a fetus and confirm pregnancy status in only one-third of all animals scanned that were actually pregnant (n=12). When scanned at a slightly later time point, that is, 24-25 days post-conception, we were able to clearly see a fetus in all guinea pigs that were actually pregnant. Hence, it was decided to scan all guinea pigs at this time point to confirm pregnancy.

In the initial scan during which the guinea pig was awake and restrained by an animal technician, it was only possible to confirm pregnancy and determine fetal number. Additionally, measurements of BPD could be taken to confirm gestational age, by comparing with published data (Turner AJ and Trudinger BJ, 2000). It was often not possible to perform a more detailed ultrasound examination and collect other fetal measurements in awake guinea pigs, as they became restless quickly. These additional measurements (abdominal circumference, femur length, placental thickness and placental diameter) could however be easily obtained under general anaesthesia, at the time of vector

injection for all guinea pigs. Initially, we also collected measurements of femur length for the fetal guinea pigs, but because of the difficulty in accurately identifying the femur, this parameter could not be acquired for all guinea pigs.

5.4 Growth-restricted guinea pigs have smaller abdominal circumferences and show a trend towards brain sparing compared to normal guinea pigs

Sonographic measurements of biparietal diameter, occipito-snout length and abdominal circumference were compared between normal and growth-restricted guinea pigs at 45 days gestational age (Figure 5.1). The results of these are summarized in Table 5.2.

A.

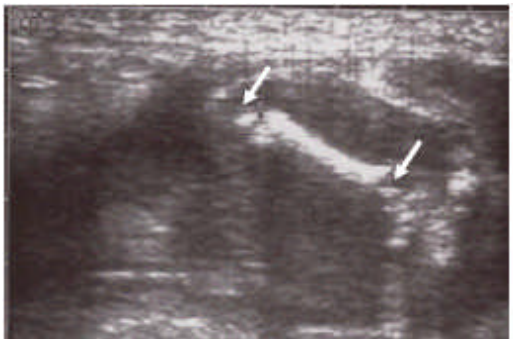

B.

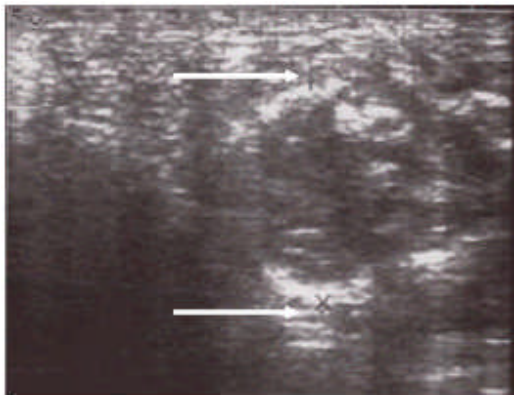

C.

D.

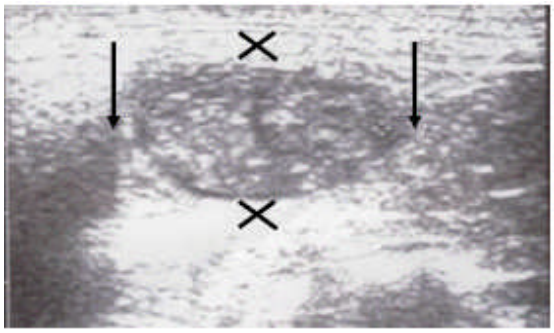

Figure 5.1 – Representative images of fetal guinea pig ultrasound measurements at 45 days of gestation.

'A' is a representative picture of femur length; measurement was taken between the two arrow heads. 'B' is a representative picture of biparietal diameter; measurement was taken between the two arrow heads. 'C' is a representative picture of abdominal circumference; measurement of the abdominal perimeter was taken. 'D' is a representative picture of the placenta; measurement between the arrow heads represents placental diameter, while measurement between the crosses represents placental thickness.

Table 5.2 – Sonographic estimation of guinea pig fetal measurements at 45 days gestational age (range 44-47 days)

Sonographic measurement	Diet		p (unpaired t-test)
	Normal *ad lib* (Mean±SD)	Nutrient-restricted (Mean±SD)	
Biparietal Diameter (BPD, mm)	16.06±0.75 (n=13)	15.53±0.70 (n=10)	0.08
Occipito-Snout Length (OSL, mm)	27.95±2.09 (n=10)	25.98±3.31 (n=9)	0.14
Head Circumference (HC, mm)	69.09±4.44 (n=10)	65.17±4.11 (n=9)	0.03
Abdominal Circumference (AC, mm)	84.25±9.25 (n=15)	71.21±11.09 (n=10)	0.004
BPD/AC	0.19±0.02 (n=13)	0.21±0.01 (n=10)	0.002
OSL/AC	0.33±0.05 (n=10)	0.36±0.04 (n=9)	0.25
HC/AC	0.82±0.09 (n=10)	0.92±0.08 (n=9)	0.07

To summarize, fetuses of guinea pigs on a nutrient restricted diet have a significantly smaller abdominal circumference at 45 days gestational age than fetuses of guinea pigs on an *ad lib* diet. BPD and OSL were also reduced in growth-restricted fetal guinea pigs, though the difference did not reach significance with the animal numbers that were analysed to date. There was a significant reduction in the head circumference of nutrient restricted guinea pigs, while the ratios of head to abdominal circumference demonstrated a trend towards being increased in the fetuses of FGR guinea pigs. This suggests that maternal nutrient restriction results in the onset of brain sparing in fetal guinea pigs.

5.5 Fetuses from guinea pigs on the nutrient-restricted diet weigh less than fetuses from guinea pigs on an ad lib diet

During the course of this Ph.D., 7 (out of 10) guinea pigs maintained on the nutrient restriction diet to assess the degree of growth restriction achieved got pregnant. Their fetuses were delivered at 44-47 dpc, and the fetal weights were compared with the weights of fetuses born to sows on an *ad lib* diet, at the same gestational age. The average fetal weight in the *ad lib* group was 35.05$\pm$3.75 g (n=16), while the average fetal weight in the nutrient restricted diet was 20.54$\pm$1.16 g (n=22), p=0.01 (unpaired t-test). Thus, the fetuses of guinea pigs on a nutrient restricted diet were 41.4% lighter than those of sows on an *ad lib* diet. This compares well with previous data (Roberts CT et al., 2001a), which achieved a 29% reduction in fetal weight at 30 days gestation and 35% reduction in fetal weight at 60 days of gestation. The difference in fetal weights between nutrient-restricted and control groups were not analysed at 45 days of gestation by this author.

5.6 Fetuses from guinea pigs on the nutrient-restricted diet have a smaller placenta than fetuses from guinea pigs on an ad lib diet

Sonographic measurements of placental dimensions (thickness and diameter) and placental weights at post-mortem were compared between the nutrient-restricted and control groups. The placental thickness was taken at its narrowest diameter for consistency, and the placental diameter was measured in the same view. It was not possible to accurately obtain a view of the placenta in a 3rd plane due to the large number of fetuses present, and the relatively large size of the ultrasound probe.

In animals that had an ultrasound examination at approximately 45 days of gestation (range 44 to 47 days), the placental thickness in the nutrient restricted group showed a trend to being smaller than the *ad lib* group. There was no,

significant difference in the placental diameters or placental areas at 45 days of gestation (Table 5.3).

Table 5.3 – Sonographic placental measurements in normal and FGR guinea pigs at 45 days (range 44-47 days) gestational age

Measurement	Group		p (unpaired t-test)
	Normal (Mean±SD)	Nutrient-restricted (Mean±SD)	
Placental thickness (mm)	13.00±1.41 (n=12)	9.18±0.97 (n=8)	0.056
Placental diameter (mm)	23.65±1.21 (n=12)	22.24±0.88 (n=8)	0.399
Placental area (mm^2)	439.06±127	388.27±83.74	0.477

The placentae of animals that had a post mortem examination at 45 days of gestation were significantly lighter in guinea pigs on the nutrient-restricted diet (3.56±0.63g, n=10) than the *ad lib* diet control group (4.72±0.91, n=22), p=0.02 (unpaired t-test).

During laparotomy surgery, it was observed that the size of the uterine and radial arteries were smaller in nutrient-restricted guinea pigs compared to normal animals. The number of radial arteries supplying each placenta was also lesser in the nutrient restricted guinea pigs.

5.7 Gene Targeting to the Utero-Placental Circulation of Pregnant Guinea Pigs

5.7.1 The guinea pig uterine artery can be injected reliably only under a dissection microscope

Initial attempts at injecting the uterine artery were carried out under direct vision. However, the small size of the artery (300-400μm diameter, Figure 5.2) and the large amount of fat that surrounded it made it difficult to inject it reliably

and repeatedly. The purchase of a dissecting microscope allowed better visualisation of the uterine arteries of the guinea pig. By elevating the fat pad on either side of the cervical canal and by shining a strong light through it, the course of the uterine artery could be seen within the fat pad as a red line, before it gives off the first radial artery branches. The uterine artery could then be seen running more superficially within the fat pad giving off radial artery branches to the 3 to 5 fetal guinea pigs within the uterus. Once the course of the lower uterine artery was identified, the fat pad was opened under an operating microscope to improve visualization. The right uterine artery runs more towards the anterior aspect of the fat pad making an anterior approach best. The left uterine artery runs more in the posterior aspect of the fat pad, therefore on the left side the fat pad was turned over to expose the posterior aspect and the uterine artery then dissected out. Intra-arterial injections with the help of a dissecting microscope have proven to be more accurate and reliable, as compared to injections under direct vision.

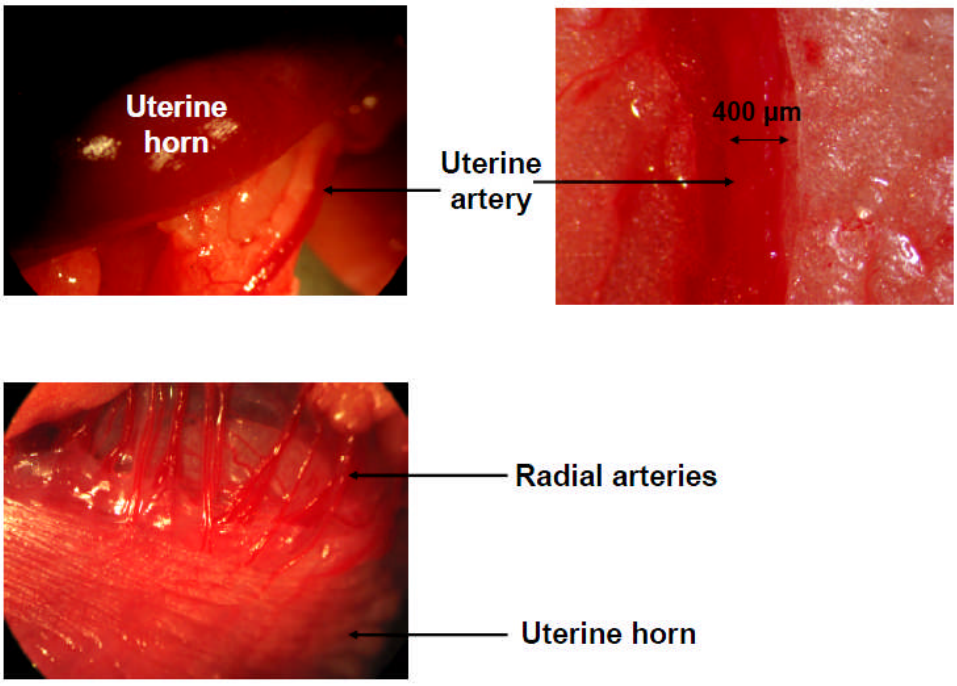

Figure 5.2 - Uterine and radial arteries in pregnant guinea pig at 45 days of gestation

5.7.2 The uterine arteries are more easily accessible at 45dpc as compared to 30dpc

In the initial phase of this study, surgeries on guinea pigs were performed at 30dpc (mid-gestation). However, the smaller size of the uterine arteries (150-250µm) made it technically challenging not only to find them within the fat pad, but also insert a needle (34 Gauge) within them to inject the vector. Hence, it was decided to perform the optimization surgeries at 45dpc (3/4 gestation) when the arteries are slightly larger (300-400µm, Figure 5.2). It was planned to operate on 30dpc animals after having gained some experience and skill at successfully injecting 45dpc animals.

5.7.3 Morbidity and mortality in pregnant guinea pigs after surgery is low

With experience we identified factors that improved fetal survival and reduced maternal mortality. These include keeping the time for sonographic measurement of fetuses to a minimum, rapidly accessing the abdomen, minimising the time needed to identify and injecting the vessels, avoiding removing the pregnant horns from the abdominal cavity, keeping the animal warm throughout surgery and during recovery, minimizing blood loss and good analgesia.

Deaths occurred initially with very long anaesthetic times (> 4 hours) due to difficulties in identifying the uterine artery, and while developing the best set up for the operating microscope. More recently, deaths have occurred when there were multiple attempts to inject the internal iliac artery associated with excessive blood loss (Table 5.4). At post mortem examination after maternal death, large blood clots over the injection sites were identified, with associated peritonitis. There is minimal bleeding after 3 minutes of occlusion over the injection site whether it is the uterine artery or the internal iliac artery. However, in cases of excessive bleeding, a longer occlusion time is required which is associated with a higher maternal and/or fetal mortality rate.

All maternal mortalities have been as a direct consequence of the surgery, either during the surgery (n=2) or within the next 24 hours (n=3). There have been no deaths attributed to the anaesthesia, and no problems with aspiration of stomach contents, or the development of diarrhea, which is a common finding if antibiotics are used. Recovery of the pregnant guinea pigs is good, and miscarriage if it occurs, is usually by day 2 post-surgically. There have been no hernias observed.

Table 5.4 - Maternal and fetal survival after surgery

Injection route	Maternal survival	Fetal survival	Comments
Uterine artery near cervix	6 out of 8	No fetal loss in mothers that survived.	Early experiments. Complicated by long anaesthetic time (>4 hrs), excessive blood loss and difficulty visualising uterine artery
Uterine artery injection or external transduction	5 out of 6	1 mother died during a 4 hour surgery Other mothers all had live fetuses at PM	Shorter anaesthetic time when extrernal gene transfer used
Internal iliac injection	4 out of 6	No fetal loss in mothers that survived.	Deaths occurred when the heating pad failed, when there was excessive blood loss and long anaesthetic time (>4 hrs)
Pluronic gel Administration	6 out of 6	One mother miscarried due to excessive uterine manipulation. No fetal morbidity or mortality in other mothers.	Simple and straightforward technique, can be performed relatively quickly compared to other techniques.

5.8 Intra-arterial injections into the uterine arteries

5.8.1 Intra-arterial injections into the uterine arteries are technically challenging even at 45dpc

We attempted Ad.LacZ injection into 16 uterine arteries from 8 pregnant guinea pigs but were only successful in 7 vessels (Table 5.5), i.e. 44% of attempts. The low success rate is primarily for two reasons – the uterine artery is deeply embedded in fat and is unsupported. A successful injection was defined as the vector seen moving down the vessel during injection. Failed injections were

due to vector being inadvertently injected into the vessel wall, leaking out of the vessel or coming out of the other side of the vessel, opposite the injection site. The dose of vector injected per artery was $1x10^{10}$ vp. The volume ranged from 500µl to 1.3ml and the duration of injection ranged from 90-112 seconds. Following injection, the vessel was occluded with a vascular clip for up to 3 minutes. If haemostasis was not achieved, adrenaline was administered to the vessel externally. Post mortem examination was carried out 2 to 5 days after injection, the earlier time points were due to unexpected maternal death or miscarriage.

Table 5.5: Uterine artery injection attempts in pregnant guinea pigs fed *ad lib*

GP no.	GA (d)	Needle size (Gauge)	Number of injection attempts per uterine artery		Volume injected (µl)	Occlusion time if successful injection (min)	Adrenaline used	Outcome
			failed	success				
231	33	31	R(2), L(4)	R(1), L(0)	500	5.5 min	Yes	Maternal death during surgery due to long anaesthetic time >4h
230	35	31	R(4), L(4)	0	500	-	No	Fetuses alive at PM (3d)
173	43	31	R(1), L(4)	R(1), L(0)	500	7 min	Yes	Fetuses alive at PM (4d)
300	45	31	R(2), L(4)	R(1), L(0)	500	5 min	Yes	Fetuses alive at PM (4d)
217	43	31	R(4), L(2)	L(1), R(0)	500	9 min	Yes	Maternal death within 24h
218	45	34	R(3), L(3)	0	500	5 min	No	1 out of 3 fetuses alive at PM (5d)
297	49	34	R(3), L(3)	R(1), L(1)	1000	8 min (L), 9.5 min (R)	Yes	Fetuses alive at PM (4d)
298	49	34	R(2), L(4)	R(1), L(0)	1300	5 min	Yes	Fetuses alive at PM (4d)

Results are presented in the order that the experiments were performed. GP: guinea pig; d: days; R: right uterine artery; L: left uterine artery; h: hours; d: days

In summary, injection of uterine arteries is more successful when using the smaller 34 Gauge needle, later in gestation and the right side is easier than the left. It was only successful in 44% of attempts, and only on both sides in 1 animal. Fetal survival was good.

5.8.2 Intra-arterial injection into the uterine artery leads to limited transgene expression in the utero-placental circulation

Injection of Ad.LacZ into the uterine arteries resulted in staining of the cervical end of the uterine arteries, the cervical end radial arteries and the radial arteries supplying fetuses in the middle of the uterus (Table 5.6 and Figure 5.3). The maternal liver and uterus were also stained. The ovarian end uterine and radial arteries were not stained.

The uterine arteries and the radial arteries to the first guinea pig fetus were transduced when only 500 μl of vector was injected, but larger volumes (1.0 ml) were needed to reach the radial arteries supplying the middle fetus (if there are 3 on one side). However, even the maximum volume that was injected (1.3 ml) was not successful in transducing the ovarian end of the uterine artery and ovarian end radial arteries.

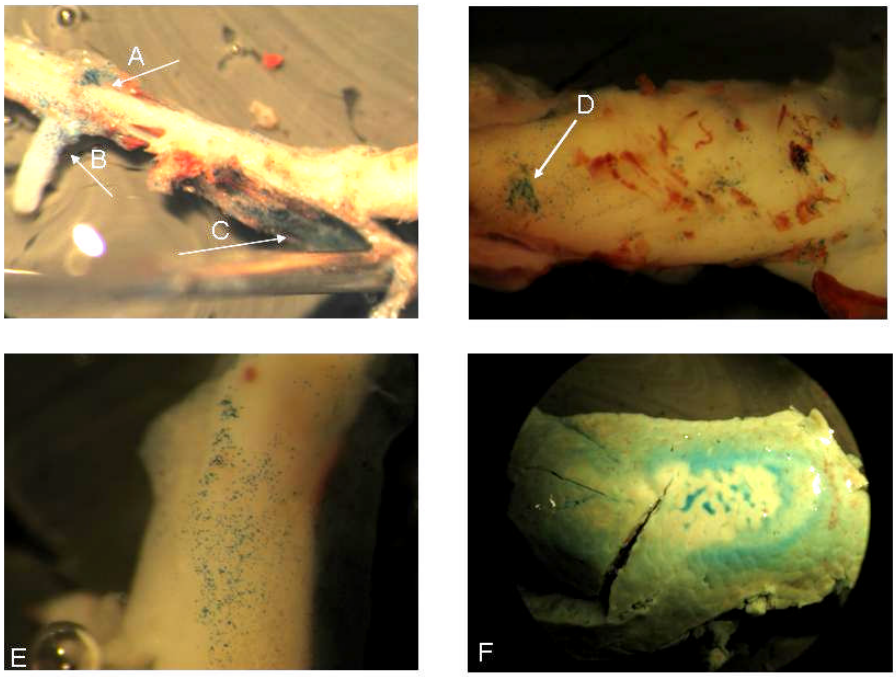

Figure 5.3 – X-gal staining of guinea pig tissue after intra-arterial administration of Ad.LacZ into the uterine arteries.

Pregnant guinea pigs received an injection of Ad.LacZ into their uterine arteries at 45 days of gestation. Maternal and fetal tissues were harvested at post-mortem examination 2-5 days later and analysed by X-gal staining. A and B – Positive expression distal to the site of injection and along the origin of a radial artery; C – positive expression on the inside wall of the uterine artery; D – positive staining on the external surface of a uterine artery; E – positive staining on the external surface of a radial artery; F – strong β-galactosidase expression in the liver.

Hence, intra-arterial administration of vector into the uterine arteries of normal pregnant guinea pigs only leads to limited/partial transduction of the utero-placental circulation that is confined to areas closest to the injection site.

Table 5.6 : Transgene expression after intra-arterial injection into the uterine artery

GP no.	GA (d)	Delivery method	Vector volume (µl)	X gal staining										
				Ut Art		Rad Art		Placenta	Fetus	Maternal liver	Uterine horn		Fat of uterus	Other tissues
				Cx end	Ov end	Cx end	Ov end				Cx end	Ov end		
231	33 $	Ut Art	500	-	-	-	-	-	-	-	-	-	-	-
230	35	Ut Art	500	-	-	-	-	-	-	+	-	-	-	
173	43	Ut Art	500	++	-	+	-	-	-	++	+	+	++	Uterine vein
300	45	Ut Art	500	+++ +	+	+++ +	-	-	-	+++	++	++	++	Uterine vein
217	43 $	Ut Art	500	-	-	-	-	-	-	-	-	-	-	-
218	45	Ut Art	500	-	-	-	-	-	-	++	+	+	+	-
297	49	Ut Art	1000	+++	-	+	-	-	-	+++	++	+	++	Uterine vein
29	49	Ut Art	1300	+++	-	+	-	-	-	+++	++	++	++	-

GP = Guinea pig; $ GP died during or shortly after surgery; GA = gestational age at administration; d = days; Ut Art = Uterine artery injection; Cx=cervical, Ov=ovarian, number of '+' signs indicates intensity of staining

5.9 External administration of Ad.LacZ to the uterine arteries of pregnant guinea pigs is technically straightforward

In those cases where repeated attempts to inject the uterine artery vessel were unsuccessful, a decision was made to study the effect of external gene transfer to the uterine and radial arteries (Table 5.7). The vector was injected into the fat pad alongside the uterine artery (n=6 vessels). In cases where the vessel could be completely exposed, the vector was dribbled upon it as it lay in the fat pad (n=2 vessels). The vessels were left to transduce for 5 minutes. Vector was also dribbled onto the radial arteries as they ran within their mesentery and left for 5 minutes before the uterus was subsequently mobilized. No vessel injection or

occlusion was used in this technique, and hence it was much less traumatic and easier to perform. We did observe however, that the vector ran off from the intended vessels which was likely to lead to widespread gene transfer rather than that local to the uteroplacental circulation.

Table 5.7: External gene transfer to uterine and radial arteries.

GP no.	GA (days)	Needle size (Gauge)	Uterine artery transduction		Volume applied to vessel (μl)
			External administration	Injection alongside vessel	
231	**33**	**31**	**na**	**L**	**500**
230	**35**	**31**	**na**	**L, R**	**500**
173	**43**	**31**	**L**	**na**	**500**
300	**45**	**31**	**L**	**na**	**500**
218	**45**	**34**	**na**	**L, R**	**500**
298	**49**	**34**	**na**	**L**	**1000**

All animals had a failed injection attempt into the uterine arteries before external vector administration was tried. na: not attempted: The side not transduced by external administration of the vector had been successfully injected by the intra-arterial route.

In summary injection alongside the vessel or dribbling the vector onto the exposed vessel was technically easy to perform. It was also probably associated with a lower morbidity and mortality when compared to intravascular injection, although this aspect of the technique could not be examined here.

5.9.1 External administration of Ad.LacZ to the uterine and radial arteries of pregnant guinea pigs leads to high expression levels, but undesirable spread of transgene expression systemically

External administration of the vector to the uterine and radial arteries resulted in positive expression in all the vessels onto which the vector was dribbled (Figure 5.4). All radial arteries expressed β-galactosidase. There was also positive β-galactosidase expression in the fat surrounding the uterine arteries, the maternal liver and uterus (Figure 5.5). There was slight staining in the placentae but none in the fetuses.

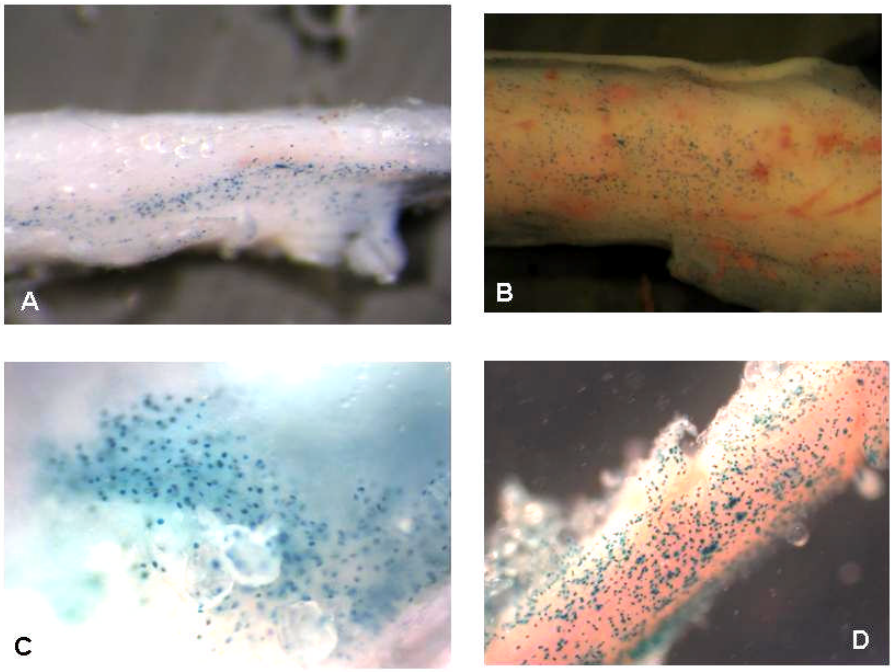

Figure 5.4 – Transgene expression in the uterine and radial arteries of guinea pigs after external administration of Ad.LacZ in PBS

The uterine and radial arteries of pregnant guinea pigs were transduced with Ad.LacZ at 45 days of gestation by external administration. Maternal and fetal tissues were harvested at post-mortem examination 2-7 days later and analysed by X-gal staining. A - Positive β-galactosidase expression in a uterine artery after Ad.LacZ was injected into the fat pad alongside the uterine artery; B – Positive transgene expression in a uterine artery after Ad.LacZ was dribbled onto the exposed vessel; C – Positive transgene expression on the inner luminal surface of a uterine artery after vector was applied externally; D – positive transgene expression on a radial artery after Ad.LacZ was dribbled on it.

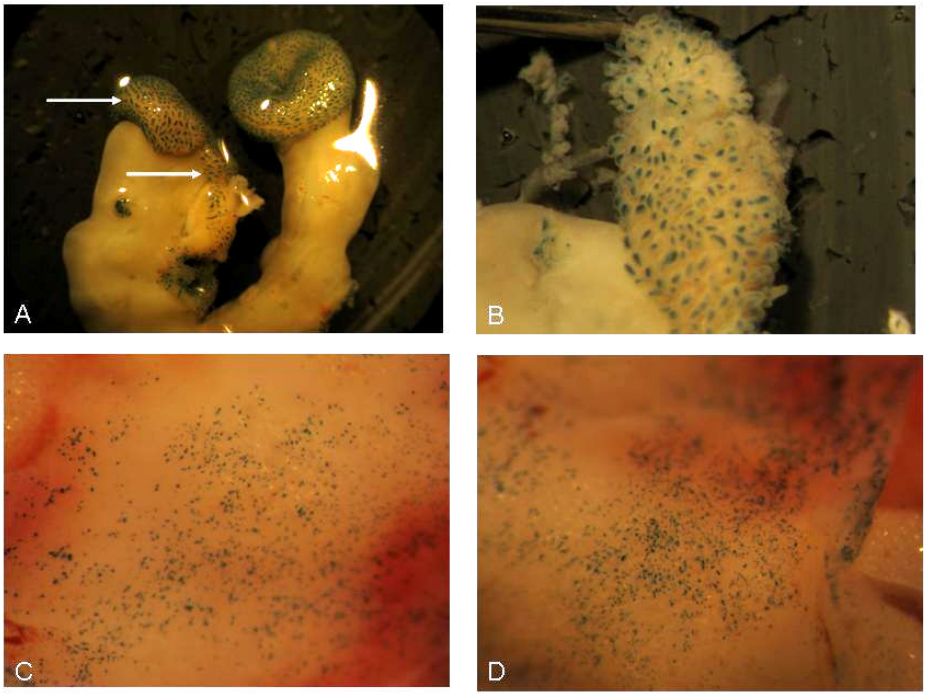

Figure 5.5 – Transgene expression in maternal tissues after external administration of Ad.LacZ to the utero-placental vasculature

The uterine and radial arteries of pregnant guinea pigs were transduced with Ad.LacZ at 45 days of gestation by external administration. Maternal and fetal tissues were harvested at post-mortem examination 2-7 days later and analysed by X-gal staining. A and B – Transgene expression in the uterine horns; C and D – Transgene expression in the fat pad surrounding the uterus

The outcome of external administration of vector to the uterine and radial arteries has been summarized in Table 5.8.

In summary, external administration of the vector to the uterine artery resulted in high levels of transgene expression in the uterine and radial arteries, but there was also viral spread and expression in the liver.

Table 5.8 : Transgene expression after external administration of vector to the uterine arteries

GP no.	GA (d)	Delivery method	Vector volume (µl)	X gal staining										
				Ut Art		Rad Art		Placenta	Fetus	Maternal liver	Uterine horn		Fat of uterus	Other tissues
				Cx end	Ov end	Cx end	Ov end				Cx end	Ov end		
231	33 $	External	500	-	-	-	-	-	-	-	-	-	-	-
230	35	External	500	+	-	+	-	-	-	+	-	-	++	-
173	43	External	500	++	-	++	++	+	-	++	++	++	++	-
300	45	External	500	++	-	+++	+++	+	-	+++	++	++	++	-
218	45	External	500	+	-	+	-	-	-	++	+	+	++	-
298	49	External	1300	++	-	++	+	-	-	+++	+	+	++	-

GP = Guinea Pig; $ GP died during or shortly after surgery; GA = gestational age at administration; d = days; Cx = cervical; Ov = ovarian The number of '+' signs indicate the intensity of staining.

5.10 Internal Iliac Injections

5.10.1 Vector injection into the internal iliac artery is more straightforward than uterine artery injection

The internal iliac artery gives off the uterine artery as one of its distal branches. Hence, we hypothesized that intra-vascular administration of vector into the internal iliac artery would lead to transduction of the utero-placental circulation, while being technically more easily achieved. We attempted to inject the internal iliac arteries of 6 normal pregnant guinea pigs (12 vessels) at 45dpc and achieved successful injection of both the internal iliac arteries of all 6 animals (Table 5.9).

Table 5.9 - Injection of the internal iliac artery: feasibility and survival (45 – 47 days of gestation)

GP no.	Needle Gauge	Number of attempts per internal iliac vessel		Volume injected (μl)	Occlusion time if successful injection (min)	Adrenaline used	Outcome
		failed	success				
301	34	L(2), R(3)	L(1), R(1)	1000	2.5 min	Yes	Fetuses alive at PM (4d)
302	34	R(2), L(2)	R(1), L(1)	R-400 L-1000	8 min	Yes	Fetuses alive at PM (4d)
94	34	R(3), L(4)	R(1), L(1)	1500	5 min	Yes	Fetuses alive at PM (3d)
331	34	R(3), L(5)	R(1), L(1)	1500	6.5 min	Yes	Fetuses alive at PM (3d)
329	34	R(5), L(6)	R(1), L(1)	1500	6 min	Yes	Maternal death within 24 hours of surgery
330	34	R(6), L(6)	R(1), L(1)	1500	5 min	Yes	Maternal death within 24 hours of surgery

GP: Guinea pig; R: right uterine artery; L: Left uterine artery; d: days

As can be inferred from Table 5.9, the internal iliac artery injection was more easily achieved than uterine artery injection, and we were able to inject the vessel in all animals, eventually. Larger volumes of vector needed more attempts to inject the vessel since the needle became dislodged from the vessel during the 1-2 minutes that were needed to deliver the volume intended, and a repeat injection was often needed. Maternal survival was generally good, but two of the four guinea pigs that received 1500 μl vector died. This is probably related more to difficulties in injecting the vessel, since 5 or 6 attempts were needed on each side to ensure that the full volume of vector was injected. This resulted in bleeding rather than vector toxicity. Fetal survival was good in all other cases.

5.10.2 Injection of vector into the internal iliac artery does not transduce the utero-placental circulation

Administration of Ad.LacZ into the internal iliac artery resulted in positive X-gal staining in the internal iliac artery, the pelvic side wall muscles, bladder, cervix and the maternal liver. There was no expression at all in the uterine/radial

arteries, the fat around the uterine arteries, the placentae or fetuses. Increasing the volume of vector injected did not lead to positive expression in the uterine artery. (Figure 5.6, Table 5.10)

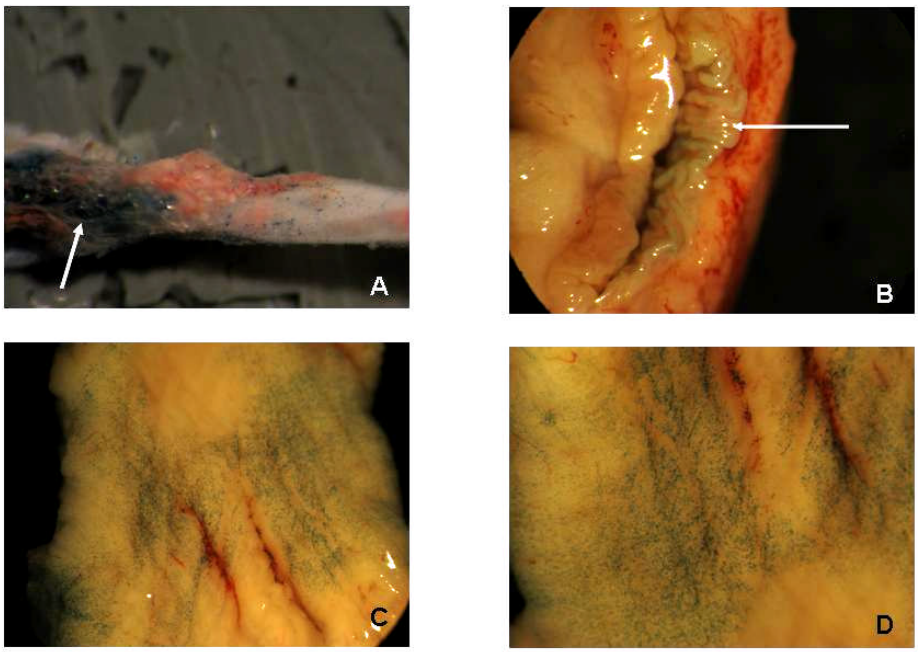

Figure 5.6 - Transgene expression in maternal tissues after intra-arterial administration of Ad.LacZ in the internal iliac arteries

Pregnant guinea pigs received an injection of Ad.LacZ into their internal iliac arteries at 45 days of gestation. Maternal and fetal tissues were harvested at post-mortem examination 3-4 days later and analysed by X-gal staining. A – Transgenic protein expression at the site of vector injection but decline in expression distally; B – Transgenic protein expression in the urinary bladder; C and D – Staining of pelvic side wall muscles from the left (C) and right (D) sides. The utero-placental blood vessels showed no positive β-galactosidase expression (not shown).

Table 5.10: Gene transfer results after internal iliac artery injection

GP	GA (d)	Vector volume (μl)	X gal staining										
			Ut Art		Rad Art		P	F	Maternal liver	Uterine horn		Ut fat	Other tissues
			Cx end	Ov end	Cx end	Ov end				Cx end	Ov end		
301	45	1000	-	-	-	-	-	-	+++	-	-	-	Pelvic muscles
302	45	R-400 L-1000	-	-	-	-	-	-	+++	-	-	-	Pelvic muscles
94	47	1500	-	-	-	-	-	-	+++	-	-	-	Pelvic muscles, Urinary bladder, cervix
331	45	1500	-	-	-	-	-	-	+++	-	-	-	Pelvic muscles, Urinary bladder, cervix
329	45 $	1500	-	-	-	-	-	-	-	-	-	-	-
330	45 $	1500	-	-	-	-	-	-	-	-	-	-	-

For each animal there are two uterine horns and results are presented together.
GP: Guinea pig; $ GP died during or shortly after surgery; GA = gestational age at administration; d= days; Cx = cervical; Ov = ovarian; P: placenta; F:fetus; Ut:uterine; Rad: radial; Art: artery; d: days

Hence, injection of vector to the internal iliac artery is not a feasible option to transduce the utero-placental circulation.

5.11 Pluronic Gel-Vector Combination

5.11.1 Administration of pluronic gel-vector combination is technically the easiest and most reliable method to transduce the utero-placental circulation

None of the intravascular injection routes so far investigated had provided the ease, reproducibility or level of local gene transfer that would be required to transduce the utero-placental circulation in the guinea pig. The easiest method of gene transfer appeared to be external administration but this was associated with high levels of systemic gene transfer, probably because the vector easily ran off from the site of application. To avoid this we investigated combining the vector with a substance that was less fluid. Pluronic gel provides such a system because of its thermodynamic properties. This gel is liquid at 4°C, but becomes solid at body temperature.

Administration of Pluronic gel-vector combination involved exposing the uterine and radial arteries by dissecting them out from the surrounding fat. The Pluronic gel-vector combination was made up over ice until use and was then drawn up into a 1ml syringe. It was then applied externally to the vessels and allowed to remain in place for 5 minutes to allow sufficient time for transduction, before mobilizing the uterine horns. In some cases parts of the uterine horns were lifted out of the peritoneal cavity to allow better visualization of the radial arteries. The uterine horns were kept warm during this time by wrapping them up in sterile gauze soaked in warm saline. With experience we observed a higher rate of fetal loss when the horn or part of it was lifted from the peritoneal cavity. To avoid this, a larger laparotomy scar was made, to well above the umbilicus which allowed the uterine horn to be manipulated to expose the radial arteries, while keeping it within the peritoneal cavity. The feasibility of this technique is presented in Table 5.11.

We found that administration of the vector by this method is relatively straightforward and quick to perform, shortening the duration of the surgery by more than half (from 3-4 hours to only 1.5 hours). Within a few seconds of laying the Pluronic gel-vector combination onto the vessel, it set to form a gelatinous mass.

Table 5.11 – Administration of vector using Pluronic gel as a vehicle: feasibility and survival (45 – 47 days of gestation)

GP no.	Number of attempts at administration		Vector volume delivered (μl)	Occlusion time if successful (min)	Adrenaline used	Outcome
	failure	success				
339	L(0), R(1)	L(1), R(0)	1000	Not required	No	Mother miscarried 24 hours after surgery
375	L(0), R(0)	L(1), R(1)	1000	Not required	No	Fetuses alive at PM (4 days)
413	L(0), R(0)	L(1), R(1)	1000	Not required	No	Fetuses alive at PM (5 days)
415	L(0), R(0)	L(1), R(1)	1000	Not required	No	Fetuses alive at PM (5 days)
319*	L(0), R(0)	L(1), R(1)	1000	Not required	No	Fetuses alive at PM (7 days)
320*	L(0), R(0)	L(1), R(1)	1000	Not required	No	Fetuses alive at PM (6 days)

* These animals only received the pluronic gel vehicle by itself, without any recombinant adenovirus.

As can be inferred from the small number of attempts required to transduce the vessels (Table 5.11), the administration of vector by this mode is technically straightforward. In one case it was not possible to administer the vector to the right uterine artery (guinea pig 339) because the vessel was very small and consequently difficult to visualize within the fat pad. This guinea pig started to miscarry the next morning, and the cause most likely was excessive manipulation of the uterine horn. There was no evidence of peritoneal inflammation, bleeding or infection at post-mortem examination.

5.11.2 Administration of vector using Pluronic gel as a vehicle leads to very high levels of localized transgene expression

Administration of Ad.LacZ using Pluronic gel as a vehicle led to very high levels of local transgenic protein expression in the uterine and radial arteries to which the vector had been applied, both on the adventitial surface and the internal

luminal surface (Figures 5.7-5.9). In fact, after X-gal histochemistry, some of the vessels appeared as if they had been spray-painted blue. The liver and uterus had minimal β-galactosidase expression in one animal and were not stained in any of the others. All other maternal and fetal tissues sampled (placentae, heart, kidney, lung, gonad, bladder, brain and adrenal) were not stained (Table 5.12). Thus, administration of Pluronic gel-vector combination achieves very high levels of localized gene transfer and expression in the utero-placental circulation. Administration of pluronic gel by itself without any Ad.LacZ in pregnant guinea pigs (n=2) did not lead to any positive X-gal staining in any maternal/fetal tissue.

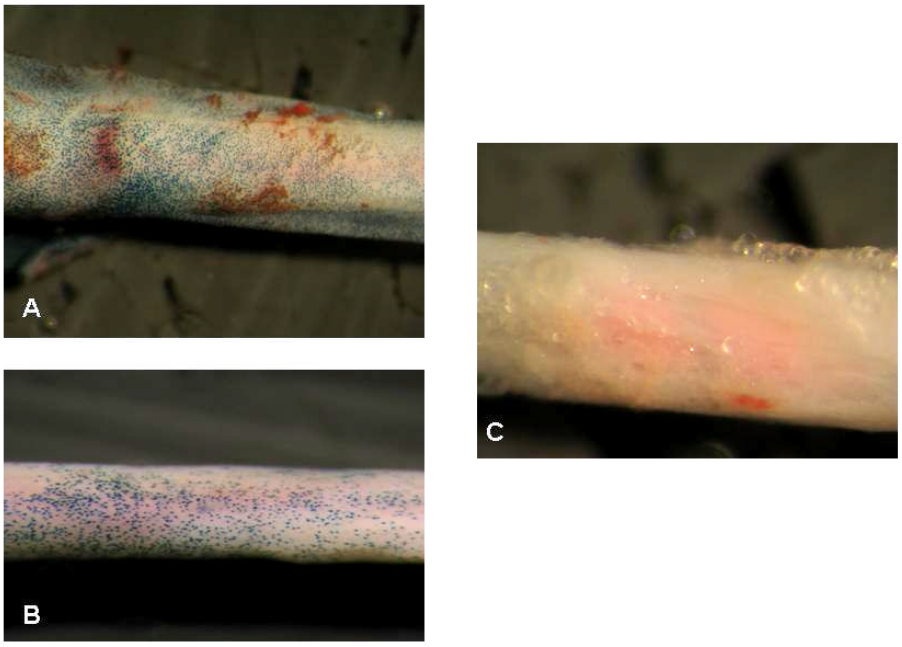

Figure 5.7 – Transgenic protein expression in the uterine arteries after external administration of Ad.LacZ using Pluronic F-127 gel as a vehicle

The uterine and radial arteries of pregnant guinea pigs were transduced with Ad.LacZ at 45 days of gestation using Pluronic F-127 as a vehicle. Maternal and fetal tissues were harvested at post-mortem examination 1-4 days later and analysed by X-gal staining. A and B – Positive transgenic protein expression in uterine arteries which had received the vector-pluronic gel combination; C – No transgenic protein expression in a uterine artery which had only received pluronic gel without Ad.LacZ.

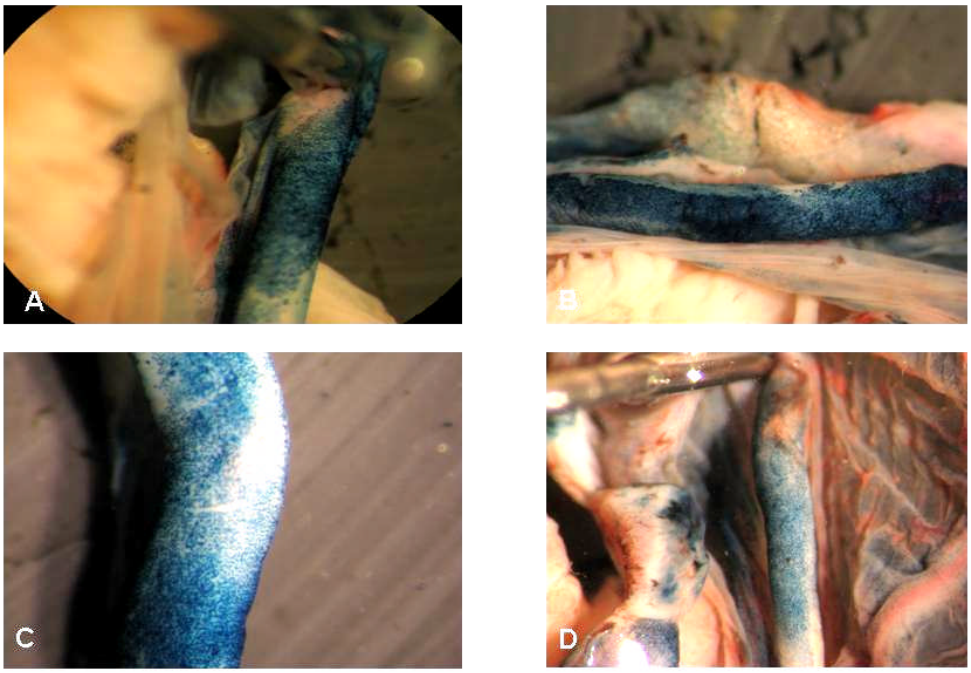

Figure 5.8 – Transgenic protein expression in the radial arteries after external administration of Ad.LacZ using Pluronic F-127 gel as a vehicle

The uterine and radial arteries of pregnant guinea pigs were transduced with Ad.LacZ at 45 days of gestation using Pluronic F-127 as a vehicle. Maternal and fetal tissues were harvested at post-mortem examination 1-4 days later and analysed by X-gal staining. A-D – Positive transgenic protein expression in radial arteries which had received the vector-pluronic gel combination.

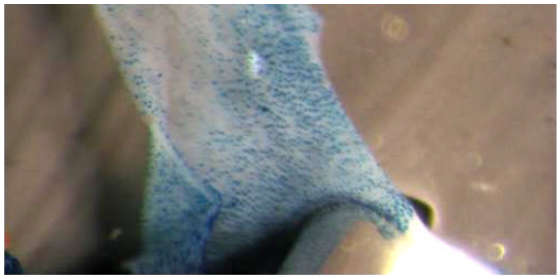

Figure 5.9 – Transgenic protein expression on the inner surface of a uterine artery after external administration of Ad.LacZ using Pluronic F-127 gel as a vehicle

The uterine and radial arteries of pregnant guinea pigs were transduced with Ad.LacZ at 45 days of gestation using Pluronic F-127 as a vehicle. Maternal and fetal tissues were harvested at post-mortem examination 1-4 days later and analysed by X-gal staining. The picture shows positive transgenic protein expression on the inner surface of a uterine artery.

Table 5.12 – Gene transfer results after administration of the vector using pluronic gel as a vehicle

GP no.	GA (d)	Vector volume (μl)	X gal staining										
			Ut Art		Rad Art		Placenta	Fetus	Maternal liver	Uterine horn		Fat of uterus	Other tissues
			Cx end	Ov end	Cx end	Ov end				Cx end	Ov end		
339	45	1000	++++	++++	++++	++++	-	-	+	+	-	++	No expression
375	46	1000	++++	++++	++++	++++	-	-	-	-	-	++	No expression
413	44	1000	++++	+++	++++	+++	-	-	-	-	-	+	No expression
415	47	1000	+++	+++	+++	+++	-	-	-	-	-	-	No expression
319 *	43	1000	-	-	-	-	-	-	-	-	-	-	No expression
320 *	46	1000	-	-	-	-	-	-	-	-	-	-	No expression

GP = Guinea Pig; GA = gestational age at administration; d = days; Cx = cervical; Ov = ovarian; * these animals only received pluronic gel by itself, without any recombinant adenovirus; The number of '+' signs indicates the intensity of staining.

The primary objective of the study in pregnant guinea pigs was to investigate how local over-expression of VEGF-A_{165} in the utero-placental circulation affects the rate of fetal growth in normal and FGR guinea pigs. Having

optimized the technique for gene targeting to the utero-placental circulation, we started to examine the long term effect of gene transfer using Pluronic gel-Ad.VEGF-A_{165} combination on the utero-placental vessels of FGR guinea pigs.

During the course of this Ph.D., an initial start was made by administering Ad.VEGF-A_{165} to three FGR guinea pigs at 45 dpc. These studies were meant to be long-term studies, with the animals being culled at 63 days (term=65 days). Unfortunately, all 3 of these studies had to be terminated prematurely, within 7 days post-administration of the vector because of experimental complications. In two of the guinea pigs, the skin sutures snapped open at day 7, and hence they had to be put down. We realized that the suture which we had been using to close the skin (3-0 Vicryl) was not robust enough to last for more than a week, and hence we decided to use 2-0 Vicryl for subsequent experiments. The third guinea pig had an eczema-like skin condition pre-operatively. Post-surgically, the condition was exacerbated and the animal appeared to in distress, having withdrawing from eating. In accordance with the Home Office Regulations, the animal had to be euthanized.

5.12 Conclusion from Gene Targeting Experiments

Based on the results of the pilot experiments described above, it was decided to administer gene therapy to the utero-placental circulation of guinea pigs using Pluronic gel as a vehicle. The advantage of this method over other methods is that it leads to very high levels of localized gene transfer and expression specifically at the site of administration. There is none to minimal transgene expression in other maternal and fetal tissues, as determined by X-gal histochemistry. It is technically straightforward and atraumatic as there is no requirement of injecting any blood vessel. External administration of the vector in pluronic gel also leads to transgene expression on the inner luminal surface. There was no evidence of any edema or inflammation at post-mortem examination. Hence, dilution of vector in Pluronic gel appeared to be the most feasible approach to administer the vector to the utero-placental circulation.

5.13 The vascular reactivity of uterine arteries from pregnant Guinea Pigs can be studied on a wire myograph

The uterine arteries from animals transduced with Ad.VEGF-A_{165}/Ad.LacZ were harvested and used for pharmacology analysis on a wire myograph. Initially, I attempted to study the vascular pharmacology of these vessels on an organ bath, but mounting on an organ bath damaged them because of their small size. This resulted in no vascular reactivity (see Discussion). Analysis was performed on Ad.VEGF-A_{165} and Ad.LacZ treated animals, who were administered the vector bilaterally at 44-47 days gestational age and terminated 2-7 days post-injection (n=3 each).

I observed a reduction in the contractile response and enhancement in relaxation in Ad.VEGF-A_{165} transduced vessels compared to Ad.LacZ transduced vessels. These results were however non-significant, probably on account of the limited number of animals studied. The results of the myography experiments have been summarized in Figures 5.10, 5.11 and Table 5.13.

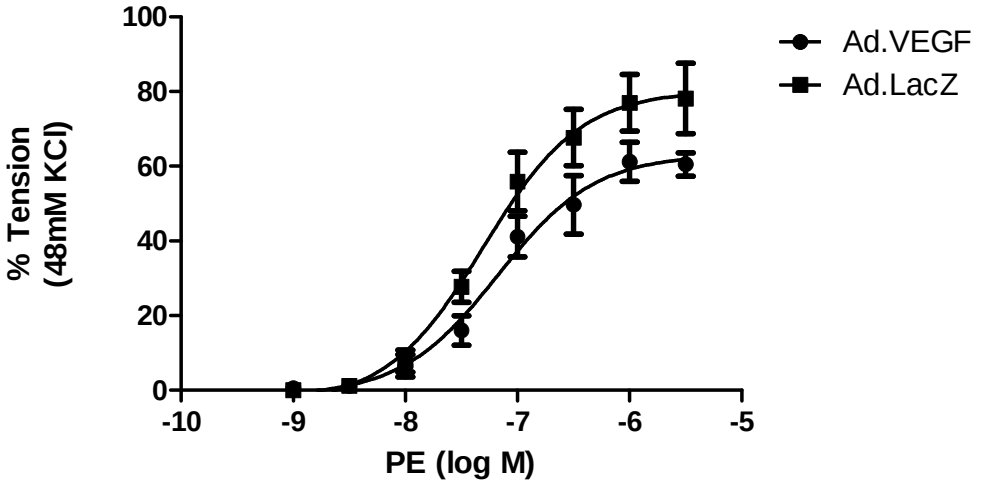

Figure 5.10 - Contractility of Ad.VEGF-A_{165} and Ad.LacZ transduced uterine arteries from nutrient restricted pregnant guinea pigs 2-7 days after gene transfer.

The uterine arteries of nutrient restricted pregnant guinea pigs were transduced with Ad.VEGF-A_{165} (n=3) or Ad.LacZ (n=3) at 43-47 days of gestation using Pluronic F-127 as a vehicle. The transduced uterine arteries were harvested at post-mortem examination 2-7 days later, cut into 1mm ring segments and analysed on a dual chambered wire myograph system. Concentration response curves to PE were conducted for each vessel in duplicate. The contractility of the vessel is expressed as a percentage of the response to KCl. PE produced concentration-dependent contractions, which were of lesser magnitude in Ad.VEGF-A_{165} transduced vessels compared to Ad.LacZ transduced vessels. Error bars denote standard error of mean.

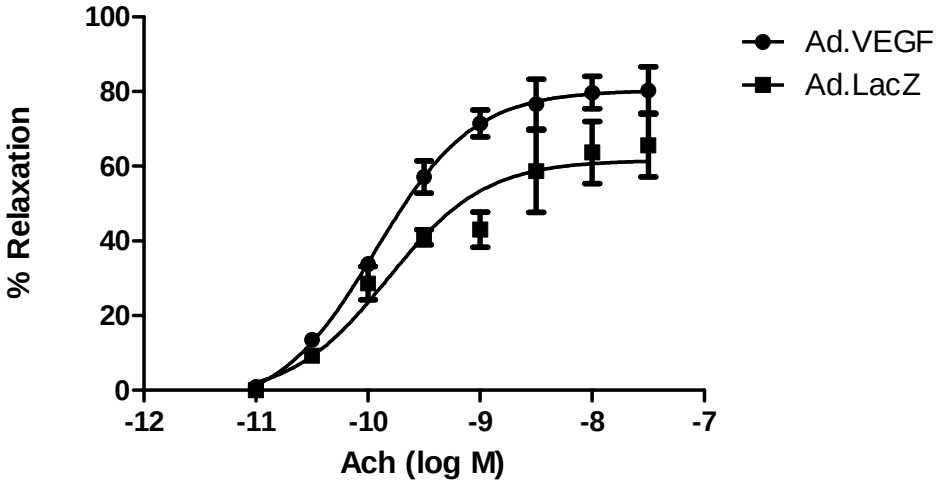

Figure 5.11 - Relaxation of Ad.VEGF-A_{165} and Ad.LacZ transduced uterine arteries from nutrient restricted pregnant guinea pigs 2-7 days after gene transfer.

The uterine arteries of nutrient restricted pregnant guinea pigs were transduced with Ad.VEGF-A_{165} (n=3) or Ad.LacZ (n=3) at 43-47 days of gestation using Pluronic F-127 as a vehicle. The transduced uterine arteries were harvested at post-mortem examination 2-7 days later, cut into 1mm ring segments and analysed on a dual chambered wire myograph system. Concentration response curves to acetylcholine (Ach) were conducted for each vessel in duplicate. The relaxation of the vessel is expressed as a percentage of inhibition of PE-produced contraction. Ach produced concentration-dependent relaxation, which was of greater magnitude in Ad.VEGF-A_{165} transduced vessels compared to Ad.LacZ transduced vessels. Error bars denote standard error of mean.

Table 5.13 – Vascular reactivity of uterine arteries from nutrient restricted pregnant guinea pigs 2-7 days after adenovirus-mediated gene transfer of VEGF-A_{165} (n=3) or β-galactosidase (n=3)

Type of response	Parameter	Ad.VEGF-A_{165}	Ad.LacZ	p
Contractility	E_{max} (Mean±SEM)	63.23±3.13 (n=3)	80.35±3.91 (n=3)	**0.327**
	EC_{50} (M)	$6.69x10^{-8}$	$4.96x10^{-8}$	
Relaxation	E_{max} (Mean±SEM)	80.35±2.11 (n=3)	61.65±3.64 (n=3)	**0.223**
	pD_2	9.93±0.08	9.82±0.19	

In summary, the vascular reactivity of uterine arteries of pregnant guinea pigs that have been transduced with Pluronic gel–Ad.VEGF-A_{165} combination can

be studied on the wire myograph. The results show a trend towards diminished vascular contractility and enhanced endothelium-dependent relaxation in vessels transduced with Ad.VEGF-A_{165} as compared with Ad.LacZ transduced vessels.

Discussion

This chapter describes the optimization of a technique of gene targeting to the utero-placental circulation of pregnant guinea pigs and analysis of vascular reactivity in transduced vessels. Having shown that local over-expression of VEGF in the utero-placental circulation of pregnant sheep leads to a sustained increase in uterine blood flow, we were interested to examine if an increase in utero-placental perfusion translated into an increase in fetal growth in FGR animal models. We chose to carry out these studies on a well documented and validated FGR animal model, the maternal nutrient restricted guinea pig (Roberts CT et al., 2001a). The advantage of using guinea pigs is that they have a haemomonochorial placentation, which is the most similar to human placentation in an animal model, with the exception of some non-human primates. Thus, experimental results obtained from pregnant guinea pigs as well as toxicology studies conducted in this species are likely to hold more relevance for clinical translation. Furthermore, they have a relatively long gestation (65 days) for a small animal, in contrast to mice, rats and rabbits. This gives the opportunity to administer therapy at mid-gestation, and study the effects of treatment for 30-35 days post-administration.

At the outset, to our knowledge, there had been no previous studies wherein different drugs/substances have been locally administered to the guinea pig uterine or radial arteries. There had been one published study which investigated the vascular anatomy of the guinea pig utero-placental circulation in detail, by administration of X-ray contrast medium into the utero-placental vessels after gaining access through femoral artery catheterization (Egund N and Carter AM, 1974). The use of X-ray guidance was not available to us and we considered that it would not be necessary, if intravascular injection under operating microscope vision was feasible.

The start of these experiments was hampered by a number of issues namely, the low conception rate of the guinea pigs, the difficulty in visualizing the uterine arteries, poor knowledge of the guinea pig utero-placental anatomy, and problems of vascular injection in small vessels. However, with time we became more skillful in the techniques needed, leading to a reduction in surgery time and improved morbidity and mortality rates

We also faced problems in getting sufficient numbers of pregnant guinea pigs when put on the nutrient restricted diet, and had to buy in some new stud boars to boost our breeding programme. Once pregnant, there were cases where pregnancy was missed on the ultrasound scan because we scanned them too early in gestation. With experience, it was realized that the optimum gestational age to confirm pregnancy by sonography was 24-25 days, at which a fetus can be reliably and easily seen.

5.14 Gene Targeting to the Utero-Placental Vasculature of pregnant Guinea pigs

In order to compare our findings in guinea pigs with results from pregnant sheep, we first attempted to transduce the utero-placental vessels by direct intra-arterial injections into the uterine artery, using a customized hand-made 34 gauge needle. While the size of the uterine artery (between 250 and 400 μm) makes it large enough for it to be injected, the vessel lies unsupported and deeply embedded in fat with a surrounding network of tributaries which made this technique extremely difficult. We were able to reliably inject the uterine artery in fewer than half of all our attempts. Of more importance to the aims of this project however was our finding that even when uterine artery injection was successful, the vector was only able to transduce the cervical end and middle of the vessel, and the radial arteries supplying the lower most fetuses. The more distal parts of the uterine artery and ovarian end radial arteries were not transduced, meaning that this end of the utero-placental vasculature would have to rely on the diffusion of transgenic VEGF from further upstream for any therapeutic benefit to be realized. Increasing the volume of vector delivered did not improve the extent of gene transfer. It is of note

that because of the very fine gauge of the needle used for these injections, it took a long time to inject 1.0-1.3 mls of vector solution, during which the needle tended to dislodge. This further added to the difficulty of the procedures.

In an angiographic study to examine the vascular anatomy of guinea pig uterine arteries, contrast medium injected into the uterine artery *in vivo*, at a rate approximating to the rate of blood flow, failed to enter the most distal radial arteries and placentae (Egund N and Carter AM, 1974). The same authors have shown that the latter are preferentially served by the ovarian arteries. I did consider injecting the vector into the ovarian arteries, but they were of even smaller diameter than the uterine arteries. It is not surprising that substances administered into the uterine artery are unable to reach the most distal radial arteries. The radial arteries follow a devious and highly tortuous path, with several branches and anastomoses. Another feature of the radial arteries is their progressive increase in caliber from their origin to the placentae. These characteristics enhance the volume of blood within the utero-placental circulation, but probably lead to the vector solution being channeled only into the radial arteries that are close to the site of injection, and none remaining to enter the distal radial arteries.

An alternative intravascular approach was used, injection of the internal iliac artery, from which originates the uterine artery. We hypothesized that the larger caliber of this vessel would improve the reliability of the intravascular injection technique, facilitate the volume of vector to be delivered over a shorter time period, and prevent needle dislodgement. The internal iliac artery in a guinea pig gives off numerous branches in the following order – cranial gluteal artery (supplying the dorsolateral wall of the pelvis and pelvic muscles), internal pudendal artery (supplying the external genitalia), vesical artery (which branches to supply the bladder, ureter and rectum), vaginal artery and uterine artery. The internal iliac artery, though not much larger in diameter than the uterine artery, was found to be easier and more reliable to inject because it is well supported on the pelvic side wall musculature, and is easily identified. Nevertheless, the technique was associated with significant fetal and maternal loss, most probably because of the long anaesthetic time required to complete the procedure. Administration of vector to the

internal iliac artery resulted in transgenic protein expression only in the pelvic muscles and bladder, and none in the uterine and radial arteries. The uterine artery is one of the most distal branches of the internal iliac artery and hence the vector solution preferentially makes it way to the more proximal branches and the organs these serve rather than the uterine and radial arteries. It was clear therefore, that the intravascular injection route would not be able to achieve the aim of transducing the uteroplacental circulation of the pregnant guinea pig.

In order to overcome this problem, it was decided to administer the vector externally to the uterine and radial arteries, diluted in PBS. While this resulted in good transduction of both cervical and ovarian ends of the uterine and radial arteries, it also led to undesirable expression of the transgenic protein in the uterine horns, the fat surrounding the uterus and maternal liver. We therefore decided to adapt this local delivery technique to reduce the run off of the vector from the vessels.

The approach adopted was to dilute the vector in Pluronic Gel, and administer it to the external surface of the uterine and radial arteries. This resulted in strong and local transgenic protein expression in the uterine and radial arteries, on both the adventitial and luminal surfaces. There appeared to be no vector expression systemically. This suggests that vector administration using Pluronic F-127 as a vehicle may be the optimum method of gene targeting to the utero-placental circulation of pregnant guinea pigs. It also resulted in shortening of the surgery time by 1.0-1.5 hours compared to other methods, thereby lowering the risk of morbidity and mortality.

Pluronics (also known as poloxamers), when dissolved in an aqueous solution exhibit the feature of reversible thermal gelation (Schmolka IR, 1972). They have the unique property of being liquid at 4°C and in a semi solid gel at room or body temperature, thus providing an attractive platform for slow release of drugs. The gelation mechanism of pluronics has been reviewed extensively (Jain NJ et al., 1998;Bohorquez M et al., 1999) . Poloxamer gels display low toxicity at therapeutically beneficial doses and do not increase serum triglycerides and cholesterol in animal models (Blonder JM et al., 1999). Medical uses of pluronic

F127 have included the controlled delivery of drugs to the eye (El-Kamel AH, 2002), nasal passage as well as parenteral and subcutaneous administration (Barichello JM et al., 1999).

Pluronic gels have been used as a vehicle for local adenoviral gene delivery previously (Iaccarino G et al., 1999;Khurana R et al., 2004;Mallawaarachchi CM et al., 2005) and shown to be safe to administer. Pluronic gels increase the transduction efficiency of adenoviral vector delivery to vascular cells in vivo (Feldman LJ et al., 1997), probably because of the slower kinetics associated with the longer term vector release from the gel or the closer proximity of viral vector to the cell surface. Because of the thermo-responsive behaviour of pluronic F-127, the gel is delivered *in vivo* over a short period of time before solidification. Our results too indicate that using a localized pluronic gel based depot of slow viral vector release facilitates greater transgene expression in comparison to other techniques. Pluronic gel has been used to deliver Ad.LacZ to the carotid artery of rats. Five days post-infection, the presence of the β-gal transgene was visualized throughout the arterial wall (Iaccarino G et al., 1999). As mentioned above, Pluronics have previously been shown to have no toxic effects, and we too did not observe any tissue edema or inflammation on gross examination at post-mortem. More detailed microscopic examination on H&E stained sections had not been performed during the course of this Ph.D., but is intended to be performed.

One of the animals that received the vector in pluronic gel suffered miscarriage. We believe this was because of excessive manipulation of the pregnant uterine horns while exposing the uterine and radial arteries, rather than the administration of the gel. There were no miscarriages observed after we amended our technique to minimize uterine manipulation.

In summary, we have shown that administration of recombinant adenoviruses using pluronic gel as a vehicle leads to robust transgenic protein expression in the utero-placental vessels, both on the adventitial and luminal surfaces. There is no vector expression in other maternal and fetal tissues.

5.15 Peri-conceptual maternal under-nutrition leads to growth restriction of fetal guinea pigs

As part of a larger project looking at the potential of local VEGF gene therapy to treat FGR in a small animal model, we created FGR in guinea pigs using a previously described method. In this model, guinea pigs are fed 70% of their *ad lib* diet from 28 days before conception to day 34 of pregnancy, and 90% of their *ad lib* diet thereafter, until term. This is reported to result in approximately 35% reduction in neonatal weights and 30% reduction in placental weight at term (Roberts CT et al., 2001a). Our findings compare very well with the findings of Roberts CT *et al*, as we observed a 40% reduction in neonatal weights and 24% reduction in placental weights (at 45 days of gestation). An important characteristic feature of this model is reduced placental vascularity in FGR guinea pigs compared to normal pregnant. This implies that the supply of both nutrients and oxygen to the developing fetus is restricted, which closely mimics the human FGR condition caused by vascular placental insufficiency.

Creating this model however, was not without problems. We observed that in a number of cases, the guinea pigs on a growth-restricted diet failed to conceive after 28 days of under-nutrition. This meant prolonging the period of restricted feeding for a further 1-2 estrus cycles (each estrus cycle of guinea pig=14-16 days days) until the hymen ruptured again. Consequently, some of the guinea pigs on the growth-restricted diet became pregnant after 28 days of under-feeding, while others became pregnant after approximately 42 or 56 days of under-feeding. One solution to this would have been that guinea pigs which failed to conceive after the initial period of nutrient restriction, were put on an *ad lib* diet for a few weeks until they regained their normal body weights, and then made to enter the experiment again. This would have increased the costs hugely, and would not have been feasible experimentally. After discussion with the original authors of this FGR model, it was decided that the most appropriate solution to this issue is to prolong the period of pre-conceptual under-nutrition in female guinea pigs that did not get pregnant the first time. They informed me that this was the strategy they adopted in their

experiments too, even though this fact has not been mentioned in any of the published papers from their group.

Thus, working with growth-restricted guinea pigs that have undergone different periods of pre-conceptual under-nutrition is one of the limitations of this model, which may influence the degree of growth restriction and the experimental outcome. Nevertheless, this model is more advantageous to work with relative to other models such as those created by uterine artery ligation. This is because the latter would involve physically obstructing blood flow in a uterine artery, and then trying to increase blood flow in it with gene therapy, which appears impossible to achieve. A physiological model is likely to be more appropriate for the kind of experiments we wish to pursue.

5.16 It is feasible to carry out fetal measurements on growth-restricted guinea pigs

During the course of developing the FGR guinea pig model, all experimental guinea pigs were scanned to collect fetal measurements by ultrasound. To our knowledge, there has only been only one other study on fetal measurement in guinea pigs by ultrasound (Turner AJ and Trudinger BJ, 2000). The authors of this study scanned only normal pregnant animals and demonstrated that ultrasound can be used successfully to study pregnancy in the guinea pig. They further showed that measurements of BPD may be used to reliably estimate gestational age in this species.

Using both normal pregnant and growth-restricted guinea pigs for our experiments, we are developing a database of fetal measurements at different gestational ages. Even with the small number of animals used so far, we observed a significant reduction in abdominal circumference in growth-restricted guinea pigs at 45 days of gestation, compared to normally grown fetuses. The biparietal diameter showed a strong trend towards reduction in the growth-restricted guinea pigs while the ratio of head to abdominal circumference showed a strong trend towards being increased in the FGR fetuses. With further animals, these parameters are likely to

reach statistical significance. These data suggest that FGR guinea pigs created by maternal nutrient restriction show evidence of brain sparing.

5.17 Transduction of guinea pig uterine arteries with Ad.VEGF-A_{165} results in a reduction of contractile response and enhancement of relaxation, compared to Ad.LacZ transduced uterine arteries

Guinea pig uterine arteries transduced with Ad.VEGF-A_{165} or Ad.LacZ were examined on a wire myograph to examine changes in vascular reactivity. I first attempted to study their vascular responses on an organ bath, as has been described previously by other groups (Weiner CP et al., 1992;Jovanovic A et al., 1997;White MM et al., 2000). However, the organ bath set-ups in our lab are not designed to experiment with any vessel smaller than a mouse aorta (~1mm in diameter). As the guinea pig uterine artery is much smaller (~400 μm diameter at 45 days gestational age), it is not unexpected that we were unable to measure its vascular reactivity on an organ bath. However, when studied on a wire myograph, which can be used to examine vessels as small as 100 μm in diameter, we were able to study the uterine artery vascular responses easily.

I observed a reduction in the contractile response of the Ad.VEGF-A_{165} transduced uterine arteries compared to Ad.LacZ injected vessels and an increase in the endothelium-dependent relaxation to acetylcholine. These results are similar to what we had observed in the sheep uterine arteries that had been transduced short-term. Statistical significance was not achieved in our results, most probably because of the limited animal numbers. Further experiments to increase animal numbers are currently in progress as part of the main project. A detailed discussion of the effects of VEGF-A_{165} over-expression on uterine artery vascular responses has already been made in Chapter 3.

Conclusion

In summary, we have described the optimization of a technique of gene targeting to the utero-placental circulation of pregnant guinea pigs using a thermo-sensitive poloxamer gel. We plan to use this technique to study the effects of VEGF-A_{165} over-expression on utero-placental vascular reactivity and fetal growth rates in an FGR model of pregnancy. After a long period of improvisation of our animal husbandry programme during which we honed our skills at time-mating of nutrient-restricted guinea pigs, we have successfully recreated the nutrient restriction FGR guinea pig model. This is characterized by reduced placental vascularity and diminished supply of both nutrients and oxygen to the developing fetuses. Experiments designed to study the effects of local Ad.VEGF-A_{165} gene therapy on fetal growth rate in this model are currently in progress in our laboratory.

Chapter 6

General Discussion

The aim of the research undertaken in this thesis was to examine the effects of local VEGF gene therapy on the utero-placental circulation, with the aim of developing a potential therapy for Fetal Growth Restriction. A number of long term physiological effects were seen in the normal sheep pregnancies examined, and the mechanism of action was studied. In addition a technique to locally transduce the uteroplacental circulation of the guinea pig was developed, with a view to studying the efficacy of VEGF gene therapy to treat FGR.

6.1 Local over-expression of VEGF leads to long term changes in uterine blood flow and vascular reactivity in pregnant sheep uterine arteries.

In this study, we found that local adenovirus-mediated over-expression of VEGF-A_{165} in the uterine arteries of mid-gestation pregnant sheep resulted in a significantly higher increase in blood flow compared to transduction with a control non-vasoreactive vector Ad.LacZ. A statistically significant increase in UABF was apparent as early as 7 days after Ad.VEGF-A_{165} injection, and was maintained for at least 28 days, where it reached a 37% increase over baseline compared to 20% on the Ad.LacZ injected side. This increase was concomitant with a significant reduction in uterine artery contractility and significant adventitial neovascularization. There was an upregulation in the level of eNOS for up to 7 days after the administration of Ad.VEGF-A_{165}, but this increase was not evident at term.

The importance of the findings presented in this thesis compared to our previously published short-term data (David AL et al., 2008) is that the increase in blood flow is maintained over at least 4 weeks, suggesting the potential for therapeutic use. Importantly, the use of 'gold standard' transit time flow probes, instead of Doppler ultrasonography (David AL et al., 2008), provided a more accurate and reliable estimate of the true increase in UABF (Abi-Nader KN et al., 2010). To our knowledge, this is the first report of a manipulation which leads to a sustained long-term increase in uterine blood flow in pregnancy, with only a single intervention. We also noted a significant increase in singleton fetal weight compared to data from historical controls using the same sheep breed. Even though encouraging at first sight, the results could have been affected by other factors such as differences in fetal growth year by year for example. Further studies on the effects of Ad.VEGF-A_{165} gene therapy on fetal growth and birthweight in cohorts of sheep with contemporaneous controls are currently ongoing.

One longitudinal case control study showed that UABF was reduced by 12.5% at 20 weeks, and by 36.7% from 24 weeks of gestation until delivery in FGR as compared to normal pregnancies (Konje JC et al., 2003). Thus, any therapy for FGR based on increasing UABF to normal levels would need to achieve a 58% increase in UABF. Even though the extent of increase in UABF in our study is less than what is expected to achieve a normal utero-placental perfusion, it must be emphasized that this treatment, if translated to the clinics, would potentially target the most severely growth-restricted fetuses, that have a birthweight of 500 grams or less. Even a small improvement in utero-placental perfusion may delay iatrogenic delivery, enhance gestation by a few days, and translate into a small increase in fetal weight. It has been shown that at the very extremes of pre-maturity, between 24-27 weeks of gestation, the median survival gained for each additional day *in utero* is 2% (Baschat AA et al., 2007). Neonatal and long term morbidity is also reduced, as gestational age and birthweight increases.

In this study, there was an acute drop in UABF in both the Ad.VEGF-A_{165}/Ad.VEGF-D and Ad.LacZ injected sides 1-3 days after vector injection. This reduction was most likely due to the vessel occlusion and trauma to the vessel wall

during vector injection which would result in vasoconstriction. UABF recovered in all experimental sheep by days 5-7 after vector injection. However, this is a point of concern if this therapy is to be applied in a clinical setting. Growth-restricted fetuses are known to be frequently hypoxemic (Akalin-Sel T et al., 1994). A minimally invasive technique such as trans-femoral uterine artery catheterization (Delotte J et al., 2009) would reduce uterine artery trauma and post-injection constriction, and has been used to inject the uterine arteries for embolization of fibroids in clinical practice. The procedure itself, and in particular the temporary occlusion of the lumen, could reduce the oxygen supply to the fetus, particularly if the other uterine artery supply was significantly compromised. Hypoxaemic FGR fetuses may have little reserve to tolerate further compromise of the uteroplacental circulation during the catheterisation procedure. This could result in immediate death of the fetus, or brain damage. It may also be possible that they may be more tolerant of a temporary interruption to the uteroplacental circulation, since they are already exposed to it chronically. Further experiments to determine the optimal vector dose and whether extra-luminal administration of vector (for instance, pluronic gel-mediated delivery) results in equally efficient gene delivery are warranted.

This thesis also investigated some of the mechanisms by which VEGF over-expression results in an increase in utero-placental perfusion. There was an upregulation in the level of eNOS short-term, while the long-term transduced vessels demonstrated increased adventitial angiogenesis, reduced vasoconstriction and reduced intima/media ratios in the Ad.VEGF transduced uterine arteries. All these appear to confer an 'arterioprotective' effect and promote the health of the uterine artery, which may be responsible for the increased uterine perfusion that we observed (discussed in 'Discussion' of Chapter 3). Experiments in endothelial cells isolated from the uterine arteries of mid-gestation pregnant sheep and infected with adenovirus vectors *in vitro* showed that infection with Ad.VEGF-A_{165} and Ad.VEGF-D, but not Ad.LacZ resulted in an increase in the levels of eNOS, iNOS and the phosphorylated (activated) form of eNOS. This further demonstrates that

VEGF over-expression contributes to increased levels of vasodilators, which is probably responsible for the increase in UABF that was observed.

This study was designed with clinical relevance in mind and was performed in sheep because many aspects of sheep fetal and vascular physiology are similar to the human. The ovine fetus is similar in size to the human fetus and has a good tolerance to *in utero* manipulations, allowing the surgical placement of catheters in both the maternal and fetal vasculature (Jellyman JK et al., 2004;Abi-Nader KN et al., 2011). The increase in uterine blood flow that occurs through the latter half of gestation is very similar for humans and sheep, increasing two and a half times in humans (from 0.3 to 0.8 L/min) while in sheep, this increase is three fold (0.4 to 1.2 L/min) (Konje JC et al., 2003;Meschia G, 1984). This increase in uterine perfusion results in an increase in the supply of substrates and oxygen to the conceptus, failure of which manifests as asymmetric FGR. The rates of oxygen and glucose consumption in both near-term sheep and human fetuses are also similar (Barry JS and Anthony RV, 2008).

However, one of the important limitations of this investigation was that it was conducted in normal pregnant and healthy sheep, rather than in an animal model of FGR. There is a possibility that young and otherwise healthy animals are able to mount an effective endogenous angiogenic response which can be further maximized by an additional stimulus like VEGF. But human patients with FGR characterized by utero-placental insufficiency and endothelial dysfunction (Yinon Y et al., 2010) would probably have a less pronounced response. A brief exposure to VEGF may be insufficient for a therapeutic effect, but chronic exposure as in the case of adenovirus-mediated over-expression may provide therapeutic benefit.

It is also important to note that the primary etiological factor for human FGR caused by utero-placental insufficiency is an inadequate remodeling of the myometrial spiral arteries, because of defective trophoblast invasion of these vessels. As a result, the uteroplacental circulation remains in a state of high resistance which causes generalized endothelial cell injury. In our studies, we have shown a significant increase in utero-placental perfusion in response to local VEGF-A_{165} over-expression, possibly on account of changes in vascular reactivity,

eNOS levels, neovascularization and uterine artery remodeling (in terms of changes in intima/media ratios). However, it is difficult to predict if the replication of similar effects in human utero-placental vessels would be sufficient to overcome the effect of inadequate trophoblast invasion to any therapeutically beneficial extent.

Furthermore, normal spiral artery remodeling by trophoblast invasion is not regulated by a single member of the VEGF family in humans. The invasive cytotrophoblasts release a number of signaling factors that play an important role in uterine invasion, including VEGF-C, PlGF and angiopoietin-2 (Zhou Y et al., 2003a). It is therefore uncertain whether over-expressing only a single molecule using local gene therapy can be of any benefit in improving a compromised uterine circulation caused by defective physiological re-modelling.

Experiments in animal species where pregnancy-induced changes in utero-placental vessels mimic the human situation would be of value. In Old World monkeys, there is remodeling of the spiral arteries following trophoblast invasion (Blankenship TN and Enders AC, 2003). The initial stages of implantation, as well as the process of invasion by the trophoblast through the uterine epithelium, are very similar in Old World monkeys and man (Enders AC, 1995). Interestingly, there have even been reports of the occurrence of PET-like symptoms spontaneously in Old World monkeys (Palmer AE et al., 1979) but it is not known whether naturally occurring FGR caused by inadequate trophoblast invasion occurs spontaneously in this species. Non-human primates are important as experimental models of human pathological pregnancy and they may be the most suitable model in which to study toxicology prior to first-in-man studies. Research in non-human primates is costly and intensive however, and would not be appropriate for the initial work up of a potential therapy, as has been explored here. Additionally, there are ethical concerns about working with them because of their very close phylogenetic relationship to humans.

Mice have the advantage of offering several transgenic models of FGR to study. These include the placental-specific *Igf2*-knockout mouse (Constancia M et al., 2002) and *eNOS*-knockout mouse (Hefler LA et al., 2001). Unfortunately, the mouse serves as a less than optimal physiological model for the development of

human utero-placental vessels. The extent of trophoblast invasion is relatively shallow in the utero-placental blood vessels of pregnant mice. In fact, transformation of the uterine arteries is more dependent on maternal factors, particularly uterine natural killer cells, rather than trophoblast invasion *per se* (Carter AM, 2007;Greenwood JD et al., 2000).

Before taking any therapy into man, its safety needs to be critically examined in pre-clinical and *ex vivo* models. Preliminary studies from our lab suggest that this treatment is safe to administer. There were no detrimental changes in maternal and fetal blood pressure following local VEGF over-expression. Histological examination of uterine artery sections showed no evidence of edema, leucocyte infiltration or inflammation. RT-PCR was not able to detect any undesirable vector expression in maternal and fetal tissues.

Further toxicology studies, including the risk of transplacental transmission are being carried out by Ark Therapeutics Ltd who manufacture the vector. These include investigating the transmission of the virus across the placental barrier in the isolated perfused human placenta, in collaboration with the Maternal and Fetal Health Research Centre, University of Manchester. The administration of very high doses of the adenoviral construct to the uterine artery of pregnant rabbits is also being performed, to determine the LD_{50} dose and to determine what toxic effects, if any, might be important.

In summary, the data presented in this thesis give hope that Ad.VEGF gene transfer to the utero-placental circulation is capable of providing long-term beneficial changes in UABF and vascular reactivity. Further work in FGR animal models is needed to determine whether this will be of therapeutic benefit for treating FGR caused by utero-placental vascular insufficiency.

6.2 It is possible to efficiently transduce the utero-placental circulation of pregnant guinea pigs by pluronic gel mediated adenoviral delivery

In the studies with pregnant sheep, an increase in fetal weight (compared to historical controls) in response to Ad.VEGF-A_{165} over-expression in the uterine arteries was apparent. However, as mentioned above, it would be more helpful to

evaluate the effects of Ad.VEGF-A_{165} gene transfer on fetal growth in an animal model of FGR. We intend to investigate this in the maternal nutrient restricted guinea pig, a species whose placentation is the closest to humans, after non-human primates.

Chapter 5 of this thesis discusses the optimization of a technique of gene targeting to the utero-placental circulation of pregnant guinea pigs. Initial attempts at intra-vascular injection into the uterine arteries of pregnant guinea pigs had a low success rate and low reproducibility. Vector delivery into the internal iliac artery unfortunately did not result in gene transfer to the uteroplacental circulation. After testing out different routes and modes of administration of the vector, administration of the vector in Pluronic gel gave the best and most consistent results in terms of local transduction efficiency. Importantly, the expression of the transgene was limited to the utero-placental vessels and there was no transgene expression in other maternal and fetal tissues. Pluronic gel has the unique property of being liquid at 4°C and in a semi-solid form at room or body temperature. It thus serves as a useful medium for the slow/controlled release of drugs over a prolonged duration of time. Previous studies on administration of adenoviral vectors using pluronic gel have shown that its use as a vehicle enhances the transduction efficiency of adenoviral vector delivery to vascular cells (Feldman LJ et al., 1997). This is believed to be because of the slower kinetics of vector release from the gel or closer proximity of the viral vector to the cell surface. Our results are in concurrence with these studies and also show that administration of the vector in pluronic gel gave the strongest transgene expression, as compared to intravascular delivery techniques. Pluronic gel at low doses has been shown to be safe to administer in our investigation as well as other studies (Feldman LJ et al., 1997;Blonder JM et al., 1999).

Having optimized a technique of gene targeting to the utero-placental vessels, this technique will be used to investigate the effects of Ad.VEGF-A_{165} gene transfer on fetal growth in FGR pregnant guinea pigs. During the course of this Ph.D., growth restricted guinea pigs were successfully created. However, because of the unanticipated and long duration of time it took to optimize the gene targeting

technique, it was only possible to perform a few experiments on Ad.VEGF-A_{165} gene transfer during this Ph.D.

At the moment, it is not known whether pluronic gel may be an optimal vehicle for gene transfer to human patients, if this therapy is translated to the clinic. This decision, to a large extent, depends on the results that are obtained from the guinea pig studies.

6.3 Insights into Prenatal Gene Therapy with VEGF to treat pathological pregnancies – An epilogue

As mentioned above, to our knowledge, the work presented in this thesis is the first report wherein a single intervention results in a sustained long-term increase in uterine artery blood flow in pregnancy. There have been several approaches to try to improve fetal growth in pathological pregnancies (Section 1.7), and while some have shown to be promising in pre-clinical studies, none have so far been of any therapeutic benefit in the clinic. There has been a general lack of research into the treatment of pathological pregnancies, such as those affected by FGR and PET. This may be because of the fear of potential risks to the developing fetus by exposure to therapeutics.

Work by only a few other groups has explored the potential of gene therapy to reverse FGR. For example, it has been demonstrated that site-specific placental gene transfer of Angiopoietin-2 using an adenoviral vector resulted in a significant increase in fetal weights in normal pregnant mice, compared to control untreated mice (Katz AB et al., 2009). Further work is being planned by these authors to study the effects of placental gene transfer on fetal growth in animal models of FGR. It is of note that there is a general paucity of drugs for severe obstetric conditions, in comparison to other health conditions. Only 17 drugs are under active development for maternal health problems, which is less than 3% of the drugs in the pipeline for cardiovascular disease and even fewer than for a single rare disease like amyotrophic lateral sclerosis. Reasons for the lack of research and development of new drugs for obstetric conditions like FGR and PET include factors such as the high costs of reproductive toxicology studies, high risk of teratogenicity and the

prohibitive expense of follow-up investigations on neonates, which need to be carried out for a mean of 6 years. Additionally, the highest returns in the bio-pharmaceutical industry typically comes from drugs taken life-long for chronic diseases with a good life expectancy. In contrast, obstetric conditions are short-lived and the number of children per woman is declining, which further limits allocations of funding towards development of drugs for conditions like FGR (Fisk NM and Atun R, 2008).

While the effects of VEGF-A_{165}/VEGF-D on uterine artery blood flow or fetal growth *per se* have not been examined before, VEGF-A_{121} gene or protein therapy was found to be beneficial and alleviated some of the adverse symptoms, including elevated blood pressure and proteinurea, in rodent models of PET (Woods AK et al., 2011;Li Z et al., 2007). Use of gene therapy (or any newly developed drug) to treat disorders of pregnancy is bound to remain a subject of controversy and debate for many years to come.

One of the limitations of the current study design which involved injection of Ad.VEGF-A_{165} and Ad.LacZ bilaterally in the same animal, was the fact that we were unable to study modulation/alteration in vascular reactivity of the placental microvasculature by VEGF. Diffusion of VEGF from the site of injection to placental microvessesls is likely to have resulted in vasodilatation and reduction in placental vascular resistance. Increased resistance in the placental microvessels is a common feature of FGR as described previously. Hence, the apparent reduction in downstream placental resistance is likely to have benefited perfusion in both the Ad.VEGF-A_{165} and Ad.LacZ transduced uterine arteries, which means that the differences in uterine blood flow that we detected between the treated and control uterine arteries are likely to have been diluted. It is possible that if both the uterine arteries of a pregnant ewe had been injected with the same vector, and an inter-animal comparison performed, we may have been able to demonstrate a more profound effect of Ad.VEGF transduction on uterine perfusion.

6.4 Ethics of Prenatal Gene Therapy

There are various ethical issues in relation to *in utero* gene therapy that need to be addressed before such therapy could be applied clinically. There is a

theoretical risk that the therapeutic gene product or vector could cause developmental aberrations to occur. Any fetal therapy or procedure poses risks of infection, immune reactions and the possibility of inducing preterm labour for the fetus. An additional challenge for procedures performed for the benefit of the fetus is that there exists the potential of risk for the mother. A conflict of interest can arise since treating the fetus may not be in the mother's best interest. In many countries, a fetus has no legal rights *per se.* Attempts have been made to resolve this moral ambiguity using the concept of 'the fetus as a patient'. This aims to provide a moral framework within which the fetus is reliably expected later to achieve the status of becoming a child and eventually a person. 'The fetus as a patient' relies on the mother's decision to continue with the pregnancy and to present the fetus for medical care (Chervenak FA and McCullough LB, 2002). However, it should be emphasized that in many societies, presently the prospective mother has a right to termination, even of a normal fetus, as well as the decision to terminate an abnormal fetus or subject it to any clinical intervention. The availability of prenatal gene therapy should not in any way infringe her autonomy in these decisions.

Currently used fetal treatments such as fetal blood transfusion for anaemia are effective and carry a low risk for the mother such that the risk-benefit analysis falls heavily on the side of treatment. For experimental prenatal gene therapy procedures, the risk-benefit analysis is uncertain and it is therefore especially important that the mother gives informed consent (Burger IM and Wilfond BS, 2000). This can be difficult since the decision to participate in a fetal gene therapy trial will occur close to the time of prenatal diagnosis of the condition. The professionals involved in counseling the parents must present the information in a non-biased way and ensure that resources are set aside for long-term surveillance of the mother and fetus after birth (David AL and Ashcroft R, 2009).

Currently some parents when faced with a severely growth-restricted baby, decide to terminate the pregnancy in a procedure that is very safe for the mother and totally effective. A prenatal gene therapy strategy will have to be extremely safe, reliable and effective at treating the disease (Coutelle C and Rodeck C, 2002). For parents who would not have continued with an affected pregnancy, a partial or no

cure of an affected child resulting in a poor quality of life would be the worst case scenario. There is a possibility to test the effectiveness of prenatal gene therapy (for FGR) *in utero*, by examining uterine and umbilical artery Dopplers and performing serial measurements of fetal parameters. This would give parents and clinicians the opportunity to terminate the pregnancy if no therapeutic benefit can be detected.

One criticism leveled at prenatal gene therapy is a belief that couples pregnant with an affected child would be unlikely to proceed with prenatal gene therapy and would opt for a termination instead. There is almost no research in this area however and the views of the general public and patient groups need to be solicited as this technology comes closer to the clinic. The general public remains concerned that ethical discussion about issues such as gene therapy, cloning and the Human Genome Project are falling behind the technology (Brown P, 2000). It is therefore important to provide adequate information that will allow the public to understand the risks and benefits of these novel techniques and to enable an educated involvement in the decision-making process along with health professionals. This will also help individuals to give informed consent as these procedures become used in clinical practice (David AL, 2005, Ph.D. Thesis).

6.5 Potential for clinical translation

If translated to the clinics, it is intended to administer this therapy to pregnant women by X-ray guided catheterization of the uterine arteries through the femoral artery. The procedure itself, and in particular the temporary occlusion of the lumen, could reduce the oxygen supply to the fetus, particularly if the other uterine artery supply was significantly compromised. Hypoxaemic FGR fetuses may have little reserve to tolerate further compromise of the uteroplacental circulation during the catheterisation procedure. This could result in immediate death of the fetus, or brain damage. On the other hand, they may be more tolerant of a temporary interruption to the uteroplacental circulation, since they are already tolerant to it. Data from sheep studies (Skillman CA et al., 1985) suggest that the uterus of the pregnant sheep is perfused to sufficient excess to protect the fetus

during short-term reductions of less that 50% UABF. In addition during the surgeries described in this thesis, the operators did not observe any deleterious effects on fetal blood pressure and heart rate following short-term occlusion of the uterine artery. Although there is a risk of profound fetal hypoxaemia or even death during the procedure, with pre-oxygenation of the mother, and sonographic fetal heart rate monitoring via the mother's abdomen this risk will be minimised. The alternative option, of not treating the fetus, carries a high risk of intra-uterine death; therefore the risk is considered acceptable. Further experiments to determine the optimal vector dose and whether extra-luminal administration of vector results in equally efficient gene delivery are required.

6.6 Future Work

Having demonstrated the long term effect of local VEGF gene therapy on UABF in pregnant sheep, future work aims to evaluate the efficacy of Ad.VEGF-A_{165} gene therapy in an ovine model of FGR, created by overfeeding the ewes during adolescence. This model is characterized by 40% reduction in UABF in mid-gestation, prior to the onset of obvious changes in fetal growth. This gives the opportunity to specifically examine the effects of Ad.VEGF-A_{165} gene therapy on a compromised utero-placental circulation, and whether it benefits fetal growth velocity. Long term outcomes in neonatal sheep born after VEGF-A_{165} gene therapy prenatally will be examined, and will provide more safety data.

There are also plans to explore the mechanism of VEGF action further in endothelial cells. We intend to knockdown the *vegf* expression in ovine UAECs by siRNA technology and then compare the effects of exogenous VEGF treatment v/s adenovirus-mediated over-expression on different signaling pathways, such as eNOS, phospho-eNOS (Ser^{1177}) and iNOS. The aim of these experiments is to study if endogenous VEGF over-expression confers an advantage over exogenous VEGF treatment, on the levels of vasodilators produced. We also intend to do similar

experiments in endothelial cells from mice wherein *vegf* has been specifically knocked out of the endothelium (Lee S et al., 2007). The importance of these studies lies in the fact that there is endothelial dysfunction in pregnancies complicated by PET and FGR (Yinon Y et al., 2010), and it is of interest to examine if endogenous VEGF over-expression can be of any benefit in endothelial cells in which cell signaling has been dysregulated because of low/absent levels of VEGF family members. Exogenous VEGF treatment was found to be of no benefit in the VEGF-knockout endothelial cells (Lee S et al., 2007).

In addition to endothelial cells, we would also like to investigate the mechanism of action and test the proposed hypothesis *in vivo*. As the premise on which this research is based is that local and sustained over-expression of VEGF in the uterine arteries results in an increase in utero-placental perfusion, we would like to evaluate this in pregnant sheep. This can be carried out by infusing an anti-VEGF antibody or sFlt-1 (which binds to VEGF) systemically into pregnant sheep shortly after Ad.VEGF/Ad.LacZ transduction of the uterine arteries. If we fail to see any difference in the increase in blood flow between the treated and control uterine arteries, it would prove that the effects on utero-placental perfusion observed are indeed VEGF-mediated.

We would also like to test if the effects observed on uterine artery blood flow are NO-mediated. This can be tested using an NO clamp. The NO clamp is a well-established technique to block NO activity *in vivo*. It involves administration of the NO synthase inhibitor L-NAME with the NO donor sodium nitroprusside to block de novo synthesis of NO while compensating for the tonic production of the gas, thereby maintaining basal vascular tone (Thakor AS et al., 2010).

One of the limitations of this work was that NO levels were not quantified in culture supernatants from endothelial cells, that had been transduced with Ad.VEGF-A_{165}, Ad.VEGF-D or Ad.LacZ. The cell culture supernatants have been preserved from all these experiments and are available for measurement of both NO levels and secreted VEGF protein levels at the different MOIs in the future.

During the course of the experiments described in this Ph.D., the technique of gene targeting to the utero-placental circulation of pregnant guinea pigs was

optimised, using a thermo-sensitive pluronic F-127 gel. This method of delivery will be used to study the effects of Ad.VEGF-A_{165} over-expression on fetal growth in an FGR model of pregnancy. This is a large-scale project funded by Action Medical Research, which aims to investigate the effects of different doses of Ad.VEGF-A_{165} and different times of administration (mid-gestation and ¾ gestation) on fetal growth.

In addition to fetal growth, it would also be helpful to determine the effects of VEGF-A_{165} over-expression on flow-mediated vasodilatory responses. As pregnancies complicated by FGR and PET are characterized by impaired flow-mediated vasodilatation (Yinon Y et al., 2010), we are interested in investigating if chronic endogenous VEGF exposure can reverse the impaired flow-mediated vasodilatory responses. We plan to do these experiments by perfusion myography, in collaboration with Prof Lucilla Poston and Dr Rachel Tribe, Division of Women's Health, St. Thomas' Hospital. We will use drugs that inhibit different components of the relaxation pathway to further analyse their relative contributions to the flow-mediated vasodilatation. L-NAME, NS-398 and Apamin would be used individually and in combination to block the effects of NO synthase, prostacyclins and EDHF respectively. NO levels will be measured in the perfusate using a colorimetric assay (Griess Method).

In the studies carried out on pregnant sheep, we were unable to measure vascular permeability of vessels transduced with Ad.VEGF-A_{165} because of experimental design and limitation of animal numbers. VEGF-A_{165} is known to profoundly increase vessel permeability leading to extravasation of leucocytes into the surrounding tissue and localised edema. Even though we did not observe any obvious changes or tissue edema at histological analysis of the maternal and fetal tissues, we plan to carry out more detailed studies on measurements of vascular permeability in the guinea pig model. These studies would be performed by administering an intra-venous injection of Evan's Blue Dye and tracking its diffusion into various tissues, particularly those around the uterine artery (like uterus and perivascular adipose tissue) (Gowen BB et al., 2010;Saria A and Lundberg JM, 1983).

Finally, before clinical application of this therapy can be contemplated, further toxicology studies need to be completed in collaboration with Ark Therapeutics Plc. These include investigating the potential of transplacental transmission in the isolated perfused human placenta, determination of LD_{50} in rabbits (a commonly used species for toxicology purposes), and the extent of vector spread in sheep and guinea pig maternal and fetal tissues by quantitative PCR.

References

Aase, K, Von Euler, G, Li, X, Ponten, A, Thoren, P, Cao, R, Cao, Y, Olofsson, B, Gebre-Medhin, S, Pekny, M, Alitalo, K, Betsholtz, C & Eriksson, U 2001. Vascular endothelial growth factor-B-deficient mice display an atrial conduction defect. *Circulation,* 104**,** 358-64.

Abi-Nader, KN, Mehta, V, Shaw, SW, Bellamy, T, Smith, N, Millross, L, Laverick, B, Filippi, E, Boyd, M, Peebles, DM & David, AL 2011. Telemetric monitoring of fetal blood pressure and heart rate in the freely moving pregnant sheep: a feasibility study. *Lab Anim,* 45**,** 50-4.

Abi-Nader, KN, Mehta, V, Wigley, V, Filippi, E, Tezcan, B, Boyd, M, Peebles, DM & David, AL 2010. Doppler ultrasonography for the noninvasive measurement of uterine artery volume blood flow through gestation in the pregnant sheep. *Reprod Sci,* 17**,** 13-9.

Acharya, G, Sitras, V, Erkinaro, T, Makikallio, K, Kavasmaa, T, Pakkila, M, Huhta, JC & Rasanen, J 2007. Experimental validation of uterine artery volume blood flow measurement by Doppler ultrasonography in pregnant sheep. *Ultrasound Obstet Gynecol,* 29**,** 401-6.

Achen, MG, Jeltsch, M, Kukk, E, Makinen, T, Vitali, A, Wilks, AF, Alitalo, K & Stacker, SA 1998. Vascular endothelial growth factor D (VEGF-D) is a ligand for the tyrosine kinases VEGF receptor 2 (Flk1) and VEGF receptor 3 (Flt4). *Proc Natl Acad Sci U S A,* 95**,** 548-53.

Adamis, AP, Shima, DT, Yeo, KT, Yeo, TK, Brown, LF, Berse, B, D'amore, PA & Folkman, J 1993. Synthesis and secretion of vascular permeability factor/vascular endothelial growth factor by human retinal pigment epithelial cells. *Biochem Biophys Res Commun,* 193**,** 631-8.

Ahmad, S & Ahmed, A 2004. Elevated placental soluble vascular endothelial growth factor receptor-1 inhibits angiogenesis in preeclampsia. *Circ Res,* 95**,** 884-91.

Ahmed, A, Li, XF, Dunk, C, Whittle, MJ, Rushton, DI & Rollason, T 1995. Colocalisation of vascular endothelial growth factor and its Flt-1 receptor in human placenta. *Growth Factors,* 12**,** 235-43.

Aiello, LP, Avery, RL, Arrigg, PG, Keyt, BA, Jampel, HD, Shah, ST, Pasquale, LR, Thieme, H, Iwamoto, MA, Park, JE & Et Al. 1994. Vascular endothelial growth factor in ocular fluid of patients with diabetic retinopathy and other retinal disorders. *N Engl J Med,* 331**,** 1480-7.

Aiumlamai, S, Fredriksson, G & Nilsfors, L 1992. Real-time ultrasonography for determining the gestational age of ewes. *Vet Rec,* 131**,** 560-2.

Akalin-Sel, T, Nicolaides, KH, Peacock, J & Campbell, S 1994. Doppler dynamics and their complex interrelation with fetal oxygen pressure, carbon dioxide pressure, and pH in growth-retarded fetuses. *Obstet Gynecol,* 84**,** 439-44.

Alexander, G 1964. Studies on the Placenta of the Sheep (Ovis Aries L.). Effect of Surgical Reduction in the Number of Caruncles. *J Reprod Fertil,* 7**,** 307-22.

Anthony, FW, Wheeler, T, Elcock, CL, Pickett, M & Thomas, EJ 1994. Short report: identification of a specific pattern of vascular endothelial growth factor mRNA expression in human placenta and cultured placental fibroblasts. *Placenta,* 15**,** 557-61.

Arduini, D & Rizzo, G 1991. Fetal renal artery velocity waveforms and amniotic fluid volume in growth-retarded and post-term fetuses. *Obstet Gynecol,* 77**,** 370-3.

Arduini, D, Rizzo, G, Mancuso, S & Romanini, C 1988. Short-term effects of maternal oxygen administration on blood flow velocity waveforms in healthy and growth-retarded fetuses. *Am J Obstet Gynecol,* 159**,** 1077-80.

Ashikari-Hada, S, Habuchi, H, Kariya, Y & Kimata, K 2005. Heparin regulates vascular endothelial growth factor165-dependent mitogenic activity, tube formation, and its receptor phosphorylation of human endothelial cells. Comparison of the effects of heparin and modified heparins. *J Biol Chem,* 280**,** 31508-15.

Ashworth, JR, Warren, AY, Baker, PN & Johnson, IR 1996. A comparison of endothelium-dependent relaxation in omental and myometrial resistance arteries in pregnant and nonpregnant women. *Am J Obstet Gynecol,* 175**,** 1307-12.

Aucott, SW, Donohue, PK & Northington, FJ 2004. Increased morbidity in severe early intrauterine growth restriction. *J Perinatol,* 24**,** 435-40.

Azuma, H, Sato, J, Hamasaki, H, Sugimoto, A, Isotani, E & Obayashi, S 1995. Accumulation of endogenous inhibitors for nitric oxide synthesis and decreased content of L-arginine in regenerated endothelial cells. *Br J Pharmacol,* 115**,** 1001-4.

Azzouz, M, Ralph, GS, Storkebaum, E, Walmsley, LE, Mitrophanous, KA, Kingsman, SM, Carmeliet, P & Mazarakis, ND 2004. VEGF delivery with retrogradely transported lentivector prolongs survival in a mouse ALS model. *Nature,* 429**,** 413-7.

Bada, HS, Das, A, Bauer, CR, Shankaran, S, Lester, B, Wright, LL, Verter, J, Smeriglio, VL, Finnegan, LP & Maza, PL 2002. Gestational cocaine exposure and intrauterine growth: maternal lifestyle study. *Obstet Gynecol,* 100**,** 916-24.

Baldwin, ME, Halford, MM, Roufail, S, Williams, RA, Hibbs, ML, Grail, D, Kubo, H, Stacker, SA & Achen, MG 2005. Vascular endothelial growth factor D is dispensable for development of the lymphatic system. *Mol Cell Biol,* 25**,** 2441-9.

Barbera, A, Jones, OW, 3rd, Zerbe, GO, Hobbins, JC, Battaglia, FC & Meschia, G 1995. Ultrasonographic assessment of fetal growth: comparison between human and ovine fetus. *Am J Obstet Gynecol,* 173**,** 1765-9.

Barichello, JM, Morishita, M, Takayama, K & Nagai, T 1999. Absorption of insulin from pluronic F-127 gels following subcutaneous administration in rats. *Int J Pharm,* 184**,** 189-98.

Barker, DJ 2006. Adult consequences of fetal growth restriction. *Clin Obstet Gynecol,* 49**,** 270-83.

Barker, DJ, Forsen, T, Uutela, A, Osmond, C & Eriksson, JG 2001. Size at birth and resilience to effects of poor living conditions in adult life: longitudinal study. *BMJ,* 323**,** 1273-6.

Barker, SG, Talbert, A, Cottam, S, Baskerville, PA & Martin, JF 1993. Arterial intimal hyperplasia after occlusion of the adventitial vasa vasorum in the pig. *Arterioscler Thromb,* 13**,** 70-7.

Barleon, B, Siemeister, G, Martiny-Baron, G, Weindel, K, Herzog, C & Marme, D 1997a. Vascular endothelial growth factor up-regulates its receptor fms-like tyrosine kinase 1 (FLT-1) and a soluble variant of FLT-1 in human vascular endothelial cells. *Cancer Res,* 57**,** 5421-5.

Barleon, B, Sozzani, S, Zhou, D, Weich, HA, Mantovani, A & Marme, D 1996. Migration of human monocytes in response to vascular endothelial growth factor (VEGF) is mediated via the VEGF receptor flt-1. *Blood,* 87**,** 3336-43.

Barleon, B, Totzke, F, Herzog, C, Blanke, S, Kremmer, E, Siemeister, G, Marme, D & Martiny-Baron, G 1997b. Mapping of the sites for ligand binding and receptor dimerization at the extracellular domain of the vascular endothelial growth factor receptor FLT-1. *J Biol Chem,* 272**,** 10382-8.

Barry, JS & Anthony, RV 2008. The pregnant sheep as a model for human pregnancy. *Theriogenology,* 69**,** 55-67.

Baschat, AA, Cosmi, E, Bilardo, CM, Wolf, H, Berg, C, Rigano, S, Germer, U, Moyano, D, Turan, S, Hartung, J, Bhide, A, Muller, T, Bower, S,

Nicolaides, KH, Thilaganathan, B, Gembruch, U, Ferrazzi, E, Hecher, K, Galan, HL & Harman, CR 2007. Predictors of neonatal outcome in early-onset placental dysfunction. *Obstet Gynecol,* 109**,** 253-61.

Baschat, AA, Gembruch, U & Harman, CR 2001. The sequence of changes in Doppler and biophysical parameters as severe fetal growth restriction worsens. *Ultrasound Obstet Gynecol,* 18**,** 571-7.

Bassett, DL 1943. The changes in the vascular pattern of the ovary of the albino rat during the estrous cycle. *Am J Anat,* 73**,** 251-264.

Bastide, A, Manning, F, Harman, C, Lange, I & Morrison, I 1986. Ultrasound evaluation of amniotic fluid: outcome of pregnancies with severe oligohydramnios. *Am J Obstet Gynecol,* 154**,** 895-900.

Bates, DO & Jones, RO 2003. The role of vascular endothelial growth factor in wound healing. *Int J Low Extrem Wounds,* 2**,** 107-20.

Batra, RK & Sharma, SWL 2002. Utility of Adenoviral Vectors in Animals Models of Human Disease I: Cancer. *In:* CURIEL, DT & DOUGLAS, JT (eds.) *Adenoviral Vectors for Gene Therapy.* New York: New York: Academic Press.

Battaglia, FC, Meschia, G, Makowski, EL & Bowes, W 1968. The effect of maternal oxygen inhalation upon fetal oxygenation. *J Clin Invest,* 47**,** 548-55.

Bauersachs, J, Popp, R, Hecker, M, Sauer, E, Fleming, I & Busse, R 1996. Nitric oxide attenuates the release of endothelium-derived hyperpolarizing factor. *Circulation,* 94**,** 3341-7.

Bekedam, DJ, Mulder, EJ, Snijders, RJ & Visser, GH 1991. The effects of maternal hyperoxia on fetal breathing movements, body movements and heart rate variation in growth retarded fetuses. *Early Hum Dev,* 27**,** 223-32.

Belgore, F, Blann, A, Neil, D, Ahmed, AS & Lip, GY 2004. Localisation of members of the vascular endothelial growth factor (VEGF) family and their receptors in human atherosclerotic arteries. *J Clin Pathol,* 57**,** 266-72.

Bell, AW, Wilkening, RB & Meschia, G 1987. Some aspects of placental function in chronically heat-stressed ewes. *J Dev Physiol,* 9**,** 17-29.

Bellomo, D, Headrick, JP, Silins, GU, Paterson, CA, Thomas, PS, Gartside, M, Mould, A, Cahill, MM, Tonks, ID, Grimmond, SM, Townson, S, Wells, C, Little, M, Cummings, MC, Hayward, NK & Kay, GF 2000. Mice lacking the vascular endothelial growth factor-B gene (Vegfb) have smaller hearts, dysfunctional coronary vasculature, and impaired recovery from cardiac ischemia. *Circ Res,* 86**,** E29-35.

Beppu, M, Obayashi, S, Aso, T, Goto, M & Azuma, H 2002. Endogenous nitric oxide synthase inhibitors in endothelial cells, endothelin-1 within the vessel wall, and intimal hyperplasia in perimenopausal human uterine arteries. *J Cardiovasc Pharmacol,* 39**,** 192-200.

Bergelson, JM, Cunningham, JA, Droguett, G, Kurt-Jones, EA, Krithivas, A, Hong, JS, Horwitz, MS, Crowell, RL & Finberg, RW 1997. Isolation of a common receptor for Coxsackie B viruses and adenoviruses 2 and 5. *Science,* 275**,** 1320-3.

Bergers, G, Brekken, R, Mcmahon, G, Vu, TH, Itoh, T, Tamaki, K, Tanzawa, K, Thorpe, P, Itohara, S, Werb, Z & Hanahan, D 2000. Matrix metalloproteinase-9 triggers the angiogenic switch during carcinogenesis. *Nat Cell Biol,* 2**,** 737-44.

Bernfield, M, Kokenyesi, R, Kato, M, Hinkes, MT, Spring, J, Gallo, RL & Lose, EJ 1992. Biology of the syndecans: a family of transmembrane heparan sulfate proteoglycans. *Annu Rev Cell Biol,* 8**,** 365-93.

Bernstein, IM, Horbar, JD, Badger, GJ, Ohlsson, A & Golan, A 2000. Morbidity and mortality among very-low-birth-weight neonates with intrauterine growth restriction. The Vermont Oxford Network. *Am J Obstet Gynecol,* 182**,** 198-206.

Bersinger, NA & Odegard, RA 2005. Serum levels of macrophage colony stimulating, vascular endothelial, and placenta growth factor in relation to later clinical onset of pre-eclampsia and a small-for-gestational age birth. *Am J Reprod Immunol,* 54**,** 77-83.

Bir, N, Yazdani, SS, Avril, M, Layez, C, Gysin, J & Chitnis, CE 2006. Immunogenicity of Duffy binding-like domains that bind chondroitin sulfate A and protection against pregnancy-associated malaria. *Infect Immun,* 74**,** 5955-63.

Bird, IM, Sullivan, JA, Di, T, Cale, JM, Zhang, L, Zheng, J & Magness, RR 2000. Pregnancy-dependent changes in cell signaling underlie changes in differential control of vasodilator production in uterine artery endothelial cells. *Endocrinology,* 141**,** 1107-17.

Blankenship, TN & Enders, AC 2003. Modification of uterine vasculature during pregnancy in macaques. *Microsc Res Tech,* 60**,** 390-401.

Blonder, JM, Baird, L, Fulfs, JC & Rosenthal, GJ 1999. Dose-dependent hyperlipidemia in rabbits following administration of poloxamer 407 gel. *Life Sci,* 65**,** PL261-6.

Bobryshev, YV, Inder, SJ, Cherian, SM, Lord, RS, Ao, PY, Hawthorne, WJ & Fletcher, JP 2001. Colonisation of prosthetic grafts by immunocompetent cells in a sheep model. *Cardiovasc Surg,* 9**,** 166-76.

Bohorquez, M, Koch, C, Trygstad, T & Pandit, N 1999. A Study of the Temperature-Dependent Micellization of Pluronic F127. *J Colloid Interface Sci,* 216**,** 34-40.

Brenner, BM & Chertow, GM 1993. Congenital oligonephropathy: an inborn cause of adult hypertension and progressive renal injury? *Curr Opin Nephrol Hypertens,* 2**,** 691-5.

Brown, DM, Kaiser, PK, Michels, M, Soubrane, G, Heier, JS, Kim, RY, Sy, JP & Schneider, S 2006. Ranibizumab versus verteporfin for neovascular age-related macular degeneration. *N Engl J Med,* 355**,** 1432-44.

Brown, P 2000. Regulations not keeping up with developments in genetics, says poll. *BMJ,* 321**,** 1369.

Brownbill, P, Mckeeman, GC, Brockelsby, JC, Crocker, IP & Sibley, CP 2007. Vasoactive and permeability effects of vascular endothelial growth factor-165 in the term in vitro dually perfused human placental lobule. *Endocrinology,* 148**,** 4734-44.

Brownbill, P, Mills, TA, Soydemir, DF & Sibley, CP 2008. Vasoactivity to and endogenous release of vascular endothelial growth factor in the in vitro perfused human placental lobule from pregnancies complicated by preeclampsia. *Placenta,* 29**,** 950-5.

Bukowski, R, Gahn, D, Denning, J & Saade, G 2001. Impairment of growth in fetuses destined to deliver preterm. *Am J Obstet Gynecol,* 185**,** 463-7.

Burger, IM & Wilfond, BS 2000. Limitations of informed consent for in utero gene transfer research: implications for investigators and institutional review boards. *Hum Gene Ther,* 11**,** 1057-63.

Carmeliet, P 2003. Angiogenesis in health and disease. *Nat Med,* 9**,** 653-60.

Carmeliet, P, Ferreira, V, Breier, G, Pollefeyt, S, Kieckens, L, Gertsenstein, M, Fahrig, M, Vandenhoeck, A, Harpal, K, Eberhardt, C, Declercq, C, Pawling, J, Moons, L, Collen, D, Risau, W & Nagy, A 1996. Abnormal blood vessel development and lethality in embryos lacking a single VEGF allele. *Nature,* 380**,** 435-9.

Carmeliet, P, Lampugnani, MG, Moons, L, Breviario, F, Compernolle, V, Bono, F, Balconi, G, Spagnuolo, R, Oosthuyse, B, Dewerchin, M, Zanetti, A, Angellilo, A, Mattot, V, Nuyens, D, Lutgens, E, Clotman, F, De Ruiter, MC, Gittenberger-De Groot, A, Poelmann, R, Lupu, F, Herbert, JM, Collen, D &

Dejana, E 1999. Targeted deficiency or cytosolic truncation of the VE-cadherin gene in mice impairs VEGF-mediated endothelial survival and angiogenesis. *Cell,* 98**,** 147-57.

Carreras, LO, Defreyn, G, Machin, SJ, Vermylen, J, Deman, R, Spitz, B & Van Assche, A 1981. Arterial thrombosis, intrauterine death and "lupus" antiocoagulant: detection of immunoglobulin interfering with prostacyclin formation. *Lancet,* 1**,** 244-6.

Carter, AM 1993. Current topic: restriction of placental and fetal growth in the guinea-pig. *Placenta,* 14**,** 125-35.

Carter, AM 2007. Animal models of human placentation--a review. *Placenta,* 28 Suppl A**,** S41-7.

Casanello, P, Gonzalez, M, Sahueza, F, Vasquez, R & Sobrevia, L 2005. Inhibition of L-arginine/nitric oxide pathway in intrauterine growth restriction is insensitive to hypoxia in human umbilical vein endothelium. *J Physiol,* 565P**,** C137.

Casanello, P & Sobrevia, L 2002. Intrauterine growth retardation is associated with reduced activity and expression of the cationic amino acid transport systems y+/hCAT-1 and y+/hCAT-2B and lower activity of nitric oxide synthase in human umbilical vein endothelial cells. *Circ Res,* 91**,** 127-34.

Celletti, FL, Waugh, JM, Amabile, PG, Brendolan, A, Hilfiker, PR & Dake, MD 2001. Vascular endothelial growth factor enhances atherosclerotic plaque progression. *Nat Med,* 7**,** 425-9.

Cellini, C, Xu, J, Arriaga, A & Buchmiller-Crair, TL 2004. Effect of epidermal growth factor infusion on fetal rabbit intrauterine growth retardation and small intestinal development. *J Pediatr Surg,* 39**,** 891-7; discussion 891-7.

Chamberlain, PF, Manning, FA, Morrison, I, Harman, CR & Lange, IR 1984. Ultrasound evaluation of amniotic fluid volume. I. The relationship of marginal and decreased amniotic fluid volumes to perinatal outcome. *Am J Obstet Gynecol,* 150**,** 245-9.

Chandra, KR & Matsumura, T 1979. Ontogenetic development of the immune system and effects of fetal growth retardation. *J Perinat Med,* 7**,** 279-90.

Chen, H, Bagri, A, Zupicich, JA, Zou, Y, Stoeckli, E, Pleasure, SJ, Lowenstein, DH, Skarnes, WC, Chedotal, A & Tessier-Lavigne, M 2000. Neuropilin-2 regulates the development of selective cranial and sensory nerves and hippocampal mossy fiber projections. *Neuron,* 25**,** 43-56.

Chervenak, FA & Mccullough, LB 2002. A comprehensive ethical framework for fetal research and its application to fetal surgery for spina bifida. *Am J Obstet Gynecol,* 187**,** 10-4.

Ciulla, TA & Rosenfeld, PJ 2009. Antivascular endothelial growth factor therapy for neovascular age-related macular degeneration. *Curr Opin Ophthalmol,* 20**,** 158-65.

Clapp, JF, 3rd, Szeto, HH, Larrow, R, Hewitt, J & Mann, LI 1981. Fetal metabolic response to experimental placental vascular damage. *Am J Obstet Gynecol,* 140**,** 446-51.

Clark, KE, Durnwald, M & Austin, JE 1982. A model for studying chronic reduction in uterine blood flow in pregnant sheep. *Am J Physiol,* 242**,** H297-301.

Clasp 1994. CLASP: a randomised trial of low-dose aspirin for the prevention and treatment of pre-eclampsia among 9364 pregnant women. CLASP (Collaborative Low-dose Aspirin Study in Pregnancy) Collaborative Group. *Lancet,* 343**,** 619-29.

Clauss, M, Weich, H, Breier, G, Knies, U, Rockl, W, Waltenberger, J & Risau, W 1996. The vascular endothelial growth factor receptor Flt-1 mediates biological activities. Implications for a functional role of placenta growth factor in monocyte activation and chemotaxis. *J Biol Chem,* 271**,** 17629-34.

Clayton, JA, Chalothorn, D & Faber, JE 2008. Vascular endothelial growth factor-A specifies formation of native collaterals and regulates collateral growth in ischemia. *Circ Res,* 103**,** 1027-36.

Cliver, SP, Goldenberg, RL, Cutter, GR, Hoffman, HJ, Davis, RO & Nelson, KG 1995. The effect of cigarette smoking on neonatal anthropometric measurements. *Obstet Gynecol,* 85**,** 625-30.

Colavitti, R, Pani, G, Bedogni, B, Anzevino, R, Borrello, S, Waltenberger, J & Galeotti, T 2002. Reactive oxygen species as downstream mediators of angiogenic signaling by vascular endothelial growth factor receptor-2/KDR. *J Biol Chem,* 277**,** 3101-8.

Colon, GP, Deveikis, JP & Dickinson, LD 1999. Revascularization of occluded internal carotid arteries by hypertrophied vasa vasorum: report of four cases. *Neurosurgery,* 45**,** 634-7.

Constancia, M, Hemberger, M, Hughes, J, Dean, W, Ferguson-Smith, A, Fundele, R, Stewart, F, Kelsey, G, Fowden, A, Sibley, C & Reik, W 2002. Placental-specific IGF-II is a major modulator of placental and fetal growth. *Nature,* 417**,** 945-8.

Coutelle, C & Rodeck, C 2002. On the scientific and ethical issues of fetal somatic gene therapy. *Gene Ther,* 9**,** 670-3.

Crampton, SP, Davis, J & Hughes, CC 2007. Isolation of human umbilical vein endothelial cells (HUVEC). *J Vis Exp***,** 183.

Crawford, BS, Davis, J & Harrigill, K 1997. Uterine artery atherosclerotic disease: histologic features and clinical correlation. *Obstet Gynecol,* 90**,** 210-5.

Creasy, RK, Barrett, CT, De Swiet, M, Kahanpaa, KV & Rudolph, AM 1972. Experimental intrauterine growth retardation in the sheep. *Am J Obstet Gynecol,* 112**,** 566-73.

Cullinan-Bove, K & Koos, RD 1993. Vascular endothelial growth factor/vascular permeability factor expression in the rat uterus: rapid stimulation by estrogen correlates with estrogen-induced increases in uterine capillary permeability and growth. *Endocrinology,* 133**,** 829-37.

David, AL. 2005. *Development of ultrasound-guided gene therapy to the sheep fetus.* Ph.D., University College London.

David, AL & Ashcroft, R 2009. Placental Gene Therapy. *Obstetrics, Gynaecology &Reproductive Medicine,* 19**,** 296-298.

David, AL, Torondel, B, Zachary, I, Wigley, V, Abi-Nader, K, Mehta, V, Buckley, SM, Cook, T, Boyd, M, Rodeck, CH, Martin, J & Peebles, DM 2008. Local delivery of VEGF adenovirus to the uterine artery increases vasorelaxation and uterine blood flow in the pregnant sheep. *Gene Ther,* 15**,** 1344-50.

Davis-Smyth, T, Chen, H, Park, J, Presta, LG & Ferrara, N 1996. The second immunoglobulin-like domain of the VEGF tyrosine kinase receptor Flt-1 determines ligand binding and may initiate a signal transduction cascade. *EMBO J,* 15**,** 4919-27.

Dechiara, TM, Efstratiadis, A & Robertson, EJ 1990. A growth-deficiency phenotype in heterozygous mice carrying an insulin-like growth factor II gene disrupted by targeting. *Nature,* 345**,** 78-80.

Dejana, E 2004. Endothelial cell-cell junctions: happy together. *Nat Rev Mol Cell Biol,* 5**,** 261-70.

Delotte, J, Novellas, S, Koh, C, Bongain, A & Chevallier, P 2009. Obstetrical prognosis and pregnancy outcome following pelvic arterial embolisation for post-partum hemorrhage. *Eur J Obstet Gynecol Reprod Biol,* 145**,** 129-32.

Dickerson, KS, Newhouse, VL, Tortoli, P & Guidi, G 1993. Comparison of conventional and transverse Doppler sonograms. *J Ultrasound Med,* 12**,** 497-506.

Dielis, AW, Castoldi, E, Spronk, HM, Van Oerle, R, Hamulyak, K, Ten Cate, H & Rosing, J 2008. Coagulation factors and the protein C system as determinants of thrombin generation in a normal population. *J Thromb Haemost,* 6**,** 125-31.

Dimmeler, S, Fleming, I, Fisslthaler, B, Hermann, C, Busse, R & Zeiher, AM 1999. Activation of nitric oxide synthase in endothelial cells by Akt-dependent phosphorylation. *Nature,* 399**,** 601-5.

Divon, MY & Hsu, HW 1992. Maternal and fetal blood flow velocity waveforms in intrauterine growth retardation. *Clin Obstet Gynecol,* 35**,** 156-71.

Doctor, BA, O'riordan, MA, Kirchner, HL, Shah, D & Hack, M 2001. Perinatal correlates and neonatal outcomes of small for gestational age infants born at term gestation. *Am J Obstet Gynecol,* 185**,** 652-9.

Dodic, M, Tangalakis, K, Moritz, K, Mcfarlane, A & Wintour, EM 1998. Fluid abnormalities occur in the chronically cannulated mid-gestation but not late gestation ovine fetus. *Pediatr Res,* 44**,** 894-9.

Doshi, N, Surti, U & Szulman, AE 1983. Morphologic anomalies in triploid liveborn fetuses. *Hum Pathol,* 14**,** 716-23.

Douglas, KA & Redman, CW 1994. Eclampsia in the United Kingdom. *BMJ,* 309**,** 1395-400.

Dubois, RN, Abramson, SB, Crofford, L, Gupta, RA, Simon, LS, Van De Putte, LB & Lipsky, PE 1998. Cyclooxygenase in biology and disease. *FASEB J,* 12**,** 1063-73.

Dumont, DJ, Jussila, L, Taipale, J, Lymboussaki, A, Mustonen, T, Pajusola, K, Breitman, M & Alitalo, K 1998. Cardiovascular failure in mouse embryos deficient in VEGF receptor-3. *Science,* 282**,** 946-9.

Dvorak, HF, Sioussat, TM, Brown, LF, Berse, B, Nagy, JA, Sotrel, A, Manseau, EJ, Van De Water, L & Senger, DR 1991. Distribution of vascular permeability factor (vascular endothelial growth factor) in tumors: concentration in tumor blood vessels. *J Exp Med,* 174**,** 1275-8.

Edwards, G, Dora, KA, Gardener, MJ, Garland, CJ & Weston, AH 1998. K+ is an endothelium-derived hyperpolarizing factor in rat arteries. *Nature,* 396**,** 269-72.

Edwards, LJ & Mcmillen, IC 2001. Maternal undernutrition increases arterial blood pressure in the sheep fetus during late gestation. *J Physiol,* 533**,** 561-70.

Egund, N & Carter, AM 1974. Uterine and placental circulation in the guinea-pig: an angiographic study. *J Reprod Fertil,* 40**,** 401-10.

El-Kamel, AH 2002. In vitro and in vivo evaluation of Pluronic F127-based ocular delivery system for timolol maleate. *Int J Pharm,* 241**,** 47-55.

Eming, SA & Krieg, T 2006. Molecular mechanisms of VEGF-A action during tissue repair. *J Investig Dermatol Symp Proc,* 11**,** 79-86.

Emmanouilides, GC, Townsend, DE & Bauer, RA 1968. Effects of single umbilical artery ligation in the lamb fetus. *Pediatrics,* 42**,** 919-27.

Enders, AC 1965. A Comparative Study of the Fine Structure of the Trophoblast in Several Hemochorial Placentas. *Am J Anat,* 116**,** 29-67.

Enders, AC 1995. Transition from lacunar to villous stage of implantation in the macaque, including establishment of the trophoblastic shell. *Acta Anat (Basel),* 152**,** 151-69.

Eremia, SC, De Boo, HA, Bloomfield, FH, Oliver, MH & Harding, JE 2007. Fetal and amniotic insulin-like growth factor-I supplements improve growth rate in intrauterine growth restriction fetal sheep. *Endocrinology,* 148**,** 2963-72.

Evans, JD & Hearing, P 2002. Adenovirus Replication. *In:* CURIEL, DT & DOUGLAS, JT (eds.) *Adenoviral Vectors for Gene Therapy.* New York: New York: Academic Press.

Facemire, CS, Nixon, AB, Griffiths, R, Hurwitz, H & Coffman, TM 2009. Vascular endothelial growth factor receptor 2 controls blood pressure by regulating nitric oxide synthase expression. *Hypertension,* 54**,** 652-8.

Faraci, FM, Sigmund, CD, Shesely, EG, Maeda, N & Heistad, DD 1998. Responses of carotid artery in mice deficient in expression of the gene for endothelial NO synthase. *Am J Physiol,* 274**,** H564-70.

Feldman, LJ, Pastore, CJ, Aubailly, N, Kearney, M, Chen, D, Perricaudet, M, Steg, PG & Isner, JM 1997. Improved efficiency of arterial gene transfer by use of poloxamer 407 as a vehicle for adenoviral vectors. *Gene Ther,* 4**,** 189-98.

Feletou, M & Vanhoutte, PM 2005. *EDHF: The Complete Story,* Boca Raton, FL, CRC Press.

Feletou, M & Vanhoutte, PM 2009. EDHF: an update. *Clin Sci (Lond),* 117**,** 139-55.

Ferrara, N 1999. Molecular and biological properties of vascular endothelial growth factor. *J Mol Med,* 77**,** 527-43.

Ferrara, N, Carver-Moore, K, Chen, H, Dowd, M, Lu, L, O'shea, KS, Powell-Braxton, L, Hillan, KJ & Moore, MW 1996. Heterozygous embryonic

lethality induced by targeted inactivation of the VEGF gene. *Nature,* 380**,** 439-42.

Ferrara, N & Henzel, WJ 1989. Pituitary follicular cells secrete a novel heparin-binding growth factor specific for vascular endothelial cells. *Biochem Biophys Res Commun,* 161**,** 851-8.

Figueroa, R & Maulik, D 2006. Prenatal therapy for fetal growth restriction. *Clin Obstet Gynecol,* 49**,** 308-19.

Fisk, NM & Atun, R 2008. Market failure and the poverty of new drugs in maternal health. *PLoS Med,* 5**,** e22.

Fleming, I & Busse, R 2003. Molecular mechanisms involved in the regulation of the endothelial nitric oxide synthase. *Am J Physiol Regul Integr Comp Physiol,* 284**,** R1-12.

Fong, GH, Rossant, J, Gertsenstein, M & Breitman, ML 1995. Role of the Flt-1 receptor tyrosine kinase in regulating the assembly of vascular endothelium. *Nature,* 376**,** 66-70.

Fong, GH, Zhang, L, Bryce, DM & Peng, J 1999. Increased hemangioblast commitment, not vascular disorganization, is the primary defect in flt-1 knock-out mice. *Development,* 126**,** 3015-25.

Fulton, D, Gratton, JP, Mccabe, TJ, Fontana, J, Fujio, Y, Walsh, K, Franke, TF, Papapetropoulos, A & Sessa, WC 1999. Regulation of endothelium-derived nitric oxide production by the protein kinase Akt. *Nature,* 399**,** 597-601.

Galan, HL, Anthony, RV, Rigano, S, Parker, TA, De Vrijer, B, Ferrazzi, E, Wilkening, RB & Regnault, TR 2005. Fetal hypertension and abnormal Doppler velocimetry in an ovine model of intrauterine growth restriction. *Am J Obstet Gynecol,* 192**,** 272-9.

Gardosi, J, Chang, A, Kalyan, B, Sahota, D & Symonds, EM 1992. Customised antenatal growth charts. *Lancet,* 339**,** 283-7.

Gardosi, JO 2005. Prematurity and fetal growth restriction. *Early Hum Dev,* 81**,** 43-9.

Gelinas, DS, Bernatchez, PN, Rollin, S, Bazan, NG & Sirois, MG 2002. Immediate and delayed VEGF-mediated NO synthesis in endothelial cells: role of PI3K, PKC and PLC pathways. *Br J Pharmacol,* 137**,** 1021-30.

Gerber, HP, Hillan, KJ, Ryan, AM, Kowalski, J, Keller, GA, Rangell, L, Wright, BD, Radtke, F, Aguet, M & Ferrara, N 1999. VEGF is required for growth and survival in neonatal mice. *Development,* 126**,** 1149-59.

Gerber, HP, Mcmurtrey, A, Kowalski, J, Yan, M, Keyt, BA, Dixit, V & Ferrara, N 1998. Vascular endothelial growth factor regulates endothelial cell survival through the phosphatidylinositol 3'-kinase/Akt signal transduction pathway. Requirement for Flk-1/KDR activation. *J Biol Chem,* 273**,** 30336-43.

Gifford, SM, Cale, JM, Tsoi, S, Magness, RR & Bird, IM 2003. Pregnancy-specific changes in uterine artery endothelial cell signaling in vivo are both programmed and retained in primary culture. *Endocrinology,* 144**,** 3639-50.

Giussani, DA, Salinas, CE, Villena, M & Blanco, CE 2007. The role of oxygen in prenatal growth: studies in the chick embryo. *J Physiol,* 585**,** 911-7.

Gleicher, N, Harlow, L & Zilberstein, M 1992. Regulatory effect of antiphospholipid antibodies on signal transduction: a possible model for autoantibody-induced reproductive failure. *Am J Obstet Gynecol,* 167**,** 637-42.

Gliki, G, Abu-Ghazaleh, R, Jezequel, S, Wheeler-Jones, C & Zachary, I 2001. Vascular endothelial growth factor-induced prostacyclin production is mediated by a protein kinase C (PKC)-dependent activation of extracellular signal-regulated protein kinases 1 and 2 involving PKC-delta and by mobilization of intracellular Ca2+. *Biochem J,* 353**,** 503-12.

Gluzman-Poltorak, Z, Cohen, T, Herzog, Y & Neufeld, G 2000. Neuropilin-2 is a receptor for the vascular endothelial growth factor (VEGF) forms VEGF-145 and VEGF-165 [corrected]. *J Biol Chem,* 275**,** 18040-5.

Goetzman, BW, Itskovitz, J & Rudolph, AM 1984. Fetal adaptations to spontaneous hypoxemia and responses to maternal oxygen breathing. *Biol Neonate,* 46**,** 276-84.

Goncalves, GA, Vassallo, PF, Dos Santos, L, Schettert, IT, Nakamuta, JS, Becker, C, Tucci, PJ & Krieger, JE 2010. Intramyocardial transplantation of fibroblasts expressing vascular endothelial growth factor attenuates cardiac dysfunction. *Gene Ther,* 17**,** 305-14.

Gowen, BB, Julander, JG, London, NR, Wong, MH, Larson, D, Morrey, JD, Li, DY & Bray, M 2010. Assessing changes in vascular permeability in a hamster model of viral hemorrhagic fever. *Virol J,* 7**,** 240.

Gragoudas, ES, Adamis, AP, Cunningham, ET, Jr., Feinsod, M & Guyer, DR 2004. Pegaptanib for neovascular age-related macular degeneration. *N Engl J Med,* 351**,** 2805-16.

Greenwood, JD, Minhas, K, Di Santo, JP, Makita, M, Kiso, Y & Croy, BA 2000. Ultrastructural studies of implantation sites from mice deficient in uterine natural killer cells. *Placenta,* 21**,** 693-702.

Griffith, TM, Edwards, DH, Lewis, MJ & Henderson, AH 1985. Evidence that cyclic guanosine monophosphate (cGMP) mediates endothelium-dependent relaxation. *Eur J Pharmacol,* 112**,** 195-202.

Grummer, MA, Sullivan, JA, Magness, RR & Bird, IM 2009. Vascular endothelial growth factor acts through novel, pregnancy-enhanced receptor signalling pathways to stimulate endothelial nitric oxide synthase activity in uterine artery endothelial cells. *Biochem J,* 417**,** 501-11.

Gryglewski, RJ 2008. Prostacyclin among prostanoids. *Pharmacol Rep,* 60**,** 3-11.

Gu, C, Rodriguez, ER, Reimert, DV, Shu, T, Fritzsch, B, Richards, LJ, Kolodkin, AL & Ginty, DD 2003. Neuropilin-1 conveys semaphorin and VEGF signaling during neural and cardiovascular development. *Dev Cell,* 5**,** 45-57.

Gulmezoglu, AM & Hofmeyr, GJ 2000. Bed rest in hospital for suspected impaired fetal growth. *Cochrane Database Syst Rev***,** CD000034.

Gulmezoglu, AM & Hofmeyr, GJ 2001. Betamimetics for suspected impaired fetal growth. *Cochrane Database Syst Rev***,** CD000036.

Gumbiner, BM & Mccrea, PD 1993. Catenins as mediators of the cytoplasmic functions of cadherins. *J Cell Sci Suppl,* 17**,** 155-8.

Hackett, GA, Campbell, S, Gamsu, H, Cohen-Overbeek, T & Pearce, JM 1987. Doppler studies in the growth retarded fetus and prediction of neonatal necrotising enterocolitis, haemorrhage, and neonatal morbidity. *Br Med J (Clin Res Ed),* 294**,** 13-6.

Haig, D 1993. Genetic conflicts in human pregnancy. *Q Rev Biol,* 68**,** 495-532.

Haig, D 1997. Parental antagonism, relatedness asymmetries, and genomic imprinting. *Proc Biol Sci,* 264**,** 1657-62.

Hales, CN, Barker, DJ, Clark, PM, Cox, LJ, Fall, C, Osmond, C & Winter, PD 1991. Fetal and infant growth and impaired glucose tolerance at age 64. *BMJ,* 303**,** 1019-22.

Hallmann, R, Horn, N, Selg, M, Wendler, O, Pausch, F & Sorokin, LM 2005. Expression and function of laminins in the embryonic and mature vasculature. *Physiol Rev,* 85**,** 979-1000.

Hamilton, WJ & Boyd, JD 1970. *The Human Placenta,* Cambridge, Heffer and Sons.

Harding, JE, Owens, JA & Robinson, JS 1992. Should we try to supplement the growth retarded fetus? A cautionary tale. *Br J Obstet Gynaecol,* 99**,** 707-9.

Haugaard, CT & Bauer, MK 2001. Rodent models of intrauterine growth restriction. *Scand J Lab Anim Sci,* 28**,** 10-22.

He, H, Venema, VJ, Gu, X, Venema, RC, Marrero, MB & Caldwell, RB 1999. Vascular endothelial growth factor signals endothelial cell production of nitric oxide and prostacyclin through flk-1/KDR activation of c-Src. *J Biol Chem,* 274**,** 25130-5.

Heaman, M & Gupton, A 1998. Perceptions of bed rest by women with high-risk pregnancies: A comparison between home and hospital. *Birth,* 25**,** 252-8.

Hecker, M, Sessa, WC, Harris, HJ, Anggard, EE & Vane, JR 1990. The metabolism of L-arginine and its significance for the biosynthesis of endothelium-derived relaxing factor: cultured endothelial cells recycle L-citrulline to L-arginine. *Proc Natl Acad Sci U S A,* 87**,** 8612-6.

Hedman, M, Hartikainen, J, Syvanne, M, Stjernvall, J, Hedman, A, Kivela, A, Vanninen, E, Mussalo, H, Kauppila, E, Simula, S, Narvanen, O, Rantala, A, Peuhkurinen, K, Nieminen, MS, Laakso, M & Yla-Herttuala, S 2003. Safety and feasibility of catheter-based local intracoronary vascular endothelial growth factor gene transfer in the prevention of postangioplasty and in-stent restenosis and in the treatment of chronic myocardial ischemia: phase II results of the Kuopio Angiogenesis Trial (KAT). *Circulation,* 107**,** 2677-83.

Hefler, LA, Reyes, CA, O'brien, WE & Gregg, AR 2001. Perinatal development of endothelial nitric oxide synthase-deficient mice. *Biol Reprod,* 64**,** 666-73.

Heistad, DD, Marcus, ML, Larsen, GE & Armstrong, ML 1981. Role of vasa vasorum in nourishment of the aortic wall. *Am J Physiol,* 240**,** H781-7.

Hemberger, M, Nozaki, T, Masutani, M & Cross, JC 2003. Differential expression of angiogenic and vasodilatory factors by invasive trophoblast giant cells depending on depth of invasion. *Dev Dyn,* 227**,** 185-91.

Henry, TD, Annex, BH, Mckendall, GR, Azrin, MA, Lopez, JJ, Giordano, FJ, Shah, PK, Willerson, JT, Benza, RL, Berman, DS, Gibson, CM, Bajamonde, A, Rundle, AC, Fine, J & Mccluskey, ER 2003. The VIVA trial: Vascular endothelial growth factor in Ischemia for Vascular Angiogenesis. *Circulation,* 107**,** 1359-65.

Hiratsuka, S, Minowa, O, Kuno, J, Noda, T & Shibuya, M 1998. Flt-1 lacking the tyrosine kinase domain is sufficient for normal development and angiogenesis in mice. *Proc Natl Acad Sci U S A,* 95**,** 9349-54.

Hitchins, MP & Moore, GE 2002. Genomic imprinting in fetal growth and development. *Expert Rev Mol Med,* 4**,** 1-19.

Ho, SS, Chan, YL, Yeung, DK & Metreweli, C 2002. Blood flow volume quantification of cerebral ischemia: comparison of three noninvasive imaging techniques of carotid and vertebral arteries. *AJR Am J Roentgenol,* 178**,** 551-6.

Hochachka, PW & Lutz, PL 2001. Mechanism, origin, and evolution of anoxia tolerance in animals. *Comp Biochem Physiol B Biochem Mol Biol,* 130**,** 435-59.

Hoefer, IE, Timmers, L & Piek, JJ 2007. Growth factor therapy in atherosclerotic disease-friend or foe. *Curr Pharm Des,* 13**,** 1803-10.

Holm, VA, Cassidy, SB, Butler, MG, Hanchett, JM, Greenswag, LR, Whitman, BY & Greenberg, F 1993. Prader-Willi syndrome: consensus diagnostic criteria. *Pediatrics,* 91**,** 398-402.

Hood, JD, Meininger, CJ, Ziche, M & Granger, HJ 1998. VEGF upregulates ecNOS message, protein, and NO production in human endothelial cells. *Am J Physiol,* 274**,** H1054-8.

Hooper, SB 1995. Fetal metabolic responses to hypoxia. *Reprod Fertil Dev,* 7**,** 527-38.

Horowitz, JR, Rivard, A, Van Der Zee, R, Hariawala, M, Sheriff, DD, Esakof, DD, Chaudhry, GM, Symes, JF & Isner, JM 1997. Vascular endothelial growth factor/vascular permeability factor produces nitric oxide-dependent hypotension. Evidence for a maintenance role in quiescent adult endothelium. *Arterioscler Thromb Vasc Biol,* 17**,** 2793-800.

Houck, KA, Ferrara, N, Winer, J, Cachianes, G, Li, B & Leung, DW 1991. The vascular endothelial growth factor family: identification of a fourth molecular species and characterization of alternative splicing of RNA. *Mol Endocrinol,* 5**,** 1806-14.

Hristova, M, Cuthill, D, Zbarsky, V, Acosta-Saltos, A, Wallace, A, Blight, K, Buckley, SM, Peebles, D, Heuer, H, Waddington, SN & Raivich, G 2010. Activation and deactivation of periventricular white matter phagocytes during postnatal mouse development. *Glia,* 58**,** 11-28.

Huang, N, Khan, A, Ashrafpour, H, Neligan, PC, Forrest, CR, Kontos, CD & Pang, CY 2006. Efficacy and mechanism of adenovirus-mediated VEGF-165 gene therapy for augmentation of skin flap viability. *Am J Physiol Heart Circ Physiol,* 291**,** H127-37.

Huang, PL, Huang, Z, Mashimo, H, Bloch, KD, Moskowitz, MA, Bevan, JA & Fishman, MC 1995. Hypertension in mice lacking the gene for endothelial nitric oxide synthase. *Nature,* 377**,** 239-42.

Hurwitz, H, Fehrenbacher, L, Novotny, W, Cartwright, T, Hainsworth, J, Heim, W, Berlin, J, Baron, A, Griffing, S, Holmgren, E, Ferrara, N, Fyfe, G, Rogers, B, Ross, R & Kabbinavar, F 2004. Bevacizumab plus irinotecan, fluorouracil, and leucovorin for metastatic colorectal cancer. *N Engl J Med,* 350**,** 2335-42.

Iaccarino, G, Smithwick, LA, Lefkowitz, RJ & Koch, WJ 1999. Targeting Gbeta gamma signaling in arterial vascular smooth muscle proliferation: a novel strategy to limit restenosis. *Proc Natl Acad Sci U S A,* 96**,** 3945-50.

Ignarro, LJ 1989. Biological actions and properties of endothelium-derived nitric oxide formed and released from artery and vein. *Circ Res,* 65**,** 1-21.

Ikeda, E, Achen, MG, Breier, G & Risau, W 1995. Hypoxia-induced transcriptional activation and increased mRNA stability of vascular endothelial growth factor in C6 glioma cells. *J Biol Chem,* 270**,** 19761-6.

Iljin, K, Karkkainen, MJ, Lawrence, EC, Kimak, MA, Uutela, M, Taipale, J, Pajusola, K, Alhonen, L, Halmekyto, M, Finegold, DN, Ferrell, RE & Alitalo, K 2001. VEGFR3 gene structure, regulatory region, and sequence polymorphisms. *FASEB J,* 15**,** 1028-36.

Illsley, NP, Aarnoudse, JG, Penfold, P, Bardsley, SE, Coade, SB, Stacey, TE & Hytten, FE 1984. Mechanical and metabolic viability of a placental perfusion system in vitro under oxygenated and anoxic conditions. *Placenta,* 5**,** 213-25.

Illsley, NP, Caniggia, I & Zamudio, S 2010. Placental metabolic reprogramming: do changes in the mix of energy-generating substrates modulate fetal growth? *Int J Dev Biol,* 54**,** 409-19.

Inoue, M, Itoh, H, Ueda, M, Naruko, T, Kojima, A, Komatsu, R, Doi, K, Ogawa, Y, Tamura, N, Takaya, K, Igaki, T, Yamashita, J, Chun, TH, Masatsugu, K, Becker, AE & Nakao, K 1998. Vascular endothelial growth factor (VEGF) expression in human coronary atherosclerotic lesions: possible pathophysiological significance of VEGF in progression of atherosclerosis. *Circulation,* 98**,** 2108-16.

Isenberg, JS, Martin-Manso, G, Maxhimer, JB & Roberts, DD 2009. Regulation of nitric oxide signalling by thrombospondin 1: implications for anti-angiogenic therapies. *Nat Rev Cancer,* 9**,** 182-94.

Jain, NJ, Aswal, VK, Goyal, PS & Bahadur, P 1998. Micellar Structure of an Ethylene Oxide−Propylene Oxide Block Copolymer: A Small-Angle Neutron Scattering Study. *J. Phys. Chem.,* 102**,** 8452-8458.

Jain, RK, Duda, DG, Clark, JW & Loeffler, JS 2006. Lessons from phase III clinical trials on anti-VEGF therapy for cancer. *Nat Clin Pract Oncol,* 3**,** 24-40.

Jellyman, JK, Gardner, DS, Fowden, AL & Giussani, DA 2004. Effects of dexamethasone on the uterine and umbilical vascular beds during basal and hypoxemic conditions in sheep. *Am J Obstet Gynecol,* 190**,** 825-35.

Jia, H, Bagherzadeh, A, Bicknell, R, Duchen, MR, Liu, D & Zachary, I 2004. Vascular endothelial growth factor (VEGF)-D and VEGF-A differentially regulate KDR-mediated signaling and biological function in vascular endothelial cells. *J Biol Chem,* 279**,** 36148-57.

Johanson, R, Lindow, SW, Van Der Elst, C, Jaquire, Z, Van Der Westhuizen, S & Tucker, A 1995. A prospective randomised comparison of the effect of continuous O2 therapy and bedrest on fetuses with absent end-diastolic flow on umbilical artery Doppler waveform analysis. *Br J Obstet Gynaecol,* 102**,** 662-5.

Jovanovic, A, Grbovic, L & Tulic, I 1994. Endothelium-dependent relaxation in response to acetylcholine in the human uterine artery. *Eur J Pharmacol,* 256**,** 131-9.

Jovanovic, A, Jovanovic, S & Grbovic, L 1997. Endothelium-dependent relaxation in response to acetylcholine in pregnant guinea-pig uterine artery. *Hum Reprod,* 12**,** 1805-9.

Kamba, T & Mcdonald, DM 2007. Mechanisms of adverse effects of anti-VEGF therapy for cancer. *Br J Cancer,* 96**,** 1788-95.

Kaneko, JJ, Harvey, JW & Bruss, M 1997. *Clinical biochemistry of domestic animals.,* San Diego, Academic Press.

Karkkainen, MJ, Saaristo, A, Jussila, L, Karila, KA, Lawrence, EC, Pajusola, K, Bueler, H, Eichmann, A, Kauppinen, R, Kettunen, MI, Yla-Herttuala, S, Finegold, DN, Ferrell, RE & Alitalo, K 2001. A model for gene therapy of human hereditary lymphedema. *Proc Natl Acad Sci U S A,* 98**,** 12677-82.

Karpanen, T, Heckman, CA, Keskitalo, S, Jeltsch, M, Ollila, H, Neufeld, G, Tamagnone, L & Alitalo, K 2006. Functional interaction of VEGF-C and VEGF-D with neuropilin receptors. *FASEB J,* 20**,** 1462-72.

Karsdorp, VH, Van Vugt, JM, Van Geijn, HP, Kostense, PJ, Arduini, D, Montenegro, N & Todros, T 1994. Clinical significance of absent or reversed end diastolic velocity waveforms in umbilical artery. *Lancet,* 344**,** 1664-8.

Katz, AB, Keswani, SG, Habli, M, Lim, FY, Zoltick, PW, Midrio, P, Kozin, ED, Herlyn, M & Crombleholme, TM 2009. Placental gene transfer: transgene screening in mice for trophic effects on the placenta. *Am J Obstet Gynecol,* 201**,** 499 e1-8.

Kaufmann, P 1981. Functional anatomy of the non-primate placenta. *Placenta (Supplement 1),* 13-28.

Kaufmann, P, Black, S & Huppertz, B 2003. Endovascular trophoblast invasion: implications for the pathogenesis of intrauterine growth retardation and preeclampsia. *Biol Reprod,* 69**,** 1-7.

Kaufmann, P & Davidoff, M 1977. The guinea-pig placenta. *Adv Anat Embryol Cell Biol,* 53**,** 5-91.

Kawabe, J, Ushikubi, F & Hasebe, N 2010. Prostacyclin in vascular diseases. - Recent insights and future perspectives. *Circ J,* 74**,** 836-43.

Kawasaki, T, Kitsukawa, T, Bekku, Y, Matsuda, Y, Sanbo, M, Yagi, T & Fujisawa, H 1999. A requirement for neuropilin-1 in embryonic vessel formation. *Development,* 126**,** 4895-902.

Keller, G, Zimmer, G, Mall, G, Ritz, E & Amann, K 2003. Nephron number in patients with primary hypertension. *N Engl J Med,* 348**,** 101-8.

Kenny, LC, Baker, PN, Kendall, DA, Randall, MD & Dunn, WR 2002. Differential mechanisms of endothelium-dependent vasodilator responses in human myometrial small arteries in normal pregnancy and pre-eclampsia. *Clin Sci (Lond),* 103**,** 67-73.

Keyt, BA, Nguyen, HV, Berleau, LT, Duarte, CM, Park, J, Chen, H & Ferrara, N 1996. Identification of vascular endothelial growth factor determinants for binding KDR and FLT-1 receptors. Generation of receptor-selective VEGF variants by site-directed mutagenesis. *J Biol Chem,* 271**,** 5638-46.

Khoury, MJ, Erickson, JD, Cordero, JF & Mccarthy, BJ 1988. Congenital malformations and intrauterine growth retardation: a population study. *Pediatrics,* 82**,** 83-90.

Khurana, R, Martin, JF & Zachary, I 2001. Gene therapy for cardiovascular disease: a case for cautious optimism. *Hypertension,* 38**,** 1210-6.

Khurana, R, Zhuang, Z, Bhardwaj, S, Murakami, M, De Muinck, E, Yla-Herttuala, S, Ferrara, N, Martin, JF, Zachary, I & Simons, M 2004. Angiogenesis-dependent and independent phases of intimal hyperplasia. *Circulation,* 110**,** 2436-43.

Kim, M, Zinn, KR, Barnett, BG, Sumerel, LA, Krasnykh, V, Curiel, DT & Douglas, JT 2002. The therapeutic efficacy of adenoviral vectors for cancer gene therapy is limited by a low level of primary adenovirus receptors on tumour cells. *Eur J Cancer,* 38**,** 1917-26.

Kingdom, J, Huppertz, B, Seaward, G & Kaufmann, P 2000. Development of the placental villous tree and its consequences for fetal growth. *Eur J Obstet Gynecol Reprod Biol,* 92**,** 35-43.

Kingdom, JC & Kaufmann, P 1997. Oxygen and placental villous development: origins of fetal hypoxia. *Placenta,* 18**,** 613-21; discussion 623-6.

Kitanaka, T, Gilbert, RD & Longo, LD 1989. Maternal responses to long-term hypoxemia in sheep. *Am J Physiol,* 256**,** R1340-7.

Kitsukawa, T, Shimizu, M, Sanbo, M, Hirata, T, Taniguchi, M, Bekku, Y, Yagi, T & Fujisawa, H 1997. Neuropilin-semaphorin III/D-mediated chemorepulsive signals play a crucial role in peripheral nerve projection in mice. *Neuron,* 19**,** 995-1005.

Koi, H, Zhang, J & Parry, S 2001. The mechanisms of placental viral infection. *Ann N Y Acad Sci,* 943**,** 148-56.

Kojda, G & Harrison, D 1999. Interactions between NO and reactive oxygen species: pathophysiological importance in atherosclerosis, hypertension, diabetes and heart failure. *Cardiovasc Res,* 43**,** 562-71.

Konje, JC, Howarth, ES, Kaufmann, P & Taylor, DJ 2003. Longitudinal quantification of uterine artery blood volume flow changes during gestation in pregnancies complicated by intrauterine growth restriction. *BJOG,* 110**,** 301-5.

Kovacevich, GJ, Gaich, SA, Lavin, JP, Hopkins, MP, Crane, SS, Stewart, J, Nelson, D & Lavin, LM 2000. The prevalence of thromboembolic events among women with extended bed rest prescribed as part of the treatment for premature labor or preterm premature rupture of membranes. *Am J Obstet Gynecol,* 182**,** 1089-92.

Kramer, MS 1987. Intrauterine growth and gestational duration determinants. *Pediatrics,* 80**,** 502-11.

Kramer, RH, Bensch, KG, Davison, PM & Karasek, MA 1984. Basal lamina formation by cultured microvascular endothelial cells. *J Cell Biol,* 99**,** 692-8.

Krebs, C, Macara, LM, Leiser, R, Bowman, AW, Greer, IA & Kingdom, JC 1996. Intrauterine growth restriction with absent end-diastolic flow velocity in the

umbilical artery is associated with maldevelopment of the placental terminal villous tree. *Am J Obstet Gynecol,* 175**,** 1534-42.

Kremer, C, Breier, G, Risau, W & Plate, KH 1997. Up-regulation of flk-1/vascular endothelial growth factor receptor 2 by its ligand in a cerebral slice culture system. *Cancer Res,* 57**,** 3852-9.

Kroll, J & Waltenberger, J 1998. VEGF-A induces expression of eNOS and iNOS in endothelial cells via VEGF receptor-2 (KDR). *Biochem Biophys Res Commun,* 252**,** 743-6.

Ku, DD, Zaleski, JK, Liu, S & Brock, TA 1993. Vascular endothelial growth factor induces EDRF-dependent relaxation in coronary arteries. *Am J Physiol,* 265**,** H586-92.

Kumasawa, K, Ikawa, M, Kidoya, H, Hasuwa, H, Saito-Fujita, T, Morioka, Y, Takakura, N, Kimura, T & Okabe, M 2011. Pravastatin induces placental growth factor (PGF) and ameliorates preeclampsia in a mouse model. *Proc Natl Acad Sci U S A,* 108**,** 1451-5.

Lackman, F, Capewell, V, Richardson, B, Dasilva, O & Gagnon, R 2001. The risks of spontaneous preterm delivery and perinatal mortality in relation to size at birth according to fetal versus neonatal growth standards. *Am J Obstet Gynecol,* 184**,** 946-53.

Lafeber, HN, Rolph, TP & Jones, CT 1984. Studies on the growth of the fetal guinea pig. The effects of ligation of the uterine artery on organ growth and development. *J Dev Physiol,* 6**,** 441-59.

Laitinen, M, Zachary, I, Breier, G, Pakkanen, T, Hakkinen, T, Luoma, J, Abedi, H, Risau, W, Soma, M, Laakso, M, Martin, JF & Yla-Herttuala, S 1997. VEGF gene transfer reduces intimal thickening via increased production of nitric oxide in carotid arteries. *Hum Gene Ther,* 8**,** 1737-44.

Lampugnani, MG, Corada, M, Caveda, L, Breviario, F, Ayalon, O, Geiger, B & Dejana, E 1995. The molecular organization of endothelial cell to cell junctions: differential association of plakoglobin, beta-catenin, and alpha-catenin with vascular endothelial cadherin (VE-cadherin). *J Cell Biol,* 129**,** 203-17.

Landrigan, PJ, Lioy, PJ, Thurston, G, Berkowitz, G, Chen, LC, Chillrud, SN, Gavett, SH, Georgopoulos, PG, Geyh, AS, Levin, S, Perera, F, Rappaport, SM & Small, C 2004. Health and environmental consequences of the world trade center disaster. *Environ Health Perspect,* 112**,** 731-9.

Lang, U, Baker, RS, Braems, G, Zygmunt, M, Kunzel, W & Clark, KE 2003. Uterine blood flow--a determinant of fetal growth. *Eur J Obstet Gynecol Reprod Biol,* 110 Suppl 1**,** S55-61.

Lash, GE, Taylor, CM, Trew, AJ, Cooper, S, Anthony, FW, Wheeler, T & Baker, PN 2002. Vascular endothelial growth factor and placental growth factor release in cultured trophoblast cells under different oxygen tensions. *Growth Factors,* 20**,** 189-96.

Lassala, A, Bazer, FW, Cudd, TA, Datta, S, Keisler, DH, Satterfield, MC, Spencer, TE & Wu, G 2010. Parenteral administration of L-arginine prevents fetal growth restriction in undernourished ewes. *J Nutr,* 140**,** 1242-8.

Lau, MM, Stewart, CE, Liu, Z, Bhatt, H, Rotwein, P & Stewart, CL 1994. Loss of the imprinted IGF2/cation-independent mannose 6-phosphate receptor results in fetal overgrowth and perinatal lethality. *Genes Dev,* 8**,** 2953-63.

Lawlor, DA, Leon, DA & Davey Smith, G 2005. The association of ambient outdoor temperature throughout pregnancy and offspring birthweight: findings from the Aberdeen Children of the 1950s cohort. *BJOG,* 112**,** 647-57.

Lee, RJ, Springer, ML, Blanco-Bose, WE, Shaw, R, Ursell, PC & Blau, HM 2000. VEGF gene delivery to myocardium: deleterious effects of unregulated expression. *Circulation,* 102**,** 898-901.

Lee, S, Chen, TT, Barber, CL, Jordan, MC, Murdock, J, Desai, S, Ferrara, N, Nagy, A, Roos, KP & Iruela-Arispe, ML 2007. Autocrine VEGF signaling is required for vascular homeostasis. *Cell,* 130**,** 691-703.

Leitich, H, Egarter, C, Husslein, P, Kaider, A & Schemper, M 1997. A meta-analysis of low dose aspirin for the prevention of intrauterine growth retardation. *Br J Obstet Gynaecol,* 104**,** 450-9.

Leppanen, P, Koota, S, Kholova, I, Koponen, J, Fieber, C, Eriksson, U, Alitalo, K & Yla-Herttuala, S 2005. Gene transfers of vascular endothelial growth factor-A, vascular endothelial growth factor-B, vascular endothelial growth factor-C, and vascular endothelial growth factor-D have no effects on atherosclerosis in hypercholesterolemic low-density lipoprotein-receptor/apolipoprotein B48-deficient mice. *Circulation,* 112**,** 1347-52.

Leung, DW, Cachianes, G, Kuang, WJ, Goeddel, DV & Ferrara, N 1989. Vascular endothelial growth factor is a secreted angiogenic mitogen. *Science,* 246**,** 1306-9.

Li, Z, Zhang, Y, Ying Ma, J, Kapoun, AM, Shao, Q, Kerr, I, Lam, A, O'young, G, Sannajust, F, Stathis, P, Schreiner, G, Karumanchi, SA, Protter, AA & Pollitt, NS 2007. Recombinant vascular endothelial growth factor 121 attenuates hypertension and improves kidney damage in a rat model of preeclampsia. *Hypertension,* 50**,** 686-92.

Limaye, V & Vadas, M 2007. *Mechanisms of Vascular Disease.,* Cambridge, Cambridge University Press.

Lithell, HO, Mckeigue, PM, Berglund, L, Mohsen, R, Lithell, UB & Leon, DA 1996. Relation of size at birth to non-insulin dependent diabetes and insulin concentrations in men aged 50-60 years. *BMJ,* 312**,** 406-10.

Liu, S, Krewski, D, Shi, Y, Chen, Y & Burnett, RT 2003. Association between gaseous ambient air pollutants and adverse pregnancy outcomes in Vancouver, Canada. *Environ Health Perspect,* 111**,** 1773-8.

Long, PA, Abell, DA & Beischer, NA 1980. Fetal growth retardation and pre-eclampsia. *Br J Obstet Gynaecol,* 87**,** 13-8.

Losordo, DW, Vale, PR, Symes, JF, Dunnington, CH, Esakof, DD, Maysky, M, Ashare, AB, Lathi, K & Isner, JM 1998. Gene therapy for myocardial angiogenesis: initial clinical results with direct myocardial injection of phVEGF165 as sole therapy for myocardial ischemia. *Circulation,* 98**,** 2800-4.

Ludman, A, Venugopal, V, Yellon, DM & Hausenloy, DJ 2009. Statins and cardioprotection--more than just lipid lowering? *Pharmacol Ther,* 122**,** 30-43.

Lumbers, ER 1997. Effects of drugs on uteroplacental blood flow and the health of the foetus. *Clin Exp Pharmacol Physiol,* 24**,** 864-8.

Lundell, A, Bergqvist, D, Mattsson, E & Nilsson, B 1993. Volume blood flow measurements with a transit time flowmeter: an in vivo and in vitro variability and validation study. *Clin Physiol,* 13**,** 547-57.

Luttun, A, Tjwa, M, Moons, L, Wu, Y, Angelillo-Scherrer, A, Liao, F, Nagy, JA, Hooper, A, Priller, J, De Klerck, B, Compernolle, V, Daci, E, Bohlen, P, Dewerchin, M, Herbert, JM, Fava, R, Matthys, P, Carmeliet, G, Collen, D, Dvorak, HF, Hicklin, DJ & Carmeliet, P 2002. Revascularization of ischemic tissues by PlGF treatment, and inhibition of tumor angiogenesis, arthritis and atherosclerosis by anti-Flt1. *Nat Med,* 8**,** 831-40.

Lyall, F, Young, A, Boswell, F, Kingdom, JC & Greer, IA 1997. Placental expression of vascular endothelial growth factor in placentae from pregnancies complicated by pre-eclampsia and intrauterine growth restriction does not support placental hypoxia at delivery. *Placenta,* 18**,** 269-76.

Lyttle, DJ, Fraser, KM, Fleming, SB, Mercer, AA & Robinson, AJ 1994. Homologs of vascular endothelial growth factor are encoded by the poxvirus orf virus. *J Virol,* 68**,** 84-92.

Macara, L, Kingdom, JC, Kaufmann, P, Kohnen, G, Hair, J, More, IA, Lyall, F & Greer, IA 1996. Structural analysis of placental terminal villi from growth-restricted pregnancies with abnormal umbilical artery Doppler waveforms. *Placenta,* 17**,** 37-48.

Maccalman, CD, Furth, EE, Omigbodun, A, Kozarsky, KF, Coutifaris, C & Strauss, JF, 3rd 1996. Transduction of human trophoblast cells by recombinant adenoviruses is differentiation dependent. *Biol Reprod,* 54**,** 682-91.

Mack, CA, Magovern, CJ, Budenbender, KT, Patel, SR, Schwarz, EA, Zanzonico, P, Ferris, B, Sanborn, T, Isom, P, Isom, OW, Crystal, RG & Rosengart, TK 1998. Salvage angiogenesis induced by adenovirus-mediated gene transfer of vascular endothelial growth factor protects against ischemic vascular occlusion. *J Vasc Surg,* 27**,** 699-709.

Magness, RR & Rosenfeld, CR 1993. Calcium modulation of endothelium-derived prostacyclin production in ovine pregnancy. *Endocrinology,* 132**,** 2445-52.

Magness, RR, Rosenfeld, CR, Hassan, A & Shaul, PW 1996. Endothelial vasodilator production by uterine and systemic arteries. I. Effects of ANG II on PGI2 and NO in pregnancy. *Am J Physiol,* 270**,** H1914-23.

Maharaj, AS & D'amore, PA 2007. Roles for VEGF in the adult. *Microvasc Res,* 74**,** 100-13.

Maharaj, AS, Saint-Geniez, M, Maldonado, AE & D'amore, PA 2006. Vascular endothelial growth factor localization in the adult. *Am J Pathol,* 168**,** 639-48.

Mallawaarachchi, CM, Weissberg, PL & Siow, RC 2005. Smad7 gene transfer attenuates adventitial cell migration and vascular remodeling after balloon injury. *Arterioscler Thromb Vasc Biol,* 25**,** 1383-7.

Mannucci, PM 1998. von Willebrand factor: a marker of endothelial damage? *Arterioscler Thromb Vasc Biol,* 18**,** 1359-62.

Manten, GT, Sikkema, MJ, Voorbij, HA, Visser, GH, Bruinse, HW & Franx, A 2007. Risk factors for cardiovascular disease in women with a history of pregnancy complicated by preeclampsia or intrauterine growth restriction. *Hypertens Pregnancy,* 26**,** 39-50.

Marinova, GV, Loyaga-Rendon, RY, Obayashi, S, Ishibashi, T, Kubota, T, Imamura, M & Azuma, H 2008. Possible involvement of altered arginase activity, arginase type I and type II expressions, and nitric oxide production in occurrence of intimal hyperplasia in premenopausal human uterine arteries. *J Pharmacol Sci,* 106**,** 385-93.

Marsh, AC, Lumbers, ER & Gibson, KJ 2002. Renal, cardiovascular and endocrine responses of fetal sheep at 0.8 of gestation to an infusion of amino acids. *J Physiol,* 540**,** 717-28.

Masuda, H, Goto, M, Tamaoki, S & Azuma, H 1999. Accelerated intimal hyperplasia and increased endogenous inhibitors for NO synthesis in rabbits with alloxan-induced hyperglycaemia. *Br J Pharmacol,* 126**,** 211-8.

Maulik, D 2006a. Fetal growth restriction: the etiology. *Clin Obstet Gynecol,* 49**,** 228-35.

Maulik, D 2006b. Management of fetal growth restriction: an evidence-based approach. *Clin Obstet Gynecol,* 49**,** 320-34.

Mayhew, TM, Ohadike, C, Baker, PN, Crocker, IP, Mitchell, C & Ong, SS 2003. Stereological investigation of placental morphology in pregnancies complicated by pre-eclampsia with and without intrauterine growth restriction. *Placenta,* 24**,** 219-26.

Mccowan, LM, Harding, JE & Stewart, AW 2005. Customized birthweight centiles predict SGA pregnancies with perinatal morbidity. *BJOG,* 112**,** 1026-33.

Mcintire, DD, Bloom, SL, Casey, BM & Leveno, KJ 1999. Birth weight in relation to morbidity and mortality among newborn infants. *N Engl J Med,* 340**,** 1234-8.

Mckeeman, GC, Ardill, JE, Caldwell, CM, Hunter, AJ & Mcclure, N 2004. Soluble vascular endothelial growth factor receptor-1 (sFlt-1) is increased throughout gestation in patients who have preeclampsia develop. *Am J Obstet Gynecol,* 191**,** 1240-6.

Mcneil, HP, Chesterman, CN & Krilis, SA 1991. Immunology and clinical importance of antiphospholipid antibodies. *Adv Immunol,* 49**,** 193-280.

Mellor, DJ, Mitchell, B & Matheson, IC 1977. Reductions in lamb weight caused by pre-mating carunclectomy and mid-pregnancy placental ablation. *J Comp Pathol,* 87**,** 629-33.

Meschia, G 1984. *Handbook of Physiology. The cardiovascular system.* , American Physiological Society.

Meschia, G, Cotter, JR, Breathnach, CS & Barron, DH 1965. The diffusibility of oxygen across the sheep placenta. *Q J Exp Physiol Cogn Med Sci,* 50**,** 466-80.

Meyer, DJ & Harvey, JW 1998. Evaluation of hepatobiliary system and skeletal muscle and lipid disorders. *In:* MEYER, DJ & HARVEY, JW (eds.). Philadelphia: W B Saunders Company.

Millauer, B, Wizigmann-Voos, S, Schnurch, H, Martinez, R, Moller, NP, Risau, W & Ullrich, A 1993. High affinity VEGF binding and developmental expression suggest Flk-1 as a major regulator of vasculogenesis and angiogenesis. *Cell,* 72**,** 835-46.

Miller, J, Turan, S & Baschat, AA 2008. Fetal growth restriction. *Semin Perinatol,* 32**,** 274-80.

Miller, SL, Chai, M, Loose, J, Castillo-Melendez, M, Walker, DW, Jenkin, G & Wallace, EM 2007. The effects of maternal betamethasone administration on the intrauterine growth-restricted fetus. *Endocrinology,* 148**,** 1288-95.

Miller, SL, Jenkin, G & Walker, DW 1999. Effect of nitric oxide synthase inhibition on the uterine vasculature of the late-pregnant ewe. *Am J Obstet Gynecol,* 180**,** 1138-45.

Miller, SL, Loose, JM, Jenkin, G & Wallace, EM 2009. The effects of sildenafil citrate (Viagra) on uterine blood flow and well being in the intrauterine growth-restricted fetus. *Am J Obstet Gynecol,* 200**,** 102 e1-7.

Mills, JL, Dersimonian, R, Raymond, E, Morrow, JD, Roberts, LJ, 2nd, Clemens, JD, Hauth, JC, Catalano, P, Sibai, B, Curet, LB & Levine, RJ 1999. Prostacyclin and thromboxane changes predating clinical onset of preeclampsia: a multicenter prospective study. *JAMA,* 282**,** 356-62.

Milner, RDG 1989. Mechanisms of overgrowth. *In:* SHARP, F, FRASER, RB & MILNER, RDG (eds.) *Fetal Growth. Proceedings of the 20th Study Group of the Royal College of Obstetricians and Gynaecologists*. London: Royal College of Obstetricians and Gynaecologists.

Moffett-King, A 2002. Natural killer cells and pregnancy. *Nat Rev Immunol,* 2**,** 656-63.

Molnar, M, Suto, T, Toth, T & Hertelendy, F 1994. Prolonged blockade of nitric oxide synthesis in gravid rats produces sustained hypertension, proteinuria, thrombocytopenia, and intrauterine growth retardation. *Am J Obstet Gynecol,* 170**,** 1458-66.

Moncada, S, Herman, AG, Higgs, EA & Vane, JR 1977. Differential formation of prostacyclin (PGX or PGI2) by layers of the arterial wall. An explanation for the anti-thrombotic properties of vascular endothelium. *Thromb Res,* 11**,** 323-44.

Moncada, S & Vane, JR 1978. Pharmacology and endogenous roles of prostaglandin endoperoxides, thromboxane A2, and prostacyclin. *Pharmacol Rev,* 30**,** 293-331.

Montone, KT, Furth, EE, Pietra, GG & Gupta, PK 1995. Neonatal adenovirus infection: a case report with in situ hybridization confirmation of ascending intrauterine infection. *Diagn Cytopathol,* 12**,** 341-4.

Morris, RK, Malin, G, Robson, SC, Kleijnen, J, Zamora, J & Khan, KS 2011. Fetal umbilical artery Doppler to predict compromise of fetal/neonatal wellbeing in a high-risk population: systematic review and bivariate meta-analysis. *Ultrasound Obstet Gynecol,* 37**,** 135-42.

Morrison, JL 2008. Sheep models of intrauterine growth restriction: fetal adaptations and consequences. *Clin Exp Pharmacol Physiol,* 35**,** 730-43.

Moulton, KS, Heller, E, Konerding, MA, Flynn, E, Palinski, W & Folkman, J 1999. Angiogenesis inhibitors endostatin or TNP-470 reduce intimal neovascularization and plaque growth in apolipoprotein E-deficient mice. *Circulation,* 99**,** 1726-32.

Naicker, T, Khedun, SM, Moodley, J & Pijnenborg, R 2003. Quantitative analysis of trophoblast invasion in preeclampsia. *Acta Obstet Gynecol Scand,* 82**,** 722-9.

Nemerow, GR 2002. Biology of Adenovirus Cell Entry. *In:* CURIEL, DT & DOUGLAS, JT (eds.) *Adenoviral Vectors for Gene Therapy.* New York: New York: Academic Press.

Nemerow, GR & Stewart, PL 1999. Role of alpha(v) integrins in adenovirus cell entry and gene delivery. *Microbiol Mol Biol Rev,* 63**,** 725-34.

Neufeld, G, Cohen, T, Gengrinovitch, S & Poltorak, Z 1999. Vascular endothelial growth factor (VEGF) and its receptors. *FASEB J,* 13**,** 9-22.

Newsome, CA, Shiell, AW, Fall, CH, Phillips, DI, Shier, R & Law, CM 2003. Is birth weight related to later glucose and insulin metabolism?--A systematic review. *Diabet Med,* 20**,** 339-48.

Nicolini, U, Hubinont, C, Santolaya, J, Fisk, NM & Rodeck, CH 1990. Effects of fetal intravenous glucose challenge in normal and growth retarded fetuses. *Horm Metab Res,* 22**,** 426-30.

Niezgoda, J, Bobek, S, Wronska-Fortuna, D & Wierzchos, E 1993. Response of sympatho-adrenal axis and adrenal cortex to short-term restraint stress in sheep. *Zentralbl Veterinarmed A,* 40**,** 631-8.

Nishijima, K, Ng, YS, Zhong, L, Bradley, J, Schubert, W, Jo, N, Akita, J, Samuelsson, SJ, Robinson, GS, Adamis, AP & Shima, DT 2007. Vascular endothelial growth factor-A is a survival factor for retinal neurons and a critical neuroprotectant during the adaptive response to ischemic injury. *Am J Pathol,* 171**,** 53-67.

O'riordan, C 2002. Humoral Immune Responses in Adenoviral Vectors for Gene Therapy. *In:* CURIEL, DT & DOUGLAS, JT (eds.) *Adenoviral Vectors for Gene Therapy.* New York: New York: Academic Press.

Obayashi, S, Beppu, M, Aso, T, Goto, M & Azuma, H 2001. 17 Beta-estradiol increases nitric oxide and prostaglandin I2 production by cultured human uterine arteries only in histologically normal specimens. *J Cardiovasc Pharmacol,* 38**,** 240-9.

Ochi, H, Matsubara, K, Kusanagi, Y, Taniguchi, H & Ito, M 1998. Significance of a diastolic notch in the uterine artery flow velocity waveform induced by uterine embolisation in the pregnant ewe. *Br J Obstet Gynaecol,* 105**,** 1118-21.

Oh, W, Omori, K, Hobel, CJ, Erenberg, A & Emmanouilides, GC 1975. Umbilical blood flow and glucose uptake in lamb fetus following single umbilical artery ligation. *Biol Neonate,* 26**,** 291-9.

Ohashi, Y, Kawashima, S, Hirata, K, Yamashita, T, Ishida, T, Inoue, N, Sakoda, T, Kurihara, H, Yazaki, Y & Yokoyama, M 1998. Hypotension and reduced nitric oxide-elicited vasorelaxation in transgenic mice overexpressing endothelial nitric oxide synthase. *J Clin Invest,* 102**,** 2061-71.

Ong, SS, Baker, PN, Mayhew, TM & Dunn, WR 2005. Remodeling of myometrial radial arteries in preeclampsia. *Am J Obstet Gynecol,* 192**,** 572-9.

Oosthuyse, B, Moons, L, Storkebaum, E, Beck, H, Nuyens, D, Brusselmans, K, Van Dorpe, J, Hellings, P, Gorselink, M, Heymans, S, Theilmeier, G, Dewerchin, M, Laudenbach, V, Vermylen, P, Raat, H, Acker, T, Vleminckx, V, Van Den Bosch, L, Cashman, N, Fujisawa, H, Drost, MR, Sciot, R, Bruyninckx, F, Hicklin, DJ, Ince, C, Gressens, P, Lupu, F, Plate, KH, Robberecht, W, Herbert, JM, Collen, D & Carmeliet, P 2001. Deletion of the hypoxia-response element in the vascular endothelial growth factor promoter causes motor neuron degeneration. *Nat Genet,* 28**,** 131-8.

Osol, G & Mandala, M 2009. Maternal uterine vascular remodeling during pregnancy. *Physiology (Bethesda),* 24**,** 58-71.

Ostrom, RS, Bundey, RA & Insel, PA 2004. Nitric oxide inhibition of adenylyl cyclase type 6 activity is dependent upon lipid rafts and caveolin signaling complexes. *J Biol Chem,* 279**,** 19846-53.

Ott, WJ 2006. Sonographic diagnosis of fetal growth restriction. *Clin Obstet Gynecol,* 49**,** 295-307.

Oyama, K, Padbury, J, Chappell, B, Martinez, A, Stein, H & Humme, J 1992. Single umbilical artery ligation-induced fetal growth retardation: effect on postnatal adaptation. *Am J Physiol,* 263**,** E575-83.

Pallotto, EK & Simmons, RA 2002. *Hypoglycemia of the Newborn In Gellis and Kagan's Current Pediatric Therapy,* Philadelphia, WB Saunders Co.

Palmer, AE, London, WT, Sly, DL & Rice, JM 1979. Spontaneous preeclamptic toxemia of pregnancy in the patas monkey (Erythrocebus patas). *Lab Anim Sci,* 29**,** 102-6.

Palmer, RM & Moncada, S 1989. A novel citrulline-forming enzyme implicated in the formation of nitric oxide by vascular endothelial cells. *Biochem Biophys Res Commun,* 158**,** 348-52.

Palmer, SK, Zamudio, S, Coffin, C, Parker, S, Stamm, E & Moore, LG 1992. Quantitative estimation of human uterine artery blood flow and pelvic blood flow redistribution in pregnancy. *Obstet Gynecol,* 80**,** 1000-6.

Papageorghiou, AT, Yu, CK & Nicolaides, KH 2004. The role of uterine artery Doppler in predicting adverse pregnancy outcome. *Best Pract Res Clin Obstet Gynaecol,* 18**,** 383-96.

Park, JE, Keller, GA & Ferrara, N 1993. The vascular endothelial growth factor (VEGF) isoforms: differential deposition into the subepithelial extracellular matrix and bioactivity of extracellular matrix-bound VEGF. *Mol Biol Cell,* 4**,** 1317-26.

Parry, S, Holder, J, Halterman, MW, Weitzman, MD, Davis, AR, Federoff, H & Strauss, JF, 3rd 1998. Transduction of human trophoblastic cells by replication-deficient recombinant viral vectors. Promoting cellular differentiation affects virus entry. *Am J Pathol,* 152**,** 1521-9.

Patel, SR, Lee, LY, Mack, CA, Polce, DR, El-Sawy, T, Hackett, NR, Ilercil, A, Jones, EC, Hahn, RT, Isom, OW, Rosengart, TK & Crystal, RG 1999. Safety of direct myocardial administration of an adenovirus vector encoding vascular endothelial growth factor 121. *Hum Gene Ther,* 10**,** 1331-48.

Peeters, LL, Sheldon, RE, Jones, MD, Jr., Makowski, EL & Meschia, G 1979. Blood flow to fetal organs as a function of arterial oxygen content. *Am J Obstet Gynecol,* 135**,** 637-46.

Pellet-Many, C, Frankel, P, Jia, H & Zachary, I 2008. Neuropilins: structure, function and role in disease. *Biochem J,* 411**,** 211-26.

Perera, FP, Tang, D, Rauh, V, Lester, K, Tsai, WY, Tu, YH, Weiss, L, Hoepner, L, King, J, Del Priore, G & Lederman, SA 2005. Relationships among polycyclic aromatic hydrocarbon-DNA adducts, proximity to the World Trade Center, and effects on fetal growth. *Environ Health Perspect,* 113**,** 1062-7.

Petrova, TV, Makinen, T & Alitalo, K 1999. Signaling via vascular endothelial growth factor receptors. *Exp Cell Res,* 253**,** 117-30.

Phillips, DI 1996. Insulin resistance as a programmed response to fetal undernutrition. *Diabetologia,* 39**,** 1119-22.

Phillips, DI, Walker, BR, Reynolds, RM, Flanagan, DE, Wood, PJ, Osmond, C, Barker, DJ & Whorwood, CB 2000. Low birth weight predicts elevated plasma cortisol concentrations in adults from 3 populations. *Hypertension,* 35**,** 1301-6.

Plate, KH, Breier, G, Millauer, B, Ullrich, A & Risau, W 1993. Up-regulation of vascular endothelial growth factor and its cognate receptors in a rat glioma model of tumor angiogenesis. *Cancer Res,* 53**,** 5822-7.

Polzin, WJ, Kopelman, JN, Robinson, RD, Read, JA & Brady, K 1991. The association of antiphospholipid antibodies with pregnancies complicated by fetal growth restriction. *Obstet Gynecol,* 78**,** 1108-11.

Preziuso, S, Taccini, E, Rossi, G, Braca, G & Renzoni, G 2002. Cutaneous haemangiosarcoma in a sheep: morphological, histopathological and immunohistochemical observations. *J Comp Pathol,* 127**,** 72.

Quinn, TP, Peters, KG, De Vries, C, Ferrara, N & Williams, LT 1993. Fetal liver kinase 1 is a receptor for vascular endothelial growth factor and is selectively expressed in vascular endothelium. *Proc Natl Acad Sci U S A,* 90**,** 7533-7.

Ravindranath, N, Little-Ihrig, L, Phillips, HS, Ferrara, N & Zeleznik, AJ 1992. Vascular endothelial growth factor messenger ribonucleic acid expression in the primate ovary. *Endocrinology,* 131**,** 254-60.

Reddy, UM, Baschat, AA, Zlatnik, MG, Towbin, JA, Harman, CR & Weiner, CP 2005. Detection of viral deoxyribonucleic acid in amniotic fluid: association with fetal malformation and pregnancy abnormalities. *Fetal Diagn Ther,* 20**,** 203-7.

Regev, RH, Lusky, A, Dolfin, T, Litmanovitz, I, Arnon, S & Reichman, B 2003. Excess mortality and morbidity among small-for-gestational-age premature infants: a population-based study. *J Pediatr,* 143**,** 186-91.

Regnault, TR, De Vrijer, B, Galan, HL, Davidsen, ML, Trembler, KA, Battaglia, FC, Wilkening, RB & Anthony, RV 2003. The relationship between transplacental O2 diffusion and placental expression of PlGF, VEGF and their receptors in a placental insufficiency model of fetal growth restriction. *J Physiol,* 550**,** 641-56.

Regnault, TR, Galan, HL, Parker, TA & Anthony, RV 2002. Placental development in normal and compromised pregnancies-- a review. *Placenta,* 23 Suppl A**,** S119-29.

Reister, F, Frank, HG, Kingdom, JC, Heyl, W, Kaufmann, P, Rath, W & Huppertz, B 2001. Macrophage-induced apoptosis limits endovascular trophoblast invasion in the uterine wall of preeclamptic women. *Lab Invest,* 81**,** 1143-52.

Reshetnikova, O, Naidenova, O & Ivaschenko, I 2002. Placental morphology in cases of fetal IUGR at 20 – 25 weeks of gestation. *Placenta,* 23**,** A33.

Reynolds, LP, Caton, JS, Redmer, DA, Grazul-Bilska, AT, Vonnahme, KA, Borowicz, PP, Luther, JS, Wallace, JM, Wu, G & Spencer, TE 2006. Evidence for altered placental blood flow and vascularity in compromised pregnancies. *J Physiol,* 572**,** 51-8.

Richter, HG, Hansell, JA, Raut, S & Giussani, DA 2009. Melatonin improves placental efficiency and birth weight and increases the placental expression of antioxidant enzymes in undernourished pregnancy. *J Pineal Res,* 46**,** 357-64.

Rissanen, TT, Korpisalo, P, Markkanen, JE, Liimatainen, T, Orden, MR, Kholova, I, De Goede, A, Heikura, T, Grohn, OH & Yla-Herttuala, S 2005. Blood flow remodels growing vasculature during vascular endothelial growth factor gene therapy and determines between capillary arterialization and sprouting angiogenesis. *Circulation,* 112**,** 3937-46.

Rissanen, TT, Markkanen, JE, Gruchala, M, Heikura, T, Puranen, A, Kettunen, MI, Kholova, I, Kauppinen, RA, Achen, MG, Stacker, SA, Alitalo, K & Yla-Herttuala, S 2003. VEGF-D is the strongest angiogenic and lymphangiogenic effector among VEGFs delivered into skeletal muscle via adenoviruses. *Circ Res,* 92**,** 1098-106.

Rivalland, ET, Clarke, IJ, Turner, AI, Pompolo, S & Tilbrook, AJ 2007. Isolation and restraint stress results in differential activation of corticotrophin-releasing hormone and arginine vasopressin neurons in sheep. *Neuroscience,* 145**,** 1048-58.

Roberts, CT, Kind, KL, Earl, RA, Grant, PA, Robinson, JS, Sohlstrom, A, Owens, PC & Owens, JA 2002. Circulating insulin-like growth factor (IGF)-I and IGF binding proteins -1 and -3 and placental development in the guinea-pig. *Placenta,* 23**,** 763-70.

Roberts, CT, Sohlstrom, A, Kind, KL, Earl, RA, Khong, TY, Robinson, JS, Owens, PC & Owens, JA 2001a. Maternal food restriction reduces the exchange surface area and increases the barrier thickness of the placenta in the guinea-pig. *Placenta,* 22**,** 177-85.

Roberts, CT, Sohlstrom, A, Kind, KL, Grant, PA, Earl, RA, Robinson, JS, Khong, TY, Owens, PC & Owens, JA 2001b. Altered placental structure induced by maternal food restriction in guinea pigs: a role for circulating IGF-II and IGFBP-2 in the mother? *Placenta,* 22 Suppl A**,** S77-82.

Robinson, CJ & Stringer, SE 2001. The splice variants of vascular endothelial growth factor (VEGF) and their receptors. *J Cell Sci,* 114**,** 853-65.

Robinson, JS, Kingston, EJ, Jones, CT & Thorburn, GD 1979. Studies on experimental growth retardation in sheep. The effect of removal of a endometrial caruncles on fetal size and metabolism. *J Dev Physiol,* 1**,** 379-98.

Robinson, NJ, Wareing, M, Hudson, NK, Blankley, RT, Baker, PN, Aplin, JD & Crocker, IP 2008. Oxygen and the liberation of placental factors responsible for vascular compromise. *Lab Invest,* 88**,** 293-305.

Robinson, V 2005. Finding alternatives: an overview of the 3Rs and the use of animals in research. *Sch Sci Rev,* 87**,** 1-4.

Romo, A, Carceller, R & Tobajas, J 2009. Intrauterine growth retardation (IUGR): epidemiology and etiology. *Pediatr Endocrinol Rev,* 6 Suppl 3**,** 332-6.

Rosati, P, Exacoustos, C, Puggioni, GF & Mancuso, S 1995. Growth retardation in pregnancy: experimental model in the rabbit employing electrically induced thermal placental injury. *Int J Exp Pathol,* 76**,** 179-81.

Rosenberg, RD 1985. Role of heparin and heparinlike molecules in thrombosis and atherosclerosis. *Fed Proc,* 44**,** 404-9.

Rosendorff, C 1997. Endothelin, vascular hypertrophy, and hypertension. *Cardiovasc Drugs Ther,* 10**,** 795-802.

Rosenfeld, PJ, Brown, DM, Heier, JS, Boyer, DS, Kaiser, PK, Chung, CY & Kim, RY 2006. Ranibizumab for neovascular age-related macular degeneration. *N Engl J Med,* 355**,** 1419-31.

Rosengart, TK, Lee, LY, Patel, SR, Sanborn, TA, Parikh, M, Bergman, GW, Hachamovitch, R, Szulc, M, Kligfield, PD, Okin, PM, Hahn, RT, Devereux, RB, Post, MR, Hackett, NR, Foster, T, Grasso, TM, Lesser, ML, Isom, OW & Crystal, RG 1999. Angiogenesis gene therapy: phase I assessment of direct intramyocardial administration of an adenovirus vector expressing VEGF121 cDNA to individuals with clinically significant severe coronary artery disease. *Circulation,* 100**,** 468-74.

Russell, WC 1998. Adenoviruses. *In:* COLLIER, L, BALOWS, A & SUSSMAN, M (eds.) *Topley and Wilson's Microbiology and Microbial Infections.* 9th ed. London: Arnold.

Ryan, HE, Lo, J & Johnson, RS 1998. HIF-1 alpha is required for solid tumor formation and embryonic vascularization. *EMBO J,* 17**,** 3005-15.

Sadler, TW 2004. *Periods of susceptibility to teratogenesis,* Lippincott Williams and Wilkins.

Samangaya, RA, Mires, G, Shennan, A, Skillern, L, Howe, D, Mcleod, A & Baker, PN 2009. A randomised, double-blinded, placebo-controlled study of the phosphodiesterase type 5 inhibitor sildenafil for the treatment of preeclampsia. *Hypertens Pregnancy,* 28**,** 369-82.

Sanlaville, D, Aubry, MC, Dumez, Y, Nolen, MC, Amiel, J, Pinson, MP, Lyonnet, S, Munnich, A, Vekemans, M & Morichon-Delvallez, N 2000. Maternal uniparental heterodisomy of chromosome 14: chromosomal mechanism and clinical follow up. *J Med Genet,* 37**,** 525-8.

Saria, A & Lundberg, JM 1983. Evans blue fluorescence: quantitative and morphological evaluation of vascular permeability in animal tissues. *J Neurosci Methods,* 8**,** 41-9.

Savvidou, MD, Yu, CK, Harland, LC, Hingorani, AD & Nicolaides, KH 2006. Maternal serum concentration of soluble fms-like tyrosine kinase 1 and vascular endothelial growth factor in women with abnormal uterine artery Doppler and in those with fetal growth restriction. *Am J Obstet Gynecol,* 195**,** 1668-73.

Say, L, Gulmezoglu, AM & Hofmeyr, GJ 2003. Maternal oxygen administration for suspected impaired fetal growth. *Cochrane Database Syst Rev***,** CD000137.

Schmolka, IR 1972. Artificial skin. I. Preparation and properties of pluronic F-127 gels for treatment of burns. *J Biomed Mater Res,* 6**,** 571-82.

Schroder, HJ 2003. Models of fetal growth restriction. *Eur J Obstet Gynecol Reprod Biol,* 110 Suppl 1**,** S29-39.

Schwartz, JE, Kovach, A, Meyer, J, Mcconnell, C & Iwamoto, HS 1998. Brief, intermittent hypoxia restricts fetal growth in Sprague-Dawley rats. *Biol Neonate,* 73**,** 313-9.

Scotland, RS, Madhani, M, Chauhan, S, Moncada, S, Andresen, J, Nilsson, H, Hobbs, AJ & Ahluwalia, A 2005. Investigation of vascular responses in endothelial nitric oxide synthase/cyclooxygenase-1 double-knockout mice: key role for endothelium-derived hyperpolarizing factor in the regulation of blood pressure in vivo. *Circulation,* 111**,** 796-803.

Seetharam, L, Gotoh, N, Maru, Y, Neufeld, G, Yamaguchi, S & Shibuya, M 1995. A unique signal transduction from FLT tyrosine kinase, a receptor for vascular endothelial growth factor VEGF. *Oncogene,* 10**,** 135-47.

Semenza, GL 2001. HIF-1, O(2), and the 3 PHDs: how animal cells signal hypoxia to the nucleus. *Cell,* 107**,** 1-3.

Sessa, WC 2009. Molecular control of blood flow and angiogenesis: role of nitric oxide. *J Thromb Haemost,* 7 Suppl 1**,** 35-7.

Shalaby, F, Rossant, J, Yamaguchi, TP, Gertsenstein, M, Wu, XF, Breitman, ML & Schuh, AC 1995. Failure of blood-island formation and vasculogenesis in Flk-1-deficient mice. *Nature,* 376**,** 62-6.

Shweiki, D, Itin, A, Soffer, D & Keshet, E 1992. Vascular endothelial growth factor induced by hypoxia may mediate hypoxia-initiated angiogenesis. *Nature,* 359**,** 843-5.

Sibai, B, Dekker, G & Kupferminc, M 2005. Pre-eclampsia. *Lancet,* 365**,** 785-99.

Sibai, BM 2004. Diagnosis, controversies, and management of the syndrome of hemolysis, elevated liver enzymes, and low platelet count. *Obstet Gynecol,* 103**,** 981-91.

Sibley, CP, Turner, MA, Cetin, I, Ayuk, P, Boyd, CA, D'souza, SW, Glazier, JD, Greenwood, SL, Jansson, T & Powell, T 2005. Placental phenotypes of intrauterine growth. *Pediatr Res,* 58**,** 827-32.

Sieroszewski, P, Suzin, J & Karowicz-Bilinska, A 2004. Ultrasound evaluation of intrauterine growth restriction therapy by a nitric oxide donor (L-arginine). *J Matern Fetal Neonatal Med,* 15**,** 363-6.

Silva, R, D'amico, G, Hodivala-Dilke, KM & Reynolds, LE 2008. Integrins: the keys to unlocking angiogenesis. *Arterioscler Thromb Vasc Biol,* 28**,** 1703-13.

Simchen, MJ, Beiner, ME, Strauss-Liviathan, N, Dulitzky, M, Kuint, J, Mashiach, S & Schiff, E 2000. Neonatal outcome in growth-restricted versus appropriately grown preterm infants. *Am J Perinatol,* 17**,** 187-92.

Simons, M, Bonow, RO, Chronos, NA, Cohen, DJ, Giordano, FJ, Hammond, HK, Laham, RJ, Li, W, Pike, M, Sellke, FW, Stegmann, TJ, Udelson, JE & Rosengart, TK 2000. Clinical trials in coronary angiogenesis: issues, problems, consensus: An expert panel summary. *Circulation,* 102**,** E73-86.

Skarsgard, ED, Amii, LA, Dimmitt, RA, Sakamoto, G, Brindle, ME & Moss, RL 2001. Fetal therapy with rhIGF-1 in a rabbit model of intrauterine growth retardation. *J Surg Res,* 99**,** 142-6.

Skillman, CA, Plessinger, MA, Woods, JR & Clark, KE 1985. Effect of graded reductions in uteroplacental blood flow on the fetal lamb. *Am J Physiol,* 249**,** H1098-105.

Smith, GC, Pell, JP & Walsh, D 2001. Pregnancy complications and maternal risk of ischaemic heart disease: a retrospective cohort study of 129,290 births. *Lancet,* 357**,** 2002-6.

Snijders, RJ, Abbas, A, Melby, O, Ireland, RM & Nicolaides, KH 1993a. Fetal plasma erythropoietin concentration in severe growth retardation. *Am J Obstet Gynecol,* 168**,** 615-9.

Snijders, RJ, Sherrod, C, Gosden, CM & Nicolaides, KH 1993b. Fetal growth retardation: associated malformations and chromosomal abnormalities. *Am J Obstet Gynecol,* 168**,** 547-55.

Snoeck, A, Remacle, C, Reusens, B & Hoet, JJ 1990. Effect of a low protein diet during pregnancy on the fetal rat endocrine pancreas. *Biol Neonate,* 57**,** 107-18.

Soker, S, Takashima, S, Miao, HQ, Neufeld, G & Klagsbrun, M 1998. Neuropilin-1 is expressed by endothelial and tumor cells as an isoform-specific receptor for vascular endothelial growth factor. *Cell,* 92**,** 735-45.

Sokol, GM, Liechty, EA & Boyle, DW 1996. Comparison of steady-state diffusion and transit time ultrasonic measurements of umbilical blood flow in the chronic fetal sheep preparation. *Am J Obstet Gynecol,* 174**,** 1456-60.

Sokol, RJ, Delaney-Black, V & Nordstrom, B 2003. Fetal alcohol spectrum disorder. *JAMA,* 290**,** 2996-9.

Sondell, M, Sundler, F & Kanje, M 2000. Vascular endothelial growth factor is a neurotrophic factor which stimulates axonal outgrowth through the flk-1 receptor. *Eur J Neurosci,* 12**,** 4243-54.

Spinillo, A, Viazzo, F, Colleoni, R, Chiara, A, Maria Cerbo, R & Fazzi, E 2004. Two-year infant neurodevelopmental outcome after single or multiple antenatal courses of corticosteroids to prevent complications of prematurity. *Am J Obstet Gynecol,* 191**,** 217-24.

Stacker, SA, Stenvers, K, Caesar, C, Vitali, A, Domagala, T, Nice, E, Roufail, S, Simpson, RJ, Moritz, R, Karpanen, T, Alitalo, K & Achen, MG 1999. Biosynthesis of vascular endothelial growth factor-D involves proteolytic processing which generates non-covalent homodimers. *J Biol Chem,* 274**,** 32127-36.

Steegers, EA, Von Dadelszen, P, Duvekot, JJ & Pijnenborg, R 2010. Pre-eclampsia. *Lancet,* 376**,** 631-44.

Stein, Z & Susser, M 1975. The Dutch famine, 1944-1945, and the reproductive process. I. Effects on six indices at birth. *Pediatr Res,* 9**,** 70-6.

Takashima, S, Kitakaze, M, Asakura, M, Asanuma, H, Sanada, S, Tashiro, F, Niwa, H, Miyazaki Ji, J, Hirota, S, Kitamura, Y, Kitsukawa, T, Fujisawa, H, Klagsbrun, M & Hori, M 2002. Targeting of both mouse neuropilin-1 and neuropilin-2 genes severely impairs developmental yolk sac and embryonic angiogenesis. *Proc Natl Acad Sci U S A,* 99**,** 3657-62.

Takei, H, Nakai, Y, Hattori, N, Yamamoto, M, Kurauchi, K, Sasaki, H & Aburada, M 2004. The herbal medicine Toki-shakuyaku-san improves the hypertension and intrauterine growth retardation in preeclampsia rats induced by Nomega-nitro-L-arginine methyl ester. *Phytomedicine,* 11**,** 43-50.

Takeshita, S, Isshiki, T, Ochiai, M, Eto, K, Mori, H, Tanaka, E, Umetani, K & Sato, T 1998. Endothelium-dependent relaxation of collateral microvessels after intramuscular gene transfer of vascular endothelial growth factor in a rat model of hindlimb ischemia. *Circulation,* 98**,** 1261-3.

Takeshita, S, Tsurumi, Y, Couffinahl, T, Asahara, T, Bauters, C, Symes, J, Ferrara, N & Isner, JM 1996a. Gene transfer of naked DNA encoding for three isoforms of vascular endothelial growth factor stimulates collateral development in vivo. *Lab Invest,* 75**,** 487-501.

Takeshita, S, Weir, L, Chen, D, Zheng, LP, Riessen, R, Bauters, C, Symes, JF, Ferrara, N & Isner, JM 1996b. Therapeutic angiogenesis following arterial gene transfer of vascular endothelial growth factor in a rabbit model of hindlimb ischemia. *Biochem Biophys Res Commun,* 227**,** 628-35.

Tamura, RK, Sabbagha, RE, Depp, R, Vaisrub, N, Dooley, SL & Socol, ML 1984. Diminished growth in fetuses born preterm after spontaneous labor or rupture of membranes. *Am J Obstet Gynecol,* 148**,** 1105-10.

Tanaka, M, Natori, M, Ishimoto, H, Miyazaki, T, Kobayashi, T & Nozawa, S 1994. Experimental growth retardation produced by transient period of uteroplacental ischemia in pregnant Sprague-Dawley rats. *Am J Obstet Gynecol,* 171**,** 1231-4.

Taylor, KJ & Holland, S 1990. Doppler US. Part I. Basic principles, instrumentation, and pitfalls. *Radiology,* 174**,** 297-307.

Teasdale, F 1985. Histomorphometry of the human placenta in maternal preeclampsia. *Am J Obstet Gynecol,* 152**,** 25-31.

Teasdale, F 1987. Histomorphometry of the human placenta in pre-eclampsia associated with severe intrauterine growth retardation. *Placenta,* 8**,** 119-28.

Tessler, S, Rockwell, P, Hicklin, D, Cohen, T, Levi, BZ, Witte, L, Lemischka, IR & Neufeld, G 1994. Heparin modulates the interaction of VEGF165 with soluble and cell associated flk-1 receptors. *J Biol Chem,* 269**,** 12456-61.

Thakor, AS, Herrera, EA, Seron-Ferre, M & Giussani, DA 2010. Melatonin and vitamin C increase umbilical blood flow via nitric oxide-dependent mechanisms. *J Pineal Res,* 49**,** 399-406.

Thakur, A, Sase, M, Lee, JJ, Thakur, V & Buchmiller, TL 2000. Ontogeny of insulin-like growth factor 1 in a rabbit model of growth retardation. *J Surg Res,* 91**,** 135-40.

Thaler, I, Manor, D, Itskovitz, J, Rottem, S, Levit, N, Timor-Tritsch, I & Brandes, JM 1990. Changes in uterine blood flow during human pregnancy. *Am J Obstet Gynecol,* 162**,** 121-5.

Thureen, PJ, Trembler, KA, Meschia, G, Makowski, EL & Wilkening, RB 1992. Placental glucose transport in heat-induced fetal growth retardation. *Am J Physiol,* 263**,** R578-85.

Tischer, E, Mitchell, R, Hartman, T, Silva, M, Gospodarowicz, D, Fiddes, JC & Abraham, JA 1991. The human gene for vascular endothelial growth factor. Multiple protein forms are encoded through alternative exon splicing. *J Biol Chem,* 266**,** 11947-54.

Tomko, RP, Xu, R & Philipson, L 1997. HCAR and MCAR: the human and mouse cellular receptors for subgroup C adenoviruses and group B coxsackieviruses. *Proc Natl Acad Sci U S A,* 94**,** 3352-6.

Trapnell, BC & Shanley, TP 2002. Innate Responses to in Vivo Adenovirus Infection. *In:* CURIEL, DT & DOUGLAS, JT (eds.) *Adenoviral Vectors for Gene Therapy.* New York: New York: Academic Press.

Trudinger, B, Song, JZ, Wu, ZH & Wang, J 2003. Placental insufficiency is characterized by platelet activation in the fetus. *Obstet Gynecol,* 101**,** 975-81.

Turner, AJ & Trudinger, BJ 2000. Ultrasound measurement of biparietal diameter and umbilical artery blood flow in the normal fetal guinea pig. *Comp Med,* 50**,** 379-84.

Tyson, JE, Kennedy, K, Broyles, S & Rosenfeld, CR 1995. The small for gestational age infant: accelerated or delayed pulmonary maturation? Increased or decreased survival? *Pediatrics,* 95**,** 534-8.

Urakami-Harasawa, L, Shimokawa, H, Nakashima, M, Egashira, K & Takeshita, A 1997. Importance of endothelium-derived hyperpolarizing factor in human arteries. *J Clin Invest,* 100**,** 2793-9.

Valdes, G, Kaufmann, P, Corthorn, J, Erices, R, Brosnihan, KB & Joyner-Grantham, J 2009. Vasodilator factors in the systemic and local adaptations to pregnancy. *Reprod Biol Endocrinol,* 7**,** 79.

Van Assche, FA & Aerts, L 1979. The fetal endocrine pancreas. *Contrib Gynecol Obstet,* 5**,** 44-57.

Van Der Zee, R, Murohara, T, Luo, Z, Zollmann, F, Passeri, J, Lekutat, C & Isner, JM 1997. Vascular endothelial growth factor/vascular permeability factor augments nitric oxide release from quiescent rabbit and human vascular endothelium. *Circulation,* 95**,** 1030-7.

Vane, JR 1994. The Croonian Lecture, 1993. The endothelium: maestro of the blood circulation. *Philos Trans R Soc Lond B Biol Sci,* 343**,** 225-46.

Vanhaesebroeck, B, Guillermet-Guibert, J, Graupera, M & Bilanges, B 2010. The emerging mechanisms of isoform-specific PI3K signalling. *Nat Rev Mol Cell Biol,* 11**,** 329-41.

Veikkola, T, Jussila, L, Makinen, T, Karpanen, T, Jeltsch, M, Petrova, TV, Kubo, H, Thurston, G, Mcdonald, DM, Achen, MG, Stacker, SA & Alitalo, K 2001. Signalling via vascular endothelial growth factor receptor-3 is sufficient for lymphangiogenesis in transgenic mice. *EMBO J,* 20**,** 1223-31.

Vestweber, D 2007. Molecular mechanisms that control leukocyte extravasation through endothelial cell contacts. *Ernst Schering Found Symp Proc***,** 151-67.

Vestweber, D 2008. VE-cadherin: the major endothelial adhesion molecule controlling cellular junctions and blood vessel formation. *Arterioscler Thromb Vasc Biol,* 28**,** 223-32.

Viita, H, Markkanen, J, Eriksson, E, Nurminen, M, Kinnunen, K, Babu, M, Heikura, T, Turpeinen, S, Laidinen, S, Takalo, T & Yla-Herttuala, S 2008. 15-lipoxygenase-1 prevents vascular endothelial growth factor A- and placental growth factor-induced angiogenic effects in rabbit skeletal muscles via reduction in growth factor mRNA levels, NO bioactivity, and downregulation of VEGF receptor 2 expression. *Circ Res,* 102**,** 177-84.

Villanueva-Garcia, D, Mota-Rojas, D, Hernandez-Gonzalez, R, Sanchez-Aparicio, P, Alonso-Spilsbury, M, Trujillo-Ortega, ME, Necoechea, RR & Nava-Ocampo, AA 2007. A systematic review of experimental and clinical studies of sildenafil citrate for intrauterine growth restriction and pre-term labour. *J Obstet Gynaecol,* 27**,** 255-9.

Vincenti, V, Cassano, C, Rocchi, M & Persico, G 1996. Assignment of the vascular endothelial growth factor gene to human chromosome 6p21.3. *Circulation,* 93**,** 1493-5.

Von Dadelszen, P, Dwinnell, S, Magee, LA, Carleton, BC, Gruslin, A, Lee, B, Lim, KI, Liston, RM, Miller, SP, Rurak, D, Sherlock, RL, Skoll, MA, Wareing, MM & Baker, PN 2011. Sildenafil citrate therapy for severe early-onset intrauterine growth restriction. *BJOG,* 118**,** 624-8.

Vonnahme, KA, Wilson, ME, Li, Y, Rupnow, HL, Phernetton, TM, Ford, SP & Magness, RR 2005. Circulating levels of nitric oxide and vascular endothelial growth factor throughout ovine pregnancy. *J Physiol,* 565**,** 101-9.

Voyta, JC, Via, DP, Butterfield, CE & Zetter, BR 1984. Identification and isolation of endothelial cells based on their increased uptake of acetylated-low density lipoprotein. *J Cell Biol,* 99**,** 2034-40.

Walker, DM, Marlow, N, Upstone, L, Gross, H, Hornbuckle, J, Vail, A, Wolke, D & Thornton, JG 2011. The Growth Restriction Intervention Trial: long-term outcomes in a randomized trial of timing of delivery in fetal growth restriction. *Am J Obstet Gynecol,* 204**,** 34 e1-9.

Wallace, JM, Aitken, RP, Milne, JS & Hay, WW, Jr. 2004. Nutritionally mediated placental growth restriction in the growing adolescent: consequences for the fetus. *Biol Reprod,* 71**,** 1055-62.

Wallace, JM, Milne, JS, Matsuzaki, M & Aitken, RP 2008. Serial measurement of uterine blood flow from mid to late gestation in growth restricted pregnancies induced by overnourishing adolescent sheep dams. *Placenta,* 29**,** 718-24.

Wallace, JM, Regnault, TR, Limesand, SW, Hay, WW, Jr. & Anthony, RV 2005. Investigating the causes of low birth weight in contrasting ovine paradigms. *J Physiol,* 565**,** 19-26.

Wallner, W, Sengenberger, R, Strick, R, Strissel, PL, Meurer, B, Beckmann, MW & Schlembach, D 2007. Angiogenic growth factors in maternal and fetal serum in pregnancies complicated by intrauterine growth restriction. *Clin Sci (Lond),* 112**,** 51-7.

Waltenberger, J, Claesson-Welsh, L, Siegbahn, A, Shibuya, M & Heldin, CH 1994. Different signal transduction properties of KDR and Flt1, two receptors for vascular endothelial growth factor. *J Biol Chem,* 269**,** 26988-95.

Wang, YP, Walsh, SW, Guo, JD & Zhang, JY 1991. The imbalance between thromboxane and prostacyclin in preeclampsia is associated with an imbalance between lipid peroxides and vitamin E in maternal blood. *Am J Obstet Gynecol,* 165**,** 1695-700.

Wareing, M, Myers, JE, O'hara, M & Baker, PN 2005. Sildenafil citrate (Viagra) enhances vasodilatation in fetal growth restriction. *J Clin Endocrinol Metab,* 90**,** 2550-5.

Weiner, CP, Thompson, LP, Liu, KZ & Herrig, JE 1992. Pregnancy reduces serotonin-induced contraction of guinea pig uterine and carotid arteries. *Am J Physiol,* 263**,** H1764-9.

Wenstrom, KD, Andrews, WW, Bowles, NE, Towbin, JA, Hauth, JC & Goldenberg, RL 1998. Intrauterine viral infection at the time of second trimester genetic amniocentesis. *Obstet Gynecol,* 92**,** 420-4.

Werner, A, Kloss, CU, Walter, J, Kreutzberg, GW & Raivich, G 1998. Intercellular adhesion molecule-1 (ICAM-1) in the mouse facial motor nucleus after axonal injury and during regeneration. *J Neurocytol,* 27**,** 219-32.

Wheeler-Jones, C, Abu-Ghazaleh, R, Cospedal, R, Houliston, RA, Martin, J & Zachary, I 1997. Vascular endothelial growth factor stimulates prostacyclin production and activation of cytosolic phospholipase A2 in endothelial cells via p42/p44 mitogen-activated protein kinase. *FEBS Lett,* 420**,** 28-32.

White, MM, Mccullough, RE, Dyckes, R, Robertson, AD & Moore, LG 2000. Chronic hypoxia, pregnancy, and endothelium-mediated relaxation in guinea pig uterine and thoracic arteries. *Am J Physiol Heart Circ Physiol,* 278**,** H2069-75.

Widdowson, EM 1971. Intra-uterine growth retardation in the pig. I. Organ size and cellular development at birth and after growth to maturity. *Biol Neonate,* 19**,** 329-40.

Widdowson, EM, Crabb, DE & Milner, RD 1972. Cellular development of some human organs before birth. *Arch Dis Child,* 47**,** 652-5.

Wigglesworth, JS 1964. Fetal growth retardation. Animal model: uterine vessel ligation in the pregnant rat. *J Path Biol.,* 88**,** 1-13.

Woodall, SM, Breier, BH, Johnston, BM, Bassett, NS, Barnard, R & Gluckman, PD 1999. Administration of growth hormone or IGF-I to pregnant rats on a reduced diet throughout pregnancy does not prevent fetal intrauterine growth retardation and elevated blood pressure in adult offspring. *J Endocrinol,* 163**,** 69-77.

Woodall, SM, Breier, BH, Johnston, BM & Gluckman, PD 1996. A model of intrauterine growth retardation caused by chronic maternal undernutrition in the rat: effects on the somatotrophic axis and postnatal growth. *J Endocrinol,* 150**,** 231-42.

Woods, AK, Hoffmann, DS, Weydert, CJ, Butler, SD, Zhou, Y, Sharma, RV & Davisson, RL 2011. Adenoviral delivery of VEGF121 early in pregnancy prevents spontaneous development of preeclampsia in BPH/5 mice. *Hypertension,* 57**,** 94-102.

Worgall, S, Wolff, G, Falck-Pedersen, E & Crystal, RG 1997. Innate immune mechanisms dominate elimination of adenoviral vectors following in vivo administration. *Hum Gene Ther,* 8**,** 37-44.

Wu, G, Bazer, FW, Davis, TA, Kim, SW, Li, P, Marc Rhoads, J, Carey Satterfield, M, Smith, SB, Spencer, TE & Yin, Y 2009. Arginine metabolism and nutrition in growth, health and disease. *Amino Acids,* 37**,** 153-68.

Wu, G, Bazer, FW, Wallace, JM & Spencer, TE 2006. Board-invited review: intrauterine growth retardation: implications for the animal sciences. *J Anim Sci,* 84**,** 2316-37.

Wu, G & Morris, SM, Jr. 1998. Arginine metabolism: nitric oxide and beyond. *Biochem J,* 336 (Pt 1)**,** 1-17.

Wutz, A & Barlow, DP 1998. Imprinting of the mouse Igf2r gene depends on an intronic CpG island. *Mol Cell Endocrinol,* 140**,** 9-14.

Xiao, D, Liu, Y, Pearce, WJ & Zhang, L 1999. Endothelial nitric oxide release in isolated perfused ovine uterine arteries: effect of pregnancy. *Eur J Pharmacol,* 367**,** 223-30.

Xiao, D, Pearce, WJ & Zhang, L 2001. Pregnancy enhances endothelium-dependent relaxation of ovine uterine artery: role of NO and intracellular Ca(2+). *Am J Physiol Heart Circ Physiol,* 281**,** H183-90.

Xiao, D & Zhang, L 2002. ERK MAP kinases regulate smooth muscle contraction in ovine uterine artery: effect of pregnancy. *Am J Physiol Heart Circ Physiol,* 282**,** H292-300.

Yamaguchi, TP, Dumont, DJ, Conlon, RA, Breitman, ML & Rossant, J 1993. flk-1, an flt-related receptor tyrosine kinase is an early marker for endothelial cell precursors. *Development,* 118**,** 489-98.

Yang, R, Thomas, GR, Bunting, S, Ko, A, Ferrara, N, Keyt, B, Ross, J & Jin, H 1996. Effects of vascular endothelial growth factor on hemodynamics and cardiac performance. *J Cardiovasc Pharmacol,* 27**,** 838-44.

Yang, X & Cepko, CL 1996. Flk-1, a receptor for vascular endothelial growth factor (VEGF), is expressed by retinal progenitor cells. *J Neurosci,* 16**,** 6089-99.

Yasuda, M, Takakuwa, K, Tokunaga, A & Tanaka, K 1995. Prospective studies of the association between anticardiolipin antibody and outcome of pregnancy. *Obstet Gynecol,* 86**,** 555-9.

Yinon, Y, Kingdom, JC, Odutayo, A, Moineddin, R, Drewlo, S, Lai, V, Cherney, DZ & Hladunewich, MA 2010. Vascular dysfunction in women with a history of preeclampsia and intrauterine growth restriction: insights into future vascular risk. *Circulation,* 122**,** 1846-53.

Yla-Herttuala, S & Martin, JF 2000. Cardiovascular gene therapy. *Lancet,* 355**,** 213-22.

Yliharsila, H, Eriksson, JG, Forsen, T, Kajantie, E, Osmond, C & Barker, DJ 2003. Self-perpetuating effects of birth size on blood pressure levels in elderly people. *Hypertension,* 41**,** 446-50.

Ylikorkala, O, Pekonen, F & Viinikka, L 1986. Renal prostacyclin and thromboxane in normotensive and preeclamptic pregnant women and their infants. *J Clin Endocrinol Metab,* 63**,** 1307-12.

Yuan, L, Moyon, D, Pardanaud, L, Breant, C, Karkkainen, MJ, Alitalo, K & Eichmann, A 2002. Abnormal lymphatic vessel development in neuropilin 2 mutant mice. *Development,* 129**,** 4797-806.

Zachary, I 2005. Signal transduction in angiogenesis. *EXS***,** 267-300.

Zachary, I, Mathur, A, Yla-Herttuala, S & Martin, J 2000. Vascular protection: A novel nonangiogenic cardiovascular role for vascular endothelial growth factor. *Arterioscler Thromb Vasc Biol,* 20**,** 1512-20.

Zachary, I & Morgan, RD 2011. Therapeutic angiogenesis for cardiovascular disease: biological context, challenges, prospects. *Heart,* 97**,** 181-9.

Zamudio, S, Baumann, MU & Illsley, NP 2006. Effects of chronic hypoxia in vivo on the expression of human placental glucose transporters. *Placenta,* 27**,** 49-55.

Zamudio, S, Wu, Y, Ietta, F, Rolfo, A, Cross, A, Wheeler, T, Post, M, Illsley, NP & Caniggia, I 2007. Human placental hypoxia-inducible factor-1alpha expression correlates with clinical outcomes in chronic hypoxia in vivo. *Am J Pathol,* 170**,** 2171-9.

Zanetta, L, Marcus, SG, Vasile, J, Dobryansky, M, Cohen, H, Eng, K, Shamamian, P & Mignatti, P 2000. Expression of Von Willebrand factor, an endothelial cell marker, is up-regulated by angiogenesis factors: a potential method for objective assessment of tumor angiogenesis. *Int J Cancer,* 85**,** 281-8.

Zezula-Szpyra, A, Gawronska, B & Skipor, J 1997. Vasa vasorum of blood and lymph vessels in the broad ligament of the sheep uterus analyzed by scanning electron microscopy. *Rocz Akad Med Bialymst,* 42 Suppl 2**,** 134-46.

Zhou, Y, Bellingard, V, Feng, KT, Mcmaster, M & Fisher, SJ 2003a. Human cytotrophoblasts promote endothelial survival and vascular remodeling through secretion of Ang2, PlGF, and VEGF-C. *Dev Biol,* 263**,** 114-25.

Zhou, Y, Genbacev, O & Fisher, SJ 2003b. The human placenta remodels the uterus by using a combination of molecules that govern vasculogenesis or leukocyte extravasation. *Ann N Y Acad Sci,* 995**,** 73-83.

Zhou, Y, Mcmaster, M, Woo, K, Janatpour, M, Perry, J, Karpanen, T, Alitalo, K, Damsky, C & Fisher, SJ 2002. Vascular endothelial growth factor ligands and receptors that regulate human cytotrophoblast survival are dysregulated in severe preeclampsia and hemolysis, elevated liver enzymes, and low platelets syndrome. *Am J Pathol,* 160**,** 1405-23.

Appendix 1 – Composition of sheep and guinea pig feed

Sheep Feed

Super Ewe & Lamb 6mm Pencils (Lillico Attlee Ltd., Surrey, UK)

This feed contains:-

Oil	5.0%
Fibre	9.0%
Selenium	0.30 mg/kg
Vitamin A	6,800 iu/kg
Vitamin D_3	2,000 iu/kg
Vitamin E	30.0 iu/kg
Protein	18.0%
Ash	8.0%

The raw ingredients of this diet include:-

10-25% Wheat
Barley
Sunflower meal
Citrus pulp
Wheatfeed
10% Rape Meal
Palm Kernel Exp
Molasses
Sun Bean Meal
Amino Green
Limestone
Vegetable Oil
Salt
Sheep Vitamin/Minerals
Calcined Magnesite
Dicalcium phosphate

Guinea Pig Feed

FD 1 (P) PL (Special Diets Services, Essex, UK)

Crude Fat	3.3%
Crude Protein	18.6%
Crude Fibre	9.7%
Crude Ash	8.8%
Vitamin A (retinol acetate)	3440 iu/kg
Vitamin D_3 (cholecalciferol)	1960 iu/kg
Vitamin E (dl-a-tocopheryl acetate)	38iu/kg
Lysine	0.89%
Methionine	0.36%
Calcium	1.17%
Phosphorous	0.92%
Sodium	0.35%
Magnesium	0.33%
Copper	21mg/kg

Appendix II – Composition of Kreb's Ringer Solution used for Pharmacology Experiments

118 mM NaCl

4.6 mM KCl

27.2 mM $NaHCO_3$

1.2 mM KH_2PO_4

1.2 mM $MgSO_4$

1.75 mM $CaCl_2$

0.03 mM Na_2EDTA

11.1 mM glucose

Appendix III – Composition of cell culture medium used for uterine artery endothelial cell experiments

The basic serum-free medium used was Endothelial Cell Basal Medium (EBM) (CC3124, Lonza, Berkshire, UK).

For routine cell culture, EBM was supplemented with fetal bovine serum (FBS) and growth factors. The supplemented medium was called Endothelial Cell Growth Medium (EGM) and had the following composition:-

EBM	450ml
FBS (10500-056, Invitrogen, UK)	50ml
Growth supplements (CC4133, Lonza, Berkshire, UK):	
Bovine brain extract	2ml
Human Epidermal Growth Factor	0.5ml
Geneticin-Amphotericin	0.5ml
Fungizone (15290-025, Invitrogen, Paisley, UK)	3.75ml

Appendix IV – Sheep post-mortem form

Date: **Animal No:** **Code:**

Fetal measurements: Fetal Weight:

Crown Rump Length: Femur Length:

Biparietal Diameter: Abdominal Circumference:

Occipito-snout Length:

Post mortem findings:

Bloods taken: Maternal Serum Maternal Plasma

Tissue samples to be collected from the **MOTHER:**

Tissue sample	code	N2	PFA
Right Uterine artery	**RU-A1**	☐	☐
Right Uterine artery 1st division	**RU-A2**	☐	☐
Right Uterine artery 2nd division	**RU-A3**	☐	☐
Right Uterine artery 3rd division	**RU-A4**	☐	☐
Right Uterus	**RU-T**	☐	☐
Right Placentome	**R-P**	☐	☐
Left Uterine artery	**LU-A1**	☐	☐
Left Uterine artery 1st division	**LU-A2**	☐	☐
Left Uterine artery 2nd division	**LU-A3**	☐	☐
Left Uterine artery 3rd division	**LU-A4**	☐	☐
Left Uterus	**LU-T**	☐	☐
Left placentome	**L-P**	☐	☐

Lung	**E-AU**	☐	☐
Heart	**E-H**	☐	☐
Ovary	**E-G**	☐	☐
Liver	**E-L**	☐	☐
Adrenal	**E-D**	☐	☐
Kidney	**E-K**	☐	☐
Spleen	**E-X**	☐	☐
Brain	**E-NC**	☐	☐
Retina	**E-Retina**	☐	☐

FETUS

Tissue samples to be collected from each **FETUS:**

Blood (serum & plasma)	**B**		
Tissue samples	**code**	**N2**	**PFA**
Membranes	**Me**	☐	☐
Umbilical cord	**U**	☐	☐
Amniotic Fluid	**AF**	☐	☐
Lung	**AU**	☐	☐
Thymus	**T**	☐	☐
Heart	**H**	☐	☐
Spleen	**X**	☐	☐
Liver	**L**	☐	☐
Gonads Female Male	**G**	☐	☐
Adrenal glands	**D**	☐	☐
Kidney	**K**	☐	☐
Brain	**NC**	☐	☐
Retina	**Retina**	☐	☐

Tissue samples collected for histology processing

Cassettes	**Tissues**
1	Left UA1
2	Left UA2
3	Left UA3
4	Left UA4
5	Left uterus Left placentomes
6	Right UA1
7	Right UA2
8	Right UA3
9	Right UA4
10	Right uterus Right placentomes
11	Maternal ovary, liver, spleen
12	Maternal kidney, adrenal, heart, lung
13	Left membranes, Left umbilical vein
14	Left gonad, liver,
15	Left spleen, adrenal, kidney
16	Left heart, lung, thymus
17	Right membranes, umbilical vein
18	Right gonad, liver
19	Right spleen, adrenal, kidney
20	Right heart, lung, thymus
21	Ewe brain, retina
22	Fetal brain, retina

Appendix V – Guinea Pig Post-mortem Form

Date: **Animal No:** **Code:**

Fetal measurements: Fetal Weight:

Brain Weight: Liver Weight:

Heart Weight: Kidney Weight:

Crown Rump Length: Femur Length:

Biparietal Diameter: Abdominal Circumference:

Occipito-snout Length:

Post mortem findings:

Bloods taken: Maternal Serum Maternal Plasma
Maternal Whole Blood

Tissue samples to be collected from the **MOTHER:**

	code	N2	PFA
Right Uterine artery	**RU-A1**	☐	☐
Right Radial artery (Cervical end 1)	**RR-A1**	☐	☐
Right Radial artery (Cervical end 2)	**RR-A2**	☐	☐
Right Radial artery (Cervical end 3)	**RR-A3**	☐	☐
Right Placenta (Cervical end 1)	**R-P1**	☐	☐
Right Placenta (Cervical end 2)	**R-P2**	☐	☐
Right Placenta (Cervical end 3)	**R-P3**	☐	☐
Right Uterus (Cervical end)	**R-UT1**	☐	☐
Right Uterus (Middle)	**R-UT2**	☐	☐
Right Uterus (Ovarian end)	**R-UT3**	☐	☐
Left Uterine artery	**LU-A1**	☐	☐

Left Radial artery (Cervical end 1)	**LR-A1**	☐	☐
Left Radial artery (Cervical end 2)	**LR-A2**	☐	☐
Left Radial artery (Cervical end 3)	**LR-A3**	☐	☐
Left Placenta (Cervical end 1)	**L-P1**	☐	☐
Left Placenta (Cervical end 2)	**L-P2**	☐	☐
Left Placenta (Cervical end 3)	**L-P3**	☐	☐
Left Uterus (Cervical end)	**L-UT1**	☐	☐
Left Uterus (Middle)	**L-UT2**	☐	☐
Left Uterus (Ovarian end)	**L-UT3**	☐	☐

Lung	**E-AU**	☐	☐
Heart	**E-H**	☐	☐
Ovary	**E-G**	☐	☐
Liver	**E-L**	☐	☐
Adrenal	**E-D**	☐	☐
Kidney	**E-K**	☐	☐
Spleen	**E-X**	☐	☐
Brain	**E-NC**	☐	☐
Retina	**E-Retina**	☐	☐

FETUS Cervical end____

Tissue samples to be collected from each FETUS:

Blood, serum & plasma			**B**		
			code	**N2**	**PFA**
Membranes			**Me**	☐	☐
Umbilical cord			**U**	☐	☐
Amniotic Fluid			**AF**	☐	☐
Lung			**AU**	☐	☐
Thymus			**T**	☐	☐
Heart			**H**	☐	☐
Spleen			**X**	☐	☐
Liver			**L**	☐	☐
Gonads	**Female**	**Male**	**G**	☐	☐
Adrenal glands			**D**	☐	☐
Kidney			**K**	☐	☐
Muscle			**M**	☐	☐
Skin			**S**	☐	☐
Brain			**NC**	☐	☐
Bone Marrow			**BM**	☐	☐

Tissue samples collected for histology processing

Cassettes	**Tissues**
1	Left UA1
2	Left RA1, Left RA2, Left RA3
3	Left uterus, Left placentae (1,2,3)
4	Right UA1
5	Right RA1, Right RA2, Right RA3
6	Right uterus, Right placentae (1,2,3)
7	Maternal ovary, liver, spleen
8	Maternal kidney, adrenal, heart, lung, thymus
9	Maternal brain
10	Maternal bone marrow
11	Fetal spleen, adrenal, kidney
12	Fetal heart, lung, thymus
13	Fetal gonad, liver
14	Fetal brain
15	Fetal muscle, skin
16	Fetal bone marrow